Deliverable 2.3 and 4.3: Training Material – Geochemical & Reactive Transport Modelling for Geological Disposal

Work Packages ACED and DONUT

This project has received funding from the European Union's Horizon 2020 research and innovation programme under grant agreement N°847593.

http://www.ejp-eurad.eu/

Document information

Project Acronym	**EURAD**
Project Title	**European Joint Programme on Radioactive Waste Management**
Project Type	**European Joint Programme (EJP)**
EC grant agreement No.	**847593**
Project starting / end date	**1st June 2019 – 30 May 2024**
Work Package No.	**2 and 4**
Work Package Title	**Asessment of the chemical evolution at the disposal cell scale** **Development and Improvement Of NUmerical methods and Tools for modelling coupled processes**
Work Package Acronym	**ACED and DONUT**
Deliverable No.	**D2.3 and D4.3**
Deliverable Title	**Training Material – Geochemical & Reactive Transport Modelling for Geological Disposal**
Lead Beneficiary	**SCK CEN and BRGM**
Contractual Delivery Date	**ACED: March 2023 / DONUT: May 2022**
Actual Delivery Date	**May 2023**
Type	**Report**
Dissemination level	**Public**
Authors	**Diederik Jacques (SCK CEN), Dmitrii Kulik (PSI), Hans Meeussen (NRG), Sergey Churakov (PSI), Francis Claret (BRGM)**

To be cited as:

Jacques, D., Kulik, D., Meeussen, H., Churakov, S., Claret, F.. (2023): Training Material – Geochemical & Reactive Transport Modelling for Geological Disposal. Final version as of xx.xx.xxxx of deliverable D2.3 and D4.3 of the HORIZON 2020 project EURAD. EC Grant agreement no: 847593.

Disclaimer

Acknowledgement

This document is a deliverable of the European Joint Programme on Radioactive Waste Management (EURAD). EURAD has received funding from the European Union's Horizon 2020 research and innovation programme under grant agreement No 847593.

Status of deliverable		
	By	Date
Delivered (Lead Beneficiary)	Diederik Jacques (SCK CEN) – ACED Francis Claret (BRGM) - DONUT	February 2023
Verified (WP Leader)	Diederik Jacques (SCK CEN) – ACED Francis Claret (BRGM) – DONUT Sergey Churakov (PSI) - FUTURE	April 2023
Reviewed (Reviewers)	Not applicable	-
Approved (PMO)	Bernd Grambow (DONUT) Louise Théodon (ACED)	May 2023
Submitted to EC (Coordinator)	Andra	04 May 2023

Executive Summary

This report contains the aims and learning outcomes, the training course description, and the abstracts, reading material and slides from the lectures given at the training course. The training was organized at the University of Bern, Switzerland on February 6-10, 2023.

Table of content

1. Introduction

Geological disposal systems for radioactive materials consist of different engineered and natural materials; this in view of the multi-barrier principle. The interaction between the contrasting materials in the near field of a disposal system (both the engineered barrier system and the host rock) will induce geochemical changes of these materials. The geochemical evolution as a consequence of physical and chemical perturbations needs to be part of the safety and performance analyses of the repository as it will influence (i) the durability of the different materials, and (ii) speciation and mobility of radionuclides. Given the time scales involved (ten thousand to hundred thousand years), assessing the evolution can only be done with numerical models in which geochemistry is linked to transport, thus with reactive transport codes.

A key aspect in these models is the geochemical model in which the geochemical state variables are calculated based on thermodynamic equilibrium and kinetic processes. These geochemical models account for aqueous speciation reactions, dissolution/precipitation based on saturation state, sorption based on mechanistic sorption models (exchange reactions, surface complexation) and possible kinetic processes (related e.g. to the dissolution of glass or clay minerals or the corrosion of steel canisters).

Reactive transport codes typically couple these chemical models to solute transport equations. State-of-the-art reactive transport codes may couple this also the water flow or heat transport. Geochemical solvers in state-of-the-art reactive transport codes are also capable of handling some (micro)biological reactions. Therefore, these codes are capable to simulate coupled thermal, hydraulic, chemical and biological (THCB) processes and possible feedback between the processes. They became a powerful tool for understanding and assessing these coupled processes and the consequences for containment.

Given the complexity of the system and the long-time scales, models typically have large computational times and many uncertainties associated with it. Recent developments in new couplings between different solvers, faster methods to solve equations including methods based on machine learning, and efficient algorithms for uncertainty analysis are crucial in the framework of the analysis of the long-term evolution, optimization and performance assessment of a radioactive waste repository.

In EURAD, the work packages ACED (Assessment of Chemical Evolution of ILW and HLW Disposal cells) DONUT (Development and improvement of numerical methods and tools for modelling coupled processes) improve and implement codes and models for assessing the geochemical evolution in the near field of a repository. In view of that, this training will continue from the state-of-the-art and introduce the new developments acquire in these work packages.

1.1 Aims

The training aims at enlarging knowledge and expertise in geochemical and coupled reactive transport modelling in the framework of disposal of radioactive waste with the focus on geological disposal. The theoretical basis will be enhanced by lectures on (i) principles of geochemical and reactive transport modelling, (ii) their applications for processes and evolution of materials in a geological disposal (cementitious materials, glass, steel, clay, granite) (iii) speciation and migration of radionuclides, and (iv) advanced topics related to uncertainty and machine learning. Practical skills will be enhanced by computer sessions in which participants will use available software to implement and analyze models for calculating properties and evolution of materials and speciation of radionuclides.

1.2 Learning outcomes

Upon completion of the training course, the participants should be able to:

- Understand the principles of geochemical thermodynamic and kinetic modelling and reactive transport modelling
- Use these principles for application in the field of radioactive waste disposal
- Transform specific research questions related to geochemical properties or evolution into a conceptual model

- Implement simple conceptual models into numerical codes for geochemical and reactive transport modelling
- Identify advanced methods for sensitivity analysis, uncertainty analysis and integration of machine learning techniques

2. Training Course Description

The one-week training is built around two pillars:

- Lectures by experts in the field on topics on
  - Geochemical and reactive transport modelling, properties and evolution of materials in the engineered barrier system of a geological disposal, geochemical properties of the host matrix, and sorption of radionuclides.
  - Advanced topics on sensitivity and uncertainty studies and surrogate learning (machine learning)
  - Demonstration of state-of-the-art codes for implementing geochemical and reactive transport models.
- Practical sessions on applying numerical codes for geochemical and reactive transport models. The course will provide training sessions for some of the more widely-used codes (PHREEQC, GEMS and ORCHESTRA, and their coupling with transport models, as HPx) between which the participant can choose. The training sessions will be built around two examples that are used in the machine learning benchmark study of ACED DONUT:
  - Ageing/leaching and/or carbonation of cementitious materials based on ordinary Portland cement,
  - Uranium sorption on clay materials.
- Delivery strategy: Classroom-based training, practical sessions

Evaluation strategy: none

3. Lectures

3.1 Lecture 1 Modelling geochemical systems – equilibrium, thermodynamics, reaction progress

Geochemical modelling aims at predicting partial equilibria between aqueous, solid and gas phases in a system of relevance for research and engineering where a solid solution may be stable over a wide range of conditions and compositions even if some or all its pure end members are unstable. Equilibrium compositions of co-existing solution phases depend on each other and on the temperature, pressure, and bulk elemental composition of the whole system. Hence, a non-linear computer-aided numerical method is needed to solve for the chemical speciation and to evaluate the partitioning of (minor) elements between phases, which is of major geochemical relevance.

A speciation algorithm requires as input the formula and standard thermodynamic properties for all chemical species, plus optional parameters of mixing in phases-solutions at temperature and pressure of interest. Such information is taken from a previously compiled and curated chemical thermodynamic database (TDB) – another crucial component of geochemical modelling along with the numerical algorithm. Methods of thermodynamic data calculation, correction and prediction are built into codes for computing thermodynamic properties of substances and chemical reactions.

At the Earth (sub)surface conditions, complete equilibria are almost never achieved. This is why modelling codes contain various tools for simulating partial equilibria or irreversible mass action processes (titration, oxidation/reduction, leaching etc.). In a partial equilibrium state, some species (e.g. atmospheric nitrogen) and/or some (solid) phases cannot react completely and thus remain in their metastable states. The saturation index logSI shows that a phase can be (i) stable in positive or zero amount when logSI ≈ 0; (ii) unstable in zero amount when logSI < 0; (iii) metastable in zero or positive amount when logSI > 0 or in positive amount when logSI < 0. Case (iii) is modeled using additional upper- or lower bound constraints on the mole amount of a species or a phase. Control on these additional constraints as functions of time, simulation step, pH, activities of ions, logSI, etc. makes it possible to simulate kinetic processes such as mineral dissolution or precipitation. This and other key concepts of geochemical thermodynamic modelling will be summarized in this talk.

Lecturer

D. Kulik, PSI, Switzerland

Reading Material

Leal A.M.M., Kulik D.A., Smith W.R., Saar M.O. (2017): An overview of computational methods for chemical equilibrium and kinetics calculations for geochemical and reactive transport modeling. Pure and Applied Chemistry 89, 597-643. doi.

Kulik D.A. (2010): Geochemical thermodynamic modelling of ion partitioning. Chapter 3 in: Ion-partitioning in ambient-temperature aqueous systems (eds. M.Prieto, H.Stoll), EMU Notes in Mineralogy 10, 65-138.

Slides

PAUL SCHERRER INSTITUT PSI

2023 EURAD Training Workshop

eurad European Joint Programme on Radioactive Waste Management

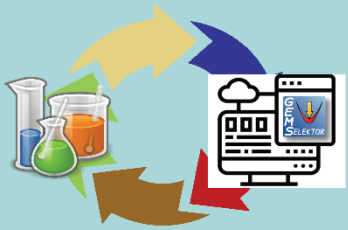

Modelling geochemical systems – Equilibrium, Thermodynamics, Reaction Progress

Dmitrii A. Kulik

Laboratory for Waste Management,

Nuclear Energy and Safety Research Department,

Paul Scherrer Institut

on behalf of GEMS Development Team

In this presentation

1. Geochemical systems: equilibrium and metastability

   Equilibrium at P,T,b: stable phases and speciation in phases-solutions

   Metastability; mineral-water reaction kinetics

2. Numerical methods to solve for geochemical speciation

   Gibbs Energy Minimization GEM, e.g. GEMS, Reaktoro

   Law of Mass Action LMA, e.g. PHREEQC, ORCHESTRA

   Forward and inverse modelling problems

3. Thermodynamic Data Bases TDB as main inputs

   Thermochemical format (substances) – $G^o(P,T)$ for GEM

   Reaction format (product- from master species) – $\log K^o(P,T)$ for LMA

What is geochemical modelling?

Goal: To improve and quantify our fundamental understanding of (slow) chemical processes in natural and engineered geochemical systems

Geochemical system: Heterogeneous, contains (non-ideal) solutions, exists in metastable (partial-equilibrium) states, "dirty" (multi-element)

Requirements: Data (bases) of standard thermodynamic properties of substances and reactions; of activity model parameters; of kinetic rate parameters

Research tools: numerical algorithms and computer codes for non-linear minimization of either total Gibbs energy or of mass balance residuals

Main types of problems: ***forward*** (find equilibrium speciation at *P,T,b*);
inverse (find some inputs from known outputs)

Relevance: (Radioactive) waste disposal, (ore) geochemistry, geothermics, cement chemistry and other areas

3 Geochemical modelling EURAD Training Workshop Univ. Bern, February 6-10, 2023

1. Geochemical systems

1. Geochemical systems: equilibrium and metastability

Equilibrium at P,T,b: stable phases and speciation in phases-solutions

Metastability; mineral-water reaction kinetics

2. Numerical methods to solve for geochemical speciation

Gibbs Energy Minimization GEM, e.g. GEMS, Reaktoro

Law of Mass Action LMA, e.g. PHREEQC, ORCHESTRA

Forward and inverse modelling problems

3. Thermodynamic Data Bases TDB as main inputs

Thermochemical format (substances) – $G^o(P,T)$ for GEM

Reaction format (product- from master species) – $\log K^o(P,T)$ for LMA

4 Geochemical modelling EURAD Training Workshop Univ. Bern, February 6-10, 2023

Phase equilibrium in a multisystem

Multisystem is a 'rich' chemical system *with (some or all):*

- *aqueous electrolyte;*
- *non-ideal gaseous fluids;*
- *non-ideal solid solutions;*
- *non-ideal (ionic) melts;*
- *adsorption, ion exchange;*
- *Many pure phases (s, l);*
- *metastable species, kinetics*

where the number of phases exceeds the number of elements and the number of species exceeds number of phases

EqDemo :: ML-B-CEM:0:Minimal-c:0:0:1:25:2:

EqIC | EqPh | EqDC | EqSurf | EqGen | 17/08/2022, 12:38

Minimal cement system with CO2 (for bench) w/b=0.5 corr straetl,…

DONUT benchmarks corrected by DK 17.08.2022

	ICnam		b	Cb	u	lgm_t
0	Al	e	0.0882688	0	-319.1387	-5.897203
1	C	e	1	1.111376e-16	-170.782	-4.58218
2	Ca	e	1.123447	-1.111376e-16	-278.7023	-2.971495
3	H	h	5.550837	-2.222752e-16	-46.8358	-2.682543
4	O	o	7.262873	9.099392e-16	-2.005843	-1.99579
5	Si	e	0.615801	-4.514965e-17	-338.43	-2.403998
6	Zz	z	0	-1.436473e-20	24.28915	0

EqStat:: Single Thermodynamic System in Project ML-B-CEM

Input: System Definition | Results: Equilibrium State

	Phase/species	L	Ty	Amount (mol)	logSI/Activity
a	aq_gen	26	a	2.332649	1.776e-09
g	gas_gen	5	g	0	-1.296
s	CSHQ	4	s	0.1181959	-5.38e-08
s	Al(OH)3am	1	s	0	-1.955
s	Al(OH)3mic	1	s	0	-1.045
s	Gibbsite	1	s	0	-0.5923
s	Kaolinite	1	s	0	1.464
s	Graphite	1	s	0	-74.17
s	CA	1	s	0	-14.92
s	CA2	1	s	0	-16.63
s	C2AH75	1	s	0	-12.66
s	C3AH6	1	s	0	-17.47
s	C4AH11	1	s	0	-25.97
s	C4AH13	1	s	0	-24.23
s	C4AH19	1	s	0	-24.03
s	CAH10	1	s	0	-7.343
s	Chabazite	1	s	0.04413437	3.555e-12
s	ZeoliteP	1	s	0	-0.07223
s	straetlingite	1	s	0	-5.279
s	C4AcH9	1	s	0	-18.98
s	C4Ac0.5H105	1	s	0	-20.57
s	C4Ac0.5H12	1	s	0	-18.84
s	C4Ac0.5H9	1	s	0	-23.57
s	C4AcH11	1	s	0	-14.98
s	Aragonite	1	s	0	-0.1438
s	Calcite	1	s	0.9999989	4.968e-10
s	lime	1	s	0	-16.09
s	Portlandite	1	s	0	-6.313
s	Quartz	1	s	0.301243	1.032
s	Silica-amorph	1	s	0.02040118	5.486e-07

Equilibrium: phases-solutions, partitioning

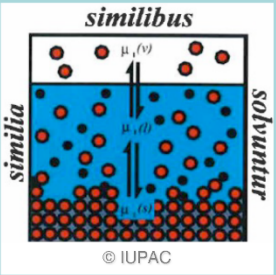

Partitioning of an ion (element) M:

- at least two *chemical components* (species) of M,
- present in at least two different *phases*,
- at least one of which is a *solution* phase

Partitioning is closely related to ***equilibrium solubility***

Uptake is usually understood as a chemical transfer of minor (trace) element *Tr* from aqueous solution into solid phase(s) upon equilibration of the system.

Measured by solid (solution) – aqueous *Tr* distribution ratios (e.g. in mole fraction)

ionic $$k_d(Tr) = \frac{x_{TrL}}{m_{Tr^{Z+}}}$$

total $$R_d(Tr) = \frac{x_{TrL}}{m_{Tr,\mathrm{tot}}}$$

From known chemical speciation, all ***distribution ratios*** can always be obtained.

Equilibrium: Aqueous-Gas-Solid

- List of species:

  $H_2O(aq)$, H^+, OH^-, Ca^{2+}, CO_3^{2-}, HCO_3^-, $H_2CO_3(aq)$; O2(g), CO2(g); CaCO3(cr)

- Mass balance equations:

  $[C]tot = mCO_3^{2-} + mHCO_3^- + mH_2CO_3(aq)$

  $[Ca]tot = mCa^{2+}$ ...

- Charge balance: $Charge = H^+ + 2Ca^{2+} - OH^- - 2CO_3^{2-} ... = 0$
- Law of mass action:

  $CaCO_{3(s)} = Ca^{2+} + CO_3^{2-}$

  $K = aCa^{2+} \times aCO_3^{2-} / aCaCO_{3(s)}$

  $HCO_3^- = H^+ + CO_3^{2-}$

  $K = aH^+ \times aCO_3^{2-} / aHCO_3^-$

- Non-ideal activity of aqueous species:

  extended Debye-Hückel model:

$$log\gamma_i = \frac{Az_i^2\sqrt{I}}{1 + a^\circ B\sqrt{I}} + \Gamma_\gamma + b_\gamma I$$

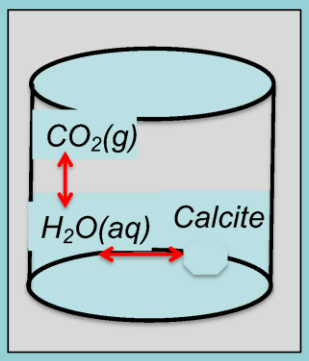

Equilibrium: many [pure] phases

- System components (C): *Na-Fe-Si-O-H*
- Phases (φ): *Arf, Rbk, Aeg, Hem, Qtz, $O_{2(g)}$, $H_2O_{(g)}$*
- Gibbs phase rule: $F = C + 2 - \phi$
- Standard Gibbs energy of mineral reaction $\Delta_r G^o(P,T)$:

  $Arf + O_{2(g)} = 3Aeg + Hem + 2Qtz + H_2O_{(g)}$

$$logK = -\frac{\Delta_r G^\circ_{(P,T)}}{ln(10)RT}$$

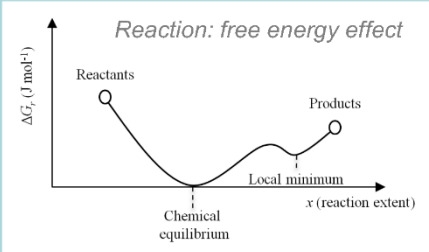

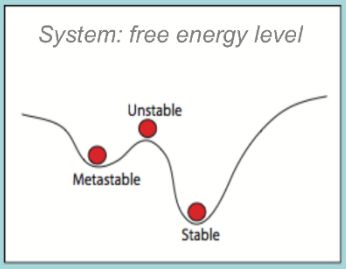

- Schreinemakers rule for metastable/stable reactions
- Pseudosections and stability diagrams (P-T-x)
- Gibbs energy minimization (e.g. Perplex, Thermocalc, Melts).

If only pure phases: linear programming (Simplex) method (PerpleX)

General case: many [non]-ideal multicomponent phases-solutions – need a non-linear Gibbs Energy Minimization algorithm

Complete equilibrium limit vs metastability

Complete equilibrium limit: ⇨
- all reactions are infinitely fast
- slow reactions over infinite time

⇩

Almost never attained at Earth surface conditions!

Metastable components: ⇨ N_2 gas in the Earth atmosphere ($4 \cdot 10^9$ years)

Metastable phases: ⇨
- Any dissolving or growing solid
- Any solid with non-reactive surface
- Any solid phase with large surface

❖ **How to account for kinetics as a** time-dependent **metastability** of mineral phases and minor element **uptake** in them in thermodynamic models and in coupled reactive transport simulations?

⇨ **Use principles of partial and local equilibria!**

9 Geochemical modelling EURAD Training Workshop Univ. Bern, February 6-10, 2023

Accounting for metastability and kinetics

Partial Equilibrium State *concept*

is used for setting up thermodynamic models of 'real-world' geochemical systems

Examples:
- Surface water open to the atmosphere
- Seawater oversaturated to dolomite
- Iron monosulfide in marine sediments
- Clinker phases in hydrated cements
- Suspension of solids with adsorption and Ostwald ripening .....

TYPICAL ASSUMPTIONS:
- ***At least one phase (reaction) is not in chemical equilibrium with the rest of the system***
- ***Dissolution of minerals is the rate-limiting step***
- ***Solid solutions dissolve stoichiometrically***
- ***Precipitation of secondary minerals is usually faster than the primary mineral dissolution***
- ***Some species (N_2atm) or solid phases are inert***

Reaction-path and process-extent models in geochemical codes ⇨

Implementations using [time-dependent]:
- ❖ ***Additional constraints on reaction species or on phases***
- ❖ ***Mineral specific surface areas and sorption capacities***
- ❖ ***Amounts of metastable phases linked to other phases***

10 Geochemical modelling EURAD Training Workshop Univ. Bern, February 6-10, 2023

'Inert' vs 'excluded' mineral phase

MB *= mass balance in system bulk composition;* ***TDB*** *= chemical thermodynamic data base*

Phase/species present:	(Over-)stable phase	Under-stable phase
Not in MB; not in TDB	Unknown (maybe large) metastability artifact	No effect on system state
Not in MB (by $\bar{n}_j = 0$) but in TDB	Known metastability ($\Omega > 1$); effect on MB	No effect on system state ($\Omega < 1$)
In TDB; amount $\bar{n}_j$ constraint in MB	System 'oversaturated' ($\Omega > 1$, precipitation)	No effect on system state ($\Omega < 1$)
In TDB; amount $\underline{n}_j$ constraint in MB	No effect on MB ($\Omega >= 1$, stable)	System 'undersaturated' ($\Omega < 1$, dissolution)
In TDB; two-side amount constraint in MB $\bar{\underline{n}}_j$	Effect on MB, metastability ($\Omega >= 1$, 'oversaturation')	Effect on MB, metastability ($\Omega < 1$, 'undersaturation')

Assuming all species formulae to be consistent with the bulk system stoichiometry;
Ω is phase stability (saturation) index.

11 Geochemical modelling EURAD Training Workshop Univ. Bern, February 6-10, 2023

2. Numerical methods

1. Geochemical systems: equilibrium and metastability

   Equilibrium at P,T,b: stable phases and speciation in phases-solutions

   Metastability; mineral-water reaction kinetics

2. Numerical methods to solve for geochemical speciation

   Gibbs Energy Minimization GEM, e.g. GEMS, Reaktoro

   Law of Mass Action LMA, e.g. PHREEQC, ORCHESTRA

   Forward and inverse modelling problems

3. Thermodynamic Data Bases TDB as main inputs

   Thermochemical format (substances) – $G^o(P,T)$ for GEM

   Reaction format (product- from master species) – $\log K^o(P,T)$ for LMA

12 Geochemical modelling EURAD Training Workshop Univ. Bern, February 6-10, 2023

Computational Geochemistry

From geochemical observations and laboratory experiments

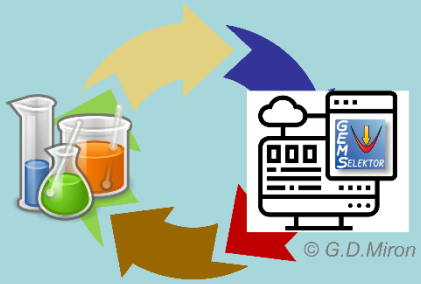

To improved understanding of (geo)chemical systems and processes

& prediction of their evolution at changing T,p,b,t conditions

Numerical methods and codes:

Gibbs Energy Minimization GEM

Minimizes total Gibbs energy of the system G(n) at boundary conditions of mass balance- (An=b), metastability constraints, and G° for all substances

Law of Mass Action LMA

Minimizes mass balance residuals at boundary conditions of LMA expressions for all product species formation reactions with their logK° values

GEM and LMA are complementary!

Shortages of LMA are advantages of GEM

13 Geochemical modelling EURAD Training Workshop Univ. Bern, February 6-10, 2023

Comparing GEM and LMA

Using slides by Prof. Alex Gysi (with modifications)

- **Aquatic geochemistry**:
- Law of mass action LMA (using **logK**), e.g. PHREEQC, Vminteq, Geochemist's Workbench

Metamorphic/igneous petrology and hydrothermal geochemistry:

- Gibbs energy minimization GEM (using **G**), e.g. PerpleX, Hch, Thermocalc, Gem-Selektor, Melts.

See also:

Leal et al. (2017), Pure and Applied Chemistry 89, Issue 5, 597-643
Kulik (2006), Chemical Geology 225, 189-212

14 Geochemical modelling EURAD Training Workshop Univ. Bern, February 6-10, 2023

Classic LMA

- Codes e.g. PHREEQC, ORCHESTRA, EQ3/6 and GWB
- Set of **master species** (CO_3^{2-}, Ca^{2+}, H^+, OH^-, $H_2O_{(aq)}$)
- Product species built from **master species** ($CO_3^{2-} + H^+ = HCO_3^-$)
- Database with equilibrium constants ($\log K_r$) at T generally at p_{sat}
- LMA minimizes mass balance residuals using Newton-Raphson method under boundary conditions of LMA for all product species
- Stable solids need to be known *a priori* (or by automated tricks)
- Redox must be set at input (Eh, pe or redox pair Fe(II)/Fe(III))
- pH set at input or by element charge balance
- Only limited (binary) solid solution models
- Fast convergence: kinetics rate laws and reactive transport models
- Easy to learn (Tableaus, F.M.M.Morel & J.Westall, MIT in 1970s)

Example: LMA Tableaux

Composition (recipe)

	H_2O	H^+	H_3PO_4	H_2CO_3	Na^+	Cl^-	Conc'n
NaH_2PO_4	0	–1	1	0	1	0	10^{-3}
Na_2CO_3	0	–2	0	1	2	0	$4x10^{-4}$
$NaHCO_3$	0	–1	0	1	1	0	10^{-4}
HCl	0	1	0	0	0	1	$3x10^{-3}$
H_2O	1	0	0	0	0	0	55.56
TOTI	55.56	$1.1x10^{-3}$	10^{-3}	$5.0x10^{-4}$	$1.9x10^{-3}$	$3.0x10^{-3}$	

LMA method was formulated in:

Brinkley, S. R., *J. Chem. Phys.*, 15,107 (1947)

Ingri, N., Kakolowicz, W., Sillén, L. G., Warnqvist, B., *Talanta,* 14, 1261 (1967)

Morel, F.; Morgan, J., *Environ. Sci. Technol.* 1972, 6 (1), 58–67

LMA reactions tableau

	H_2O	H^+	H_3PO_4	H_2CO_3	Na^+	Cl^-	log *K*
H_3PO_4	0	0	1	0	0	0	0
$H_2PO_4^-$	0	–1	1	0	0	0	–2.16
HPO_4^{2-}	0	–2	1	0	0	0	–7.20
PO_4^{3-}	0	–3	1	0	0	0	–21.71
H_2CO_3	0	0	0	1	0	0	0
HCO_3^-	0	–1	0	1	0	0	–6.35
CO_3^{2-}	0	–2	0	1	0	0	–16.68
Na^+	0	0	0	0	1	0	0
Cl^-	0	0	0	0	0	1	0
H^+	0	1	0	0	0	0	0
OH^-	1	–1	0	0	0	0	–14.00
H_2O	1	0	0	0	0	0	0

Speciation upon acid-base titration

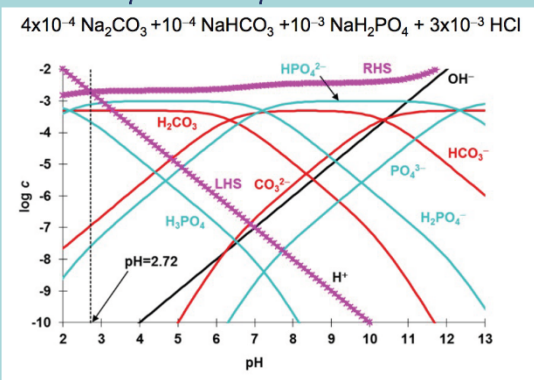

http://faculty.washington.edu/markbenj/CEE543/Slides_10-18-12.pdf

Why (do I prefer) GEM?

*Because **GEM can solve for phase speciation in complex chemical systems** with*

- ***many** (non)ideal solid, liquid, aqueous, gaseous **solutions** with various mixing models, including sublattice solutions and phase separation*
- *calculation of **intrinsic redox** states (f_{O2}, pe, Eh) and pH from the bulk chemical composition in wide T,P ranges*
- *multiple sorption phases with **multi-surface-site complexation**, implemented with- or without mole balances for "surface site ligands"*
- *multiple **metastability constraints** and simulation of mineral dissolution/ precipitation **kinetics***
- ***inverse modeling**, advanced robustness and sensitivity studies of model setup and results (GEMSFITS)*
- *and all other things that LMA speciation codes can do too!*

17 Geochemical modelling EURAD Training Workshop Univ. Bern, February 6-10, 2023

Classic GEM

- e.g. GEM-Selektor, Hch, ChemSage, Reaktoro codes
- Mass balance using **(IC) independent components** (H, O, Al, …) and electric charge Z
- Chemical species are **(DC) dependent components** (aqueous species, minerals, gases…) constructed from IC
- Uses database with standard Gibbs energy (G^o) at P,T for each DC
- Gibbs energy minimization (GEM) to solve for equilibrium state
- pH, activities and redox (pe, Eh) calculated from minimization
- Slower convergence, but more output data from a single calculation: e.g. dual solution, phase volumes, fugacity, etc…
- Solves for equilibria in systems with complex non-ideal solutions
- Coupling with reactive transport models (Kulik et al., 2013)
- Steeper learning curve than LMA (need to know what you're doing)
- Born in 1958 (White, Johnson & Dantzig, 1958, GEM for gas mixture)

18 Geochemical modelling EURAD Training Workshop Univ. Bern, February 6-10, 2023

Forward Thermodynamic Modelling

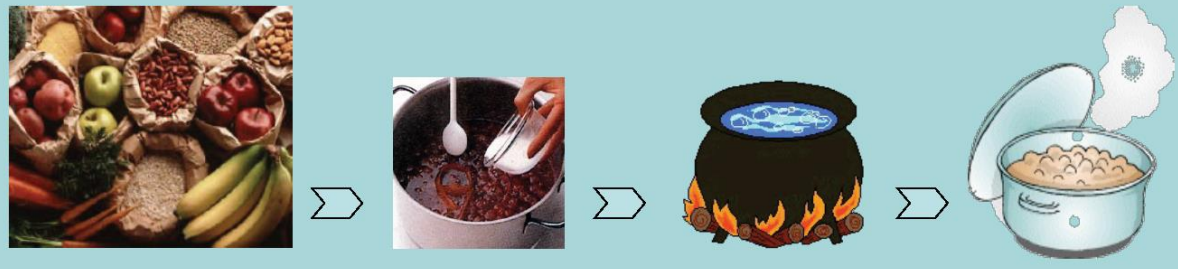

Ingredients → **Recipe** → **Cooking** → **Done**

In terms of chemical thermodynamics "cooked" at *T,P* of interest

Feasible phases and components → **Initial state (bulk composition, *b*)** → **Equilibration, chemical mass transfer** → **Final state n(*x*); stable speciation**

Forward Problem in GEM Formulation

Goal: Calculate (unknown) equilibrium phase assemblage and speciation in the system defined by T, p, b, g^o, and parameters of mixing in solution phases.

= Find amounts of dependent components $n^{(x)} = \{ n^{(x)}_j, j \in L\}$ that

$$G(n^{(x)}) \Rightarrow \min \quad \text{s. t. } A \cdot n^{(x)} = n^{(b)} \qquad \text{(Problem F)}$$

where $n^{(b)} = \{ n^{(b)}_i, i \in N\}$ is the input vector of bulk system composition (b)

$A = \{a_{ij}, i \in N, j \in L\}$ is a matrix of formula stoichiometry coefficients of species;

and $G(n^{(x)})$ is the total Gibbs energy $G(n^{(x)}) = \sum_j n_j^{(x)} \upsilon_j, \quad j \in L$

where υ_j is the chemical potential of *j*-th dependent component

$$\upsilon_j = g_j^o / RT + \ln C_j + \ln \gamma_j + \Xi, \quad j \in L$$

Linear vs Non-Linear Minimization

*System contains **pure phases only**:*
*A **linear programming (LP) problem**, solution always on an apex of the polyhedron of (MB) constraints*

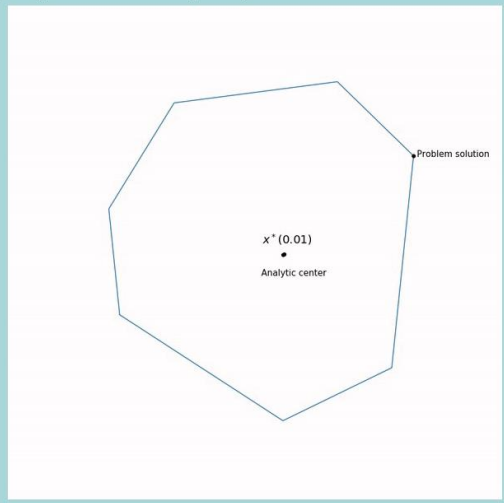

Solved using Simplex LP method

*System contains **phases-solutions** (e.g. gas mixture, aqueous, ss or ls):*
*A **non-inear minimization problem***

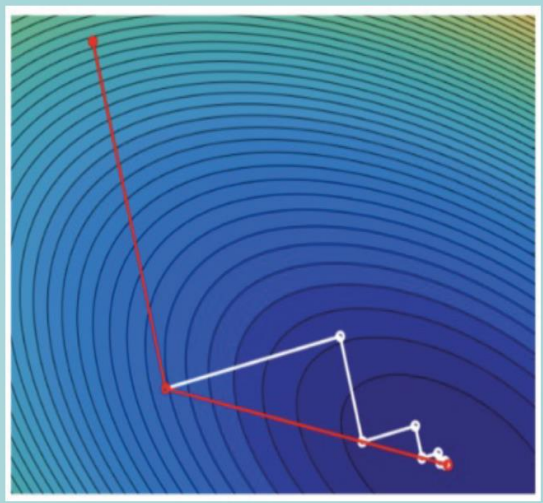

Steepest descent, IPM, etc. method

Non-Linear GEM: Ideal vs Non-Ideal Solutions

Chemical potential of species j in solution

$$\upsilon_j = {g_j^o}/{RT} + \ln C_j + \ln \gamma_j + \Xi, \quad j \in L$$

$$G(n^{(x)}) = \sum_j n^{(x)} \upsilon_j$$

Activity terms introduce non-linearity of G(x)

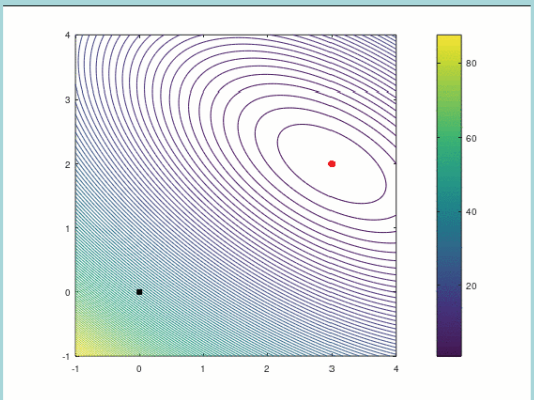

Ideal solutions: simple G(x) shape (convex, polyhedron of constraints)

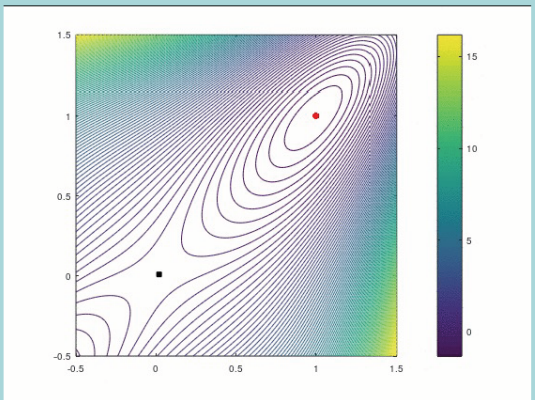

Non-ideal solutions: complex G(x) shape (pseudoconvex?)

Non-ideal [solid] solutions

Subregular binary Margules model (in Thompson-Waldbaum form)

Excess Gibbs energy:

$$G_m^E = RT\left(x_1 \ln f_1 + x_2 \ln f_2\right) = x_1 x_2 \left(W_{12} x_2 + W_{21} x_1\right)$$

W_{12}, W_{21} - *interaction parameters (f(T,P))*

End-member activity coefficients:

$$RT \ln f_1 = \left(2W_{21} - W_{12}\right)x_2^2 + 2\left(W_{12} - W_{21}\right)x_2^3$$

$$RT \ln f_2 = \left(2W_{12} - W_{21}\right)x_1^2 + 2\left(W_{21} - W_{12}\right)x_1^3$$

Regular model: $W_{12} = W_{21} = W_G$ *and* $W_G = RT\alpha_0$

Relation to the Guggenheim model:

$$W_{12} = RT\left(\alpha_0 - \alpha_1\right); W_{21} = RT\left(\alpha_0 + \alpha_1\right)$$

Many more models for complex mixtures have been suggested

Strong non-ideality: Miscibility gaps

If excess Gibbs energy $G^{ex} > 0$, at some intermediate bulk system composition, two SS phases of different compositions may become stable instead of one

Simple criterion (Glynn, 1991) for the regular SS model $W_G = RT\alpha_0$

Binodal miscibility gap is possible at $\alpha_0 \geq 2.0$

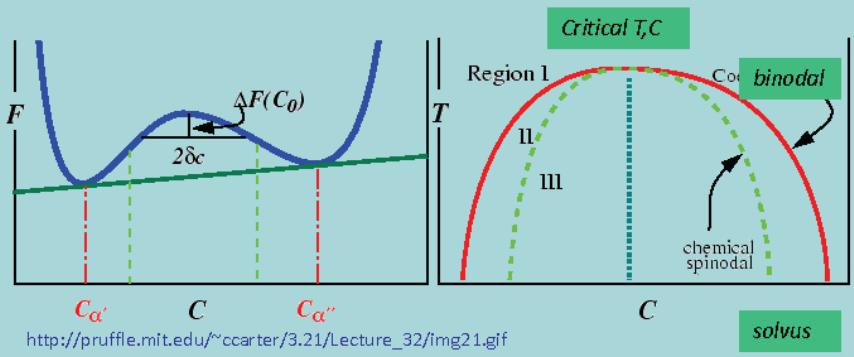

http://pruffle.mit.edu/~ccarter/3.21/Lecture_32/img21.gif

GEM can compute a binodal solvus using two SS phases with the same model

Example: Solvus (binodal)

Alkali feldspar solvus, asymmetric multicomponent formulation

Sanidine $KAlSi_3O_8$
Albite $NaAlSi_3O_8$
Anorthite $CaAl_2Si_2O_8$

Van Laar solid solution model

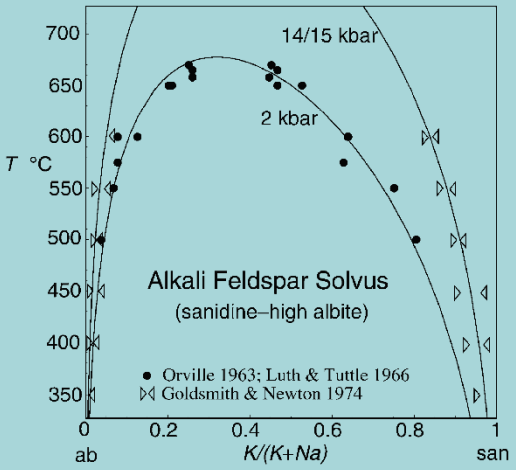

Holland and Powell, Contr. Mineral. Petrol. 2003

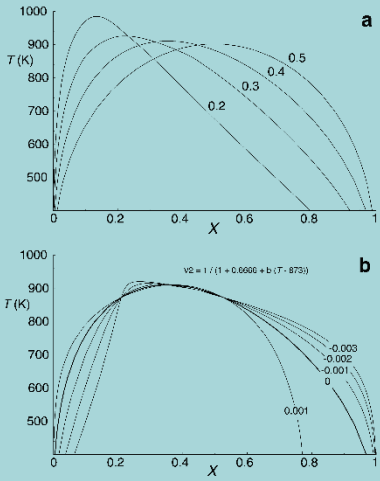

Fig. 2a, b Solvus shapes calculated using the van Laar model. **a** Varying the asymmetry parameter $\upsilon_2 = \frac{\Delta_r}{r \cdot \upsilon_1}$ for constant W, and **b** varying the temperature-dependence of υ_2 for constant W and a value for υ_2 0.6 at the critical temperature

Example: Solvus in alkali feldspar (binodal)

Test project "Solvus"

- *Sequential temperature change (P mode)*
- *Change T at constant P*
- *Output of solid solution composition as a function of P-T*

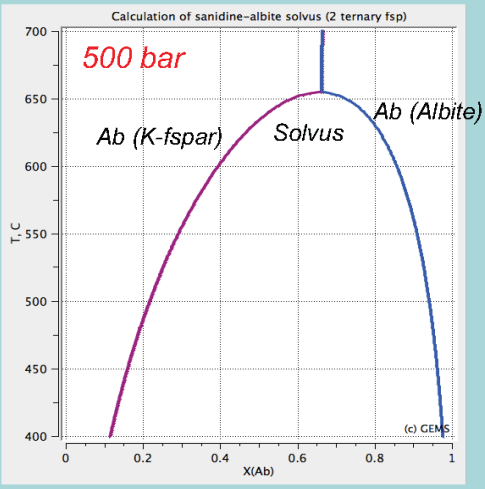

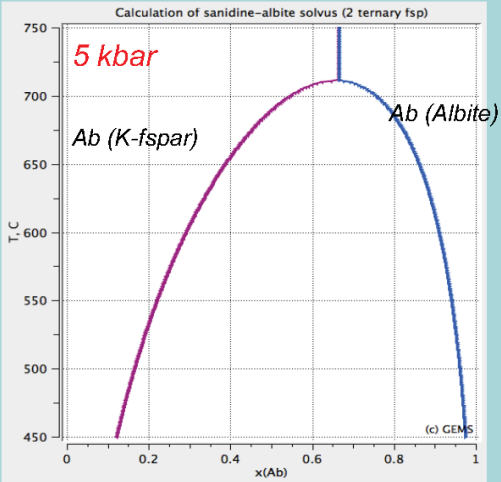

Irreversible processes: Reaction-path sims

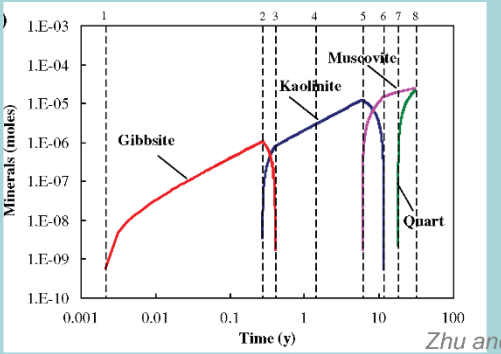

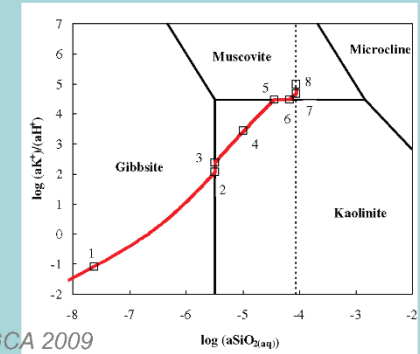

Zhu and Lu, GCA 2009

- *Sequential bulk composition change*
- *Change x at constant P-T*
- *Output: pH and moles of secondary minerals formed*

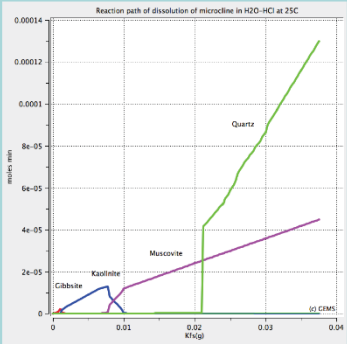

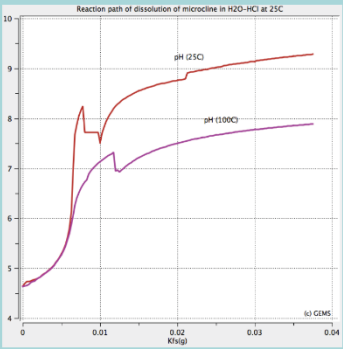

Water-rock interaction (reaction path)

Geochemical equilibrium modeling of CO_2 sequestration in basalt [glass] using MINES'18 chemical thermodynamic database

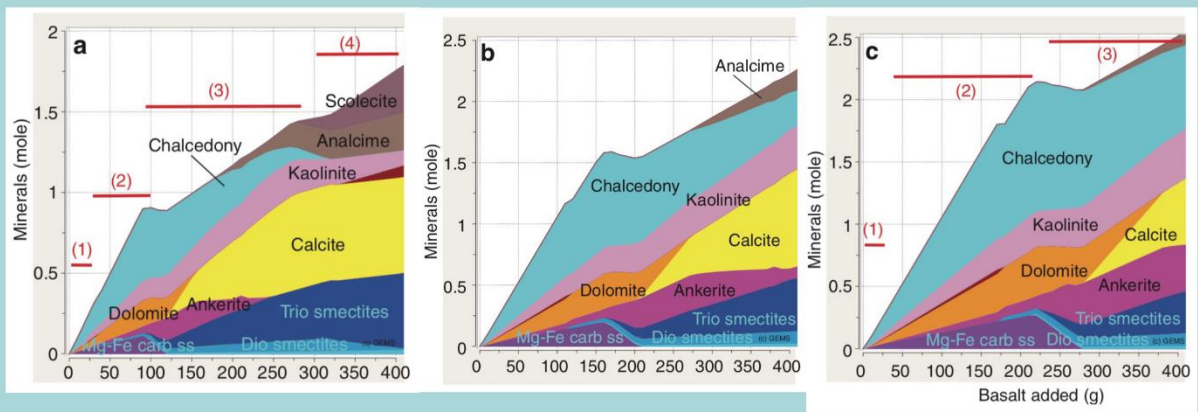

Secondary mineralogy as a function of basaltic glass addition at T = 50° C and pCO_2 of (a) 20, (b) 40 and (c) 100 bar, simulated in GEM-Selektor with MINES TDB *Gysi, Pure Appl. Chem. (2017)*

Thermodynamic modelling of sorption

ClaySor model

B&B (2SPNE SC/CE) model for Na-conditioned illite

Bayens & Bradbury (2009): Geoch. Cosmoch. Acta 73, 990-1003

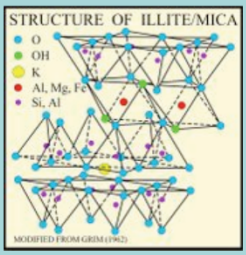

Planar 'clay' sites: cation exchange capacity: CEC = 0.225 eq/kg

Edge sites: surface complexation

Capacities: $\equiv S^{S}OH$: 2 mmol/kg

$\equiv S^{W1}OH$: 40 mmol/kg

$\equiv S^{W2}OH$: 40 mmol/kg

$\log_{10}K$ (protolysis on edges)

Protolysis reactions	$\equiv S^{S}OH$	$\equiv S^{W1}OH$	$\equiv S^{W2}OH$
$\equiv SOH + H^+ \Leftrightarrow \equiv SOH_2^+$	4.0	4.0	8.5
$\equiv SOH \Leftrightarrow \equiv SO^- + H^+$	-6.2	-6.2	-10.5

Metals adsorption on edges

$$=S^{X}OH + Me^{+z} + yH_2O \leftrightarrow =S^{X}OMe(OH)_y^{z-(y+1)} + (y+1)H^+$$

Kd of Eu(III) on 1 g/L illite, vs pH

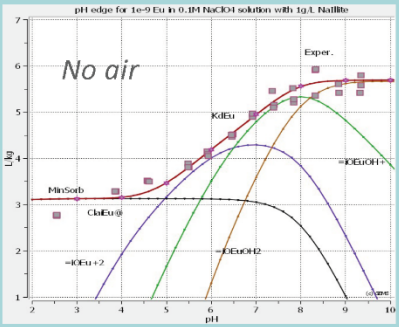

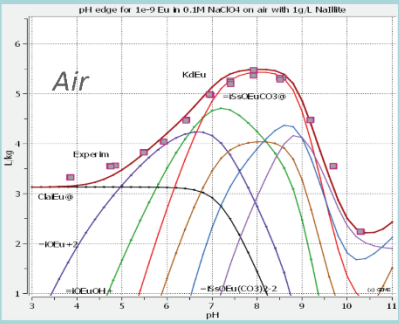

Mineral-water reaction kinetics

Trace element uptake depends on calcite growth rate

Growth surface entrapment?

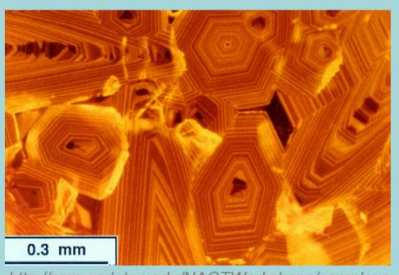

http://serc.carleton.edu/NAGTWorkshops/complexsystems/workshop2010/participants/dutrow.html

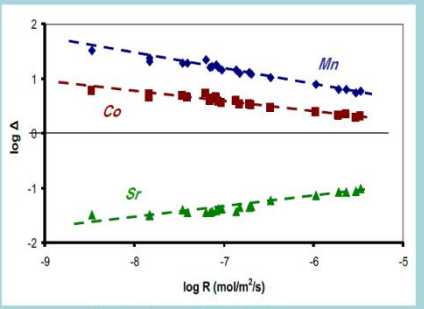

Data from Lorens, GCA 45,1981

Seeded growth of calcite:
Wolthers (2012) rate equation; Experimental data: *Dreybrodt et al. (1997)*

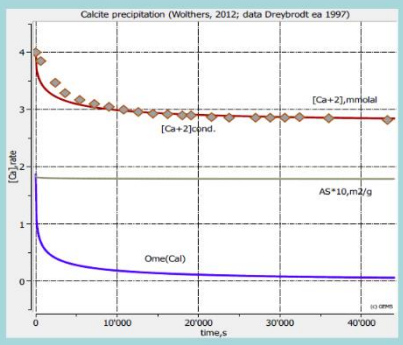

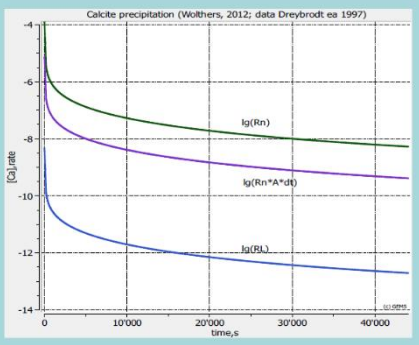

Mineral-water reaction kinetics sims

Kinetics can be simulated as a series of partial equilibria governed by rate equations

AMR — *Time step duration Δt, time t, net kinetic rate $R_{n,k,t}$ surface area $A_{k,t}$ of k-th solid (solution) phase*

$$\overline{n}_{k,t+\Delta t} = n_{k,t} + A_{k,t} R_{n,k,t} \Delta t \quad \text{if} \quad \log_{10} \Omega_k > \varepsilon$$

$$\underline{n}_{k,t+\Delta t} = n_{k,t} - A_{k,t} R_{n,k,t} \Delta t \quad \text{if} \quad \log_{10} \Omega_k < -\varepsilon$$

Surface area

$$A_{k,t} = A_{S,k} M_{M,k} n_{k,t}$$

$A_{S,k}$: specific surface area; $M_{M,k}$: molar mass; $n_{k,t}$: amount (mol) of k-th phase

Stability index of k-th phase

$$\Omega_k = \sum_j \hat{x}_j = \sum_j \exp\left(\hat{\eta}_j - g_j^o / RT - \ln \lambda_j - \Xi_k\right)$$

Standard-state Gibbs energy — *Activity coefficient* — *To-mole-fraction conversion term*

$n_{k,t}$

Dual-solution chemical potential

$$\hat{\eta}_j = \sum_i a_{ij} \hat{u}_i^{(b)}$$

Can LMA method be improved?

- *Equilibrium speciation codes based on the conventional LMA approach require tentative addition or removal of phases so that all mass action equations remain **valid***
- *Common practice for >30 years in aquatic geochemistry literature (Morel & Morgan, 1972; Reed, 1982; Bethke 2007); MINEQL, PHREEQC, GWB, MINTEQ, ORCHESTRA, …*

Leal, Kulik, Kosakowski, Saar (2016), Adv. Water Res. 96, 405–422

Consider reactions like

product — master species

$$CaCO_3 + H^+ \rightleftharpoons Ca^{2+} + HCO_3^-$$

$$K_{CaCO_3} = \frac{a_{Ca^{2+}} \cdot a_{HCO_3^-}}{a_{H^+} \cdot a_{CaCO_3}}$$

Calcite is stable (valid)

$$K_{CaCO_3} \neq \frac{a_{Ca^{2+}} \cdot a_{HCO_3^-}}{a_{H^+} \cdot a_{CaCO_3}}$$

Calcite is unstable (to be removed)

xLMA method: LMA input, GEM power

Leal, Kulik, Kosakowski, Saar (2016), Adv. Water Res. 96, 405–422.

The GEM problem:

$$\min_n G = \sum_{i=1}^{N} n_i \mu_i$$

s.t.

$$\mu(n) - A^T y - z = 0$$
$$An - b = 0$$
$$n_i z_i = 0$$
$$n_i, z_i \geq 0$$

using

$$\mu_i = \mu_i^o + RT \ln a_i$$

activity

$$w_i = \exp\left(-\frac{z_i}{RT}\right)$$

Stability-related factor in GEM

xLMA method: LMA input, GEM power

Leal, Kulik, Kosakowski, Saar (2016), Adv. Water Res. 96, 405–422.

The GEM problem:

$$\min_n G = \sum_{i=1}^{N} n_i \mu_i$$

s.t.

$$\mu(n) - A^T y - z = 0$$
$$An - b = 0$$
$$n_i z_i = 0$$
$$n_i, z_i \geq 0$$

using

$$\mu_i = \mu_i^o + RT \ln a_i$$

activity

Conventional LMA equations:

$$K_m = \prod_{i=1}^{N} a_i^{\nu_{mi}}$$

$$0 \rightleftharpoons \sum \nu_{mi} \alpha_i$$

$$\ln K = \nu(\ln a + z)$$

missing!

$$w_i = \exp\left(-\frac{z_i}{RT}\right)$$

Stability-related factor: missing in all old LMA codes

xLMA method: LMA input, GEM power

Leal, Kulik, Kosakowski, Saar (2016), Adv. Water Res. 96, 405–422. *Runs in Reaktoro framework (reaktoro.org)*

The GEM problem:

$$\min_n G = \sum_{i=1}^{N} n_i \mu_i$$

s.t.

$$\mu(n) - A^T y - z = 0$$
$$An - b = 0$$
$$n_i z_i = 0$$
$$n_i, z_i \geq 0$$

using

$$\mu_i = \mu_i^o + RT \ln a_i$$

activity

Conventional LMA equations:

$$K_m = \prod_{i=1}^{N} a_i^{\nu_{mi}}$$

$$0 \rightleftharpoons \sum \nu_{mi} \alpha_i$$

$$\ln K = \nu(\ln a + z)$$

missing!

Extended xLMA equations:

$$K_m = \prod_{i=1}^{N} (a_i w_i)^{\nu_{mi}}$$

"extended activity"

$$w_i = \exp\left(-\frac{z_i}{RT}\right)$$

Stability-related factor: missing in all old LMA codes, but renders xLMA the full power of GEM!

35 Geochemical modelling EURAD Training Workshop Univ. Bern, February 6-10, 2023

Reaktoro v2: xGEM and xLMA all-in-one

Reaktoro
for Python and C++
© Allan Leal

Open source computational framework developed in C++ and Python to simulate chemically reactive processes.
https://reaktoro.org

- **Common** The module in Reaktoro in which methods and classes commonly used in other modules are implemented
- **Core** The module in Reaktoro in which core classes and methods are defined
- **Equilibrium** The module in Reaktoro in which classes and methods for chemical equilibrium calculations are implemented
- **Kinetics** The module in Reaktoro in which classes and methods for chemical kinetics calculations are implemented
- **Math** The module in Reaktoro in which math related methods and classes are implemented
- ▼ **Models** The module in Reaktoro in which various thermodynamic and reaction models are implemented
  - **Activity Models** The module in Reaktoro in which activity models for phases are implemented
  - **Reaction ReactionRate Models** The module in Reaktoro in which kinetic rate models for reactions are implemented
  - **Standard Thermodynamic Models** The module in Reaktoro in which standard thermodynamic models for species and reactions are implemented
  - **Surface Area Models** The module in Reaktoro in which surface area models are implemented
- **Singletons** The module in Reaktoro in which default databases for critical properties, elements, dissociation reactions and others are implemented
- **Utils** The module in Reaktoro in which utility classes and methods are defined
- **Water** The module in Reaktoro in which thermodynamic and electrostatic models for water are implemented

36 Geochemical modelling EURAD Training Workshop Univ. Bern, February 6-10, 2023

Solving inverse problems massively: GEMSFITS

- *A tool for **multi-property, multiple parameters optimization** against various types of experiments or geochemical data*
- *Uses **state of the art optimization library** (Nlopt)*
- *Has a **graphical user interface***
- *Maintains a **Database of experiments**, tasks, results*
- *Goodness of fit, sensitivity analysis, correlation coefficients, **parameter confidence intervals** using **Monte Carlo sampling***

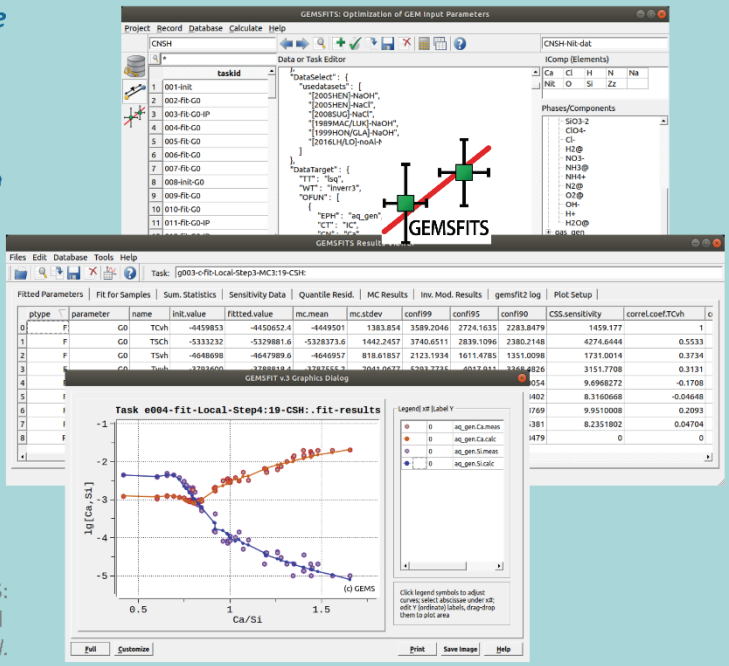

Miron G.D., Kulik D.A., et al. (2015). GEMSFITS: Code package for optimization of geochemical model parameters and inverse modeling. *Appl. Geochem*. 55, 28-45

https://gems.web.psi.ch/GEMSFITS

3. Thermodynamic data bases

1. Geochemical systems: equilibrium and metastability

   Equilibrium at P,T,b: stable phases and speciation in phases-solutions

   Metastability; mineral-water reaction kinetics

2. Numerical methods to solve for geochemical speciation

   Gibbs Energy Minimization GEM, e.g. GEMS, Reaktoro

   Law of Mass Action LMA, e.g. PHREEQC, ORCHESTRA

   Forward and inverse modelling problems

3. Thermodynamic Data Bases TDB as main inputs

   Thermochemical format (substances) – $G^o(P,T)$ for GEM

   Reaction format (product- from master species) – $\log K^o(P,T)$ for LMA

Standard thermodynamic properties at *P,T*

www.thermohub.org/thermofun

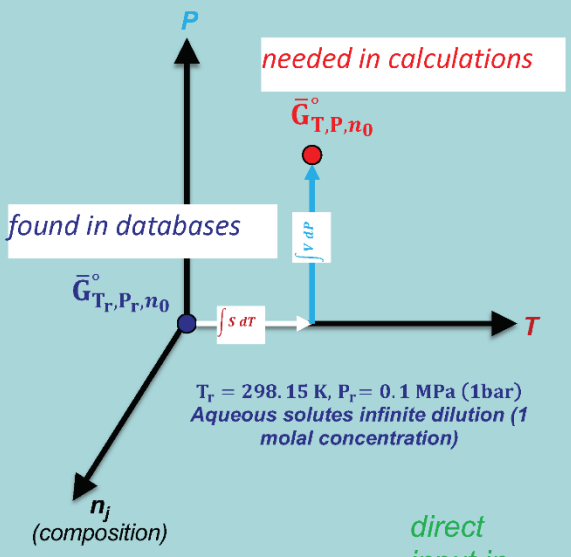

direct input in GEM

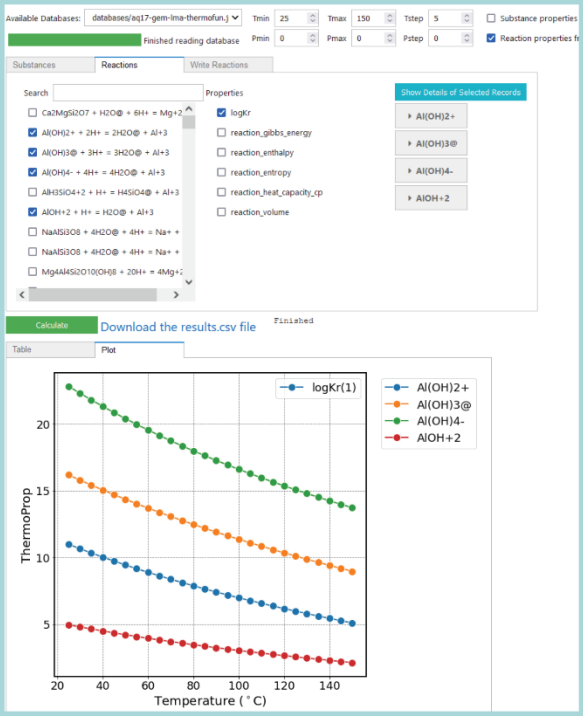

Miron et al. 2020, Goldschmidt conf.

G°(P,T) thermochemical databases (for GEM)

Defined at standard (P0=1bar, T0=298.15K) *and reference* ($\gamma = 1$) *states*

- elemental chemical formula of substance *j* *(formation from elements)*
- standard molar Gibbs energy, $G^o_{T0,j} = \Delta_f G^o_{T0,j} = -\mathrm{RT}\ln K^o_{f,T0,j}$
- standard molar enthalpy, $H^o_{T0,j} = \Delta_f H^o_{T0,j}$ J/mol
- standard molar absolute entropy, $S^o_{T0,j}$ J/K/mol
- standard molar volume $V^o_{P0,T0,j}$ [f(P,T) coefficients] J/bar
- standard molar heat capacity (constant P) $Cp^o_{T0,j}$ [f(T) coefficients]
- aqueous species: HKF EoS (P,T) coefficients, partial molal properties

Thermochemical conventions:
$G^o_{T0,element} = 0$
$H^o_{T0,element} = 0$

GEM calculations require input formulae, $G^o_{P,T,j}$, $V^o_{P,T,j}$ *(optional* $H^o_{P,T,j}$ *for heat effects). The* $H^o_{T0,j}$ *or* $S^o_{T0,j}$, $Cp^o_{T,j} = f(T)$, $V^o_{P,T,j} = f(P,T)$, *EoS coeffs are needed for converting* $G^o_{T0,j} \Rightarrow g^o_{P,T,j}$, $V^o_{P0,T0,j} \Rightarrow V^o_{P,T,j}$, *and* $H^o_{T0,j} \Rightarrow h^o_{P,T,j}$

A logK° thermodynamic dataset can be generated from GEM formulae-$G^o_{T0,j}$ *dataset upon choosing "master species" and constructing formation reactions for other species (with loss of* $G^o_{T0,j}$ *values for master species from logK° values of reactions)*

GEMS3 Built-in Thermodynamic Databases

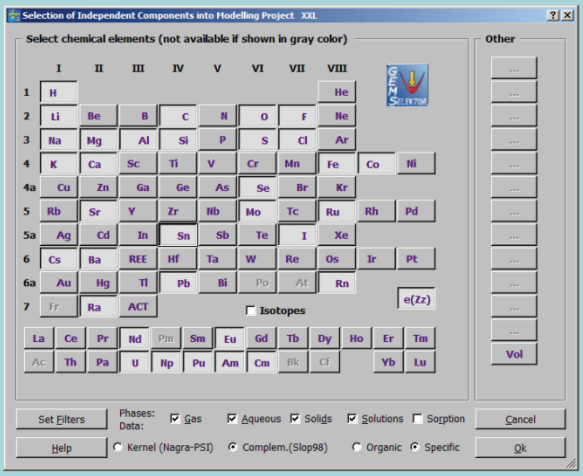

PSI-Nagra v 11/07 TDB

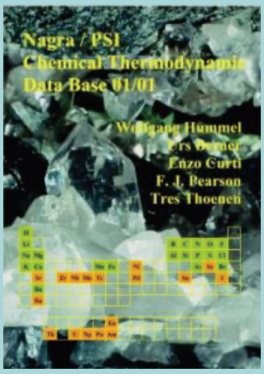

log*K* at 1 bar 25 C

Extended with *T,P* corrections from S92

Specific: Cemdata '18

Specific: HERACLES

Specific: MINES'19

Complementary: SUPCRT92 (G^o etc.)

DComp and ReacDC data record formats

logK° thermodynamic databases (for LMA)

Defined at standard (P0=1bar, T0=298.15K) *and reference* ($\gamma = 1$) *states*

Such thermodynamic datasets may contain lists of primary /secondary master species and of product species, with elemental formulae of them

For product species:

- stoichiometry of formation reaction from master species
- equilibrium constant of formation reaction, $K^o_{j,P0,T0}$ or $\log_{10} K^o_{j,P0,T0}$
- standard Gibbs energy effect of reaction, $\Delta_r G^o_{T0,j} = -\mathrm{RTln}K^o_{P0,T0,j}$ J/mol
- standard entropy effect of reaction, $\Delta_r S^o_{T0,j}$
- standard enthalpy effect of reaction, $\Delta_r H^o_{T0,j} = \Delta_r G^o_{T0,j} + T0 \cdot \Delta_r S^o_{T0,j}$
- standard heat capacity effect of reaction, $\Delta_r Cp^o_{T0,j}$
- standard molar volume effect of reaction, $\Delta_r V^o_{T0,j}$

LMA calculations require input stoichiometry of reactions, $\log_{10} K^o_{j,P,T}$, $\Delta_r V^o_{P,T,j}$.
Values of $\Delta_r S^o_{T0,j}$ or $\Delta_r H^o_{T0,j}$, $\Delta_r Cp^o_{T0,j}$, $\Delta_r V^o_{T0,j}$ *are needed for converting* $\log_{10} K^o_{j,P0,T0} \Longrightarrow \log_{10} K^o_{j,P,T}$, *usually as* $\log_{10} K^o_{j,P,T} = f(P,T)$ *polynomial coefficients*

A logK° thermodynamic dataset can be converted into a GEM $G^o_{T0,j}$ *dataset after adding the missing information (elemental formulae, standard properties of master species)*

Hybrid / dual (G° / logK°) TDBs for GEM or LMA

Provide thermodynamic datasets for both GEM and LMA

Most convenient TDBs & tools, long tradition

SUPCRT92 ⟹ CHNOSZ, SUPCRTBL

PSI-Nagra 12/07 [GEMS], GEM-Selektor

CEMDATA07 to **CEMDATA18** (Empa)

THERMODDEM (BRGM)

ThermoHub **ThermoMatch**

ThermoFun

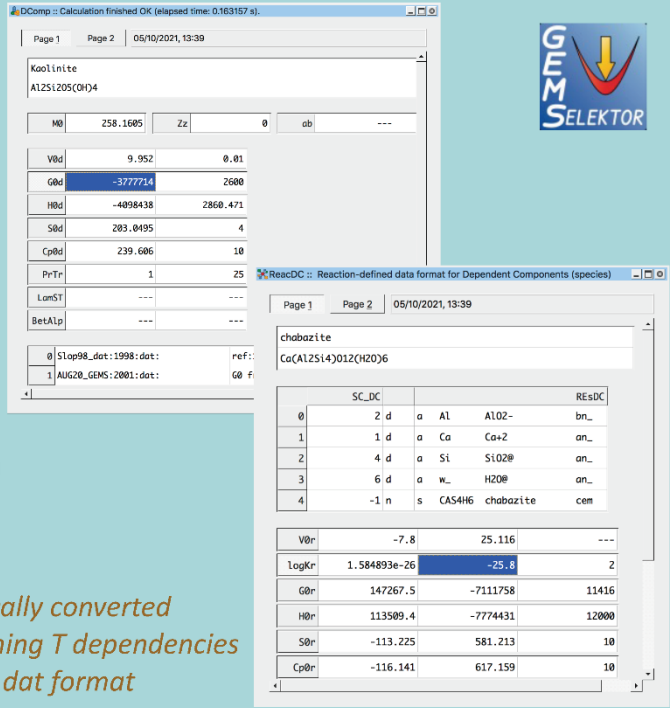

Recent story of success:
Cemdata18 TDB for GEM was automatically converted using TermoMatch into LMA form (retaining T dependencies up to 100 °C) and exported to PHREEQC .dat format

Acknowledgments

Thanks for attention! Questions?

- Partial financial support from Nagra (Wettingen) is gratefully acknowledged

My sincere gratitude to Dan, Barbara, Alex, Enzo, Georg, Allan, Nikos, and many other people for helpful discussions!

3.2 Lecture 2 - Thermodynamic modelling of cementitious systems and their evolution

Hydraulic binders such as cement paste, mortar and concrete show rapid and complex evolution of pore water composition and mineral assemblage during hydration. Thermodynamic equilibrium calculations are a valuable tool to understand the consequences of different factors such as cement composition, hydration, leaching or temperature on the composition and the properties of a hydrated cementitious system on a chemical level. Equilibrium calculations can be used to compute the stable phase assemblages based on the solution composition as well as to model the stable phase assemblage in completely hydrated cements and thus to assess the influence of the chemical composition on the hydrate assemblage. In combination with a kinetic model, thermodynamic calculations can also be used to follow changes during hydration or, in combination with transport models, to calculate the interaction of cementitious systems with the environment. In all these applications, thermodynamic equilibrium calculations have been a valuable addition to experimental studies deepening our understanding of the processes that govern cementitious systems and interpreting experimental observations.

Lecturer

Barbara Lothenbach, EMPA, Switzerland

Reading Material

Lothenbach, B., *Thermodynamic equilibrium calculations in cementitious systems.* Materials and Structures, 2010: p. DOI 10.1617/s11527-010-9592-x.

Lothenbach, B., K. Scrivener, and R.D. Hooton, *Supplementary cementitious materials.* Cement and Concrete Research, 2011. **41**(12): p. 1244-1256.

Lothenbach, B., et al., *Influence of limestone on the hydration of Portland cements.* Cem. Concr. Res., 2008. **38**(6): p. 848-860.

Slides

Willkommen
Welcome
Bienvenue

Empa
Materials Science and Technology

Thermodynamic modelling of cementitious systems and their evolution

Barbara Lothenbach
Empa, Concrete & Asphalt Laboratory, Dübendorf, Switzerland
Institute of Geology, University of Berne, Switzerland
NTNU,. Department of Structural Engineering, Trondheim, Norway

Cements and Concrete

Empa

1

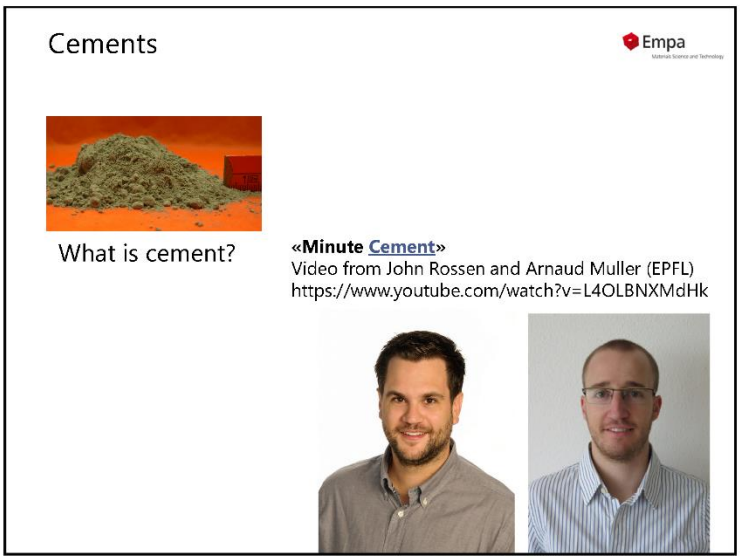
Cements
Empa
What is cement?
«Minute Cement»
Video from John Rossen and Arnaud Muller (EPFL)
https://www.youtube.com/watch?v=L4OLBNXMdHk

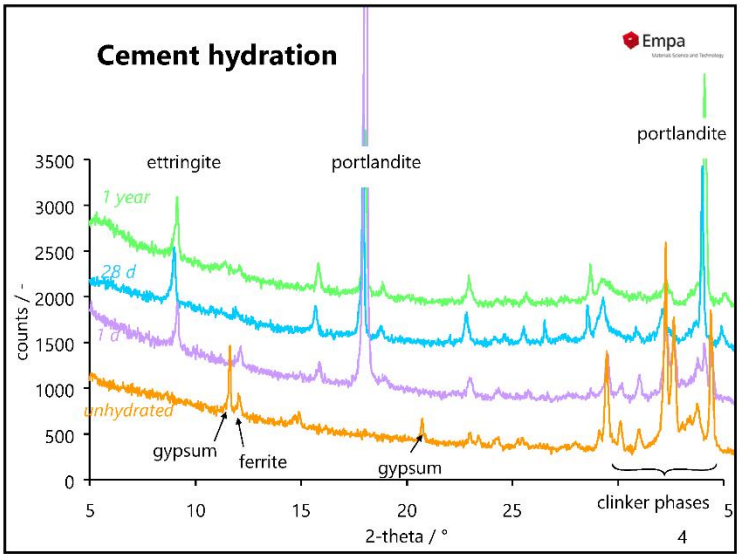
Cement hydration
Empa
ettringite
portlandite
portlandite
1 year
28 d
1 d
unhydrated
gypsum
ferrite
gypsum
clinker phases
counts / -
2-theta / °
3500
3000
2500
2000
1500
1000
500
0
5
10
15
20
25
5
4

2

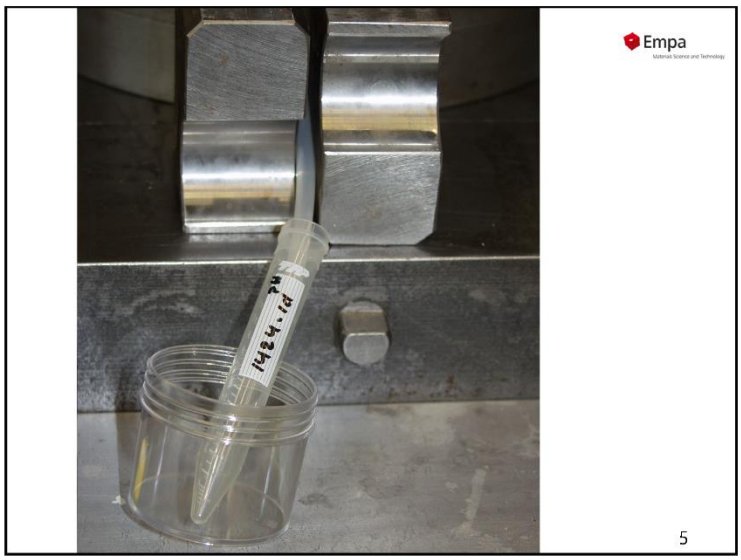
Empa
5

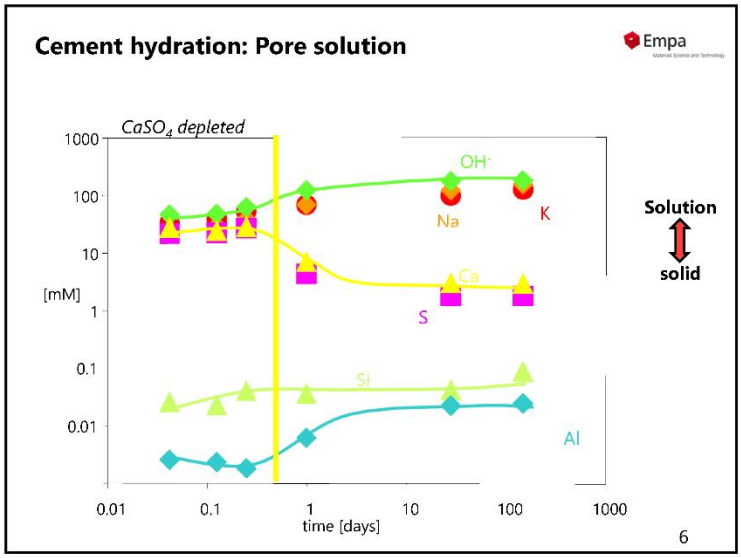
Cement hydration: Pore solution
Empa
$CaSO_4$ depleted
1000
100
10
[mM]
1
0.1
0.01
OH⁻
Na
K
Ca
S
Si
Al
0.01
0.1
1
10
100
1000
time [days]
Solution
solid
6

3

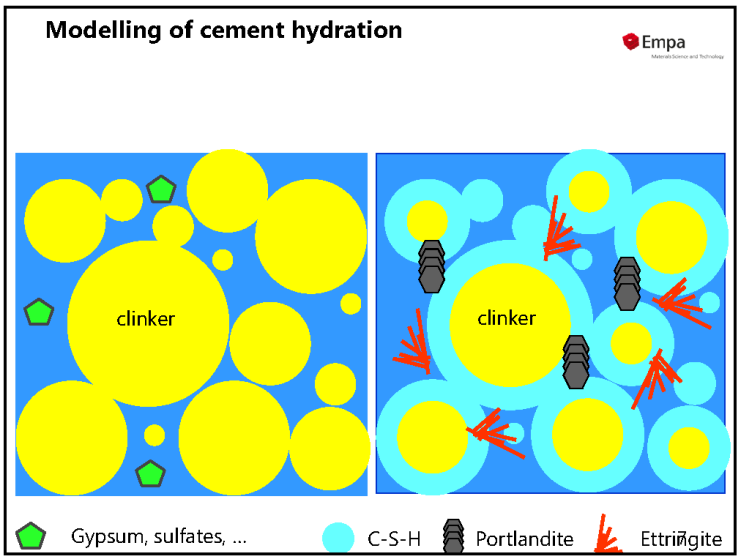
Modelling of cement hydration
Empa
clinker
clinker
Gypsum, sulfates, ...
C-S-H
Portlandite
Ettringite
7

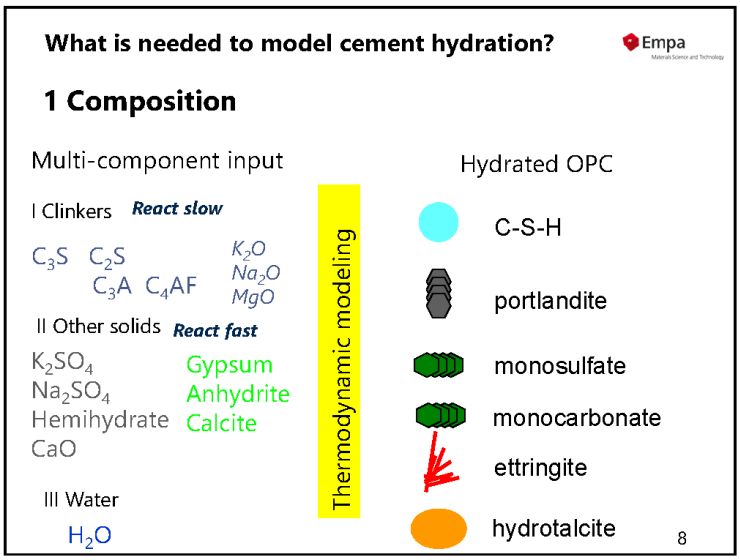
What is needed to model cement hydration?
Empa
1 Composition
Multi-component input
I Clinkers React slow
C_3S C_2S C_3A C_4AF
K_2O Na_2O MgO
II Other solids React fast
K_2SO_4
Na_2SO_4
Hemihydrate
CaO
Gypsum
Anhydrite
Calcite
III Water
H_2O
Thermodynamic modeling
Hydrated OPC
C-S-H
portlandite
monosulfate
monocarbonate
ettringite
hydrotalcite
8

What is needed to model hydration?

Empa

2 Reactivity of clinker phases

based on empirical data, measured data, dissolution rates,...

$$R_t = \frac{K_1}{N_1}(1-\alpha_t)(-\ln(1-\alpha_t))^{(1-N_1)}$$

$$R_t = \frac{K_2 \times (1-\alpha_t)^{2/3}}{1-(1-\alpha_t)^{1/3}}$$

$$R_t = K_3 \times (1-\alpha_t)^{N_3}$$

All parameters (K_i, N_i) from Parrot and Killoh (1984)

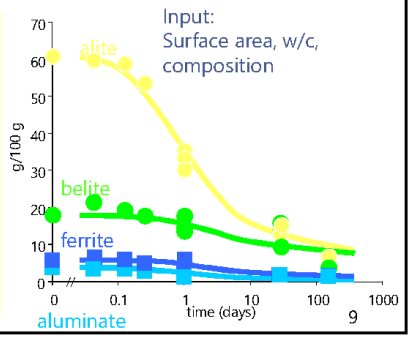

9

What is needed to model hydration?

Empa

3 Thermodynamic data

Chemical equilibria:

Anhydrite $CaSO_4$

$CaSO_4^0$

Ca^{2+} SO_4^{2-}

$CaOH^+$

OH^- H^+

H_2O

Gypsum $CaSO_4 \cdot 2H_2O$

Generic data

Equilibrium calculations with geochemical software:
PHREEQC
GEMS
...

Complex formation

$K = \{CaOH^+\}/\{Ca^{2+}\}\cdot\{OH^-\} = 10^{1.22}$

$K = \{CaSO_4^0\}/\{Ca^{2+}\}\cdot\{SO_4^{2-}\} = 10^{2.3}$

$K = \{H^+\}\cdot\{OH^-\} = 10^{-14.00}$

Solubility products

$K_{S0} = \{Ca^{2+}\}\cdot\{SO_4^{2-}\} = 10^{-4.58}$

$K_{S0} = \{Ca^{2+}\}\cdot\{OH^-\}^2 = 10^{-5.20}$

$$K_{s0} = e^{-\frac{\Delta G_r^\circ}{RT}}; \Delta G_r^\circ = \sum_i \nu_i \Delta G_f^\circ$$

5

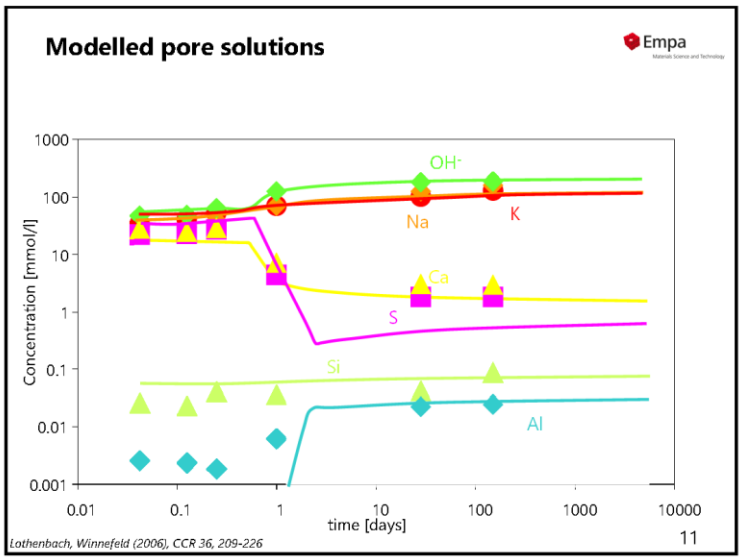
Modelled pore solutions
Empa
Concentration [mmol/l]
1000
100
10
1
0.1
0.01
0.001
OH-
Na
K
Ca
S
Si
Al
0.01
0.1
1
10
100
1000
10000
time [days]
Lothenbach, Winnefeld (2006), CCR 36, 209-226
11

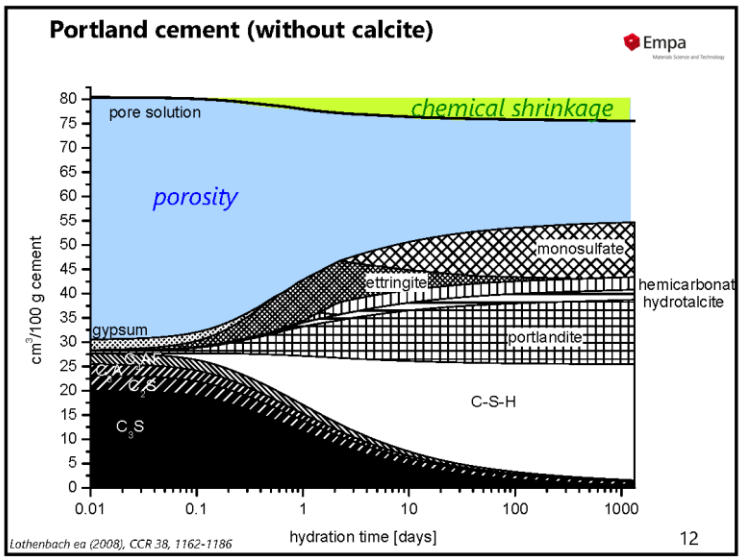
Portland cement (without calcite)
Empa
cm³/100 g cement
80
75
70
65
60
55
50
45
40
35
30
25
20
15
10
5
0
pore solution
chemical shrinkage
porosity
monosulfate
ettringite
hemicarbonat
hydrotalcite
gypsum
portlandite
C-S-H
C3S
0.01
0.1
1
10
100
1000
hydration time [days]
Lothenbach ea (2008), CCR 38, 1162-1186
12

6

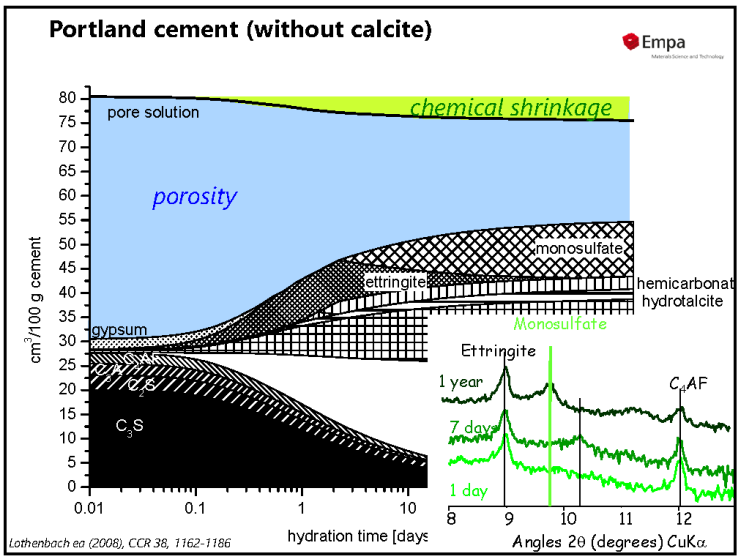
Portland cement (without calcite)
Empa
pore solution
chemical shrinkage
porosity
monosulfate
ettringite
hemicarbonat
hydrotalcite
gypsum
Monosulfate
Ettringite
1 year
7 days
1 day
C_4AF
C_2S
C_3S
cm³/100 g cement
hydration time [days
Angles 2θ (degrees) CuKα
Lothenbach ea (2008), CCR 38, 1162-1186

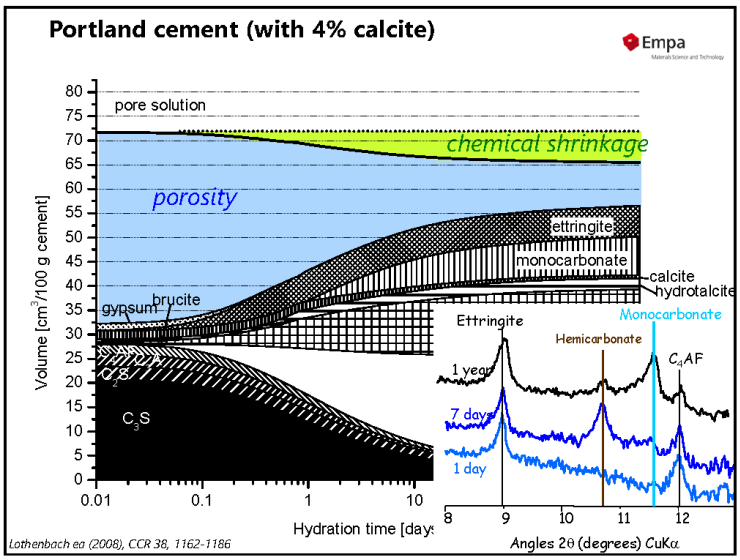
Portland cement (with 4% calcite)
Empa
pore solution
chemical shrinkage
porosity
ettringite
monocarbonate
calcite
hydrotalcite
brucite
gypsum
Ettringite
Monocarbonate
Hemicarbonate
1 year
7 days
1 day
C_4AF
C_2S
C_3S
Volume [cm³/100 g cement]
Hydration time [days
Angles 2θ (degrees) CuKα
Lothenbach ea (2008), CCR 38, 1162-1186

7

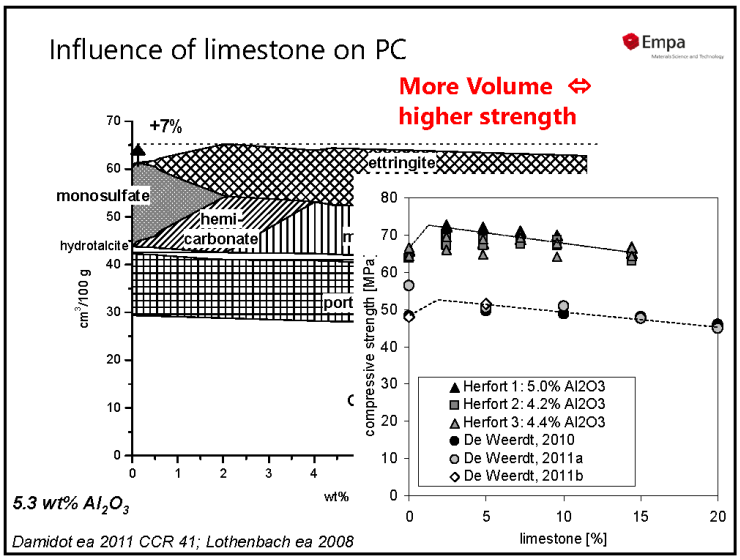
Influence of limestone on PC
Empa
More Volume ⇔
higher strength
+7%
ettringite
monosulfate
hemi-
carbonate
hydrotalcite
cm³/100 g
wt%
5.3 wt% Al2O3
compressive strength [MPa]
limestone [%]
Herfort 1: 5.0% Al2O3
Herfort 2: 4.2% Al2O3
Herfort 3: 4.4% Al2O3
De Weerdt, 2010
De Weerdt, 2011a
De Weerdt, 2011b
Damidot ea 2011 CCR 41; Lothenbach ea 2008

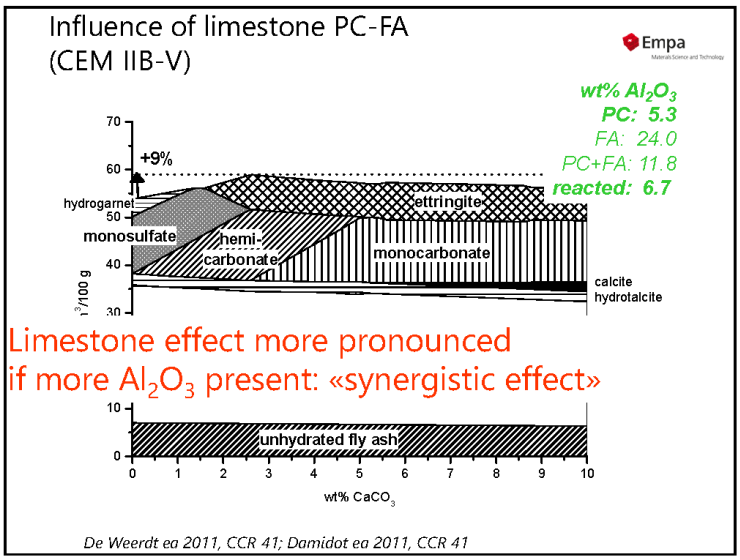
Influence of limestone PC-FA
(CEM IIB-V)
Empa
wt% Al2O3
PC: 5.3
FA: 24.0
PC+FA: 11.8
reacted: 6.7
+9%
hydrogarnet
ettringite
monosulfate
hemi-
carbonate
monocarbonate
calcite
hydrotalcite
Limestone effect more pronounced
if more Al2O3 present: «synergistic effect»
unhydrated fly ash
wt% CaCO3
De Weerdt ea 2011, CCR 41; Damidot ea 2011, CCR 41

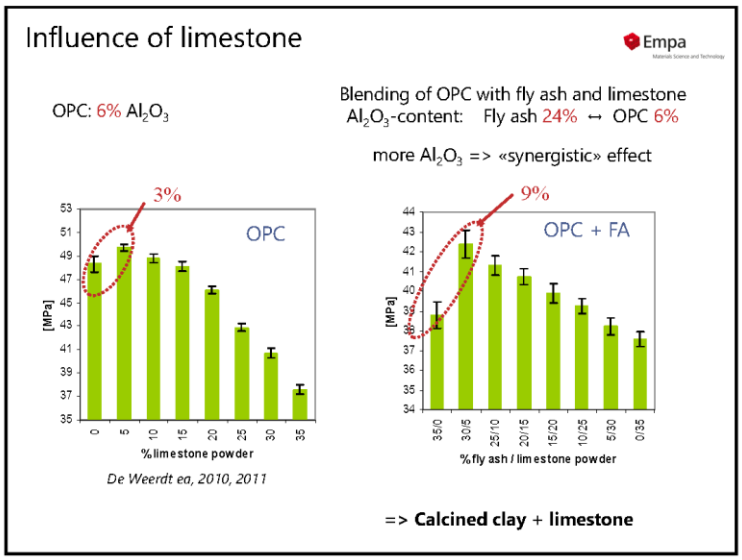
Influence of limestone
Empa
OPC: 6% Al_2O_3
Blending of OPC with fly ash and limestone
Al_2O_3-content: Fly ash 24% ↔ OPC 6%
more Al_2O_3 => «synergistic» effect
3%
OPC
[MPa]
%limestone powder
De Weerdt ea, 2010, 2011
9%
OPC + FA
[MPa]
%fly ash / limestone powder
=> Calcined clay + limestone

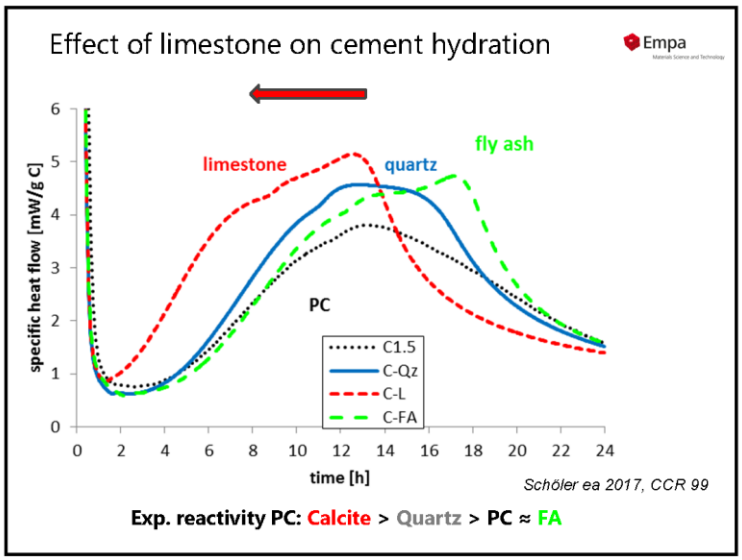
Effect of limestone on cement hydration
Empa
limestone
quartz
fly ash
PC
C1.5
C-Qz
C-L
C-FA
specific heat flow [mW/g C]
time [h]
Schöler ea 2017, CCR 99
Exp. reactivity PC: Calcite > Quartz > PC ≈ FA

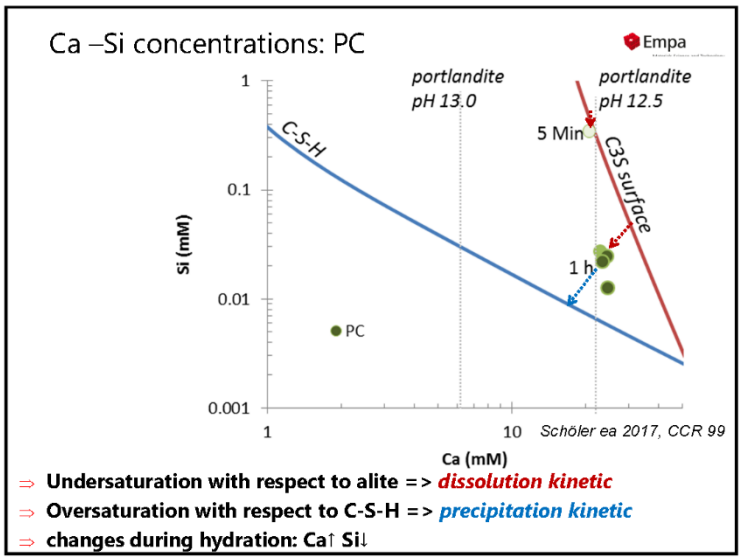
Ca –Si concentrations: PC
Empa
portlandite
pH 13.0
portlandite
pH 12.5
5 Min
C-S-H
C3S surface
1 h
PC
Si (mM)
1
0.1
0.01
0.001
1
10
Ca (mM)
Schöler ea 2017, CCR 99
⇒ Undersaturation with respect to alite => dissolution kinetic
⇒ Oversaturation with respect to C-S-H => precipitation kinetic
⇒ changes during hydration: Ca↑ Si↓

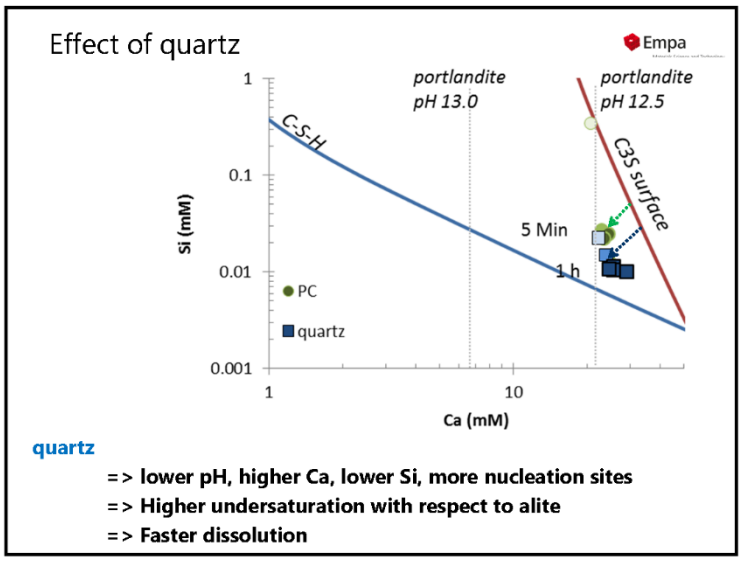
Effect of quartz
Empa
portlandite
pH 13.0
portlandite
pH 12.5
C-S-H
C3S surface
5 Min
1 h
PC
quartz
Si (mM)
1
0.1
0.01
0.001
1
10
Ca (mM)
quartz
=> lower pH, higher Ca, lower Si, more nucleation sites
=> Higher undersaturation with respect to alite
=> Faster dissolution

10

Effect of limestone

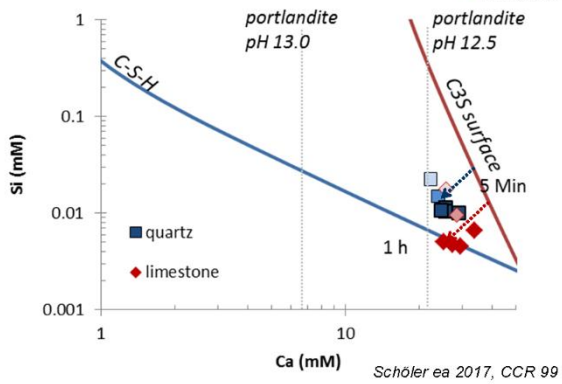

Schöler ea 2017, CCR 99

Limestone => Higher alite undersaturation => Faster dissolution

- Very strong nucleation => faster C-S-H formation
- More undersaturation => faster dissolution

Effect of surface area

Empa

- More surface
  - More reaction
- **Calcite**
  - Very strong nucleation
  - => faster C-S-H formation
  - More undersaturation => faster dissolution

Berodier+Scrivener 2014, JACerS 97

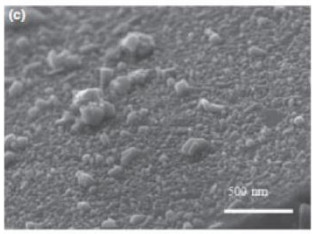

Nucleation on calcite (1.5 h)

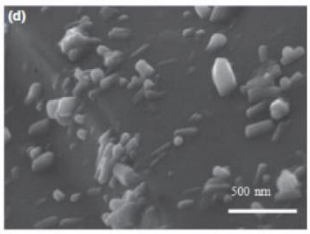

Nucleation on clinker surface (1.5 h)

11

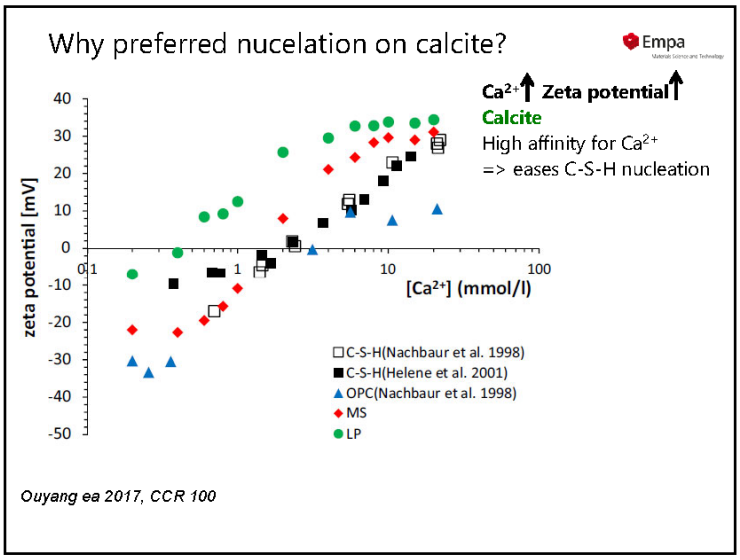
Why preferred nucelation on calcite?
Empa
Ca^{2+} ↑ Zeta potential ↑
Calcite
High affinity for Ca^{2+}
=> eases C-S-H nucleation
zeta potential [mV]
40
30
20
10
0
-10
-20
-30
-40
-50
0.1
1
10
100
[Ca^{2+}] (mmol/l)
C-S-H(Nachbaur et al. 1998)
C-S-H(Helene et al. 2001)
OPC(Nachbaur et al. 1998)
MS
LP
Ouyang ea 2017, CCR 100

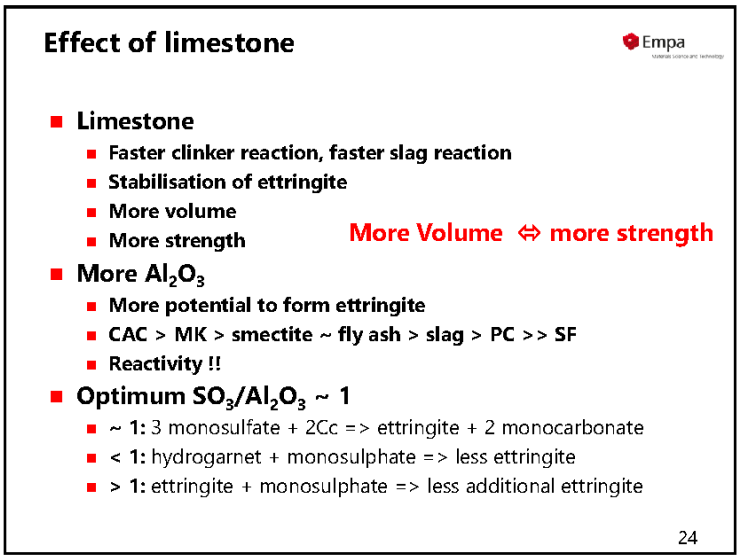
Effect of limestone
Empa
Limestone
Faster clinker reaction, faster slag reaction
Stabilisation of ettringite
More volume
More strength
More Volume ⇔ more strength
More Al_2O_3
More potential to form ettringite
CAC > MK > smectite ~ fly ash > slag > PC >> SF
Reactivity !!
Optimum SO_3/Al_2O_3 ~ 1
~ 1: 3 monosulfate + 2Cc => ettringite + 2 monocarbonate
< 1: hydrogarnet + monosulphate => less ettringite
> 1: ettringite + monosulphate => less additional ettringite
24

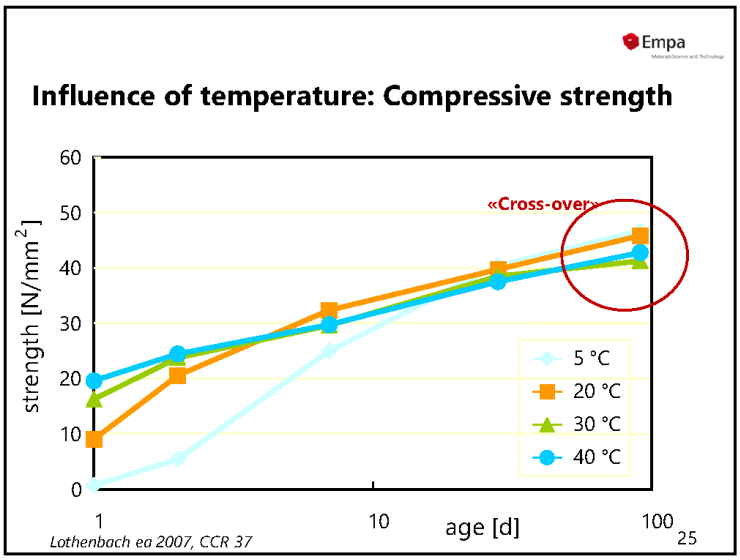
Empa
Influence of temperature: Compressive strength
«Cross-over»
strength [N/mm²]
60
50
40
30
20
10
0
1
10
100
age [d]
5 °C
20 °C
30 °C
40 °C
Lothenbach ea 2007, CCR 37
25

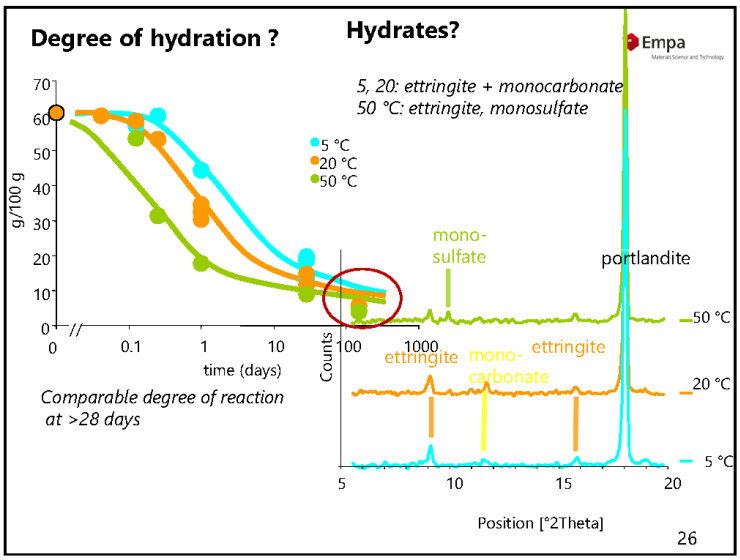
Degree of hydration ?
Hydrates?
Empa
5, 20: ettringite + monocarbonate
50 °C: ettringite, monosulfate
g/100 g
70
60
50
40
30
20
10
0
0
0.1
1
10
100
1000
time (days)
5 °C
20 °C
50 °C
mono-
sulfate
portlandite
Counts
ettringite
mono-
carbonate
ettringite
50 °C
20 °C
5 °C
5
10
15
20
Position [°2Theta]
Comparable degree of reaction
at >28 days
26

13

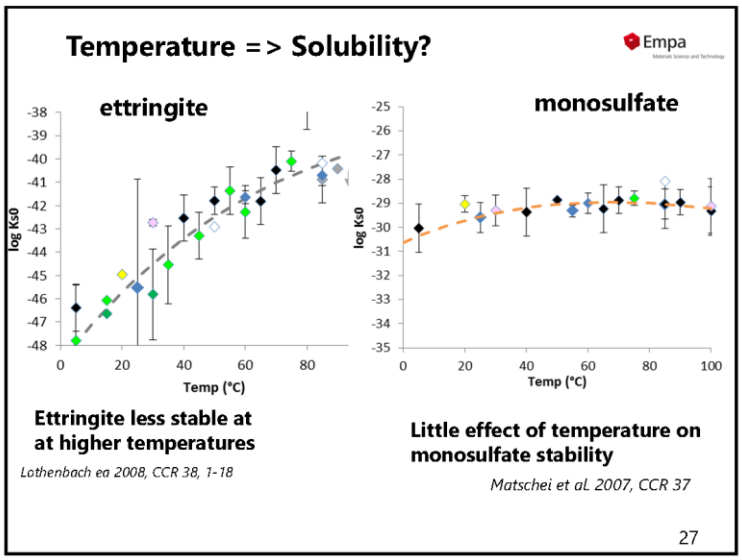
Temperature => Solubility?
Empa
ettringite
monosulfate
log Ks0
Temp (°C)
Ettringite less stable at at higher temperatures
Lothenbach ea 2008, CCR 38, 1-18
Little effect of temperature on monosulfate stability
Matschei et al. 2007, CCR 37
27

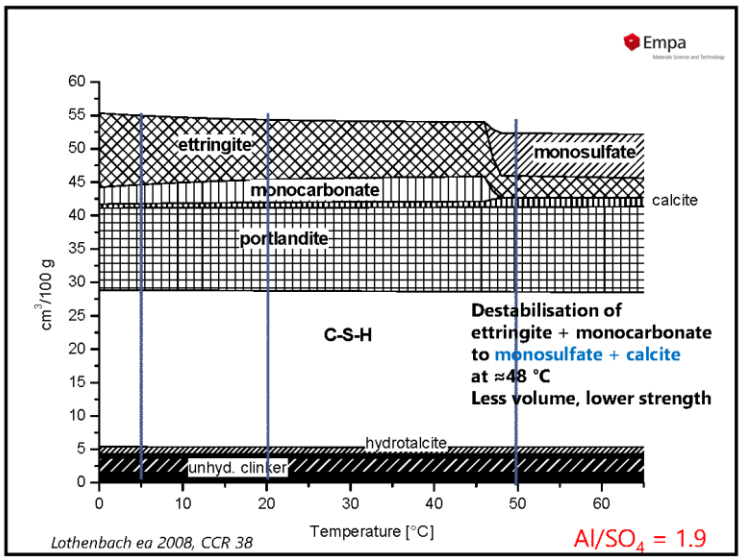
Empa
ettringite
monosulfate
monocarbonate
calcite
portlandite
C-S-H
Destabilisation of ettringite + monocarbonate to monosulfate + calcite at ≈48 °C
Less volume, lower strength
hydrotalcite
unhyd. clinker
cm³/100 g
Temperature [°C]
Lothenbach ea 2008, CCR 38
Al/SO4 = 1.9

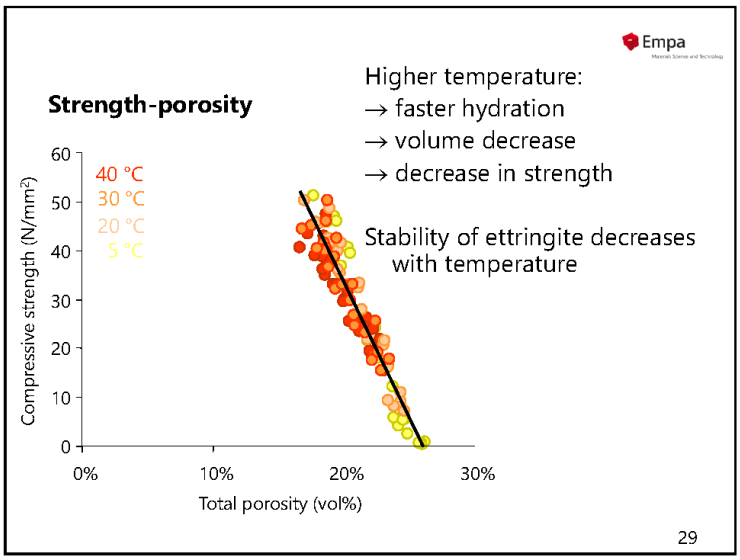
Empa
Strength-porosity
Higher temperature:
→ faster hydration
→ volume decrease
→ decrease in strength
Stability of ettringite decreases with temperature
40 °C
30 °C
20 °C
5 °C
Compressive strength (N/mm²)
60
50
40
30
20
10
0
0%
10%
20%
30%
Total porosity (vol%)
29

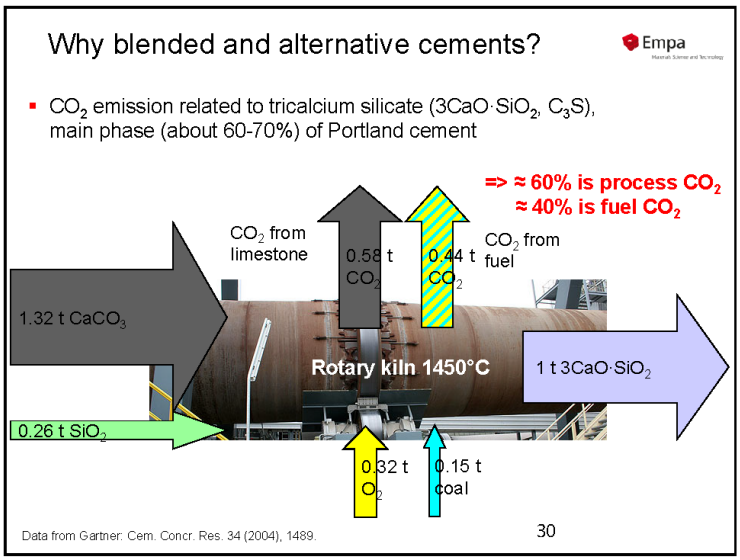
Why blended and alternative cements?
Empa
CO2 emission related to tricalcium silicate (3CaO·SiO2, C3S), main phase (about 60-70%) of Portland cement
=> ≈ 60% is process CO2
≈ 40% is fuel CO2
CO2 from limestone
0.58 t CO2
0.44 t CO2
CO2 from fuel
1.32 t CaCO3
Rotary kiln 1450°C
1 t 3CaO·SiO2
0.26 t SiO2
0.32 t O2
0.15 t coal
Data from Gartner: Cem. Concr. Res. 34 (2004), 1489.
30

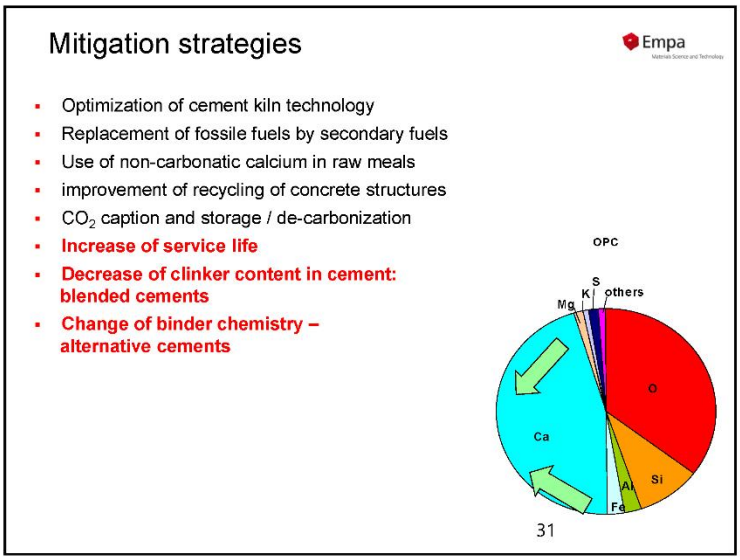
Mitigation strategies
Empa
Optimization of cement kiln technology
Replacement of fossile fuels by secondary fuels
Use of non-carbonatic calcium in raw meals
improvement of recycling of concrete structures
CO_2 caption and storage / de-carbonization
Increase of service life
Decrease of clinker content in cement: blended cements
Change of binder chemistry – alternative cements
OPC
S
K
others
Mg
O
Ca
Si
Al
Fe
31

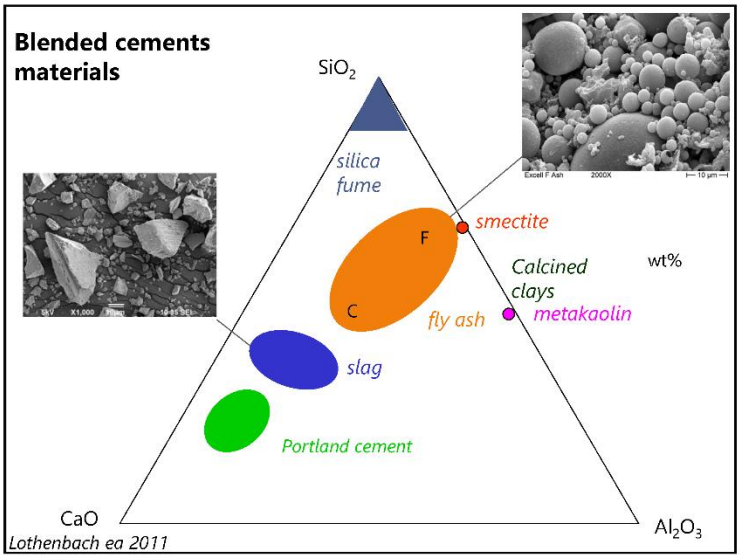
Blended cements materials
SiO_2
silica fume
smectite
F
Calcined clays
wt%
C
fly ash
metakaolin
slag
Portland cement
CaO
Al_2O_3
Lothenbach ea 2011

16

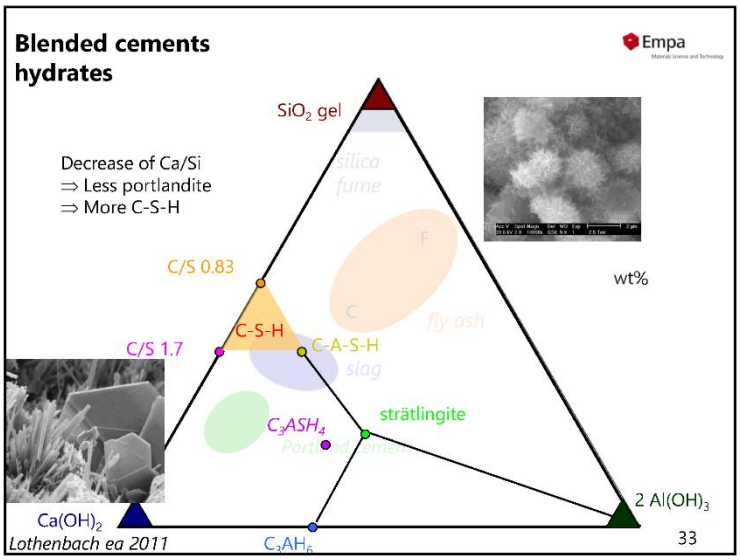
Blended cements hydrates
Empa
SiO2 gel
Decrease of Ca/Si
⇒ Less portlandite
⇒ More C-S-H
silica fume
F
C
fly ash
slag
C/S 0.83
C/S 1.7
C-S-H
C-A-S-H
strätlingite
C3ASH4
wt%
2 Al(OH)3
Ca(OH)2
C3AH6
Lothenbach ea 2011
33

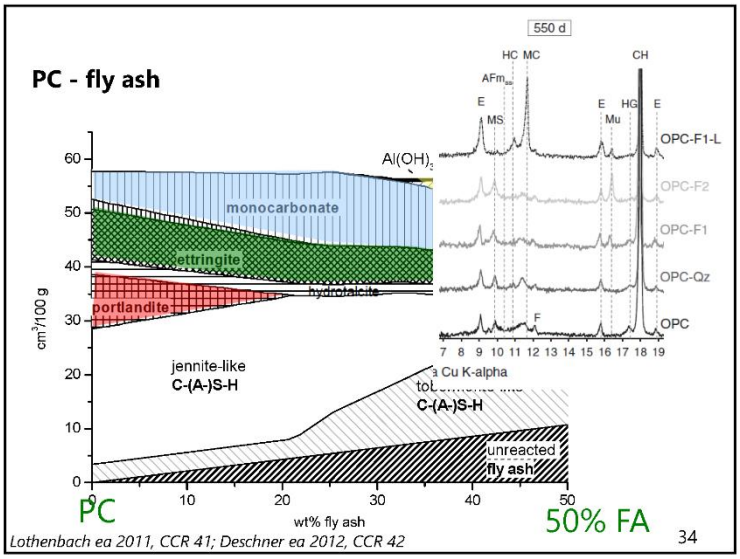
PC - fly ash
550 d
HC MC
CH
AFm
E
MS
E
Mu
HG
E
OPC-F1-L
OPC-F2
OPC-F1
OPC-Qz
OPC
F
7 8 9 10 11 12 13 14 15 16 17 18 19
Cu K-alpha
Al(OH)3
monocarbonate
ettringite
portlandite
hydrotalcite
cm³/100 g
jennite-like
C-(A-)S-H
C-(A-)S-H
unreacted
fly ash
wt% fly ash
PC
50% FA
Lothenbach ea 2011, CCR 41; Deschner ea 2012, CCR 42
34

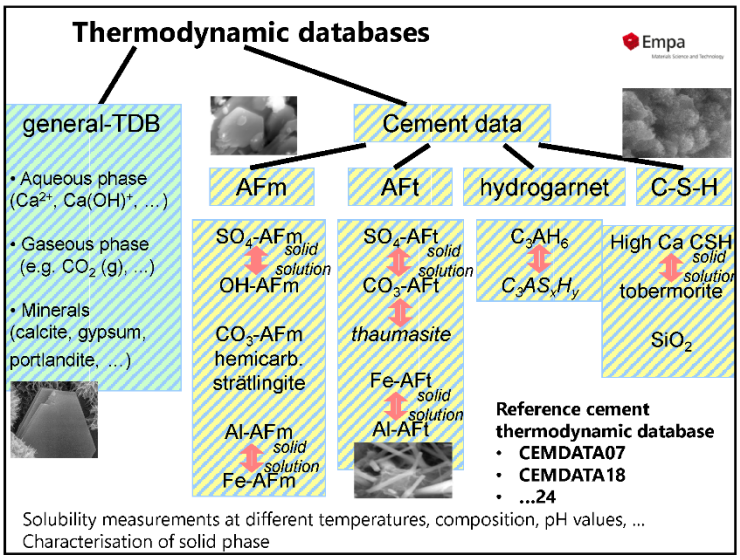
Thermodynamic databases
Empa
general-TDB
• Aqueous phase (Ca^{2+}, $Ca(OH)^+$, ...)
• Gaseous phase (e.g. CO_2 (g), ...)
• Minerals (calcite, gypsum, portlandite, ...)
Cement data
AFm
AFt
hydrogarnet
C-S-H
SO_4-AFm
solid solution
OH-AFm
CO_3-AFm
hemicarb.
strätlingite
Al-AFm
solid solution
Fe-AFm
SO_4-AFt
solid solution
CO_3-AFt
thaumasite
Fe-AFt
solid solution
Al-AFt
C_3AH_6
$C_3AS_xH_y$
High Ca CSH
solid solution
tobermorite
SiO_2
Reference cement thermodynamic database
• CEMDATA07
• CEMDATA18
• ...24
Solubility measurements at different temperatures, composition, pH values, ...
Characterisation of solid phase

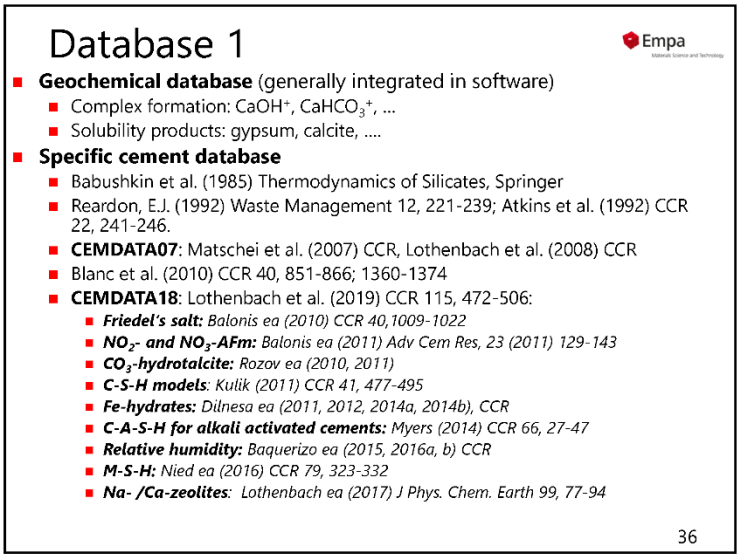
Database 1
Empa
Geochemical database (generally integrated in software)
Complex formation: $CaOH^+$, $CaHCO_3^+$, ...
Solubility products: gypsum, calcite, ...
Specific cement database
Babushkin et al. (1985) Thermodynamics of Silicates, Springer
Reardon, E.J. (1992) Waste Management 12, 221-239; Atkins et al. (1992) CCR 22, 241-246.
CEMDATA07: Matschei et al. (2007) CCR, Lothenbach et al. (2008) CCR
Blanc et al. (2010) CCR 40, 851-866; 1360-1374
CEMDATA18: Lothenbach et al. (2019) CCR 115, 472-506:
Friedel's salt: Balonis ea (2010) CCR 40,1009-1022
NO_2- and NO_3-AFm: Balonis ea (2011) Adv Cem Res, 23 (2011) 129-143
CO_3-hydrotalcite: Rozov ea (2010, 2011)
C-S-H models: Kulik (2011) CCR 41, 477-495
Fe-hydrates: Dilnesa ea (2011, 2012, 2014a, 2014b), CCR
C-A-S-H for alkali activated cements: Myers (2014) CCR 66, 27-47
Relative humidity: Baquerizo ea (2015, 2016a, b) CCR
M-S-H: Nied ea (2016) CCR 79, 323-332
Na- /Ca-zeolites: Lothenbach ea (2017) J Phys. Chem. Earth 99, 77-94
36

Cemdata

Cemdata18 database: Standard thermodynamic properties at 25 °Ca and 1 atm. Update of Cemdata07

The data are fully compatible with the GEMS version of the PSI/Nagra thermodynamic database [6, 7].

	log K_{50}°	$\Delta_f G^{\circ}$ [kJ/mol]	$\Delta_f H^{\circ}$ [kJ/mol]	S° [J/K/mol]	a_0 [J/K/mol]	a_1	a_2	a_3	V° [cm^3/mol]	Ref
(Al-)ettringite[a,b,c]	-44.9	-15205.94	-17535	1900	1939	0.789			707	[3, 4]
$C_6As_3H_{30}$[c]		-14728.1	-16950.2	1792.4	1452	2.156			708	[8]
$C_6As_3H_{13}$		-10540.6	-11530.3	1960.4	970.7	1.483			411	[8]
$C_6As_3H_9$		-9540.4	-10643.7	646.6	764.3	1.638			361	[8]
tricarboaluminate[a]	-46.5	-14565.64	-16792	1858	2042	0.559	$-7.78\cdot10^6$		650	[3, 4]
Fe-ettringite[b]	-44.0	-14282.36	-16600	1937	1922	0.855	$2.02\cdot10^6$		717	[3, 9]
Thaumasite	-24.75	-7564.52	-8700	897.1	1031	0.263	$-3.40\cdot10^6$		330	[10]
C_3AH_6[d]	-20.50	-5008.2	-5537.3	422	290	0.644	$-3.25\cdot10^6$		150	[11, 12]
*$C_3AS_{0.41}H_{5.18}$[**d]*	*-25.35*	*-5192.9*	*-5699*	*399*	*310*	*0.566*	*$-4.37\cdot10^6$*		*146*	*[12]*
*$C_3AS_{0.84}H_{4.32}$[**e]*	*-26.70*	*-5365.2*	*-5847*	*375*	*331*	*0.484*	*$-5.55\cdot10^6$*		*142*	*[12]*
C_3FH_6[***]	*-26.30*	*-4122.8*	*-4518*	*870*	*330*	*1.237*	*$-4.74\cdot10^6$*		*155*	*[12]*
$C_3FS_{0.84}H_{4.32}$[e,f]	-32.50	-4479.9	-4823	840	371	0.478	$-7.03\cdot10^6$		149	[12]
$C_3A_{0.5}F_{0.5}S_{0.84}H_{4.32}$[e]	-30.20	-4926.0	-5335	619	367	0.471	$-8.10\cdot10^6$		146	[12]
$C_3FS_{1.34}H_{3.32}$	-34.20	-4681.1	-4994	820	395	0.383	$-8.39\cdot10^6$		145	[12]
C_4AH_{19}[g]	-25.45	-8749.9	-10017.9	1120	1163	1.047		-1600	369	[11, 13]
C_4AH_{13}		-7325.7	-8262.4	831.5	208.3	3.13			274	[13]
C_4AH_{11}		-6841.4	-7656.6	772.7	0.0119	3.56	$1.34\cdot10^{-7}$		257	[13]
$C_2AH_{7.5}$	-13.80	-4695.5	-5277.5	450	323	0.728			180	[11]
CAH_{10}	-7.60	-4623.0	-5288.2	610	151	1.113		3200	193	[11]
C_4AsH_{16}		-8726.8	-9930.5	975.0	636	1.606			351	[13, 14]
C_4AsH_{14}[g]		-8252.9	-9321.8	960.9	1028.5				332	[13, 14]
C_4AsH_{12}[h]		-7778.4	-8758.6	791.6	175	2.594			310	[13, 14]
$C_4AsH_{10.5}$		-7414.9	-8311.9	721	172	2.402			282	[13, 14]
C_4AsH_9		-7047.6	-7845.5	703.6	169	2.211			275	[13, 14]
C_4AcH_{11}	-31.47	-7337.46	-8250	657	618	0.982	$-2.59\cdot10^6$		262	[3, 4]
C_4AcH_9		-6840.3	-7618.6	640.6	192.4	2.042			234	[13]
$C_4Ac_{0.5}H_{12}$	-29.13	-7335.97	-8270	713	664	1.014	$-1.30\cdot10^6$	-800	285	[3, 4]
$C_4Ac_{0.5}H_{10.5}$		-6970.3	-7813.3	668.3	0.0095	2.836	$1.07\cdot10^{-7}$		261	[13]
$C_4Ac_{0.5}H_9$		-6597.4	-7349.7	622.5	0.0088	2.635	$9.94\cdot10^{-8}$		249	[13]

Database: Cemdata18

Empa

- **PC:**
  Focus on **Portland cements and Portland-blends**
  - CSHQ (Kulik): Ca/Si 0.67 – 2.2 (portlandite limits to Ca/Si ≈ **1.6**)
  - $(KOH)_{2.5}SiO_2H_2O$) and $(NaOH)_{2.5}SiO_2H_2O$) to **estimate** alkali uptake
  - Very stable hydrotalcite from Atkins: $Mg_4Al_2O_{10}$ $10H_2O$
- **AAM18**
  Focus on **alkali activated materials**
  - CSHT (Kulik) with Na uptake and Al-uptake (in bridging site) (Myers ea 2014) Ca/Si **0.67 – 1.5**
  - Less stable hydrotalcite, variable Mg/Al (Myers ea 2015) $Mg_4Al_2O_{10}$ $10H_2O$, $Mg_6Al_2O_{12}$ $12H_2O$, $Mg_8Al_2O_{14}$ $14H_2O$

Cannot be used at the same time

Further CSH models activated by introducing additional solid solutions in «Phase»:

- Tob-jennite (Kulik and Kersten 2001, Lothenbach and Winnefeld 2006)
- CSHT (Kulik 2011)

All details in Lothenbach et al. (2019) CCR 115, 472-506

New CSH model with alkali, earth alkali and Al uptake in progress:

Kulik ea (2022) CCR 151, 106585; Miron ea (2022) CCR 152, 106667; Miron ea (2022) M&S 55(8), 212; Miron ea (2023) in preparation

38

19

AFm phases: solid solutions

C_4AH_{13} – monosulfate: solid solution

Characteristics
solid solutions:
- XRD peak shift

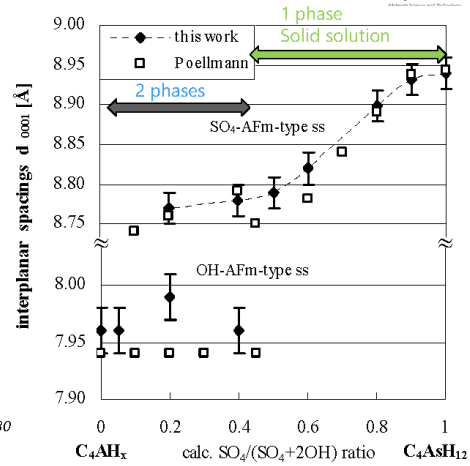

Matschei et al (2007) CCR 37, 118-130

AFm phases: solid solutions

C_4AH_{13} – monosulfate: solid solution

Characteristics
solid solutions:
- XRD peak shift
- change of concentrations

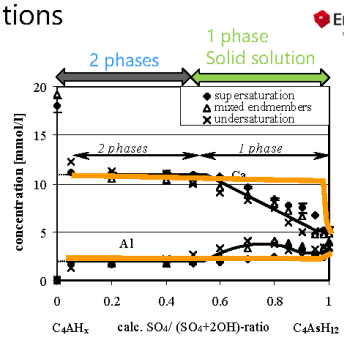

- solid solution: miscibility gap 0.03-0.5
- no solid solution

Further reading:
J. Bruno, D. Bosbach, D. Kulik and A. Navrotsky
Chemical Thermodynamics of Solid Solutions of Interest in Nuclear Waste Management
Nea, Chemical Thermodynamics Vol. 10 (2007)

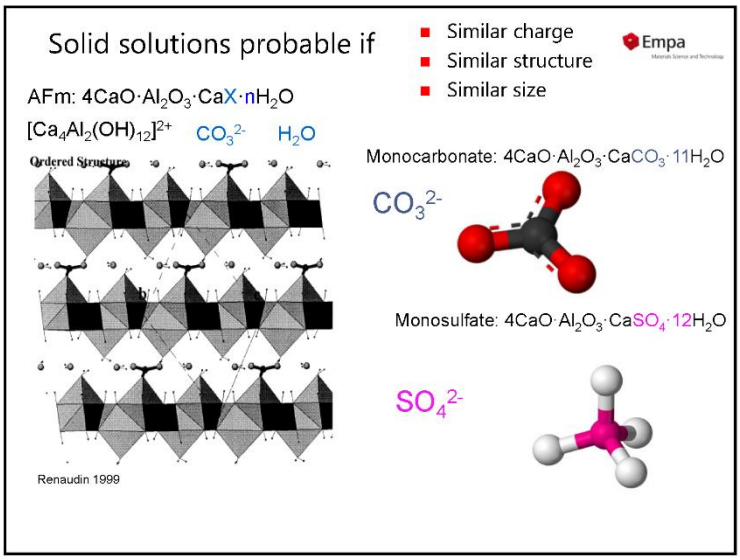
Solid solutions probable if
Similar charge
Similar structure
Similar size
Empa
AFm: 4CaO·Al2O3·CaX·nH2O
[Ca4Al2(OH)12]2+ CO32- H2O
Ordered Structure
Renaudin 1999
Monocarbonate: 4CaO·Al2O3·CaCO3·11H2O
CO32-
Monosulfate: 4CaO·Al2O3·CaSO4·12H2O
SO42-

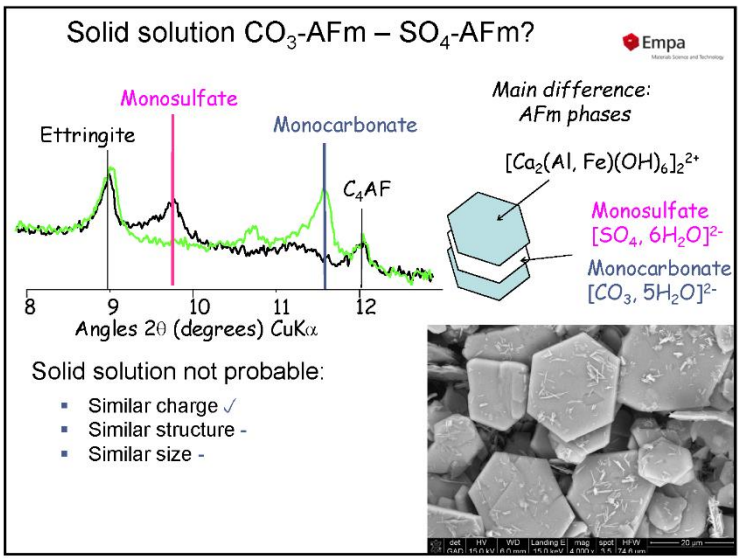
Solid solution CO3-AFm – SO4-AFm?
Empa
Monosulfate
Ettringite
Monocarbonate
C4AF
8
9
10
11
12
Angles 2θ (degrees) CuKα
Main difference:
AFm phases
[Ca2(Al, Fe)(OH)6]2 2+
Monosulfate
[SO4, 6H2O]2-
Monocarbonate
[CO3, 5H2O]2-
Solid solution not probable:
Similar charge ✓
Similar structure -
Similar size -

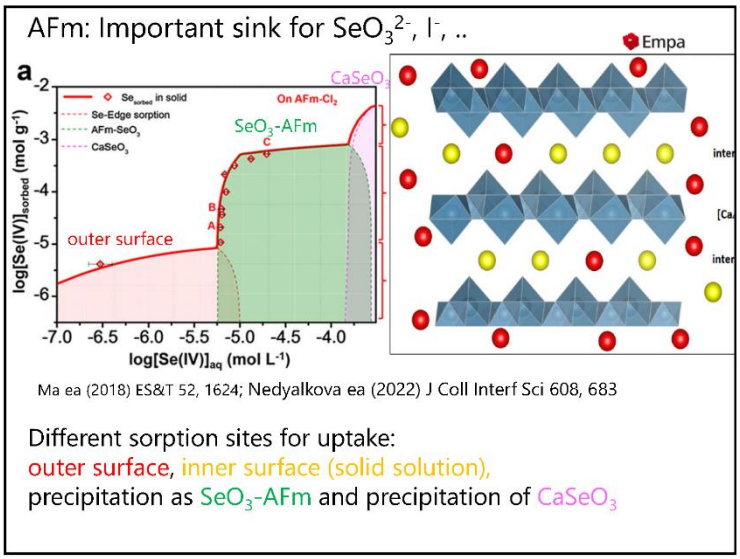
AFm: Important sink for SeO_3^{2-}, I^-, ..
Empa
a
Se_{sorbed} in solid
Se-Edge sorption
AFm-SeO_3
$CaSeO_3$
On AFm-Cl_2
SeO_3-AFm
$CaSeO_3$
outer surface
log[Se(IV)]sorbed (mol g-1)
log[Se(IV)]aq (mol L-1)
Ma ea (2018) ES&T 52, 1624; Nedyalkova ea (2022) J Coll Interf Sci 608, 683
Different sorption sites for uptake:
outer surface, inner surface (solid solution),
precipitation as SeO_3-AFm and precipitation of $CaSeO_3$

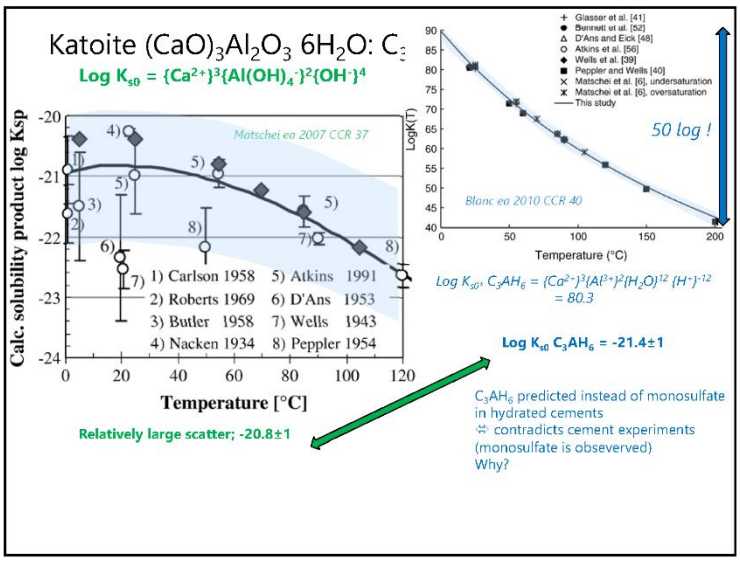
Katoite $(CaO)_3Al_2O_3$ $6H_2O$: C_3
Log K_{s0} = $\{Ca^{2+}\}^3\{Al(OH)_4^-\}^2\{OH^-\}^4$
Matschei ea 2007 CCR 37
Calc. solubility product log Ksp
Temperature [°C]
1) Carlson 1958
2) Roberts 1969
3) Butler 1958
4) Nacken 1934
5) Atkins 1991
6) D'Ans 1953
7) Wells 1943
8) Peppler 1954
Relatively large scatter; -20.8±1
Glasser et al. [41]
Bennett et al. [52]
D'Ans and Eick [48]
Atkins et al. [56]
Wells et al. [39]
Peppler and Wells [40]
Matschei et al. [6], undersaturation
Matschei et al. [6], oversaturation
This study
50 log !
Blanc ea 2010 CCR 40
LogK(T)
Temperature (°C)
Log K_{s0}, C_3AH_6 = $\{Ca^{2+}\}^3\{Al^{3+}\}^2\{H_2O\}^{12}\{H^+\}^{-12}$ = 80.3
Log K_{s0} C_3AH_6 = -21.4±1
C_3AH_6 predicted instead of monosulfate in hydrated cements
☹ contradicts cement experiments (monosulfate is obseverved)
Why?

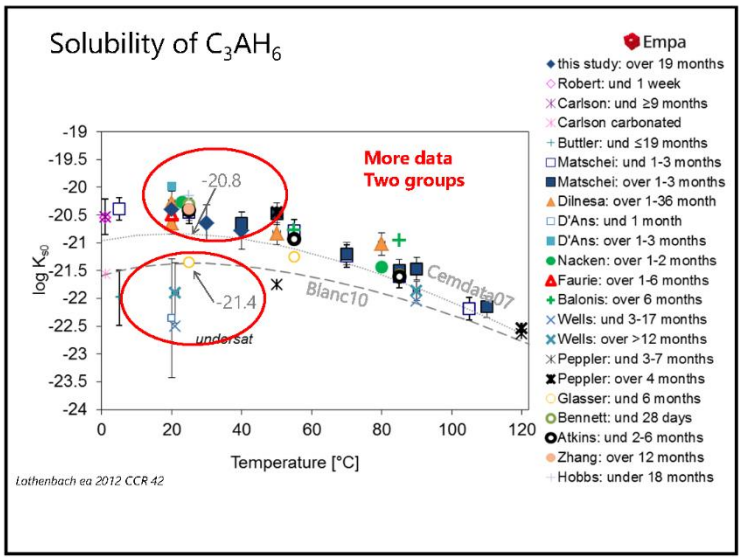
Solubility of C_3AH_6
Empa
More data
Two groups
-20.8
-21.4
undersat
Blanc10
Cemdata07
log K_{s0}
Temperature [°C]
this study: over 19 months
Robert: und 1 week
Carlson: und ≥9 months
Carlson carbonated
Buttler: und ≤19 months
Matschei: und 1-3 months
Matschei: over 1-3 months
Dilnesa: over 1-36 month
D'Ans: und 1 month
D'Ans: over 1-3 months
Nacken: over 1-2 months
Faurie: over 1-6 months
Balonis: over 6 months
Wells: und 3-17 months
Wells: over >12 months
Peppler: und 3-7 months
Peppler: over 4 months
Glasser: und 6 months
Bennett: und 28 days
Atkins: und 2-6 months
Zhang: over 12 months
Hobbs: under 18 months
Lothenbach ea 2012 CCR 42

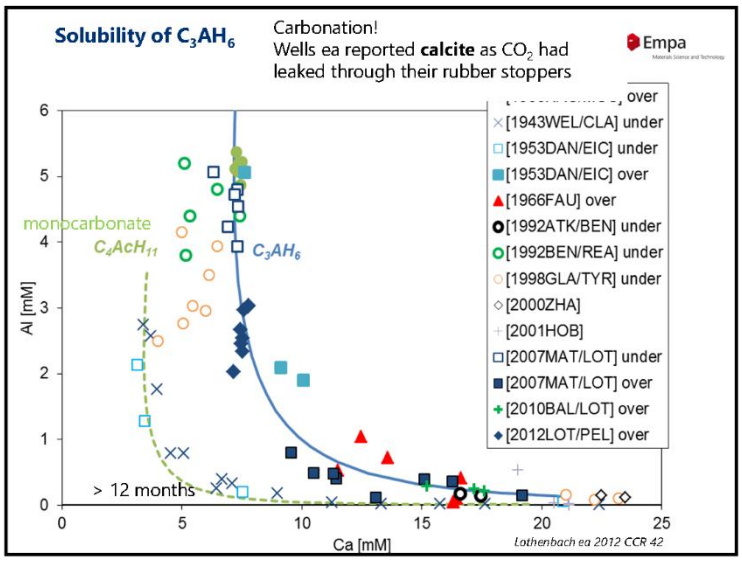
Solubility of C_3AH_6
Carbonation!
Wells ea reported **calcite** as CO_2 had leaked through their rubber stoppers
Empa
monocarbonate
C_4AcH_{11}
C_3AH_6
> 12 months
Al [mM]
Ca [mM]
[1943WEL/CLA] under
[1953DAN/EIC] under
[1953DAN/EIC] over
[1966FAU] over
[1992ATK/BEN] under
[1992BEN/REA] under
[1998GLA/TYR] under
[2000ZHA]
[2001HOB]
[2007MAT/LOT] under
[2007MAT/LOT] over
[2010BAL/LOT] over
[2012LOT/PEL] over
Lothenbach ea 2012 CCR 42

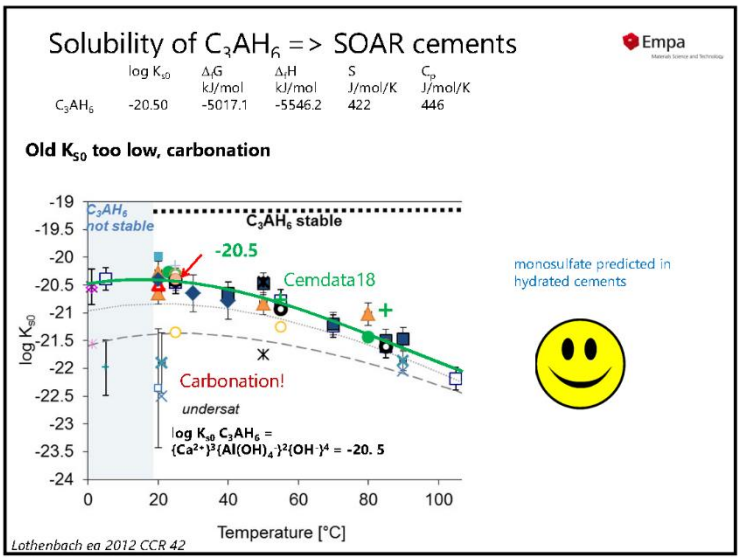
Solubility of C_3AH_6 => SOAR cements
Empa
log K_{s0} | $\Delta_f G$ kJ/mol | $\Delta_f H$ kJ/mol | S J/mol/K | C_p J/mol/K
C_3AH_6 | -20.50 | -5017.1 | -5546.2 | 422 | 446
Old K_{S0} too low, carbonation
C_3AH_6 not stable
C_3AH_6 stable
-20.5
Cemdata18
Carbonation!
undersat
log K_{s0} C_3AH_6 = $\{Ca^{2+}\}^3\{Al(OH)_4^-\}^2\{OH^-\}^4$ = -20. 5
log K_{s0}
Temperature [°C]
monosulfate predicted in hydrated cements
Lothenbach ea 2012 CCR 42

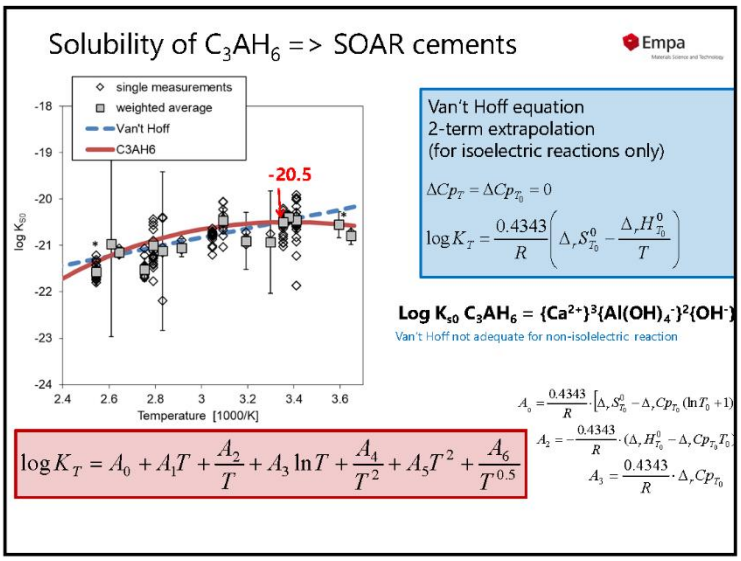
Solubility of C_3AH_6 => SOAR cements
Empa
single measurements
weighted average
Van't Hoff
C3AH6
-20.5
log K_{s0}
Temperature [1000/K]
Van't Hoff equation
2-term extrapolation
(for isoelectric reactions only)
$\Delta Cp_T = \Delta Cp_{T_0} = 0$
$\log K_T = \frac{0.4343}{R}\left(\Delta_r S^0_{T_0} - \frac{\Delta_r H^0_{T_0}}{T}\right)$
Log K_{s0} C_3AH_6 = $\{Ca^{2+}\}^3\{Al(OH)_4^-\}^2\{OH^-\}$
Van't Hoff not adequate for non-isolelectric reaction
$A_0 = \frac{0.4343}{R}\cdot[\Delta_r S^0_{T_0} - \Delta_r Cp_{T_0}(\ln T_0 + 1)]$
$A_2 = -\frac{0.4343}{R}\cdot(\Delta_r H^0_{T_0} - \Delta_r Cp_{T_0} T_0)$
$A_3 = \frac{0.4343}{R}\cdot\Delta_r Cp_{T_0}$
$\log K_T = A_0 + A_1 T + \frac{A_2}{T} + A_3 \ln T + \frac{A_4}{T^2} + A_5 T^2 + \frac{A_6}{T^{0.5}}$

24

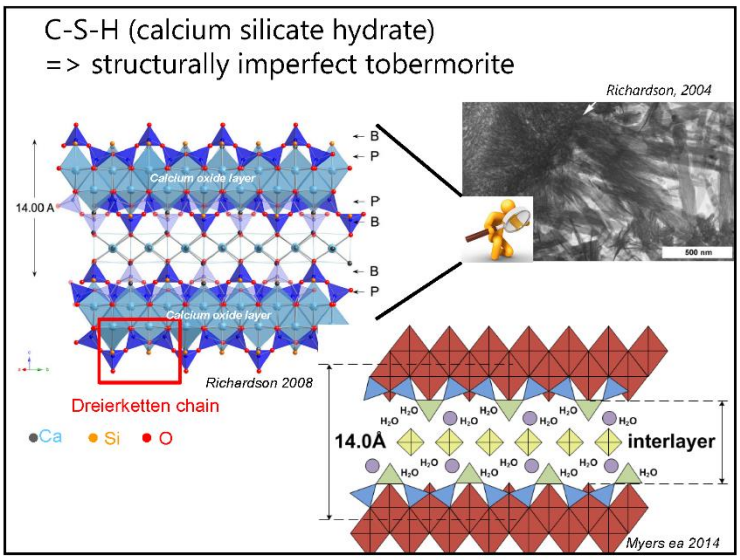
C-S-H (calcium silicate hydrate)
=> structurally imperfect tobermorite
Richardson, 2004
Calcium oxide layer
14.00 A
B
P
Richardson 2008
Dreierketten chain
Ca
Si
O
14.0Å
interlayer
Myers ea 2014

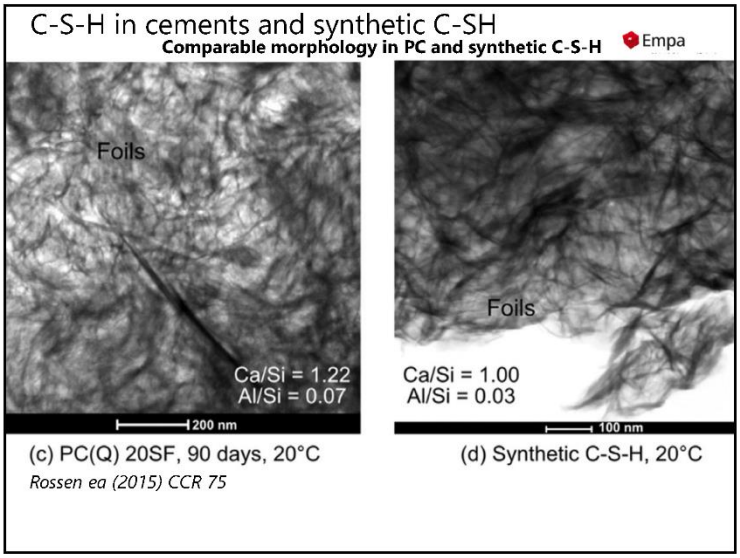
C-S-H in cements and synthetic C-SH
Comparable morphology in PC and synthetic C-S-H
Empa
Foils
Ca/Si = 1.22
Al/Si = 0.07
200 nm
Foils
Ca/Si = 1.00
Al/Si = 0.03
100 nm
(c) PC(Q) 20SF, 90 days, 20°C
(d) Synthetic C-S-H, 20°C
Rossen ea (2015) CCR 75

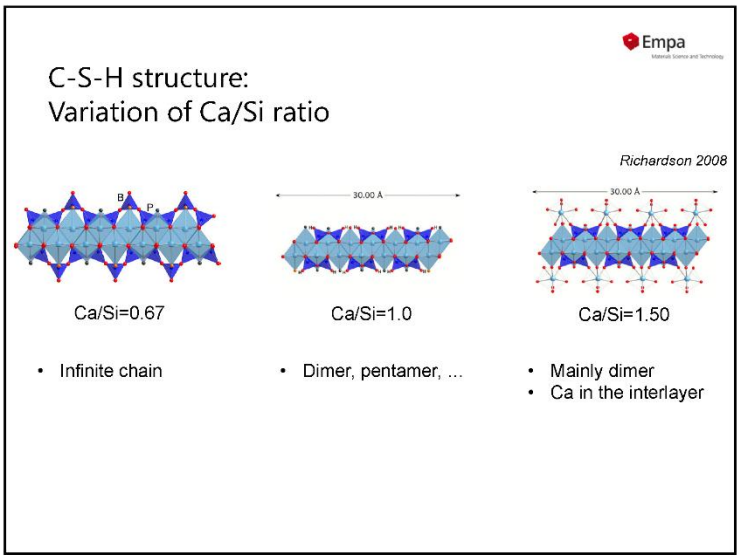
Empa
C-S-H structure:
Variation of Ca/Si ratio
Richardson 2008
30.00 Å
30.00 Å
Ca/Si=0.67
Ca/Si=1.0
Ca/Si=1.50
• Infinite chain
• Dimer, pentamer, ...
• Mainly dimer
• Ca in the interlayer

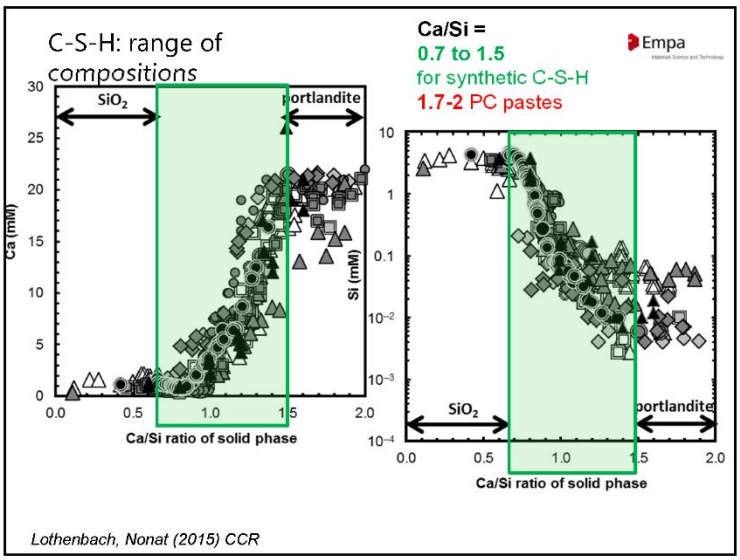
C-S-H: range of compositions
Ca/Si =
0.7 to 1.5
for synthetic C-S-H
1.7-2 PC pastes
Empa
SiO2
portlandite
Ca (mM)
Si (mM)
Ca/Si ratio of solid phase
Lothenbach, Nonat (2015) CCR

26

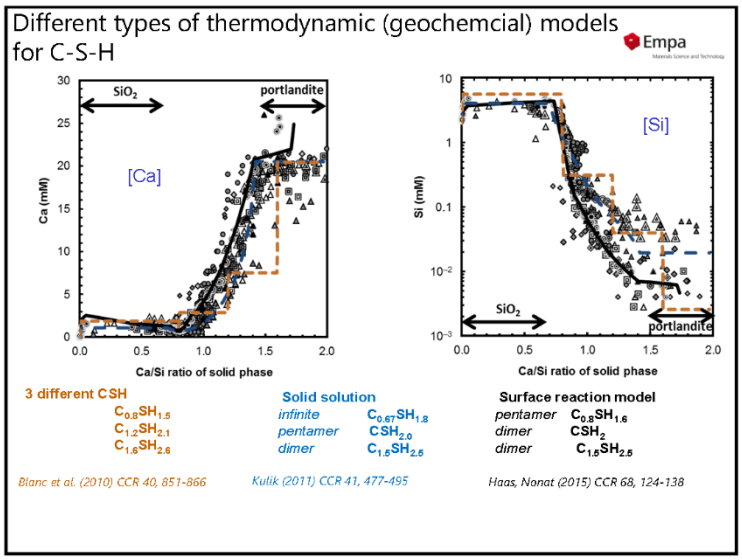
Different types of thermodynamic (geochemcial) models for C-S-H
Empa
SiO2
portlandite
[Ca]
Ca (mM)
Ca/Si ratio of solid phase
[Si]
Si (mM)
3 different CSH
C0.8SH1.5
C1.2SH2.1
C1.6SH2.6
Solid solution
infinite C0.67SH1.8
pentamer CSH2.0
dimer C1.5SH2.5
Surface reaction model
pentamer C0.8SH1.6
dimer CSH2
dimer C1.5SH2.5
Blanc et al. (2010) CCR 40, 851-866
Kulik (2011) CCR 41, 477-495
Haas, Nonat (2015) CCR 68, 124-138

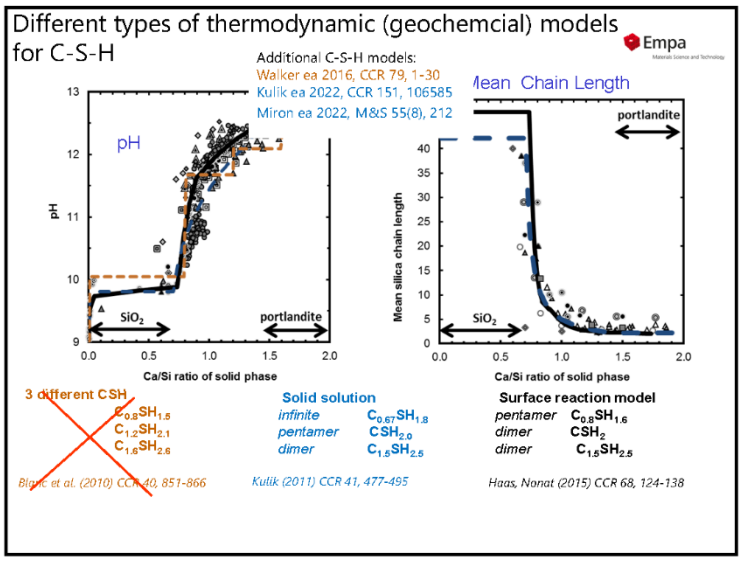
Different types of thermodynamic (geochemcial) models for C-S-H
Empa
Additional C-S-H models:
Walker ea 2016, CCR 79, 1-30
Kulik ea 2022, CCR 151, 106585
Miron ea 2022, M&S 55(8), 212
Mean Chain Length
pH
SiO2
portlandite
Mean silica chain length
Ca/Si ratio of solid phase
3 different CSH
C0.8SH1.5
C1.2SH2.1
C1.6SH2.6
Solid solution
infinite C0.67SH1.8
pentamer CSH2.0
dimer C1.5SH2.5
Surface reaction model
pentamer C0.8SH1.6
dimer CSH2
dimer C1.5SH2.5
Blanc et al. (2010) CCR 40, 851-866
Kulik (2011) CCR 41, 477-495
Haas, Nonat (2015) CCR 68, 124-138

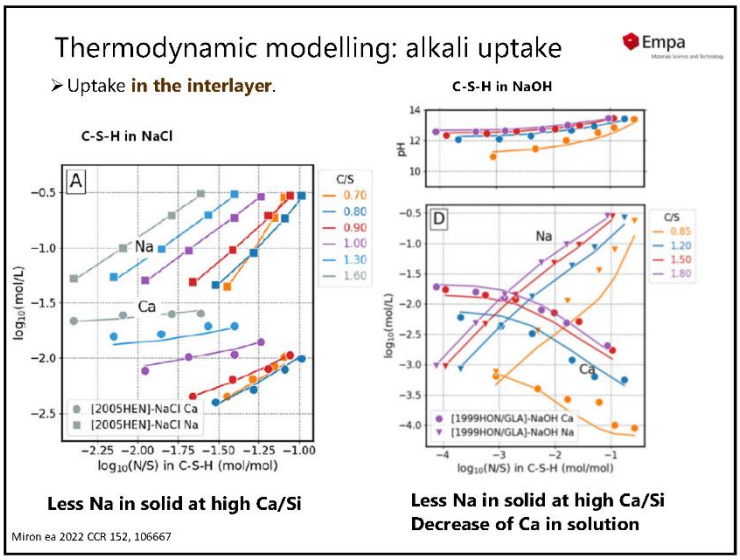
Thermodynamic modelling: alkali uptake
Empa
➢ Uptake in the interlayer.
C-S-H in NaCl
C-S-H in NaOH
A
D
Na
Ca
C/S
0.70
0.80
0.90
1.00
1.30
1.60
0.85
1.20
1.50
1.80
pH
log10(mol/L)
log10(N/S) in C-S-H (mol/mol)
[2005HEN]-NaCl Ca
[2005HEN]-NaCl Na
[1999HON/GLA]-NaOH Ca
[1999HON/GLA]-NaOH Na
Less Na in solid at high Ca/Si
Less Na in solid at high Ca/Si
Decrease of Ca in solution
Miron ea 2022 CCR 152, 106667

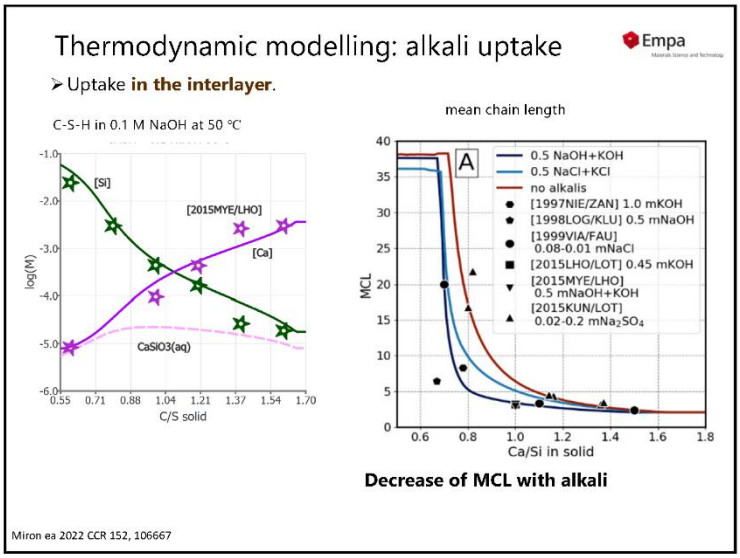
Thermodynamic modelling: alkali uptake
Empa
➢ Uptake in the interlayer.
C-S-H in 0.1 M NaOH at 50 °C
[Si]
[2015MYE/LHO]
[Ca]
CaSiO3(aq)
log(M)
C/S solid
mean chain length
A
0.5 NaOH+KOH
0.5 NaCl+KCl
no alkalis
[1997NIE/ZAN] 1.0 mKOH
[1998LOG/KLU] 0.5 mNaOH
[1999VIA/FAU] 0.08-0.01 mNaCl
[2015LHO/LOT] 0.45 mKOH
[2015MYE/LHO] 0.5 mNaOH+KOH
[2015KUN/LOT] 0.02-0.2 mNa2SO4
MCL
Ca/Si in solid
Decrease of MCL with alkali
Miron ea 2022 CCR 152, 106667

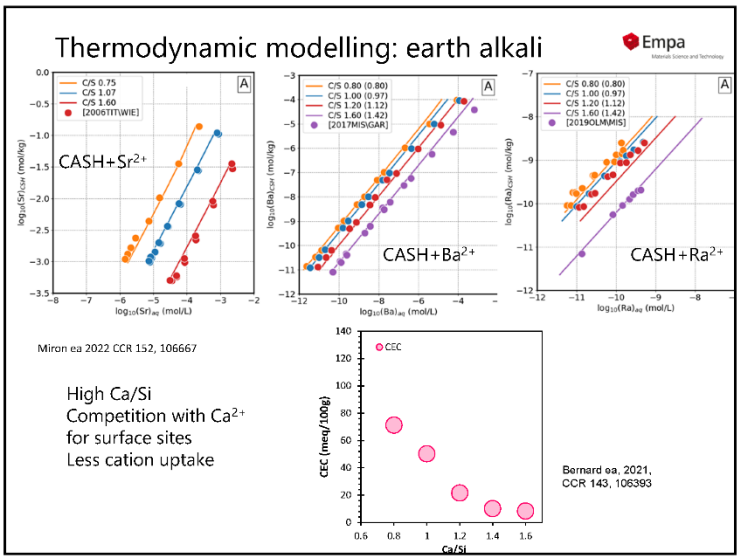
Thermodynamic modelling: earth alkali
Empa
CASH+Sr2+
CASH+Ba2+
CASH+Ra2+
Miron ea 2022 CCR 152, 106667
High Ca/Si
Competition with Ca2+
for surface sites
Less cation uptake
CEC
CEC (meq/100g)
Ca/Si
Bernard ea, 2021,
CCR 143, 106393

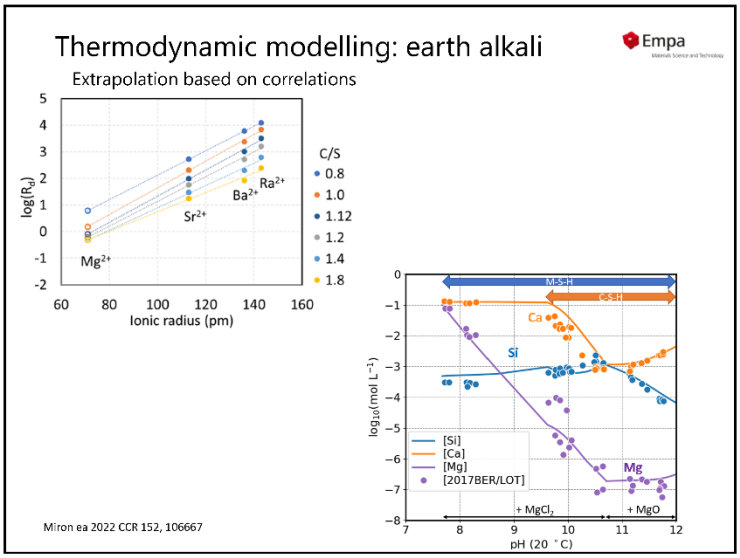
Thermodynamic modelling: earth alkali
Empa
Extrapolation based on correlations
log(Rd)
Ionic radius (pm)
C/S
0.8
1.0
1.12
1.2
1.4
1.8
Mg2+
Sr2+
Ba2+
Ra2+
M-S-H
C-S-H
Ca
Si
Mg
[Si]
[Ca]
[Mg]
[2017BER/LOT]
+ MgCl2
+ MgO
pH (20 °C)
Miron ea 2022 CCR 152, 106667

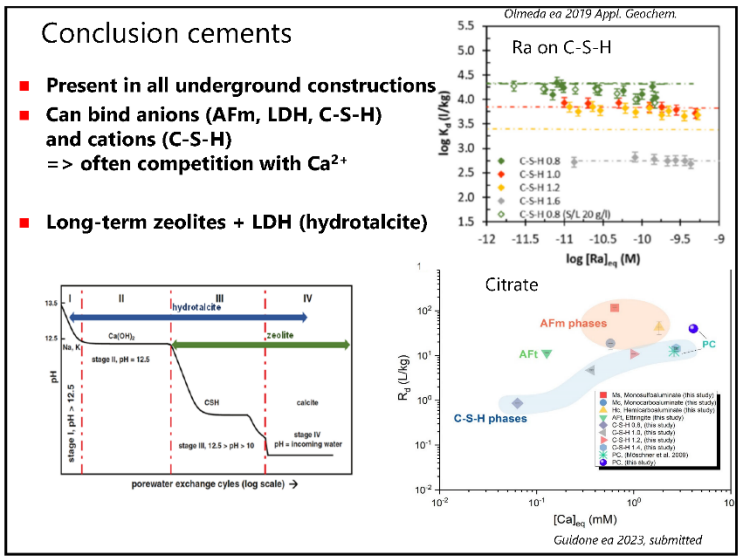
Conclusion cements
Present in all underground constructions
Can bind anions (AFm, LDH, C-S-H) and cations (C-S-H)
=> often competition with Ca2+
Long-term zeolites + LDH (hydrotalcite)
Olmeda ea 2019 Appl. Geochem.
Ra on C-S-H
log Kd (l/kg)
log [Ra]eq (M)
C-S-H 0.8
C-S-H 1.0
C-S-H 1.2
C-S-H 1.6
C-S-H 0.8 (S/L 20 g/l)
hydrotalcite
zeolite
Ca(OH)2
stage II, pH = 12.5
CSH
calcite
stage IV
pH = incoming water
stage III, 12.5 > pH > 10
stage I, pH > 12.5
pH
porewater exchange cyles (log scale)
Citrate
AFm phases
AFt
PC
C-S-H phases
Rd (L/kg)
[Ca]eq (mM)
Guidone ea 2023, submitted

3.3 Lecture 3 - Geochemistry of the host rock and natural barrier material (pore water chemistry, mineralogy, fracture-matrix)

In the framework of nuclear waste disposal, the natural geochemical conditions play a major role in the long-term stability of the materials used in the disposal (clays, concrete and cement phases, metals, glass…). The speciation of the radionuclides is also determined by the water chemistry and consequently, their potential out-diffusion from the disposal site or from the host rock. This lecture presents a strategy of data acquisition for determining the porewater chemistry of clay host rock and the global rock-water-gas equilibria. The main artifacts susceptible to change drastically the porewater chemistry are also described with the countermeasures that can insure a proper acquisition. Reliable experiments and the redundancy of the acquisition will allow to feed a numerical model following the phase rule adapted to a system considering also the ion exchange reactions. This critical review is focused on the methods that have been developed during the last two decades assuring and allowing a robust determination of the porewater chemistries in clayrocks and shales.

Lecturer

Eric C. Gaucher, Rock-Water-Interaction group. University of Bern, Switzerland

Reading Material

Gaucher, E.C., Tournassat, C., Pearson, F., Blanc, P., Crouzet, C., Lerouge, C. and Altmann, S. (2009) A robust model for pore-water chemistry of clayrock. Geochimica et Cosmochimica Acta 73, 6470-6487.

Lassin, A., Marty, N.C., Gailhanou, H., Henry, B., Trémosa, J., Lerouge, C., Madé, B., Altmann, S. and Gaucher, E.C. (2016) Equilibrium partial pressure of CO_2 in Callovian–Oxfordian argillite as a function of relative humidity: Experiments and modelling. Geochimica et Cosmochimica Acta 186, 91-104.

Pearson, F., Tournassat, C. and Gaucher, E.C. (2011) Biogeochemical processes in a clay formation in situ experiment: Part E–Equilibrium controls on chemistry of pore water from the Opalinus Clay, Mont Terri Underground Research Laboratory, Switzerland. Applied geochemistry 26, 990-1008.

Tournassat, C., Vinsot, A., Gaucher, E.C. and Altmann, S. (2015) Chemical conditions in clay-rocks, Developments in clay science. Elsevier, pp. 71-100.

Wersin, P., Mazurek, M., Gimmi, T (2022) Porewater chemistry of Opalinus Clay revisited: Findings from 25 years of data collection at the Mont Terri Rock Laboratory. Applied Geochemistrythis, 138, 105234.

Slides

TRAINING COURSE:
Geochemical & Reactive Transport Modelling for Geological Disposal

Eric C. Gaucher
Rock-Water Interaction
Institute of Geological Sciences

Geochemistry of the host rock and natural barrier material

(pore water chemistry, mineralogy, fracture-matrix)

How to develop a strategy for geochemical data acquisition and modelling to define PoreWater chemistry in clay formations?

Geochimical data acquisition for Nuclear Waste storage in deep geological formations

- Geochemists must answer the following questions:
  - What is the chemistry of the porewater of the host rock?
    - pH, Eh, TDS, major elements, minor elements
  - What is the chemistry of the surrounding aquifers?

  - How can understanding the past and present help us predict the future of the system?
  - How is the system buffered (or not) by the mineralogy of the host rocks?
  - How can the system evolve through interaction with concrete, glass, metals, gallery atmosphere, bacterial activity?
  - How are radioelements transported (or trapped) in geological environments?

Clay rocks: an environment difficult to study

- Clay rocks are a compact, reduced and reactive system that can be chemically strongly modified by:
  - drilling fluids contamination,
  - oxidation,
  - dehydration,
  - bacterial activity,
  - degassing…

- After two decades, we have established a list of experiments which are necessary for a complete acquisition of the chemical parameters.

Generic example of the evolution of the concentration of an aqueous component (SO_4) in the porewater (PW) of a clayey formation and in the surrounding rock formations including the aquifers (groundwater: GW)

AqEx: Aqueous Extraction
AD: Advective displacement
SQ: Squeezing
GW: Groundwater

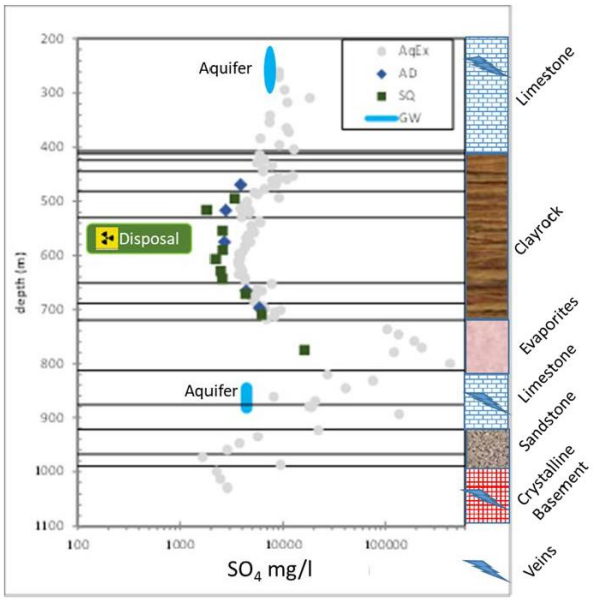

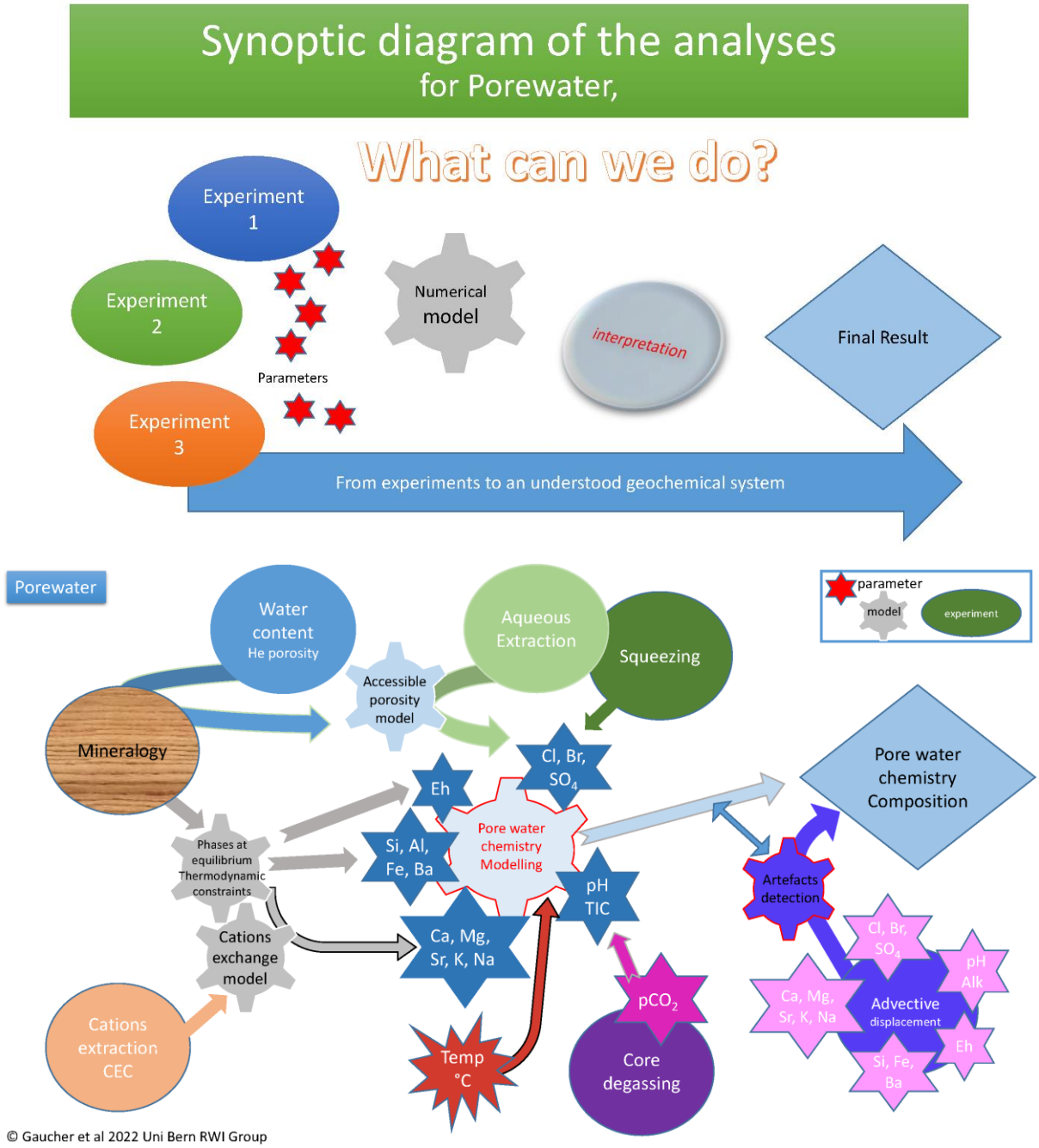
Synoptic diagram of the analyses
for Porewater,
What can we do?
Experiment 1
Experiment 2
Experiment 3
Parameters
Numerical model
interpretation
Final Result
From experiments to an understood geochemical system
Porewater
Water content
He porosity
Aqueous Extraction
Squeezing
parameter
model
experiment
Accessible porosity model
Mineralogy
Cl, Br, SO4
Eh
Pore water chemistry Composition
Phases at equilibrium Thermodynamic constraints
Si, Al, Fe, Ba
Pore water chemistry Modelling
pH TIC
Artefacts detection
Cations exchange model
Ca, Mg, Sr, K, Na
Cl, Br, SO4
pH Alk
Ca, Mg, Sr, K, Na
Advective displacement
Eh
Si, Fe, Ba
pCO2
Cations extraction CEC
Temp °C
Core degassing
© Gaucher et al 2022 Uni Bern RWI Group

Reception of samples

Lab experiments

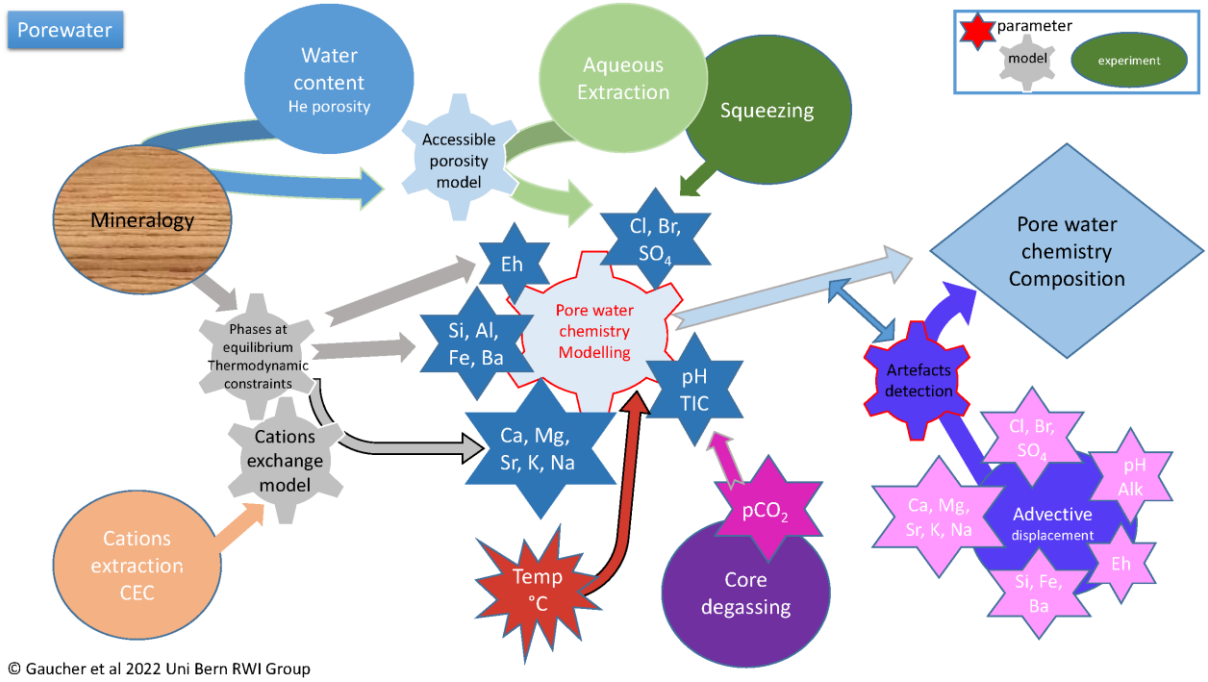

Mineralogy

Callovian-Oxfordian Formation Paris Basin France

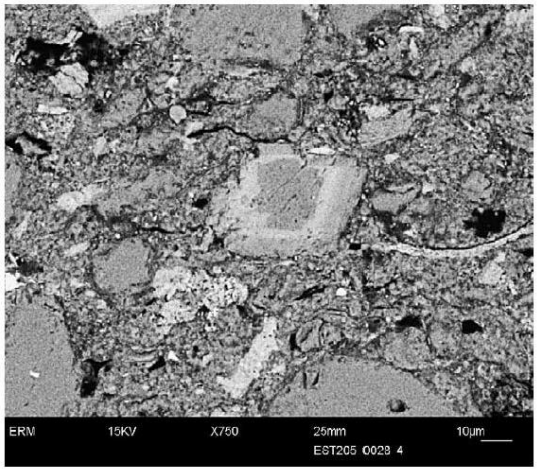

Fig. 5. Scanning Electron Micrograph. Sample EST05474 (432.4 m). Mg-calcite with a variable composition from the centre to the border.

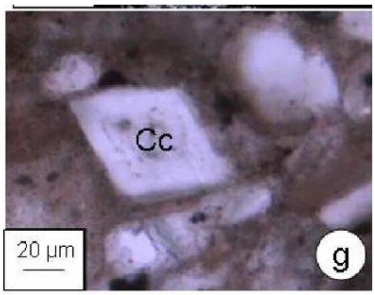

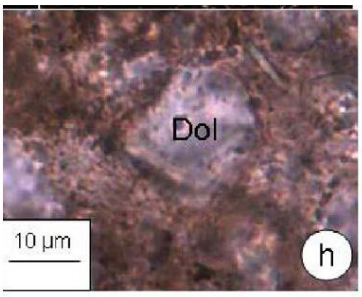

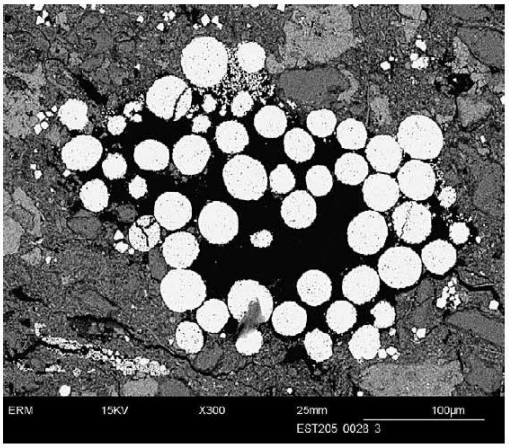

Fig. 6. Scanning Electron Micrograph. Sample EST05505 (442 m). Pyritosphere with organic matter (black).

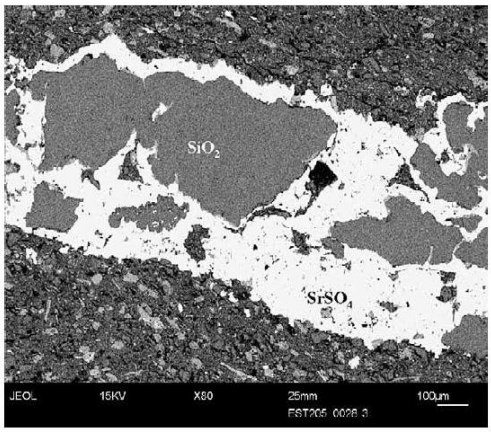

Fig. 7. Scanning Electron Micrograph. Sample EST05632 (475 m). Bioclast filled with celestite and chalcedony (?).

Selection of minerals for rock-water equilibrium model

List of minerals from Optical microscopy, X-Ray diffraction, Scanning electron microscopy, TEM…

The diagenetic studies are essential because they allow to identify the last phases which precipitated.

Lerouge, C., Grangeon, S., Claret, F., Gaucher, E., Blanc, P., Guerrot, C., Flehoc, C., Wille, G. and Mazurek, M. (2014) Mineralogical and isotopic record of diagenesis from the Opalinus Clay formation at Benken, Switzerland: Implications for the modeling of pore-water chemistry in a clay formation. Clay. Clay. Miner. 62, 286-312.

Lerouge, C., Grangeon, S., Gaucher, E.C., Tournassat, C., Agrinier, P., Guerrot, C., Widory, D., Fléhoc, C., Wille, G., Ramboz, C., Vinsot, A. and Buschaert, S. (2011) Mineralogical and isotopic record of biotic and abiotic diagenesis of the Callovian-Oxfordian clayey formation of Bure (France). Geochim. Cosmochim. Acta 75, 2633-2663.

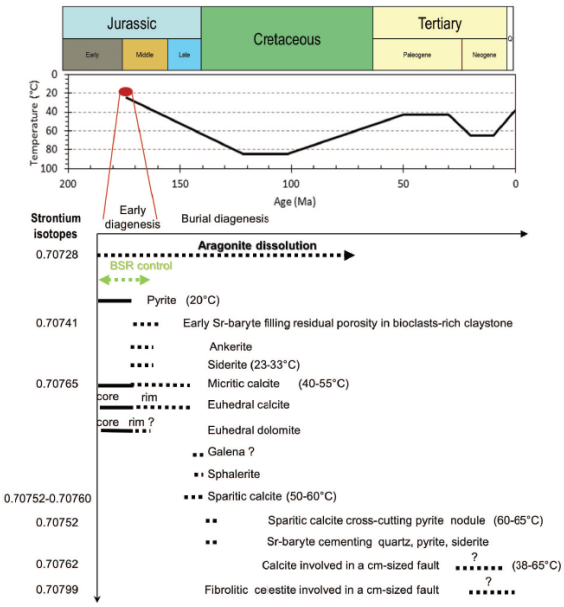

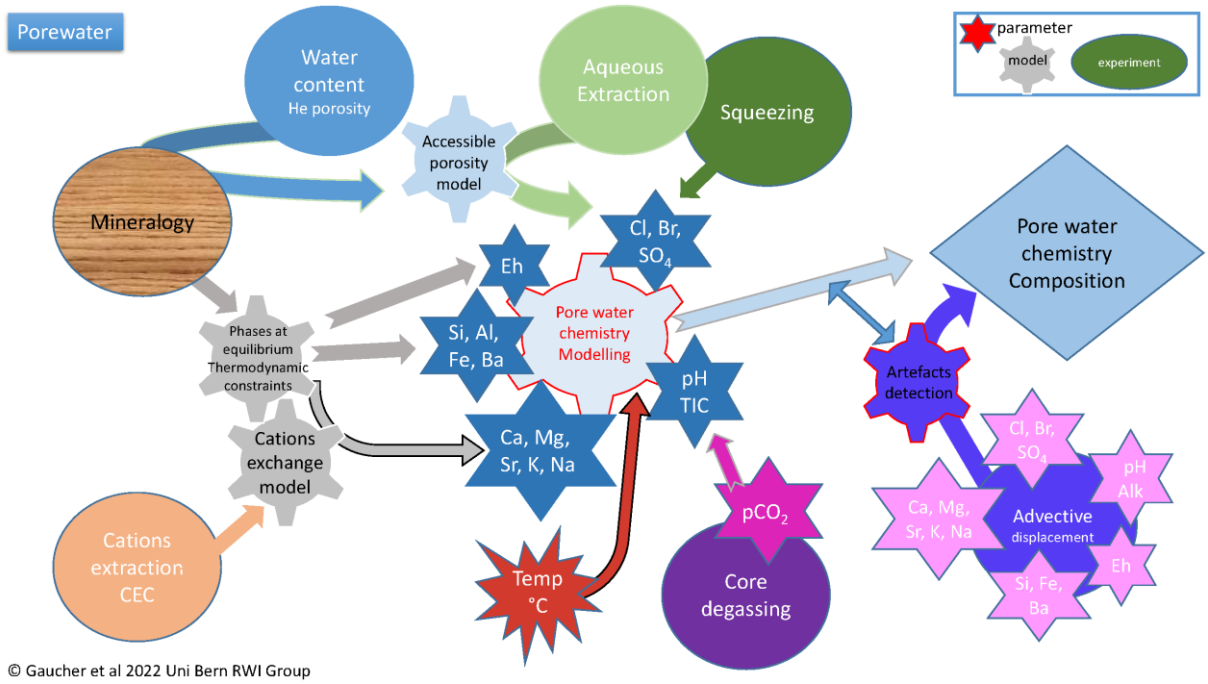

Squeezing experiment

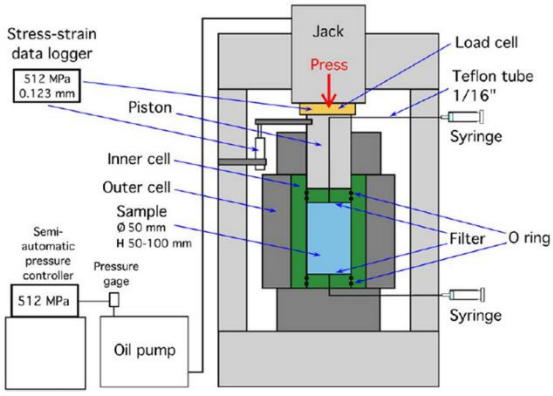

Deviation of chloride concentrations at high squeezing pressures

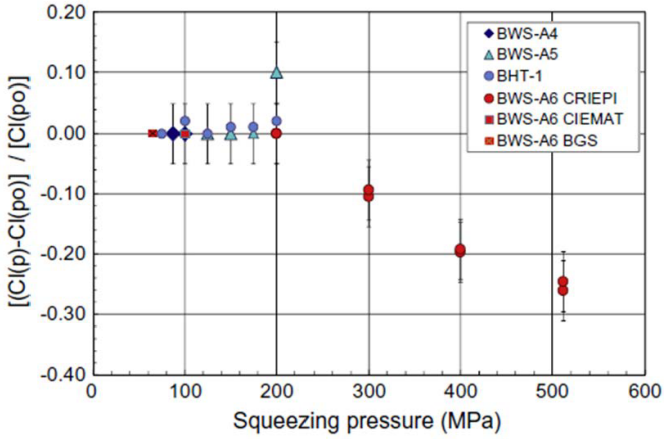

Artifacts with Squeezing experiment

Mazurek, M., Oyama, T., Wersin, P. and Alt-Epping, P. (2015) Pore-water squeezing from indurated shales. Chem. Geol. 400, 106-121.

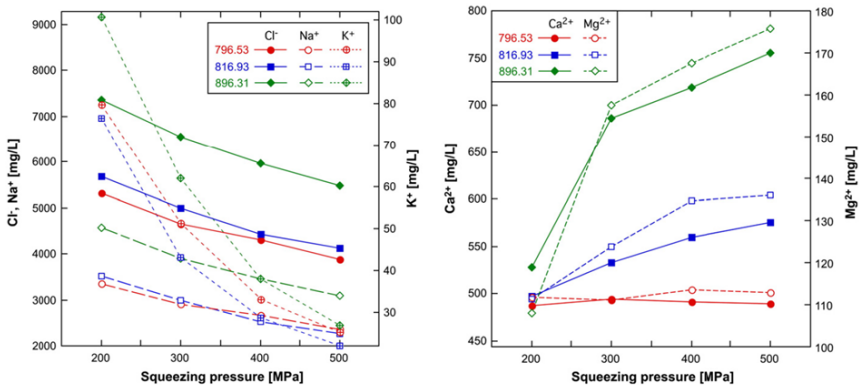

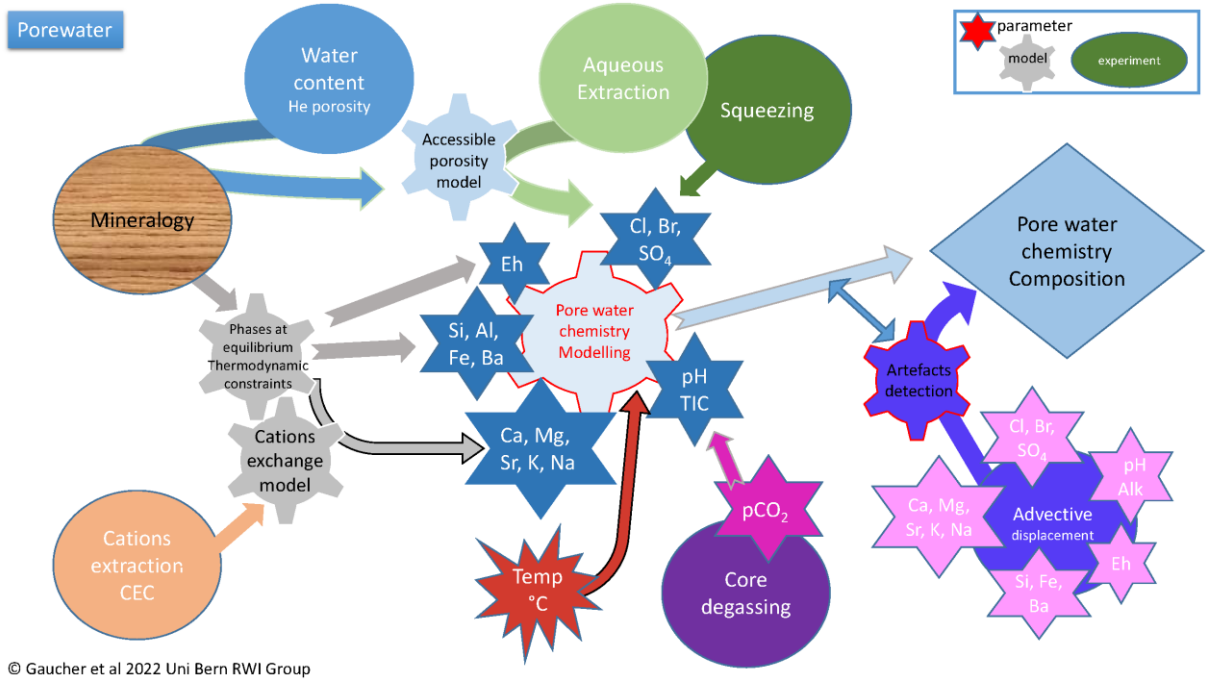

Advective displacement experiment

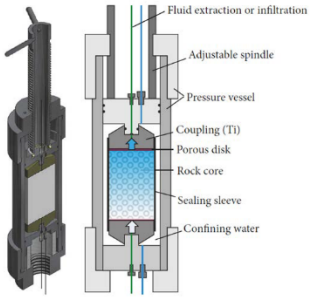

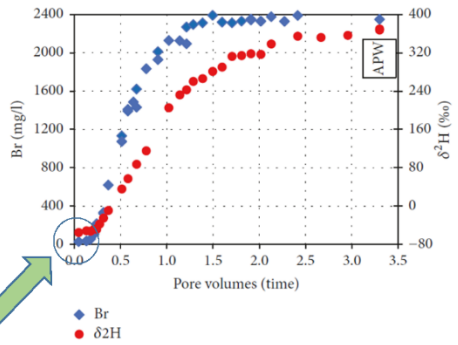

The first aliquots are representative of the PW

Global characterization of the chemistry of the PW

Breakthrough of Artificial PoreWater APW spiked with deuterated water and bromide versus time expressed as pore volume (water content) from Mäder, 2018

Mäder, U. (2018) Advective Displacement Method for the Characterisation of Pore Water Chemistry and Transport Properties in Claystone. Geofluids 2018, 8198762.

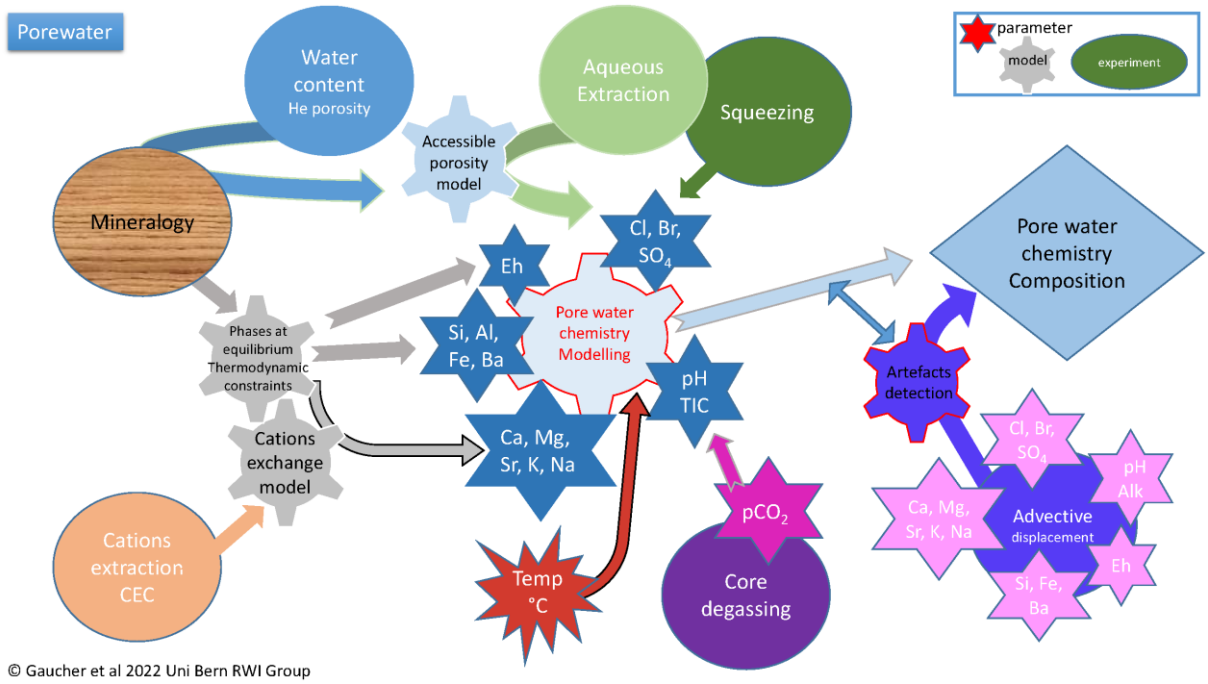

Cation Exchange Capacity (CEC) measurements + Cationic occupancy of the surface sites

Origin of the permanent basal charge in clays

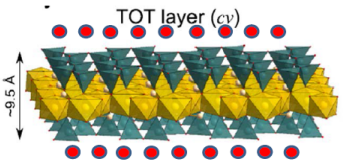

Smectite(MX80)
$Na_{0.409}K_{0.024}Ca_{0.009}(Si_{3.738}Al_{0.262})(Al_{1.598}Mg_{0.214}Fe_{0.208})O_{10}(OH)_2$

Montmorillonite-Na
$Na_x(Si_8)(Al_{4-x}Mg_x)O_{20}(OH)_4$ — Substitution of Al^{3+} by Mg^{2+}

Bedellite-Na
$Na_x(Si_{8-x}Al_x)(Al_4)O_{20}(OH)_4$ — Substitution of Si^{4+} by Al^{3+}

Nontronite-Na
$Na_x(Si_{8-x}Al_x)(Fe_4)O_{20}(OH)_4$ — Substitution of Si^{4+} by Al^{3+}

Experiment with Ni-ethylenediamine
$X_2Ca + [(Ni(en)_3]^{2+} \Leftrightarrow X_2[(Ni(en)_3] + Ca^{2+}$

Ion exchange equilibria

Homovalent exchange

$Na^+ + K\text{-}X \Leftrightarrow Na\text{-}X + K^+$

$$K_{Na/K} = \frac{a_{Na-X}\, a_{K^+}}{a_{K-X}\, a_{Na^+}}$$

Heterovalent exchange

$2\,Na^+ + Ca\text{-}X2 \Leftrightarrow 2\,Na\text{-}X + Ca^{2+}$

$$K_{Na/Ca} = \frac{(a_{Na-X})2\, a_{Ca^{2+}}}{a_{Ca-X2}(a_{Na^+})2}$$

Replace activities of exchanger species by equivalent fractions (meq/CEC)

$$[Na-X] = \beta_{Na\_X} = \frac{meq(Na-X)}{CEC} \quad \text{and} \quad CEC = \Sigma meq_i$$

$$K^{G-T}_{Na/K} = \frac{[Na-X]}{[K-X]}\frac{a_{K^+}}{a_{Na^+}} \qquad K^{G-T}_{Na/Ca} = \frac{[Na-X]^2}{[Ca-X_2]}\frac{a_{Ca^{2+}}}{(a_{Na^+})^2}$$

G-T: Gaines-Thomas convention

Ion exchange – selectivity coefficients

Equation: $Na^+ + 1/i\, I\text{-}X_i \leftrightarrow Na\text{-}X + 1/i\, I^{i+}$ with $K_{Na\backslash I} = \frac{[Na\text{-}X]\,[I^{i+}]^{1/i}}{[I\text{-}X_i]^{1/i}\,[Na^+]} = \frac{\beta_{Na}\,[I^{i+}]^{1/i}}{\beta_I^{1/i}\,[Na^+]}$

Ion I^+	$K_{Na\backslash I}$	Ion I^{2+}	$K_{Na\backslash I}$	Ion I^{3+}	$K_{Na\backslash I}$
Li^+	1.2 (0.95-1.2)	Mg^{2+}	0.50 (0.4-0.6)	Al^{3+}	0.6 (0.5-0.9)
K^+	0.20 (0.15-0.25)	Ca^{2+}	0.40 (0.3-0.6)	Fe^{3+}	?
NH_4^+	0.25 (0.2-0.3)	Sr^{2+}	0.35 (0.3-0.6)		
Rb^+	0.10	Ba^{2+}	0.35 (0.2-0.5)		
Cs^+	0.08	Mn^{2+}	0.55		
		Fe^{2+}	0.6		
		Co^{2+}	0.6		
		Ni^{2+}	0.5		
		Cu^{2+}	0.5		
		Zn^{2+}	0.4 (0.3-0.6)		
		Cd^{2+}	0.4 (0.3-0.6)		
		Pb^{2+}	0.3		

Selectivity coefficients relative to Na^+ (Gaines-Thomas convention), Appelo & Postma (1993)

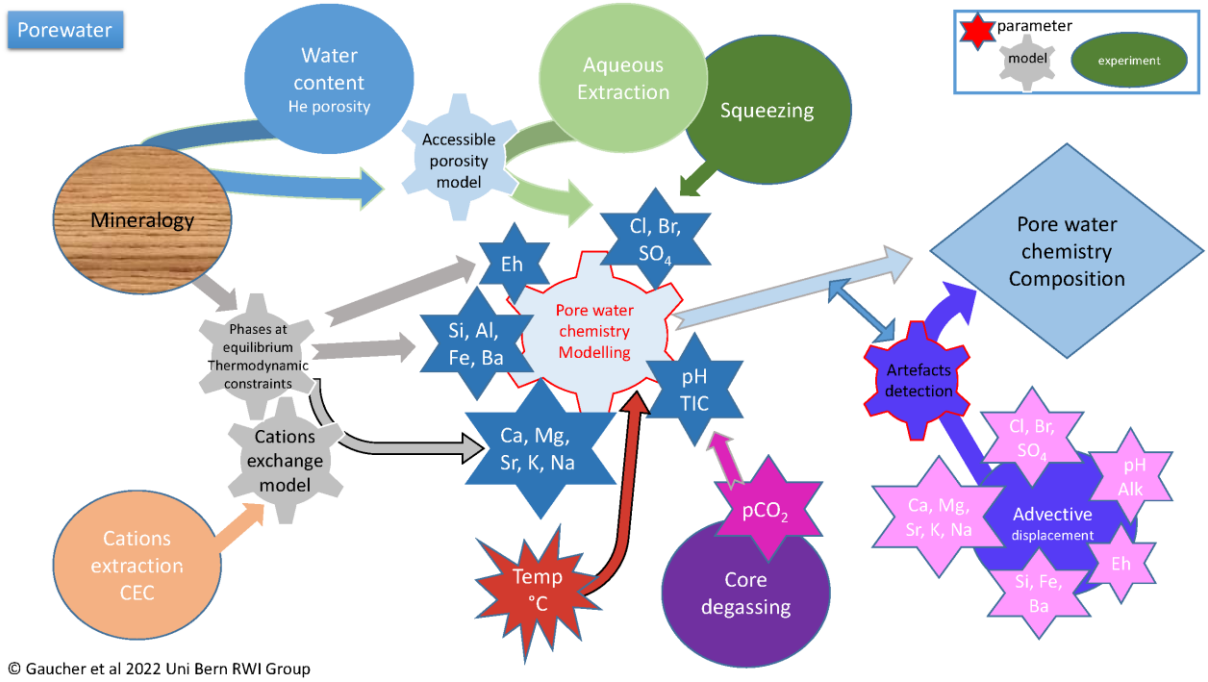

PCO_2 measure => a way to control the carbonate system and the pH

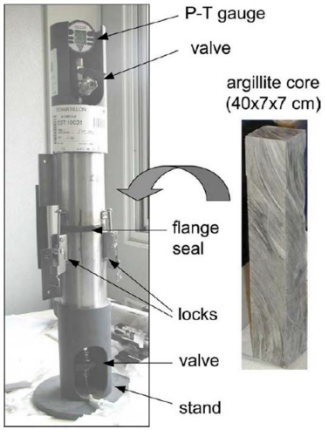

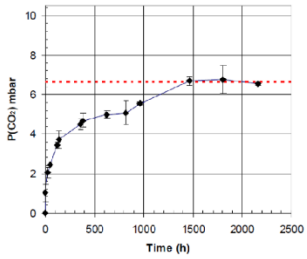

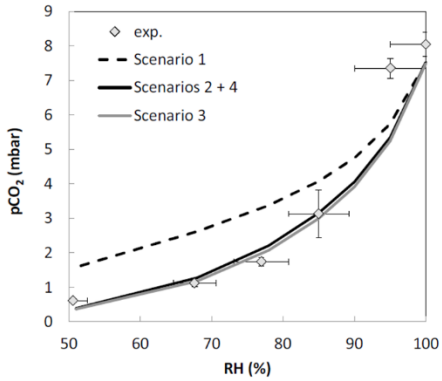

Evolution of the partial pressure of CO_2 as a function of the relative humidity. Symbols are experimental data and lines are various model calculations (From Lassin et al., 2016)

PCO_2 measure

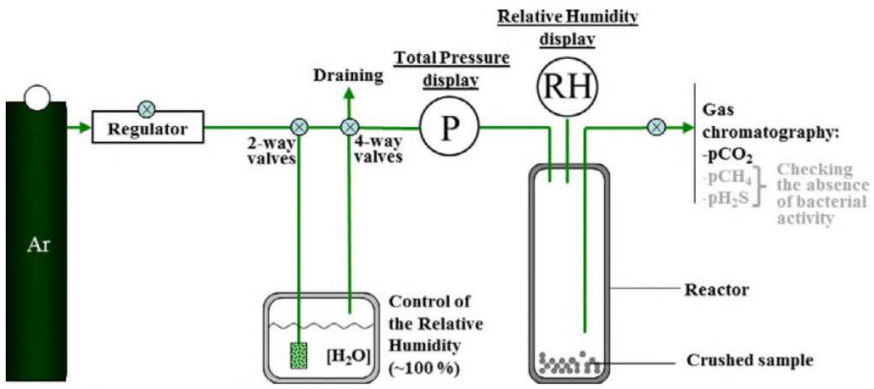

Example of experimental set up for pCO_2 measurement at a known relative humidity (from Lassin et al., 2016)

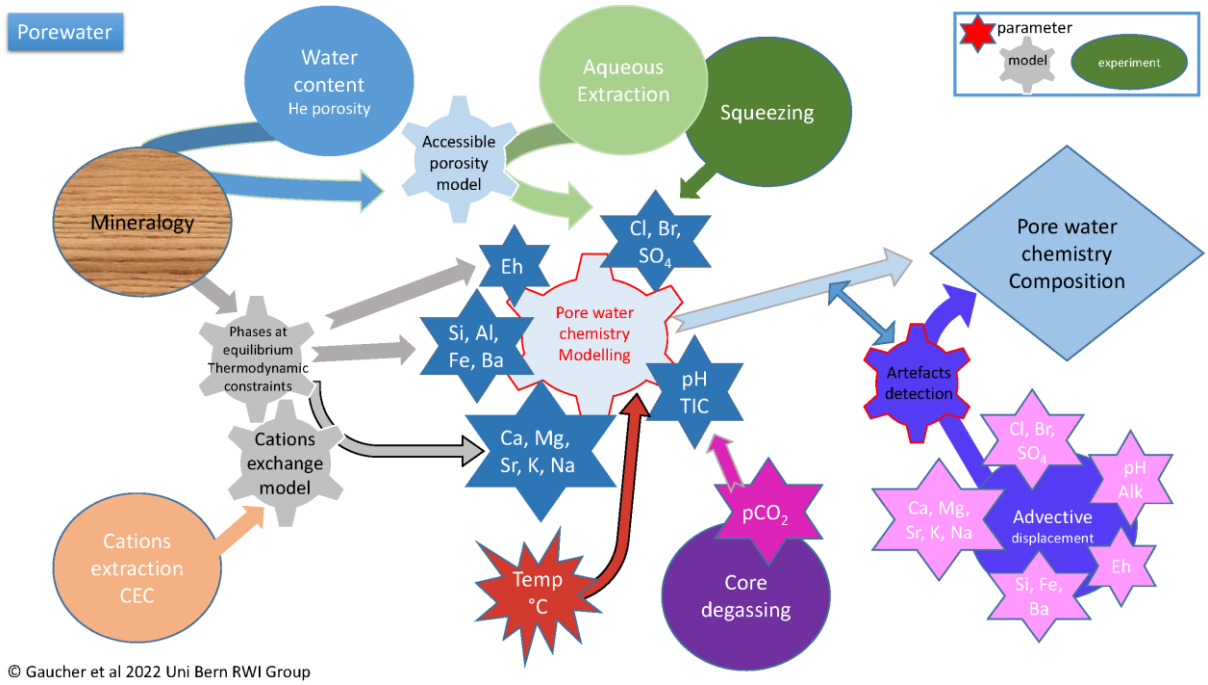

Modeling with the phase rule

The number of phases is equal to the number of components.
If we want to know the concentrations of Na, K, Mg, Ca, Sr, C, S, Cl, Br, Al, Si, Fe with the Eh and the pH, we should have 14 constraints for 14 elements

The conservative tracers, Cl^- and Br^- are fixed (AqEx, AD, SQ).

Knowing the relative occupancy of the cations on the clay surface (CEC Experiment) and choosing a selectivity coefficient for each exchange reaction allows calculating the concentration in solutions of the major cations (Na, K, Ca, Mg, Sr). Na, K, Mg, Ca, Sr are interdependent and knowing one constraint (Na concentration) is enough to calculate the other concentrations.

To constrain 8 parameters (Na, C, S, Al, Si, Fe, Eh and pH), 8 phases are required. In the model of Gaucher et al., 2009 (or Pearson et al., 2011, Tremosa et al., 2012) theses phases are: water, calcite, celestite, illite, quartz, siderite, pyrite, chlorite.

Control tests can be made. It is possible to compare the modelled pCO_2 to the values obtained by the core degassing. Dolomite should be also at equilibrium.

Modeling

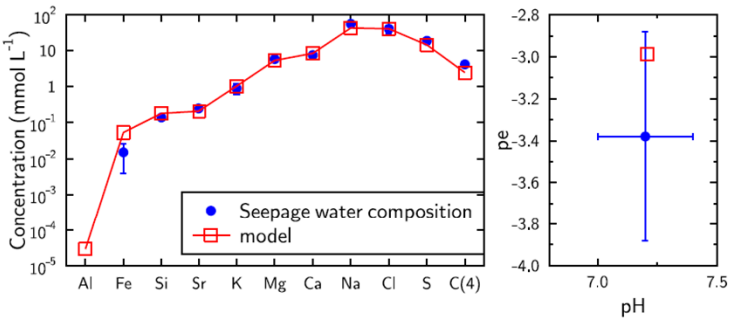

Example of fully constrained porewater model in the system pH, pe, Na, K, Mg, Ca, Sr, C, S, Cl, Al, Si, Fe, (COx, Bure, France) after Gaucher et al., 2009

Phreeqc Modeling

```
SELECTED_OUTPUT
-file Appendix 2.prn
-reset false
-pH true
-pe true
-totals Cl S(6) Na K Ca Mg Fe Sr
-molalities CoxNa CoxK Cox2Ca Cox2Mg Cox2Sr Cox2Fe

EXCHANGE_MASTER_SPECIES

Cox Cox-

EXCHANGE_SPECIES

Cox- = Cox-
log_k 0

Cox- + Na+ = CoxNa
log_k 0

Cox- + K+ = CoxK
log_k 1.2

2 Cox- + Ca+2 = Cox2Ca
log_k 0.7

2 Cox- + Mg+2 = Cox2Mg
log_k 0.7

2 Cox- + Fe+2 = Cox2Fe
log_k 0.8

2 Cox- + Sr+2 = Cox2Sr
log_k 0.6
```

```
#####################################
# First calculation block: preequilibration
#####################################
SOLUTION 1
pe -1
Na 150 charge
Cl 41
S(6) 66
EXCHANGE 1
CoxNa 108.24
CoxK 41.7
Cox2Ca 154.9
Cox2Mg 60.2
Cox2Fe 1.2
Cox2Sr 7.37
SAVE SOLUTION 1
END

#####################################
# Second calculation block: equilibration with celestite
#####################################

USE SOLUTION 1
EXCHANGE 2
CoxNa 1.0824
CoxK 0.417
Cox2Ca 1.549
Cox2Mg 0.602
Cox2Fe 0.012
Cox2Sr 0.0737
EQUILIBRIUM_PHASES 2
Celestite 0 0
END
```

```
#######################################
# Third calculation block: equilibration with COX mineralogy:
# Daphnite_14A / Illite-Mg case
#######################################

USE SOLUTION 2
USE EXCHANGE 2
EQUILIBRIUM_PHASES 3
Celestite 0 1
Calcite 0 1
Quartz,alpha 0 1
Pyrite  0 1
Daphnite_14A 0 1
Illite-Mg  0 1
END

#######################################
# Fourth calculation block: equilibration with COX mineralogy:
# Chlorite_Cca-2 / Illite-Mg case
#######################################

USE SOLUTION 2
USE EXCHANGE 2
EQUILIBRIUM_PHASES 4
Celestite 0 1
Calcite 0 1
Dolomite 0 1
Siderite 0 1
Quartz,alpha 0 1
Pyrite  0 1
Chlorite_Cca-2 0 1
Illite-Mg  0 1
END

#######################################
```

```
#######################################
# Fifth calculation block: equilibration with COX mineralogy:
# Chlorite_Cca-2 / Illite_IMt-2 case
#######################################

USE SOLUTION 2
USE EXCHANGE 2
EQUILIBRIUM_PHASES 5
Celestite 0 1
Calcite 0 1
Dolomite 0 1
Siderite 0 1
Quartz,alpha 0 1
Pyrite  0 1
Chlorite_Cca-2 0 1
Illite_IMt-2  0 1
END

#######################################
# Sixth calculation block: equilibration with COX mineralogy:
# Daphnite_14A / Illite_IMt-2 case
#######################################

USE SOLUTION 2
USE EXCHANGE 2
EQUILIBRIUM_PHASES 5
Celestite 0 1
Calcite 0 1
Dolomite 0 1
Siderite 0 1
Quartz,alpha 0 1
Pyrite  0 1
Daphnite_14A 0 1
Illite_IMt-2  0 1
SAVE SOLUTION 2
END
```

> Take Home message

— The combination of proven experiments provides a data set that can be used in numerical modeling.
— The numerical modeling is based on thermodynamic constraints including ion exchange reactions.
— Comparison with underground laboratory data shows the robustness of the modeling.
— The numerical model of the intact host rock can be used to calculate chemical disturbance and radionuclide transport.

References

Gaucher, E.C., Tournassat, C., Pearson, F., Blanc, P., Crouzet, C., Lerouge, C. and Altmann, S. (2009) A robust model for pore-water chemistry of clayrock. Geochimica et Cosmochimica Acta 73, 6470-6487.

Lassin, A., Marty, N.C., Gailhanou, H., Henry, B., Trémosa, J., Lerouge, C., Madé, B., Altmann, S. and Gaucher, E.C. (2016) Equilibrium partial pressure of CO_2 in Callovian–Oxfordian argillite as a function of relative humidity: Experiments and modelling. Geochimica et Cosmochimica Acta 186, 91-104.

Pearson, F., Tournassat, C. and Gaucher, E.C. (2011) Biogeochemical processes in a clay formation in situ experiment: Part E–Equilibrium controls on chemistry of pore water from the Opalinus Clay, Mont Terri Underground Research Laboratory, Switzerland. Applied geochemistry 26, 990-1008.

Tournassat, C., Vinsot, A., Gaucher, E.C. and Altmann, S. (2015) Chemical conditions in clay-rocks, Developments in clay science. Elsevier, pp. 71-100.

Wersin, P., Mazurek, M., Gimmi, T (2022) Porewater chemistry of Opalinus Clay revisited: Findings from 25 years of data collection at the Mont Terri Rock Laboratory. Applied Geochemistrythis, 138, 105234.

3.4 Lecture 4 - Reactive Transport – Pore to Continuum scale

Reactive transport in the Earth and Environmental Sciences is at a crossroads today. The discipline has reached a level of maturity well beyond what could be demonstrated even 15 years ago. This is shown now by the successes with which complex and in many cases coupled behavior have been described in a number of natural Earth environments, ranging from corroding storage tanks leaking radioactive Cs into the vadose zone (Steefel et al. 2003), to field scale sorption behavior of uranium (Li et al. 2011) to the successful prediction of mineral and pore solution profiles in a 226 ka chemical weathering profile (Maher et al. 2009), to the prediction of ion transport in compacted bentonite and clay rocks (Tournassat and Steefel 2015; Tournassat and Steefel, 2019; Steefel and Tournassat, 2021).
So, is the "reactive transport problem" solved? Where do we go from here? This is the crossroads we are at now as we decide what are the challenges that need to be faced so as to continue advancing the field. Arguably the most significant challenges we now face are associated with the huge range of length scales that need to be addressed, since these extend from the molecular to nanoscale to pore scale all the way up to the watershed and continental scale. Across this extreme range of scales, the constitutive equations and parameters that are used to describe reactive transport processes often change as well, thus requiring mathematical and numerical models to become "scale aware". Charged porous media offers special challenges, since ion mobility can be strongly affected by electrostatic interactions, and this can lead to effects such as anion exclusion that are not captured by Fick's Law (Tournassat and Steefel 2015; Tournassat and Steefel, 2019). Where the charged porous media involves nanoscale porosity, off-diagonal coupling effects on transport between such master variables as fluid pressure, electrical current and chemical composition may become important (Tournassat and Steefel 2019: Steefel and Tournassat, 2021). At the watershed and continental scales, reactive transport is further complicated by the coupling with diverse Earth surface processes, including subsurface and surface water, vegetation, and the atmosphere, all played out typically in highly heterogeneous and transient settings. Interest has also increased in the effects of geomechanics on reactive transport ("chemo-mechanical effects), of which pressure solution is one of the examples (Hu et al., 2021).

Lecturer

Carl I. Steefel, Lawrence Berkeley National Laboratory, United States

Reading Material

Steelel C.I and M Hu (2022) Reactive transport modeling of mineral precipitation and carbon trapping in discrete fracture networks. *Water Resources Research*. DOI: 10.1029/2022WR032321

Hu, M. C.I. Steefel, J.R. Rutqvist (2021) Microscale mechanical-chemical modeling of granular salt: Insights for creep. *Journal of Geophysical Research Solid Earth*. doi: 10.1029/2021JB023112

Steefel, C.I. and Yang, L. (2021) Secondary magnesite formation from forsterite under CO_2 sequestration conditions via coupled heterogeneous nucleation and crystal growth. *Geochimica et Cosmochimica Acta* 311: 29.42.

Steefel, C.I. and C. Tournassat (2021) A model for discrete fracture-clay rock interaction incorporating electrostatic effects on transport. *Computational Geosciences* 25 (1): 395-410. DOI: 10.1007/s10596-020-10012-3.

Steefel, C.I. (2019) Reactive transport at the crossroads. *Reviews in Mineralogy and Geochemistry* 85: 1-26.

Tournassat, C.M., Steefel, C.I. (2019) Reactive transport modeling of coupled processes in nanoporous media. *Reviews in Mineralogy and Geochemistry* 85: 75-109.

Tournassat, C., C.I Steefel (2015) Ionic transport in nano-porous clays with consideration of electrostatic effects. *Reviews in Mineralogy and Geochemistry* 80: 287-329.

Steefel, C.I., S.B. Yabusaki, K.U. Mayer (2015) Reactive transport benchmarks for subsurface environmental simulation. *Computational Geosciences* 19: 439-443. DOI: 10.1007/s10596-015-9499-2.

Steefel, C.I., Appelo, C.A.J., Arora, B., Jacques, D., Kalbacher, T., Kolditz, O., Lagneau, V., Lichtner, P.C., Mayer, K.U., Meeussen, J.C.L. and Molins, S., 2015. Reactive transport codes for subsurface environmental simulation. Computational Geosciences, 19(3), pp.445-478.

Molins, S., D. Trebotich, C. I. Steefel, and C. Shen (2012) An investigation of the effect of pore scale flow on average geochemical reaction rates using direct numerical simulation. *Water Resources Research* 48, W03527, DOI:10.1029/2011WR011404.

Steefel, C.I., K. Maher, 2009, Fluid-rock interaction: A reactive transport approach. *Reviews in Mineralogy and Geochemistry* 70: 485-532, DOI: 10.2138/rmg.2009.70.11.

Maher, K., C.I. Steefel, A.F. White, and D.A. Stonestrom, 2009, The role of reaction affinity and secondary minerals in regulating chemical weathering rates at the Santa Cruz Soil Chronosequence, California, *Geochim. Cosmochim. Acta*, 73, 2804–2831.

Li, L., C.I. Steefel, L. Yang, 2008, Scale dependence of mineral dissolution rates within single pores and fractures, *Geochimica Cosmochimica Acta* 72(2), 360-377.

Steefel, C.I, D. DePaolo, and P.C. Lichtner, 2005, Reactive transport modeling: An essential tool and a new research approach for the Earth sciences, *Earth and Planetary Science Letters* 240: 539-558.

Steefel, C.I., Carroll, S., Zhao, P., and Roberts, S. (2003), Cesium migration in Hanford sediment: A multi-site cation exchange model based on laboratory transport experiments. *J. of Contaminant Hydrology* 67, 219-246.

Steefel, C.I. and Van Cappellen, P.C. (1998) Reactive transport modeling of natural systems. *J. Hydrology* 209, 1-7.

Steefel, C.I. and Lichtner, P.C. (1998) Multicomponent reactive transport in discrete fractures: I. Controls on reaction front geometry. *J. Hydrology* 209, 186-199.

Steefel, C.I. and Lichtner, P.C. (1998) Multicomponent reactive transport in discrete fractures: II. Infiltration of hyperalkaline groundwater at Maqarin, Jordan, a natural analogue site. *J. Hydrology* 209, 200-224.

Steefel, C.I. and MacQuarrie, K.T.B. (1996) Approaches to modeling reactive transport in porous media. In Reactive Transport in Porous Media (P.C. Lichtner, C.I. Steefel, and E.H. Oelkers, eds.), *Reviews in Mineral*ogy 34, 83-125. DOI: 10.1515/9781501509797-005

Steefel, C.I., and Lasaga, A.C. (1994) A coupled model for transport of multiple chemical species and kinetic precipitation/dissolution reactions with application to reactive flow in single phase hydrothermal systems. *American Journal of Science* 294, 529-592.

Steefel, C.I., and Lichtner, P.C. (1994) Diffusion and reaction in rock matrix bordering a hyperalkaline fluid-filled fracture. *Geochimica et Cosmochimica Acta* 58, 3592-3612.

Steefel, C.I. and Van Cappellen, P. (1990) A new kinetic approach to modeling water-rock interaction: The role of nucleation, precursors, and Ostwald ripening. *Geochimica et Cosmochimica Acta*, 54, 2657-2677.

Slides

Energy Geosciences
EARTH & ENVIRONMENTAL SCIENCES AREA

Eurad Training

Reactive Transport: Pore to Continuum Scales

Carl Steefel
Lawrence Berkeley National Laboratory

February 7, 2023

BERKELEY LAB

U.S. DEPARTMENT OF ENERGY | Office of Science

2

Coupled Processes and Scales

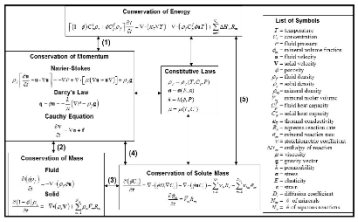

Coupled Processes

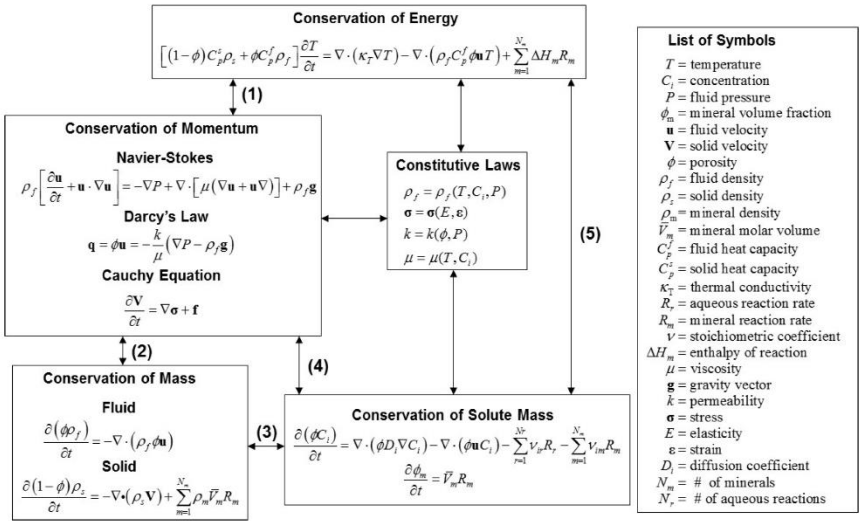

Steefel, DePaolo, & Lichtner, 2005

4

Challenge of Multiscale in Earth and Environmental Sciences

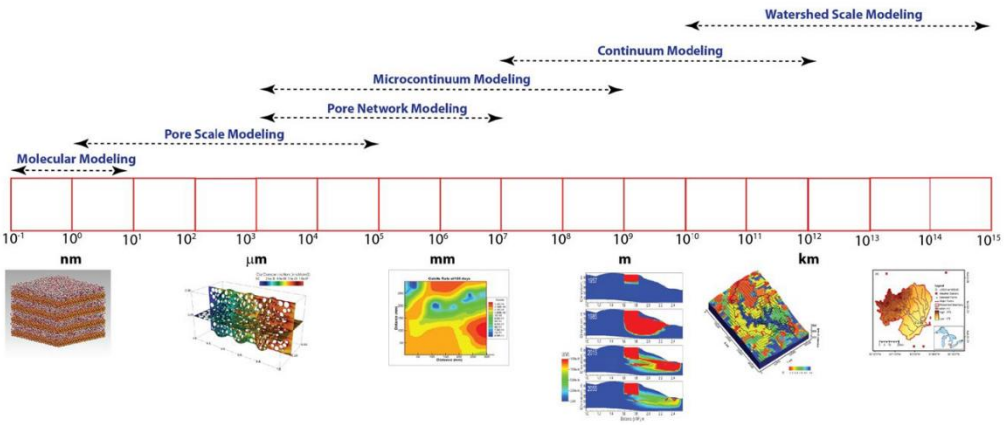

Pore to Continuum Scale

- Continuum models
  - Solid, liquid, and gas all coexist in space within REV
  - Reactions treated as if taking place throughout control volume
  - Fluid phase is well mixed (no gradients in concentration or rate)
- Pore scale models
  - Solid, gas, and liquid interfaces resolved
  - Gradients in concentration and reaction rate can develop

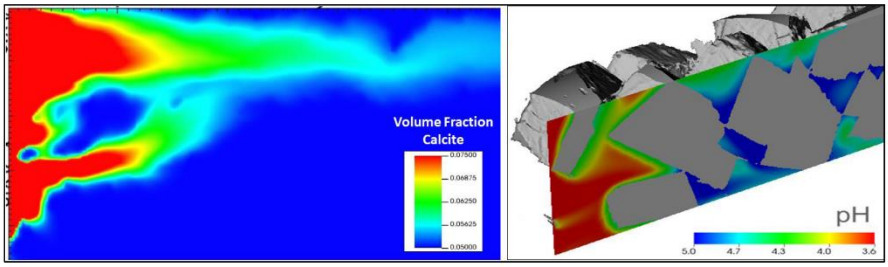

Steefel, 2019

Equations: Pore to Continuum Scale

	Pore Scale	Continuum or Darcy Scale
Flow	$\frac{\partial \boldsymbol{u}}{\partial t} + (\boldsymbol{u} \cdot \nabla)\boldsymbol{u} + \nabla p = \nu \Delta \boldsymbol{u}$ $\nabla \cdot \boldsymbol{u} = 0$	$\boldsymbol{q} = -\frac{\boldsymbol{k}}{\mu} \nabla p$ $\nabla \cdot (\boldsymbol{k} \nabla p) = 0$
Transport	$\frac{\partial c}{\partial t} = \nabla \cdot (D \nabla c) - \nabla \cdot (\boldsymbol{u} c)$	$\boldsymbol{\theta} \frac{\partial c}{\partial t} = \nabla \cdot (\mathcal{D} \nabla c) - \nabla \cdot (\boldsymbol{q} c)$ *where* $\mathcal{D} = \boldsymbol{\theta} \boldsymbol{\tau} D + \boldsymbol{\alpha}_L \lvert \boldsymbol{u} \rvert$
Reaction	$-D \nabla c \cdot \boldsymbol{n} = k\, f(\boldsymbol{c})$	$r = k\, \boldsymbol{A}\, f(\boldsymbol{c})$

Pore Scale Approaches

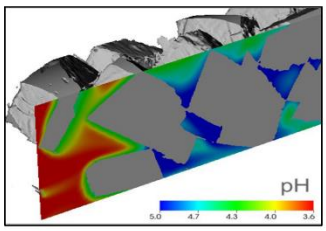

Direct Numerical Simulation of Pore Scale Reactive Transport

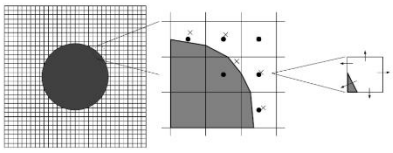

- Sharp interface resolution with Embedded Boundary (EB) method
- Fixed time divergence theorem for conservative discretization of fluxes

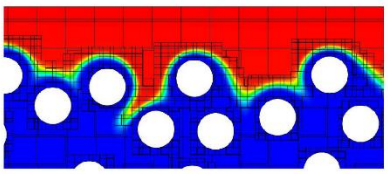

Adaptive mesh refinement (AMR)

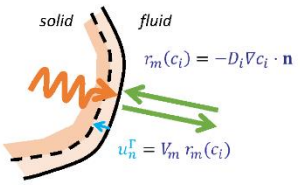

Direct resolution of reactive interfaces

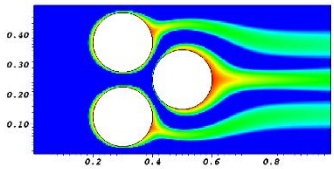

Moving reactive interphases influenced by Navier-Stokes flow and diffusion

Molins et al, 2014; Trebotich et al, 2014

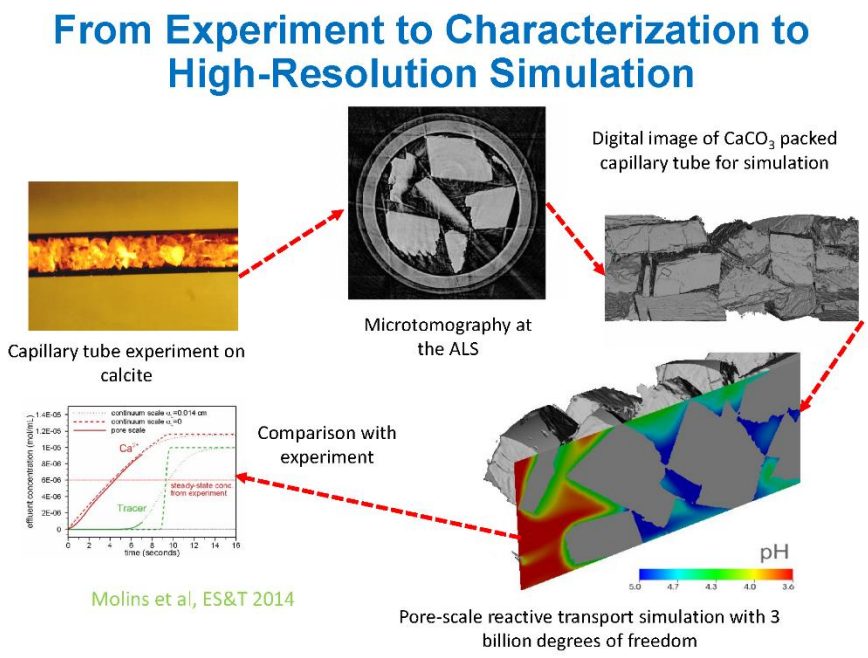

Fracture Evolution in the Duperow Dolomite

High resolution pore scale model showing mineral dissolution and wormholing

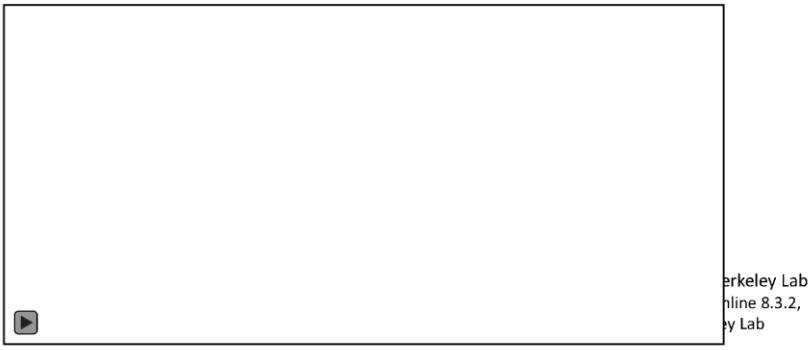

$scCO_2$ saturated brine injected into fracture from left side

Microscale MC Modeling of Granular Salt Creep

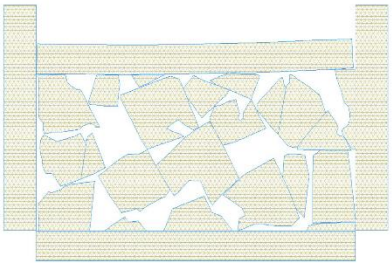

Geometry of the halite grains after pressure solution

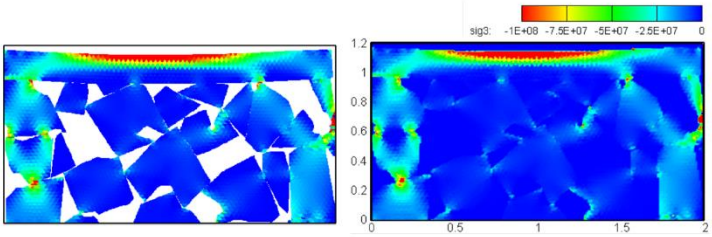

Minimum principal stress after reaching equilibrium of compaction induced by pressure solution

(Hu, Steefel, and Rutqvist, 2021)

11

Thermodynamic-Kinetic Model for Pressure Solution

1. Assume that thermodynamic pressure is approximately equal to the minimum principal stress
2. Include dependence of Gibbs free energy on pressure

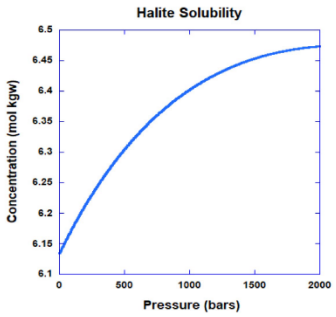

Solubility as a function of pressure (Anderson, 2005):

$$\ln K_P = \ln K_{P=1} - \Delta V_r \left(\frac{P-1}{RT}\right)$$

Helgeson–Kirkham–Flowers-modified-Redlich–Rosenfeld (HKFmoRR) to calculate partial molar volumes as function of pressure and temperature (Appelo et al, 2014)

$$\Delta V_r = \boxed{V_{m,Na^+} + V_{m,Cl^-}} - V_{Halite}$$

Calculated as function of pressure and ionic strength

Transition state theory (TST) rate law for the kinetics of halite (Alkattan et al, 1997):

$$r = -Ak\left(1 - \frac{Q}{K_P}\right)$$

Ion activity product:

$$Q = a_{Na^+}a_{Cl^-} = [\gamma_{Na^+}C_{Na^+}][\gamma_{Cl^-}C_{Cl^-}]$$

Reactive transport equations for Na+ and Cl-

$$\frac{\partial(\varphi C_{Na^+})}{\partial t} = \nabla \cdot (\varphi^m D_{Na^+}\nabla C_{Na^+}) - r$$

$$\frac{\partial(\varphi C_{Cl^-})}{\partial t} = \nabla \cdot (\varphi^m D_{Cl^-}\nabla C_{Cl^-}) - r$$

(Hu, Steefel, Rutqvist, 2021)

12

Stress Effects on Concentration

Minimum principal stress (Unit: Pa)

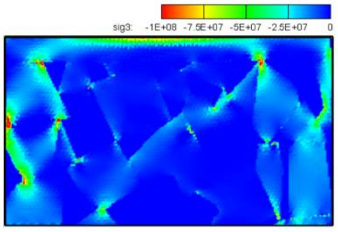

$$\ln K_{(P)} = \ln K_{(P=1)} - \Delta V_r \left(\frac{P-1}{RT} \right)$$

$$r = Ak \left(1 - \frac{Q}{K_{(P)}} \right)$$

Sodium concentration after 2 hours

Sodium concentration after 10,000 hours

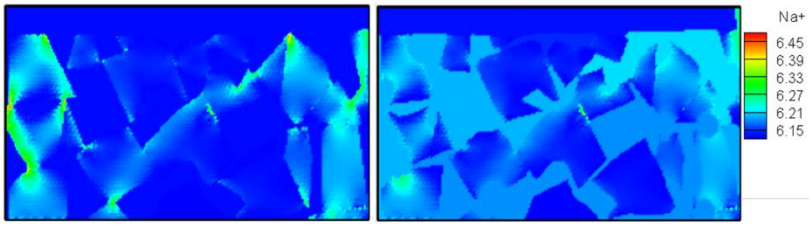

(Hu, Steefel, Rutqvist, 2021)

13

Pressure Solution within Halite Grain Pack

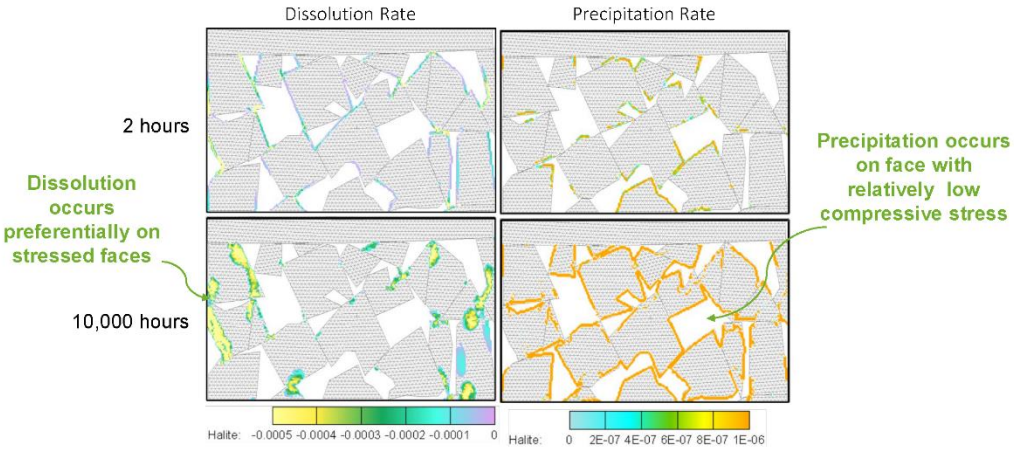

(Hu, Steefel, Rutqvist, 2021)

14

Micro-Continuum Approaches

Reviews in Mineralogy & Geochemistry
Vol. 80 pp. 217-246, 2015

7

Micro-Continuum Approaches for Modeling Pore-Scale Geochemical Processes

Carl I. Steefel and Lauren E. Beckingham
Earth Sciences Division
Lawrence Berkeley National Laboratory
Berkeley, California 94720, USA
cisteefel@lbl.gov

Gautier Landrot
Synchrotron SOLEIL
91192 Gif sur Yvette, France

INTRODUCTION

The recent profusion of microscopic characterization methods applicable to Earth Science materials, many of which are described in this volume (Anovitz and Cole 2015, this volume; Noiriel 2015, this volume), suggests that we now have an unprecedented new ability to consider geochemical processes at the pore scale. These new capabilities offer the potential for a paradigm shift in the Earth Sciences that will allow us to understand and ultimately quantify such enigmas as the apparent discrepancy between laboratory and field rates (White

Volume-Averaged Mineral Maps from Cranfield Pilot CO_2 Injection Site

Volume averaged over 16 µm² from 4 µm BSE data

Landrot et al, 2012;
Steefel et al., 2015

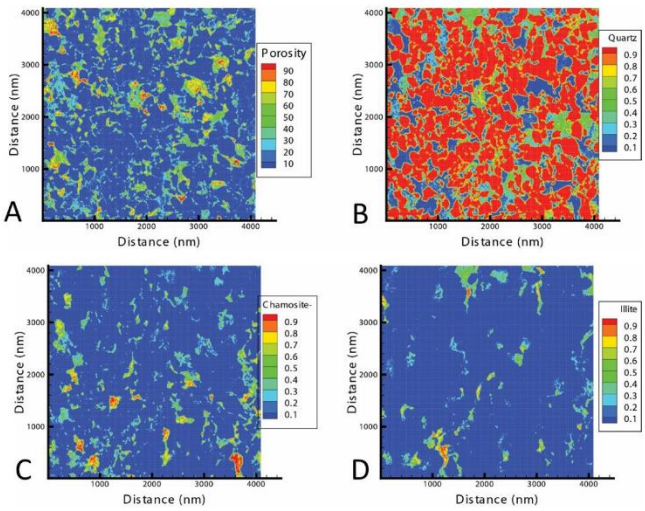

Micro-Continuum Modeling Approach

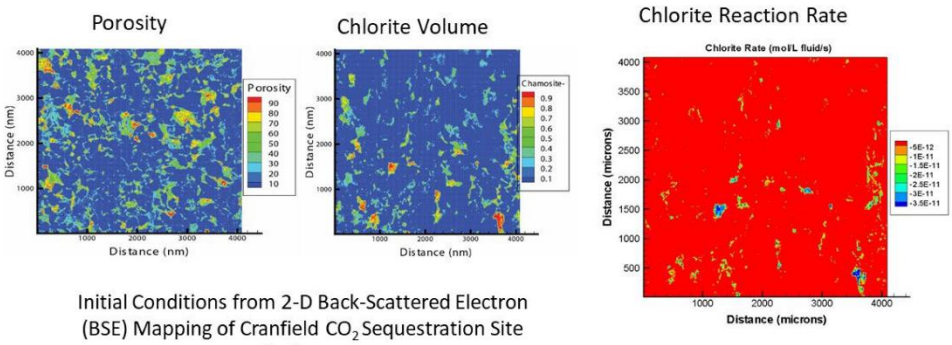

Initial Conditions from 2-D Back-Scattered Electron (BSE) Mapping of Cranfield CO_2 Sequestration Site Sediment

Combination of microscopic chemical mapping and micro-continuum modeling quantifies the reactivity in physically and chemically heterogeneous materials

Steefel et al., 2015

Reactivity of Sediments, Nagaoka Japan

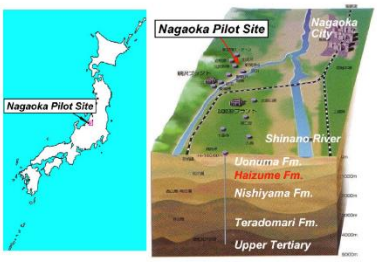

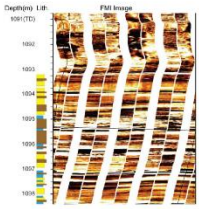

Haizume Formation
Predominantly sandstone
Thin layers of shales (siltstone to mudstone) interbedded within sandstone layers

Mineralogy (XRD)
Abundant quartz, plagioclase, K-feldspar, smectite and pyroxene

40 t CO_2/day, total of 10 kt CO_2 stored
CO_2 injection period: 7/2003 –1/2005

Injection depth = 1100 m
T = 48°C
P = 108 bars

k = 6 mD
Thickness = 60 m

2-D SEM-BSE & QEMSCAN of Nagaoka Sediment

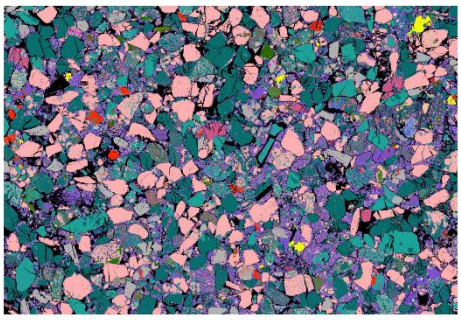

Mineral	(A) Abundance %	(B) Accessible % (all BSE pores)	(C) Accessible % (connected macro and micro pores)
Quartz	27.64	20.16	13.71
Plagioclase	22.65	19.48	14.54
Smectite	16.99	32.43	36.33
K-feldspar	13.38	8.06	6.87
Pyroxene	7.21	7.22	11.10
AlSitrap	2.74	1.63	3.73
Biotite	2.58	2.57	5.17
Amphibole	1.85	1.46	1.94
Others	1.41	2.44	2.65
Fe Hydroxide	1.22	1.07	0.82
Chlorite	1.17	1.34	1.31
Kaolinite	0.41	1.08	1.21
Pyrite	0.36	0.41	0.23
Serpentine	0.29	0.52	0.31
Ca-phosphate	0.07	0.08	0.06
Calcite	0.03	0.06	0.03

Sediment dominated by smectite, plagioclase, pyroxene + volcanic glass

Beckingham et al, 2016

Characterization Approach for Nagaoka Sediment

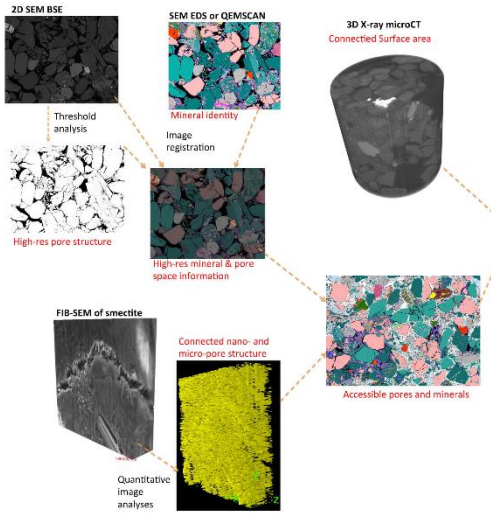

Mineral specific accessible surface area

Mineral	Accessible SA (m^2/g)
Quartz	9.95E-03
Plagioclase	1.06E-02
Smectite	9.23
K-feldspar	4.98E-03
Pyroxene	8.06E-03
AlSitrap	2.71E-03
Biotite	3.75E-03
Amphibole	1.41E-03
Others	1.92E-03
Fe Hydroxide	5.94E-04
Chlorite	9.49E-04
Kaolinite	8.79E-04
Pyrite	1.68E-04
Serpentine	2.26E-04
Ca-phosphate	4.02E-05
Calcite	2.14E-05

Beckingham et al, 2016, Geochimica

Nagaoka Experimental Approach

1. Disaggregated sediment experiments in well-stirred reactor
2. Compare with intact coreflood experiments (pore structure intact)

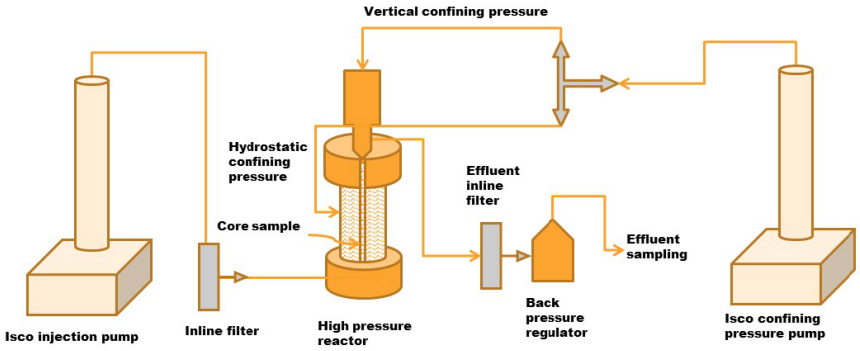

Disaggregated Sediment Experiment

Fit with mineral volume percentages from QEMSCAM Mapping—All grains accessible

Cation leaching (Ca+Na+K > SiO_2) in glass phase over first 300 hours

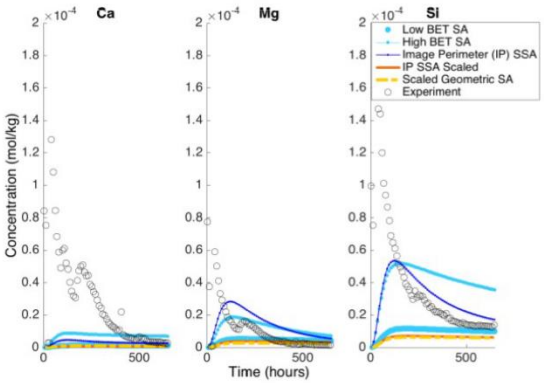

Including Grain Size Distribution and Glass

Grain Size Distribution

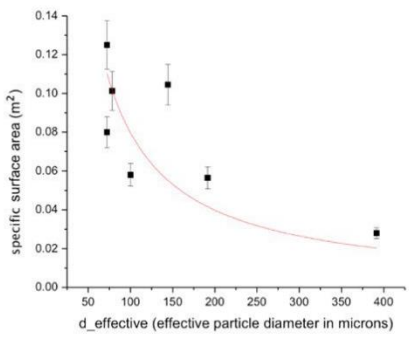

With and without glass phase

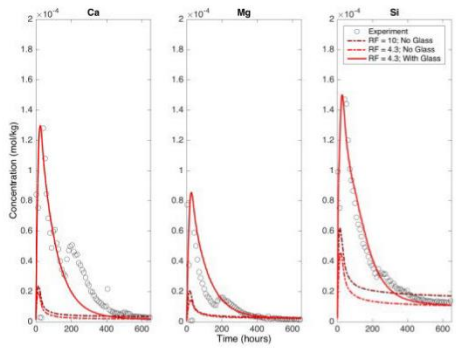

Core Modeling with Pore-Accessible Reactive Surface Area

<u>10x lower specific surface area</u> compared to disaggregated sediment

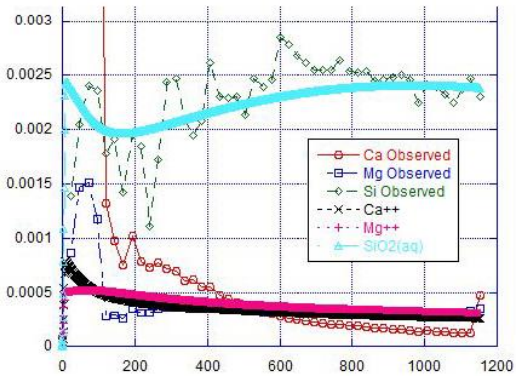

2

Earth's Critical Zone

3

Critical Zone

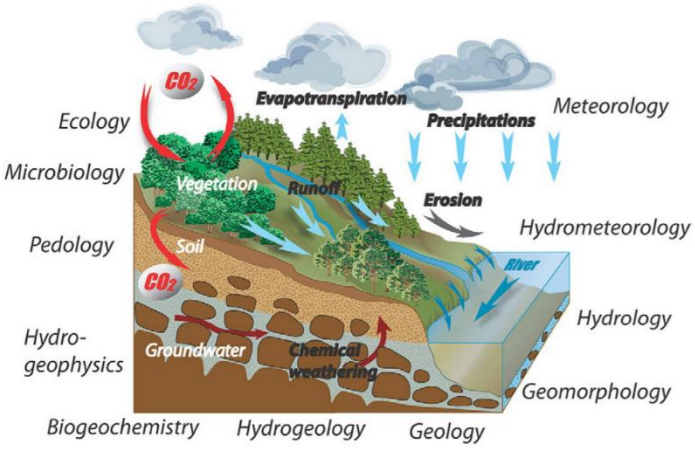

Earth's Critical Zone: Watershed Scale

Figure courtesy Erica Woodburn, LBNL

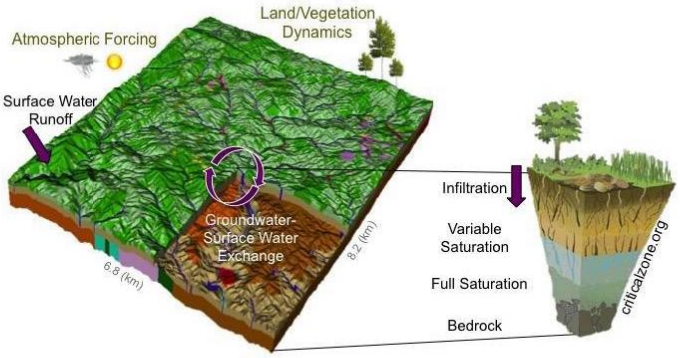

Figure courtesy SERC Carleton College

4

5

East River Watershed (Colorado)

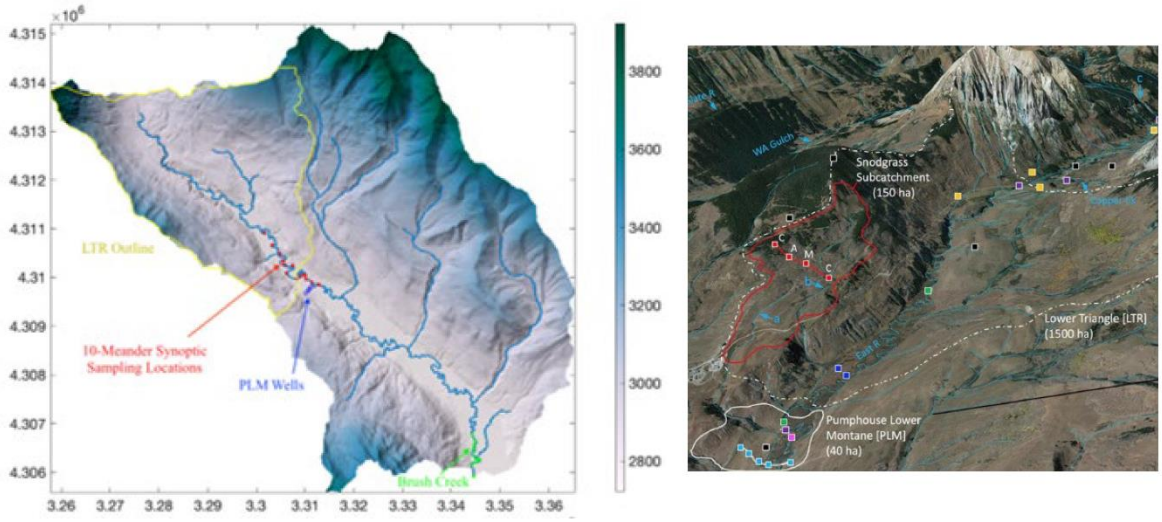

Watershed Function High Performance Computing

Computational Grid for Copper Creek, East River Watershed

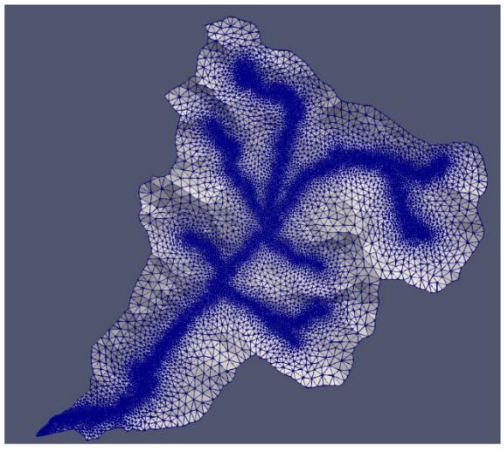

Calculated Ca Concentration in Dry Summer

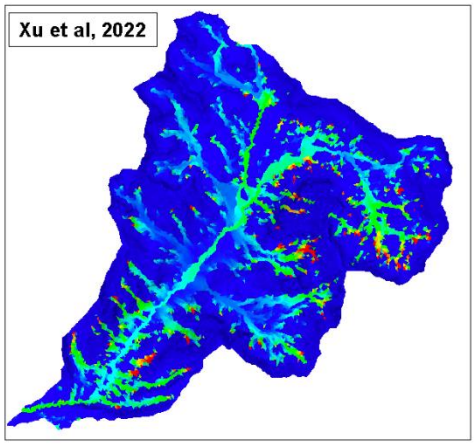

Southern Sierra Critical Zone Observatory

Ackerer, Steefel, et al, 2021

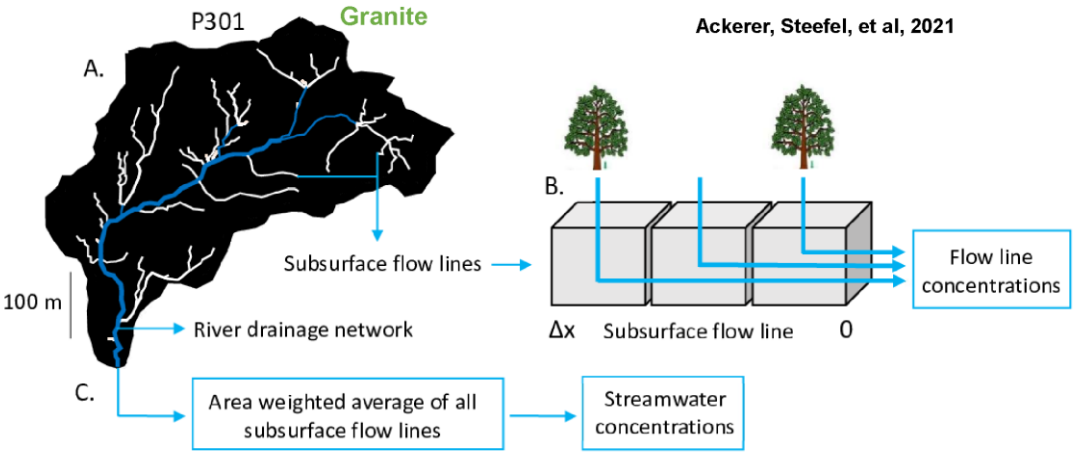

7

8

Chemical Weathering (and Negative Emissions)

9

CO_2 System

$$\underbrace{CO_2(g)}_{\text{Carbon Dioxide Gas}} \rightarrow \underbrace{CO_2(aq)}_{\text{Dissolved Carbon Dioxide}}$$

$$\underbrace{CO_2(aq)}_{\text{Dissolved Carbon Dioxide}} + H_2O \rightarrow \underbrace{H_2CO_3}_{\text{Carbonic Acid}}$$

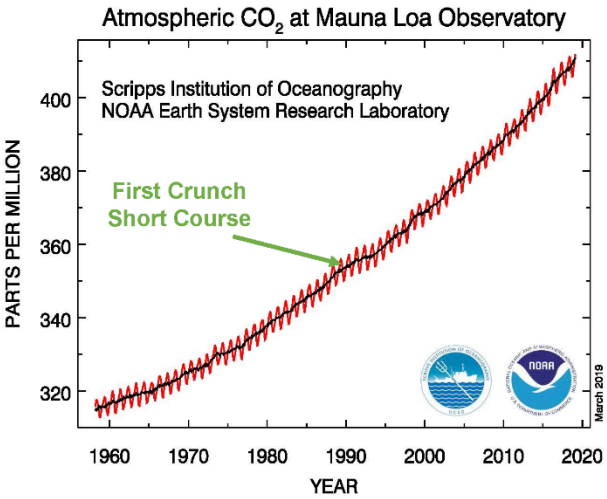

Chemical Weathering

$$\underbrace{CaAl_2Si_2O_8}_{\text{Feldspar}} + \underbrace{CO_2}_{\text{Carbon Dioxide}} + \underbrace{H^-}_{\text{Hydrogen Ion}} + 3\,H_2O \rightarrow$$

$$\underbrace{HCO_3^-}_{\text{Bicarbonate}} + \underbrace{Ca^{2+}}_{\text{Calcium Ion}} + \underbrace{2\,SiO_2}_{\text{Silica}} + \underbrace{2\,Al(OH)_3}_{\text{Aluminum Hydroxide}}$$

$$\underbrace{HCO_3^-}_{\text{Bicarbonate}} + \underbrace{Ca^{2+}}_{\text{Calcium Ion}} \rightarrow \underbrace{CaCO_3}_{\text{Calcite}} + \underbrace{H^+}_{\text{Hydrogen Ion}}$$

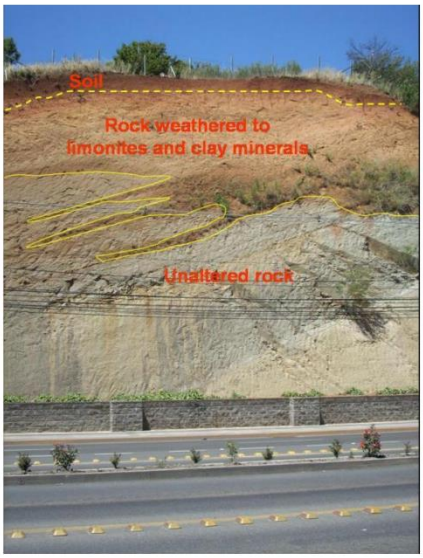

Carbon Capture in Basaltic Rocks (Negative Emissions)

- Reactive transport behavior in fracture networks mostly not considered previously
- Reactive transport behavior arises from highly focused but often connected flow paths
  - Flow in matrix typically minor
  - Fluid mixing may be important
- Fracture intersections may act like pore throats do at the pore scale
  - Can be locus of mineral precipitation having an outsized effect
- Hypotheses:
  - Flow connectivity as key control?
  - Connectivity easily modified due to mineral precipitation

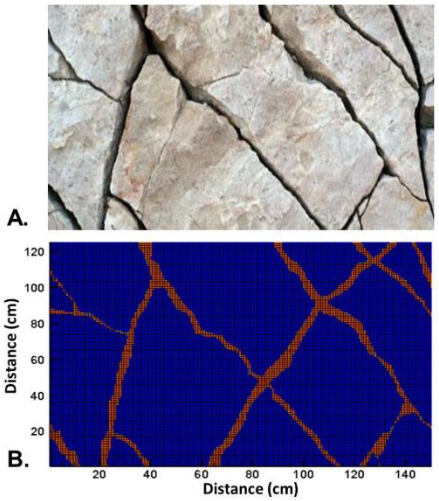

Steefel and Hu, submitted

CO_2 Reaction with Forsterite→ Magnesite

Forsterite as proxy for ultramafic and mafic rocks

$$\underbrace{Mg_2SiO_4}_{Forsterite} + 2CO_2 \rightarrow \underbrace{2MgCO_3}_{Magnesite} + SiO_2(aq)$$

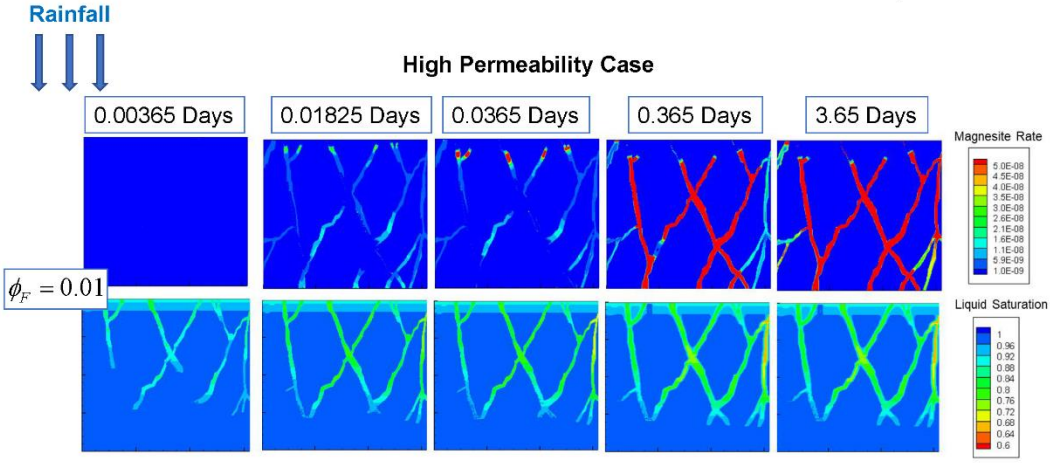

Steefel and Hu, WRR, 2022

Subsurface CO_2 Trapping Mechanisms

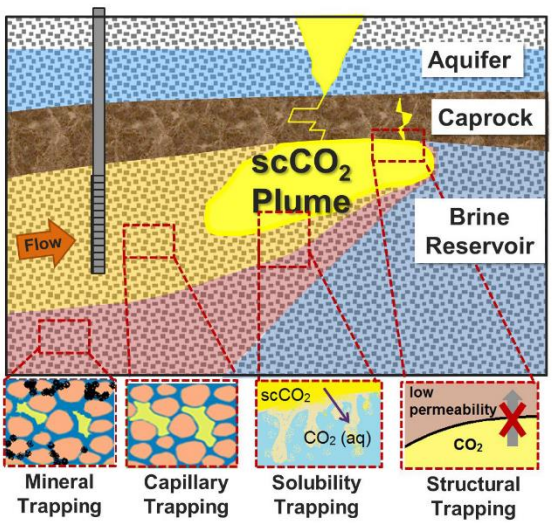

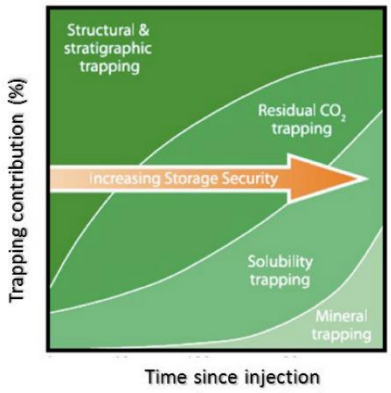

Time Scale?

13

Contaminant Hydrology

Redox Ladder

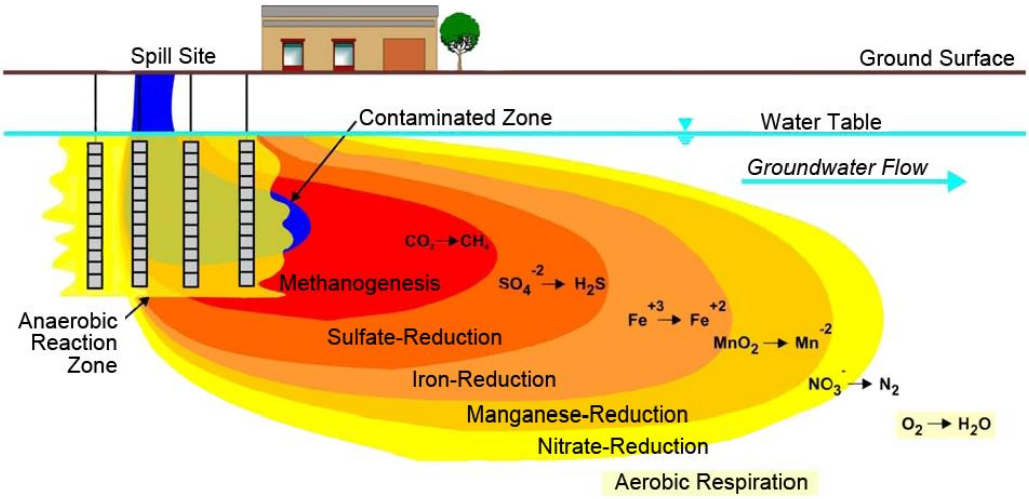

Environmental Remediation

- Gas (carbon) leak is reducing, so inject oxygen to facilitate breakdown by microbes

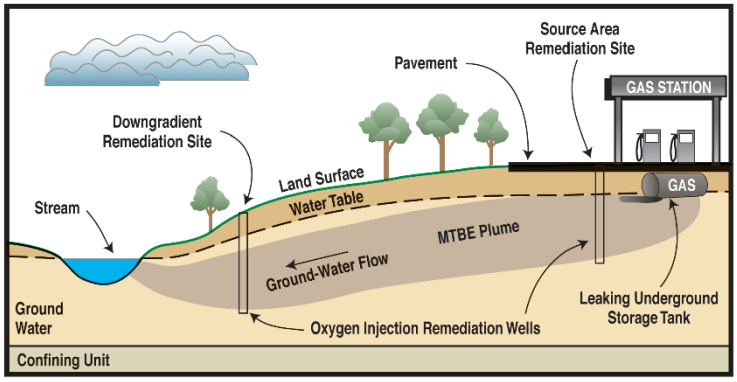

Hanford 200E Area Uranium Plume

Used supercomputer to carry out 3D flow and reactive transport calculations

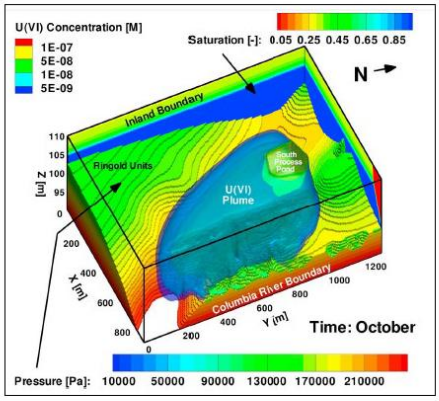

Hammond et al, 2010

Hanford Nuclear Reservation, Washington

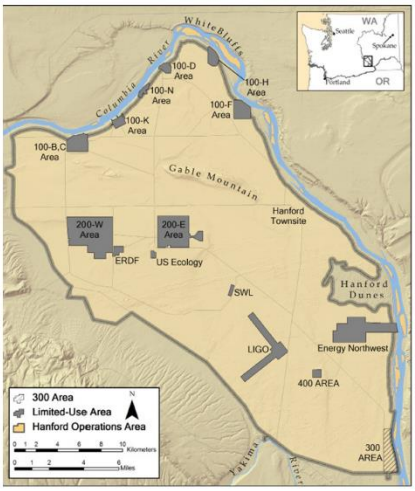

- 1942-1990 plutonium production for nuclear weapons
- 200,000 m^3 of high level radioactive waste, including abundant fission products (^{137}Cs, ^{90}Sr)
- Nuclear waste stored in 177 underground tanks, 70 of which leaked
- Stored in single shelled stainless steel tanks, with radioactive waste heat production resulting in boiling of concentrated (most sodium nitrate) corrosive liquids—some very high pH, some low pH depending on treatment

Cs Migration below Hanford SX-108 Tank

- Greatest mobility of ^{137}Cs was below the Hanford SX-108 tanks
- Abject failure of K_d models spawned a major Science and Technology Program at Hanford funded by the U.S. Department of Energy

Expected position of ^{137}Cs front based on K_d (linear distribution coefficient) transport modeling

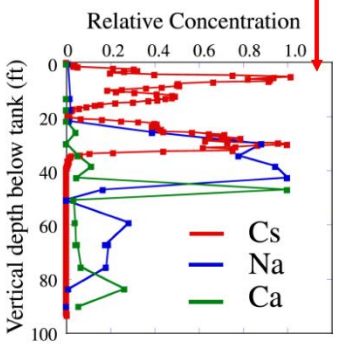

Concentration-Dependent K_d: Effects on Contaminant Migration

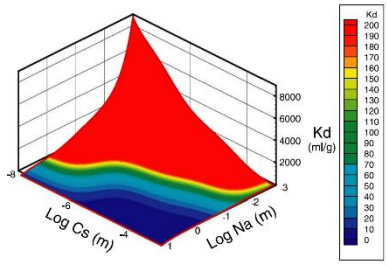

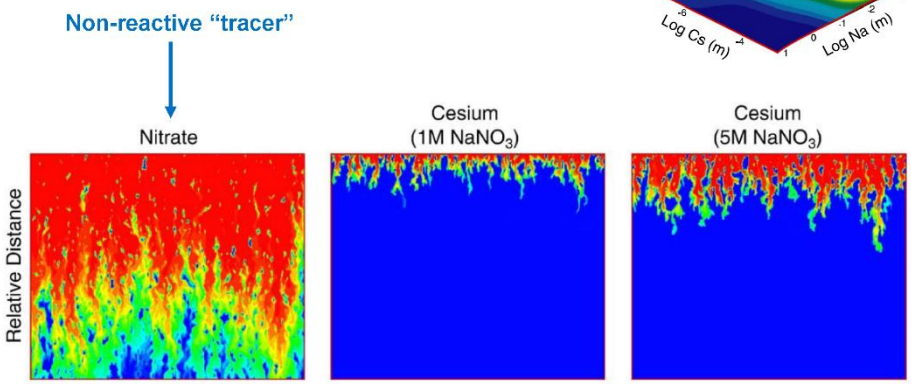

21

Clays and Clay Rocks

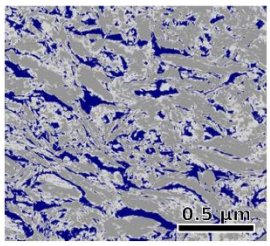

Energy Geosciences
EARTH & ENVIRONMENTAL SCIENCES AREA

Importance of Clays and Clay Rocks

LBNL BES GEOSCIENCES

Shale Reservoirs

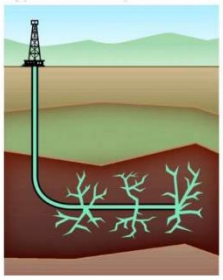

Nuclear Waste Disposal in Clay and Clay Rocks

Sedimentary Basin Pressure Anomalies

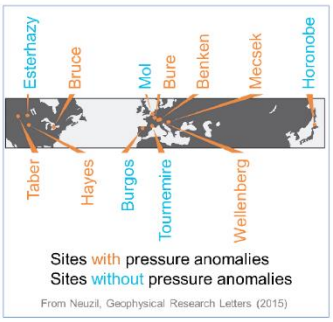

Serpentinization

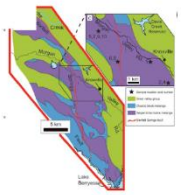

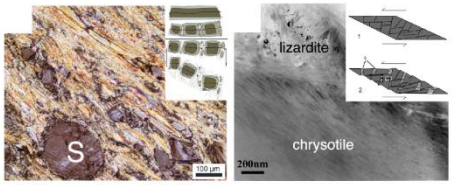

22

Energy Geosciences
EARTH & ENVIRONMENTAL SCIENCES AREA

Electrical Double Layer in Clay

LBNL BES GEOSCIENCES

Electrical Double Layer (EDL)

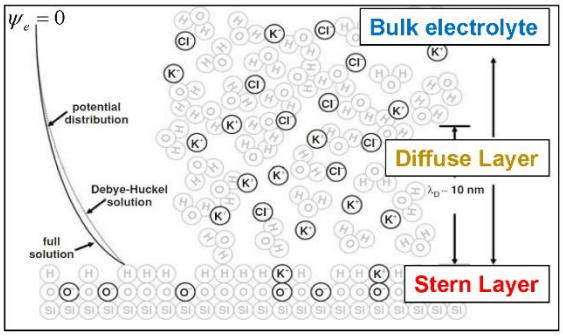

Modified after Kirby, 2010

Chloride Distribution from TEM

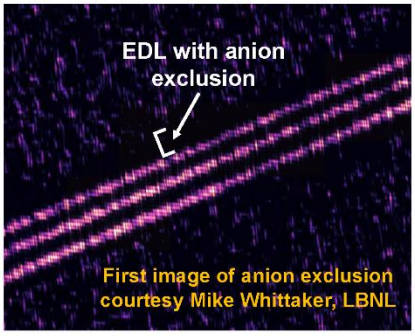

What features of clay EDLs explain the anomalous behavior of clay rocks?

U.S. DEPARTMENT OF ENERGY | Office of Science

23

Simulating DR-A Test in Opalinus Clay with Mean Electrostatic Potential Model

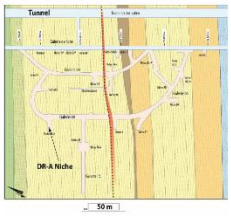

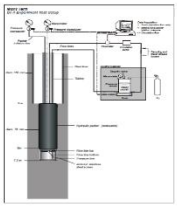

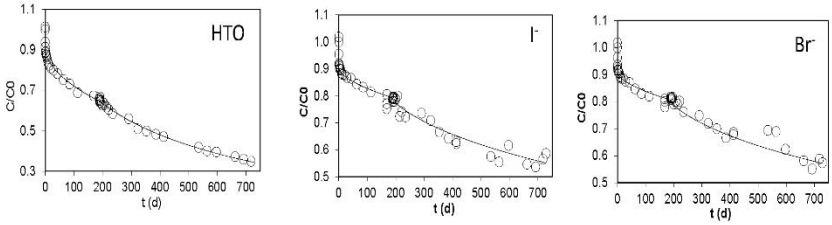

Decrease in HTO (uncharged) > anions

Soler et al, 2019

Uphill Diffusion in Clays

Gradient in $NaClO_4$ concentration from 0.5M to 0.1M

Experiment and data from Glaus et al, 2013

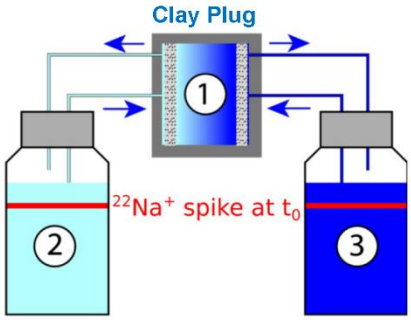

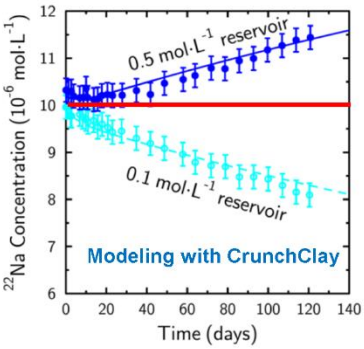

Tournassat and Steefel, 2019

Why is uphill diffusion occurring for the ^{22}Na when no concentration gradient is present?

25

Scales and Models for Clay EDLs

Molecular Scale

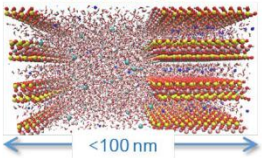

Pore/Particle Scale

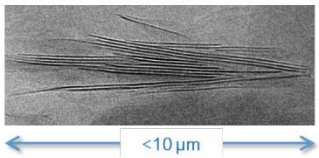

Continuum Scale

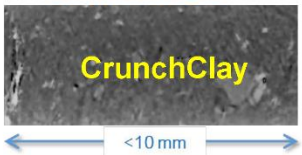

$$\frac{d^2\psi_e(y)}{dy^2} = -\frac{1}{\varepsilon}\sum_i z_i F C_{i,0} \exp\left(\frac{-z_i F \psi_e(y)}{RT}\right)$$

$$\sum_i z_i F \overline{C_{i,DL}} = \sum_i z_i F C_{i,0} \exp\left(\frac{-z_i F \psi_M}{RT}\right) = -Q_{DL}$$

Molecular Dynamics

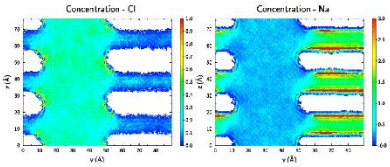

Tournassat et al 2015

Poisson-Boltzmann Equation

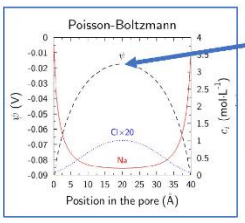

$$\pi_P = k_B T \sum_{i=1}^{N} (\overline{C}_i - {}^{B}C_i)$$

Swelling pressure from EDL overlap

Tournassat and Steefel, 2019

Dual Continuum Approach

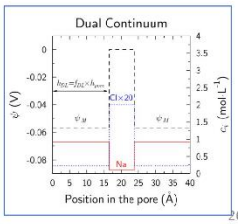

26

Diffusive Transport in Unfractured and Fractured Shale

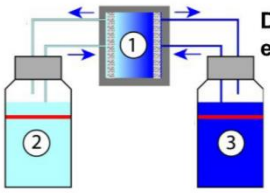

Diffusion cell expt (SLAC)

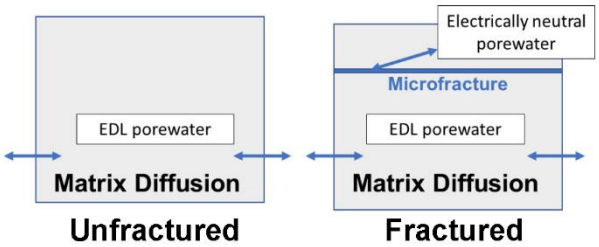

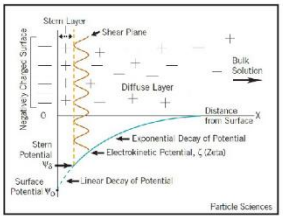

Anion exclusion due to electrical double layer (EDL)

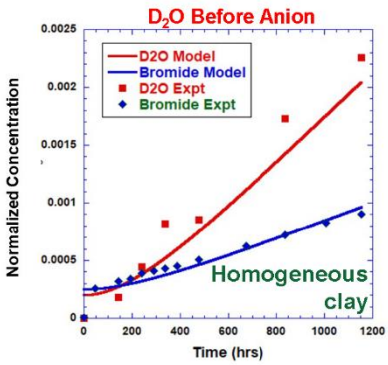

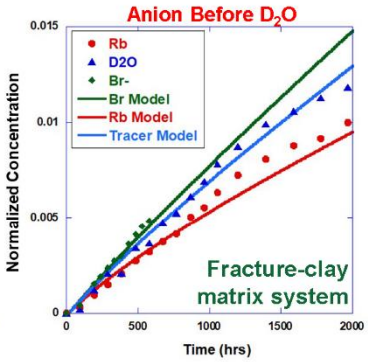

Summary

- Reactive transport modeling has come a long way in its ability to describe important observations/processes
- Earth's critical zone is the area of most intense interest presently
- Much more model development is needed:
  - Chemo-mechanical coupling
  - Electrostatic effects on reactive transport
  - Vegetation-hydrology-geochemistry interaction in Critical Zone
  - …

3.5 Lecture 5 - Speciation of radionuclides – Including thermodynamic databases

To develop adequate strategies for radioactive waste management as well as to properly assess the impact of radionuclide migration in a repository system and/or the environment, radionuclide speciation calculations are needed. The assessment of radionuclide mobility in these systems is essential for the safety demonstration of the repository. One of the key factors influencing the rate of radionuclide transport out of the repository is the solubility of radionuclides released into the aqueous environment and their speciation. For this reason, the ability to model radionuclide speciation under repository conditions is an important issue when assessing the safety of a disposal system.

In this models, thermodynamic data on the stability of the complexes formed are really important. One of the particularities, which makes very challenging these models is that the different chemical properties of each radionuclides results in different speciation, migration and mobilization processes.

Lecturer

Vanessa Montoya, SCK CEN, Belgium

Reading Material

Gaona, X., Montoya, V., Colàs, E., Grivé, M. and Duro, L., 2008. Review of the complexation of tetravalent actinides by ISA and gluconate under alkaline to hyperalkaline conditions. Journal of Contaminant Hydrology, 102(3-4), pp.217-227.

Duro, L., Montoya, V., Colàs, E. and García, D., 2010. Groundwater equilibration and radionuclide solubility calculations. Nuclear Waste Management Organization Technical Report NWMO TR-2010-02. Toronto, Canada.

Montoya, V., Noseck, U., Mattick, F., Britz, S., Blechschmidt, I. and Schäfer, T., 2022. Radionuclide geochemistry evolution in the Long-term In-situ Test (LIT) at Grimsel Test Site (Switzerland). Journal of Hazardous Materials, 424, p.127733

Slides

Speciation of radionuclides
Including thermodynamic databases

Vanessa Montoya

03.03.2023

1

Speciation of radionuclides
Introduction

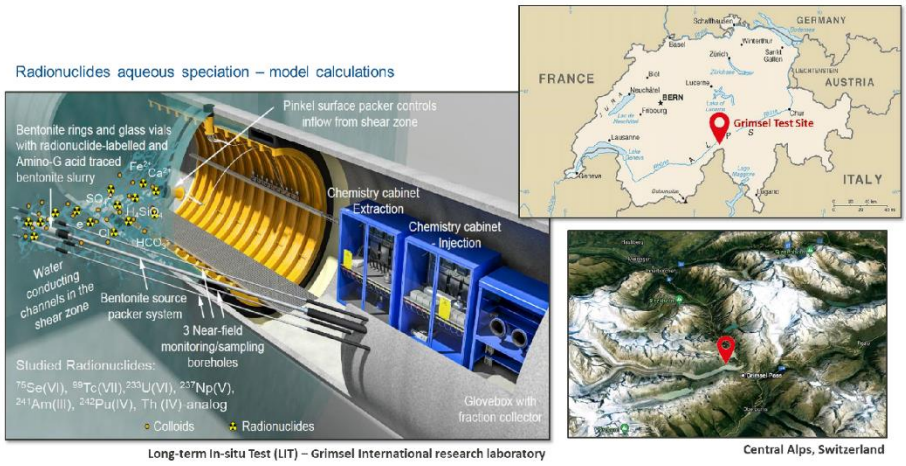

Montoya, V., et al. (2022).. *Journal of Hazardous Materials, 424, 127733.*

2

Speciation of radionuclides
Introduction

- **Chemical model + thermodynamic model**
- **Aquatic speciation** (relevant species, intrinsic colloids, …)
- **Redox** (calculation of predominance fields, Eh measurements, exp. Validation)
- **Solid phases** (relevant solids, crystalline vs. amorphous, particle size,…)
- **Thermodynamic databases** (NEA-TDB, extended TDBs…)

3

Speciation of radionuclides
Introduction

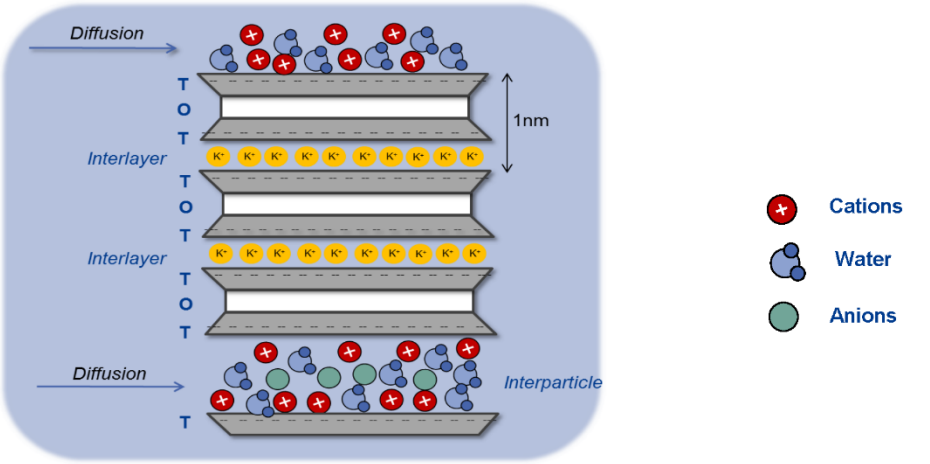

4

Theory
Chemical model

Chemical processes occurring in the system

$$\frac{\partial SC_i}{\partial t} = \Gamma_i(C_i \dots C_m)$$

5

Theory
Chemical reactions

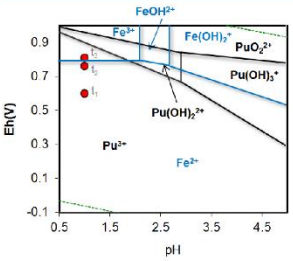

Thermodyn.

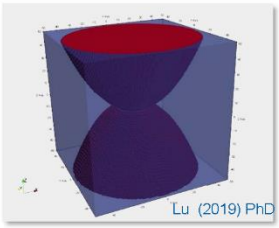

Kinetics

Duro et al. (2010) NWMO

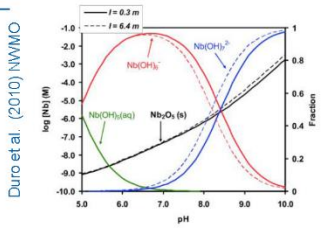

Aqueous speciation

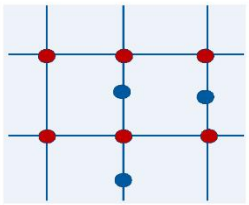

Solid solutions

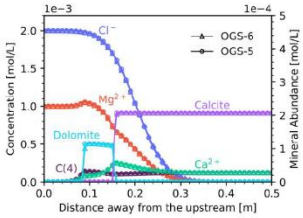

Precipitation/dissolution

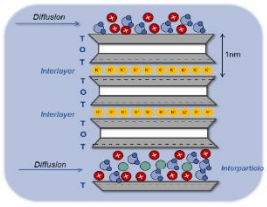

Surface reactions

6

Theory
Aqueous speciation

Thermodynamic databases

Fast reactions - Thermodynamics

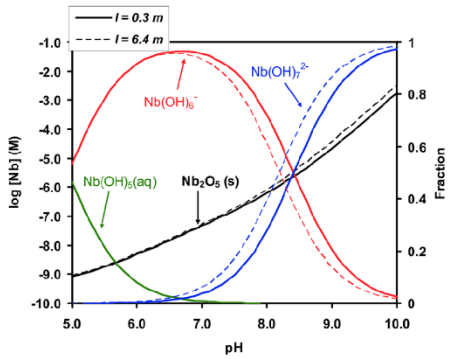

Duro et al. (2010) NWMO TR-2010-02

Product

$$\underbrace{a\ \mathbf{A}^+\ (aq) + b\ \mathbf{B}^-\ (aq)}_{\text{Reactants}} = \mathbf{A_aB_b}\ (aq)$$

Gibbs Energy

$$\Delta G_r = RT \ln K$$

$$K = \frac{[A_aB_b]}{[A]^a[B]^b}$$

Equilibrium constant

R → Universal gas constant = 0.082 atm·l/mol·K = 8.31 J/mol·K
T → Temperature (K) T = 273.15 + t(ºC)

7

Theory
Aqueous speciation – accounting for the salinity

$$\log(\gamma_i) = -z_i^2\left(\frac{A\sqrt{I_m}}{1+Ba_i\sqrt{I_m}}\right)$$

Extended Debye-Hückel

$$a = m\,\gamma_i$$

$$I = \frac{1}{2}\sum mz^2$$

$$\log(\gamma_i) = -z_i^2\left(\frac{A\sqrt{I_m}}{1+Ba_i\sqrt{I_m}}\right) + \sum_k \varepsilon(i,k,I_m)m_k$$

Specific Ionic Theory (SIT)

$$\log(\gamma_i) = -z_i^2\left(\frac{A\sqrt{I_m}}{1+b\sqrt{I_m}} + \frac{2}{b}\ln\left(1+b\sqrt{I_m}\right)\right) + \sum_c\sum_a m_c m_a B'_{ac} + \sum_c\sum_{c'} m_c m_{c'}\phi'_{cc'}$$
$$+\sum_a\sum_{a'} m_a m_{a'}\phi'_{aa'} + \sum_a m_a\left(2B_{ia} + ZC_{ia}\right) + \sum_c m_c\left(2\phi_{ic} + \sum_a m_a\psi_{ica}\right)$$
$$+\sum_a\sum_{a'} m_a m_{a'}\psi_{iaa'} + |z_i|\sum_c\sum_a m_c m_a C_{ac} + 2\sum_n m_n\lambda_{ni}$$

PITZER

Salinity

8

Theory
Aqueous speciation

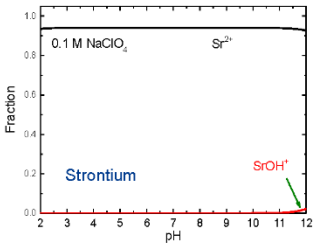

Montoya et al. (2018) Geochimica et Cosmochimica Acta 223, 1-20

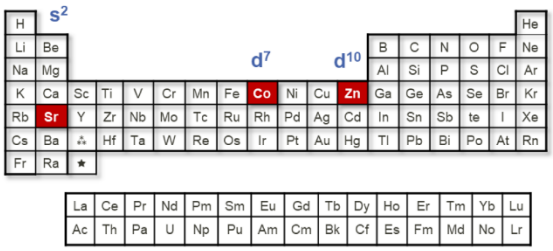

Zinc speciation

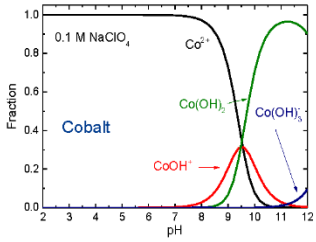

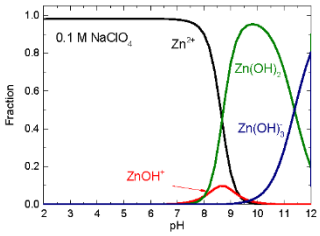

All chemicals behave differently in aqueous solution

	r (Å)
Sr^{2+}	1.18
Co^{2+}	0.74
Zn^{2+}	0.74

9

Theory
Aqueous speciation

Acid / Base reactions

pH = - log [H⁺]

Acid < neutral (pH = 7) < basic

Redox $A^{2+} = A^{3+} + e^-$

pe = - log [e⁻]

$$E_h = E^0 - \frac{RT}{nF} ln \frac{[Ox]}{[Red]} \qquad p_e = \frac{E_h}{0.059}$$

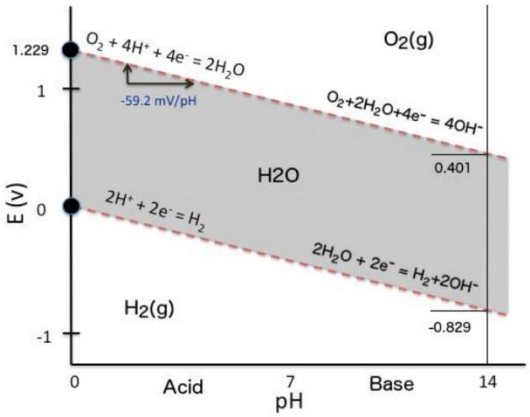

R → Universal gas constant = 0.082 atm·l/mol·K = 8.31 J/mol·K

10

Theory
Aqueous speciation

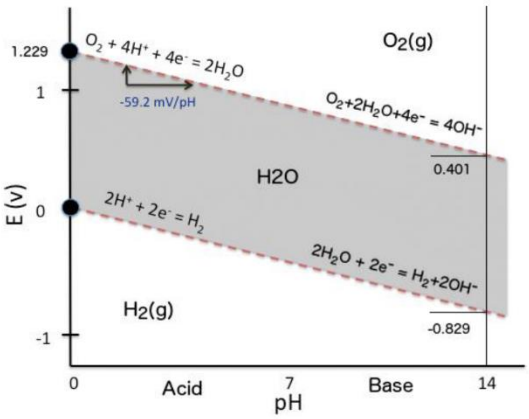

11

Theory
Precipitation / dissolution – Interaction solid / fluid

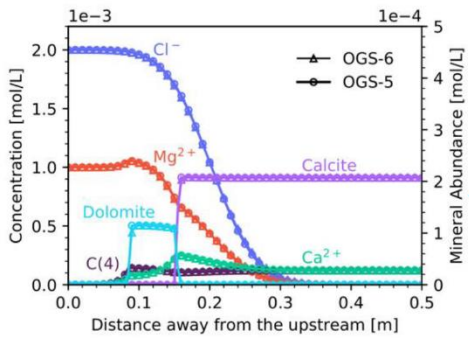

Thermodyn. Fast reactions

C (s) = a **A**$^+$ (aq) + b **B**$^-$ (aq)

Equilibrium constant ⟷ Solubility product $K = [A]^a[B]^b$

$$S.I = log\frac{[A]^a[B]^b}{K}$$

Saturation index
- S. I < 0
- S. I = 0
- S. I > 0

12

Theory
Chemical + thermodynamic model

Aqueous species distribution **Solubility** **Redox**

Uncertanties: Data uncertainty + systematic uncertainties (chem. model…)

13

Theory
Thermodynamic databases

Thermodynamic databases

– Examples of available databases:

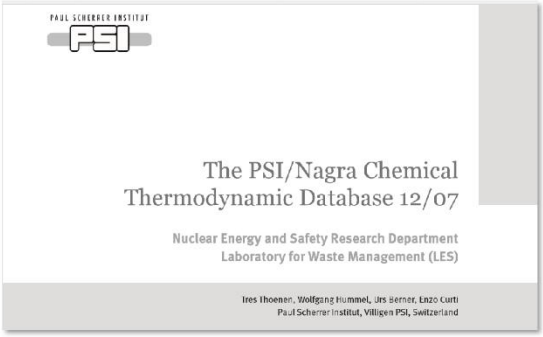

14

Theory
Thermodynamic databases

Thermodynamic databases

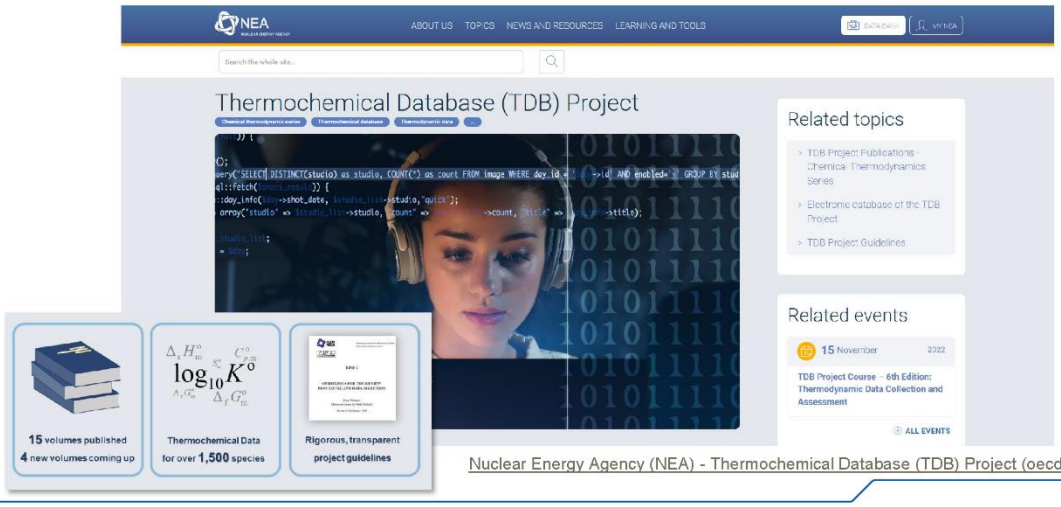

Nuclear Energy Agency (NEA) - Thermochemical Database (TDB) Project (oecd-nea.org)

15

Theory
Thermodynamic databases

Thermodynamic databases

Chemical Reviews — Review

Actinide (oxidation state)	Complexing ligand	Electrolyte matrix
Thorium(IV)	OH^-	NaCl
Protactinium(IV, V)	F^-	$NaClO_4$
Neptunium(IV, V, VI)	Cl^-	$MgCl_2$
Plutonium(III, IV, V, VI)	SO_4^{2-}	$CaCl_2$
Americium(III)	NO_3^-	(TMA-Cl)
Curium(III)	PO_4^{3-}	(NO_3^-)
[Uranium(IV, VI)]	CO_3^{2-}	**Temperature range**
	silicates	10 – 200°C

Altmaier, M., et al. (2013).. *Chemical reviews, 113(2), 901-943*

16

Theory
Thermodynamic databases

Table 7. Speciation scheme and stability constants selected for An(IV)–ISA and An(IV)–GLU complexes forming in alkaline to hyperalkaline conditions

Species	$\log_e\beta°$			
	Th	U	Np	Pu
$An(OH)_4(ISA)^-$	−11.5±1.5 a,e	−6.8±0.9 d	−4.06±0.62 a,k	−3.8±1.6 b,l,m
$An(OH)_4(ISA)_2^{2-}$	−11.2±1.5 b,f	−4.9±1.0 b,j	−2.20±0.62 a,k	0.4±1.1 b,l,m
$CaAn(OH)_4(ISA)_2(aq)$	−4.0±0.4 a,c,e,g,h			
$An(OH)_4(GLU)^-$	−13.2±1.0 b,i	−5.2±1.0 b,j	−3.5±1.1 d	−2.8±1.5 b,l,n
$An(OH)_4(GLU_{-H})^{2-}$	−22.4±1.0 b,i			
$CaTh(OH)_4(GLU)_2(aq)$	−0.8±0.1 a,h			

a. recalculated in this work; b. determined in this work from the available experimental data; c. average of the available data; d. determined by LFER; e. Vercammen et al. (2001); f. Rai et al. (2004); g. Tits et al. (2002); h. Tits et al. (2005); i. Felmy (2004); j. Warwick et al. (2004); k. Rai et al. (2003); l. Moreton (1993); m. Greenfield et al. (1995); n. Cross et al. (1989).

Gaona, X., *Journal of Contaminant Hydrology* 102, no. 3-4 (2008): 217-227.

17

Theory
Thermodynamic databases

Thermodynamic databases

Altmaier, M., et al. (2013).. *Chemical reviews, 113(2), 901-943*

18

Theory
Solid phases – solubility limit

Thermodynamic data based on estimations:
Analogy with Ln(III) and An(III) as a function of ionic radii.

$Pu^{3+} + CO_3^{2-} + H_2O = \mathbf{Pu(CO_3)(OH)(s)} + 1H^+$

Crystal radius stracted from Shannon (1976)

19

Theory
Solid phases – crystallinity & particle size

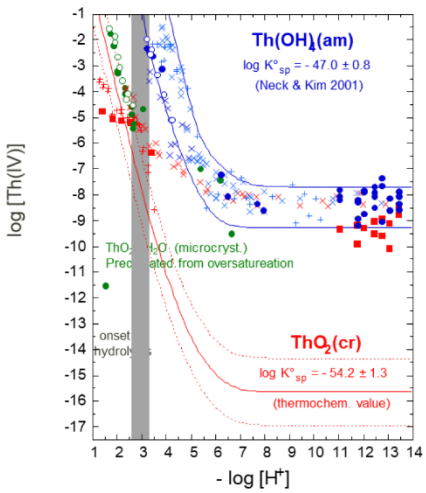

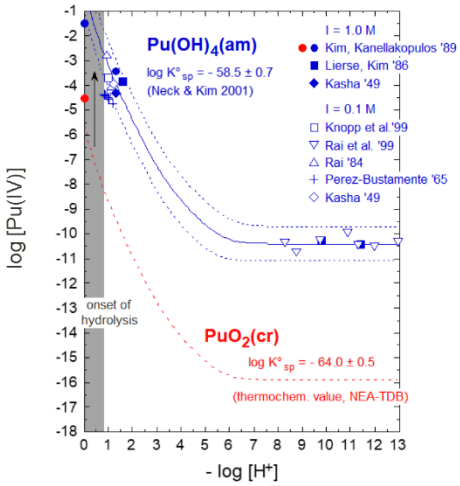

20

Theory
Precipitation / dissolution – Interaction solid / fluid

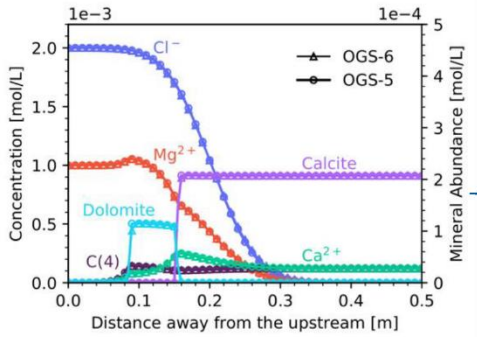

Kinetics Slow reactions

C (s) = a **A**⁺ (aq) + b **B**⁻ (aq)

Kinetic law → different orders

$$\frac{\partial c_i}{\partial t} = K_{Kin}[A]^n$$

$$\frac{\partial c_i}{\partial t} = K_{Kin}[A]^n[B]^y$$

$$\frac{\partial c_i}{\partial t} = K_{Kin}$$

....

21

Theory
Surface reactions

➢ **Diffusion in Na-illite**

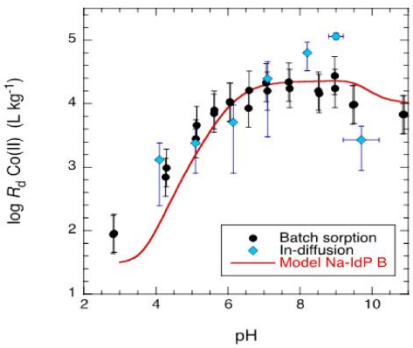

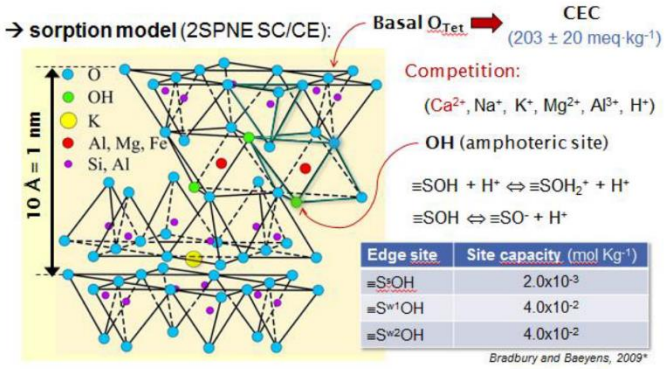

Montoya et al. (2018). Geochim. Cosmochim. Acta, 2018, 223, 1

22

Theory
Solid solutions

$R_xB_{(1-x)}A = x\,\mathbf{R}^+ + (1-x)\,\mathbf{B}^+ + A^-$

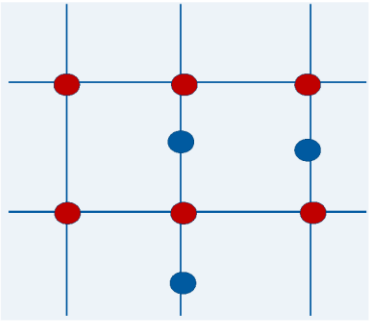

$$K_{BA} = \frac{[A][B]}{[BA]} = \frac{[A][B]}{X_{BA}\,\gamma_{BA}}$$ End member BA

$$K_{RA} = \frac{[A][R]}{[RA]} = \frac{[A][B]}{X_{RA}\,\gamma_{RA}}$$ End member RA

$$\ln \gamma_{RA} = \chi_{BA}^2 \left(a_0 - a_1 (3\chi_{RA} - \chi_{BA})\right)$$ Non-ideal solid-solutions

23

Theory
Temperature

Data estimation procedures are of especial interest when the influence of temperature is taken into account. Virial equations classically used to account for temperature variations in thermodynamic databases require a good knowledge on the temperature dependence of heat capacities. Nevertheless, heat capacity data of radionuclides are seldom available. In the absence of experimental information on the temperature dependence of the standard heat capacities, the simplification described by the Van't Hoff equation (no effect of temperature on reaction enthalpy) can provide a reasonable estimate of temperature effect on stability for many systems. The application of the Van't Hoff equation is especially accurate below 100 °C, when changes in temperature are not very important (few tens of degrees) or in the case of isocoulombic reactions (Grenthe et al., 1997).

The application of the Vant'Hoff equation needs values for the e given temperature and the enthalpy of reaction. Enthalpies can l

$$\ln \frac{K_2}{K_1} = \frac{\Delta_r H^\ominus}{R} \left(\frac{1}{T_1} - \frac{1}{T_2} \right).$$

methods, although formation/reaction entropy and enthalpy of solid phases are

24

Theory
Temperature

Low permeability of Opalinus Clay (anisotropic material)

– Conduction is the only heat transfer mechanism

– Diffusion is the only mass transport mechanism

Temperature can affect transport parameters and geochemistry.

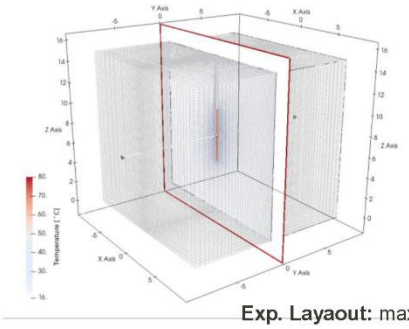

Exp. Layaout: max. 80°C

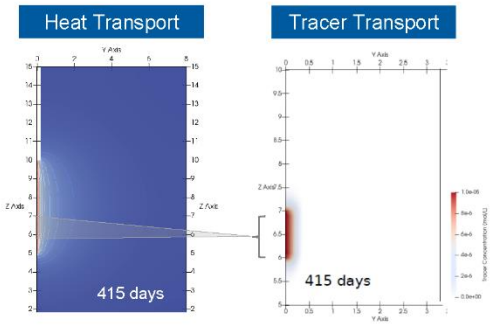

25

Questions?

03.03.2023

26

3.6 Lecture 6 - Molecular aspect and thermodynamic modelling of sorption phenomena

Lecture provides introduction into

- molecular mechanism of sorption phenomena by molecular simulations and spectroscopy

- physical and chemical processes at mineral surface interface

- foundation for development and application of mechanistic thermodynamic models for sorption

- assessments of model uncertainties

Lecturer

Sergey Churakov, PSI, Switzerland

Reading Material

B. Baeyens, M. and M. Fernandes (2018). Adsorption of heavy metals including radionuclides. Surface and Interface Chemistry of Clay Minerals. R. Schoonheydt, C. T. Johnston and F. Bergaya, Elsevier**:** 125-172.

Churakov, S. V., W. Hummel and M. Marques Fernandes (2020). "Fundamental Research on Radiochemistry of Geological Nuclear Waste Disposal." Chimia **74**(12): 1000-1009.

Keri, A., R. Dahn, M. Marques Fernandes, A. C. Scheinost, M. Krack and S. V. Churakov (2020). "Iron Adsorption on Clays Inferred from Atomistic Simulations and X-ray Absorption Spectroscopy." Environmental Science & Technology **54**: 1886-11893

Slides

WP FUTURE

Sorption Phenomena: Thermodynamic modelling and Molecular scale sorption mechanisms

Sergey V. Churakov

The project leading to this application has received funding from the European Union's Horizon 2020 research and innovation programme under grant agreement n° 847593.

08/02/2023 Joint Training Event ACED-DONUT-FUTURE 1

OUTLINE

- Retention and transport mechanics radionuclides
- Sorption mechanism and fluid-surface interaction
- Structure and properties of clay minerals
- Development and validation of sorption models
- Types and sources of uncertainties
- Application of sorption models in Safety Assessment Studies

ACKNOWLEDGEMENT

- Maria Marques
- Dan Miron
- Dmitrii Kulik

Retention and transport in porous media

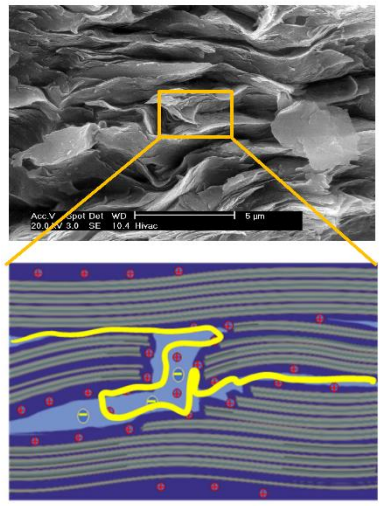

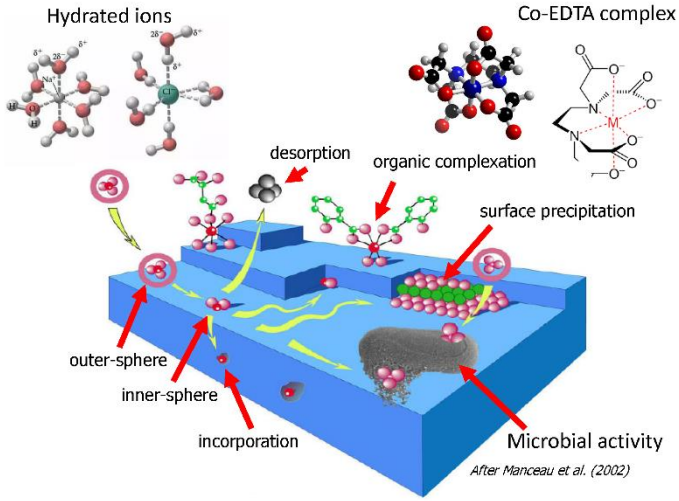

- Knowledge on uptake mechanisms is essential for predictions of radionuclides and contaminants transport in the geosphere

Solubility & solution chemistry

We cannot dissolve unlimited amounts of a solid in water.

$$NaCl_{(s)} \leftrightarrow Na^{+}_{aq} + Cl^{-}_{aq}$$

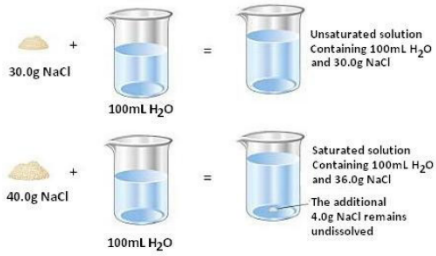

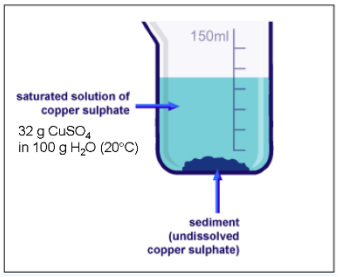

Many salts (e.g. NaCl, $CuSO_4$) dissolve in the order of grams per 100 g H_2O, but most radionuclides are limited to very low concentrations.

$$UO_{2,(s)} + 2H_2O \leftrightarrow U^{4+}_{aq} + 4OH^{-}_{aq}$$
$$K_{sp,\,UO_2} = \{U^{4+}\}_{aq}\{OH^{-}\}^{4}_{aq} \cong 10^{-56}$$

Pore water solution is saturated with respect to rock forming minerals.

Solubility & complexation

Metal ions (Me) are in equilibrium with solids and several complexes (X).

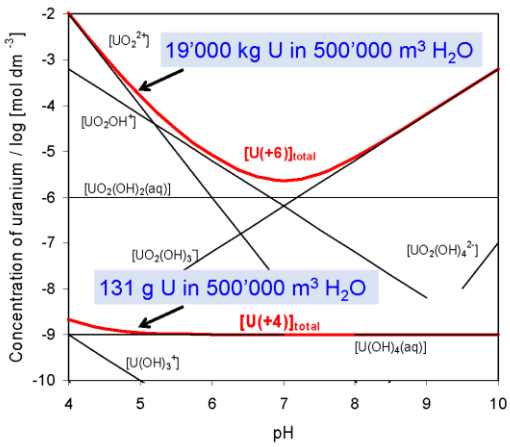

Solubility product

$$UO_{2,(s)} + 2H_2O \leftrightarrow U^{4+}_{aq} + 4OH^{-}_{aq}$$

$$K_{sp,\,UO_2} = \frac{\{U^{4+}\}_{aq}\{OH^{-}\}^{4}_{aq}}{\{H_2O\}_{aq}=1\,\{UO_2\}_{s}=1} = \{U^{4+}\}_{aq}\{OH^{-}\}^{4}_{aq} \cong 10^{-56}$$

Aqueous complexation equilibrium

$$U^{4+}_{aq} + OH^{-}_{aq} \leftrightarrow U(OH)_{4,(aq)}$$

$$K_{sp,\,UO_2}K = \frac{U(OH)_{4,(aq)}}{\{U^{4+}\}_{aq}\{OH^{-}\}^{4}_{aq}\{UO_2\}_{s}=1} \cong 10^{47}$$

Solubility

$$\sum_{tot,aq} Me = [Me]^{n+}_{aq} + [MeX_i]^{m+/-}_{aq} + [MeX_j]^{p+/-}_{aq} \ldots$$

Sorption

Is empirically defined esperimental measurements of

solid/liquid distribution coefficient R_d

— The quantity of a solute sorbed by a solid, per unit weight of solid, divided by the quantity of the solute dissolved in the water per unit volume of water.

$$R_d = \frac{[C]_{sorbed}}{M_{solid}} : \frac{[C]_{eq}}{V_{aq}} = \frac{C_{init} - C_{eq}}{C_{eq}} : \frac{V_{aq}}{M_{solid}} \; [L/kg]$$

C_{init} is the total initial nuclide concentration $[\frac{mol}{L}]$,

$[C]_{eq} \equiv [C]_{dissolved}$ is the total equilibrium aqueous nuclide concentration $[\frac{mol}{L}]$

V_{aq} is the volume of the liquid phase [L = dm³],

M_{solid} is the mass of the solid phase [kg]

Phyllosilicates structure & reactivity

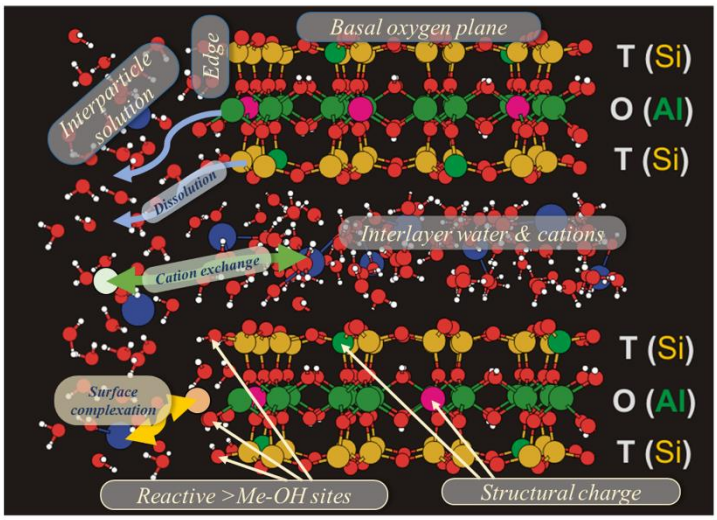

Churakov & Schliemann (2021) AIPEA Educational Series (AES) doi: 10.14644/AES.003

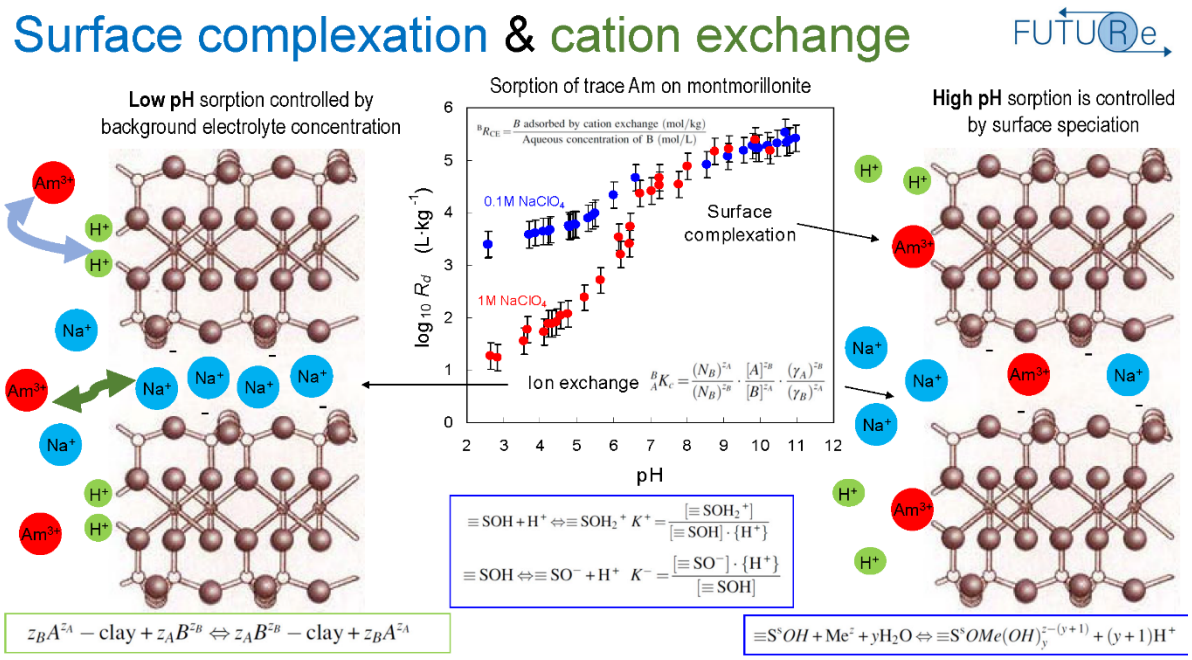

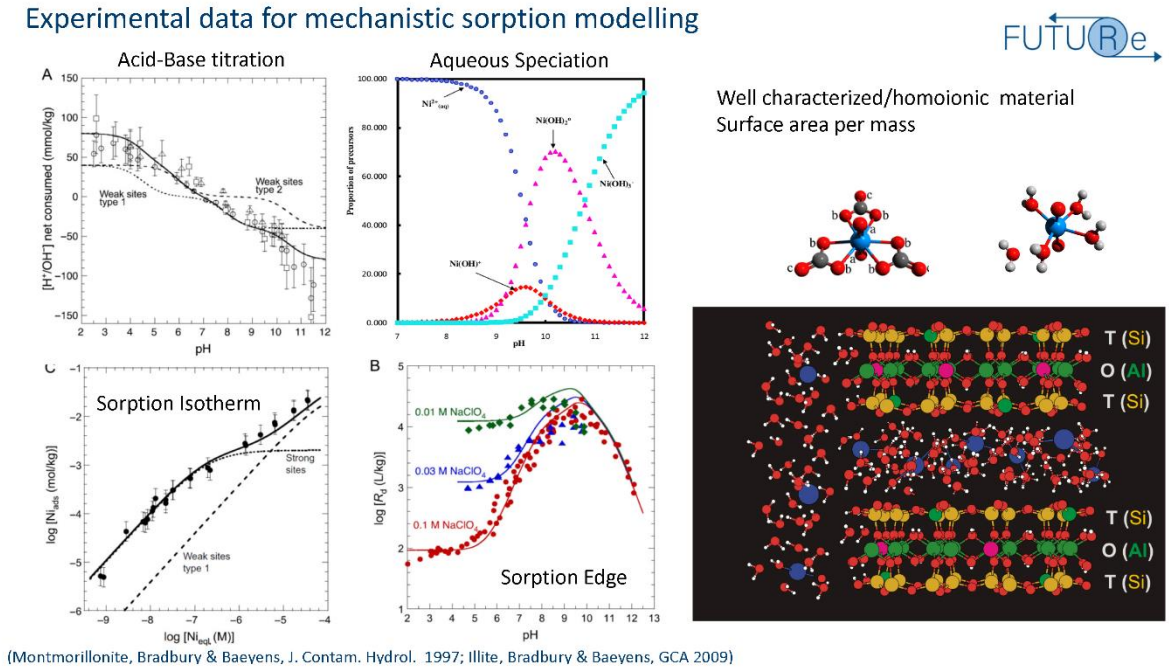

(Montmorillonite, Bradbury & Baeyens, J. Contam. Hydrol. 1997; Illite, Bradbury & Baeyens, GCA 2009)

Generalised 2SPNE SC/CE model: Case study Eu

(Montmorillonite, Bradbury & Baeyens, J. Contam. Hydrol. 1997; Illite, Bradbury & Baeyens, GCA 2009)

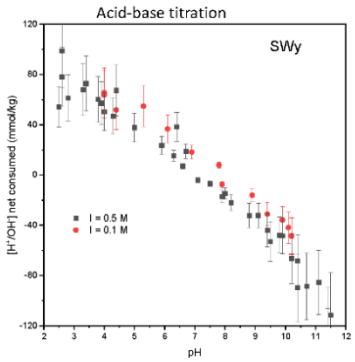

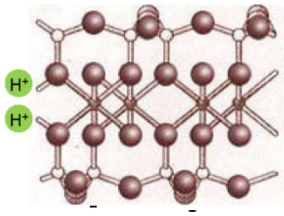

$$\equiv SOH + H^+ \Leftrightarrow \equiv SOH_2^+ \quad K^+ = \frac{[\equiv SOH_2^+]}{[\equiv SOH]\cdot\{H^+\}}$$

$$\equiv SOH \Leftrightarrow \equiv SO^- + H^+ \quad K^- = \frac{[\equiv SO^-]\cdot\{H^+\}}{[\equiv SOH]}$$

Generalised 2SPNE SC/CE model: Case study Eu

(Montmorillonite, Bradbury & Baeyens, J. Contam. Hydrol. 1997; Illite, Bradbury & Baeyens, GCA 2009)

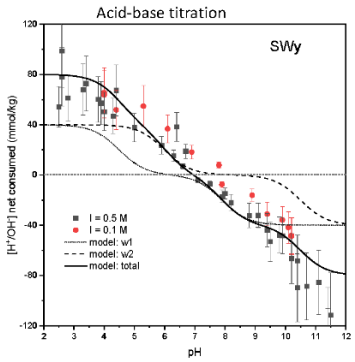

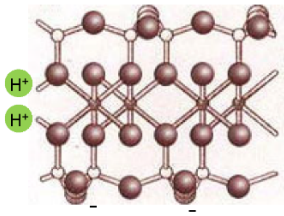

$$\equiv SOH + H^+ \Leftrightarrow \equiv SOH_2^+ \quad K^+ = \frac{[\equiv SOH_2^+]}{[\equiv SOH]\cdot\{H^+\}}$$

$$\equiv SOH \Leftrightarrow \equiv SO^- + H^+ \quad K^- = \frac{[\equiv SO^-]\cdot\{H^+\}}{[\equiv SOH]}$$

Protolysis reactions	log K_{IdP}	log K_{Mont}
$\equiv S^{W1}OH + H^+ \Leftrightarrow \equiv S^{W1}OH_2^+$	4.0	4.5
$\equiv S^{W1}OH \Leftrightarrow \equiv S^{W1}O^- + H^+$	-6.2	-7.9
$\equiv S^{W2}OH + H^+ \Leftrightarrow \equiv S^{W2}OH_2^+$	8.5	6.0
$\equiv S^{W2}OH \Leftrightarrow \equiv S^{W2}O^- + H^+$	-10.5	-10.5

Site type	Site capacities (mmol kg^{-1})
$\equiv S^{W1}OH$	40
$\equiv S^{W2}OH$	40
CEC (IdP)	225
CEC (Mont)	870

Stepwise modelling of sorption edge

Site type	Site capacities (mmol kg^{-1})
$\equiv S^{W1}OH$	40
$\equiv S^{W2}OH$	40
CEC (IdP)	225
CEC (Mont)	870

Protolysis reactions	log K_{IdP}	log K_{Mont}
$\equiv S^{W1}OH + H^+ \Leftrightarrow \equiv S^{W1}OH_2^+$	4.0	4.5
$\equiv S^{W1}OH \Leftrightarrow \equiv S^{W1}O^- + H^+$	-6.2	-7.9
$\equiv S^{W2}OH + H^+ \Leftrightarrow \equiv S^{W2}OH_2^+$	8.5	6.0
$\equiv S^{W2}OH \Leftrightarrow \equiv S^{W2}O^- + H^+$	-10.5	-10.5

Eu(III) aqueous speciaton in 0.1 $NaClO_4$

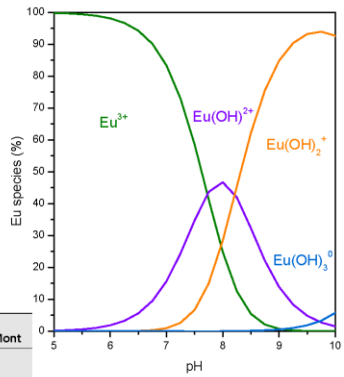

Eu(III) sorption onto Na-SWy-1 (carbonate free) in 0.1 $NaClO_4$

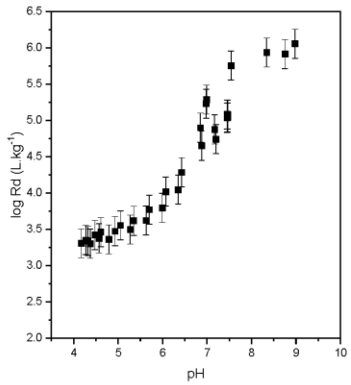

$[Eu]_{aq} \sim 10^{-8}$

Bradbury, M. H. and B. Baeyens (2011). Applied Clay Science 52: 27–33.

Stepwise modelling of sorption edge

Cation exchange reactions:

CE: 3Na-clay + $Eu^{3+} \Leftrightarrow$ Eu-clay + $3Na^+$ $K_c = 29$

Site type	Site capacities (mmol kg^{-1})
$\equiv S^{W1}OH$	40
$\equiv S^{W2}OH$	40
CEC (IdP)	225
CEC (Mont)	870

Protolysis reactions	log K_{IdP}	log K_{Mont}
$\equiv S^{W1}OH + H^+ \Leftrightarrow \equiv S^{W1}OH_2^+$	4.0	4.5
$\equiv S^{W1}OH \Leftrightarrow \equiv S^{W1}O^- + H^+$	-6.2	-7.9
$\equiv S^{W2}OH + H^+ \Leftrightarrow \equiv S^{W2}OH_2^+$	8.5	6.0
$\equiv S^{W2}OH \Leftrightarrow \equiv S^{W2}O^- + H^+$	-10.5	-10.5

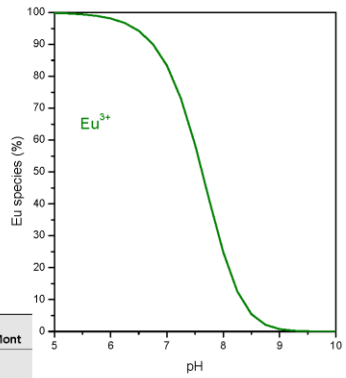

free Eu^{3+} cation

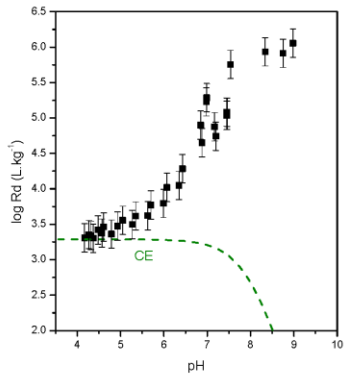

$[Eu]_{aq} \sim 10^{-8}$

Bradbury, M. H. and B. Baeyens (2011). Applied Clay Science 52: 27–33.

Stepwise modelling of sorption edge

Surface complexation reactions:

1: $\equiv S^{s}OH + Eu^{3+} \Leftrightarrow \equiv S^{s}OEu^{2+} + H^{+}$ $\log {}^{S}K_1 = 1.6$

Site type	Site capacities (mmol kg^{-1})
$\equiv S^{W1}OH$	40
$\equiv S^{W2}OH$	40
CEC (IdP)	225
CEC (Mont)	870

Protolysis reactions	log K_{IdP}	log K_{Mont}
$\equiv S^{W1}OH + H^{+} \Leftrightarrow \equiv S^{W1}OH_2^{+}$	4.0	4.5
$\equiv S^{W1}OH \Leftrightarrow \equiv S^{W1}O^{-} + H^{+}$	-6.2	-7.9
$\equiv S^{W2}OH + H^{+} \Leftrightarrow \equiv S^{W2}OH_2^{+}$	8.5	6.0
$\equiv S^{W2}OH \Leftrightarrow \equiv S^{W2}O^{-} + H^{+}$	-10.5	-10.5

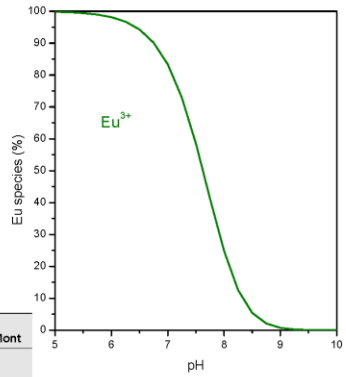

free Eu^{3+} cation

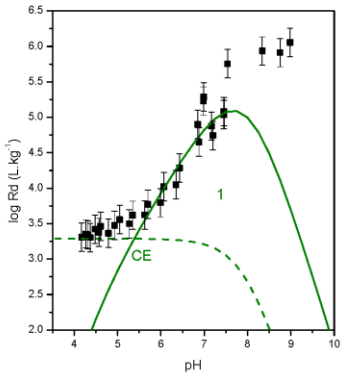

$[Eu]_{aq} \sim 10^{-8}$

Bradbury, M. H. and B. Baeyens (2011). Applied Clay Science 52: 27–33.

Stepwise modelling of sorption edge

2: $\equiv S^{s}OH + Eu^{3+} + H_2O \Leftrightarrow \equiv S^{s}OEuOH^{+} + 2H^{+}$ $\log {}^{S}K_2 = -5.9$

Site type	Site capacities (mmol kg^{-1})
$\equiv S^{W1}OH$	40
$\equiv S^{W2}OH$	40
CEC (IdP)	225
CEC (Mont)	870

Protolysis reactions	log K_{IdP}	log K_{Mont}
$\equiv S^{W1}OH + H^{+} \Leftrightarrow \equiv S^{W1}OH_2^{+}$	4.0	4.5
$\equiv S^{W1}OH \Leftrightarrow \equiv S^{W1}O^{-} + H^{+}$	-6.2	-7.9
$\equiv S^{W2}OH + H^{+} \Leftrightarrow \equiv S^{W2}OH_2^{+}$	8.5	6.0
$\equiv S^{W2}OH \Leftrightarrow \equiv S^{W2}O^{-} + H^{+}$	-10.5	-10.5

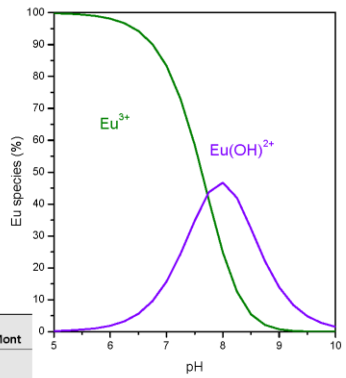

Eu-monohydroxy complex

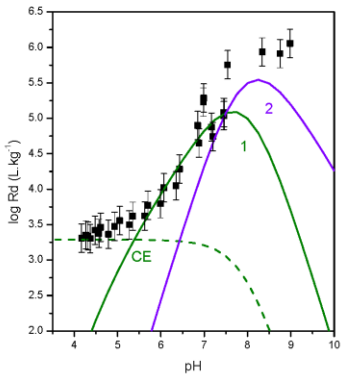

$[Eu]_{aq} \sim 10^{-8}$

Bradbury, M. H. and B. Baeyens (2011). Applied Clay Science 52: 27–33.

Stepwise modelling of sorption edge

3: $\equiv S^{s}OH + Eu^{3+} + 2H_2O \Leftrightarrow \equiv S^{s}OEu(OH)_2 + 3H^+$ $\log {}^{S}K_3 = -14.2$

Site type	Site capacities (mmol kg^{-1})
$\equiv S^{W1}OH$	40
$\equiv S^{W2}OH$	40
CEC (IdP)	225
CEC (Mont)	870

Protolysis reactions	log K_{IdP}	log K_{Mont}
$\equiv S^{W1}OH + H^+ \Leftrightarrow \equiv S^{W1}OH_2^+$	4.0	4.5
$\equiv S^{W1}OH \Leftrightarrow \equiv S^{W1}O^- + H^+$	-6.2	-7.9
$\equiv S^{W2}OH + H^+ \Leftrightarrow \equiv S^{W2}OH_2^+$	8.5	6.0
$\equiv S^{W2}OH \Leftrightarrow \equiv S^{W2}O^- + H^+$	-10.5	-10.5

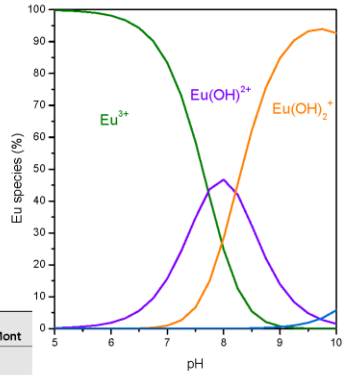

Eu-dihydroxy complex

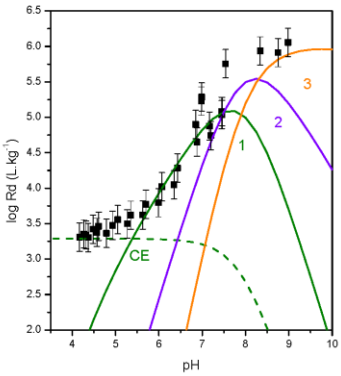

$[Eu]_{aq} \sim 10^{-8}$

Bradbury, M. H. and B. Baeyens (2011). Applied Clay Science 52: 27–33.

Complete sorption model

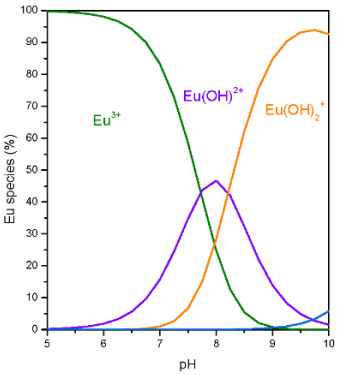

Eu-dihydroxy complex

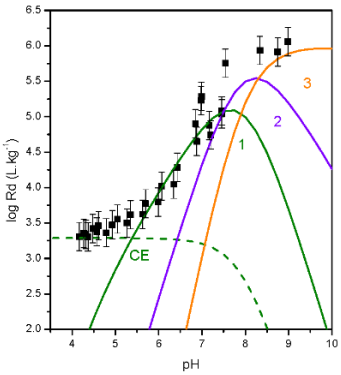

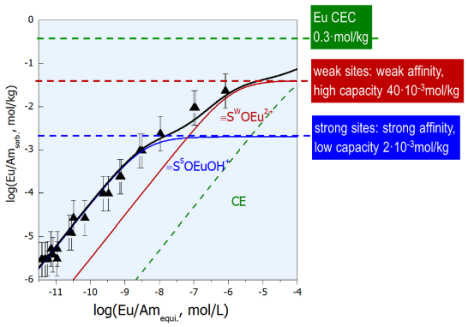

Surface complexation reactions:

1: $\equiv S^{s}OH + Eu^{3+} \Leftrightarrow \equiv S^{s}OEu^{2+} + H^+$ $\log {}^{S}K_1$ 1.6

2: $\equiv S^{s}OH + Eu^{3+} + H_2O \Leftrightarrow \equiv S^{s}OEuOH^+ + 2H^+$ $\log {}^{S}K_2$ -5.9

3: $\equiv S^{s}OH + Eu^{3+} + 2H_2O \Leftrightarrow \equiv S^{s}OEu(OH)_2 + 3H^+$ $\log {}^{S}K_3$ -14.2

CE: $3Na\text{-}clay + Eu^{3+} \Leftrightarrow Eu\text{-}clay + 3Na^+$

$\equiv S^{W}OH + Eu^{3+} \Leftrightarrow \equiv S^{W}OEu^{2+} + H^+$

$\equiv S^{S}OH + Eu^{3+} + H_2O \Leftrightarrow \equiv S^{S}OEuOH^+ + 2H^+$

Bradbury, M. H. and B. Baeyens (2011). Applied Clay Science 52: 27–33.

Generalised Cs model for illite

To model the sorption isotherm on illite:
- 3 site types are required: Frayed Edge Sites (FES), Type II sites and Planar sites
- Selectivity coefficients of Cs with respect to other cations e.g. Na and K are required

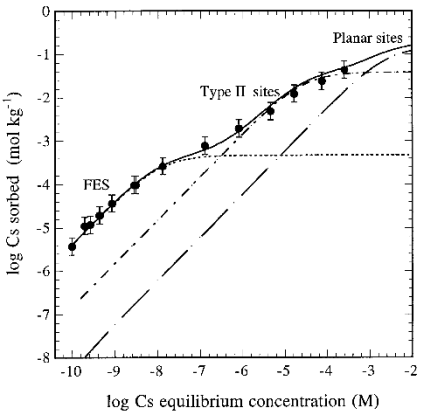

Cs sorption model summary

Site type	Site capacity CEC illite = 200 meq kg^{-1}
FES	0.25 % of CEC
Type II	20 % of CEC
Planar	80 % of CEC

Cation exchange reaction	Log K_c
Na-FES + K ⇔ K-FES + Na Na-FES + Cs ⇔ Cs-FES + Na	2.4 7.0
Na-II + K ⇔ K-II + Na Na-II + Cs ⇔ Cs-II + Na	2.1 3.6

(Bradbury & Baeyens, 2000)

Cation diffusion in the interlayer of montmorillonite

Molecular dynamics simulation
Cs (Yellow) – Na (Blue) -Montmorillonite

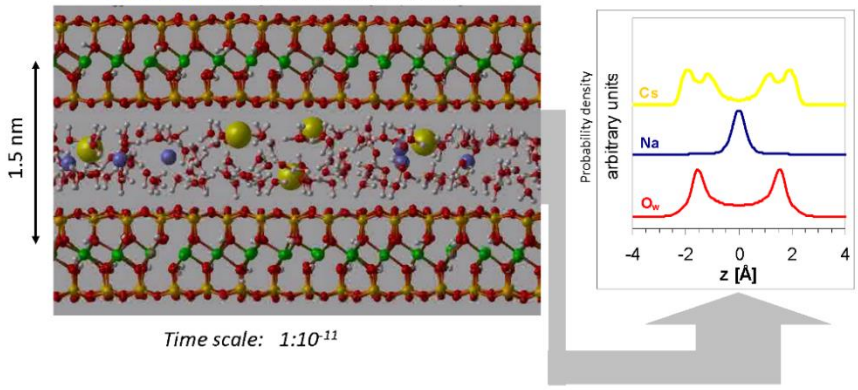

Time scale: 1:10^{-11}

T=300K, P=1bar

Froideval, et al.(2011) J. Nuc. Mat. 416, 242-251

Molecular Nature of Cs sorption

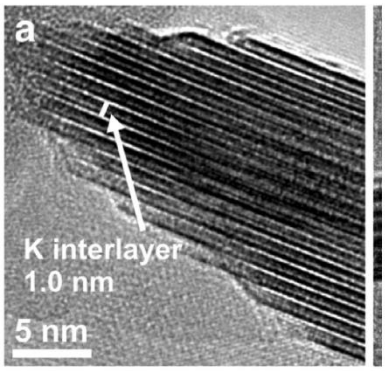

Fuller et al. (2015) Appl. Clay Sci
http://dx.doi.org/10.1016/j.clay.2015.02.008

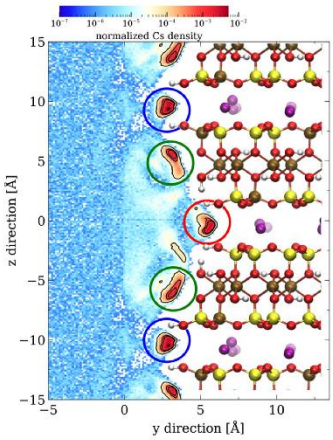

Krejci P. (2023) in prep.

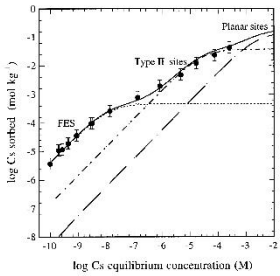

Extended X-ray Absorption Fine Structure (EXAFS)

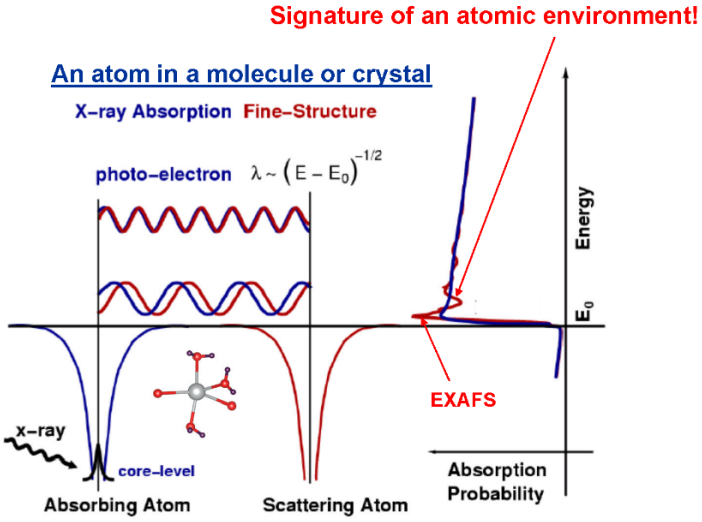

EXAFS spectroscopy: structural information at an atomistic scale!

XAS analysis and molecular structures

Conventional XAS data modelling

1) Measure of XAS spectrum
2) Fit shell model
3) Interatomic distances consistent with presumed structure?

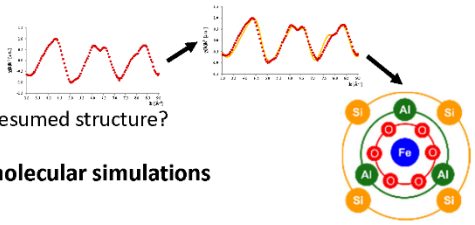

Interpretation of XAS data based on molecular simulations

I) Measure of XAS spectrum
II) Molecular modelling of potential structures
III) Calculation of XAS spectra based on simulated structures
IV) Linear fit of calculated XAS spectra to measured ones

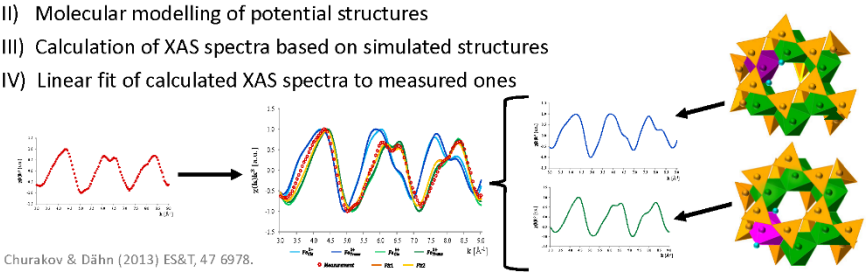

Churakov & Dähn (2013) ES&T, 47 6978.

Mechanistic sorption model: Zn/Ni sorption on illite

3 site types are required: Strong sites (SS), Weak sites (WS) and Cation exchange sites (CE)

Selectivity coefficients of Zn/Ni with respect to Na are required for the 3 sites

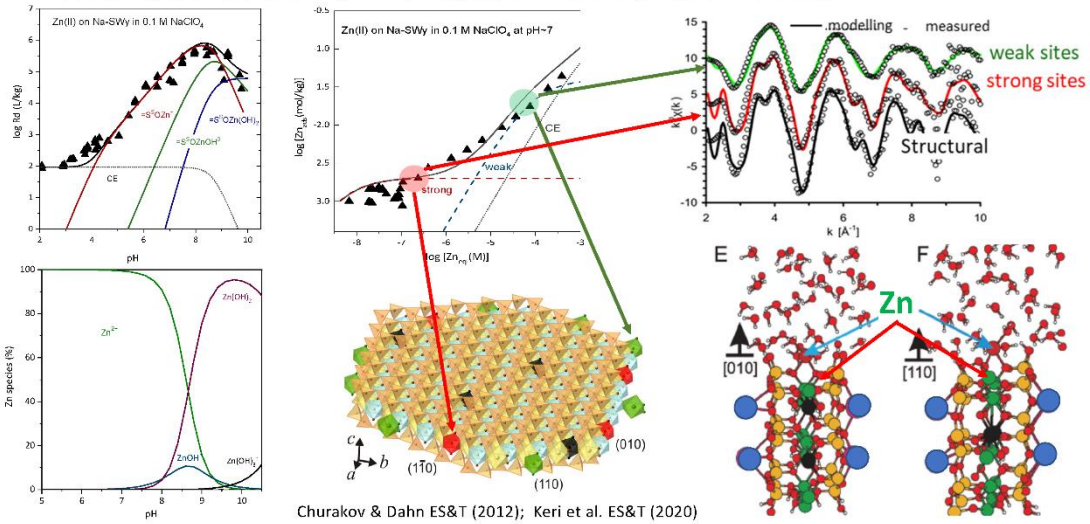

Churakov & Dahn ES&T (2012); Keri et al. ES&T (2020)

Leaching mechanism: Octahedral sheet

Ab initio metadynamics simulations: (010) DFT(PBE)-D3; 298K

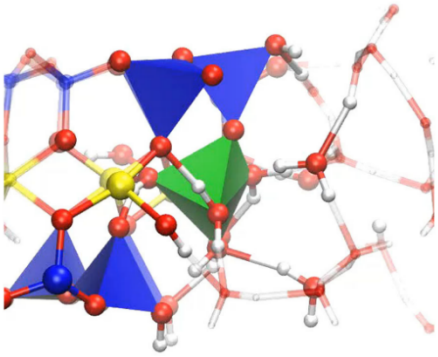

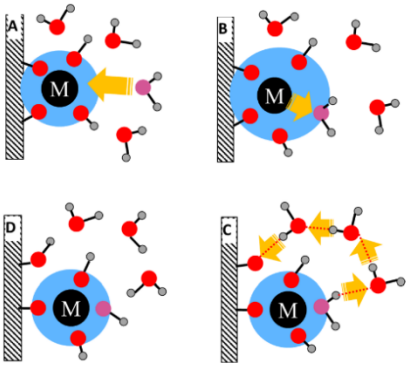

Complex multistep reaction kinetics:

- Step by step changes of dentisity;
- Solvent exchange;
- Several concurrent reaction pathways;

Schliemann & Churakov (2021) Geochim Cosm. Acta. 293, 438-460; Schliemann & Churakov (2021) Geochim Cosm. Acta. 307, 42-55.

Model parameter uncertainties

- "Synthetic datasets" by randomly sampling from a distributions according to the error intervals
- "Repeat the parameter estimation" → **standard deviation & mean**

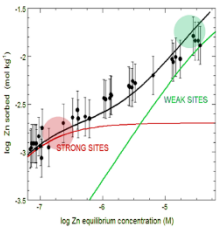

Uncertainities estimate Ni sorption sites on Illite

	Fit by eye	GEMSFITS
Surface complexation on strong sites		$\log {}^{SC}K$
$=^{S}SOH + Ni^{2+} \leftrightarrows =^{S}SONi^{+} + H^{+}$	0.6	0.76 ±0.05
$=^{S}SOH + Ni^{2+} + H_2O \leftrightarrows =^{S}SONiOH^{0} + 2H^{+}$	-8.4	-8.21 ±0.24
$=^{S}SOH + Ni^{2+} + 2H_2O \leftrightarrows =^{S}SONi(OH)_2^{-} + 3H^{+}$	-18.0	-17.96 ±0.13
Surface complexation on weak sites		
$=^{W1}SOH + Ni^{2+} \leftrightarrows =^{W1}SONi^{+} + H^{+}$	-1.8	-1.84 ±0.14
Cation exchange on planar sites		$\log K_{ex}$
$2Na\text{-}IdP + Ni^{2+} \leftrightarrows Ni\text{-}IdP + 2Na^{+}$	1.04	0.44 ±0.09

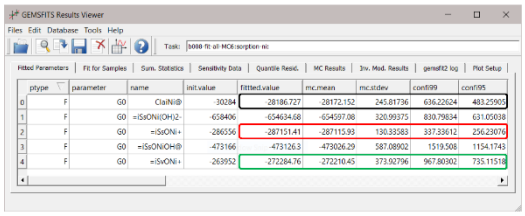

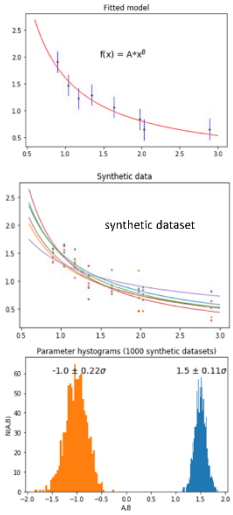

Anderson, G. M., 1976. Error propagation by Monte Carlo method in geochemical calculations. Bradbury and Baeyens (2009); [2] Marques Fernandes et al. (2015)

Curtesy of Dan Miron

Generalised bottom up approach for RN uptake

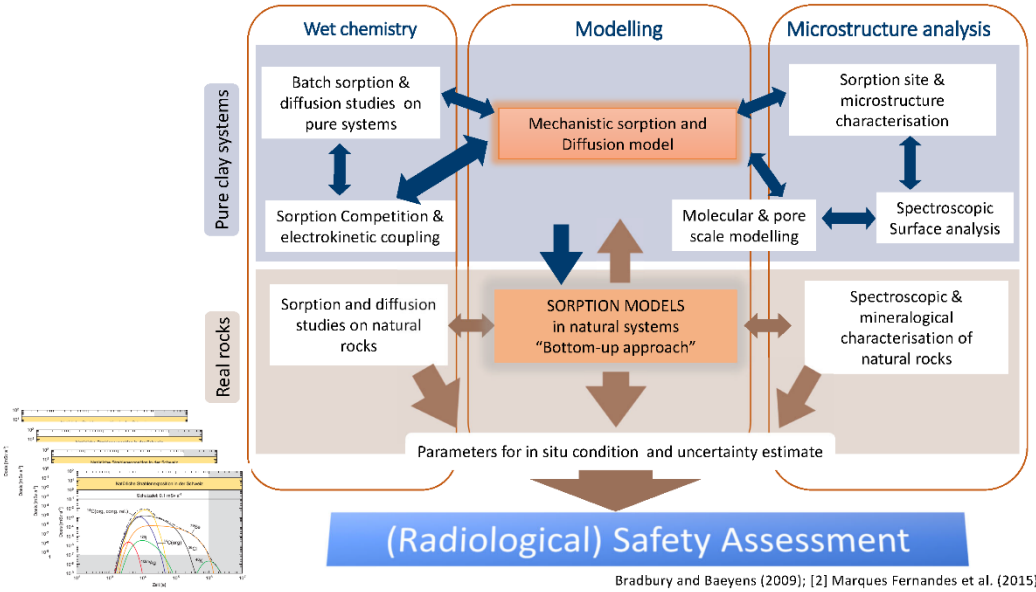

Bradbury and Baeyens (2009); [2] Marques Fernandes et al. (2015)

Derivation of sorption databases for safety assesment

Ni trace sorption edge on illite

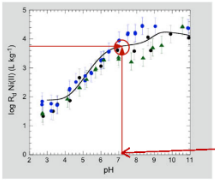

Opalinus Clay mineralogy

Mineral	wt.%
Illite	24
Illite/smectite mixed layer	9
Chlorite	9
Kaolinite	18
Quartz	20
Calcite	13
Dolomite + ankerite	0.4
K-Feldspar	2
Plagioclase	0.9
Siderite	4
Pyrite	1

Opalinus Clay porewater

Parameter	
pH	7.20
log pCO_2 (bar)	-2.20
Ionic strength (M)	0.23
Dissolved constituents(M)	
Na	1.64×10^{-1}
K	2.60×10^{-3}
Mg	9.65×10^{-3}
Ca	1.25×10^{-2}
Cl	1.60×10^{-1}
HCO_3/CO_3	2.51×10^{-3}
SO_4	2.47×10^{-2}
Si	1.78×10^{-4}

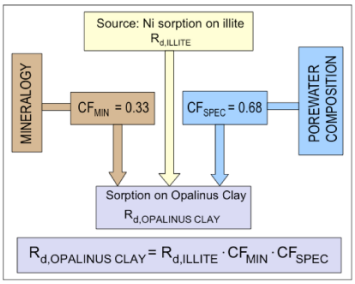

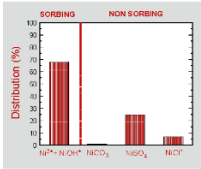

$$D_a^i = \frac{D_e^i}{\varepsilon + \rho_{bd} K_d^i}$$

Major parameters variability:

- Pore water chemistry & in situ conditions
- Mineralogical composition variations
- Reversibility and kinetics
- **Model parameter uncertainty**

Bradbury and Baeyens (2009);

Summary an outlook

- High quality experimental data are the basis for the development of the mechanistic sorption models
- Good understanding of sorption mechanism for uptake of monovalent and divalent cations as well as some actinides has been obtained by molecular simulations and spectroscopy
- Combination of molecular spectroscopy and simulations is particularly important for discrimination of co-existing surface complexes on different surfaces
- Further application and development of molecular simulations should allow for direct estimation of the sorption complexation constants

3.7 Lecture 7 - Modelling of kinetically controlled processes in radioactive waste disposal, from radiolytic corrosion to microbial activity

Reactive transport modelling (RTM) has been important for assessing the long-term performance of the geologic disposal of radioactive waste. RTM is capable of great generality since it can be applied to a wide range of natural processes, as well as to engineering issues such as metal corrosion or bentonite alteration. This requires an understanding how the various barriers evolve through space and time. Mass transfers are often driven by diffusion or very slow advective flows, which allows to model the geochemical reactions under thermodynamic equilibrium. But some key slow processes intrinsically remain under a kinetic control.

In a first stage, we will recall the main kinetic rate laws that are commonly used for RTM, such as the transition state theory with catalytic or inhibiting effects, Arrhenius dependency with temperature or the Monod microbial kinetic laws. We will also focus on the importance of reactive surfaces for heterogenous solid/liquid kinetics. Then we will introduce more specialized kinetic models, such as glass dissolution with passivating altered layer. Eventually, we will give an overview of kinetic databases.

In a second stage, we will study RTM applications where kinetics plays a key role using the reactive transport code HYTEC: 1) the radiolytic auto-dissolution of spent nuclear fuels driven by oxidants produced by the irradiation of water, 2) the corrosion of carbon steel canister driven by sulfato-reducing bacteria, 3) the long-term coupled evolution of the glass / steel / cement / claystone multi-barrier in a disposal cell.

Lecturer

L. De Windt, Mines Paris, France

Reading Material

Brantley, S.L., Kubicki, J.D., White, A.F. (2008). Kinetics of Water-Rock Interaction, Springer-Verlag (New York, US).

De Windt, L., Spycher, N. (2019). Reactive transport modeling: a key performance assessment tool for the geologic disposal of nuclear waste, Elements Vol. 15, 99.

van der Lee, J., De Windt, L., Lagneau, V., Goblet, P. (2003). Module-oriented modeling of reactive transport with HYTEC, Computers and Geosciences 29, 265.

Slides

TRAINING COURSE: Geochemical & RT Modeling for Geological Disposal

Bern, 06 – 10 Feb 2023

Modelling of kinetically controlled processes in radioactive waste disposal: from radiolytic corrosion to microbial activity

Laurent De Windt

1

Academics

2

Geosciences Dpt., Paris School of Mines (F)

Applied geochemistry
radioactive waste disposal and environmental chemistry (DISCO, ACED European Projects)

Reactive transport modeling (RTM) code
HYTEC

Dewindtite crystal

$Pb_3(H(UO_2)_3O_2(PO_4)_2)_2 \cdot 12H_2O$

Phosphate family,
named by Professor M.A. Schoep of the University of Ghent (Belgium) in memory of his student Jean DeWindt-
a distant cousin?, drowned in Lake Tanganyika in Congo.

Cr Acad Sci Paris 174 (1922)

Outlines

3 MINES PARIS

1. **Context: kinetics and radwaste diposals**

2. **Main kinetic laws commonly used for RTM**
   a. Mineral dissolution/precipitation with catalytic or inhibiting effects
   b. Reactive surfaces
   c. Arrhenius dependency with temperature
   d. Monod microbial kinetics
   e. Sources of kinetic data

3. **Examples of application to radwaste disposals**
   a. Glass / steel / cement / claystone multi-barrier
   b. Radiolytic dissolution of spent nuclear fuels
   c. Steel corrosion driven by sulfato-reducing bacteria

A few readings

4 MINES PARIS

Geochemical kinetics
Brantley, S.L., Kubicki, J.D., White, A.F. (2008). Kinetics of Water-Rock Interaction, Springer-Verlag (New York, US).

among many other very good books

Application of RTM to radwaste disposals
De Windt, L., Spycher, N. (2019). Reactive transport modeling: a key performance assessment tool for the geologic disposal of nuclear waste, Elements Vol. 15, 99.

The HYTEC RTM code
van der Lee, J., De Windt, L., Lagneau, V., Goblet, P. (2003). Module-oriented modeling of reactive transport with HYTEC, Computers and Geosciences 29, 265.

Context

RTM and radwaste disposals

5 MINES PARIS

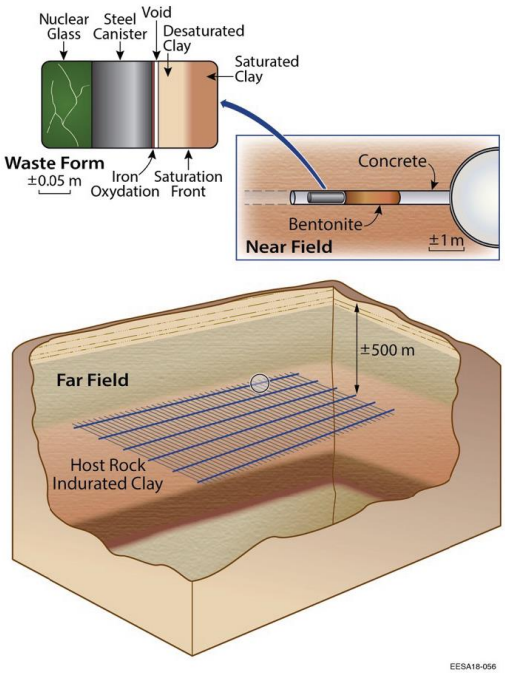

- Reactive transport modelling (RTM) are important for assessing the long-term performance of the geologic disposal of radioactive waste
- RTM can be applied to a wide range of natural processes, as well as to engineering issues such as metal corrosion or bentonite alteration
- This requires an understanding how the various barriers evolve through space and time

De Windt et al. (2019), Elements

Context

Typical processes that need kinetic modeling

6 MINES PARIS

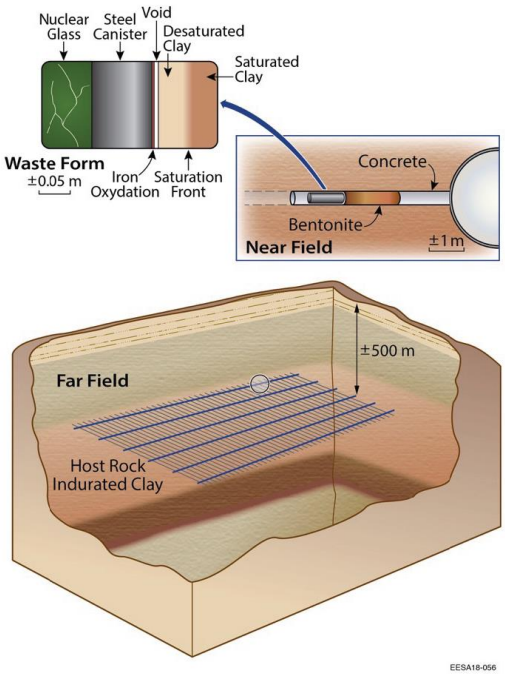

- Mass transfers are often driven by diffusion or very slow advective flows, which allows to model the geochemical reactions under thermodynamic equilibrium; i.e. the "characteristic time" is long
- But some key slow processes intrinsically remain under a kinetic control, such as
  - Vitrified wastes (nuclear glasses) due to their amorphous state
  - Corrosion of metals that are never stable in water, e.g. Mg(0) and Fe(0)
  - Radiolytic-enhanced processes
  - Microbially-driven reactivity
  - To a lesser extent: clay dissolution, cement carbonation or hydration

Kinetics in RTM

Mineral dissolution

7 MINES PARIS

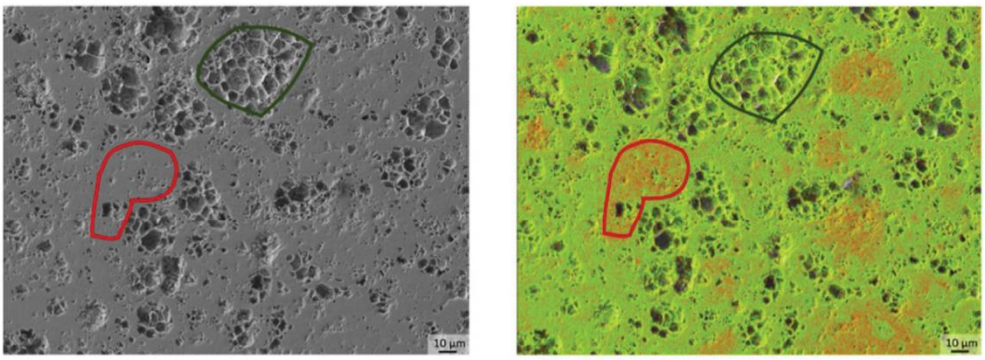

SEM image of a heterogeneous MOx fuel $U_{1-x}Pu_xO_2$
after leaching in carbonated water;

the corrosion pits corresponds to the UO_2-enriched zones whereas PuO_2-aggregates remain stable

Kinetic notions of reactive surface, thermodynamic effects, influence of the solution

Kerleger et al. (2020), JNM

Kinetics in RTM

Mineral dissolution

8 MINES PARIS

"Transition state theory" with catalytic or inhibiting effects

$$\frac{d[M]}{dt} = -kA_v$$

[M] = mineral concentration [mol/L]
k = intrinsic kinetic rate constant [mol/m²/s]
A_v = volumic reactive surface area [m²/L]

$$\frac{d[M]}{dt} = kA_v\left(\left(\frac{Q}{K_s}\right)^p - 1\right)$$

Q = Ion Activity Products
K_s = thermodynamic equilibrium constant
p = empirical fitted parameter

$$\frac{d[M]}{dt} = kA_v\prod_i (A_i)^{a_i}\left(\left(\frac{Q}{K_s}\right)^p - 1\right)$$

"Catalyst" if a_i is positive
or "inhibitor" if a_i is negative
Can combine several dependencies

Example: calcite dissolution in acidic media

$$\frac{d[M]}{dt} = kA_v(H^+)^1\left(\left(\frac{(Ca^{2+})(CO_3^{2-})}{K_{Calcite}}\right) - 1\right)$$

Kinetics in RTM
Mineral dissolution

9 MINES PARIS

"Transition state theory" with catalytic or inhibiting effects

$$\frac{d[M]}{dt} = -kA_v$$

Mineral dependency
Heterogeneous kinetics, surface controlled

$$\frac{d[M]}{dt} = kA_v\left(\left(\frac{Q}{K_s}\right)^p - 1\right)$$

Thermodynamic equilibrium dependency

$$(\Omega - 1) \quad \left(\exp\left(\frac{\Delta G}{RT}\right) - 1\right)$$

$$\frac{d[M]}{dt} = kA_v\prod_i (A_i)^{a_i}\left(\left(\frac{Q}{K_s}\right)^p - 1\right)$$

Aqueous solution dependency

Example: calcite dissolution in acidic media

$$\frac{d[M]}{dt} = kA_v(H^+)^1\left(\left(\frac{(Ca^{2+})(CO_3^{2-})}{K_{Calcite}}\right) - 1\right)$$

Kinetics in RTM
Mineral dissolution

10 MINES PARIS

$$CaCO_{3(s)} + H^+_{(aq)} = Ca^{2+}_{(aq)} + HCO^-_{3(aq)} \qquad r = k_1 a_{H^+}$$

$$CaCO_{3(s)} + H_2CO_{3(aq)} = Ca^{2+}_{(aq)} + 2HCO^-_{3(aq)} \qquad r = k_2 a_{H_2CO_3^*}$$

$$CaCO_{3(s)} + H_2O_{(aq)} = Ca^{2+}_{(aq)} + HCO^-_{3(aq)} + OH^-_{(aq)} \qquad r = k_3 a_{H_2O}$$

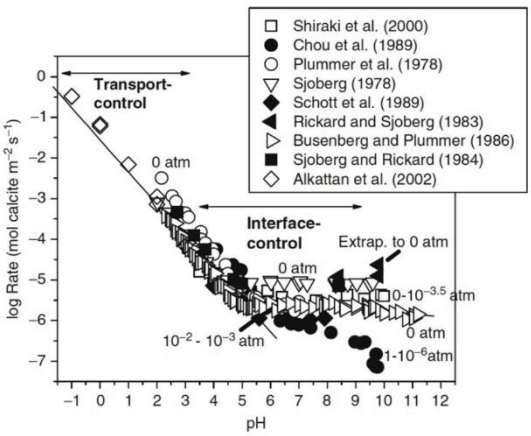

Kinetics of calcite dissolution vs. the chemistry of the solution

In Brantley et al. (2008)

Kinetics in RTM
Mineral dissolution

11 MINES PARIS

$$r = k_H a_{H^+}^n + k_{OH} a_{OH^-}^m$$

Kinetics of albite ($NaAlSi_3O_8$) dissolution vs. the pH of the solution

$$r = k_H [\equiv SOH_2^+]^{q_1} + = k_{OH} [\equiv SO^-]^{q_2}$$

Assumption of a control by surface sites

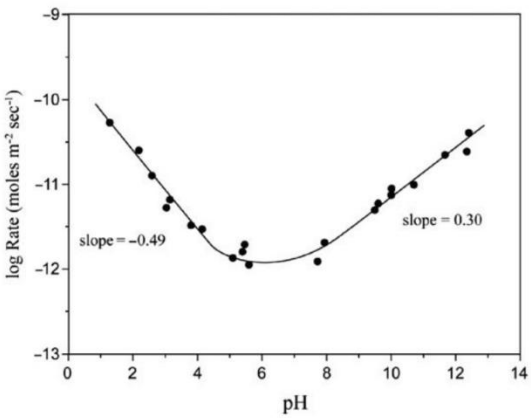

In Brantley et al. (2008)

Kinetics in RTM
Mineral dissolution

12 MINES PARIS

Kinetics of Al_2O_3 dissolution vs. the nature of the ligand L in solution

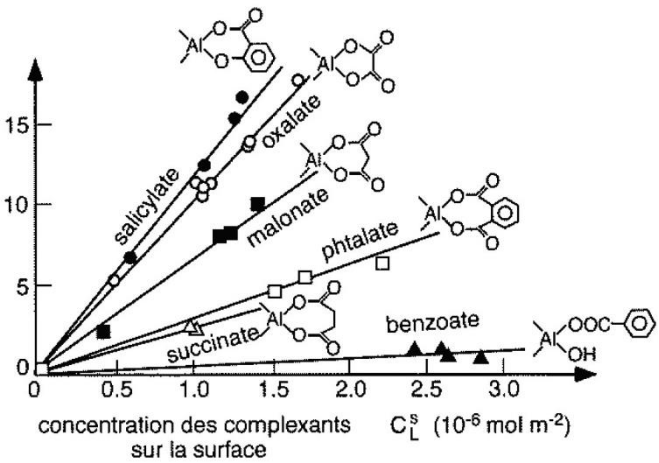

$$\frac{d[M]}{dt} = k_L [\equiv Al - L]$$

In Sigg et al. (2014)

Kinetics in RTM

Reactive surface

13 MINES PARIS

$$\frac{d[M]}{dt} = kA_v\left(\left(\frac{Q}{K_s}\right)^p - 1\right)$$

$$A_v = A_s[M] \longleftrightarrow A_s = \frac{3}{\rho r}$$

Specific surface [m²/g ; m²/mol]
Homogeneous suspension of spherical particles with constant radius

Alternative evolution of surfaces

$$A = A_0\left(\frac{M_0}{M}\right)^{\frac{2}{3}}$$

Reactive surface increases while the spherical particles dissolves

$$A = constant$$

Dissolution progressing in depth along the full surface

Kinetics in RTM

Reactive surface

14 MINES PARIS

Alternative evolution of surfaces (cond't)

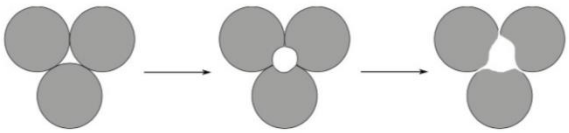

Dissolution in a porous media

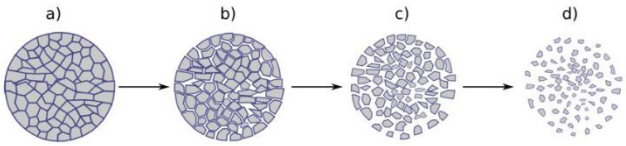

Dissolution of ceramic-like solid (e.g. UOx fuel)

Important to discriminate between
- calculated geometric surface
- BET measured surfaces, i.e. surface roughness

Kinetics in RTM

Mineral precipitation

15 MINES PARIS

- Very often, one assumes that the dissolution law can be "reversed"

$$\frac{d[M]}{dt} = kA_v\left(\left(\frac{Q}{K_s}\right)^p - 1\right)$$

Q > Ks, i.e. positive sign (formation) with a thermodynamic effect: the further from equilibrium, the faster the reaction

A minimum (nucleus) surface can be provided

- The correct theory of precipitation kinetics is complex and not always operational for "real" applications, e.g.
  - nucleation barrier vs. critical oversaturation Ω_c
  - homogenous vs. heterogeneous nucleation, then crystal growth

Kinetics in RTM

Mineral precipitation

16 MINES PARIS

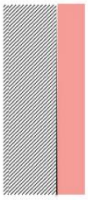

Epitaxial linear growth

$$\frac{d[Toberm]}{dt} = k\,A_v\,(\Omega - 1)$$

$$\longrightarrow \frac{d[Toberm]}{dt} = k\,A_v$$

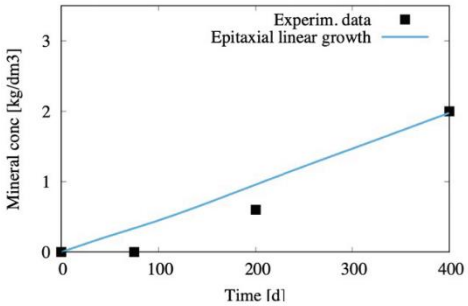

Example: precipitation of tobermorite (crystallized C-S-H) at the cement/clay interface at 70°

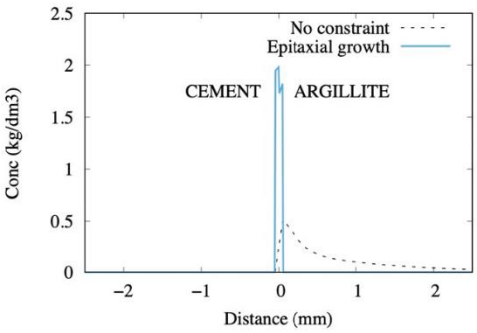

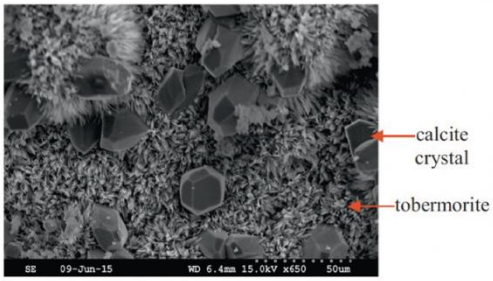

Lalan et al. CCR (2019)

Kinetics in RTM

Arrhenius law

17 MINES PARIS

- The speed of a reaction generally increases with the temperature

$$k(T) = A \exp\left(\frac{-E_A}{RT}\right)$$

k = intrinsic kinetic rate constant [mol/m²/s]
A = pre-exponential factor
E_A = activation energy [kJ/mol]
T in °K

- More operational formulation

$$\lg k_T = \lg k_{T_0} - \frac{E_a}{2{,}3R}\left(\frac{1}{T} - \frac{1}{T_0}\right)$$

EA [kJ/mol]	Diffusion in water	Diffusion in solids	Fe corrosion	Clay dissolution	Quartz dissolution
Approxim.	20	500	25	60	90

Kinetics in RTM

Microbial kinetics

18 MINES PARIS

The presence of micro-organisms catalyzes reactions

Microbiologically-mediated multistep reactions

Monod equations, derived from enzyme catalysis laws (Michaelis Menten)

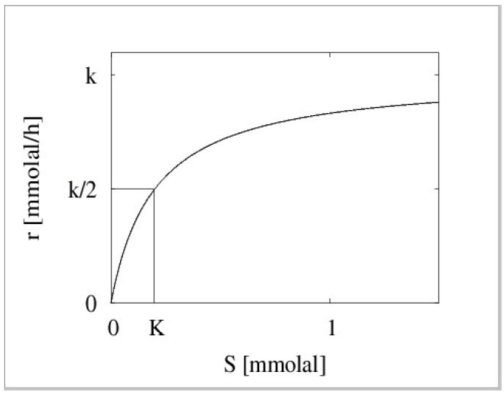

$$M = \prod_k \left(\frac{S_k^{a_k}}{K_k^{a_k} + S_k^{a_k}}\right)^{b_k}$$

when S << K, rate ∝ [S]

when S >> K, maximum constant rate

K = half of the maximum constant rate

Kinetics in RTM

Microbial kinetics

19 MINES PARIS

Ex.: methanogen bacteria $CO_2 + 4\ H_2 \rightarrow CH_4 + 2\ H_2O$

$$r = k\left(\frac{[H_2]}{[H_2]+K_D}\right)$$

Catalyzed

$$r = k'[B]\left(\frac{[H_2]}{[H_2]+K_D}\right)$$

Catalyzed and population growth
B is the active biomass

$$r = k'[B]\left(\frac{[H_2]}{[H_2]+K_D}\right)\left(\frac{K_I}{[CH_4]+K_I}\right)$$

Catalyzed, population growth, and inhibition (poison)

Kinetics in RTM

Microbial kinetics

20 MINES PARIS

Anabolism= growth and then sustainability of the biomass vs. death (steady state)

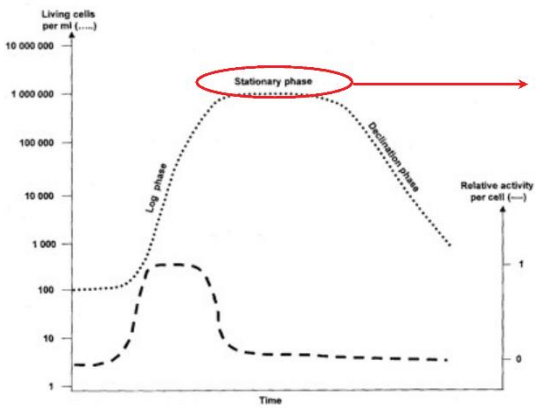

$$r = k'[B]\left(\frac{[H_2]}{[H_2]+K_D}\right)$$

Biofilm = bacterial community, contained in a matrix of exopolymers, adhering to a surface

Kinetics in RTM

Source of kinetic data

21 MINES PARIS

Mostly from individual papers from the literature

Brantley, Kubicki, White (2008). Kinetics of Water-Rock Interaction, Springer-Verlag (New York, US).

Palandri & Kharaka, Y. K. (2004). *A compilation of rate parameters of water-mineral interaction kinetics for application to geochemical modeling*. REPORT 2004-1068, Geological Survey Menlo Park CA.

Table 29. Clay Group Mineral Dissolution Rate Parameters.

	Acid Mechanism			Neutral Mechanism		Base Mechanism		
	[a]log k	[b]E	[c]n	[a]log k	[b]E	[a]log k	[b]E	[c]n
kaolinite	-11.31	65.9	0.777	-13.18	22.2	-17.05	17.9	-0.472
[d]montmorillonite	-12.71	48.0	0.220	-14.41	48.0	-14.41	48.	-0.130
[e]smecite	-10.98	23.6	0.340	-12.78	35.0	-16.52	58.9	-0.400

Marty et al. (2015). A database of dissolution and precipitation rates for clay-rocks minerals, *Applied Geochemistry* 55.

Outlines

22 MINES PARIS

1. **Context: kinetics and radwaste diposals**

2. **Main kinetic laws commonly used for RTM**
   a. Mineral dissolution/precipitation with catalytic or inhibiting effects
   b. Reactive surfaces
   c. Arrhenius dependency with temperature
   d. Monod microbial kinetics
   e. Sources of kinetic data

3. **Examples of application to radwaste disposals**
   a. Glass / steel / cement / claystone multi-barrier
   b. Radiolytic dissolution of spent nuclear fuels
   c. Steel corrosion driven by sulfato-reducing bacteria

Long-term evolution of multi-barrier

Generic configuration

23 MINES PARIS

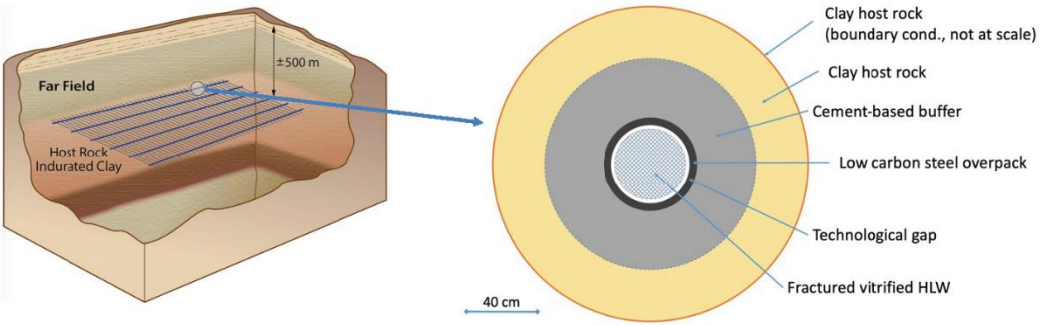

Long-term evolution of multi-barrier

Modeling approach

24 MINES PARIS

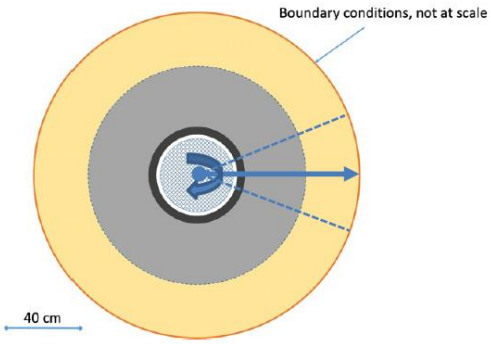

Reactive transport modeling with HYTEC (De Windt, Elements, 2019)

- **thermodynamics** (ThermoChimie) + kinetics ==> 150 aqueous species, 35 minerals, 20 sorption sites
- **1D – radial** (axi-symmetry)
- **diffusion**-driven (with & **without porosity/D_{eff} evolution**)
- **water-saturated** conditions
- (non)-**isothermal** conditions

- **PA sensitivity** analysis on
  - buffer thickness 5 – **30** – 100 **cm**
  - buffer composition **CEM I – concrete** vs. cement/bentonite grout

Long-term evolution of multi-barrier
Clay and cement-type materials

25 MINES PARIS

Callovo-Oxfordian claystone (Marty et al., 2015)

- carbonate/clay/quartz – **pH = 7**
- **low** porosity (18%) and diffusion coeff D_{eff} ($3x10^{-11}$ m^2/s)

CEM I concrete (Kosakowski, 2020) – **30 cm**

- CEM I + limestone aggregates (>70 vol%) – **pH > 13**
- **low** porosity (11%) and diffusion coeff D_{eff} ($1x10^{-11}$ m^2/s)

$$\frac{d[M]}{dt} = \left(-k_{OH}\,(OH^-)^n - k_{neutral}\right)\left(1 - \frac{Q}{K_s}\right)$$

Kinetic coupling: cement/clay interactions will slow down when pH will decrease

Long-term evolution of multi-barrier
Carbon-steel overpack

26 MINES PARIS

Generalized anaerobic corrosion

- Fe(0) – **5 cm** thick
- "breaching" when non-corroded thickness < 1.5 cm (ACED)
- empirical kinetic rate pH-dependent

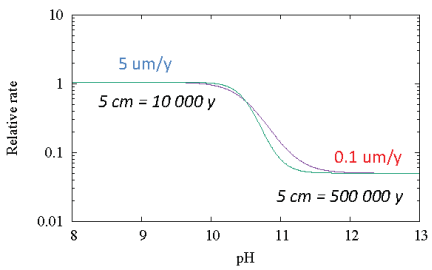

Corrosion will speed up when pH will decrease

Steel corrosion products

- Fe-oxides, e.g. **goethite, magnetite**
- Fe-carbonates, e.g. **siderite**
- Fe-silicates, e.g. **greenalite**
- *(Fe-sulfides, e.g. mackinawite, not included)*

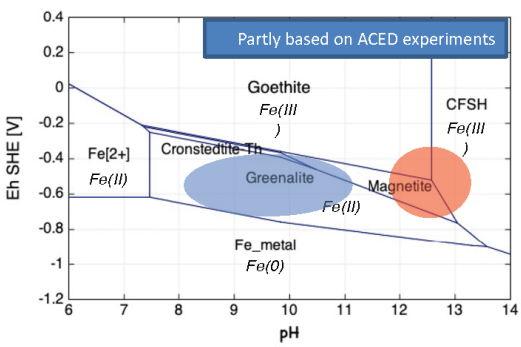

Long-term evolution of multi-barrier
Nuclear Glass

27 MINES PARIS

Borosilicate International Simple **Glass ISG**

Empirical kinetic rate law initial (**CEA papers** and De Windt, MRS, 2006)

$$\frac{d[glass]}{dt} = r_o(T, pH, Si) - r_{residual}(T)$$
$$= -k_{0,pH}\,(H^+)^{-0.4}\,A_v\left(1 - \frac{C_{Si}}{C^*_{Si}}\right) - k_r\,A_v$$

Dissolution will slow down when pH will decrease

Glass dissolution sustained by the environment

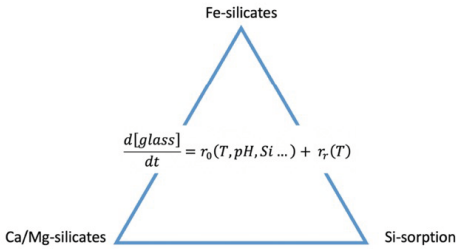

- Operational for 5.0 ≤ pH ≤ 10.5, T = 25 – 90 °C
- Cracking ratio of the glass block

Long-term evolution of multi-barrier
Glass/steel/cement/claystone – 30 cm & 40 000 years

28 MINES PARIS

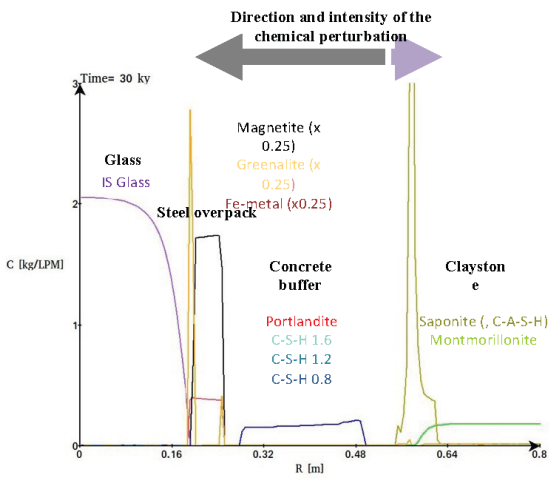

Not all minerals shown; modeling still in progress, rather pessimistic for ISG

1. **Main driving force of the whole system is the cement phase degradation by the clay host-rock**
2. The lost of high-pH conditions leads to the speed-up of C-steel corrosion
3. Overpack breaching leads to the income of aqueous solution in contact with the nuclear glass, which releases Boron; Fe(0)/Fe-silicates sustains glass dissolution

Long-term evolution of multi-barrier

Comment on the C-steel overpack

29 MINES PARIS

C-STEEL OVERPACK

- Corrosion rate is significantly enhanced only when C-S-H 0.8 becomes predominant
- Corrosion products zonation:
  - Glass/steel => Fe(II)-silicate
  - Inner zones => magnetite
  - Steel/degraded-concrete => Fe(II)-silicate (siderite)
- Possibility of clogging by the corrosion products

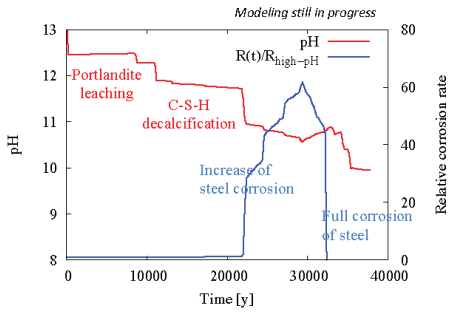

Evolution with time at the steel/cement interface

Radiolytic dissolution of spent-fuel

Disposal cell and experimental set-up

30 MINES PARIS

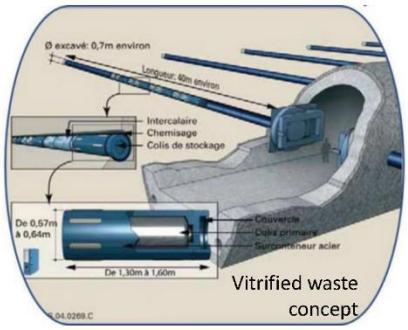

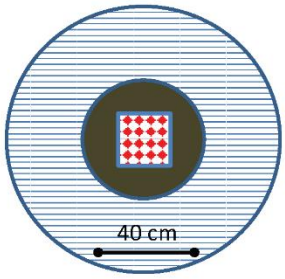

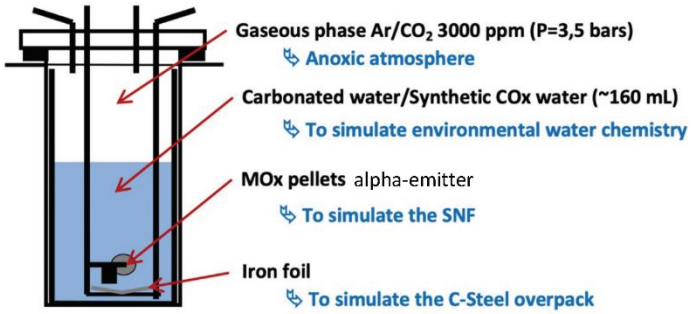

Radiolytic dissolution of spent-fuel

Main processes

31 MINES PARIS

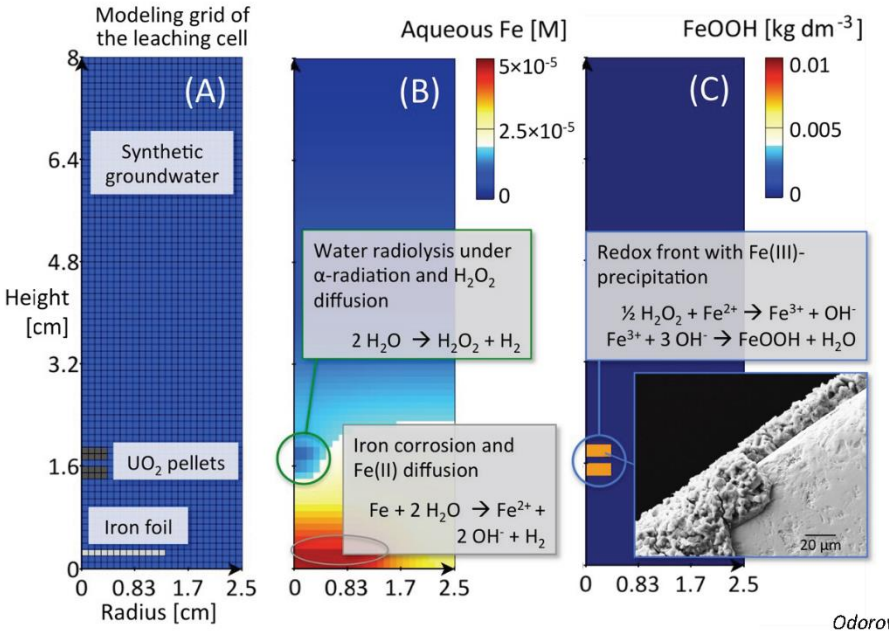

Odorowski et al. GCA (2017)

Radiolytic dissolution of spent-fuel

Kinetic laws

32 MINES PARIS

Kinetics constraints

H_2O_2 alpha-radiolytic production

$$\frac{d[H_2O_2(aq)]}{dt} = +k_{rad} \times A_{MOx}$$

H_2O_2 disproportionation on the pellet surfaces

$$\frac{d[H_2O_2(aq)]}{dt} = -k_{dispMOx} \times A_{UOx} \times [H_2O_2(aq)]$$

$$H_2O_2 => H_2O + 0.5O_2$$

UOx oxidation by H_2O_2

$$\frac{d[\mathbf{U}Ox]}{dt} = -k_{ox}^{H_2O_2} \times A_{UOx} \times [H_2O_2(aq)]$$

$$UO_2 + 2H^+ + H_2O_2(aq) \rightarrow UO_2^{2+} + 2H_2O$$

UOx dissolution under reducing conditions

$$\frac{d[\mathbf{U}Ox]}{dt} = -k_{red} \times A_{UOx}$$

$$UO_2 + H_2O \rightleftharpoons U(OH)_4(aq)$$

Anoxic iron corrosion by water

$$\frac{d[Fe]}{dt} = -k_{anox} \times A_{\mathbf{Fe}}$$

$$Fe + 2H_2O \rightarrow Fe^{2+} + 2OH^- + H_2(aq)$$

Radiolytic dissolution of spent-fuel

Examples of modeling results (COx + metallic iron)

33

MINES PARIS

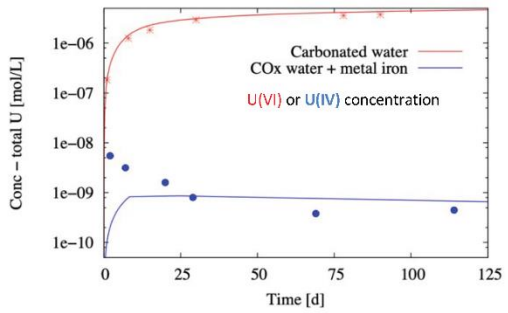

$$\frac{1}{2}H_2O_2 + Fe^{2+} \rightarrow Fe^{3+} + OH^-$$

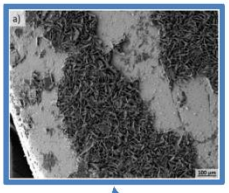

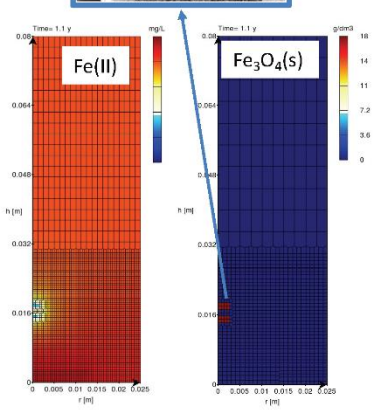

- **Full scavenging** of radiolytic oxidants by Fe(II), redox front location at the MOX pellets, magnetite precipitation

Radiolytic dissolution of spent-fuel

Location of the redox front

34

MINES PARIS

Dissolved Fe(II)

Dissolved H_2O_2

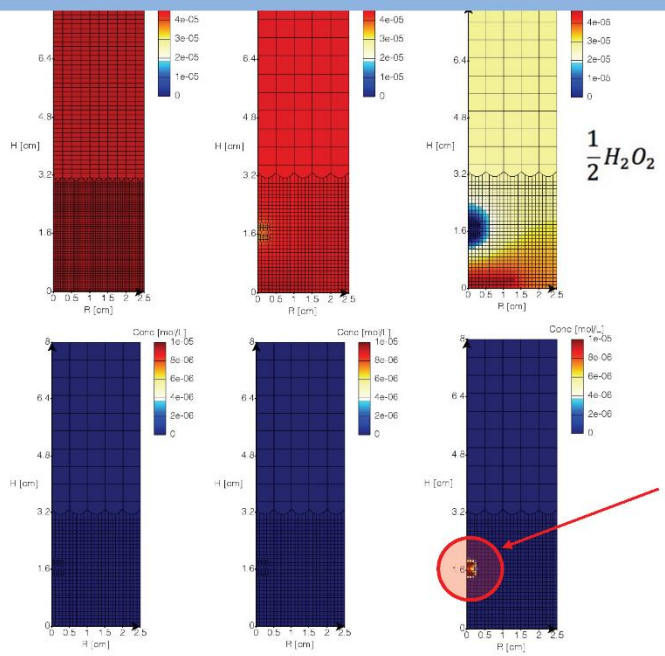

$$\frac{1}{2}H_2O_2 + Fe^{2+} \rightarrow Fe^{3+} + OH^-$$

Zone of MOX oxidation and U(VI) release

Increase of the H_2O_2 production rate

Bio-corrosion of steel

Experimental set-up

35 MINES PARIS

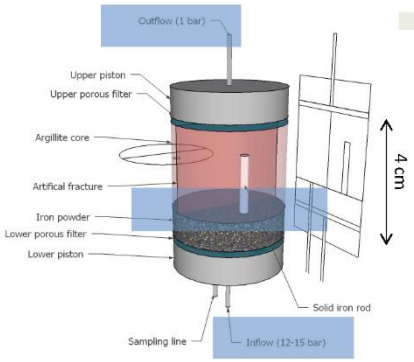

Materials + heterogeneities

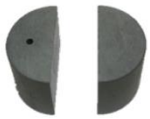

Artificially cracked Tournemire argillite (Tournemire URL)

Massive iron rod

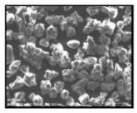

Iron powder (< 60 µm)

- Bacteria initially inoculated and then sampled at the powder/argillite interface
  - thermophilic, anaerobic and hydrogenotrophic
  - SRB: $SO_4^{2-} + 4\,H_2 \rightarrow HS^- + 3\,H_2O + OH^-$ *Thermodesulfovibrio hydrogeniphilus*

Chautard et al (2012), Proc. Chem.

Bio-corrosion of steel

Modeling of BSR activity and pore water chemistry

36 MINES PARIS

$$SO_4^{2-} + 4\,H_2 \rightarrow HS^- + 3\,H_2O + OH^-$$

$$r_{BSR} = k\,[B] \times \left(\frac{[H_2]}{[H_2] + K_D}\right)\left(\frac{[SO_4]}{[SO_4] + K_A}\right)$$

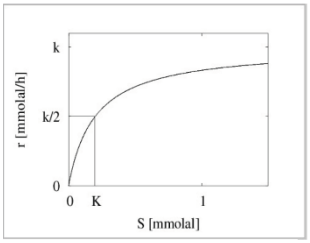

Monod-like kinetics

Species	Pore water	KA, KD
SO_4	≈ 11 mmol/L	(0.05 mmol/L)
H_2	After corrosion ≥ 100 mmol/L	(0.005 mmol/L)

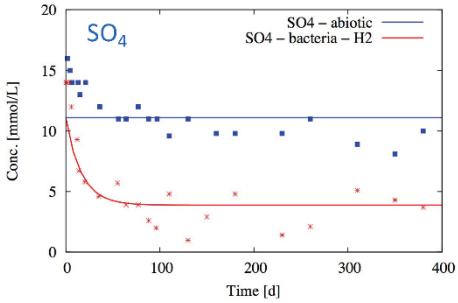

Inverse modeling on BSR rate r_{BSR}

	Time [day]	SO4 consumption rate [mmol.L^{-1}.d^{-1}]
With bacteria(*)	0 – 100	2.1
	100 – 300	1.6
	300 – 400	0.5

Bio-corrosion of steel

Observed corrosion products

37 MINES PARIS

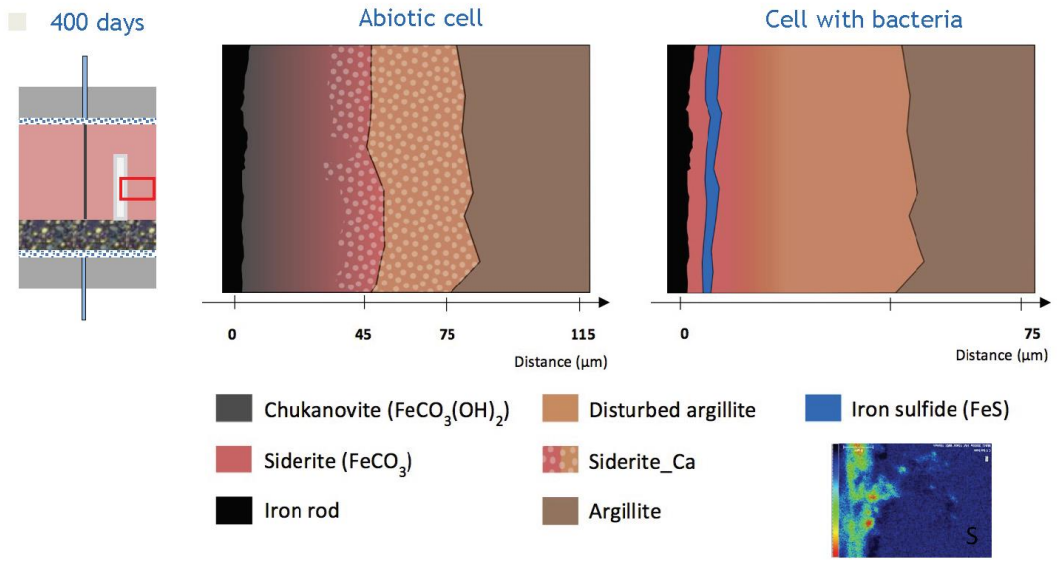

Bio-corrosion of steel

Modeling of corrosion processes

38 MINES PARIS

Magnetite = kinetics

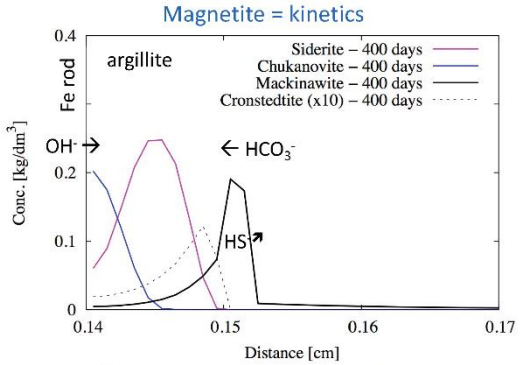

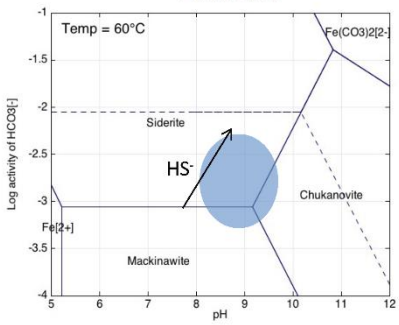

(1) rod/argillite proximity => carbonated corrosion products

(2) Reducing D_{eff} in the corrosion layer => spatial segregation of OH^- source (rod) and HCO_3 source (argillite) => $Fe_2(OH)_2CO_3$ and $FeCO_3$

(3) BSR activity => FeS precipitation and increase in siderite stability

With bacteria

Concluding remark

The unusual timeframe of radwaste disposal for humanity

39 MINES PARIS

@Geluck

Outlines

40 MINES PARIS

1. **Context: kinetics and radwaste diposals**

2. **Main kinetic laws commonly used for RTM**
   a. Mineral dissolution/precipitation with catalytic or inhibiting effects
   b. Reactive surfaces
   c. Arrhenius dependency with temperature
   d. Monod microbial kinetics
   e. Sources of kinetic data

3. **Examples of application to radwaste disposals**
   a. Glass / steel / cement / claystone multi-barrier
   b. Radiolytic dissolution of spent nuclear fuels
   c. Steel corrosion driven by sulfato-reducing bacteria

3.8 Lecture 8 - Integration of processes at larger scale – sensitivity (uncertainty) analyses

This lecture will present:

1) Conceptual and numerical reactive transport models for HLW radioactive waste disposal at the disposal cell scale. The reactive transport models simulate the geochemical evolution of HLW disposal cells in granite and clay for a time span of 50,000 years. The model considers the vitrified waste, the carbon-steel canister, the saturated bentonite buffer and the host rock. These models have been performed within the context of the ACED Work Package of the EURAD Joint Project.

2) Local sensitivity analyses of model predictions: methods and results.

3) Global sensitivity analyses: description of the methods and results obtained with the VARS (Variogram Analysis of Response Surface) method. These results have been obtained within the context of the DONUT Work Package of the EURAD Joint Project

4) Ongoing international initiatives (JOSA Group

Lecturer

Javier Samper, University of A Coruña, Spain

Reading Material

Claret, F, A Dauzeres, D Jacques, P Sellin, B Cochepin, L De Windt, J Garibay-Rodriguez, J Govaerts, O Leupin, A Mon, L Montenegro, V Montoya, N I. Prasianakis, J Samper & J Talandier, (2022). Modelling of the long-term evolution and performance of engi-neered barrier system, EPJ Nuclear Sci. Technol. 8, 41. https://doi.org/10.1051/epjn/2022038.

Claret, F., J Samper, J Samper II, AC Samper, A Mon, B Pisani, C López, C Yang, (2023). UDC Contribution to the "Report describing numerical improvement and developments and their application to treat uncertainty when dealing with coupled processes". WP DONUT. EURAD Joint Program. Deliverable D4.7 of the EURAD Joint Project. EC Grant Agreement no: 847593

JOSA: Uncertainty Quantification and Sensitivity Analysis in Geologial Disposal: Joint Sensitivity Group (JOSA) Group: Volume 1. https://www.osti.gov/servlets/purl/1822591.

Mon, A, J Samper, L Montenegro, A Naves, & J Fernández, (2017). Long-term nonisothermal reactive transport model of compacted bentonite, concrete and corrosion products in a HLW repository in clay, J Cont Hydrol, Vol 197: 1-16. http://dx.doi.org/10.1016/j.jconhyd.2016.12.006.

Mon, A, J. Samper, L Montenegro, E Torres, MJ Turrero, J Cuevas, & L De Windt, (2023). Reactive transport models of geochemical interactions at the iron/bentonite interface in lab corrosion tests, Applied Clay Sciences, (submitted).

Samper, J., L. Montenegro, L. De Windt, V. Montoya, J. Garibay-Rodríguez, D. Grigaliuniene, A. Narkuniene, & P. Poskas, (2021). Conceptual model formulation for a mechanistic based model implementing the initial SOTA knowledge (models and parameters) in existing numerical tools. Deliverable D2.16 of the EURAD Joint Project. EC Grant Agreement no: 847593.

Slides

UNIVERSIDADE DA CORUÑA

EURAD Training
Geochemical & Reactive Transport Modelling for Geological Disposal training

eurad
European Joint Programme on Radioactive Waste Management

LECTURE 8: INTEGRATION OF PROCESSES AT LARGER SCALE – SENSITIVITY (UNCERTAINTY) ANALYSES

Javier Samper

University of A Coruña
j.samper@udc.es

This project has received funding from the European Union's Horizon 2020 research and innovation programme 2014-2018 under grant agreement N°847593

UNIVERSIDADE DA CORUÑA

EURAD Training
Geochemical & Reactive Transport Modelling for Geological Disposal training

INTRODUCTION & MOTIVATION

- **The conceptual bases of the geochemical and reactive transport models for geological disposal are developed from lab and in situ tests**
- **Reactive transport models often integrate many thermal, hydrodynamic and chemical processes**
- **Models constructed from lab and in situ tests must be scaled up to the scale of the disposal cell**
- **Numerical models are simplified representations of some parts of the repository and therefore have uncertainties**
- **Model uncertainties are analyzed and quantified by sensitivity analyses**
- **This lecture addresses these issues based on the work done in EURAD within ACED & DONUT Work Packages**
- **The presentation has two parts**
  - Conceptual and numerical reactive transport models for HLW radioactive waste disposal at the disposal cell scale
  - Sensitivity and uncertainty methods for such reactive transport models

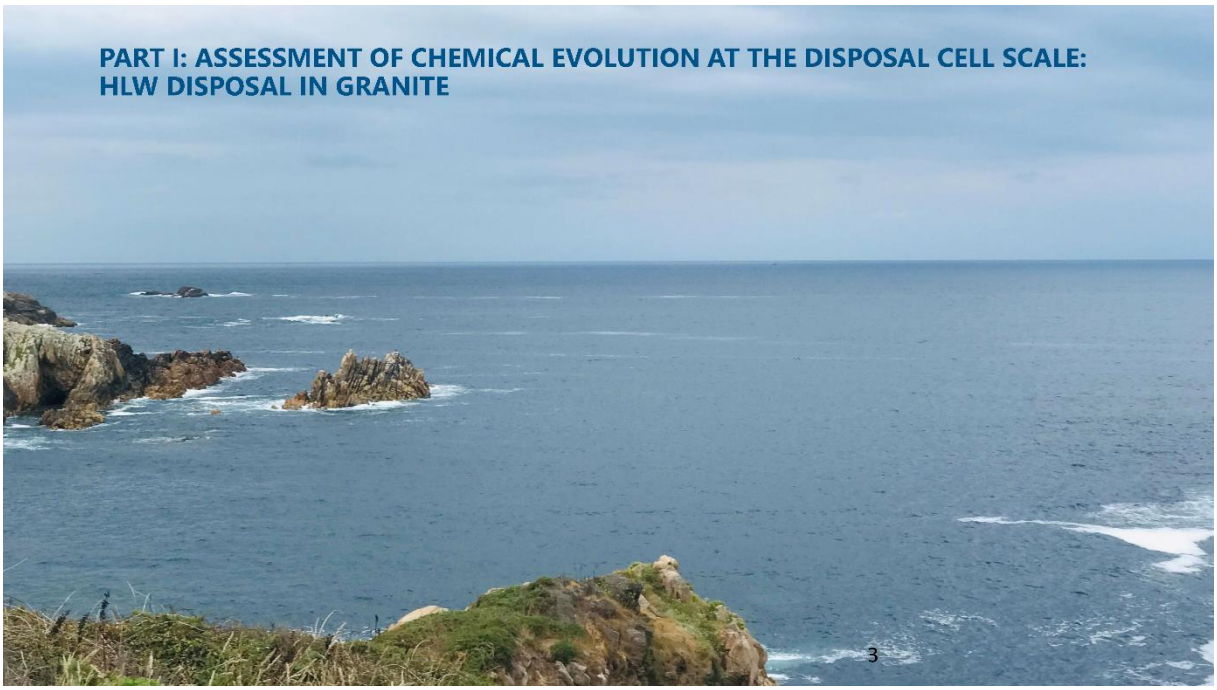

UNIVERSIDADE DA CORUÑA

EURAD Training
Geochemical & Reactive Transport Modelling for Geological Disposal training

OUTLINE OF PART I

- Modelling approach
- Description of the disposal cell concept in granite
- Conceptual model & narrative evolution
- Mathematical & numerical model
- Computer code
- Model results
- Sensitivity analysis

February 10th, 2023 Lecture 8: Integration of processes at larger scale – sensitivity (uncertainty) analyses

UNIVERSIDADE DA CORUÑA

Geochemical & Reactive Transport Modelling for Geological Disposal training

REFERENCE CONCEPT FOR HLW DISPOSAL IN GRANITE

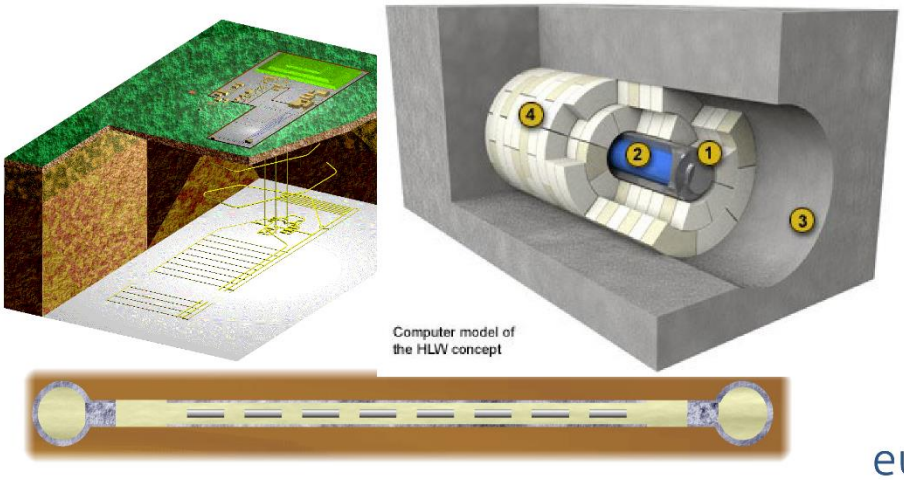

February 10th, 2023 Lecture 8: Integration of processes at larger scale – sensitivity (uncertainty) analyses

UNIVERSIDADE DA CORUÑA

Geochemical & Reactive Transport Modelling for Geological Disposal training

DESCRIPTION OF REPRESENTATIVE CONCEPT FOR HLW IN GRANITE

- **HLW disposal in granite**
  - Vitrified waste
  - Steel canister
  - Gap
  - Liner
  - Bentonite buffer
    - Compacted FEBEX bentonite (b=75 cm)
  - Granitic host rock
    - Spanish Reference Granite

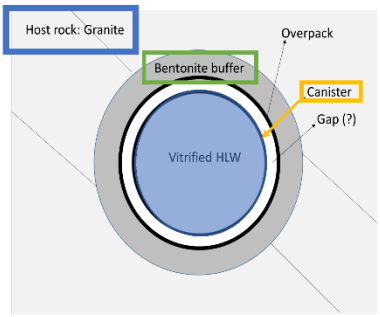

February 10th, 2023 Lecture 8: Integration of processes at larger scale – sensitivity (uncertainty) analyses

UNIVERSIDADE DA CORUÑA

Geochemical & Reactive Transport Modelling for Geological Disposal training

CONCEPTUAL MODEL & NARRATIVE EVOLUTION: TIME STAGES

- **Geochemical and temperature evolution periods**
- **The conceptual model considers 3 periods**
- **Period I covers the oxic transient stage with unsaturated conditions**
- **Period II starts when the buffer is fully saturated**
  - Nonisothermal
  - Anoxic canister corrosion
  - Interactions of corrosion products and buffer material
- **Period III starts after canister failure**
  - Glass dissolution
  - Interactions of glass with corrosion products and uncorroded canister
- **Simulation time horizon: $5{\cdot}10^4$ years**

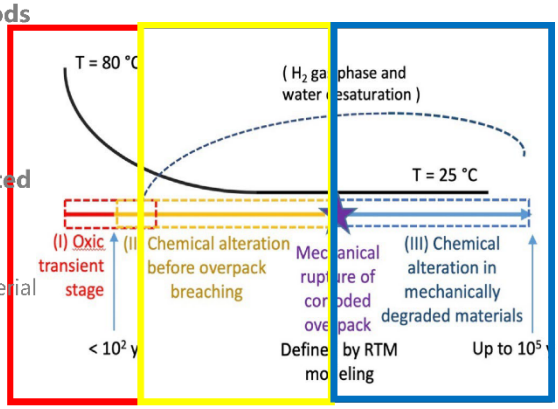

Taken from D2.16

February 10th, 2023 Lecture 8: Integration of processes at larger scale – sensitivity (uncertainty) analyses

UNIVERSIDADE DA CORUÑA

Geochemical & Reactive Transport Modelling for Geological Disposal training

CONCEPTUAL MODEL: GEOCHEMICAL PROCESSES

- **Canister corrosion**
  - Leads to the precipitation of corrosion products (CP)
  - The precipitation of corrosion products (CP) near the canister decreases the porosity of the bentonite and may clog the pores
- **Interactions of CP and bentonite**
  - Bentonite cementation due to the precipitation of CP and SiO_2 coming from montmorillonite transformation
  - Replacement of bentonite minerals by Fe-rich smectites and non-swelling Fe-rich phyllosilicates
  - Dissolution & alteration of montmorillonite
- **Glass dissolution**
  - The interactions of vitrified glass and corrosion products start in Period III after canister failure
  - The vitrified glass is not treated as a boundary condition. Instead, it is considered explicitly in the reactive transport model and coupled with the canister, the buffer and host-rock evolution

February 10th, 2023 Lecture 8: Integration of processes at larger scale – sensitivity (uncertainty) analyses

UNIVERSIDADE DA CORUÑA

EURAD Training
Geochemical & Reactive Transport Modelling for Geological Disposal training

MATHEMATICAL AND NUMERICAL MODEL

- The numerical model includes Periods II and III
- Partial desaturation of the buffer is disregarded
- Solute diffusion is the main transport process
- Nonisothermal conditions
- The excavation damaged zone (EDZ) is disregarded in the base case
- The focus is on the steel canister which protects the vitrified glass
- The stainless-steel envelope (0.5 cm thick) is disregarded & the technological gap is assumed to be filled with corrosion products in Period II

Time evolution of temperature at canister/bentonite & bentonite /granite interfaces

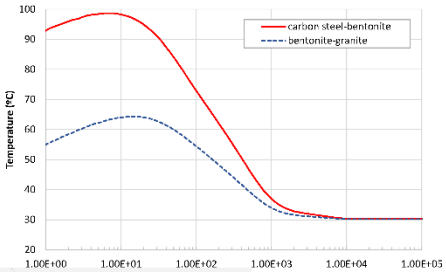

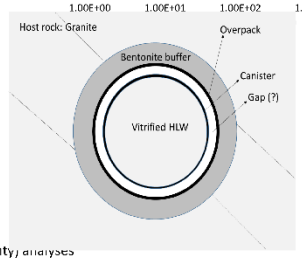

February 10th, 2023 Lecture 8: Integration of processes at larger scale – sensitivity (uncertainty) analyses

UNIVERSIDADE DA CORUÑA

EURAD Training
Geochemical & Reactive Transport Modelling for Geological Disposal training

MATHEMATICAL AND NUMERICAL MODEL

- **Glass dissolution model and rate**
  - The ISG (the International Simple Glass) is used
  - A simple congruent glass dissolution model is used
  - The glass dissolution rate has two terms:
    - First-order silica-dependent rate law & a long-term residual rate

[wt.%]	SiO_2	Na_2O	B_2O_3	Al_2O_3	CaO	ZrO_2
ISG	56.2	12.2	17.3	6.0	5.0	3.3

$$\frac{d[glass]}{dt} = -k_{0,pH}\,(H^+)^{-0.4}\,A_v\left(1-\frac{C_{Si}}{C^*_{Si}}\right) - k_r\,A_v$$

- C_{Si} = concentration of dissolved silica; C^*_{Si} = threshold concentration of dissolved silica
- A_v = glass reactive surface; k_r and $k_{0,pH}$ = kinetic parameters
- The rate is valid for 7 < pH < 9.5 (the rate is assumed to reach a threshold value for pH > 9.5)

- **Interactions of glass and corrosion products**
  - Glass dissolution takes up protons and water and releases Si, Al, B, Ca, Na, Zr

'ISG' 7.7016 7 +0.023 'al+3' +0.096 'b(oh)4-' +0.017 'ca+2' +0.076 'na+' +0.180 'h4(sio4)' -0.103 'h+' -0.5005 'h2o'

  - The precipitation of iron silicates and phyllosicates is a sink of the silica released by the vitrified glass

February 10th, 2023 Lecture 8: Integration of processes at larger scale – sensitivity (uncertainty) analyses 10

UNIVERSIDADE DA CORUÑA

EURAD Training
Geochemical & Reactive Transport Modelling for Geological Disposal training

MATHEMATICAL AND NUMERICAL MODEL

- **Carbon-steel canister: corrosion & failure**
  - Corrosion rate: Constant and time-varying depending on T, pH, Eh and reactive surface area
  - The canister
    - Porous material filled with corrosion products. All the canister corrodes simultaneously
    - Fails when the thickness is 1.5 cm
- **Canister/bentonite interface**
  - Anaerobic steel corrosion, Fe diffusion, Fe sorption and precipitation of corrosion products
- **Geochemical conceptual model for the bentonite**
  - Aqueous complexation, acid/base, redox; mineral dissolution/precipitation, cation exchange and surface complexation of protons and Fe on three types of sorption sites (LEA)
- **Porosity feedback effect caused by mineral dissolution/precipitation is considered in a sensitivity case**

February 10th, 2023 Lecture 8: Integration of processes at larger scale – sensitivity (uncertainty) analyses

UNIVERSIDADE DA CORUÑA

EURAD Training
Geochemical & Reactive Transport Modelling for Geological Disposal training

MATHEMATICAL AND NUMERICAL MODEL

- **1D axi-symmetric model**
- **Advection in granite & diffusion in bentonite**
- **Multicomponent reactive transport**
  - 14 chemical components
  - Aqueous complexation, acid base & redox reactions
  - Equilibrium mineral dissolution/precipitation: calcite, gypsum, quartz, magnetite, siderite, goethite, greenalite
  - Kinetic reactions: glass dissolution & canister corrosion
  - Cation exchange: Na^+, Ca^{2+}, Mg^{2+}, K^+, Fe^{2+}
  - Surface complexation (3 sites)
- **Canister corrosion 1.4 µ/y**
  - 3.5 cm corroded after 25000 years

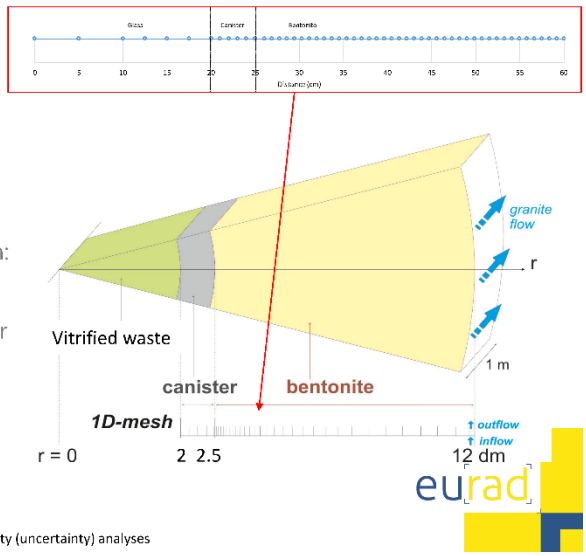

February 10th, 2023 Lecture 8: Integration of processes at larger scale – sensitivity (uncertainty) analyses

UNIVERSIDADE DA CORUÑA

EURAD Training
Geochemical & Reactive Transport Modelling for Geological Disposal training

COMPUTER CODE

- **CORE^{2D} V5: Developed by UDC**

eurad

February 10th, 2023 Lecture 8: Integration of processes at larger scale – sensitivity (uncertainty) analyses

UNIVERSIDADE DA CORUÑA

EURAD Training
Geochemical & Reactive Transport Modelling for Geological Disposal training

MODEL RESULTS

- **The time evolution at selected locations (interfaces) and the spatial distribution at selected times of:**
  - pH and redox potential
  - Concentrations of the dissolved species
  - Concentrations of exchanged cations and surface complexes
  - Mineral volume fractions
  - Changes in porosity

eurad

February 10th, 2023 Lecture 8: Integration of processes at larger scale – sensitivity (uncertainty) analyses

UNIVERSIDADE DA CORUÑA

Geochemical & Reactive Transport Modelling for Geological Disposal training

MODEL RESULTS FOR THE BASE RUN

- **pH spatial distribution**

Period II

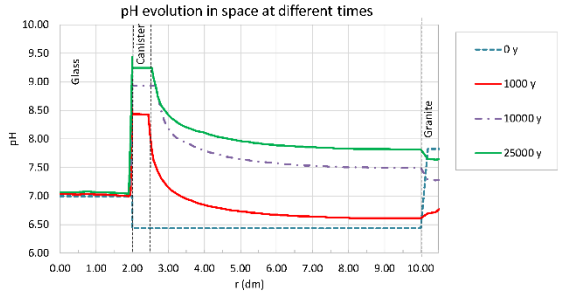

Period III

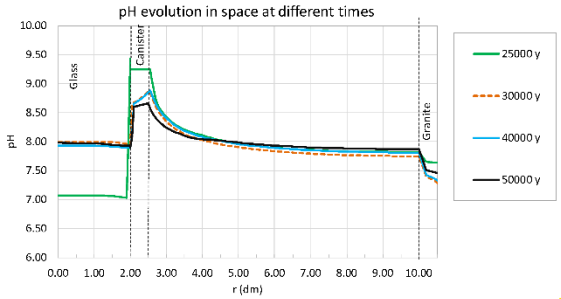

February 10th, 2023 Lecture 8: Integration of processes at larger scale – sensitivity (uncertainty) analyses

UNIVERSIDADE DA CORUÑA

Geochemical & Reactive Transport Modelling for Geological Disposal training

MODEL RESULTS FOR THE BASE RUN IN PERIOD II

Mineral volume fractions

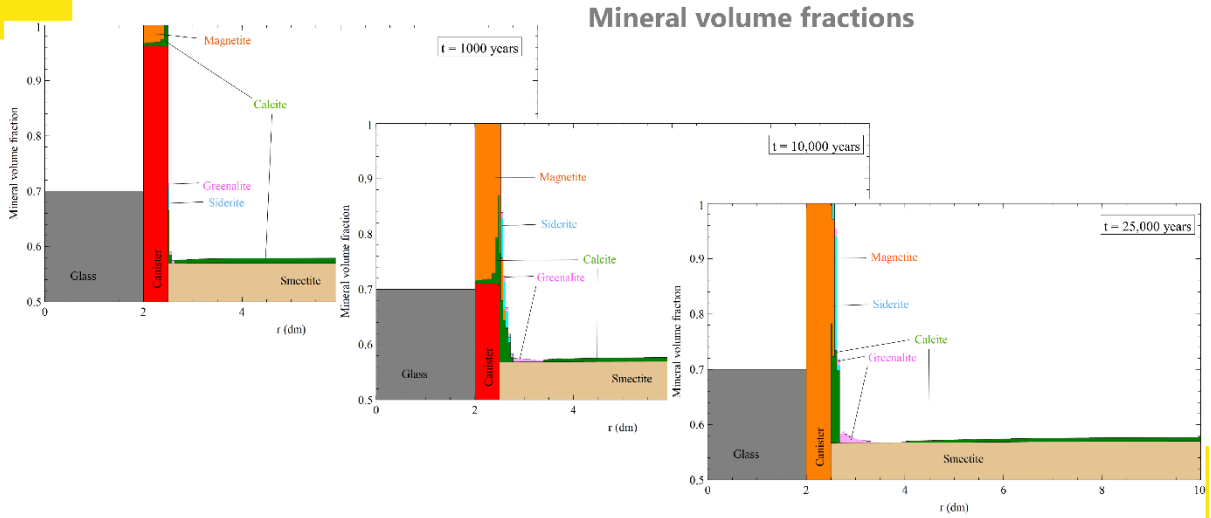

February 10th, 2023 Lecture 8: Integration of processes at larger scale – sensitivity (uncertainty) analyses

UNIVERSIDADE DA CORUÑA

Geochemical & Reactive Transport Modelling for Geological Disposal training

MODEL RESULTS FOR THE BASE RUN IN PERIOD III

Mineral volume fractions

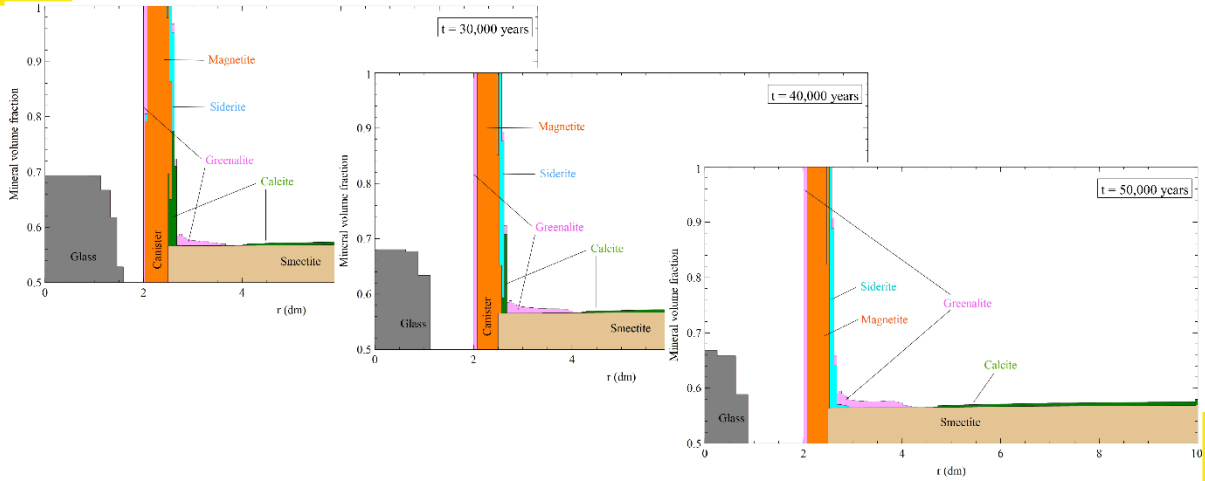

February 10th, 2023 Lecture 8: Integration of processes at larger scale – sensitivity (uncertainty) analyses

UNIVERSIDADE DA CORUÑA

Geochemical & Reactive Transport Modelling for Geological Disposal training

MODEL RESULTS FOR THE BASE RUN

- **Glass dissolution rate**

Glass (vol)

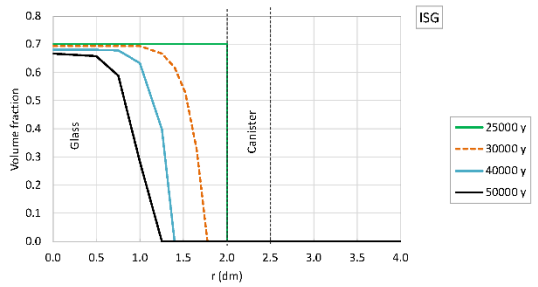

Glass dissol. rate

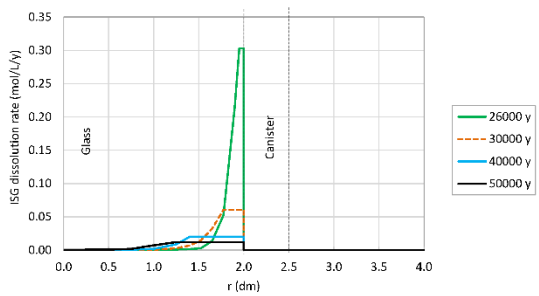

February 10th, 2023 Lecture 8: Integration of processes at larger scale – sensitivity (uncertainty) analyses

UNIVERSIDADE DA CORUÑA

EURAD Training
Geochemical & Reactive Transport Modelling for Geological Disposal training

MODEL RESULTS FOR THE BASE RUN

- **Glass dissolution rate & dissolved silica concentration**
  - Selected times: $3{\cdot}10^4$ & $5{\cdot}10^4$ years
  - The peak of the dissolution rate is at the dissolution front where the concentration of dissolved silica decreases

$3{\cdot}10^4$ years

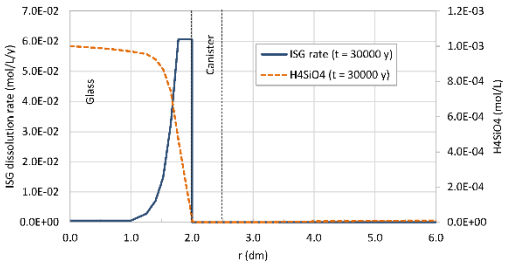

$5{\cdot}10^4$ years

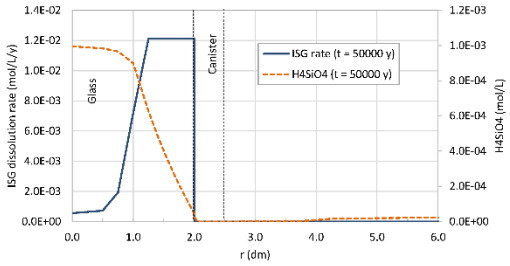

February 10th, 2023 Lecture 8: Integration of processes at larger scale – sensitivity (uncertainty) analyses

UNIVERSIDADE DA CORUÑA

EURAD Training
Geochemical & Reactive Transport Modelling for Geological Disposal training

MODEL RESULTS OF THE BASE RUN AT THE END OF PERIOD II

- Canister corrosion leads to an increase in pH and the concentration of dissolved Fe^{2+}
- Magnetite precipitates in the canister and in the bentonite (1 cm band)
- Siderite and greenalite precipitate
  - In the canister near the bentonite interface
  - In the bentonite: small amount in a thin band
- The bentonite near the canister gets enriched in exchanged and sorbed Fe^{2+}
- The calculated porosity
  - Decreases in the canister due to magnetite precipitation reaching clogging before 10,000 years
  - Decreases in the bentonite (1 cm from the C/B interface) due to calcite, siderite and greenalite precipitation

February 10th, 2023 Lecture 8: Integration of processes at larger scale – sensitivity (uncertainty) analyses

UNIVERSIDADE DA CORUÑA

EURAD Training
Geochemical & Reactive Transport Modelling for Geological Disposal training

MODEL RESULTS FOR THE BASE RUN AT THE END OF PERIOD III

- Glass dissolution increases with time and shows a dissolution front which moves into the glass
- Glass dissolution leads to an increase of pH and dissolved $H_4(SiO_4)$ concentration in the glass
- $H_4(SiO_4)$ diffuses into the canister and the bentonite causing greenalite precipitation mainly at the G/C & C/B interfaces
- Final pH values: 7.93 to 7.98 in the glass, 7.89 to 8.66 in the canister and 7.86 to 8.57 in the bentonite
- Magnetite re-dissolves after 25,000 years in the canister near the G/C interface while greenalite precipitates. Siderite precipitates at the C/B interface
- The bentonite near the canister gets enriched in exchanged and sorbed Fe^{2+}
- The calculated porosity
  - Increases in the glass due to glass dissolution
  - Decreases in the canister and the bentonite due to calcite, magnetite, siderite and greenalite precipitation

eurad

February 10th, 2023 Lecture 8: Integration of processes at larger scale – sensitivity (uncertainty) analyses

UNIVERSIDADE DA CORUÑA

EURAD Training
Geochemical & Reactive Transport Modelling for Geological Disposal training

SENSITIVITY ANALYSES

- **Sensitivity cases for HLW disposal in granite**
  - Sensitivity case 1: ISG with different saturation threshold
  - Sensitivity case 2: SRG with a larger Cl- concentration in granitic porewater
  - Variant 1: SRG with an EDZ and a larger hydraulic conductivity of the host rock
  - Variant 2: Czech Reference Crystalline Roc
- **Other sensitivity cases:**
  - Porosity feedback effect
  - Corrosion rate depending on temperature and saturation index
  - Earlier canister failure with a shorter duration of Period II

eurad

February 10th, 2023 Lecture 8: Integration of processes at larger scale – sensitivity (uncertainty) analyses

UNIVERSIDADE DA CORUÑA

EURAD Training
Geochemical & Reactive Transport Modelling for Geological Disposal training

SENSITIVITY ANALYSIS

- **Model results are not sensitive to**
  - The increase of Cl- concentration in the granite boundary water
  - The chemical composition of the granite porewater
  - Smectite dissolution
- **Model results are sensitive to**
  - Porosity feedback effect
  - Corrosion rate depending on temperature and saturation index
  - Earlier canister failure with a shorter duration of Period II

February 10th, 2023 Lecture 8: Integration of processes at larger scale – sensitivity (uncertainty) analyses

UNIVERSIDADE DA CORUÑA

EURAD Training
Geochemical & Reactive Transport Modelling for Geological Disposal training

SENSITIVITY ANALYSIS

- **Sensitivity to the threshold silica concentration for ISG dissolution**
  - The change in C_{Si^*} leads to a change in the glass dissolution front, but it does not affect the computed pH.

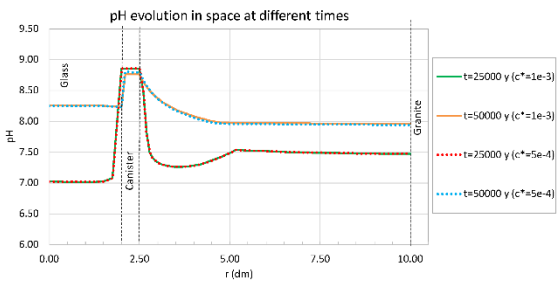

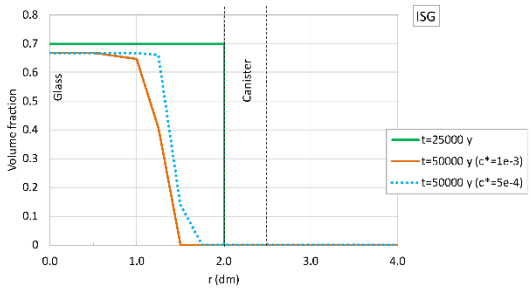

February 10th, 2023 Lecture 8: Integration of processes at larger scale – sensitivity (uncertainty) analyses

UNIVERSIDADE DA CORUÑA

EURAD Training
Geochemical & Reactive Transport Modelling for Geological Disposal training

ONGOING & FUTURE WORK

- **Develop abstracted models**
  - Lower Fidelity (physically based) models
    - simplified (e.g. dimensionality, geometry, transport or geochemical processes, parameterization)
    - key output of interest is obtained more easily
    - the accuracy is acceptable
  - Response Surface Surrogates:
    - simulate the input-output relationships of the complex model with a statistical relationship
    - Data – driven methods

eurad

25

February 10th, 2023 Lecture 8: Integration of processes at larger scale – sensitivity (uncertainty) analyses

UNIVERSIDADE DA CORUÑA

EURAD Training
Geochemical & Reactive Transport Modelling for Geological Disposal training

EXAMPLE OF MODEL ABSTRACTION

- **Mesh discretization**
  - pH at 50,000 years: with less refined grid is smaller
  - Magnetite precipitation with less refined grid is larger

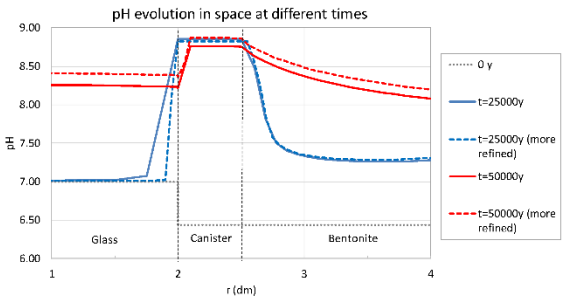

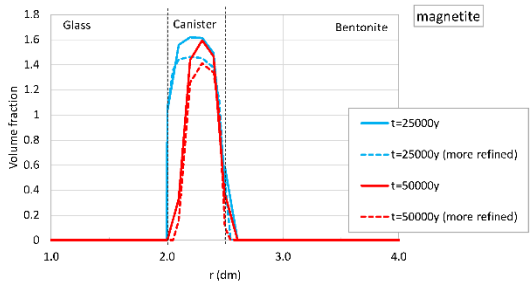

eurad

February 10th, 2023 Lecture 8: Integration of processes at larger scale – sensitivity (uncertainty) analyses

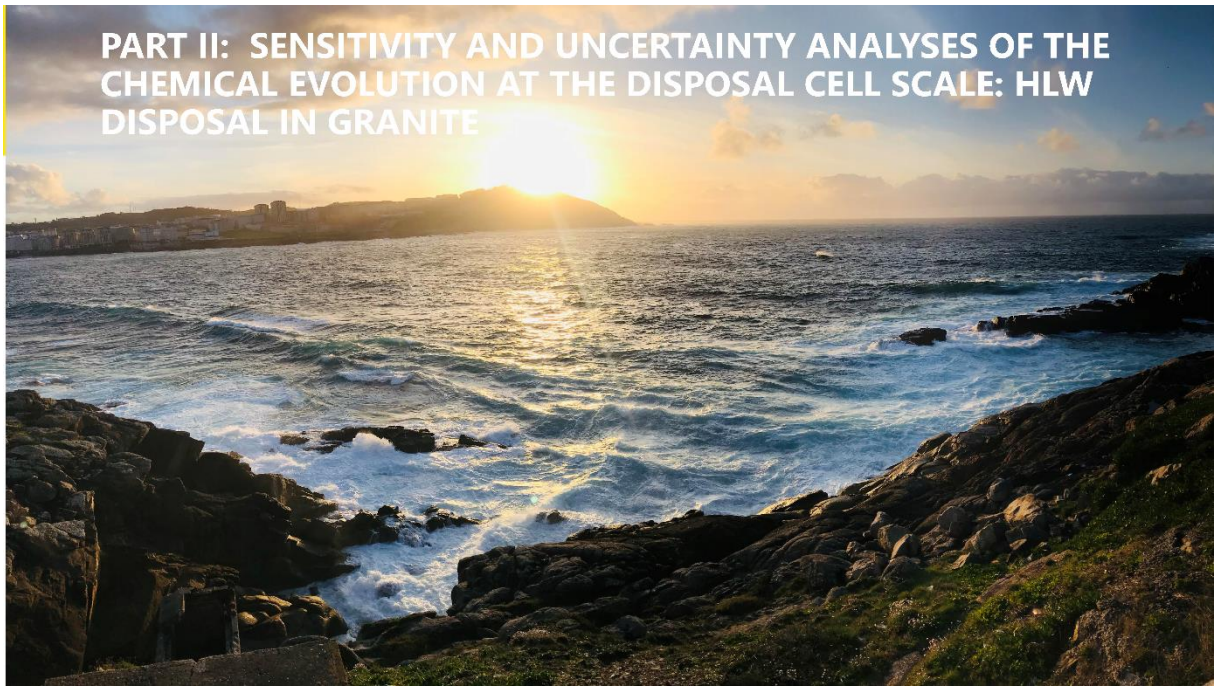

UNIVERSIDADE DA CORUÑA

Geochemical & Reactive Transport Modelling for Geological Disposal training

OUTLINE

- **Introduction & motivation**
- **Methods of global sensitivity and uncertainty analysis**
- **VARS (Variogram Analysis of Response Surface) method**
  - Description
  - Parameters
  - Numerical implementation
  - VARS results
  - Future and ongoing work
- **Ongoing international initiatives on sensitivity analysis (JOSA Group)**

February 10th, 2023 Lecture 8: Integration of processes at larger scale – sensitivity (uncertainty) analyses 28

UNIVERSIDADE DA CORUÑA

Geochemical & Reactive Transport Modelling for Geological Disposal training

INTRODUCTION

- **The predictions of numerical models have uncertainties**
- **Sensitivity analysis**
  - Classical approach:
    - Local nature
    - Change one parameter at a time
    - Sensitivity analysis results are "incomplete" and may even be erroneous
  - Modern & recent approaches: Global methods

pH at the canister/bentonite interface

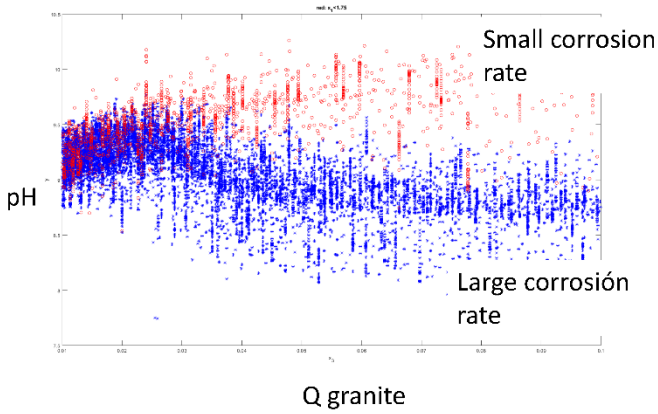

eurad

29

February 10th, 2023 Lecture 8: Integration of processes at larger scale – sensitivity (uncertainty) analyses

UNIVERSIDADE DA CORUÑA

Geochemical & Reactive Transport Modelling for Geological Disposal training

GLOBAL METHODS OF SENSITIVITY ANALYSIS

- **Monte Carlo simulations of Z for a large number of parameter combinations**

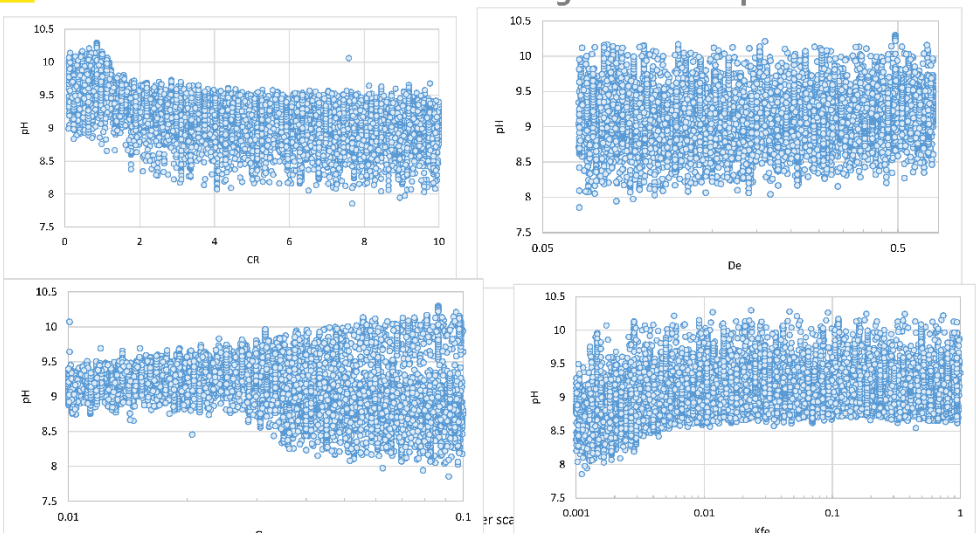

UNIVERSIDADE DA CORUÑA

Geochemical & Reactive Transport Modelling for Geological Disposal training

GLOBAL METHODS OF SENSITIVITY ANALYSIS

- **Monte Carlo simulations of Z for a large number of parameter combinations: what to do ?**

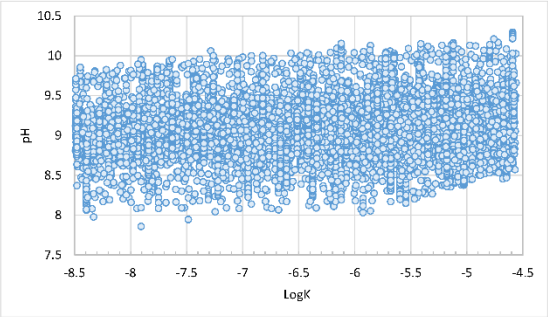

eurad

February 10th, 2023 Lecture 8: Integration of processes at larger scale – sensitivity (uncertainty) analyses

UNIVERSIDADE DA CORUÑA

Geochemical & Reactive Transport Modelling for Geological Disposal training

GLOBAL METHODS OF SENSITIVITY ANALYSIS

- **Provide a global measure of the sensitivity of a model output Z to changes in model parameters**
- **Derivative-based methods: Morris "Elementary Effects"**
  - Quantify the average mean change in Z due to perturbations in each input parameter
  - Identify the dominant parameters
- **Variance-based methods: Sobol indexes**
  - Quantify the contributions of each parameter x_i to the total variance of the output Z
  - The total Sobol index quantifies the contribution of x_i to the variance of Z
  - Provide measures of the "interactions" among parameters
- **Morris and Sobol methods require performing thousands of Monte Carlo simulations to get statistically significant results**

UNIVERSIDADE DA CORUÑA | EURAD Training: Geochemical & Reactive Transport Modelling for Geological Disposal training

GLOBAL METHODS OF SENSITIVITY ANALYSIS

- **VARS (Variogram Analysis of Response Surfaces**
  - Method proposed by Razavi & Gupta (WRR, 2016)
  - Provides a comprehensive and efficient tool to analyse the structure of the response surface or model output Z
  - VARS includes Morris and Sobol methods as particular
  - The number of simulations required by VARS is smaller than those of Morris and Sobol methods

UNIVERSIDADE DA CORUÑA | EURAD Training: Geochemical & Reactive Transport Modelling for Geological Disposal training

VARS: DESCRIPTION OF THE METHOD

- **Analyzes the structure of a response function Z based on the directional variograms $\gamma(h_i)$ for each variable**
  - $\boldsymbol{\theta} = (x_1, x_2, \dots, x_i, \dots)$ = Parameter vector
  - h_i = increment in i-th parameter
  - The variogram $\gamma(h_i)$ is half the variance of the increment $Z(\boldsymbol{\theta} + h_i) - Z(\boldsymbol{\theta})$
- **Variograms are computed from Monte Carlo simulations**
  - The response function is evaluated at many parameter combinations

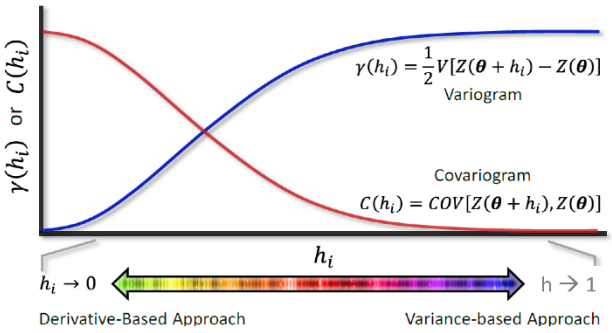

February 10th, 2023 Lecture 8: Integration of processes at larger scale – sensitivity (uncertainty) analyses 34

UNIVERSIDADE DA CORUÑA | Geochemical & Reactive Transport Modelling for Geological Disposal training

VARS: DESCRIPTION OF THE METHOD

- **VARS includes the Morris and the Sobol methods as particular cases**
  - The limit of the variogram for $h_i \rightarrow 0$ is "similar" to the Morris effects
    - VARS-ABE: Mean absolute elementary effects
  - The limit for $h_i \rightarrow 1$ is linked to the Sobol sensitivity index
    - VARS-TO: Sobol
- **IVARS-50**

$$IVARS-50 = \int_0^{0.5} \gamma(h_i)\, dh_i$$

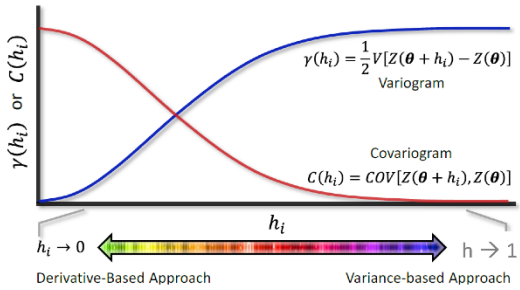

Summary Derivations:

If $h_i \rightarrow 0 \Rightarrow$

$$\gamma(h_i) \propto V\left[\frac{dZ}{d\theta_i}\right] \propto E\left[\left(\frac{dZ}{d\theta_i}\right)^2\right]$$

"Elementary Effects" based Metrics of Morris

$h \rightarrow 1 \Rightarrow \gamma(h_i) = V(Z)$

Variance of Response Surface

$$S_i^{TO} = \frac{\gamma(h_i) + E[C_{\boldsymbol{\theta}_{-i}}(h_i)]}{V(Z)}$$

"Total-Order Effects" of Sobol'

UNIVERSIDADE DA CORUÑA | Geochemical & Reactive Transport Modelling for Geological Disposal training

VARS: DESCRIPTION OF THE METHOD

- Parameters x_i are normalized into [0, 1] intervals
- Each axis is discretized with constant parameter increments Δh (ressolution)
- Perform quasi Montecarlo simulations by defining first the so-called "star centers"
  - Latin hypercube sampling (LHS), Halton, …
- Draw lines parallel to the axes & evaluate the response function Z at all the discretized points
- Estimate the variogram $\gamma(h_i)$ of Z along each direction from the values of (Z_i, x_i)
- **(see https://www.youtube.com/watch?v=YxeMdA8QIfU)**

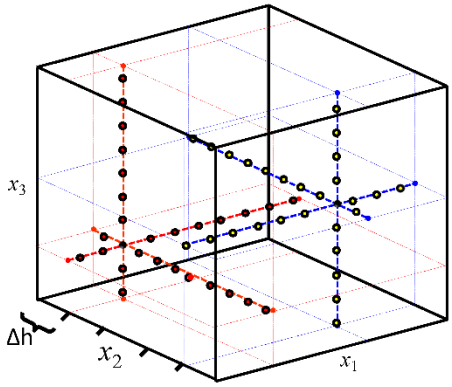

UNIVERSIDADE DA CORUÑA | Geochemical & Reactive Transport Modelling for Geological Disposal

VARS: PARAMETERS

- **Long-term geochemical evolution in a HLW repository in granite**
  - Corrosion products & interactions with bentonite
- **Parameters**
  - Corrosion rate (CR)
  - Bentonite diffusion coefficient
  - Granite flux (Q_{gra})
  - Fe selectivity coefficient
  - Magnetite equilibrium constant
    - Log-K
- **Distributions**
  - Log-uniform except for corrosion rate

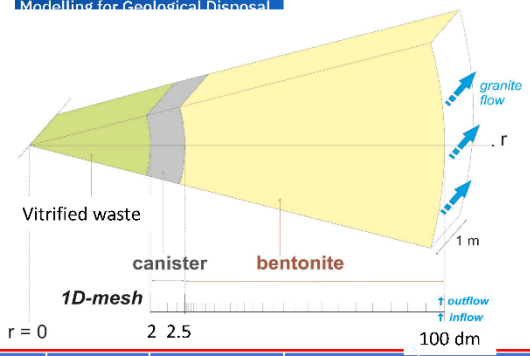

Parameter	Name	L Bound	U Bound	PDF	Units
1 (CR)	Corrosion rate	0.1	10	Uniform	µm/y
2 (De)	Bentonite dif	0.0631	0.631	Log-uniform	dm2/y
3 (Q^{gra})	Granite flow	0.01	0.1	Log-uniform	L/y
4 (Fe^{ksel})	Fe Selectivity	0.001	1	Log-uniform	-
5 (log K)	Log K magnetite	-8.56	-4.56	Uniform	-

February 10th, 2023 Lecture 8: Integration of processes at larger scale – sensitivity (uncertainty) analyses 37

UNIVERSIDADE DA CORUÑA | Geochemical & Reactive Transport Modelling for Geological Disposal training

VARS IMPLEMENTATION

- **Computer codes**
  - CORE^{2D} V5 for reactive transport modelling
  - VARS Matlab version (open access)
- **Reactive transport simulations were performed on a HPC infrastructure (FinisTerrae II cluster from the Galician Supercomputing Center, CESGA, www.cesga.es)**
- **CPU time for 27600 simulations**
  - 3 months of wall time
  - Equivalent to nearly 25 CPU-years
  - CPU time reduction by a factor of 100

February 10th, 2023 Lecture 8: Integration of processes at larger scale – sensitivity (uncertainty) analyses 38

UNIVERSIDADE DA CORUÑA

Geochemical & Reactive Transport Modelling for Geological Disposal training

VARS RESULTS

- pH after $5 \cdot 10^4$ years
- IVARS50 vs number of star centers
- Results get stable after 100 star centers
- The largest the IVARS-50 the largest the importance
- $I_{CR} > I_Q > I_{Fe\ sel} >> I_{De} > I_{Kmag}$

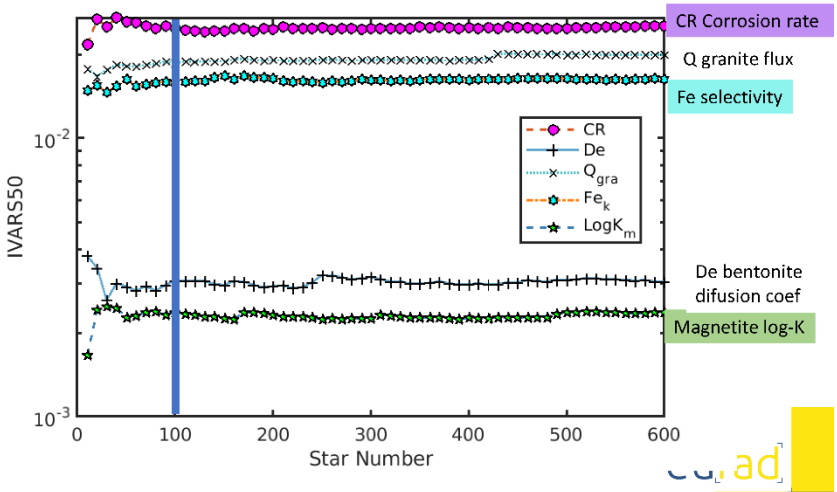

February 10th, 2023 Lecture 8: Integration of processes at larger scale – sensitivity (uncertainty) analyses 39

UNIVERSIDADE DA CORUÑA

Geochemical & Reactive Transport Modelling for Geological Disposal training

VARS RESULTS

- pH after $5 \cdot 10^4$ years
- Directional variograms
- 3 main parameters
- The variograms $\gamma(h_i)$
  - Provide indexes (IVARS-0, IVARS-50, IVARS-100)
  - Can be used to construct metamodels with Gaussian Processes
    - Additional advantage of VARS

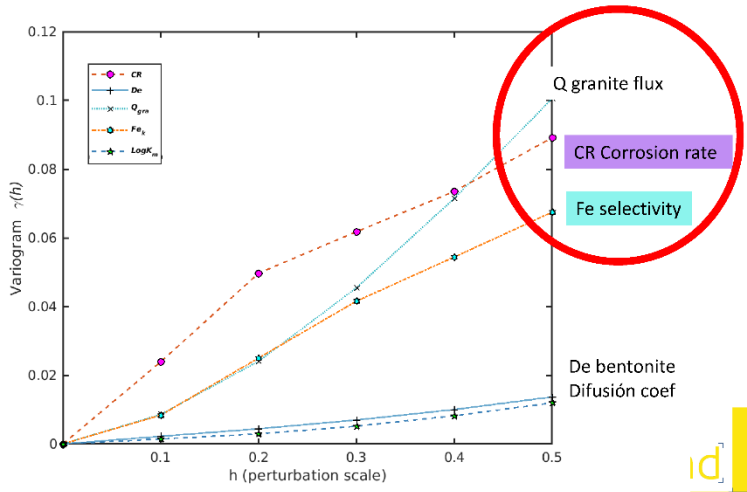

February 10th, 2023 Lecture 8: Integration of processes at larger scale – sensitivity (uncertainty) analyses 40

UNIVERSIDADE DA CORUÑA

Geochemical & Reactive Transport Modelling for Geological Disposal training

VARS RESULTS

- pH after $5 \cdot 10^4$ years
- VARS indicators
- IVARS-50
- VARS-TO: Sobol
- VARS-ABE: Mean absolute elementary effects
- Comparison of IVARS-50, VARS-TO & VARS-ABE
  - All give similar results
  - Small differences for some parameters

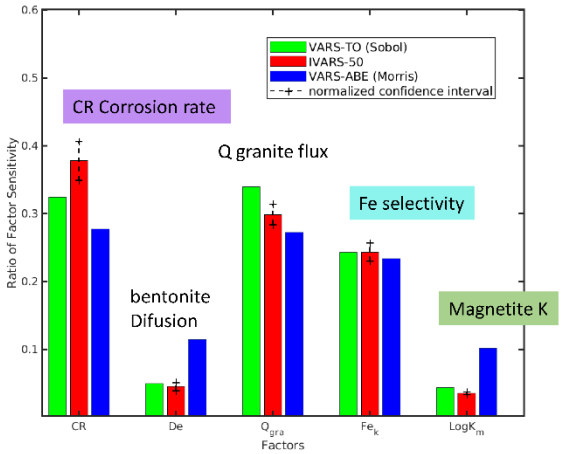

UNIVERSIDADE DA CORUÑA

Geochemical & Reactive Transport Modelling for Geological Disposal training

CONCLUSIONS

- VARS analysis of the computed pH after $5 \cdot 10^4$ years for a HLW repository in granite has been presented
- 5 parameters were considered
- Most influential parameters are
  - Corrosion rate, granite flux and Fe selectivity
- Morris, Sobol and VARS (IVARS-50) provide similar results in terms of rankings and significance

UNIVERSIDADE DA CORUÑA

EURAD Training
Geochemical & Reactive Transport Modelling for Geological Disposal training

VARS ONGOING & FUTURE WORK

- **VARS method**
  - Increase the number of parameters
  - Consider additional model outputs
    - pH at several times: 10 k years , 25 k years and 50 k years
    - Other output variables such as
      - Redox potential, mineral volume fractions, dissolved Fe, sorbed Fe & exchanged Fe
  - Numerical aspects
    - How to deal with failed runs?
    - Sensitivity to numerical simplifications
      - Space & time discretization
      - Convergence tolerances
  - Construct metamodels & perform sensitivity analyses with both RT models and metamodels

eurad

February 10th, 2023 Lecture 8: Integration of processes at larger scale – sensitivity (uncertainty) analyses 43

UNIVERSIDADE DA CORUÑA

EURAD Training
Geochemical & Reactive Transport Modelling for Geological Disposal training

OTHER INTERNATIONAL SENSITIVITY INITIATIVES

- **JOSA: Joint Sensitivity Analysis Working Group**
- **Volunteer initiative to develop and test sensitivity and uncertainty methods for radioactive waste disposal**
- **Test cases are prepared by some groups**
- **Different groups apply different methods and model results are compared**
- **Available results are compiled in Volume 1 published by SNL (USA)**
- **https://www.osti.gov/servlets/purl/1822591**
- **Volume 2 is in progress**
- **Contact persons**
  - Laura Swile: lpswile@sandia.gov
  - Dirk Becker: Dirk-Alexander.Becker@grs.de

eurad

February 10th, 2023 Lecture 8: Integration of processes at larger scale – sensitivity (uncertainty) analyses 44


UNIVERSIDADE DA CORUÑA
Geochemical & Reactive Transport Modelling for Geological Disposal training
THANK YOU VERY MUCH!
Acknowledgements
Authors from UDC Team: Javier Samper, Alba Mon, Luis Montenegro, Aurora-Core Samper-Pilar, Acacia Naves, Bruno Pisani, Javier Samper-Pilar
Authors from ENRESA: Enrique García
Collaboration with
Carlos López (Uruguay)
Changbing Yang (San Antonio, Texas, USA)
February 10th, 2023
Lecture 8: Integration of processes at larger scale – sensitivity (uncertainty) a

3.1 Lecture 9 - Machine learning for accelerating reactive transport model simulations and analysis

In several areas of geosciences it is of interest to conduct multiphysics simulations. Typically the involved processes are non-linear and strongly coupled. Reactive transport model (RTM) simulations can be computationally-demanding, especially when large grids and/or long simulation periods are considered. Furthermore, even for small domains and simulation periods, model analysis tasks that require repeated model runs such as sensitivity analysis or the inverse modelling of laboratory or underground experiments, can quickly become intractable, since in these cases several thousands of such model simulations are needed. In this lecture, we will review different situations where nonlinear regression by machine learning (ML) methods, such as artificial neural networks (NNs), can help to: a) make the coupling between codes and scales, b) accelerate parts of RTM codes, and c) accelerate the full RTM simulations for sensitivity analysis and uncertainty quantification. Parameter upscaling may be facilitated via ML interfaces. At the same time, in a typical RTM simulation the geochemical calculations are responsible for the largest part of the total computing cost. The geochemical solver can be replaced by a metamodel (or surrogate model) which is several orders of magnitude faster. Coupling the geochemical solver metamodel with the transport model can lead to a significant speed up of the computations. Finally, we illustrate how ML can be used to surrogate the full RTM over some input and boundary conditions, such that sensitivity analysis, uncertainty propagation and/or inverse modelling become possible. The computational acceleration provided by machine the learning techniques is a crucial component of the digital twin technology.

Lecturer

Nikoloas Prasianakis, PSI, Switzerland

Eric Laloy, SCK CEN, Belgium

Reading Material

Churakov, S. V., Prasianakis, N. I. 2018. Review of the current status and challenges for a holistic process-based description of mass transport and mineral reactivity in porous media. American journal of science, 318(9), 921-948. https://doi.org/10.2475/09.2018.03

Laloy E., Jacques, D. 2019. Emulation of CPU-demanding reactive transport models: a comparison of gaussian processes, polynomial chaos expansion, and deep neural networks. Comput Geosci 23(5):1193–1215. https://doi.org/10.1007/s10596-019-09875-y.

Laloy E., Jacques D. 2022. Speeding up reactive transport simulations in cement systems by surrogate geochemical modeling: deep neural networks and k-nearest neighbors. Transp Porous Media 143(2):433–462. https://doi.org/10.1007/s11242-022-01779-3.

Prasianakis, N. I., Haller, R., Mahrous, M., Poonoosamy, J., Pfingsten, W., Churakov, S. V. 2020. Neural network based process coupling and parameter upscaling in reactive transport simulations. Geochimica et Cosmochimica Acta, 291, 126-143. https://doi.org/10.1016/j.gca.2020.07.019

Slides

PAUL SCHERRER INSTITUT

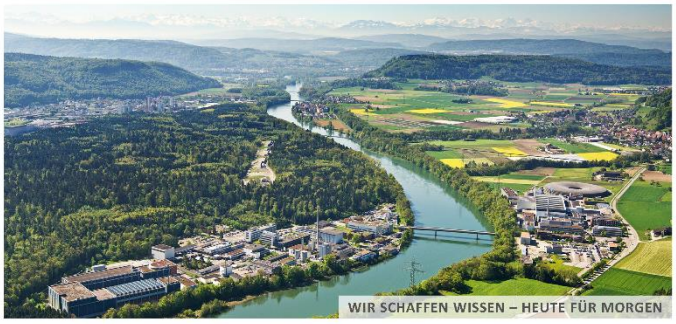

Nikolaos Prasianakis :: Laboratory for Waste management :: Paul Scherrer Institut

Machine learning for accelerating reactive transport model simulations and analysis

EURAD Training, Bern 10.02.2023

In collaboration with:
M. Mahrous,
Y. Yang (FZJ), J. Poonoosamy (FZJ),
G. Kosakowski, W. Pfingsten, D. Miron,
E. Curti, D. Kulik, S.V. Churakov

PAUL SCHERRER INSTITUT

ETH-Domain: Paul Scherrer Institut

Page 2

PAUL SCHERRER INSTITUT

Nuclear Waste Management concept: Geological disposal

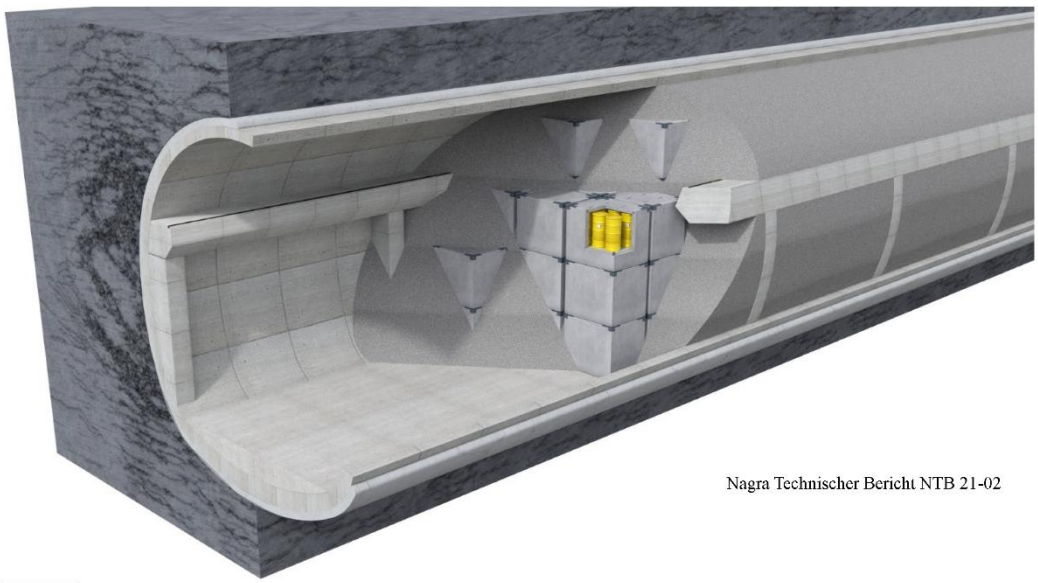

PAUL SCHERRER INSTITUT

Motivation:
Subsurface processes are governed by dissolution precipitation processes

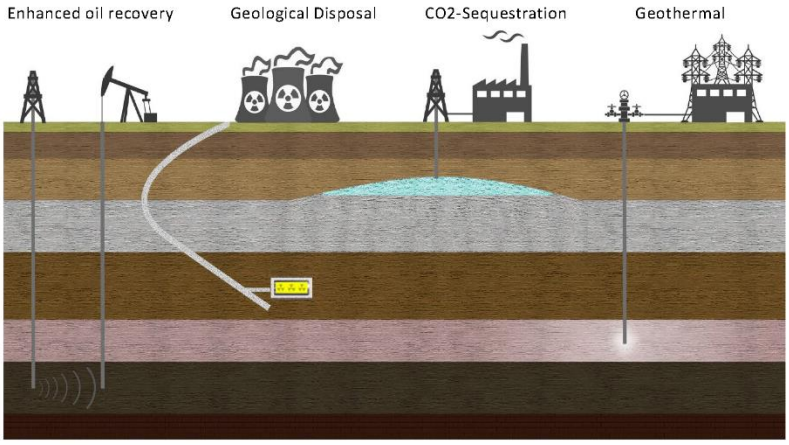

Graphic: M. Mahrous

Multiscale description is necessary

Page 4

Motivation: Geochemical digital twins

Digital Twin is a modelling based tool of increased realism. For geochemical applications, it should cover several spatial and temporal scales, as well as all major underlying mechanisms.

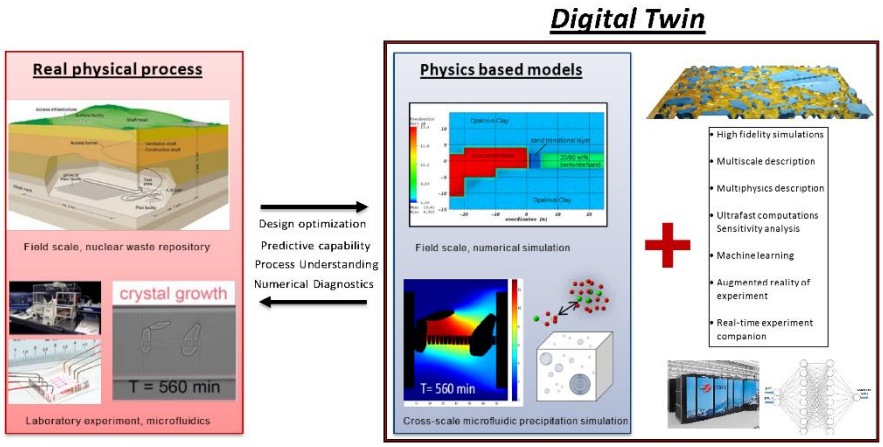

Geochemical evolution of repository is governed by mass transport and phase changes: all scales matter

Processes occurring at the atomic- and pore- scale control the evolution of the geochemical systems. Currently, there exist several mature numerical tools, and good process understanding, at each scale.

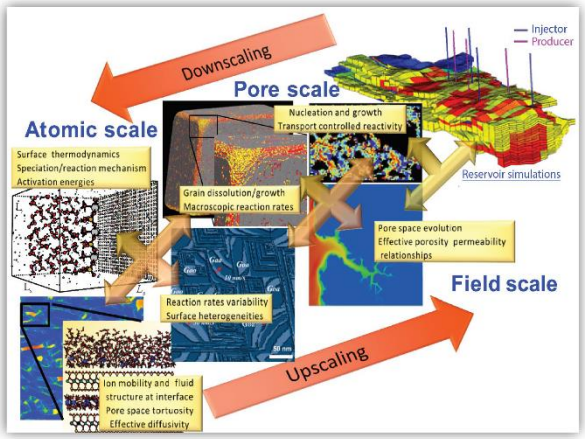

Churakov & Prasianakis, *Holistic process-based description of mass transport and mineral reactivity in porous media.* **Am. J. Science, 318 (9)** 921-948 (2018)

EURAD-DONUT
Development and Improvement
Of **NU**merical methods and **T**ools
for modelling coupled processes

Questions:
How to couple heterogeneous codes and processes ?
How to accelerate calculations ?

Evolution of dissolution and precipitation during 140 hours
blue: celestine volumetric fraction,
yellow: baryte volumetric fraction

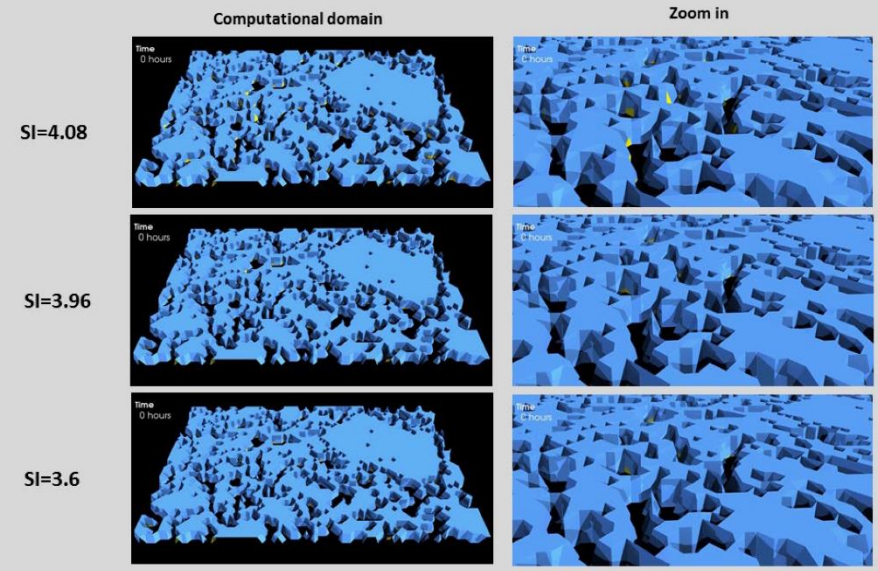

Lattice Boltzmann Simulation

Prasianakis, N. I., Curti, E., Kosakowski, G., Poonoosamy, J., & Churakov, S. V. (2017). *Deciphering pore-level precipitation mechanisms.* ***Scientific reports***, 7(1), 13765.

Page 7

PAUL SCHERRER INSTITUT

Well established tools and process understanding exists at each scale: pore-scale benchmark example.

Such an example is the pore-scale dissolution benchmark with evolving fluid-solid interfaces.
A calcite rock is dissolved due to the convective flow of acid solution.
Six different codes participated and gave similar results.

Remaining Challenges: ***Transfer information and connect the scales / codes, Accelerate Calculations***

Institute:	Oak Ridge National Laboratory	PSI	Lawrence Berkeley National Laboratory	Université de Paris-Est Marne-la-Vallée	University of Florida	Stanford University / brgm
Participant code:	**dissolFoam**	**Lattice Boltzmann**	**Chombo Crunch**	**Vortex method**	**dissolFoam**	**OpenFoam-DBS**

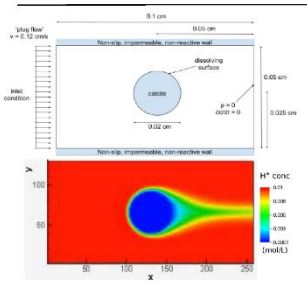

H+ Concentration contours pH=2

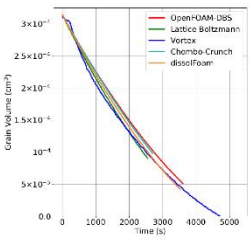

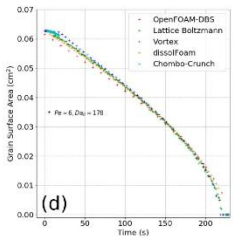

Molins et al, *Simulation of mineral dissolution at the pore scale with evolving fluid-solid interfaces: Review of approaches and benchmark problem set*, **Computational Geosciences, 1-34** (2020), https://doi.org/10.1007/s10596-019-09903-x

PAUL SCHERRER INSTITUT

Challenges

- Bridging heterogeneous codes which describe processes at different scales
- Accelerate reactive transport numerical simulations without loss of accuracy
- Accelerate sensitivity analysis without loss of accuracy
- How to exploit high performance computing (Parallel CPU/GPU Supercomputers)

machine learning is the key enabling technology

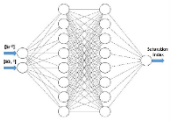

"**Machine learning** is the subset of *artificial intelligence (AI)* that focuses on building systems that learn, or improve performance, based on the data they consume" source: Oracle.com

"**Deep learning** is a subset of machine learning in which multi-layered neural networks 'learn' from large amounts of data" source: IBM.com

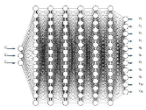

Seite 9

PAUL SCHERRER INSTITUT

Bridging heterogeneous codes at different scales

Example: upscaling pore-level results to macroscopic codes

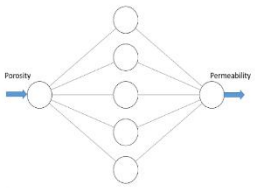

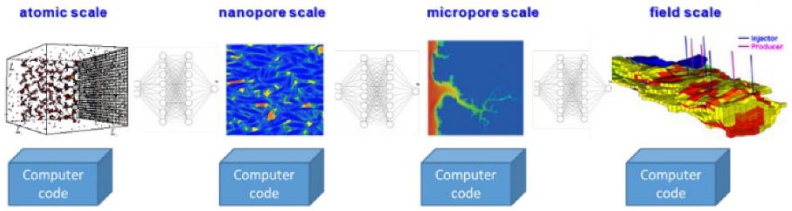

Prasianakis, N.I., Haller, R., Mahrous, M., Poonoosamy, J., Pfingsten, W. and Churakov, S.V., **(2020)**. Neural network based process coupling and parameter upscaling in reactive transport simulations. ***Geochimica et Cosmochimica Acta***, *291*, pp.126-143.

*This document is property of PSI. No unauthorized reproduction or disclosure is permitted

Page 10

PAUL SCHERRER INSTITUT

Upscaling pore-level results to macroscopic codes
Calcite rock acidification: case specific porosity-permeability correlations, extracted from detailed pore-level simulations.

$$H^+ + CaCO_3 \rightarrow Ca^{2+} + HCO^-_3$$

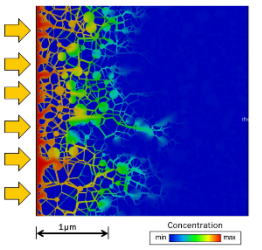

Evolution of porous medium (calcite matrix) due to reactive transport (dissolution)

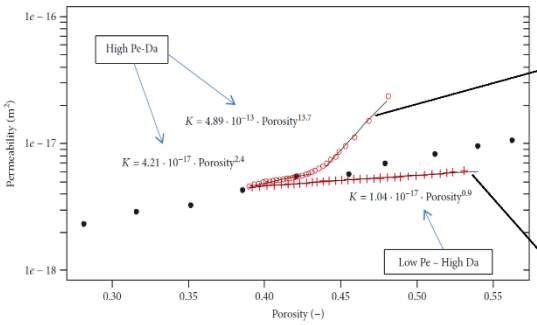

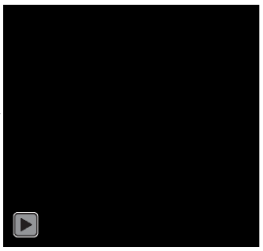

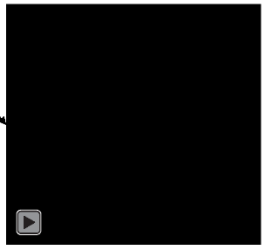

Kozeny-Carman equation **fails !**

$$K = a \cdot porosity^b$$

Prasianakis, N.I., et al. Upscaling Strategies of Porosity-Permeability Correlations in Reacting Environments from Pore-Scale Simulations. ***Geofluids*** 9260603 (2018).

PAUL SCHERRER INSTITUT

Bridging heterogeneous codes at different scales: Upscaling of Pore level porosity-permeability correlations to macroscopic darcy scale code

Communication and interfacing of heterogeneous codes at different spatial scales can be based on neural networks.
The scale specific mechanisms and their dependence on several parameters can be used as the training input.

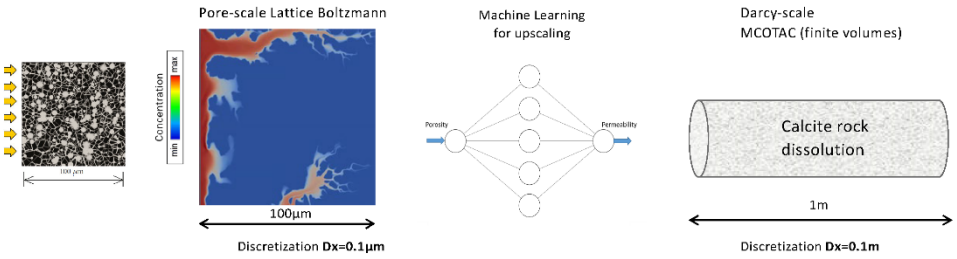

Trained neural networks are light and robust functions that can be easily integrated in any code, written in any of the major programming languages.

Prasianakis, N.I., Haller, R., Mahrous, M., Poonoosamy, J., Pfingsten, W. and Churakov, S.V., **(2020)**.
Neural network based process coupling and parameter upscaling in reactive transport simulations. ***Geochimica et Cosmochimica Acta***, *291*, pp.126-143.

12

Passing information from pore-scale level codes to Macroscopic codes: Process can be automated.

During dissolution/precipitation, the permeability-porosity correlations deviate from typical Kozeny-Carman, and depend highly on the chemical and flow gradients. The Peclet (Pe) and Damkohler (Da) numbers dictate the evolution paths (e.g. wormhole formation / face dissolution).

$$H^+ + CaCO_3 \rightarrow Ca^{2+} + HCO^-_3$$

Permeability (K) – porosity correlation: $K = a \cdot porosity^b$

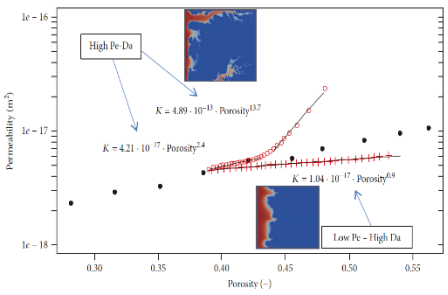

Machine Learning for upscaling

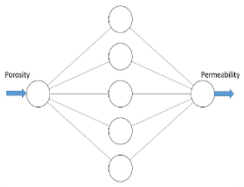

Calcite porosity distribution during acidification along the macroscopic domain for two different approaches

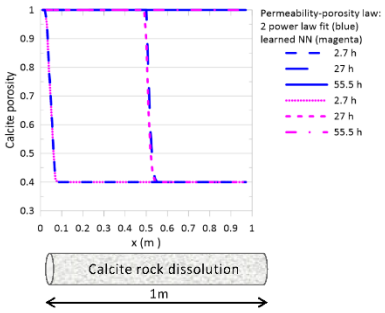

If data exist, the neural network can represent higher dimension parameter spaces:
e.g. **porosity / diffusivity-permeability correlations as functions of** ***K=f(Pe, Da, initial porosity, heterogeneity,…)***

13

Machine Learning for accelerating codes: chemical reactions

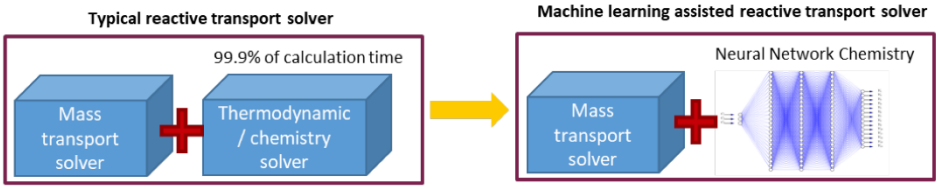

Accelerating chemistry in the field of combustion, reactive flows (1996 -)

Christo, F. C. et al."Artificial neural network implementation of chemistry with PDF simulation of H2/CO2 flames." Combustion and Flame 106, no. 4 (**1996**): 406-427.

Accelerating geochemistry and geochemical reactive transport calculations (2016 -)

Jatnieks, J., De Lucia, M., Dransch, D. and Sips, M., (**2016**). Data-driven surrogate model approach for improving the performance of reactive transport simulations. Energy Procedia, 97, pp.447-453.

Guerillot, D. R., and J. Bruyelle, 3rd EAGE Integrated Reservoir Modelling 504 (**2016**).

Leal, A., Kyas S., Kulik D., Saar, M. arXiv:1708.04825 (**2017**), *Transport in Porous Media* (**2020**).

Laloy, E., and Jacques, D., *Computational Geosciences* 23, no. 5 (**2019**): 1193-1215.

Prasianakis, N.I., Haller, R., Mahrous, M., Poonoosamy, J., Pfingsten, W. and Churakov, S.V., (**2020**). *Geochimica et Cosmochimica Acta*, *291*, pp.126-143.

Laloy, E. and Jacques, D., Transport in Porous Media (**2022**), DOI: 10.1007/s11242-022-01779-3

Seite **14**

PAUL SCHERRER INSTITUT

Numerical diagnostics and digital twins

Lab on a chip experiment (Celestine precipitation)
Augmented reality via modeling diagnostics

"Need for Speed"

NVIDIA CUDA · MATLAB · python · TensorFlow · Keras

Page 15

PAUL SCHERRER INSTITUT

Accelerating reactive transport simulations for Geochemical Digital Twins

JÜLICH FORSCHUNGSZENTRUM

Radionuclide transport: Ra retention due to precipitation → solid solutions **(Ba,Sr,Ra)SO4**

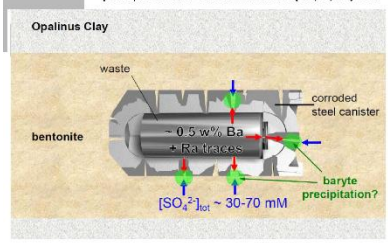

Lab on a chip
Microfluidic reactor
(**µm** scale)

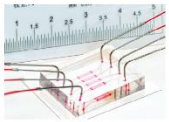

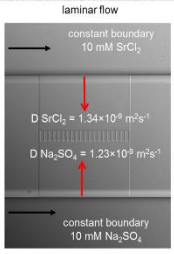

$SrCl_{2(aq)} + Na_2SO_{4(aq)} \rightarrow SrSO_{4(s)} + 2NaCl_{(aq)}$

Injection of fresh 10 mM $SrCl_2$ and 10 mM Na_2SO_4 mixture → celestine precipitation, crystal growth

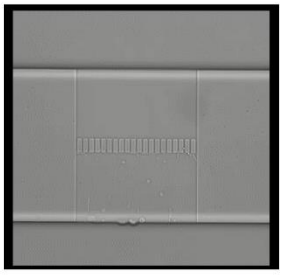

Experiments: J. Poonoosamy et al. (FZ-Jülich)

Lattice Boltzmann pore-level reactive transport simulations

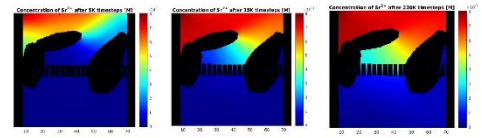

Evolution of Concentration of Sr^{+2}

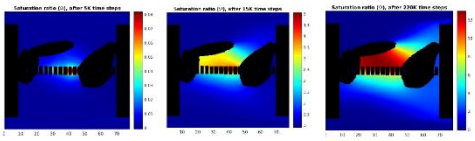

Evolution of Saturation ratio

Poonoosamy, J., Westerwalbesloh, C., Deissmann, G., Mahrous, M., Curti, E., Churakov, S.V., Klinkenberg, M., Kohlheyer, D., Von Lieres, E., Bosbach, D., Prasianakis, N.I., A microfluidic experiment and pore scale modelling diagnostics for assessing mineral precipitation and dissolution in confined spaces, ***Chemical Geology, 528, 5, 119264 (2019)***

16

PAUL SCHERRER INSTITUT PSI

Lab on a chip: design and concept

JÜLICH FORSCHUNGSZENTRUM

μscale

Advantages: miniaturized environment, shorter time-scales, small quantities of reactants, continuous monitoring, parallel

Challenges : in-situ conditions of flow and chemistry unknown, control of experiment, manufacturing, design of experiment

Typical lab experiment (**cm** scale)

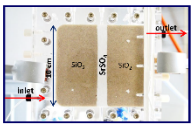

Microfluidic reactor (**μm** scale)

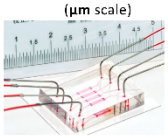

laminar flow

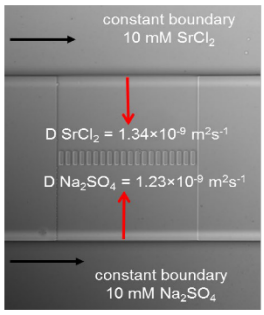

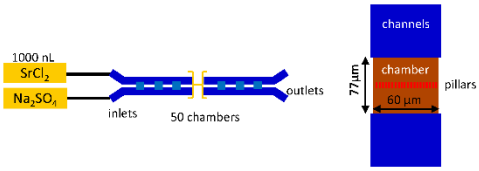

$SrCl_{2(aq)} + Na_2SO_{4(aq)} \rightarrow SrSO_{4(s)} + 2NaCl_{(aq)}$

Collaboration with J. Poonoosamy, FZ-Jülich, Germany

Page 17

PAUL SCHERRER INSTITUT PSI

Digital Twin and Numerical diagnostics

JÜLICH FORSCHUNGSZENTRUM

Augmented reality by combining cross scale lattice Boltzmann modelling diagnostics. Numerical model includes:
a classical nucleation theory (CNT) implementation (nanoscale processes), multicomponent transport, kinetic reactions.

Injection of 10 mM $SrCl_2$ and 10 mM Na_2SO_4 → celestine precipitation, crystal growth

Layers of diagnostics

Evolution of experiment (camera)

Local flow-field and streamlines visualization (numerically calculated, experimentally verified).

Spatial resolution of velocity field at different stages of the experiment (numerically calculated)

Local species concentrations, saturation ratio (numerically calculated, interplay of advection/diffusion)

Local precipitation rates at fluid-solid interface, prediction of directional differential growth (numerically calculated, color: precipitation rate)

Poonoosamy, J., Westerwalbesloh, C., Deissmann, G., Mahrous, M., Curti, E., Churakov, S.V., Klinkenberg, M., Kohlheyer, D., Von Lieres, E., Bosbach, D., Prasianakis, N.I., A microfluidic experiment and pore scale modelling diagnostics for assessing mineral precipitation and dissolution in confined spaces, ***Chemical Geology, 528, 5, 119264 (2019)***

PAUL SCHERRER INSTITUT PSI

Digital Twin and Numerical diagnostics

JÜLICH FORSCHUNGSZENTRUM

Augmented reality by combining cross scale lattice Boltzmann modelling diagnostics. Numerical model includes: a classical nucleation theory (CNT) implementation (nanoscale processes), multicomponent transport, kinetic reactions.

Injection of 10 mM $SrCl_2$ and 10 mM Na_2SO_4 → celestine precipitation, crystal growth

Layers of diagnostics

Evolution of experiment (camera)

Local flow-field and streamlines visualization (numerically calculated, experimentally verified).

Spatial resolution of velocity field at different stages of the experiment (numerically calculated)

Local species concentrations, saturation ratio (numerically calculated, interplay of advection/diffusion)

Local precipitation rates at fluid-solid interface, prediction of directional differential growth (numerically calculated, color: precipitation rate)

Poonoosamy, J., Westerwalbesloh, C., Deissmann, G., Mahrous, M., Curti, E., Churakov, S.V., Klinkenberg, M., Kohlheyer, D., Von Lieres, E., Bosbach, D., Prasianakis, N.I., A microfluidic experiment and pore scale modelling diagnostics for assessing mineral precipitation and dissolution in confined spaces, ***Chemical Geology, 528, 5, 119264 (2019)***

PAUL SCHERRER INSTITUT PSI

Digital Twin and Numerical diagnostics

JÜLICH FORSCHUNGSZENTRUM

Augmented reality by combining cross scale lattice Boltzmann modelling diagnostics. Numerical model includes: a classical nucleation theory (CNT) implementation (nanoscale processes), multicomponent transport, kinetic reactions.

Injection of 10 mM $SrCl_2$ and 10 mM Na_2SO_4 → celestine precipitation, crystal growth

Layers of diagnostics

Evolution of experiment (camera)

Local flow-field and streamlines visualization (numerically calculated, experimentally verified).

Spatial resolution of velocity field at different stages of the experiment (numerically calculated)

Local species concentrations, saturation ratio (numerically calculated, interplay of advection/diffusion)

Local precipitation rates at fluid-solid interface, prediction of directional differential growth (numerically calculated, color: precipitation rate)

Poonoosamy, J., Westerwalbesloh, C., Deissmann, G., Mahrous, M., Curti, E., Churakov, S.V., Klinkenberg, M., Kohlheyer, D., Von Lieres, E., Bosbach, D., Prasianakis, N.I., A microfluidic experiment and pore scale modelling diagnostics for assessing mineral precipitation and dissolution in confined spaces, ***Chemical Geology, 528, 5, 119264 (2019)***

PAUL SCHERRER INSTITUT PSI

Digital Twin and Numerical diagnostics

JÜLICH FORSCHUNGSZENTRUM

Augmented reality by combining cross scale lattice Boltzmann modelling diagnostics. Numerical model includes:
a classical nucleation theory (CNT) implementation (nanoscale processes), multicomponent transport, kinetic reactions.

Injection of 10 mM $SrCl_2$ and 10 mM Na_2SO_4 → celestine precipitation, crystal growth

Layers of diagnostics

Evolution of experiment (camera)

Local flow-field and streamlines visualization (numerically calculated, experimentally verified).

Spatial resolution of velocity field at different stages of the experiment (numerically calculated)

Local species concentrations, saturation ratio (numerically calculated, interplay of advection/diffusion)

Local precipitation rates at fluid-solid interface, prediction of directional differential growth (numerically calculated, color: precipitation rate)

Poonoosamy, J., Westerwalbesloh, C., Deissmann, G., Mahrous, M., Curti, E., Churakov, S.V., Klinkenberg, M., Kohlheyer, D., Von Lieres, E., Bosbach, D., Prasianakis, N.I., A microfluidic experiment and pore scale modelling diagnostics for assessing mineral precipitation and dissolution in confined spaces, ***Chemical Geology, 528, 5, 119264 (2019)***

PAUL SCHERRER INSTITUT PSI

Digital Twin and Numerical diagnostics

JÜLICH FORSCHUNGSZENTRUM

Augmented reality by combining cross scale lattice Boltzmann modelling diagnostics. Numerical model includes:
a classical nucleation theory (CNT) implementation (nanoscale processes), multicomponent transport, kinetic reactions.

Injection of 10 mM $SrCl_2$ and 10 mM Na_2SO_4 → celestine precipitation, crystal growth

Layers of diagnostics

Evolution of experiment (camera)

Local flow-field and streamlines visualization (numerically calculated, experimentally verified).

Spatial resolution of velocity field at different stages of the experiment (numerically calculated)

Local species concentrations, saturation ratio (numerically calculated, interplay of advection/diffusion)

Local precipitation rates at fluid-solid interface, prediction of directional differential growth (numerically calculated, color: precipitation rate)

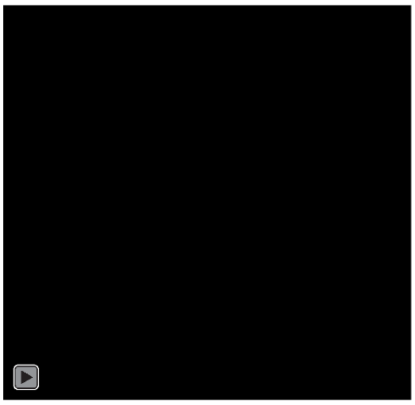

Poonoosamy, J., Westerwalbesloh, C., Deissmann, G., Mahrous, M., Curti, E., Churakov, S.V., Klinkenberg, M., Kohlheyer, D., Von Lieres, E., Bosbach, D., Prasianakis, N.I., A microfluidic experiment and pore scale modelling diagnostics for assessing mineral precipitation and dissolution in confined spaces, ***Chemical Geology, 528, 5, 119264 (2019)***

PAUL SCHERRER INSTITUT

Simple speciation, complex reactive transport and phase change setup: celestine precipitation

For the digital twin of the microfluidic experiment it is necessary to calculate at each time step, and at each node the chemical speciation and the saturation index (SI). Local SI drives the precipitation kinetics.

Injection of fresh 10 mM $SrCl_2$ and 10 mM Na_2SO_4 mixture
→ celestine precipitation, crystal growth

Evolution of Concentration of Sr^{+2}

Evolution of Saturation ratio

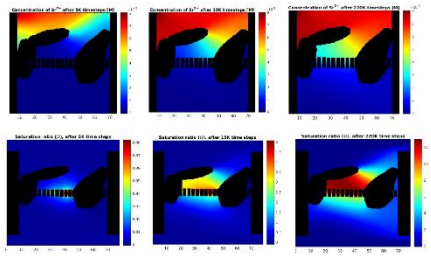

Typical workflow for calculation of SI: Knowing the concentrations of primary species, an external LMA solver, e.g. GEMS / PHREEQC / ORCHESTRA is invoked for the calculation of the chemical speciation

Primary Species: $[Sr]_{total}$, $[Cl]_{total}$, $[Na]_{total}$, $[S]_{total}$ → Exact LMA GEMS PHREEQC → Secondary Species: $SrSO_{4\,(aq)}$, Na^+, Cl^-, $NaSO4^-$, Sr^{+2}, $SO4^{-2}$ →

$$SI_{celestine} = log_{10}\frac{\{Sr^{+2}\}\{SO_4^{-2}\}}{K_{sp}}$$

PAUL SCHERRER INSTITUT

Accelerating geochemistry, and accuracy considerations Comparison of Exact LMA, Lookup table, Neural Network

Exact LMA GEMS PHREEQC **Vs**

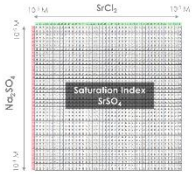

Vs

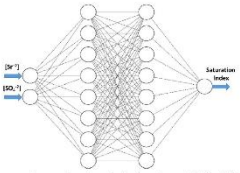

Exact LMA coupled to lattice Boltzmann (LB)

40x40 lookup table generated from exact LMA, coupled to LB

Neural network trained on 70% of the lookup table entries, RMSE=6.64 * 10^{-3}, coupled to LB

Evolution of the domain average supersaturation for the different methods: exact LMA, lookup table (linear interpolation), neural network with 2 hidden layers.

In this setup, ANN proves to be orders of magnitude faster compared to LMA and extremely accurate also compared to lookup table.

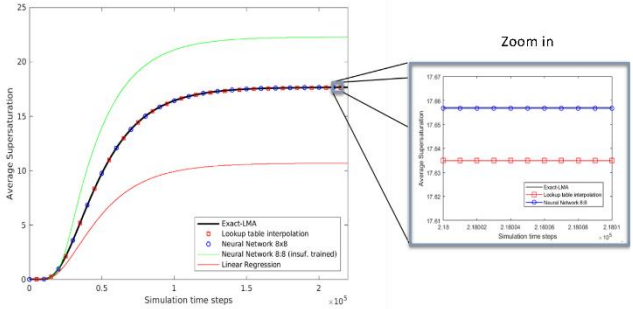

Prasianakis, N.I., Haller, R., Mahrous, M., Poonoosamy, J., Pfingsten, W. and Churakov, S.V., (**2020**). Neural network based process coupling and parameter upscaling in reactive transport simulations. ***Geochimica et Cosmochimica Acta***, ***291***, pp.126-143.

Page 24

PAUL SCHERRER INSTITUT

High Performance Computing: Transport is fast, chemistry is slow, hybrid computer architecture

Current supercomputers allow to simulate geometries with > 10 billion voxels (grid points). Most advanced systems have hybrid CPU/GPU computational nodes. Transport and chemical calculations take place at every voxel, at every timestep

Swiss Supercomputing Center (CSCS)
Piz Daint Nvidia Tesla P100 GP-GPUs

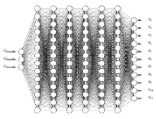

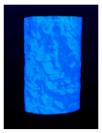

X-ray tomogram
(1 Billion Voxels)

Comparision of Calculations per second

Chemistry GEMS / PHREEQC	Transport (flow) Lattice Boltzmann	Chemistry Neural Network
1 CPU-core ~ 1'000/s	1 CPU-core, 4 species ~ 1'000'000/s	1 CPU-core (depending on system) ->more than 1'000'000/s
1 GPU -> **Impossible** **Code not available**	1 GPU, 4 species -> 100'000'000/s	1 GPU -> more than 50'000'000/s

➡ For high performance computing, where problem can be solved entirely in parallel GPU/CPU architectures (Lattice Boltzmann), **surrogate modelling is an enabling step**.

In this setup, ANN proves to be orders of magnitude faster **(10'000 times !!!)** compared to LMA and extremely accurate also compared to lookup table. **Overall speed up** > **1'000x**

Page 25

PAUL SCHERRER INSTITUT

Cement Clay interfaces

- Laboratory and field experiments show a porosity reduction on the clay side
- Necessity to predict the transport properties of altered interfaces through experiments and numerical simulations

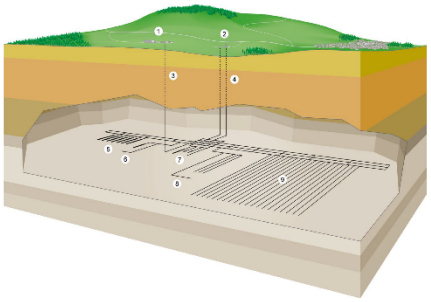

Illustration of a combined repository for SF/HLW and for L/ILW (NTB-21-01, 2022)

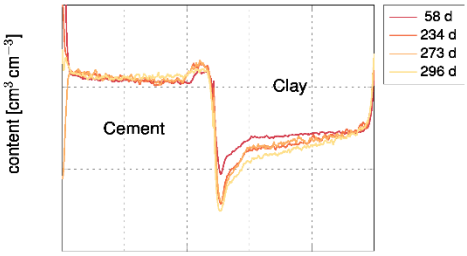

Time evolution of the water content in the OPC-Na montmorillonite laboratory sample C5 over a time of ~300 days. (Shafizadeh, Gimmi, Van Loon, Churakov et al.)

Page 26

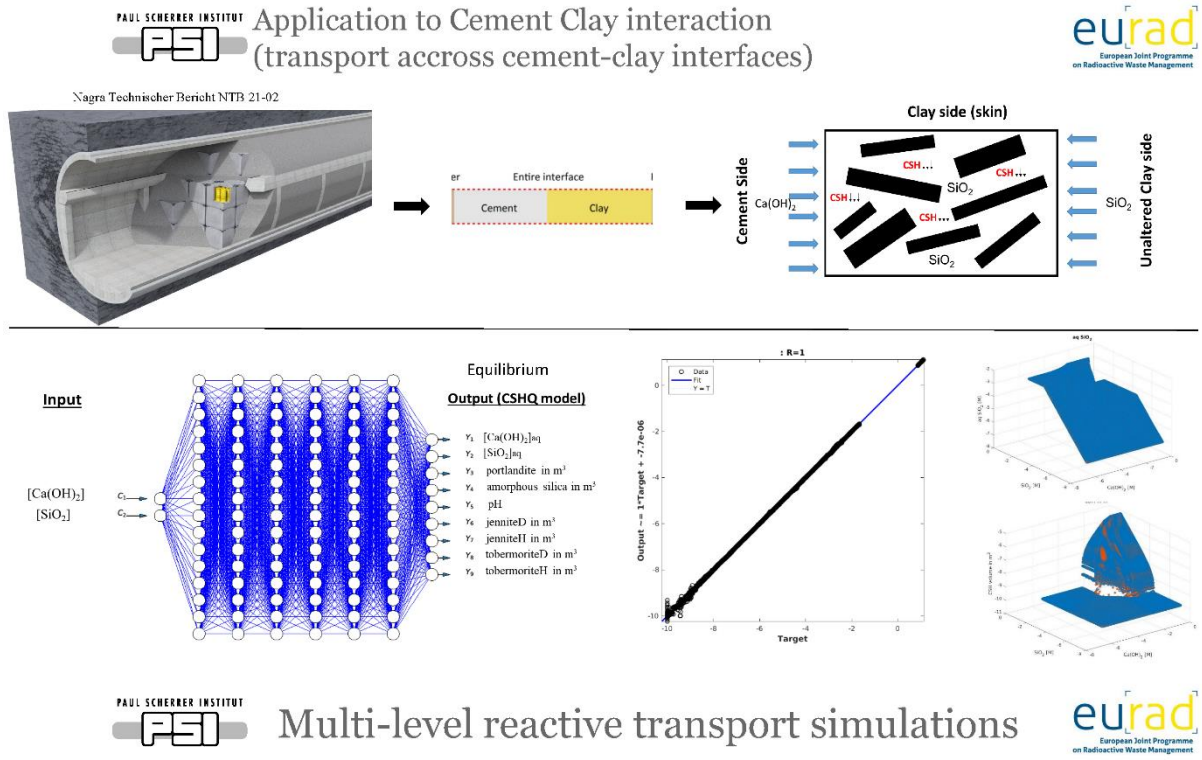
PAUL SCHERRER INSTITUT
Application to Cement Clay interaction
(transport accross cement-clay interfaces)
eurad
European Joint Programme on Radioactive Waste Management
Nagra Technischer Bericht NTB 21-02
Entire interface
Cement
Clay
Clay side (skin)
Cement Side
Unaltered Clay side
Ca(OH)2
SiO2
CSH...
Input
Equilibrium
Output (CSHQ model)
[Ca(OH)2]
[SiO2]
portlandite in m³
amorphous silica in m³
pH
jenniteD in m³
jenniteH in m³
tobermoriteD in m³
tobermoriteH in m³
Target

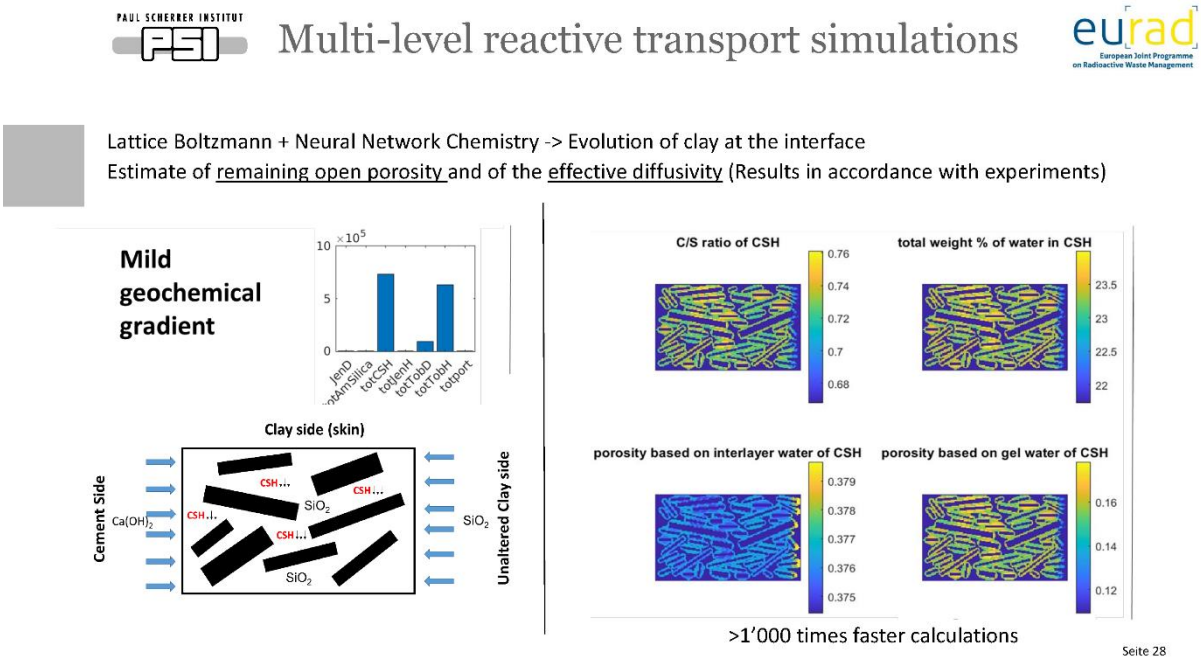
PAUL SCHERRER INSTITUT
Multi-level reactive transport simulations
eurad
European Joint Programme on Radioactive Waste Management
Lattice Boltzmann + Neural Network Chemistry -> Evolution of clay at the interface
Estimate of remaining open porosity and of the effective diffusivity (Results in accordance with experiments)
Mild geochemical gradient
totCSH
totJenH
totTobD
totTobH
totport
Clay side (skin)
Cement Side
Unaltered Clay side
C/S ratio of CSH
total weight % of water in CSH
porosity based on interlayer water of CSH
porosity based on gel water of CSH
>1'000 times faster calculations
Seite 28

EURAD DONUT: Machine Learning and geochemistry benchmark: so far > 10 modelling teams

- CROSS-EURAD Collaborative effort Participants inside/outside EURAD continue to join
- Meetings every 1-2 months to discuss progress
- Joint Development of methodologies and codes. Modelling teams are working closely together.
- Open source software is heavily used.

several machine learning techniques are explored within EURAD-DONUT
e.g. ***polynomial chaos expansion, Gaussian processes, reduced base approach***

29

Next generation of computational tools: Initiative for open online platforms (*Prototype stage*)

As simple as it gets…

- Education
- Collaboration
- Demonstration

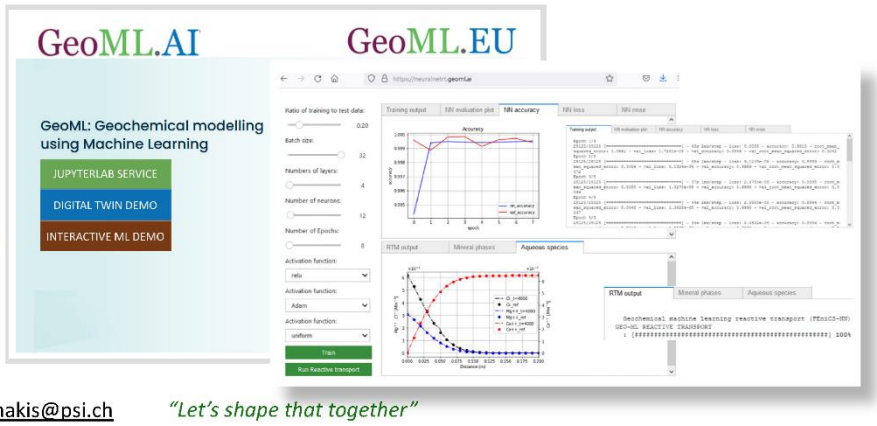

contact: nikolaos.prasianakis@psi.ch *"Let's shape that together"*

Seite 30

Summary

- Ever increasing realism of multiphysics simulations **is an enabling technology** for **process understanding and design optimization** of future nuclear waste repositories
- **Machine learning** can assist in **bridging** the scales and physics in multiscale multiphenomena simulations and in **accelerating** numerical simulations.
- This is especially important for conducting **sensitivity and uncertainty analysis**. Metamodels can accelerate sensitivity analysis (see presentation of E. Laloy)
- **Neural networks** must be trained carefully to achieve the desired accuracy. More research is needed to identify better the fields of application. Full potential is yet to be explored. Should be used when lookup-tables become enormously large.
- **Digital twins** can assist in the interpretation and the steering of laboratory experiments. The potential is yet to be explored.

Page 31

Wir schaffen Wissen – heute für morgen

Acknowledgements: Nagra, SNF, BFE, EU

Page 32

sck cen
Belgian Nuclear Research Centre

Machine learning for accelerating reactive transport model simulations and analysis

Eric Laloy

EURAD training course, 10/02/2023

Content

- Why and how nonlinear regression using ML can be useful in RTM simulation
- Brief overview of three popular ML methods for regression
  - kNN (lookup table + interpolation)
  - Gaussian processes (GP, "non parametric")
  - Artificial neural networks (NN, parametric & high-dimensional)
- Examples
  - Surrogate geochemical modeling to accelerate 2D RT simulations in a cement system
  - Full RTM surrogate modeling to enable uncertainty analysis (SA, UP, Inverse modeling) for the 1D transport of UVI in a soil column
- Outlooks

sck cen | Reference

2
ISC: Restricted

Why ML is useful?

- Geochemical calculations typically consume most of the computational time of RT simulations, say 80% to 90%
- Over large domains and/or for long simulation periods, RT simulations may become intractable (see table with times by Nikoleos)
  - Replace the geochemical solver of the RTM by a trained ML surrogate model
  - Some recent works : Huang et al. (2018), Guérillot and Bruyelle (2019), Leal et al. (2020), Prasianakis et al. (2020), De Lucia and Kühn (2021), Laloy and Jacques (2022), Demirer et al. (2022)
- Even for small domain and simulation period, CPU-time might be quite long, thereby preventing tasks such as SA, Uncertainty propagation, inverse modeling (model calibration)
  - Emulate output(s) of interest for the full RTM (flow + geochemistry), for given initial and boundary conditions
  - Laloy and Jacques (2019)

sck cen | Reference 3 ISC: Restricted

Nonlinear regression methods

- **kNN** regression
- y* given by weighted mean of the k nearest points to x*

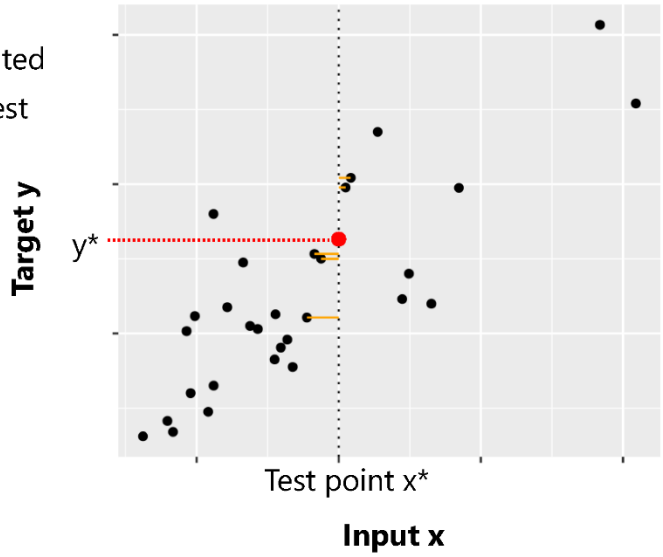

sck cen | Reference 4 ISC: Restricted

Some nonlinear regression methods

- **GP** $f(\mathbf{x}) = GP[m(\mathbf{x}), k(\mathbf{x}, \mathbf{x}')]$

$$\overline{f}(\mathbf{x}^*) = \mathbf{k}_*^{\mathrm{T}}(\mathbf{K} + \sigma_n \mathbf{I})^{-1}\mathbf{y} = \sum_{i=1}^{n} \alpha_i k_*(\mathbf{x}_i, \mathbf{x}_*)$$

$$V[f(\mathbf{x}^*)] = k_*(\mathbf{x}_*, \mathbf{x}_*) - \mathbf{k}_*^{\mathrm{T}}(\mathbf{K} + \sigma_n \mathbf{I})^{-1}\mathbf{k}_*$$

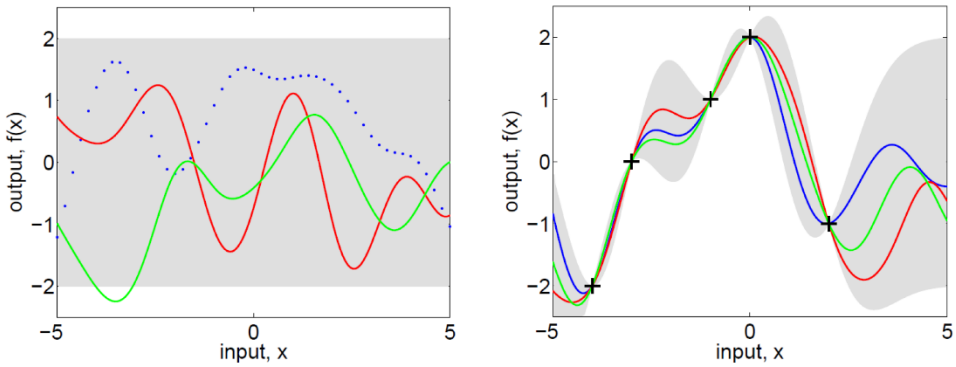

(a), prior (b), posterior

sck cen | 5 ISC: Restricted

Some nonlinear regression methods

- Feedforward fully connected **DNN**

$$\boldsymbol{M}(\mathbf{x}) = f_3\{\mathbf{W}_3 f_2[\mathbf{W}_2 f_1(\mathbf{W}_1\mathbf{x} + \mathbf{b}_1) + \mathbf{b}_2] + \mathbf{b}_3\}$$

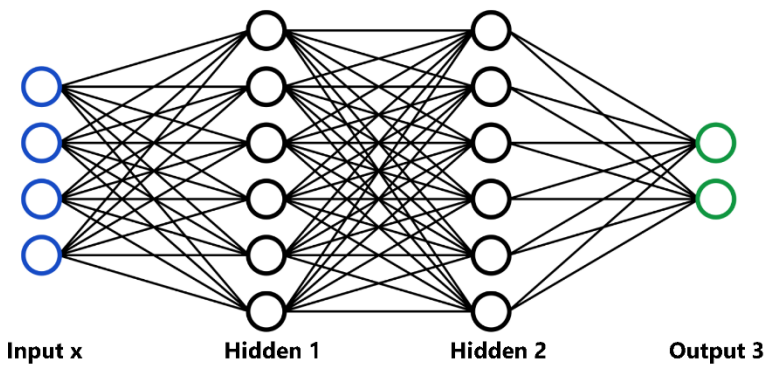

sck cen | Reference 6 ISC: Restricted

Full RTM surrogate modeling

- Problem
  - Desorption of U(VI) from radionuclide-contaminated sediment
  - Multi-rate surface complexation with dual domain mass transfer and alternating hydrochemical composition at the column inlet
  - 13 input parameters
  - Output: times series of dissolved U(VI) concentration (mol/l) in the outflow node of the mobile domain
  - 500 runs in 17 days (4-core parallel)

sck cen | Reference

7
ISC: Restricted

Full RTM surrogate modeling

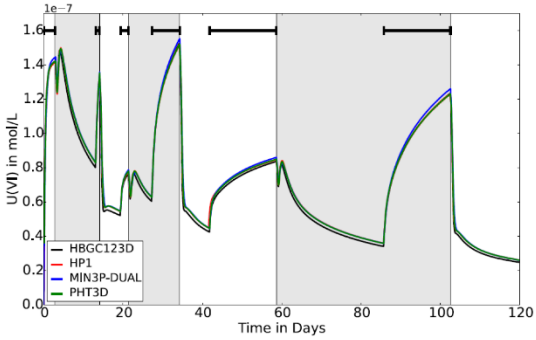

- ML methods: DNN, GP, PCE
- Tasks: (1) plain emulation, (2) global sensitivity analysis (GSA), (3) uncertainty propagation (UP), and (4) probabilistic calibration or inversion
- Training: 25, 75, 175 and 500 samples

sck cen | Reference

8
ISC: Restricted

Plain emulation

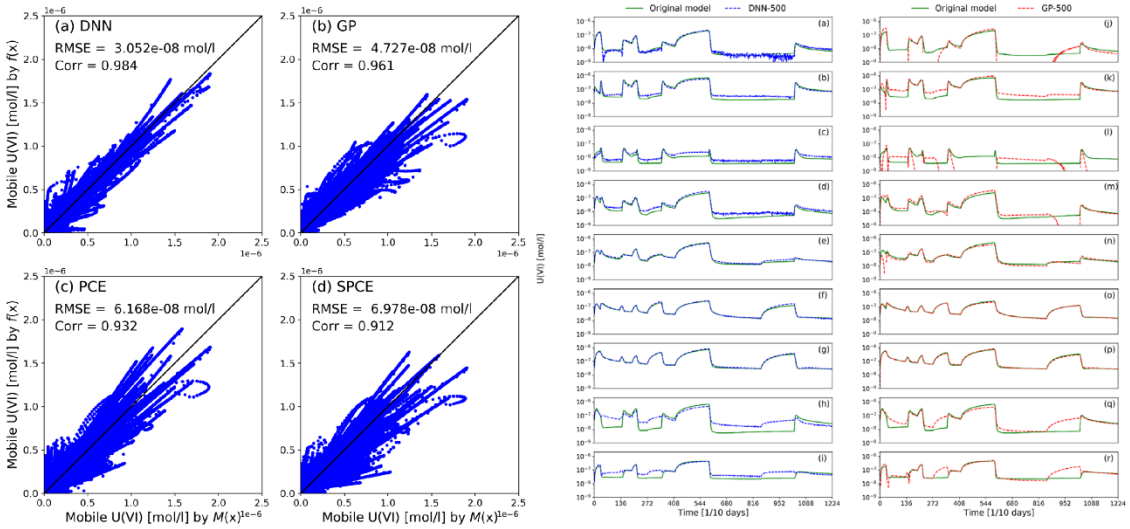

sck cen | Reference

9
ISC: Restricted

Sensitivity analysis

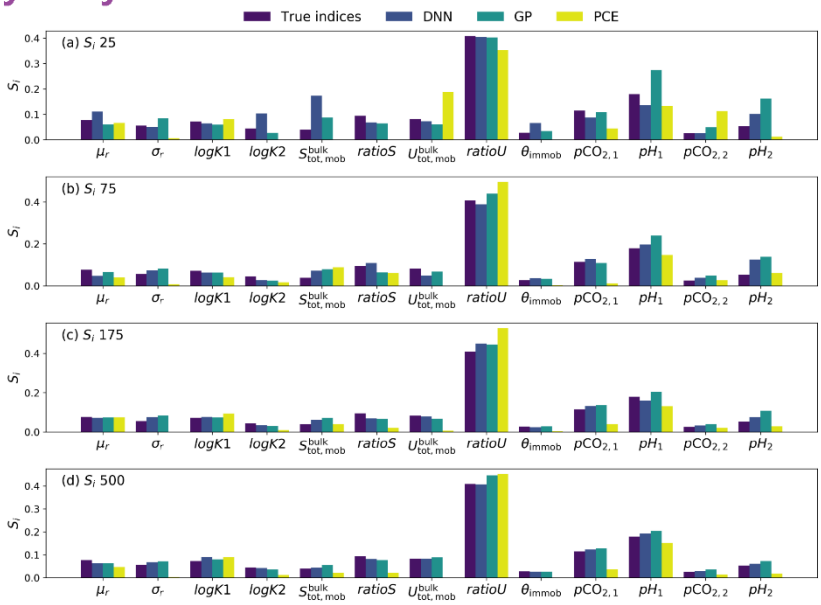

sck cen | Reference

10
ISC: Restricted

Uncertainty propagation

DNN-75	GP-75	PCE-75	DNN-175	GP-175	PCE-175	DNN-500	GP-500	PCE-500
p_{MAX}, true value is 0.0166								
0.0207	0.0041	0.0156	0.0207	0	0	0.0166	0.0166	0.0250
μ_{MAX} (10^{-7} mol/l), true value is 5.346								
5.066	5.029	5.176	5.048	5.000	5.064	5.357	5.125	5.211
σ_{MAX} (10^{-7} mol/l), true value is 3.786								
3.605	3.083	2.961	3.520	3.033	2.898	3.557	3.284	3.531

sck cen | Reference

11
ISC: Restricted

Inverse modeling

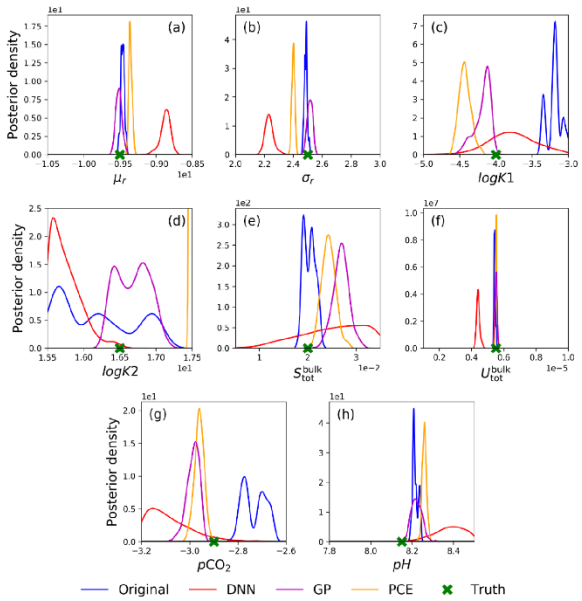

sck cen | Reference

12
ISC: Restricted

Surrogate geochemical modeling within the RTM

- Replace PHREEQC in HPx RT model by trained
  - kNN
  - DNN
  - Speedup > 1000 on a GPU vs single-threaded PHREEQC for 10,000 predictions at once
- After each transport step calculated by Hydrus
  - The C++ written HPx main module calls the Python-based kNN or DNN emulator
  - For each node, emulation of aqueous concentrations from total amounts and re-calculation of the solid amounts
  - For each node and time step, mass balance is honored, but potentially wrong distribution between aqueous and solid phases

sck cen | Reference 13 ISC: Restricted

Problems

- 2D leaching from hardened cement paste, 61x61 (3721) and 121x121 (14641) nodes, advective flow
- Portlandite, C-S-H solid-solution (CSHQ model of Kulik, 2011)
- CaO-SiO_2 system
  - 2 inputs (total Ca, and Si) – 4 outputs (aqueous Ca, H, O and Si)
- CaO-SiO_2-Al_2O_3-CO_2-SO_3 system
  - Calcite, straetlingite, monocarboaluminate and ettringite 5 inputs (total Ca, Si, Al, C and S) – 7 outputs (aqueous Ca, Si, Al, S, C, O, H

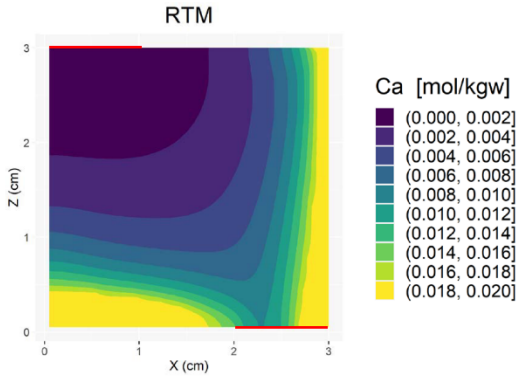

- PHREEQC consumes 80% to 90% of HPx computational budget using 4-cores parallelization (or 94% to 97% on a single-thread)

sck cen | Reference 14 ISC: Restricted

$CaO\text{-}SiO_2$ system

DNN Speedup > 1000 (DNN-GPU versus single-thread PHREEQC)

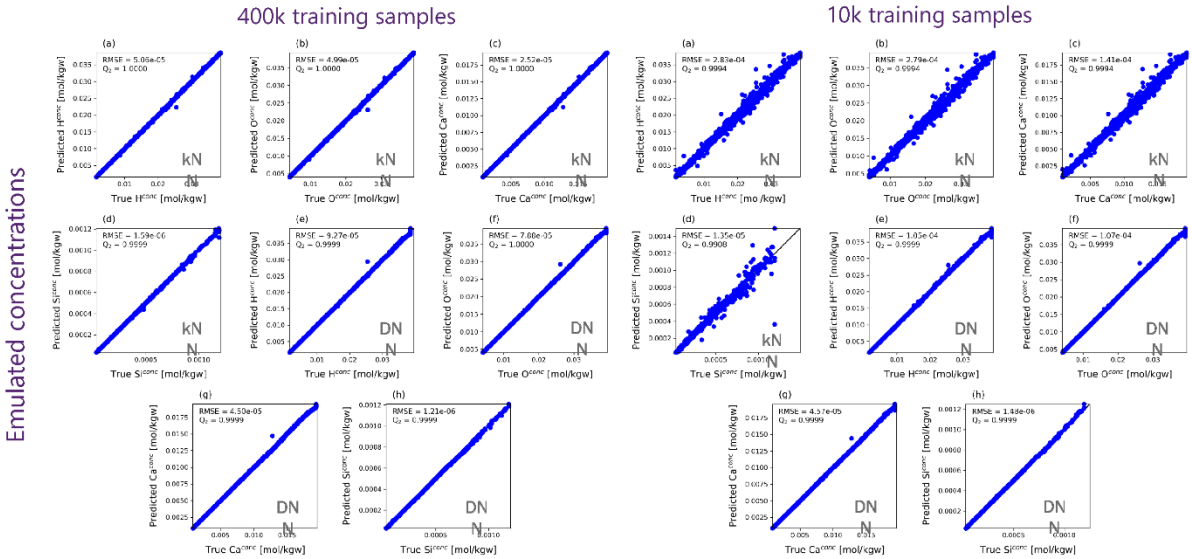

$CaO\text{-}SiO_2$ system

Ca-Si –2D aqueous concentration maps at given time step

DNN & kNN speedup of 7 (max = 7.7) against HP-4 cores, 24.5 (max = 28.5) against HP-1 core

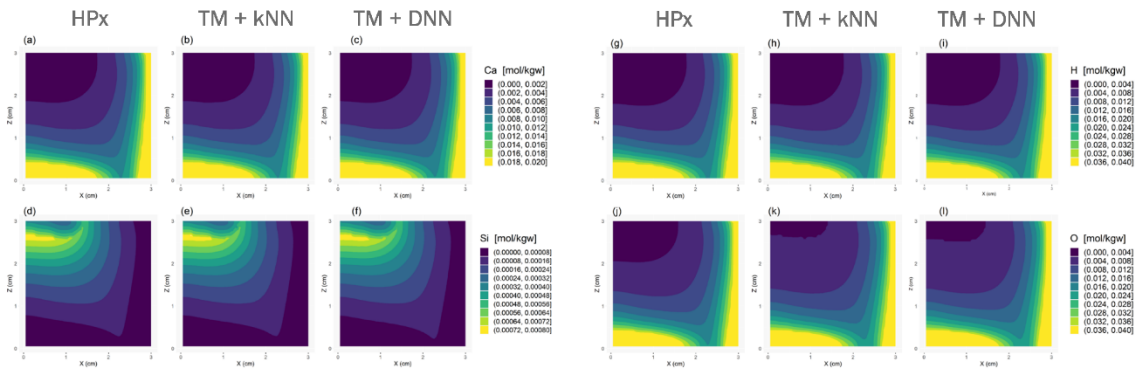

$CaO\text{-}SiO_2$ system

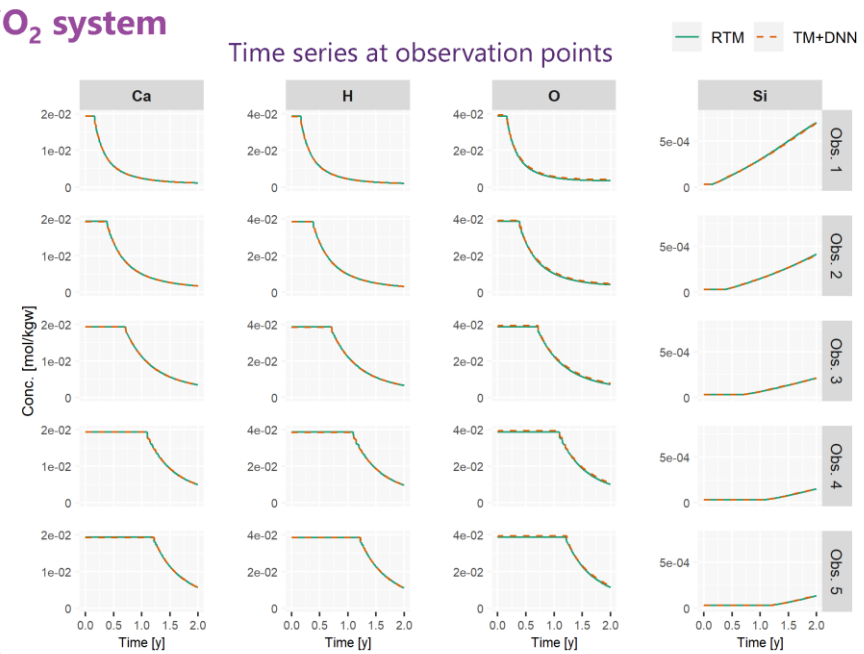

sck cen | Referer

17
ISC: Restricted

$CaO\text{-}SiO_2$ system

Ca-Si –2D solid amount maps at given time step

DNN & kNN speedup of 7 (max = 7.7) against HP-4 cores, 24.5 (max = 28.5) against HP-1 core

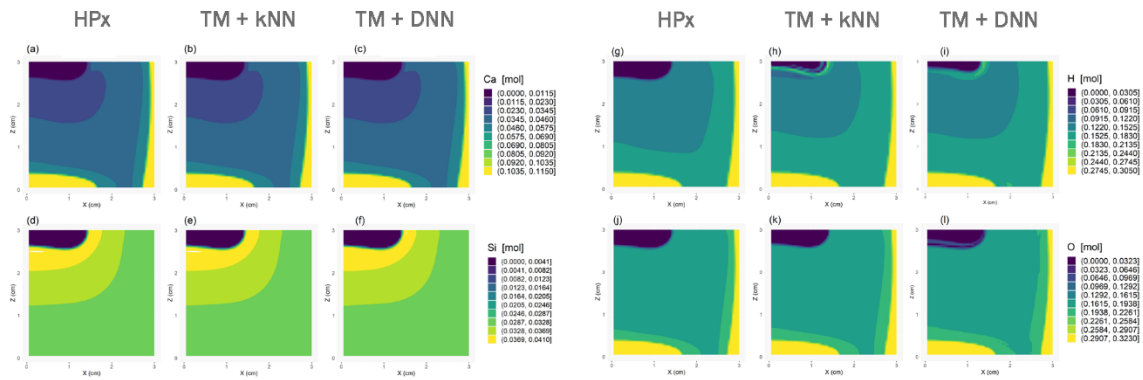

sck cen | Reference

18
ISC: Restricted

CaO-SiO_2-Al_2O_3-CO_2-SO_3 system

- Here training an emulator from a set of samples that cover the whole possible input space **does not work**
- Good accuracy in training/testing split test but poor accuracy in reactive transport simulation!
- This even if the emulator is trained with up to 4,000,000 samples obtained either by LHS or by a low-discrepancy sequence (e.g., Sobol, also called QMC sampling) that more uniformly covers the input space
- For this problem the input (5 total amounts) and output (7 aqueous concentrations) spaces are quite nonlinearly related and both cover 6 to 10 orders of magnitudes depending on the considered chemical element.
- Our considered solution
  - Run a cheap reactive transport simulation: small domain / time period and collect input-output pairs. This simulation indicates potentially interesting directions in the input space.
  - Enrich this dataset by kernel density sampling (KDE).
  - Train the emulators using the ensemble of samples created in steps 1 and 2.

sck cen | Reference 19 ISC: Restricted

CaO-SiO_2-Al_2O_3-CO_2-SO_3 system

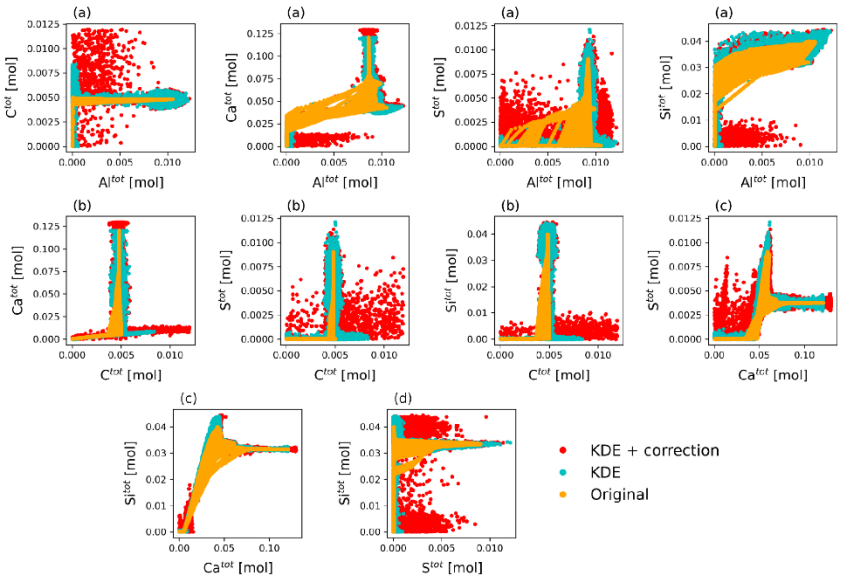

sck cen | Reference 20 ISC: Restricted

$CaO-SiO_2-Al_2O_3-CO_2-SO_3$ system

DNN speedups
8.2 (max = 9) against HP-4c
30.3 (max = 33.1) against HP-1c

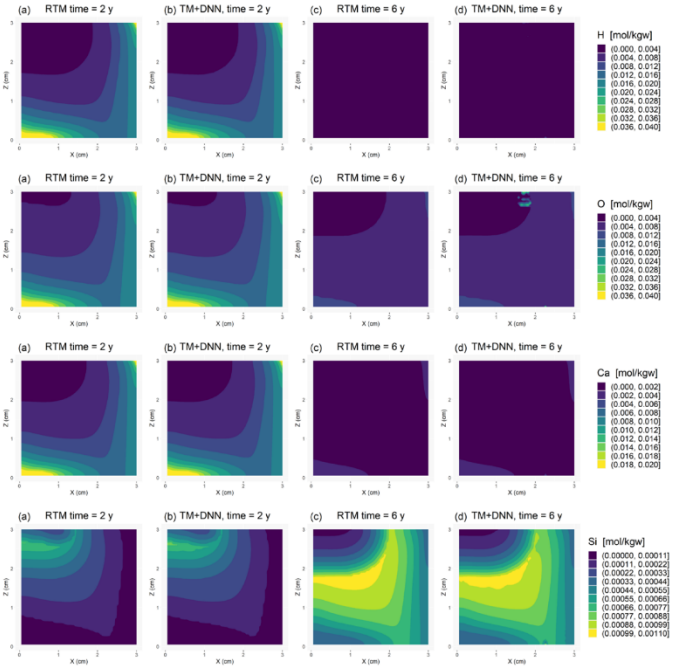

$CaO-SiO_2-Al_2O_3-CO_2-SO_3$ system

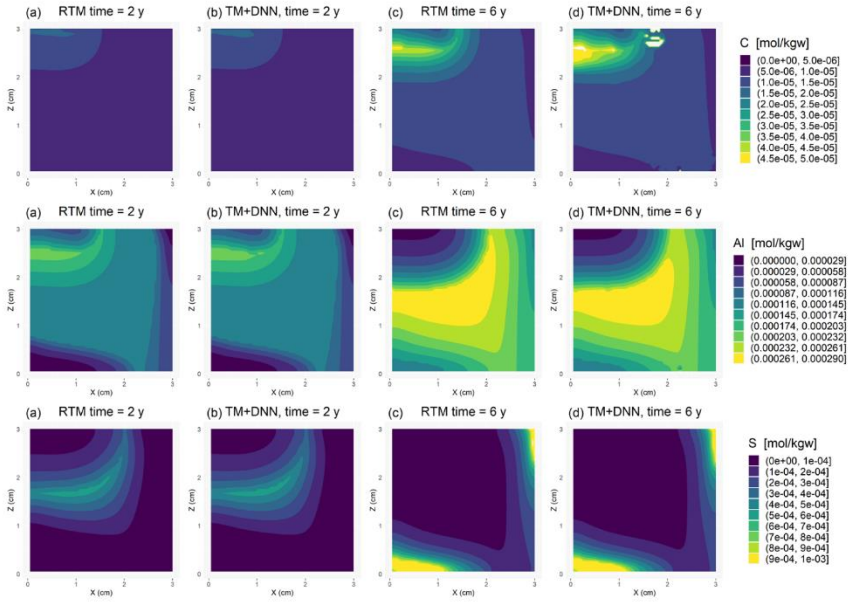

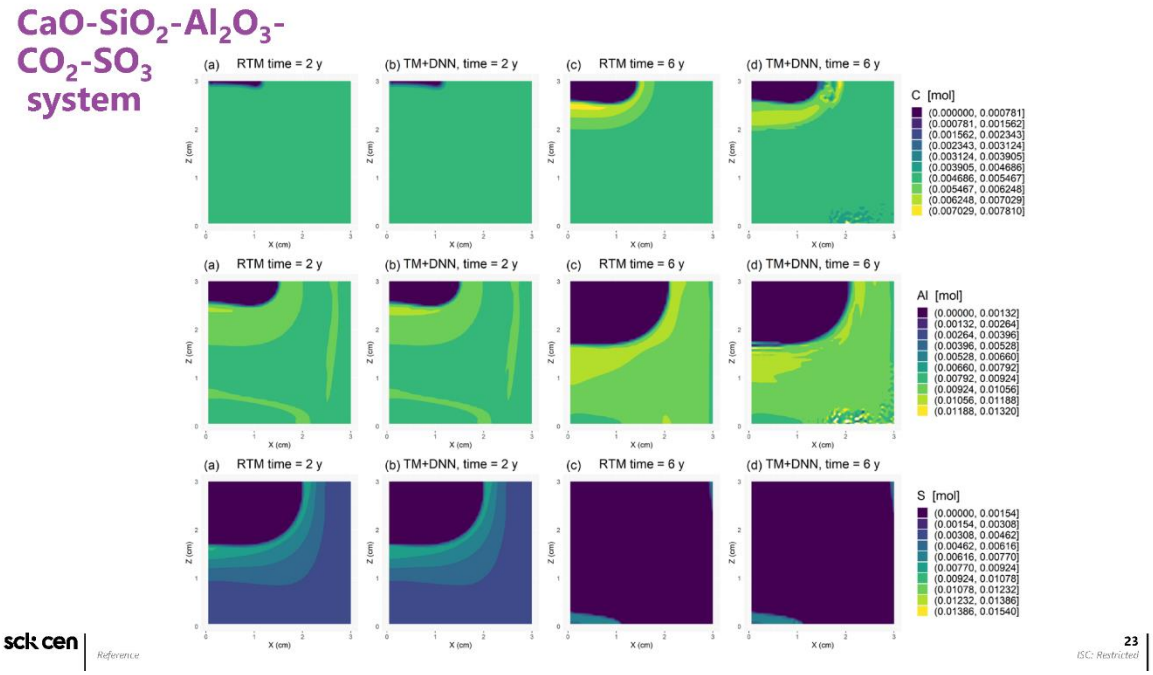
CaO-SiO2-Al2O3-CO2-SO3 system
(a) RTM time = 2 y
(b) TM+DNN, time = 2 y
(c) RTM time = 6 y
(d) TM+DNN, time = 6 y
C [mol]
(0.000000, 0.000781]
(0.000781, 0.001562]
(0.001562, 0.002343]
(0.002343, 0.003124]
(0.003124, 0.003905]
(0.003905, 0.004686]
(0.004686, 0.005467]
(0.005467, 0.006248]
(0.006248, 0.007029]
(0.007029, 0.007810]
Al [mol]
(0.00000, 0.00132]
(0.00132, 0.00264]
(0.00264, 0.00396]
(0.00396, 0.00528]
(0.00528, 0.00660]
(0.00660, 0.00792]
(0.00792, 0.00924]
(0.00924, 0.01056]
(0.01056, 0.01188]
(0.01188, 0.01320]
S [mol]
(0.00000, 0.00154]
(0.00154, 0.00308]
(0.00308, 0.00462]
(0.00462, 0.00616]
(0.00616, 0.00770]
(0.00770, 0.00924]
(0.00924, 0.01078]
(0.01078, 0.01232]
(0.01232, 0.01386]
(0.01386, 0.01540]
X (cm)
Z (cm)
sck cen
Reference
23
ISC: Restricted

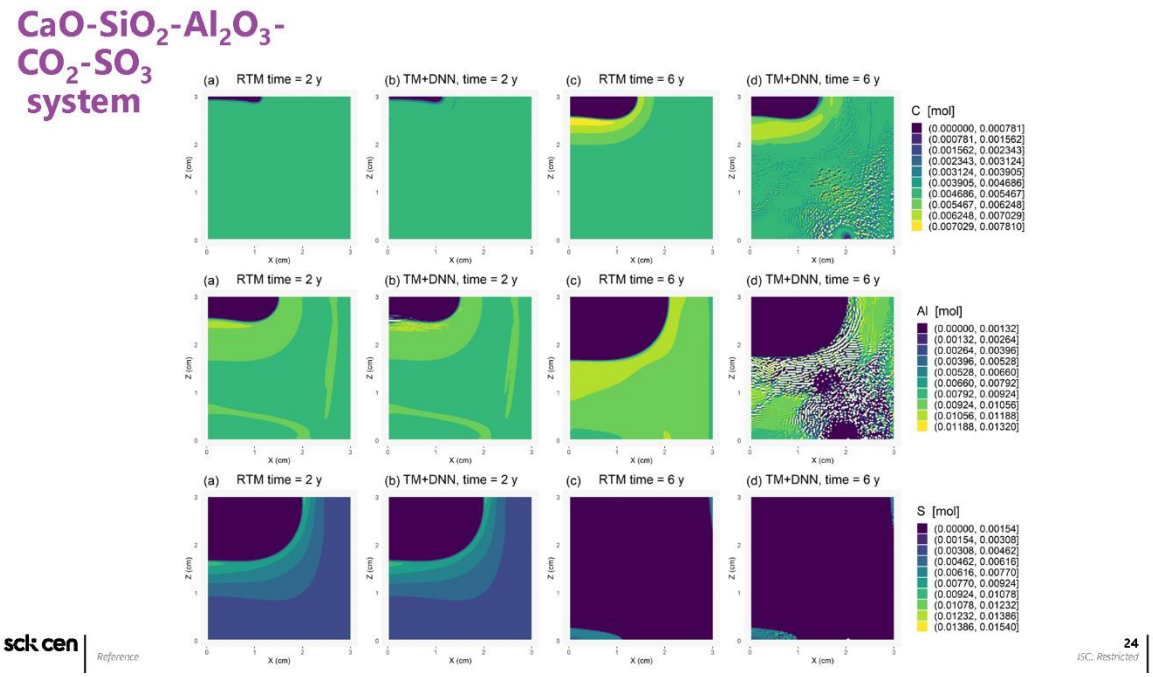
CaO-SiO2-Al2O3-CO2-SO3 system
(a) RTM time = 2 y
(b) TM+DNN, time = 2 y
(c) RTM time = 6 y
(d) TM+DNN, time = 6 y
C [mol]
(0.000000, 0.000781]
(0.000781, 0.001562]
(0.001562, 0.002343]
(0.002343, 0.003124]
(0.003124, 0.003905]
(0.003905, 0.004686]
(0.004686, 0.005467]
(0.005467, 0.006248]
(0.006248, 0.007029]
(0.007029, 0.007810]
Al [mol]
(0.00000, 0.00132]
(0.00132, 0.00264]
(0.00264, 0.00396]
(0.00396, 0.00528]
(0.00528, 0.00660]
(0.00660, 0.00792]
(0.00792, 0.00924]
(0.00924, 0.01056]
(0.01056, 0.01188]
(0.01188, 0.01320]
S [mol]
(0.00000, 0.00154]
(0.00154, 0.00308]
(0.00308, 0.00462]
(0.00462, 0.00616]
(0.00616, 0.00770]
(0.00770, 0.00924]
(0.00924, 0.01078]
(0.01078, 0.01232]
(0.01232, 0.01386]
(0.01386, 0.01540]
X (cm)
Z (cm)
sck cen
Reference
24
ISC: Restricted

Conclusions

- Full RTM emulation especially useful for SA and calibration
- Replacing geochemical solver in RT model by ML
  - Using a GPU, kNN and DNN are very fast - close to optimal speedup in RT simulation
  - For our "simple" cement case study, replacing geochemical solver (PHREEQC) by an emulator in a RTM (HP) works well
  - For our or more complex cement case study, no emulator that is globally accurate over the whole possible input space could be devised offline
  - Building training set based on a cheap/lower fidelity full reactive transport simulation: not fully satisfying
  - DNN extremely sensitive to representativeness of training set, kNN is more robust but will suffer from the curse of dimensionality at some point
- Outlooks
  - Quality of training set
  - Implement an accept/reject criterion of the ML predictions, enrich kNN training set online by full calculation data
  - Physics Informed Neural Networks (PINN)

sck cen | Reference

25
ISC: Restricted

4. Codes

4.1 Code 1 – GEM – Selektor

GEMS (https://gems.web.psi.ch) has been developed at PSI during 23 years. To date, GEMS is the most popular freely-available open-source GEM code and TDB kit for geochemical modelling, with >10'000 downloads and ca. 1'000 active users (CemGEMS web app, https://cemgems.app has >530 registered users), and about 1'400 publications where it has been used. Main parts of GEMS are: GEM-Selektor code; GEMS3K numerical library for use in coupled codes; and GEMSFITS coupled code for inverse modelling and parameterization.

The GEM-Selektor GUI code is used for the forward thermodynamic modelling (in Equillibria mode) and for manipulation with input thermodynamic and reaction formats (in Database mode). The forward problem is to find mole amounts *n* and activities *a* of chemical species in an equilibrium state defined by pressure *p*, temperature *T* and bulk elemental composition *b*. This is done in the GEMS3K code library by applying the IPM-3 GEM algorithm (Kulik et al., 2013), now available also with C, C++11 and Python 3 interfaces. From GEM results, any species concentrations, activity coefficients in any phase, partition and fractionation coefficients of elements between phases, and saturation indices can be obtained. The applicability of GEM is limited only by the knowledge of standard-state molar properties of end members and interaction parameters for phase-solutions (some provided in database files supplied with the code).

If some of GEM outputs are known from the experiments or from observations, then some input thermodynamic properties or interaction parameters of models of mixing can be retrieved by solving inverse thermodynamic modelling problems. This is the purpose of the GEMSFITS (Miron et al., 2015) code that has been successfully used recently in a number of funded projects.

Lecturer

Dmitrii Kulik, PSI, Switzerland

Reading Material

Kulik D.A., Winnefeld F., Kulik A., Miron G.D., Lothenbach B. (2021): CemGEMS – an easy-to-use web application for thermodynamic modeling of cementitious materials. RILEM Technical Letters, 6, 36-52, doi.

Miron G.D., Kulik D.A., Dmytrieva S.V., Wagner T. (2015): GEMSFITS: Code package for optimization of geochemical model parameters and inverse modeling. Applied Geochemistry 55, 28-45. doi.

Kulik, D.A., Wagner T., Dmytrieva S.V., Kosakowski G., Hingerl F.F., Chudnenko K.V., Berner U. (2013): GEM-Selektor geochemical modelling package: revised algorithm and GEMS33K numerical kernel for coupled simulation codes. Computational Geosciences 17, 1-24, .doi

Slides

PAUL SCHERRER INSTITUT PSI

2023 EURAD Training Workshop

eurad European Joint Programme on Radioactive Waste Management

GEMS SELEKTOR

GEMS = Gibbs Energy Minimization Software for thermodynamic modelling

Dmitrii A. Kulik

Laboratory for Waste Management,

Nuclear Energy and Safety Research Division,

Paul Scherrer Institut

on behalf of GEMS Development Team

In this presentation

GEMS SELEKTOR

1. Basics of GEM method and GEM-Selektor code
2. Single systems including optional metastability
3. Examples: Cement and clay systems for DONUT

Downloads, technical info, publications: PSI team

https://gems.web.psi.ch/

What is GEMS?

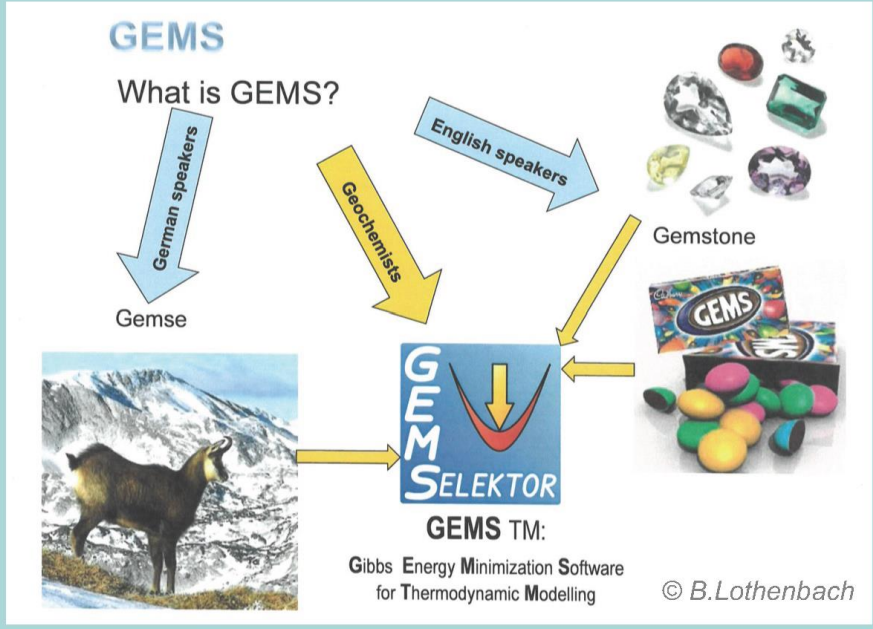

GEMS is a geochemical modeling software collection based on Gibbs Energy Minimization (GEM)

Developed, used and provided from PSI since 2000

3 Geochemical modelling EURAD Training Workshop Univ. Bern, February 6-10, 2023

GEMS architecture

GEM-Selektor v3 Code Package

Developed collaboratively at PSI LES, CosyLab CH

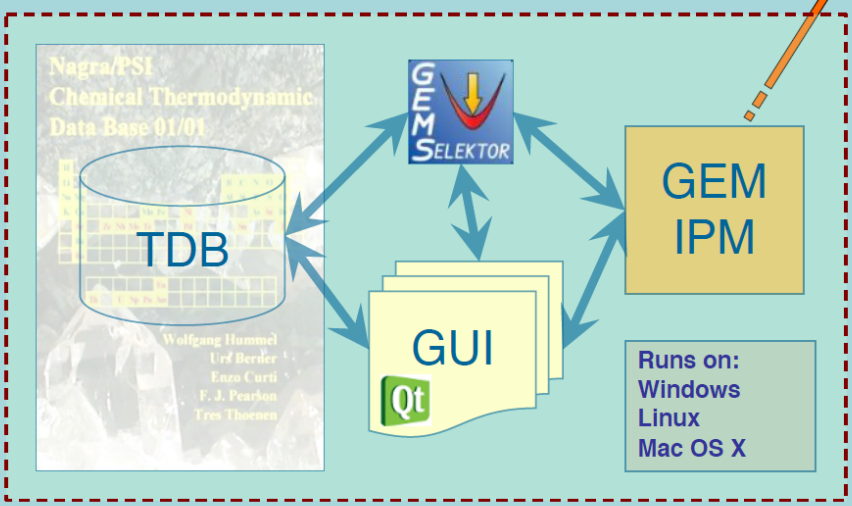

- Integrated
- Interactive
- User-friendly
- User scripts
- Runtime help
- Graphics
- Written in C/C++
- Built on Qt4
- Modular code
- Modular database

https://gems.web.psi.ch/ (download, techinfo, test projects)

4 Geochemical modelling EURAD Training Workshop Univ. Bern, February 6-10, 2023

GEMS3 built-in thermodynamic databases

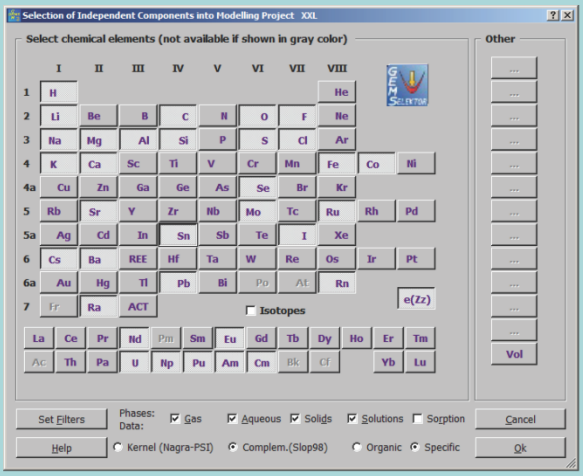

PSI-Nagra v 11/07 TDB

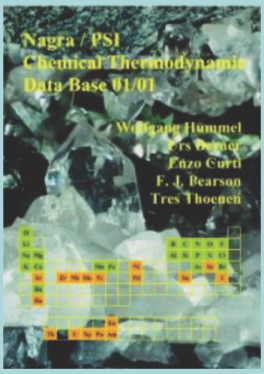

log*K* at 1 bar 25 C

Extended with *T,P* corrections from S92

Specific: Cemdata '18

Specific: HERACLES

Specific: MINES'19

Complementary: SUPCRT92 (*G*° etc.)

DComp and ReacDC data record formats

1. Basics of GEMS

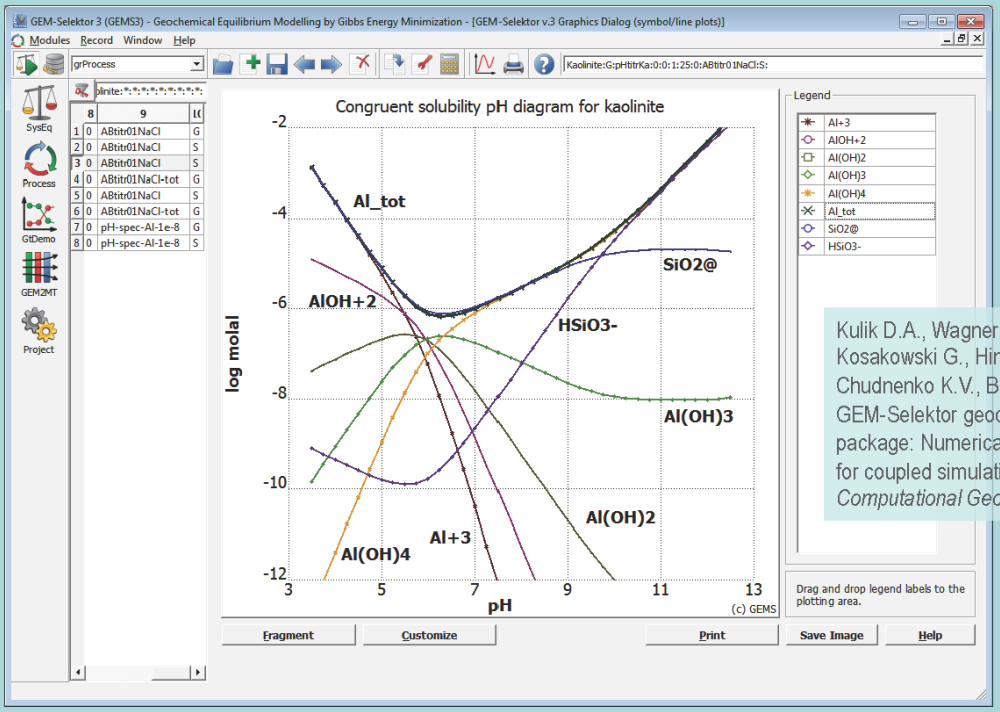

Kulik D.A., Wagner T., Dmytrieva S.V., Kosakowski G., Hingerl F.F., Chudnenko K.V., Berner U. (2013): GEM-Selektor geochemical modeling package: Numerical kernel GEMS3K for coupled simulation codes. *Computational Geosciences*

Two modes of GEM-Selektor operation

Equilibria calculation mode

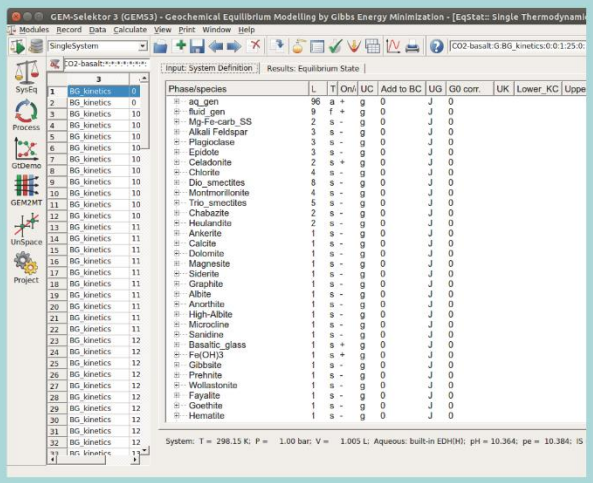

- *Calculate chemical equilibria of minerals-fluids*
- *Calculate processes for rock alteration: cooling, fluid mixing, leaching etc…*

Thermodynamic database mode

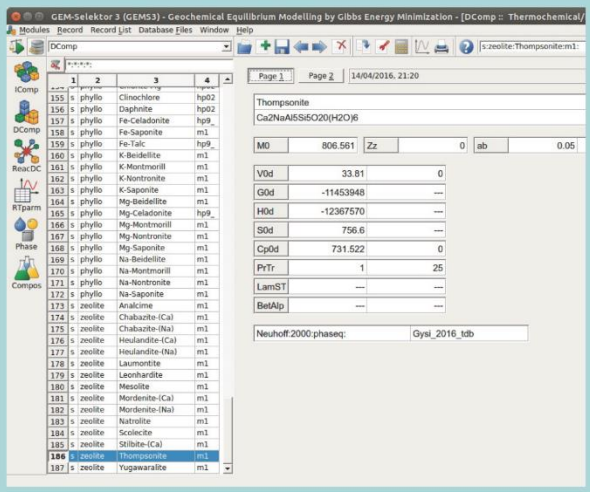

- *Thermodynamic properties of minerals and fluids*
- *Solution models: solid solutions, non-ideal gas…*
- *Prepare complex rock or fluids compositions*

The Database Mode

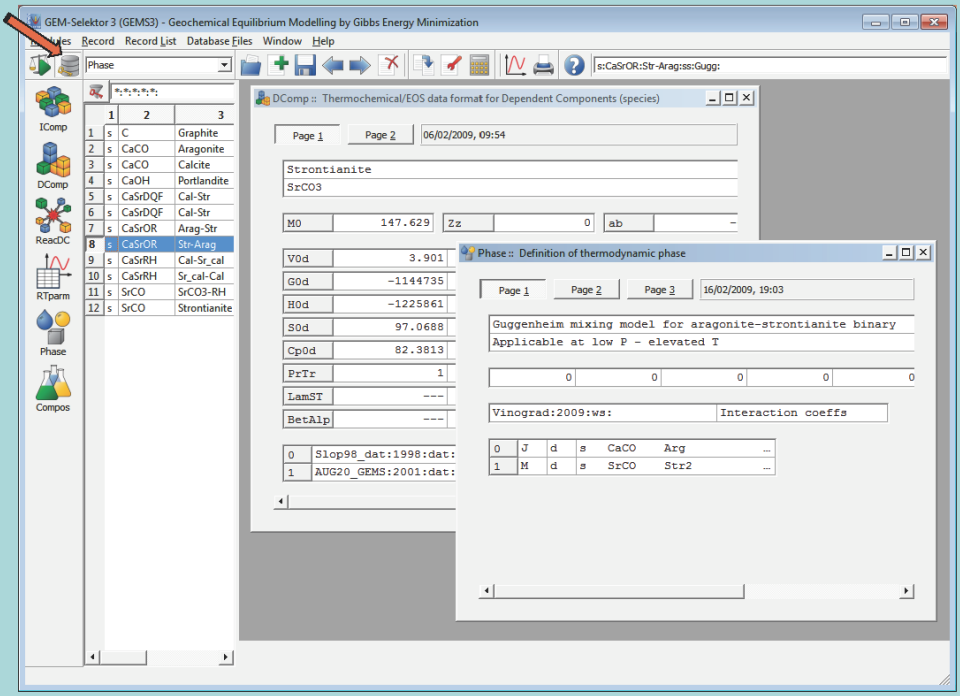

To manage thermodynamic parameters for substances, reactions, and phases; predefined compositions; references, etc.

Data arranged in database records of several types

Export/import of the data and management of database files possible

Main Database Mode options

Vertical toolbar on left side

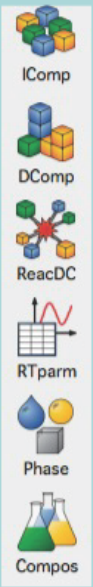

- **IComp:** add/edit an **independent component** (e.g. Al, H, O, Si ...).
- **DComp:** add/edit thermodynamic properties of a **dependent component** (e.g. quartz, kaolinite, Al^{3+}, $CO_{2(g)}$ ...)
- **ReacDC:** add/configure/edit a **reaction-defined dependent component** (e.g. $Al)OH_3(s)$ using $Al(OH)_3(s)+H^+= Al^{3+}+3OH^-$; logK = ...)
- **RTparm:** plot thermodynamic properties vs P-T for a DComp or ReacDC
- **Phase:** define/configure/edit a **phase definition** (pure or a mixture e.g. mineral, mineral solid solution, gas mixtures).
- **Compos:** add/edit a **composition object** to be used as input **entity** in the simulations (e.g. granite, fluid, acid ...)

9 Geochemical modelling EURAD Training Workshop Univ. Bern, February 6-10, 2023

The Equilibria Calculation mode

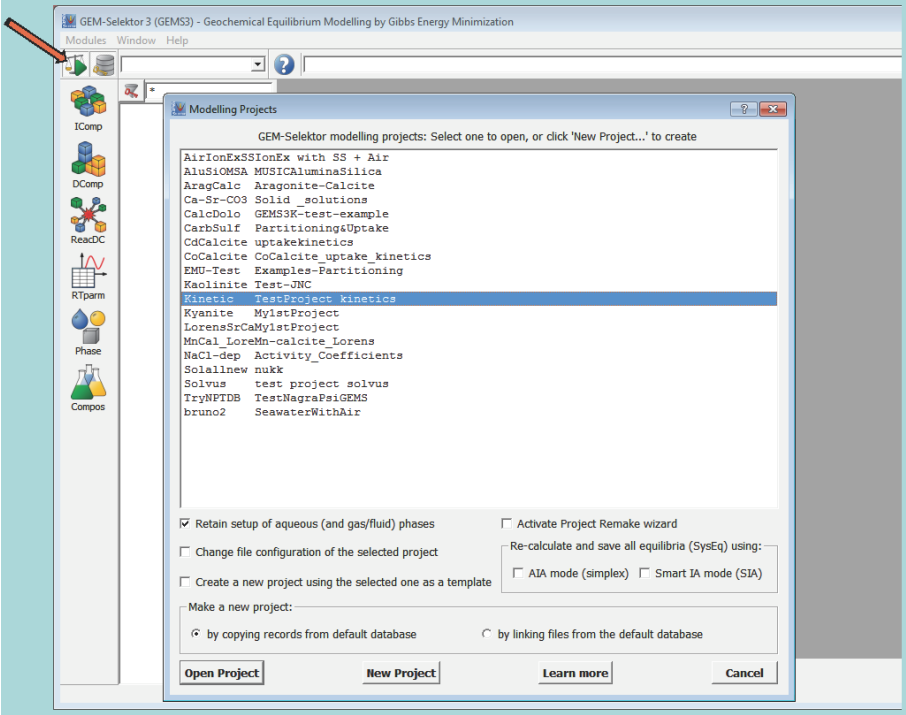

To set up CSDs (Chemical System Definitions) and compute equilibrium states in them

CSD records are kept in Modeling Projects

Create new or open an existing project

Tabular and graphic presentation of results

Export/import of results and data

10 Geochemical modelling EURAD Training Workshop Univ. Bern, February 6-10, 2023

Equilibria Mode

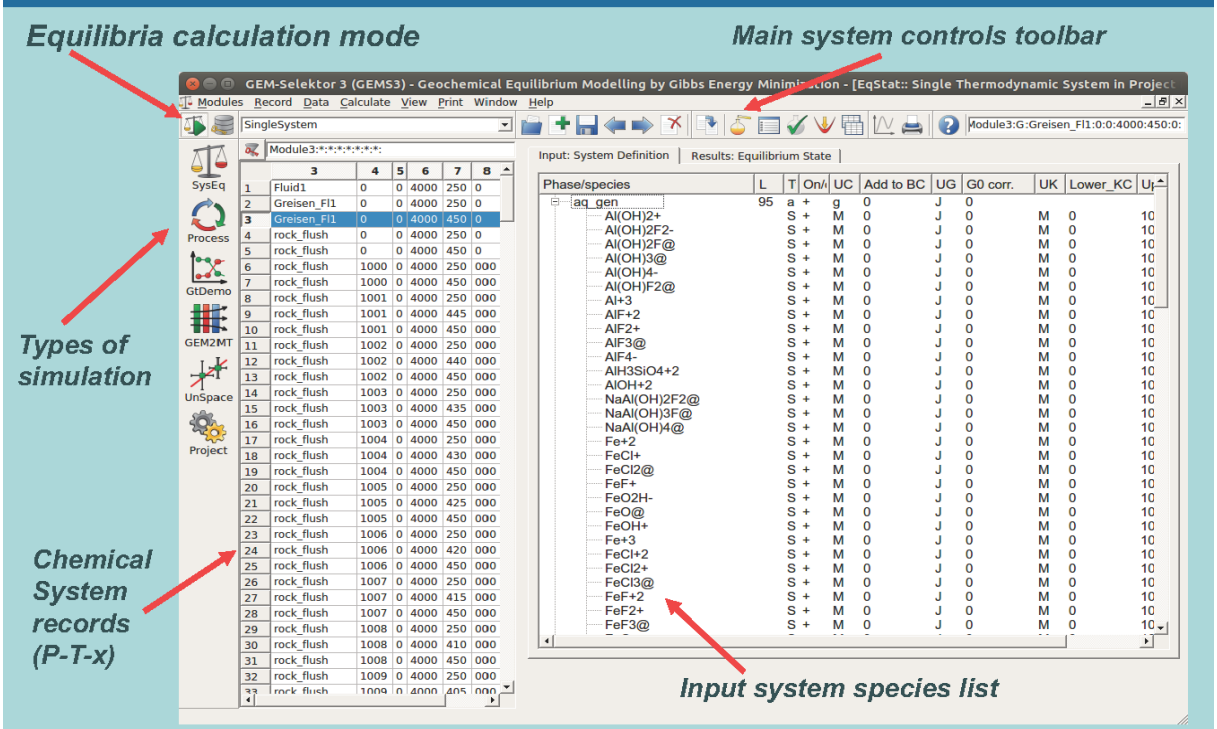

Main Equilibria Mode options

Vertical toolbar on left side

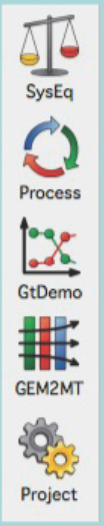

- **SysEq:** create/compute/modify an equilibrium state (speciation, pH, redox, concentrations, stable minerals) for a single chemical system
- **Process simulator:** create/compute/modify a series of equilibrium states (starting from a single parent chemical system) subject to variations in P-T-x.
  - (P) P-T variable; bulk composition (b) fixed -> cooling
  - (S) Reaction path (titration), fluid mixing; composition (b) variable
  - (G) Inverse titrations, e.g. pH – solubility diagram
  - (R) Flow-through cell reactor (flushing or leaching of a rock by a fluid)
- **GtDemo:** Collect and plot selected (and transformed) modeling results
- **GEM2MT:** Define and run a 1-D reactive transport modeling simulation
- **Project:** Tune up the GEM numerical controls and other project settings

Workflow of a single equilibrium calculation

- *Define a new system (b, P, T)*
- *Set up and check the input bulk chemical composition (b)*
- *Calculate equilibrium speciation (x)*

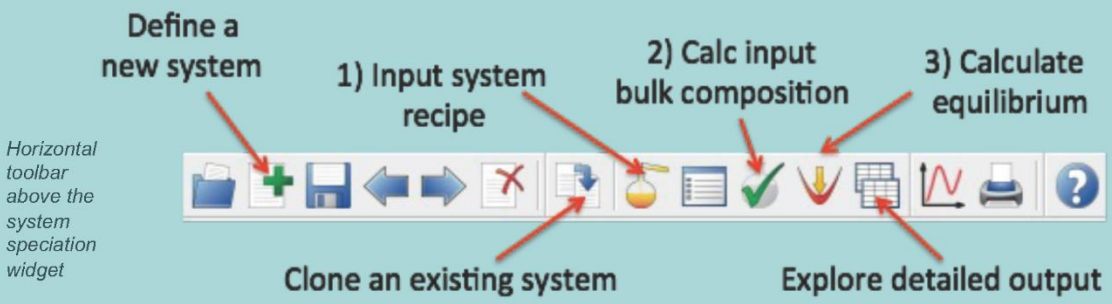

Proceed from the left to the right! *Watch tooltips!*

Forward calculation of equilibrium state

Compositions *Initial state* *Equilibrium*

Recipe

1) Ingredients

Gibbsite 10 g
H_2O 1000 g
NaCl 0.1 moles
HCl 0.1 moles

© Alex Gysi

2) Mix the ingredients and prepare for cooking 100°C p_{sat}

Independent components (IC)

Al	0.128 moles
Cl	0.2 moles
H	111.5 moles
Na	0.1 moles
O	55.89 moles

3) The soup is cooked!

Dependent components (DC)

pH	2.40
$Al(OH)^{+2}$	9.64-04 m
$Al(OH)_2+$	9.65-06 m
$Al(OH)_3@$	1.15-07 m
$Al(OH)_4-$	1.23e-10 m
Al^{+3}	0.031 m
...	

Chemical mass conservation

Ax = b

Input bulk composition in moles of IC (b)

EqIC | EqPh | EqDC | EqSurf | EqGen | 09/10/2016, 11:26

---

*Dual solution vector **u***

	ICnam	b	Cb	u	lgm t	m t	ICnam
0	Al e	0.62959143	5.5511151e-17	-78.056309	-2.5679522	0.0027042561	Al e
1	Cl e	3.6241344	5.6920614e-17	-27.730922	0.66751843	4.6507012	Cl e
2	F e	0.0046318636	-2.1684043e-19	-60.243903	-2.2259301	0.0059438782	F e
3	Fe ...	0.39594963	-4.3368087e-18	-10.677829	-0.29848367	0.50294018	Fe ...

Output speciation in moles of DC (x)

EqIC | EqPh | EqDC | EqSurf | EqGen | 09/10/2016, 11:26

	DCnam	x	lga	gamma	my
0	Al(OH)2+	3.2463557e-08	-7.7112597	0.46669187	4.1659134e-08
1	Al(OH)2F2-	1.5935912e-06	-6.0202786	0.46669187	2.0449894e-06
2	Al(OH)2F@	2.1426425e-05	-4.4605393	1.2594958	2.7495642e-05
3	Al(OH)3@	3.2965844e-07	-6.2734248	1.2594958	4.2303698e-07
4	Al(OH)4-	1.7356844e-05	-4.9831848	0.46669187	2.2273317e-05
5	Al(OH)F2@	2.6555582e-06	-5.3673331	1.2594958	3.4077675e-06
6	Al+3	1.3458628e-12	-15.542995	0.00016584348	1.7270898e-12

15 Geochemical modelling EURAD Training Workshop Univ. Bern, February 6-10, 2023

Forward problem in GEM formulation

Goal: Calculate (unknown) equilibrium phase assemblage and speciation in the system defined by T, p, b, g^o, and parameters of mixing in solution phases.

= Find amounts of dependent components $n^{(x)} = \{ n^{(x)}_j, j \in L\}$ that

$$G(n^{(x)}) \Rightarrow \min \quad \text{s. t.} \quad A \cdot n^{(x)} = n^{(b)} \qquad \text{(Problem F)}$$

where $n^{(b)} = \{ n^{(b)}_i, i \in N\}$ is the input vector of bulk system composition (b)

$A = \{a_{ij}, i \in N, j \in L\}$ is a matrix of formula stoichiometry coefficients of species;

and $G(n^{(x)})$ is the total Gibbs energy $G(n^{(x)}) = \sum_j n_j^{(x)} \upsilon_j, \quad j \in L$

where υ_j is the chemical potential of j-th dependent component

$$\upsilon_j = g_j^o / RT + \ln C_j + \ln \gamma_j + \Xi, \quad j \in L$$

Terms non-linear relative to $n^{(x)}$ (in phases-solutions)

16 Geochemical modelling EURAD Training Workshop Univ. Bern, February 6-10, 2023

Non-linear GEM: Ideal vs non-ideal solutions

Chemical potential of species j in solution

$$\upsilon_j = g_j^o / RT + \ln C_j + \ln \gamma_j + \Xi, \quad j \in L \qquad G(n^{(x)}) = \sum_j n^{(x)} \upsilon_j$$

Activity terms introduce non-linearity of G(x)

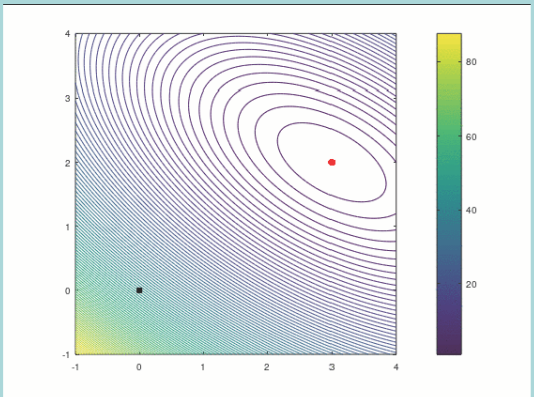

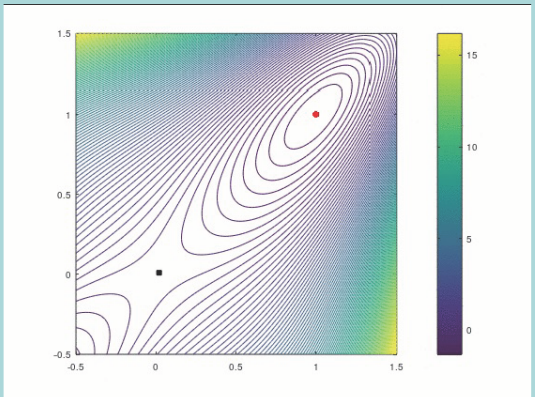

Ideal solutions: simple G(x) shape (convex, in polyhedron of constraints)

Non-ideal solutions: complex G(x) shape (pseudoconvex?), special initial guess

Interior Points Method (IPM) of GEM

IPM algorithm finds simultaneously the *primal* $\hat{n}^{(x)}$ and the *dual* u solutions of problem (F) using *Karush-Kuhn-Tucker* necessary and sufficient conditions:

$$\upsilon - A^T u \geq 0; \quad \Longleftarrow \quad \text{Stability (dual thermodynamics)}$$

$$A\hat{n}^{(x)} = n^{(b)}; \quad \hat{n}^{(x)} \geq 0; \quad \Longleftarrow \quad \text{Mole balance, non-negativity}$$

$$\hat{n}^{(x)}\left(\upsilon - A^T u\right) = 0 \quad \Longleftarrow \quad \text{Orthogonality (DC selection)}$$

The first condition, re-written with indexes, is

$$g_j^o / RT + \ln C_j + \ln \gamma_j + \Xi - \sum_i a_{ij} u_i \geq 0, \quad j \in L, \quad i \in N$$ implying that

$$\upsilon_j \geq \eta_j, \; j \in L, i \in N$$ where $$\eta_j = \sum_i a_{ij} u_i, \; j \in L, i \in N$$ is the *dual* chemical potential

Equilibrium chemical potential of a partitioned element or compound is the same in all phases

Activities of species from GEM dual solution

For any species in any phase present in equilibrium, the first Karush-Kuhn-Tucker condition $\upsilon - \mathrm{A}^T u \geq 0$ expands into a generic *DualTh equation* $\eta_j = \upsilon_j$, or

$$\sum_i \mathrm{a}_{ij} u_i = \frac{g^o_{j,T}}{RT} + \ln C_j + \ln \gamma_j + \Xi \qquad \text{(GDTE)}$$

Activity of any component in any multi-component phase at equilibrium is:

$$\ln a_j = \sum_i \mathrm{a}_{ij} u_i - {g^o_j}/{RT}, \quad j \in L, \quad i \in N \qquad \text{(DTAE)}$$

Compare with a traditional calculation of "primal" activities:

$$\ln a_j = \ln C_j + \Xi + \ln \gamma_j$$

Both concentration C_j and activity coefficient γ_j are functions of the primal solution $\hat{n}^{(x)}$

19 Geochemical modelling EURAD Training Workshop Univ. Bern, February 6-10, 2023

Calculation of pe, Eh and pH in GEMS v3

For aqueous electron e_{aq}, $\ln a_e = -1 \cdot u_{\mathrm{Charge}}$. By defining $\mathrm{pe} = -\log_{10} a_e$

$$\mathrm{pe} = -\frac{1}{\ln 10}\left(-u_{\mathrm{Charge}}\right)$$

No e- species molality or activity coefficient is needed!

Because $\mathrm{pe} \cdot RT \cdot \ln 10 = F \cdot \mathrm{Eh}$

$$\mathrm{Eh} = \frac{RT}{F} \cdot u_{\mathrm{Charge}}$$

Volts, F = 96485 C·mol^{-1} is the Faraday's constant

$$\mathrm{pH} = -\frac{1}{\ln 10}\left(u_{\mathrm{H}} + u_{\mathrm{Charge}}\right)$$

Corresponds to defining $\mathrm{pe} = -\log_{10} a(H+)$ and conventional $g^o(\mathrm{H}^+) = 0$ at any T and p

No H+ species molality and activity coefficient is required!

DualTh-calculated activities and their functions are more accurate than primal ones

20 Geochemical modelling EURAD Training Workshop Univ. Bern, February 6-10, 2023

Calculation of species fugacity or activity

Relative activity of a gas can be defined as $\mu_j - \mu_j^o = RT \ln a_j = RT\left(\ln f_j - \ln f^o\right)$

where the standard-state fugacity $f^o = 1$ bar. Hence

$$\ln f_j = \sum_i a_{ij} u_i - g_j^o / RT, \quad j \in L_g, \quad i \in N$$

DTAE

Example: fugacity of ideal methane (CH_4) at T = 25 °C in any system containing C and H

$$\log_{10} f_{CH_4,g} = 1/\ln 10 \left[u_C + 4u_H - (-20.44)\right]$$

No CH_4,g or even no gas phase needs to be present in the mass balance

For any stable (solid) solution, the activity of any end-member is found from DTAE

Example: strontianite $SrCO_3$ in any stable SS

$$\log_{10} a_{Stront.,s} = 1/\ln 10 \left[u_{Sr} + u_C + 3u_O - (-461.77)\right]$$

Calculation of phase stability index: Proof

For a single-component (pure substance) phase, DTAE yields the saturation index SI:

$$\Omega_{Sp} = \frac{1}{\ln 10}\left(\sum_i a_{ip} u_i - g_p^o / RT\right), \quad p \in L_p, \quad i \in N$$

Proof: For an ionic solid BL, compare with usual definition

$$10^{\Omega_{S,BL}} = Q_{S,BL} / K_{S,BL} = \left(a_{B+} a_{L-}\right) / K_{S,BL}$$

Activities of aqueous ions and their product $Q_{S,BL}$ can be found using DTAE:

$$\ln Q_{S,BL} = \left[u_B + u_{Charge} - g_{B+}^o / RT\right] + \left[u_L - u_{Charge} - g_{L-}^o / RT\right] = u_B + u_L - \left(g_{B+}^o + g_{L-}^o\right) / (RT)$$

solubility product $K_{S,BL}$ is defined as

$$\ln K_{S,BL} = -\left(g_{B+}^o + g_{L-}^o\right) / (RT) + g_{s,BL}^o / (RT)$$

Substitution results in

$$\Omega_{S,BL} = \frac{1}{\ln 10} \ln\left(Q_{S,BL} / K_{S,BL}\right) = \frac{1}{\ln 10}\left(u_B + u_L - g_{s,BL}^o / RT\right)$$

which is the proof

Phase stability indices in GEM-Selektor output

Chemical potential *of j-th compound from GEM dual solution u:* ⇨ $\hat{\eta}_j = \sum_{i \in N} a_{ij} \hat{u}_i$

⇧ ⇩

GEM SELEKTOR ⇨ ***Stability (saturation) index*** *for a k-th phase-solution of I_k species:*

⇩

$$\Omega_k = \sum_{j \in I_k} \hat{x}_j = \sum_{j \in I_k} \exp\left(\hat{\eta}_j - \frac{g_j^o}{RT} - \ln\gamma_j - \Xi_k\right)$$

'dual' estimate of mole fraction — *'primal' activity coefficient*

⇩

Stability (saturation) index for a k-th pure phase (j-th species) ⇨ $\Omega_k = \exp\left(\hat{\eta}_j - \frac{g_j^o}{RT}\right)$

$\log_{10}\Omega_k$	$< -\varepsilon_\Omega$	$> -\varepsilon_\Omega$ & $< +\varepsilon_\Omega$	$> +\varepsilon_\Omega$
phase:	under-stable	stable	over-stable

SysEq Recipe 2: 'CalciteSW' at 400 bar 3 C

ICnam	u
C ...	-177.14693
Ca ...	-318.71489
Cl ...	-21.618519
H ...	-52.113967
Na ...	-149.752
Nit ...	2.8605319
O ...	1.8574335
Sr ...	-327.7595
Zz ...	35.44269

Calculate stability index of:

Calcite Cal $CaCO_3$
Aragonite Arg $CaCO_3$
Portlandite $Ca(OH)_2$

and compare with 'EqPh' 'Fa'

'Mtparm' window

						gTP
63	s	CaCO	Arg ...	d	+	-1125074.6
64	s	CaCO	Cal ...	d	+	-1125730.2
65	s	CaOH	Portlandite ...	d	+	-893931.09

'EqPh' page in 'EqDemo' window

		PHnam	Xa	Fa
0	a	aq_gen	54.809148	-7.0994752e-012
1	g	gas_gen	0	-0.86149778
2	s	Graphite	0	-76.996523
3	s	Aragonite	0	-0.12401373
4	s	Calcite	0.09381742	-2.7511445e-008
5	s	Portlandite	0	-12.98278
6	s	Strontianite	0	-1.0188954

2. Phase metastability and kinetics

Partial Equilibrium State *concept*

is used for setting up thermodynamic models of 'real-world' geochemical systems

Examples:
- Surface water open to the atmosphere
- Seawater oversaturated to dolomite
- Iron monosulfide in marine sediments
- Clinker phases in hydrated cements
- Suspension of solid with adsorption and Ostwald ripening .....

TYPICAL ASSUMPTIONS:

- ***At least one phase (reaction) is not in chemical equilibrium with the rest of the system***
- ***Dissolution of minerals is the rate-limiting step***
- ***Solid solutions dissolve stoichiometrically***
- ***Precipitation of secondary minerals is usually faster than the primary mineral dissolution***
- ***Some species (N_2atm) or solid phases are inert***

Reaction-path and process-extent models in geochemical codes ⇨

Implementations using time-dependent:

- ***Additional constraints on reaction species or on phases***
- ***Mineral specific surface areas and sorption capacities***
- ***Amounts of metastable phases linked to other phases***

The simplest form of GEM IPM

The IPM algorithm finds simultaneously the *primal* $\hat{n}^{(x)}$ and the *dual* u solutions of the problem (F) using *Karush-Kuhn-Tucker* necessary and sufficient conditions:

$$\upsilon - \mathrm{A}^T u \geq 0;$$ ⟸ Stability (dual thermodynamics)

$$\mathrm{A}\hat{n}^{(x)} = n^{(b)}; \quad \hat{n}^{(x)} \geq 0;$$ ⟸ Mole balance, non-negativity

$$\hat{n}^{(x)}\left(\upsilon - \mathrm{A}^T u\right) = 0$$ ⟸ Orthogonality (DC selection)

Metastability can be controlled here !

The first condition, re-written with indexes, is

$$g_j^o / RT + \ln C_j + \ln \gamma_j + \Xi - \sum_i \mathrm{a}_{ij} u_i \geq 0, \quad j \in L, \quad i \in N$$ implying that

$$\upsilon_j \geq \eta_j, \; j \in L, i \in N$$ where $$\eta_j = \sum_i \mathrm{a}_{ij} u_i, \; j \in L, i \in N$$ is the *dual* chemical potential

Metastability constraints in GEM IPM 3

At given *T, p, b, g°, and parameters of mixing in solution phases,* ***find***

such amounts of species (dependent components) $n^{(x)} = \{ n^{(x)}_j, j \in L\}$ *that*

$$G(n^{(x)}) \Rightarrow min \quad \text{s. t.}$$
$$A \cdot n^{(x)} = n^{(b)}$$
← *Mole balance*

Total Gibbs energy function:

$$G(n^{(x)}) = \sum_j n_j^{(x)} \upsilon_j, \quad j \in L$$

υ_j *is primal chemical potential of j-th species*

$$\upsilon_j = g_j^o / RT + \ln C_j + \ln \gamma_j + \Xi, \quad j \in L$$

AND

Extended *KKT conditions for a partial equilibrium state*

$$\left.\begin{aligned} &\upsilon_j - \hat{\eta}_j \geq 0, \\ &(\upsilon_j - \hat{\eta}_j)\hat{n}_j^{(x)} = 0, \; \hat{n}_j^{(x)} \geq 0 \end{aligned}\right\}, \quad j \in D_0 \qquad n_j$$

Dissolution

$$\left.\begin{aligned} &\upsilon_j - \hat{\eta}_j \geq 0, \\ &(\upsilon_j - \hat{\eta}_j)(\underline{n}_j^{(x)} - \hat{n}_j^{(x)}) = 0 \end{aligned}\right\}, \quad j \in D_1 \qquad \underline{n}_j$$

Precipitation

$$\left.\begin{aligned} &\upsilon_j - \hat{\eta}_j \geq 0, \\ &(\upsilon_j - \hat{\eta}_j)(\hat{n}_j^{(x)} - \overline{n}_j^{(x)}) = 0 \end{aligned}\right\}, \quad j \in D_2 \qquad \overline{n}_j$$

Both

$$\left.\begin{aligned} &\upsilon_j - \hat{\eta}_j + p_j \geq 0, \\ &(\upsilon_j - \hat{\eta}_j + \hat{p}_j)(\underline{n}_j^{(x)} - \hat{n}_j^{(x)}) = 0, \\ &\hat{p}_j \geq 0, \quad \hat{p}_j(\hat{n}_j^{(x)} - \overline{n}_j^{(x)}) = 0 \end{aligned}\right\}, \quad j \in D_3 \qquad \underline{n}_j, \; \overline{n}_j$$

$$\sum_j \mathrm{a}_{ij} \hat{n}_j^{(x)} = n_i^{(b)}, \quad i \in N, \; j \in L$$ *Common balance*

$\hat{p}_j$ *Lagrange multiplier conjugate to j-th non-trivial two-side constraints*

(Karpov et al., 2001, Geochemistry International)

Setting additional metastability restrictions

System: Portlandite + 1 kg water + N_2-O_2 air
(data from PSI/Nagra TDB)

Recipe 0: **'PortlKin'** at 1 bar 25 C, var. 0

Property	Name	Quantity	Units
xa_	Aqua	1	kg
xd_	Portlandite	0.05	mol
bi_	Nit	0.0016	mol
bi_	O	0.0004	mol

Saturation

Complete equilibrium:

pH = 12.47; IS= 0.05 *m*

$[Ca]_{aq}$ = 0.0203 *m*

n(Portlandite) = 0.02971 mol

Ω(Portlandite) = 1.0

Recipe 0: **'PortlKin'** at 1 bar 25 C, var. 1

Property	Name	Quantity	Units
xa_	Aqua	1	kg
xd_	Portlandite	0.05	mol
bi_	Nit	0.0016	mol
bi_	O	0.0004	mol
dul_	Portlandite	0.01	mol

+ upper amount constraint in MB

Oversaturation

Partial equilibrium:

pH = 12.73; IS= 0.096 *m*

$[Ca]_{aq}$ = 0.04 *m*

n(Portlandite) = 0.01 mol

Ω(Portlandite) = **4.75**

27 Geochemical modelling EURAD Training Workshop Univ. Bern, February 6-10, 2023

Additional metastability restrictions: Dissolution

System: Portlandite + 1 kg water + N_2-O_2 air

Recipe 1: **'PortlKin'** at 1 bar 25 C, var. 0

Property	Name	Quantity	Units
xa_	Aqua	1	kg
xd_	Portlandite	0.02	mol
bi_	Nit	0.0016	mol
bi_	O	0.0004	mol

Undersaturation

Complete equilibrium:

pH = 12.47; IS= 0.05 *m*

$[Ca]_{aq}$ = 0.02 *m*

n(Portlandite) = 0 mol

Ω(Portlandite) = 0.967

Recipe 1: **'PortlKin'** at 1 bar 25 C, var. 1

Property	Name	Quantity	Units
xa_	Aqua	1	kg
xd_	Portlandite	0.02	mol
bi_	Nit	0.0016	mol
bi_	O	0.0004	mol
dll_	Portlandite	0.01	mol

+ lower amount constraint in MB

Undersaturation

Partial equilibrium:

pH = 12.20; IS= 0.027 *m*

$[Ca]_{aq}$ = 0.01 *m*

n(Portlandite) = 0.01 mol

Ω(Portlandite) = **0.183**

28 Geochemical modelling EURAD Training Workshop Univ. Bern, February 6-10, 2023

Outlook for metastability/kinetics models

- Hardcode the nucleation, precipitation, dissolution and uptake models to make them usable in GEMS3K-based coupled RMT codes
- Implementation of various cases, mineral reaction kinetic rate laws in GEMS TKinMet class library
- Implementation of Trace element uptake kinetic models; parameterization on the data for calcite, sulfates, etc.
- Development of model scenarios relevant in repository performance (SKIN), geothermics, etc.
- Model sensitivity studies, evaluation of parameter uncertainties, long-time extrapolations

Next training: Check out and test the "Kinetics" test project
(look at Process simulators and Phase definitions for calcite, portlandite)

29 Geochemical modelling EURAD Training Workshop Univ. Bern, February 6-10, 2023

3. Examples: Cement & clay systems

Preparations (assuming GEM-Selektor already installed)

1. Check in what folder the DB.default folder of GEM-Selektor is located (e.g. C:\Users\you\GEMS\Gems3-app\Resources\DB.default)
2. In web browser, navigate to https://www.empa.ch/web/s308/thermodynamic-data and download Cemdata18.1 for GEMS
3. Unzip the downloaded zip file (contains a directory named "DB.default") into a temporary directory, e.g. as \Temp\DB.default
4. Copy all files from \Temp\DB.default into DB.default folder (see #1.)
5. Start GEM-Selektor and create a new modelling project
   In the widget for selection of DB modules, make choices as shown:
6. In the widget for selection of Independent Components, click to choose Al, C, Ca, Cl, H, K, Mg, Na, Nit, O, S, Si, Zz and proceed
7. In the appearing System key widget, give a name and proceed
8. In the appearing Recipe widget, construct a recipe of the system
9. Click on "Check BCC" toolbar button and then to "Equilibrate"
10. Explore the results in the main Equilibrium Mode widget

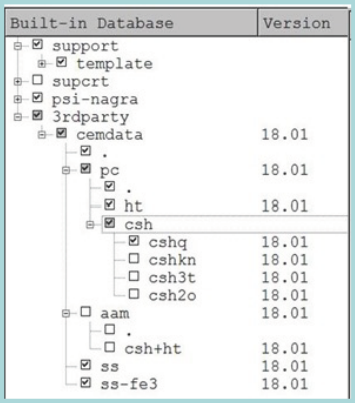

30 Geochemical modelling EURAD Training Workshop Univ. Bern, February 6-10, 2023

Simplified cement systems (DONUT)

Bulk elemental compositions of simplified cement systems used in DONUT ML benchmarking and training project (moles), w/b ratio 0.5, 1 bar 25 °C

Element	Simple-C	Simple	Minimal-C	Minimal	Primitive-C	Primitive
Al	0.0882688	0.0882688	0.0882688	0.0882688	0	0
C	0.001	0	1	0	0.96	0
Ca	1.123447	1.123447	1.123447	1.123447	1.123447	1.123447
Cl	0	0	0	0	0	0
H	5.550837	5.550837	5.550837	5.550837	5.550837	5.550837
K	0.02186929	0.02186929	0	0	0	0
Mg	0	0	0	0	0	0
Na	0	0	0	0	0	0
Nit	0	0	0	0	0	0
O	5.463155	5.386216	7.262873	5.262873	7.05047	5.13047
S	0.0624491	0.03746946	0	0	0	0
Si	0.615801	0.615801	0.615801	0.615801	0.615801	0.615801
Zz	0	0	0	0	0	0

See "Cement-systems.xslx" files for recipes and other settings, hands-on sessions

31 Geochemical modelling EURAD Training Workshop Univ. Bern, February 6-10, 2023

UO_2-montmorillonite systems (DONUT)

Bulk compositions of simplified UO_2-clay systems used in DONUT ML benchmarking and training project (moles of independent components), 1 g/L clay, 1 bar 25 °C

Element	MontU-mini-c	MontU-mini	MontU-prim-c	MontU-prim
C	0.00044	0	3.3E-07	0
Ca	0.001	0.001	0	0
Cl	0.102	0.102	0.1	0.1
Clay	0.00087	0.00087	0.00087	0.00087
Ess	2E-06	2E-06	2E-06	2E-06
Esv	4E-05	4E-05	4E-05	4E-05
Esw	4E-05	4E-05	4E-05	4E-05
H	110.5111	110.5105	110.512	110.3677
N	0	0	0	0
Na	0.10142	0.100871	0.100871	0.100871
Nit	0.00001	0.00001	0.00001	0.00001
O	55.25689	55.25546	55.25618	55.18407
U	1E-09	1E-09	1E-09	9E-08
Zz	0	0	0	0

See "ClaySorU-systems.xslx" files for recipes and other settings, hands-on sessions, use project "ML-B-MontU"

Nit atmospheric (non-reactive) nitrogen
N reactive nitrogen

Montmorillonite sorption:
Clay ion-exchange site
Ess strong edge site
Esv weak edge site type 1
Esw weak edge site type 2

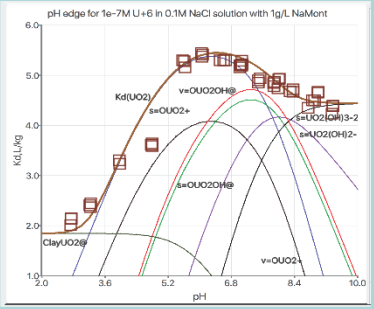

32 Geochemical modelling EURAD Training Workshop Univ. Bern, February 6-10, 2023

Acknowledgments

Thank you! Q&A?

- Partial financial support from Nagra (Wettingen) is gratefully acknowledged

Thanks to Alex, Dan, Barbara, Enzo, Georg, Allan, and other people for help and discussions, and Diederik for invitation to this workshop

Enjoy GEMS SELEKTOR **and check for updates!**

33 Geochemical modelling EURAD Training Workshop Univ. Bern, February 6-10, 2023

4.2 Code 2 – ORCHESTRA

In this presentation I will give an overview of the motivation for developing ORCHESTRA, in what ways it is similar and different from other codes, and what implications this has for chemical and reactive transport modelling.

The ORCHESTRA code has a similar application area as e.g. PHREEQC and GEMS, but was specifically developed to allow users to create their own model extensions.

To make this possible, the internal structure of ORCHESTRA is quite different from that of other chemical solver codes. (Although its use is very similar)

In case of ORCHESTRA chemical (and physical) models (expressions, equations) are not defined in its source code but in a separate text file that is read as input. So all chemical models can be inspected, adapted or extended by users.

So whereas standard codes allow users to compose chemical models systems from a fixed set of predefined building blocks, (such as chemical elements, aqueous species, solid phases and a set of adsorption models etc.) ORCHESTRA makes it possible to extend this set and is therefore often used e.g. for adsorption model development, or other non-standard chemical applications.

However, for the "standard" chemical processes that are the subject of this course the existing set of models will be sufficient.

ORCHESTRA comes with a large set of predefined chemical (adsorption) models, and a graphical user interface that enables users to set up chemical systems by selecting substances and reactions from thermodynamic databases.

This graphical user interface also allows to generate stability/predominance diagrams.

ORCHESTRA is written in Java, but within the DONUT project a C++ version of the chemical solver was developed to facilitate integration with other (transport or PYTHON) codes.

Lecturer

Hans Meeussen, NRG, The Netherlands

Reading Materials

www.meeussen.nl/orchestra

ORCHESTRA: An Object-Oriented Framework for Implementing Chemical Equilibrium Models | Environmental Science & Technology (acs.org)

Slides

1

Modelling reactive transport processes with **ORCHESTRA**

Hans Meeussen, NRG Petten & TU Delft, 6 February 2023

EURAD course modelling reactive transport processes

2

Overview

- Personal background (education, work/research experience, teaching
- Chemical modelling code development (ORCHESTRA)
- Comparison with GEMS/ PHREEQC
  - What is the same what is different
  - What are advantages/disadvantages
- Demonstration

Background

3

- MSc Wageningen University (1982-1988)
  - Environmental Science, **Software engineering**
- PhD Wageningen University (1988-1992)
  - **Soil chemistry**, Cyanide chemical behavior in soils
- Post doc Wageningen University (1992-1994)
  - Modelling **reactive transport processes** (leaching behavior of waste/building materials, adsorption model development)
- Macaulay (now Hutton) research institute, Aberdeen, Scotland, (1994-2000)
  - Modeling reactive transport process in soils, starting **ORCHESTRA** development
- ECN (2001-2010)
  - Modelling contaminant leaching from waste materials)
- **NRG (2010-**
  - Modelling migration of radionuclides in waste, soil, rock and concrete,
- **TU Delft (2021-**
  - Teaching reactive transport processes, coupling ORCHESTRA solver with TU Delft models
- Vanderbilt University Nashville (2006-
  - Long term US-DOE funded collaboration modelling radionuclide migration in cementitious materials

Area of expertise: reactive transport processes

4

Horizon 2020 DONUT project: Development and Improvement Of NUmerical methods and Tools for modelling coupled processes

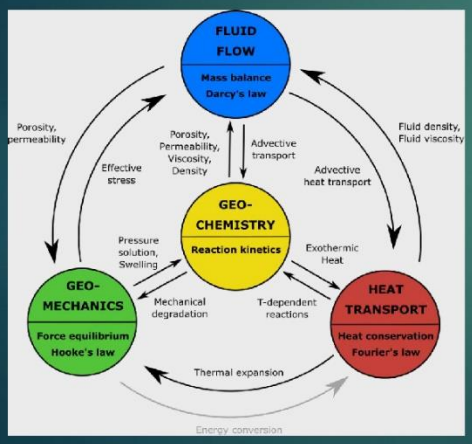

- **Coupled** Thermo, Hydro, Mechanical Chemical (**THMC**) models are used in evaluating waste disposal facilities/scenarios
- **Predict evolution** of waste packages, repository and behavior of nuclides
- (e.g. **PREDIS, ACED, CORI** projects, etc.)
- **Geo-chemistry** plays **central** role
- Takes up **most of the calculation** time (90%)
- Is relatively **complex**
- **Existing modules (e.g. PHREEQC, GEMS, ORCHESTRA)** are used

What is a (geo) chemical solver

5

- Calculates equilibrium composition of set of chemical substances (species) and set of chemical reactions,
  - by iteratively solving set of non-linear equations,
  - or by minimizing set of functions (Gibbs free energy of system)
- **Input:**
  - Set of chemical reactions thermodynamic constants (from database)
  - total amounts of elements (or components, master species)
- **Output:** concentrations of individual chemical species
  - **Including:** distribution over species with different mobility (e.g. dissolved, precipitated, gaseous, colloidal etc.

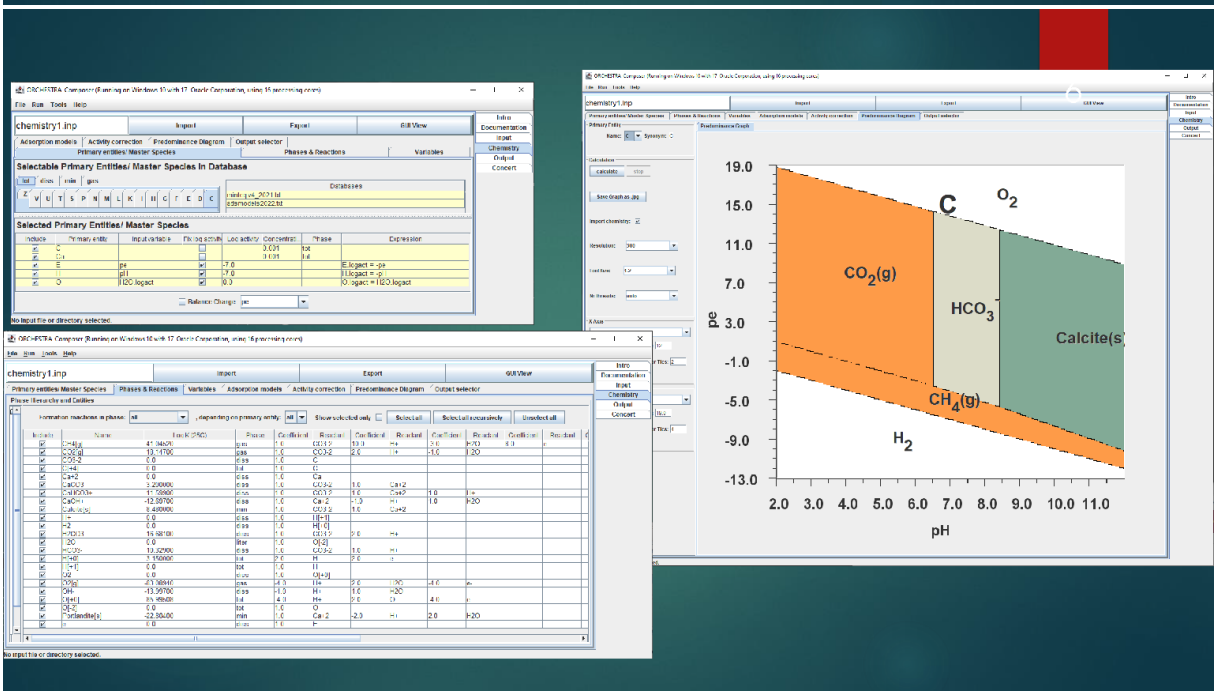

What is special about modelling chemical processes (in comparison with modelling physical processes)

7

- **Physical models** (equations) are often **literally coded** (Python, Matlab, COMSOL, Fortran, C++ etc.)
- For **chemical models** this becomes (very) **tedious** for systems consisting of more than a handful of chemical reactions
- Therefore **standard codes** (e.g. PHREEQC, GEMS) are used as chemical solver modules
- Combined with **standard databases** with thermodynamic constants

Consequences:

→ set of chemical (e.g. adsorption) **models** that can be used is **determined by solver code**

→ This is fine for "standard models"

→ But a challenge for new model development (modification of solver source code necessary)

- Alternative approach more suitable for model development (Wageningen University)

Code structure

8

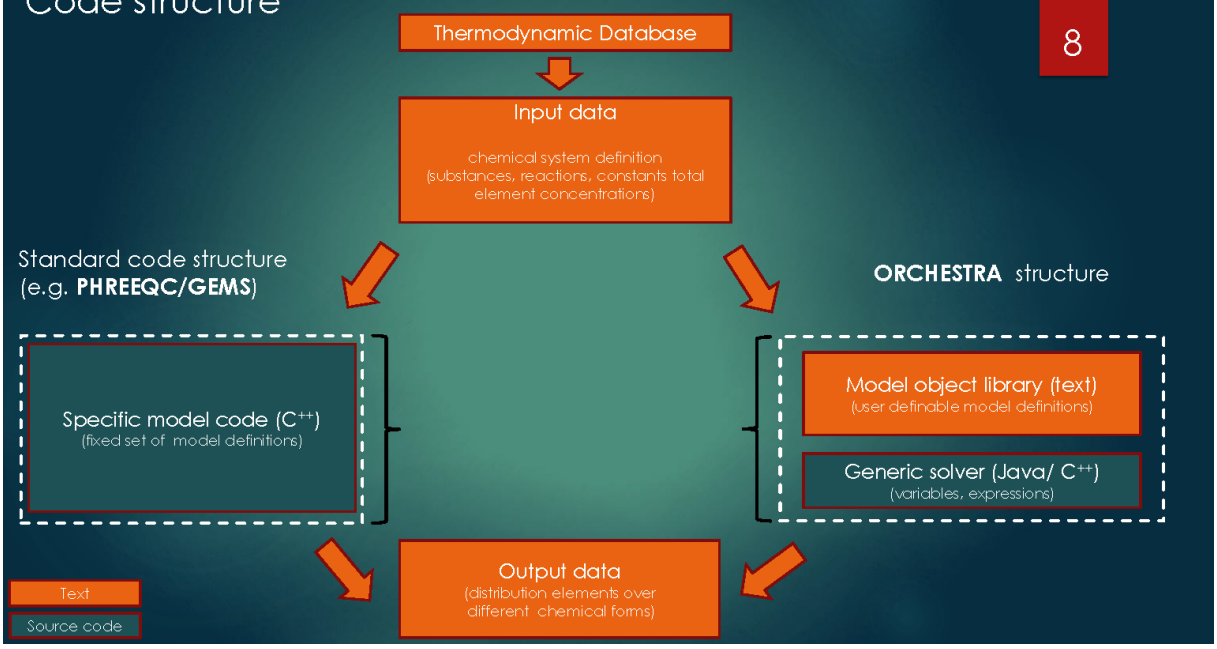

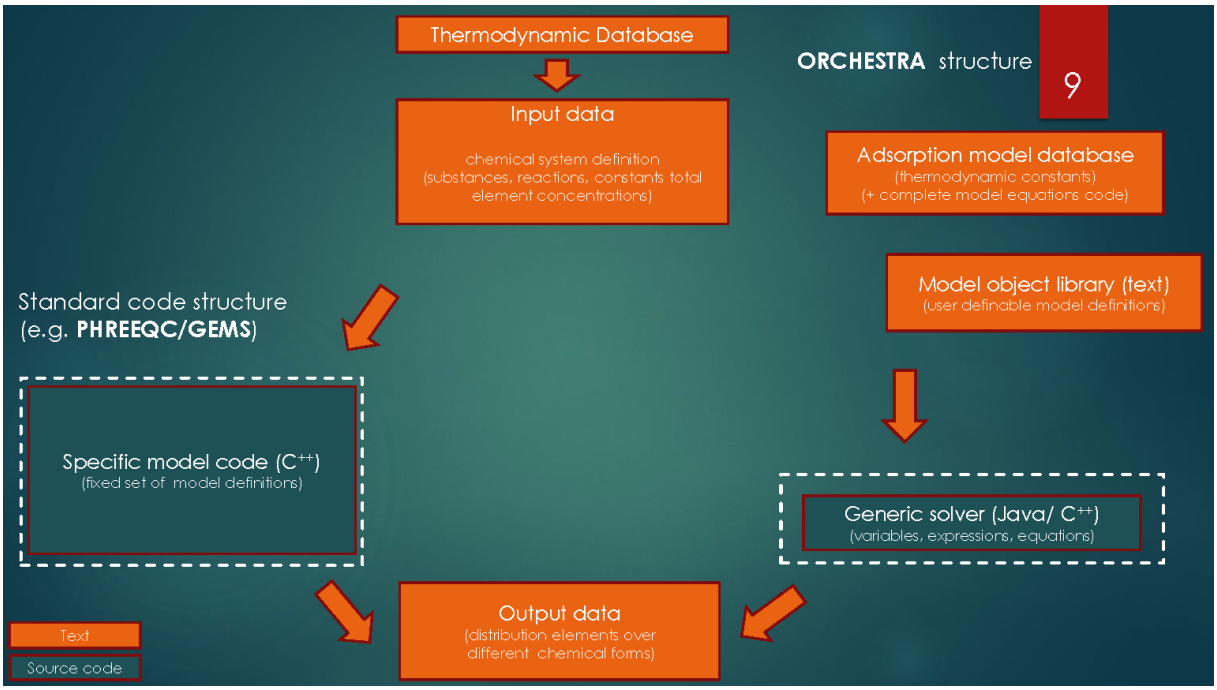
Thermodynamic Database
ORCHESTRA structure
9
Input data
chemical system definition
(substances, reactions, constants total element concentrations)
Adsorption model database
(thermodynamic constants)
(+ complete model equations code)
Model object library (text)
(user definable model definitions)
Standard code structure
(e.g. PHREEQC/GEMS)
Specific model code (C++)
(fixed set of model definitions)
Generic solver (Java/ C++)
(variables, expressions, equations)
Output data
(distribution elements over different chemical forms)
Text
Source code

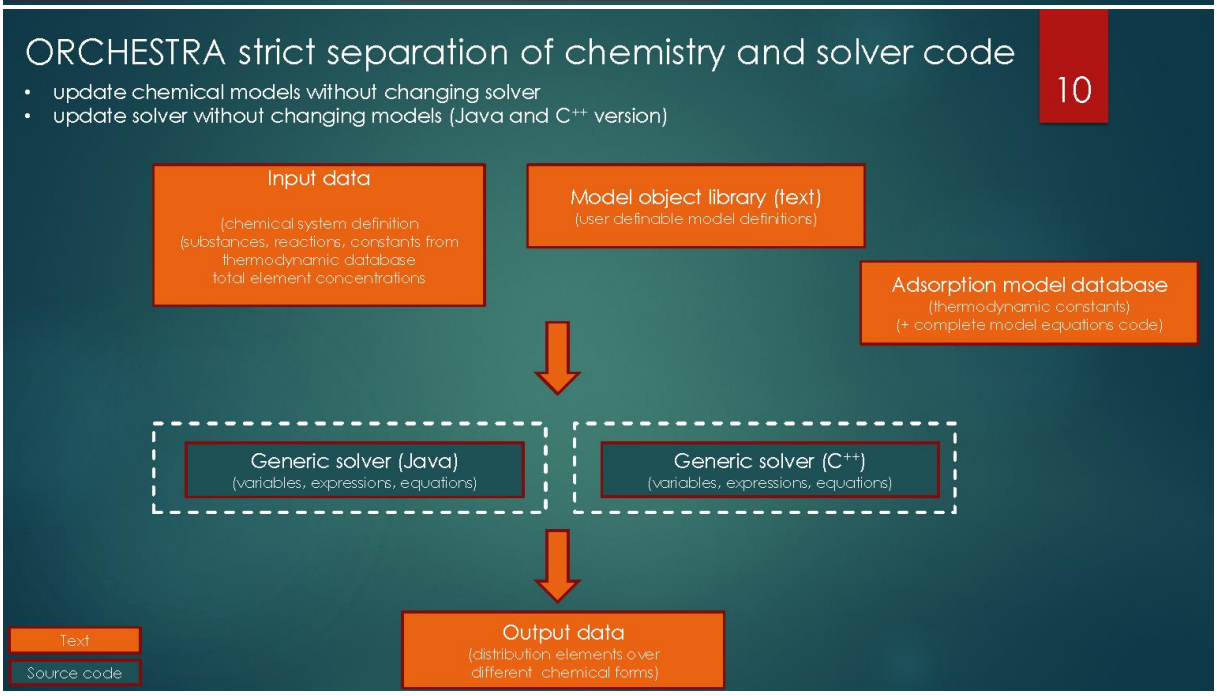
ORCHESTRA strict separation of chemistry and solver code
10
update chemical models without changing solver
update solver without changing models (Java and C++ version)
Input data
(chemical system definition
(substances, reactions, constants from thermodynamic database
total element concentrations
Model object library (text)
(user definable model definitions)
Adsorption model database
(thermodynamic constants)
(+ complete model equations code)
Generic solver (Java)
(variables, expressions, equations)
Generic solver (C++)
(variables, expressions, equations)
Output data
(distribution elements over different chemical forms)
Text
Source code

ORCHESTRA solver structure

11

- Chemical models **extendable** by users
- Large **State-of-the art** (adsorption) model library
- Ideal for **combining** "standard chemistry" with **user-defined** chemical-physical-biological model development
  (clay swelling, concrete expansion, rock salt deformation, Nernst-Planck diffusion etc.)
- However: For standard models the new structure behaves just as traditional structure and models can be defined with **Graphical User Interface**

Challenges:

- Using increased flexibility requires more knowledge
- Increased flexibility challenge for user interface and for documentation

12

Demonstration

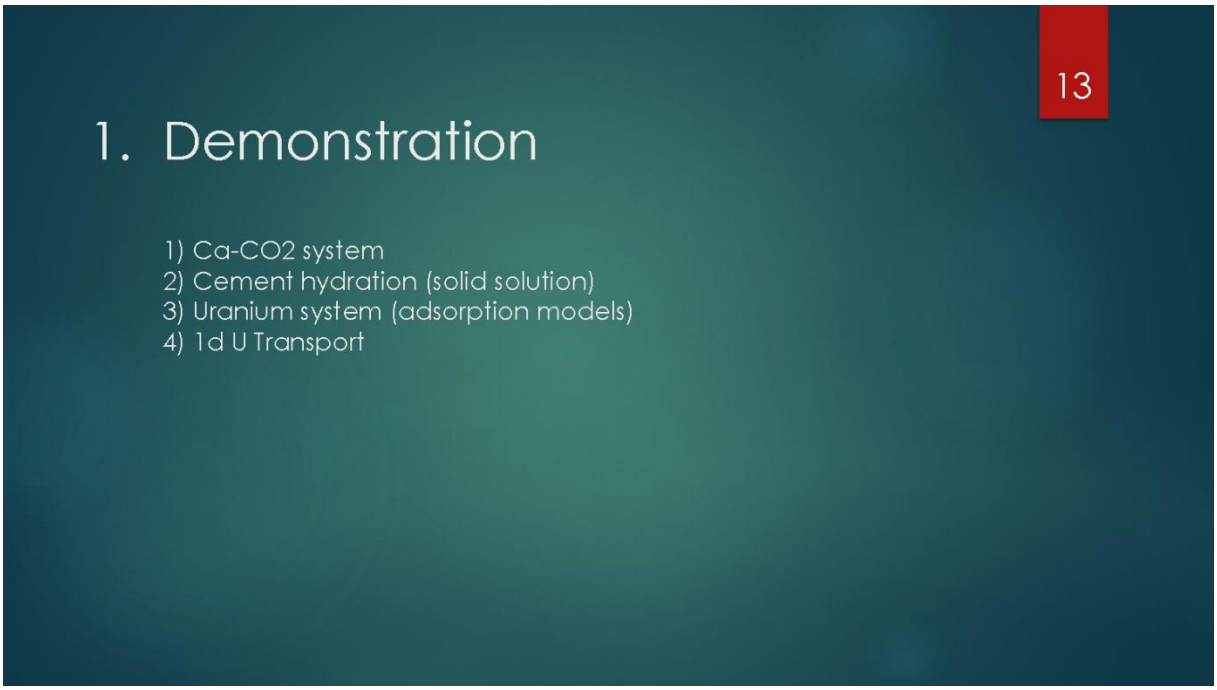
13
1. Demonstration
1) Ca-CO2 system
2) Cement hydration (solid solution)
3) Uranium system (adsorption models)
4) 1d U Transport

4.3 Code 3 – PHREEQC

The geochemical solver PHREEQC is a powerful geochemical code for aqueous speciation, mineral equilibria, multi-site cation exchange, complex surface complexation modelling, exchange with a gas-phase, solid solutions and kinetic reactions. It gives a large flexibility for modelling different geochemical systems and experimental set-ups including titration, speciation plots, etc. Moreover, PHREEQC has the possibility to perform one-dimensional advective-dispersive transport under steady-state flow conditions and multi-dimensional diffusive transport. The current version is 3.7.3. The wrappers iPHREEQC and PHREEQCRM provides libraries to work with PHREEQC from Excel, python, R, fortran, C++, … In one or another form, PHREEQC has been coupled with different transport solvers which can be used for different areas and research questions for several engineering and environmental application

In this presentation, we focus further on the PHREEQC version embedded in the HPx software. Originally, it referred to coupling of PHREEQC-3 to the HYDRUS family of flow and transport codes. The framework developed for that coupling has been extended to different geochemical solvers and transport solvers. Now, HPx refers to the core that handles geochemical calculations and the exchange of the relevant state variables to transport solvers. Beside a fresh GUI for smooth project-oriented implementations of geochemical problems (HPGeoChemistry), the PHREEQC version in HPx is extended with additional scripting languages, using of inline variables, and an alternative plotting definition. HPx also couples HYDRUS 1D and 2D for unsaturated transient-variable water flow, multicomponent transport and heat transfer with different geochemical solvers (PHREEQC and ORCHESTRA) and can uses python libraries for surrogate modelling. The framework is also used to couple the geochemical solvers with MS3D-USGS.

Lecturer

Diederik Jacques, SCK CEN, Belgium

Reading Materials

PHREEQC website: https://www.usgs.gov/software/phreeqc-version-3

HYDRUS 5.0 website: https://www.pc-progress.com/en/Default.aspx?hydrus

Jacques, D., et al., *Modeling Coupled Hydrologic and Chemical Processes: Long-Term Uranium Transport following Phosphorus Fertilization.* Vadose Zone Journal, 2008. **7**(2): p. 698-711.

Jacques, D., et al., *Modelling coupled water flow, solute transport and geochemical reactions affecting heavy metal migration in a podzol soil.* Geoderma, 2008. **145**(3-4): p. 449-461.

Jacques, D., et al., *The HPx software for multicomponent reactive transport during variably-saturated flow: Recent developments and applications.* JOURNAL OF HYDROLOGY AND HYDROMECHANICS, 2018. **66**(2): p. 211-226.

Parkhurst, D.L. and L. Wissmeier, *PhreeqcRM: A reaction module for transport simulators based on the geochemical model PHREEQC.* Advances in Water Resources, 2015. **83**(0): p. 176-189.

Charlton, S.R. and D.L. Parkhurst, *Modules based on the geochemical model PHREEQC for use in scripting and programming languages.* Computers & Geosciences, 2011. **37**(10): p. 1653-1663.

Slides

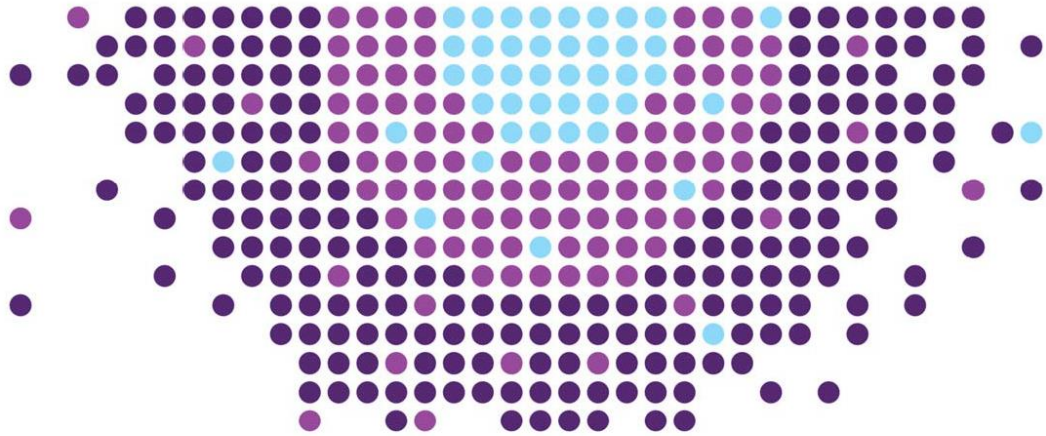

sck cen
Belgian Nuclear Research Centre

D. Jacques - 06/02/2023

PHREEQC

"Modelling workflow"

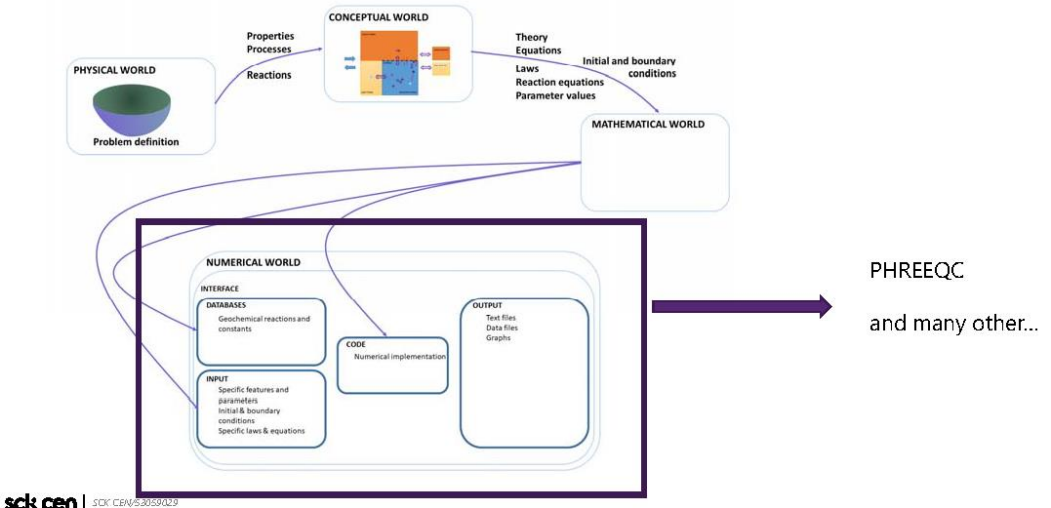

PHREEQC

and many other...

sck cen | SCK CEN/S3059/029

2
ISC: Restricted

Problem solving environment

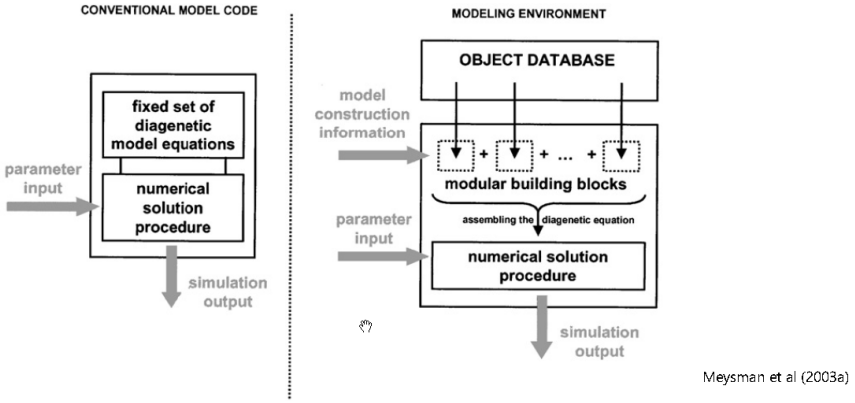

Meysman et al (2003a)

sck cen | SCK CEN/53059029

3
ISC: Restricted

Conceptual continuum representation

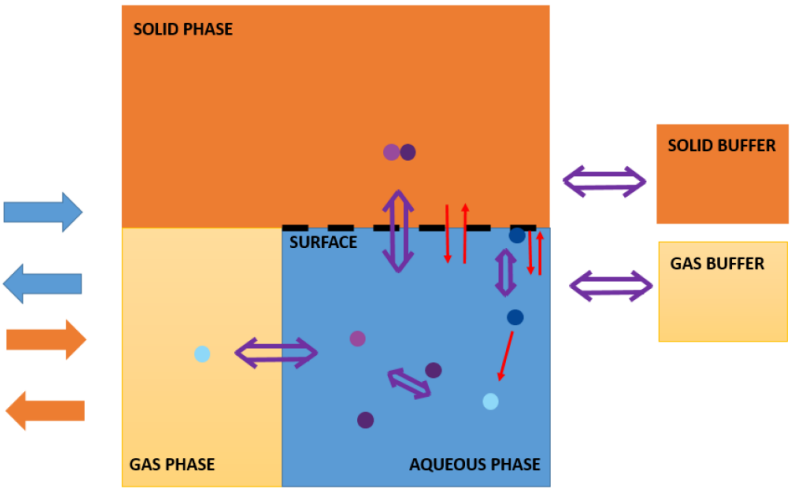

sck cen | SCK CEN/5305902

4
ISC: Restricted

PHREEQC

- Developed/maintained by USGS https://www.usgs.gov/software/phreeqc-version-3
- Two main developers: David Parkhurst (USGS), Tony Appelo (The Netherlands)
- Written in C
- Originally batch program – ASCI files (free format) define input
  - Notepad++ integration (https://www.hydrochemistry.eu/)
- Futher developments
  - iPHREEQC – A Microsoft COM for allowing easy integration in other software
  - PHREEQCRM – wrapper to ease coupling with transport models
  - PHREEQCI(nteractive) - GUI

sck cen | SCK CEN/S3059029

5
ISC: Restricted

Databases

Database	T-P range	Pressure correction	Corrected P range	Aqueous activity coefficient model	Fugacity coefficients	Number of species	Sources
phreeqc.dat	<200 °C, <1 kb	Appelo et al. (2014)	up to ~1 kb	mixed WATEQ[1] and Davies equation	Peng-Robinson	~310[2]	Appelo et al. (2014)
amm.dat	<200 °C, <1 kb	Appelo et al. (2014)	up to ~1 kb	mixed WATEQ and Davies equation	Peng-Robinson	~310[2]	Appelo et al. (2014)
iso.dat	0.01–100 °C at 1 bar	N.A.	N.A.	mixed WATEQ and Davies equation	Ideal gas law	~330	Thorstenson and Parkhurst (2002, 2004)
wateq4f.dat	0.01–100 °C at 1 bar	N.A.	N.A.	mixed WATEQ and Davies equation	Ideal gas law	~770	Ball and Nordstrom (1991)
llnl.dat	0.01–100 °C at 1 bar, 100–300 °C along P_{SAT}	SUPCRT92	N.A.	B-dot	Ideal gas law	~2590	Greg M. Anderson; EQ3/6[3]
core10.dat	0.01–100 °C at 1 bar, 100–300 °C along P_{SAT}	Appelo et al. (2014) & P_{cor} log K in SUPCRT92	up to ~1 kb	B-dot	Peng-Robinson	~630	Neveu et al. (2017)
carbfix.dat	0.01–100 °C at 1 bar, 100–300 °C along P_{SAT}	Appelo et al. (2014) & P_{cor} log K in SUPCRT92	up to ~1 kb	B-dot	Peng-Robinson	~660	Voigt et al. (2018)
sit.dat	15–50 °C at 1 bar	N.A.	N.A.	SIT	Ideal gas law	~2300	Amphos 21, BRGM and HydrAsa for ANDRA
minteq.dat	0.01–100 °C at 1 bar	N.A.	N.A.	mixed WATEQ and Davies equation	Ideal gas law	~1610	Allison et al. (1991)
minteq.v4.dat	0.01–100 °C at 1 bar	N.A.	N.A.	Mostly Davies equation	Ideal gas law	~1990	Allison et al. (1991)
pitzer.dat	<200 °C, <1 kb	Appelo et al. (2014)	up to ~1 kb	Pitzer equation	Peng-Robinson	~120	Plummer et al. (1988)
frezchem.dat	−73–25 °C at 1 bar	Appelo et al. (2014)	up to ~1 kb	Pitzer equation	Peng-Robinson	~70	Spencer et al. (1990), Marion and Farren (1999), and Marion (2001)
ColdChem.dat	−73–25 °C at 1 bar	N.A.	N.A.	Pitzer equation	N.A.	~40	Toner and Catling (2017)
geothermal.dat	0.01–100 °C at 1 bar, 100–300 °C along P_{SAT}	SUPCRTBL	N.A.	B-dot	Ideal gas law	~1050	SuperPhreeqc (Zhang et al., 2020)
diagenesis.dat	0.01–100 °C at 1 bar, 100–200 °C along P_{SAT}	Appelo et al. (2014) & P_{cor} log K in SUPCRTBL	up to ~1 kb	WATEQ equation	Peng-Robinson	~1050	SuperPhreeqc (Zhang et al., 2020)
BL.dat	Up to 1000 °C and 5 kb (variable T isobaric)	SUPCRTBL	up to 5 kb	B-dot	Ideal gas law	~1050	SuperPhreeqc (Zhang et al., 2020)

sck cen | SCK CEN/S3059029

6
ISC: Restricted

Some "hardcoded" processes

Activity correction models

- Davies
- Extended DH
- B-dot
- SIT
- Pitzer

Sorption models

- Exchange
  - Different conventions
- Surface complexation
  - Non electrostatic
  - Diffuse double layer
  - Triple layer (CD-music)
  - Constant capacitance
- DDL composition
  - Donnan
  - Explicite

Equilibrium with gas phase

- +
- Peng-Robison for high pressure and temperature

Isotopes

sck cen | SCK CEN/53059029

7
ISC: Restricted

Some "hardcoded" processes

Equilibrium with solid phases

- Pure phases
- Solid-solutions
  - Ideal
  - Binary non-ideal

Transport

- Multidimensional diffusion
- 1D Advective-dispersive
- Multi-species diffusion/electro-migration/surface layer diffusion
- Transport of collodis

Kinetics

- Two solvers
  - Runge-Kutta
  - Stiff ODE solver

Rate equations are defined by the user
And scripted in an old school BASIC language
But it has accessibility to all geochemical variables

sck cen | SCK CEN/53059029

8
ISC: Restricted

Flexible input format

- (Many) keywords (with specific identifiers)
- Copy/delete/modify option of chemical entities
- INCLUDE$

⇒Allow to model simple batch to complex mixed equilibrium-kinetic reactions paths

- Graphing possibilities

sck cen | SCK CEN/S3059/029

9
ISC: Restricted

New ways of working with PHREEQC to overcome tedious input scripting

PhreePlot is a program for making geochemical plots and fitting geochemical models to observations with **PHREEQC** (https://www.phreeplot.org/)

Predominance plots

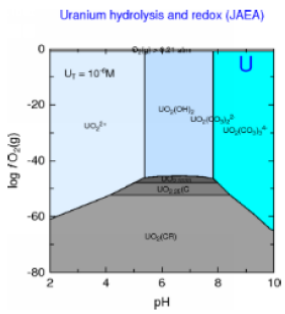

Speciation plots

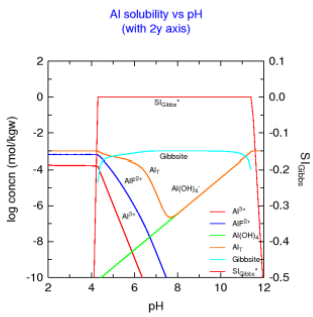

Fitting

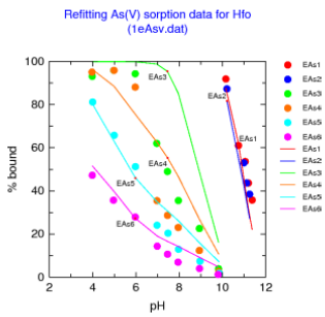

sck cen | SCK CEN/S3059/029

Note – phreeqc has been combined with generic fitting tools (e.g. ucode) as well

10
ISC: Restricted

New ways of working with PHREEQC to overcome tedious input scripting

Python

PhreeqPy: https://www.phreeqpy.com/

Phreeqpyton: https://github.com/Vitens/phreeqpython

R

Phreeqc:R Interface: https://rdrr.io/cran/phreeqc/

tidyverse: https://github.com/paleolimbot/tidyphreeqc

sck cen | SCK CEN/53059029 | 11 | ISC: Restricted

New ways of working with PHREEQC to overcome tedious input scripting

Gibbsstudio (https://gibbsstudio.io/)

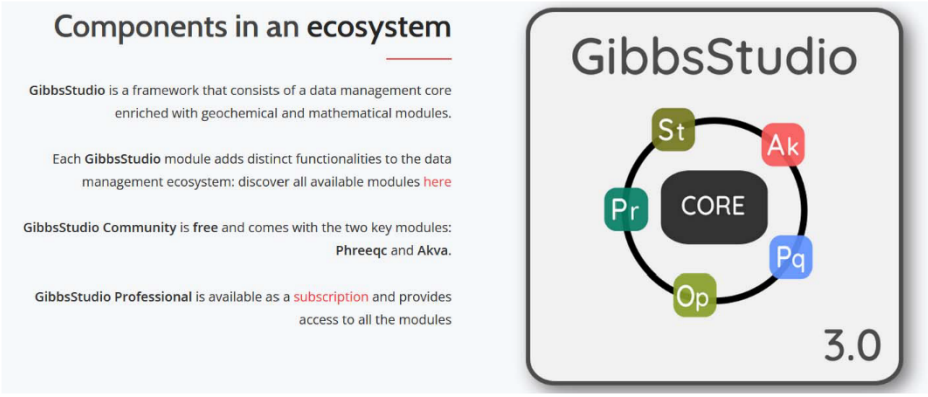

sck cen | SCK CEN/53059029 | 12 | ISC: Restricted

sck cen | SCK CEN/53059029

13
ISC: Restricted

HP1 - How it started... 1999

Rien van Genuchten

Dirk Mallants

Diederik Jacques

Hello from C++

Hello from Fortran

Jirka Simunek

Mirek Senja

sck cen | SCK CEN/53059029

14
ISC: Restricted

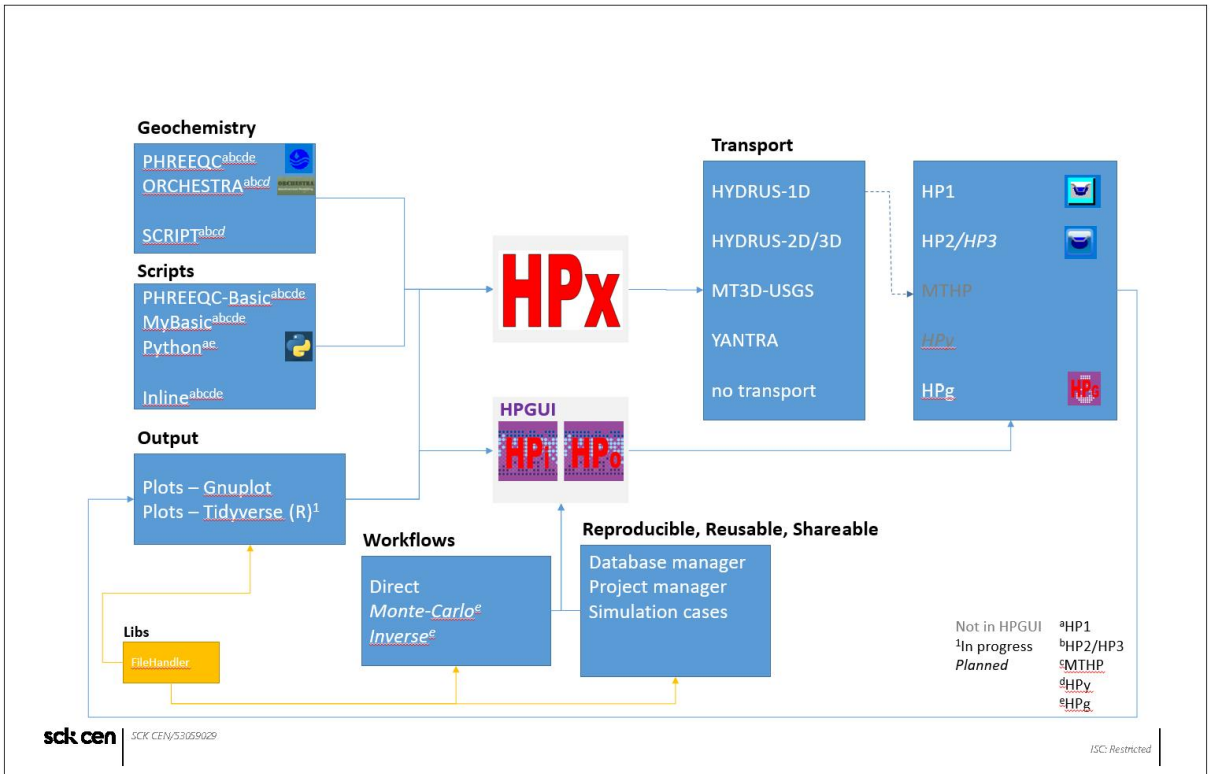
Geochemistry
PHREEQC[abcde]
ORCHESTRA[abcd]
SCRIPT[abcd]
Scripts
PHREEQC-Basic[abcde]
MyBasic[abcde]
Python[ae]
Inline[abcde]
Output
Plots – Gnuplot
Plots – Tidyverse (R)[1]
Libs
FileHandler
HPx
HPGUI
Transport
HYDRUS-1D
HYDRUS-2D/3D
MT3D-USGS
YANTRA
no transport
HP1
HP2/HP3
MTHP
HPv
HPg
Workflows
Direct
Monte-Carlo[e]
Inverse[e]
Reproducible, Reusable, Shareable
Database manager
Project manager
Simulation cases
Not in HPGUI
[1]In progress
Planned
[a]HP1
[b]HP2/HP3
[c]MTHP
[d]HPv
[e]HPg
sck cen
SCK CEN/53059029
ISC: Restricted

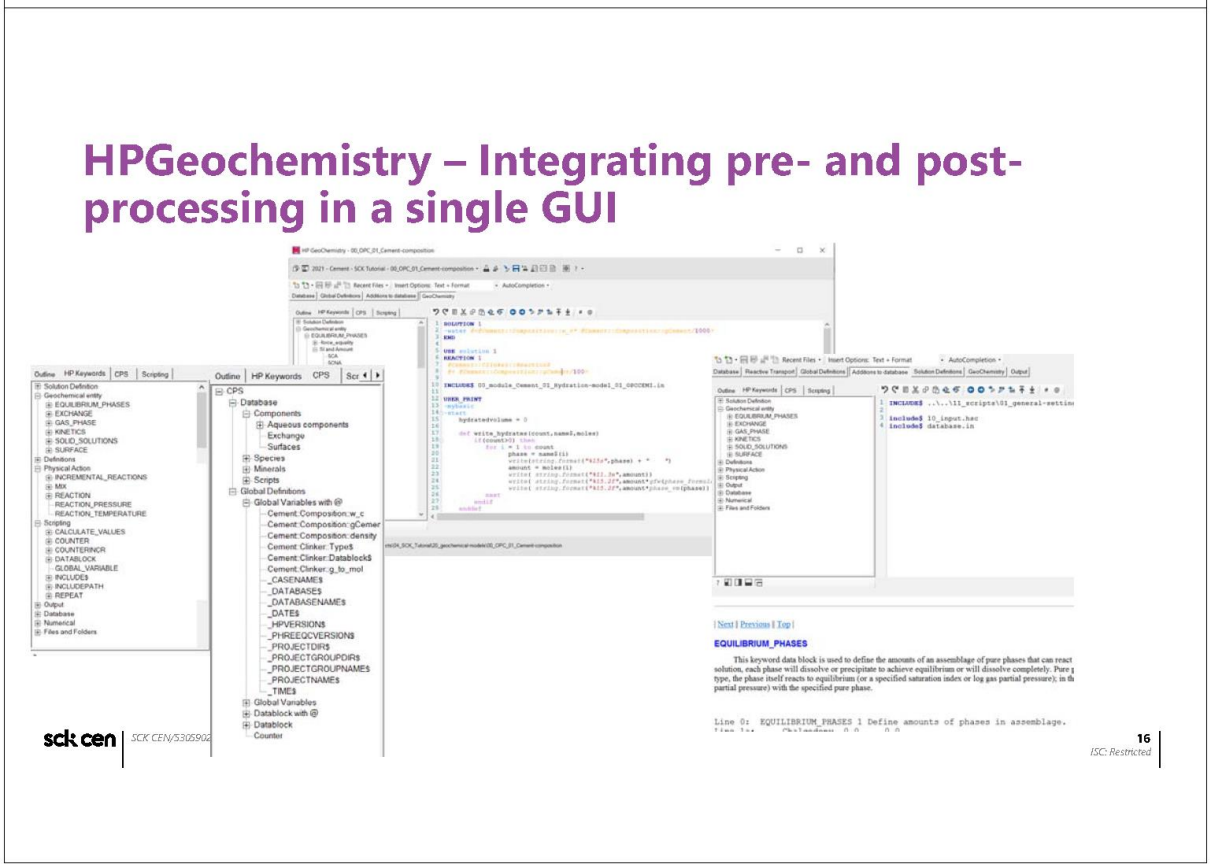
HPGeochemistry – Integrating pre- and post-processing in a single GUI
sck cen
SCK CEN/53059029
16
ISC: Restricted

HPGeochemistry – Integrating pre- and post-processing in a single GUI

Text files: Phreeqc.out

Data files

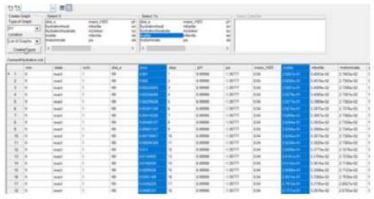

Graphs

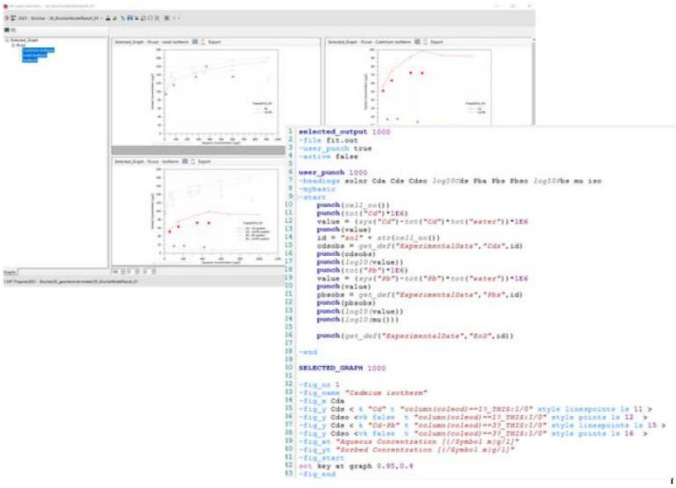

sck cen | SCK CEN/53059029

HPGeochemistry – GUI

Managed Projects

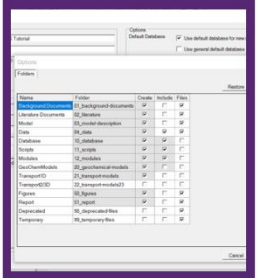

Re-use of "modules"
Integrated in HYDRUS
Easy exchange

User-defined input forms

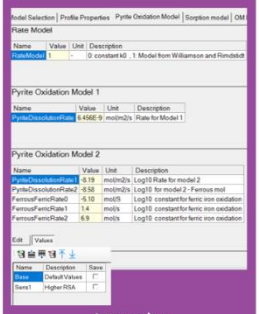

Automation
Set parameters and model options
Define different cases

Flexible scripting language

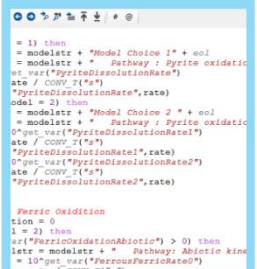

Including all PHREEQC functions
and more
Structured BASIC + OO

sck cen | SCK CEN/53059029

18
ISC: Restricted

Cement chemistry – Hydration & ageing

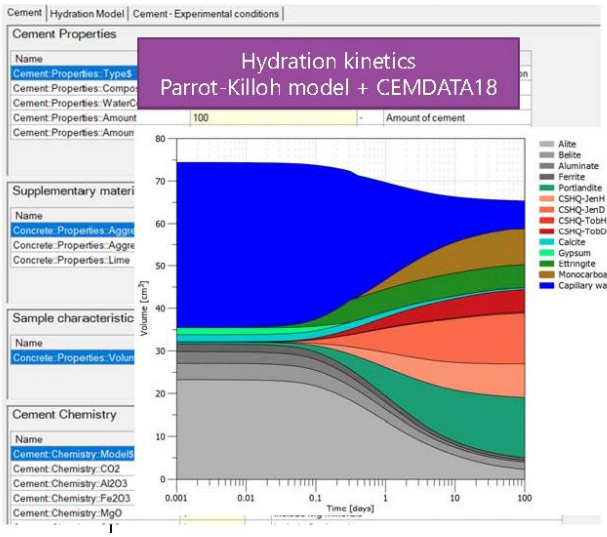

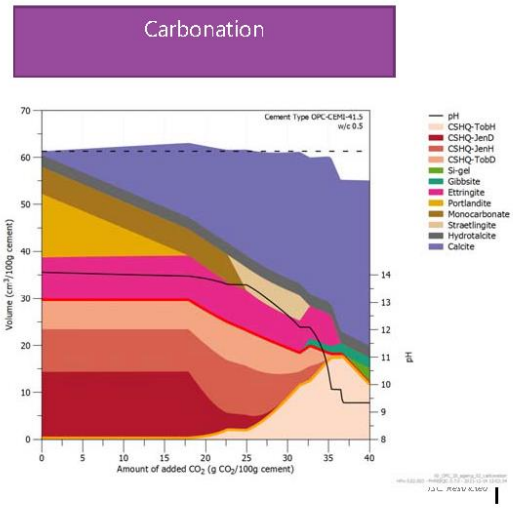

1D/2D(/3D) reactive transport integrated in HYDRUS 5.0

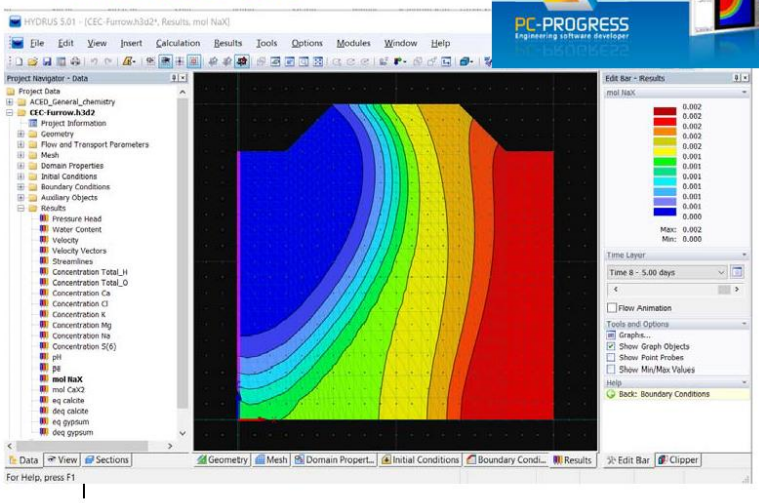

- License needed
- But for 1D
  - Free version HYDRUS 4.17 available on website
  - With HPx GUI: 4.18 available on request

20
ISC: Restricted

Alternative solver ORCHESTRA (DONUT)

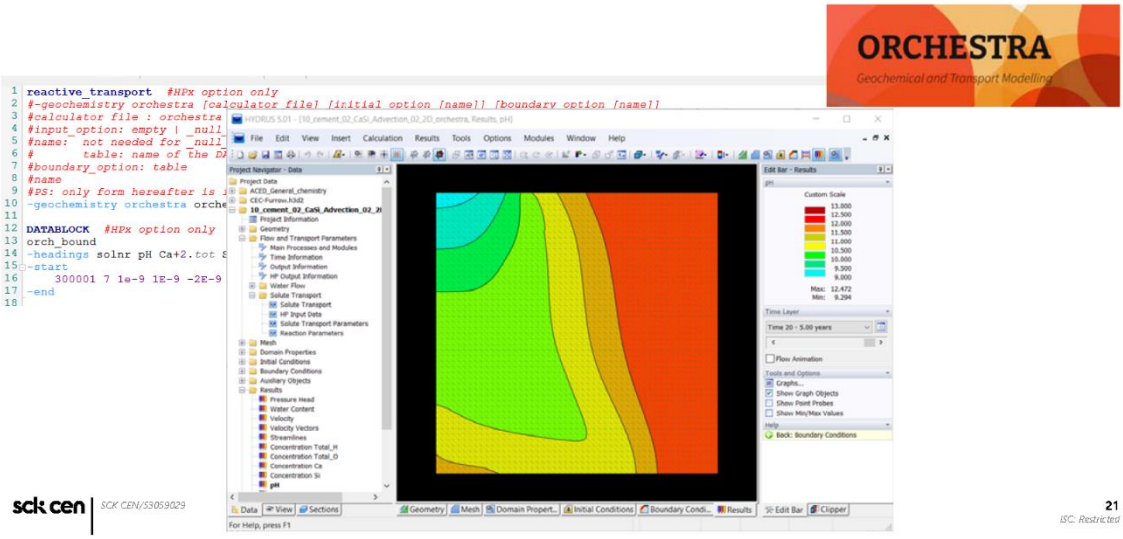

ORCHESTRA: EURAD-DONUT – Cement leaching

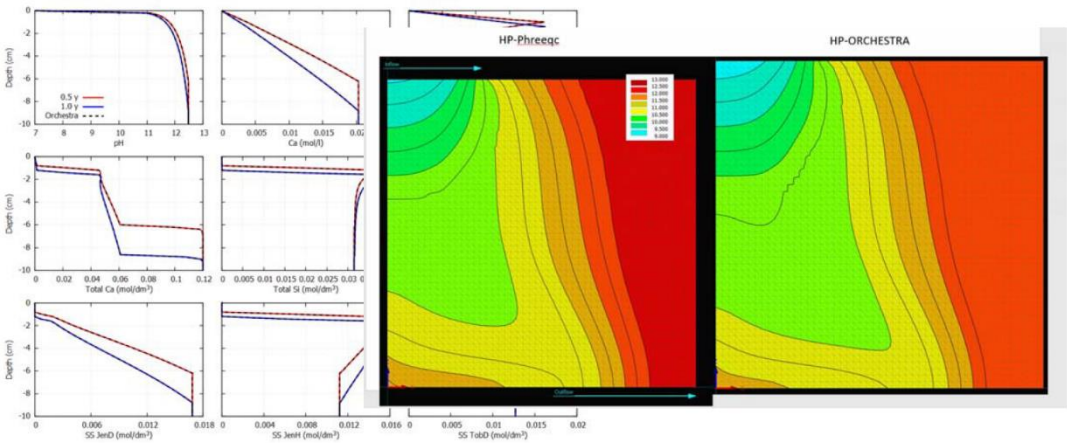

Alternative solver "Script"

Alternative geochemical model
Surrogate modelling

```
REACTIVE_TRANSPORT
-geochemistry function CementModel_kNN

#Geochemical Surrogate Model
CALCULATE_VALUES
CementModel_kNN
-python
-start
if 'initialization' not in globals():
    print("Initialization")
    import rtm as rtm
    import phreeqc as phrq
    import sys
    sys.path.append("C:\\Users\\djacques\\AppData\\Local\\Programs\\Python\\Python37\\Lib\\site-packages")
    sys.path.append("D:\\HP Scripts\\Python\\Surrogate Models")
    sys.path.append("C:\\Users\\djacques\\AppData\\Local\\Continuum\\anaconda3\\Lib\\site-packages")
    import numpy as np
    import Surrogate as Surrogate
    initialization = 1
    SolidMoles=rtm.GetInitialConditions()
    Components = rtm.GetComponents()
    dir = phrq.get_var("_FOLDERTRAINGS")
    ParSet = Surrogate.LoadParSet(indir = dir, infile = "Training03.dat")
    kNN, ExtrakNN = Surrogate.BuildkNN(ParSet,Components, prefix="Sys", suffix="Conc")
    print(ExtrakNN)
    step = 0
step = step + 1
if step==100:
    boutprint = True
    step = 0
else:
    boutprint = False
AqConc = rtm.GetAqConcentrations()
WaterContent = rtm.GetWaterContent()
AqConc, SolidMoles, NewDim = Surrogate.EvalSurrogate('kNN',kNN,ExtrakNN, AqConc,WaterContent,SolidMoles,outprint=False)
for par in NewDim:
    entity.modify("reaction",5000,"r","CaO",par[0])
    entity.modify("reaction",5000,"r","SiO2",par[1])
    d=entity.run(5000,retvalue=True,punch=True)
    list->Add(d)
```

Note
Calling Python from PHREEQC is a reverse alternative to the phreeqc "embedding" in python

Can be used for
- Monte Carlo simulation
- ...

Cement chemistry – Transport

- CEBAMA – Experiments SCK CEN

Boom Clay solution (0.4% CO_2)
Saturated Cement/concrete
Boom Clay solution (0.4% CO_2)

Batch experiment → Diffusion controlled

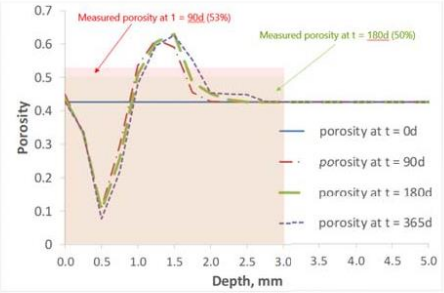

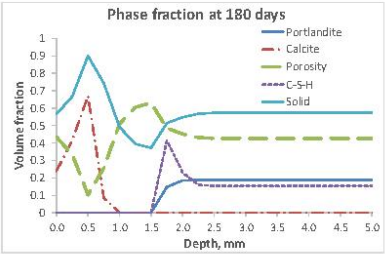

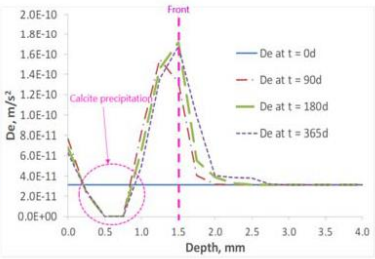

Changes in composite diffusivity

Duration	Measured	Predicted
90d	3.3%	3.1%
180d	10.2%	4.0%

MTHP

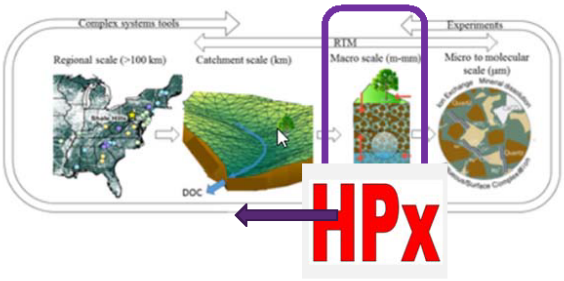

MT3D-USGS

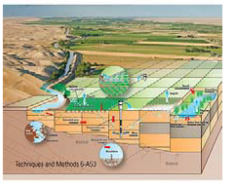

MCP package

New multi-component package

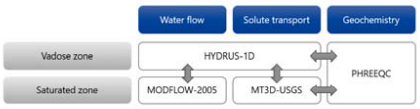

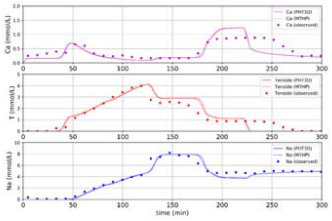

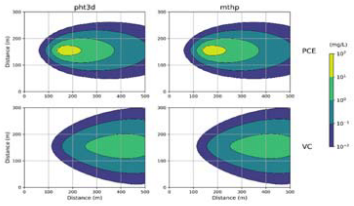

sck cen | SCK CEN/S3059029

25
ISC: Restricted

SCK CEN
Belgian Nuclear Research Centre

Foundation of Public Utility

Registered Office: Avenue Herrmann-Debrouxlaan 40 – BE-1160 BRUSSELS
Operational Office: Boeretang 200 – BE-2400 MOL

sck cen | SCK CEN/S3059029

26
ISC: Restricted

4.4 Code 4 – iCP

The interface Comsol PhreeqC, or iCP, is a reactive transport simulator that couples two standalone simulation softwares: Comsol Multiphysics® and the geochemical simulator PhreeqC. iCP maximizes the synergies between these codes, providing a numerical platform that can efficiently simulate a wide number of multiphysics problems coupled with geochemistry. iCP is a powerful tool for those consultants or researchers who need to tackle coupled geochemical problems. The flexibility and wide applicability of iCP make it suitable for a large number of modelling challenges, which cover most of the needs of both industry and academia.

In this introduction to iCP we will give a brief overview of the implementation of the tool and its capabilities. We will also demonstrate these capabilities with several examples of iCP applications to reactive transport modelling in the nuclear waste management sector including coupled thermo-hydro-chemical processes, fracture flow, multiphase flow and mechanics

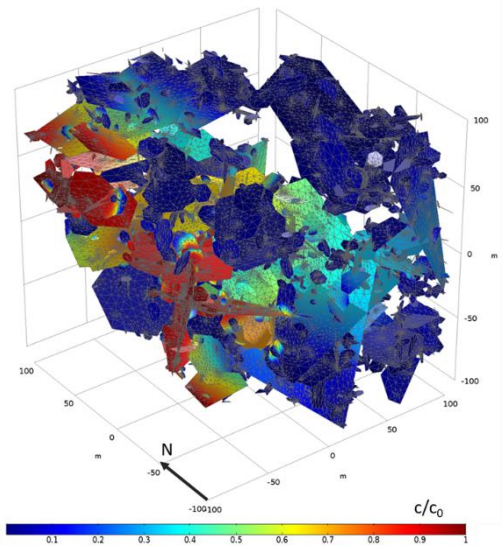

Lecturer

Emilie Coenen, Amphos21, Spain

Reading Material

Nardi, A., Idiart, A., Trinchero, P., de Vries, L. M., and J. Molinero. Interface COMSOL-PHREEQC (iCP), an efficient numerical framework for the solution of coupled multiphysics and geochemistry. Computers & Geosciences 69 (2014): 10-21.

More information on iCP can be found on the Techlabs webpage of Amphos 21: https://techlabs.amphos21.com/technology/interface-comsol-phreeqc/

Slides

AMPHOS 21

member of RSK

Introduction to iCP

Emilie Coene, 07/02/2023

www.amphos21.com

www.rskgroup.com/rsk-businesses/

Amphos 21 Group

We are a scientific, technical and strategic consulting to the service of the environment and the economic and social development.

We are a team of **+230 professionals** with high technical skills and innovative mindset. Geologists, Chemists, Hydrogeologists, Geochemists, Engineers, Mathematicians, Physicists, Biologists, Environmentalists and Economists to the service of sectors such as :

- **Mining**
- **Nuclear**
- **Water Resources**
- **Sustainability, Energy, Climate Change**
- **Oil&Gas**

Integrated Innovative and efficient solutions developed with a quantitative approach.

We have been working for 29 years in a global world. From our 3 offices in Europe and Latin America, we develop projects in more than 20 countries.

Since January 2021, we are part of **RSK Group**

A21

OUR MISSION

Our driving force is reducing the environmental impact associated with industrial and economic activities needed for the development of our society.

Project diversification

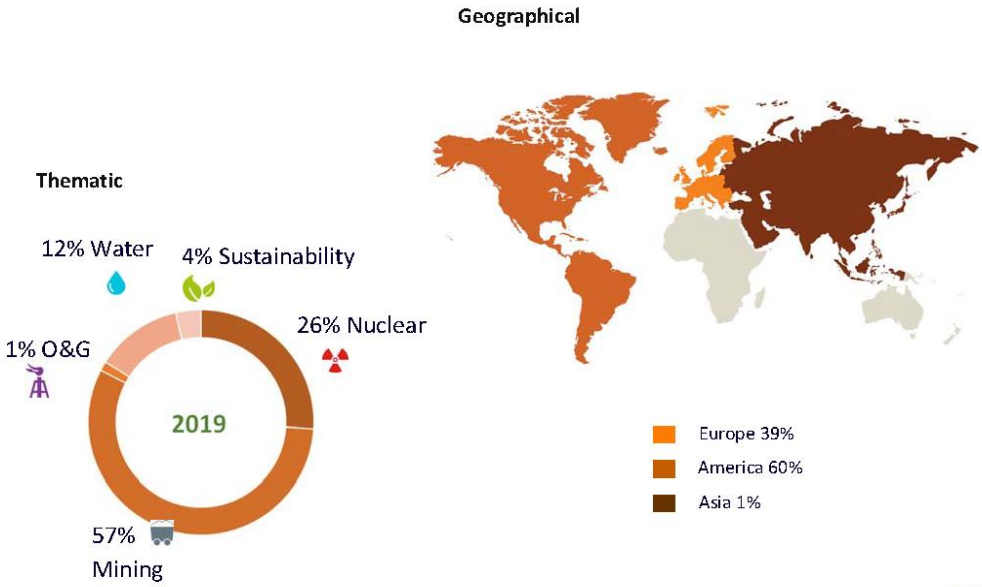

AMPHOS 21 – Modelling Solutions

We perform advanced numerical modelling to provide quantitative solutions to our clients.

iCP: interface COMSOL - PHREEQC

iCP
interface COMSOL PHREEQC

- iCP is an interface to couple Comsol Multiphysics with the geochemical simulator Phreeqc. The result is a tool for solving a wide range of coupled multiphysics and geochemical problems.
- iCP is part of the interfacing **M**ultiphysics **and** **Ge**ochemistry (iMaGe) platform.

iMaGe
an Amphos21 initiative

SKB POSIVA ANDRA JÜLICH KIT AMPHOS 21

Our partners

iCP is ….

- an **interface** that couples two standalone simulation programs: COMSOL and PHREEQC.
- able to **maximize their synergies**.
- **flexible and powerful**. The **wide range of application** of the two coupled codes result in an extensive list of modelling possibilities.

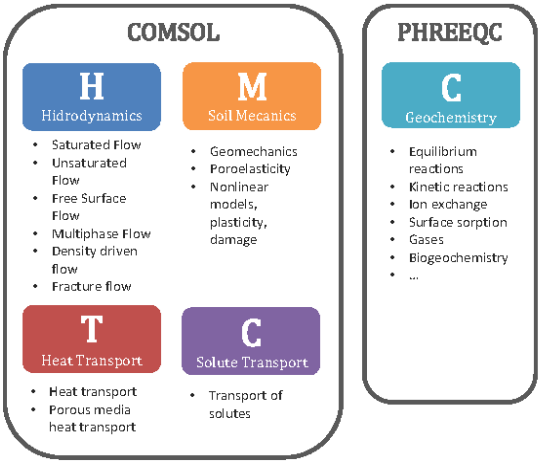

Implementation details

Flow of information overview

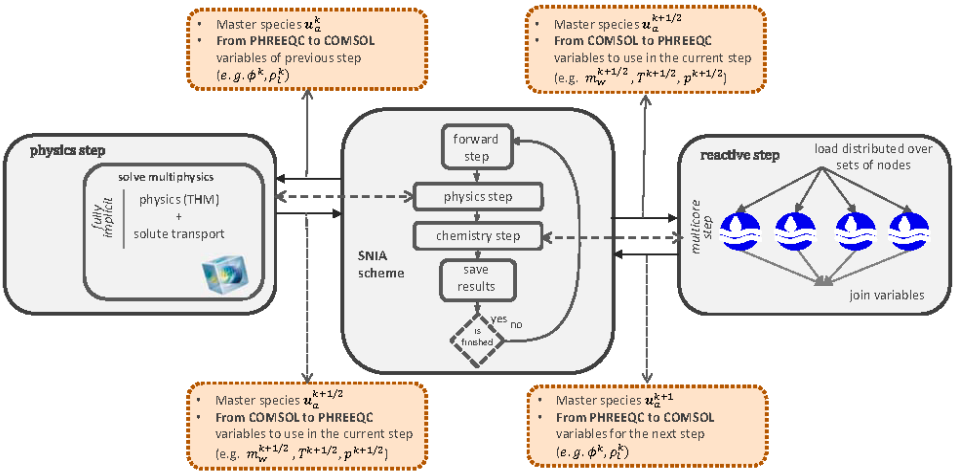

iCP capabilites

- iCP application examples:
  - **HCM modelling of concrete degradation**
  - HCM model of bentonite sealing
  - Reactive transport in fractured media
  - Coupled multiphase flow and reactive transport

Hydro-chemo-mechanical modelling of concrete degradation in SFL

- Objectives:
  - Evaluate concrete degradation taking into account both the chemical degradation and mechanical loading
  - Implement Mazars mechanical damage model (1986)
  - Implement a chemical damage model to study the impact of calcium leaching and sulphate attack on the mechanical properties of the concrete

Idiart A., Laviña M., Coene E. (2019). Modelling of concrete degradation – Hydro-chemo-mechanical processes. SKB Report R 19-12

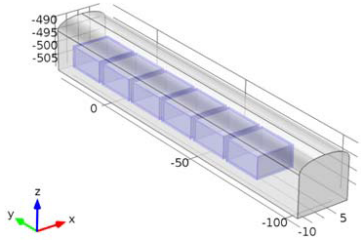

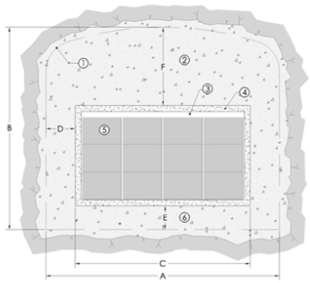

Hydro-chemo-mechanical modelling of concrete degradation in SFL

- The water flux thourgh the repository is calculated with Darcy's law:

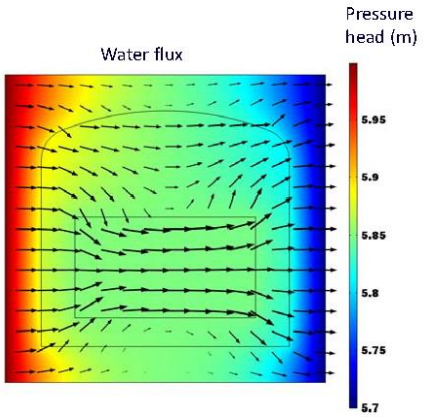

Hydro-chemo-mechanical modelling of concrete degradation in SFL

- Calcium leaching, 100.000 years:

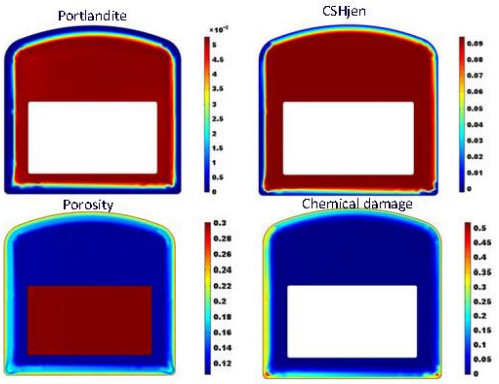

Mechanical damage, base case

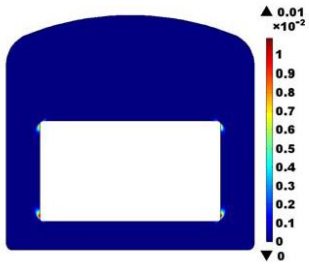

Mechanical damage, glaciation

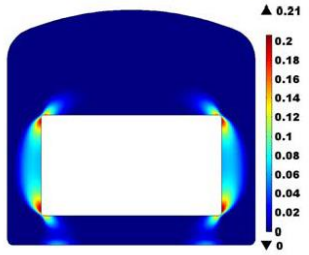

Hydro-chemo-mechanical modelling of concrete degradation in SFL

- Sulphate attack: Ettringite and thaumasite precipitation generate a volumetric expansion and cause mechanical damage in the concrete

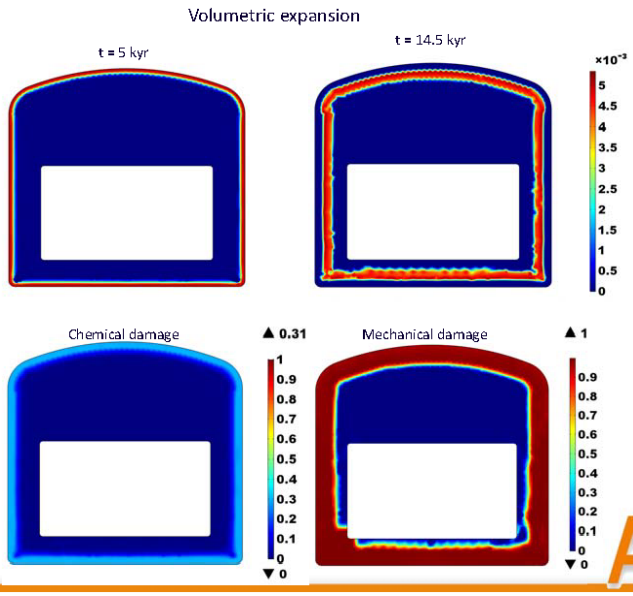

iCP capabilites

- iCP application examples:
  - HCM modelling of concrete degradation
  - **HCM model of bentonite sealing**
  - Reactive transport in fractured media
  - Coupled multiphase flow and reactive transport

HCM modelling of sealing components in Cigéo

- Andra bentonite-based sealing component for Cigéo
  - Main function: limit porewater movement (radionuclide migration) and provide mechanical support
  - Performance linked to swelling pressure development and stability
  - Challenges: high number of coupled processes and large timescales involved

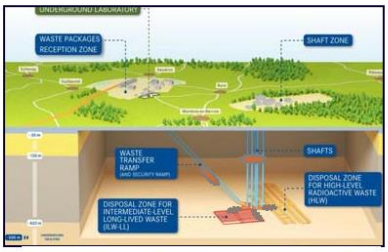

Diagram of the Industrial Centre for Geological Disposal, Cigeo [1]

- Processes under study:
  - Resaturation of the sealing system
  - Two-phase flow hydraulic gas transient phase (H_2 gas)
  - HM swelling of bentonite-based materials – Barcelona Basic Model
  - Reactive transport (chemical gradients between components)
  - Impact of geochemical alteration on HM response

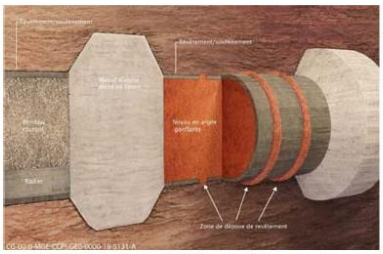

Detail of gallery bentonite-based sealing component

Idiart, A., Laviña, M., Pasteau, A., Cochepin, B., 2020b. Hydro-chemo-mechanical modelling of long-term evolution of bentonite swelling. Applied Clay Science 195, 105717. https://doi.org/10.1016/j.clay.2020.105717

HCM modelling of sealing components in Cigéo

- Seal alteration after 20ky of interaction:
  - High pH plume from concrete degradation
  - Little Mt dissolution
  - Cation exchange in bentonite interlayer

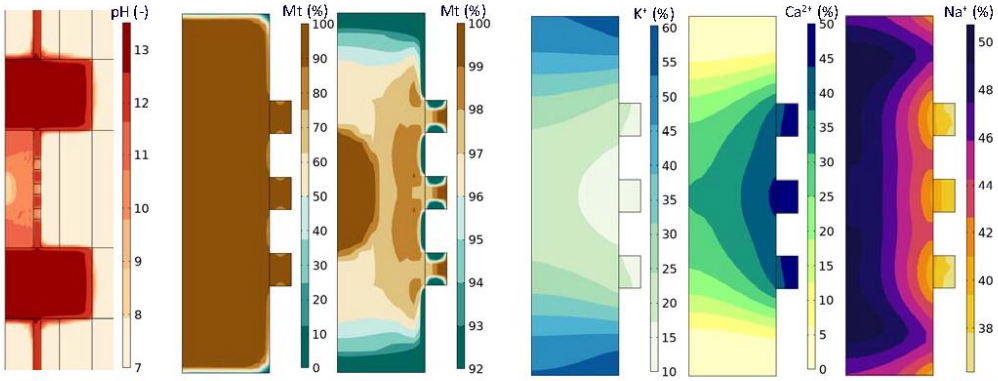

HCM modelling of sealing components in Cigéo

- Impact of chemistry on mechanical performance:
  - Relative (based on HM results) swelling pressure in the seal after 20ky
  - Highly affected by Mt dissolution and K+ uptake from the concrete plugs

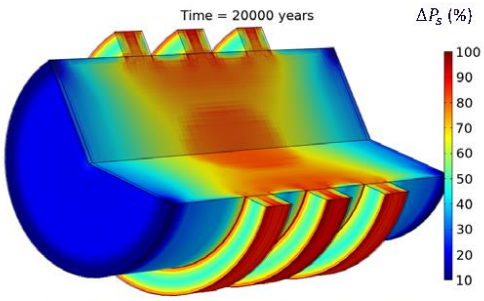

Relative swelling pressure (%) distribution due to geochemical alteration

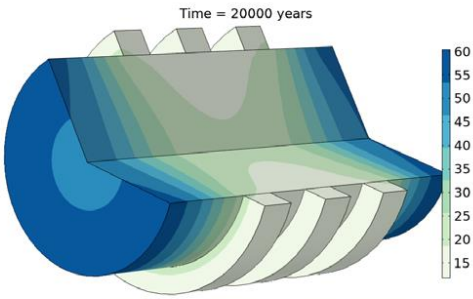

Potassium fraction (%) distribution in bentonite exchanger

iCP capabilites

- iCP application examples:
  - HCM modelling of concrete degradation
  - HCM model of bentonite sealing
  - **Reactive transport in fractured media**
  - Coupled multiphase flow and reactive transport

3D RTM of a discrete fracture network including the matrix effect.

3D fractured carbonated media (200x200x200 m) which includes a discrete fracture network (DFN) generated in Mafic (Miller et al, 1999), with 3,531 hexagonal fractures. Magnesium-rich groundwater flows through the fractures leading to calcite dissolution and eventually dolomite formation.

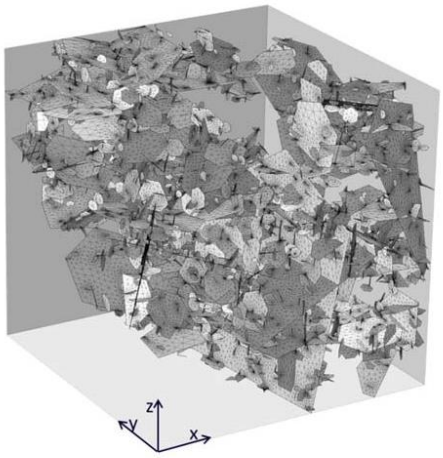

3D RTM of a discrete fracture network including the matrix effect.

Boundary Conditions: a prescribed hydraulic head (Dirichlet boundary condition) is imposed along the fractures of the east boundary and at the west boundary.

Boundary conditions

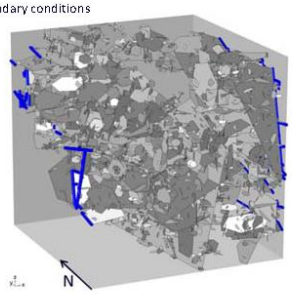

Transmisivity distribution

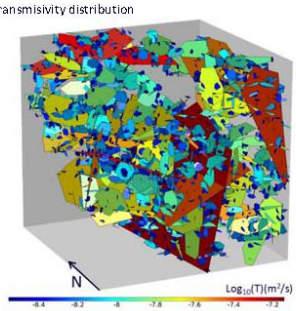

Component	Concentration (mol/kg$_w$) for the initial condition	Concentration (mol/kg$_w$) imposed at the inlet of the fracture
Ca	1.227×10^{-4}	1×10^{-14}
C	1.227×10^{-4}	1.7×10^{-14}
Mg	1.0×10^{-5}	$\mathbf{1.0 \times 10^{-3}}$
Cl	1.0×10^{-4}	2.0×10^{-3}
T (ºC)	25	25
Pe	4	4
pH	7.0	7.0

3D RTM of a discrete fracture network including the matrix effect.

Normalized chloride distribution at the end of the simulation for the fractures.

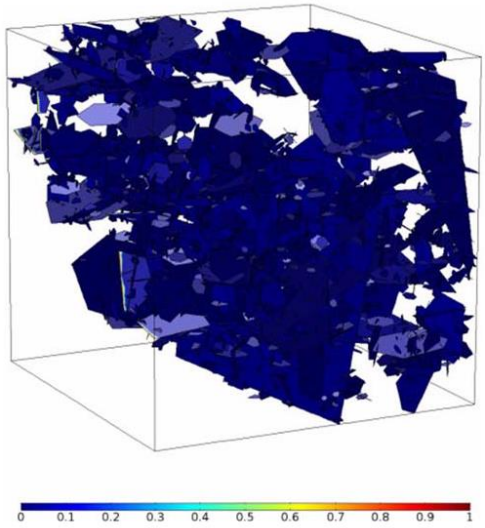

3D RTM of a discrete fracture network including the matrix effect.

Normalized chloride distribution at the end of the simulation for the fractures (left) and the matrix at 0.25 meters of the fractures (centre) and 0.75 meters of the fractures (right).

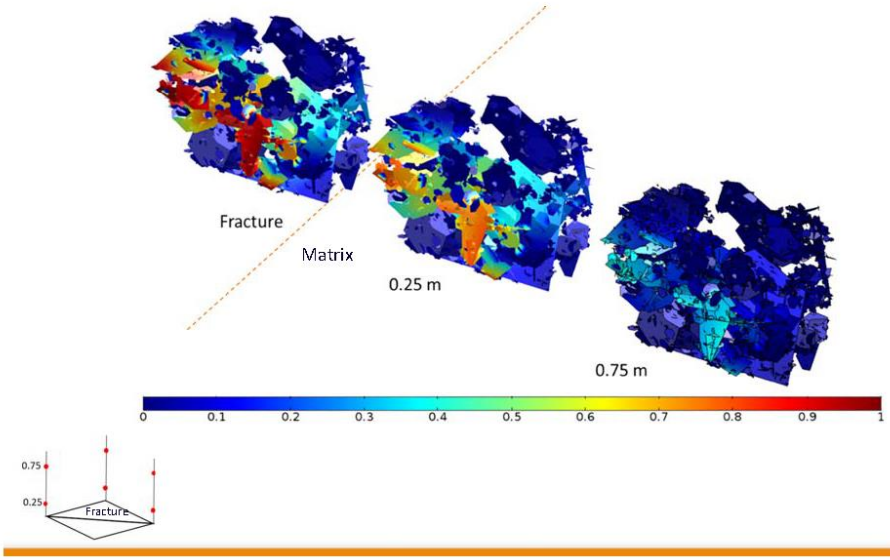

3D RTM of a discrete fracture network including the matrix effect.

Animation showing the concentration of calcite, tracer and dolomite at the end of the simulation for the fractures

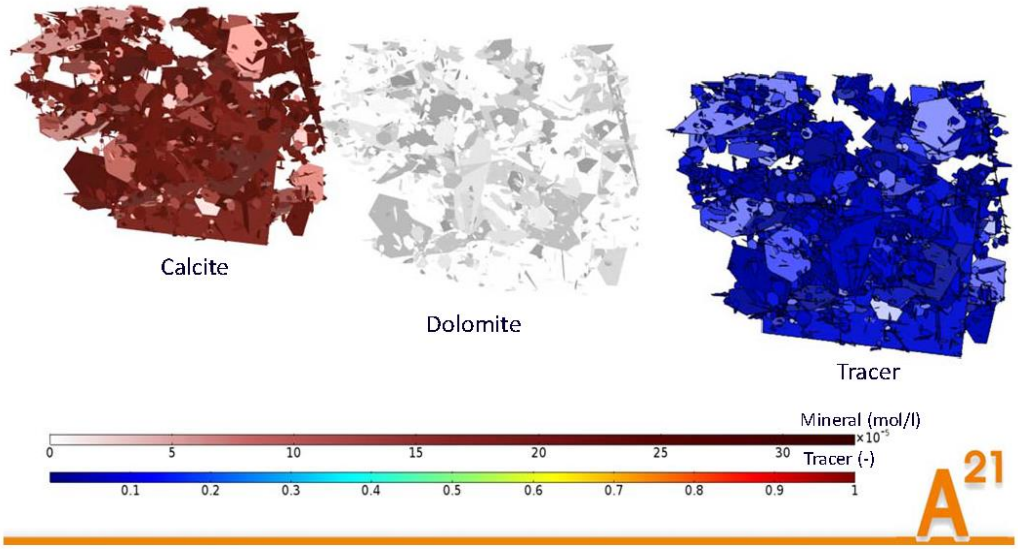

3D RTM of a discrete fracture network including the matrix effect.

Results

Concentration of calcite, tracer and dolomite at the end of the simulation for the fractures

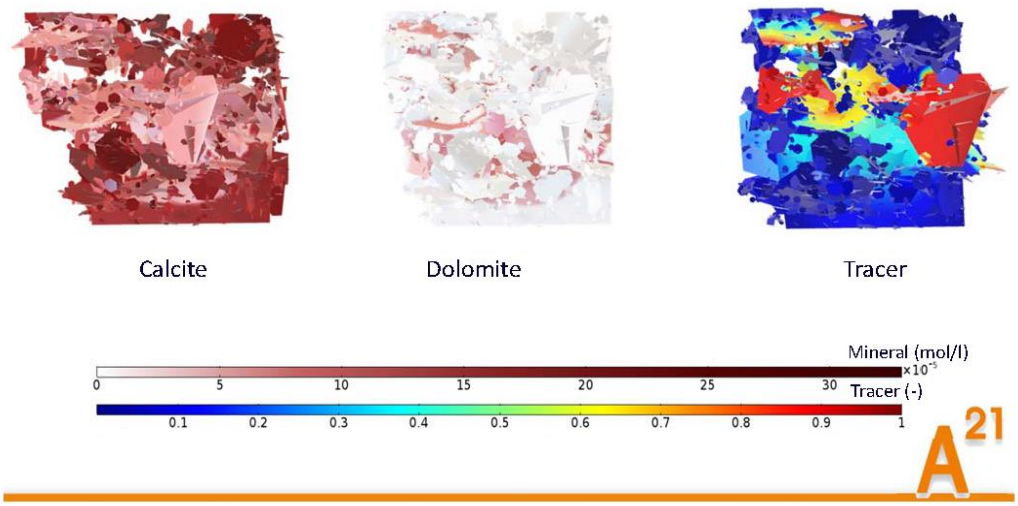

iCP capabilites

- iCP application examples:
  - HCM modelling of concrete degradation
  - HCM model of bentonite sealing
  - Reactive transport in fractured media
  - **Coupled multiphase flow and reactive transport**

Otway Fault Project: Modelling shallow injection of CO_2

- Feasibility study of an t of CO_2 injection, controlled release and monitoring experimen in a shallow fault.
- Aims:
  - Implement a 3D geological model of Port Campbell Limestone
  - Develop a multiphase flow model to simulate the injection and migration of CO_2 next to a fault
  - Predict the final distribution of CO_2 (gas, dissolved and precipitated as mineral phase) during 200 days.

Otway Fault Project: Modelling shallow injection of CO_2

- Injection of 25 tons of CO_2 during 50 days
- Evolution of the CO_2 bubble

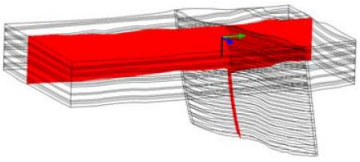

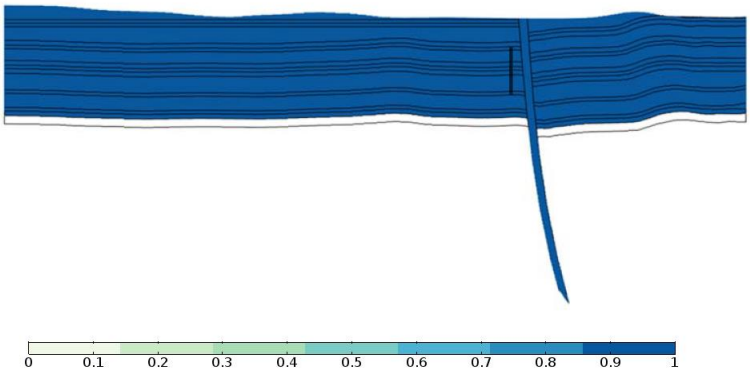

Otway Fault Project: Modelling shallow injection of CO_2

Carbonate concentration (mol/kgw)

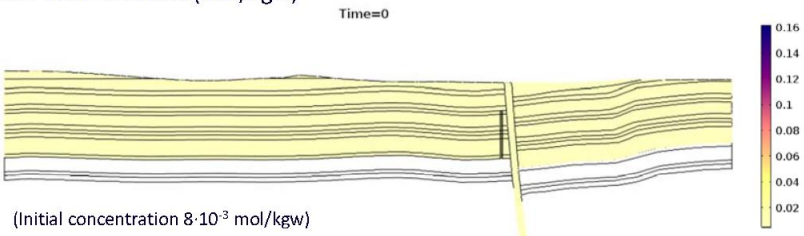

(Initial concentration $8 \cdot 10^{-3}$ mol/kgw)

Calcite concentration (mol/l med)

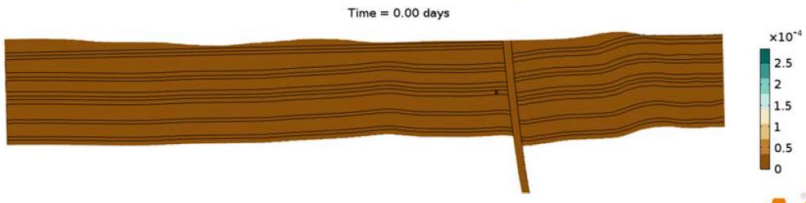

Otway Fault Project: Modelling shallow injection of CO_2

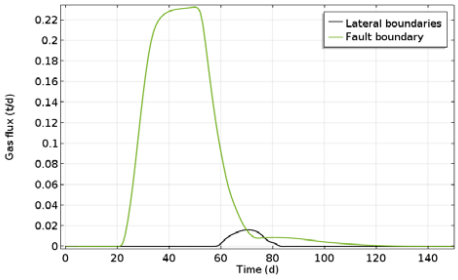

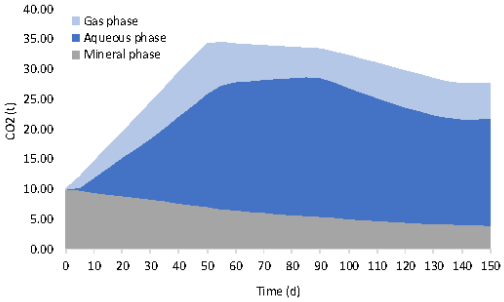

Resources

- Techlabs page of iCP:
  - General information
  - Free trial license
  - Blog posts and posters
  - FAQ
- Paper: Nardi et al. 2014
- iCP Project in ResearchGate: https://www.researchgate.net/project/iCP-interface-Comsol-Phreeqc

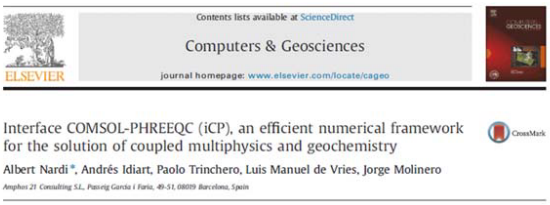

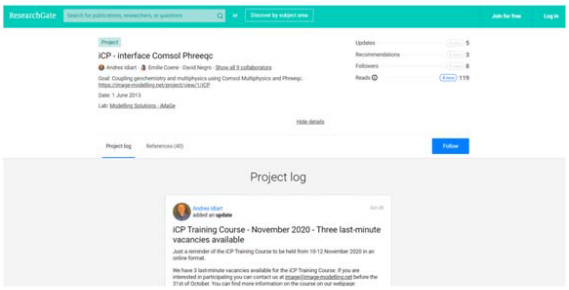

4.5 Code 5 – CRUNCH

For abstract, see section 3.4.

Lecturer

C.I. Steefel, Lawrence Berkeley National Laboratory, United States

Reading Material

For abstract, see section 3.4

Slides

Introduction to Reactive Transport Modeling with CrunchTope/CrunchClay

Carl Steefel
Christophe Tournassat

February 7, 2023
Eurad Training
Bern, Switzerland

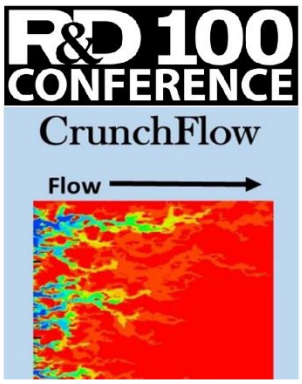

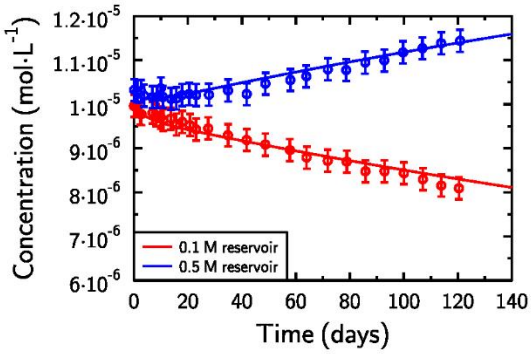

Acknowledgments

- This work was supported by the Director, Office of Science, Basic Energy Sciences, Chemical Sciences, Geosciences, and Biosciences Division, of the U.S. Department of Energy under Contract No. DE-AC02-05CH11231 to Lawrence Berkeley National Laboratory.
- Additional support was provided by the Center for Nanoscale Control of Geologic CO_2, an Energy Frontier Research Center funded by the U.S. Department of Energy, Office of Science, Basic Energy Sciences.
- This work was supported as part of the Watershed Function Science Focus Area at Lawrence Berkeley National Laboratory funded by the U.S. Department of Energy, Office of Science, Biological and Environmental Research.

Latest CrunchTope/CrunchClay Executables

CrunchTope Release v2.10 (Feb.6, 2023)

https://github.com/ClSteefel/CrunchTope/releases/tag/v2.10

Intel® oneAPI DPC++/C++ Compiler Runtime for Windows

Intel® Fortran Compiler Runtime for Windows

Latest Install Package for Windows/Linux/Mac

```
git clone -b release https://gitlab.com/petsc/petsc
```

CrunchTope Source
https://github.com/ClSteefel/CrunchTope

Intel oneAPI Compilers

https://www.intel.com/content/www/us/en/developer/tools/oneapi/toolkits.html#gs.paa9c0

Transport and Reaction Processes

Closed versus Open Systems

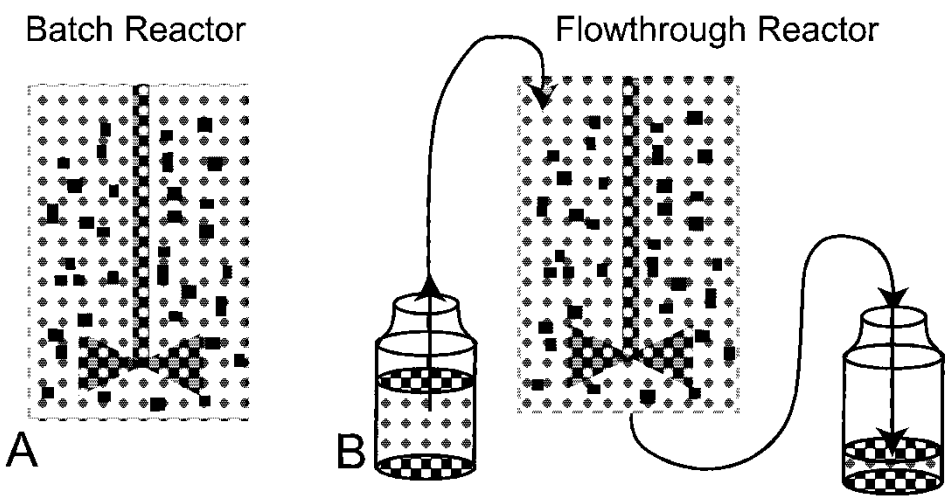

Characteristic Reaction and Transport Times

Conservation Equation

$$\frac{dM}{dt} = J_{in} - J_{out} - R = C_{in}Q_{in} - C_{out}Q_{out} - R$$

Steady State

$$R = kC_{out}V = C_{in}Q_{in} - C_{out}Q_{out}$$

Residence Time

$$\tau_{res} = V / Q$$

Ratio of Characteristic Times

$$\frac{k}{\tau_{res}} = \frac{kV}{Q} = \frac{(C_{in} - C_{out})}{C_{out}}$$

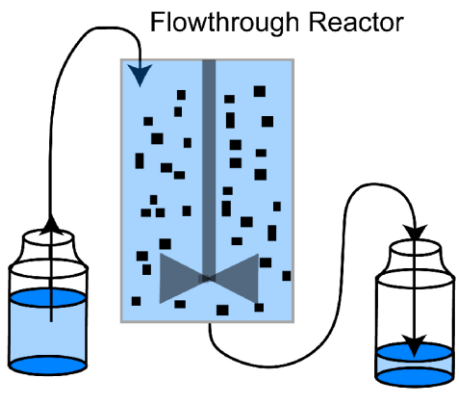

t = time
M = mass of solute
Q = volumetric flow rate
V = volume of reactor
C = concentration of solute
R = reaction rate

Advective Transport

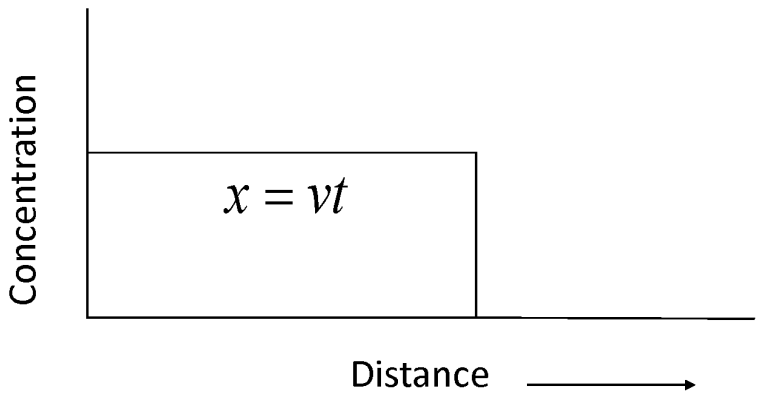

$$J_{adv} = \phi v C_i$$

Diffusive Transport

Fick's 1st Law

$$J_i = -D_i \frac{\partial C_i}{\partial x}$$

Diffusive flux is proportional to the concentration gradient

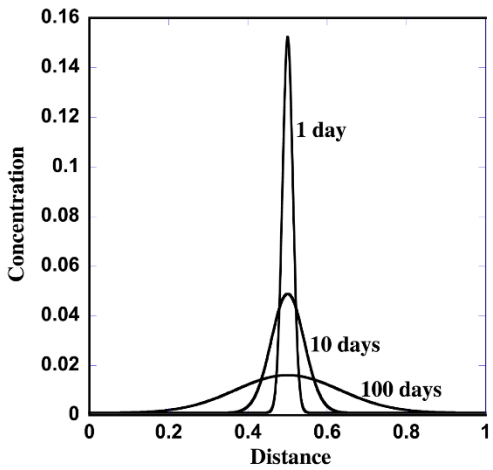

Fick's 2nd Law

$$\frac{\partial C_i}{\partial t} = \frac{\partial}{\partial x}\left[J_i\right] = -D_i \frac{\partial^2 C_i}{\partial x^2}$$

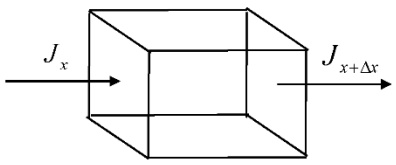

Hydrodynamic Dispersion

Treatment of dispersive flux as a Fickian process

$$J_i^{disp} = -D_h \frac{\partial C_i}{\partial x}$$

Dispersion coefficient

$$D_L = \alpha_L V_i ; D_T = \alpha_T V_i$$

Does not capture the time dependence of the dispersion coefficient, which grows as the plume advances

Overestimates mixing and its effect on reactions

Taylor-Aris Dispersion

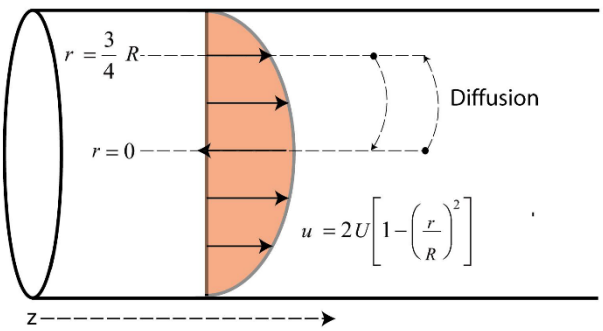

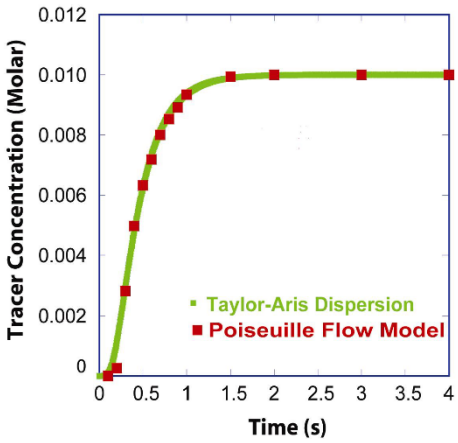

$$D_{Tay}^{*} = D + \frac{U^2 R^2}{48 D}$$

Macrodispersion

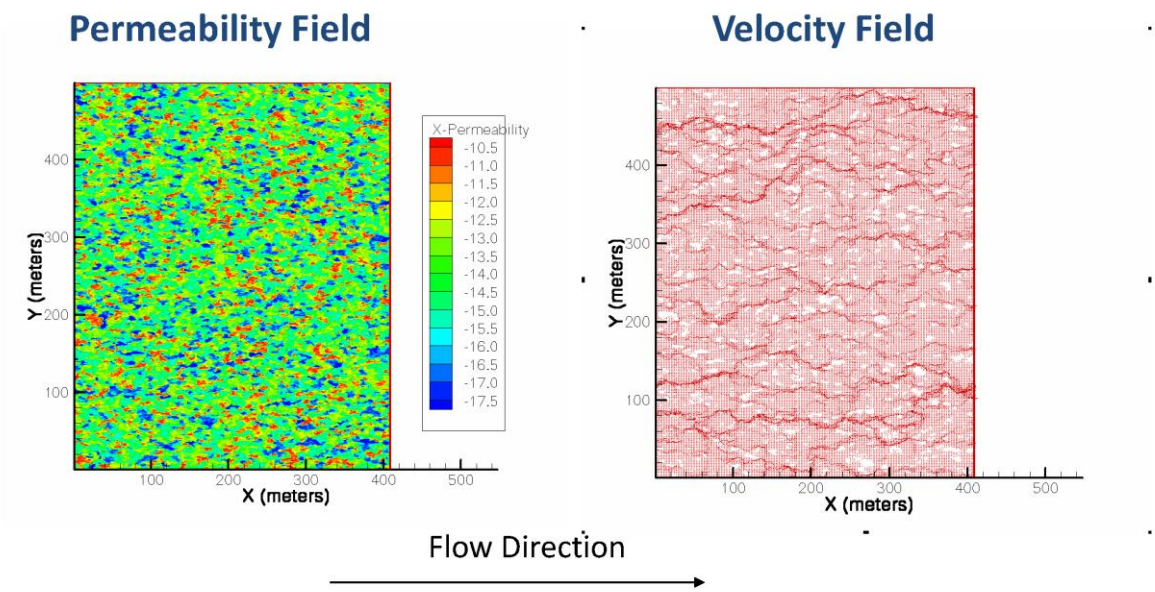

Macrodispersion

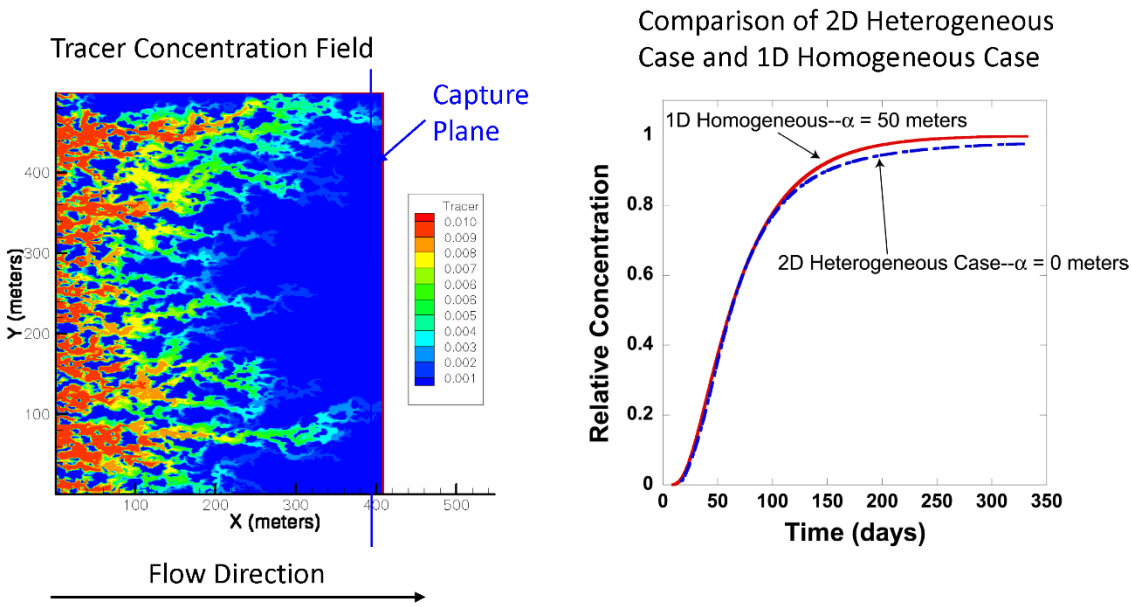

Non-Dimensional Numbers
Péclet and Damköhler

Advection-dispersion-reaction equation

$$\frac{\partial C_i}{\partial t} = -v\frac{\partial C_i}{\partial x} + D^*\frac{\partial^2 C_i}{\partial x^2} - Ak(C - C_{eq})$$

Non-dimensional form of advection-dispersion-reaction equation

$$\frac{\partial C_i}{\partial t'} = \frac{1}{Pe}\frac{\partial^2 C_i}{\partial x'^2} - \frac{\partial C_i}{\partial x'} - Da_I(C - C_{eq})$$

Péclet number

$$Pe = \frac{t'_A}{t'_D} = \frac{vl}{D^*}$$

Damköhler I number

$$Da_I = \frac{t'_R}{t'_A} = \frac{Akl}{v}$$

Damköhler II number

$$Da_{II} = \frac{t'_R}{t'_D} = \frac{Akl^2}{D^*}$$

Effect of Peclet Number

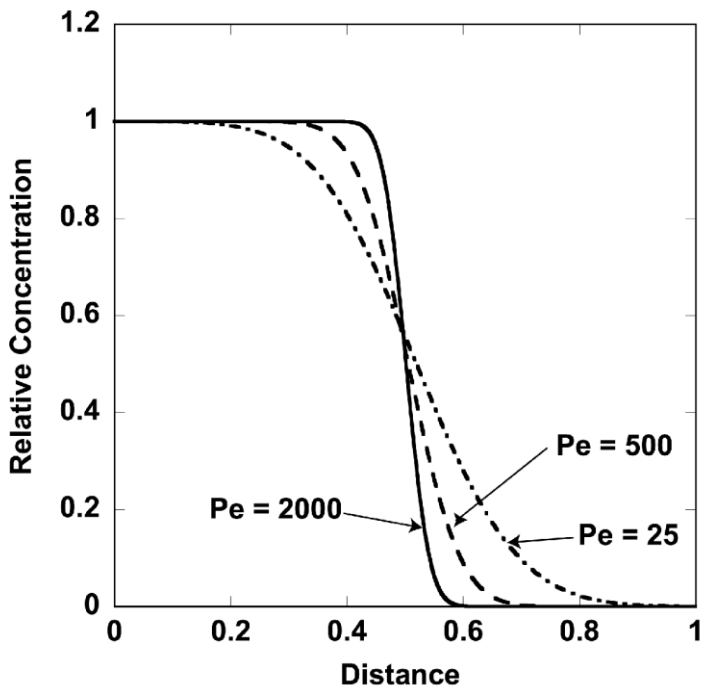

Effect of Damköhler Number

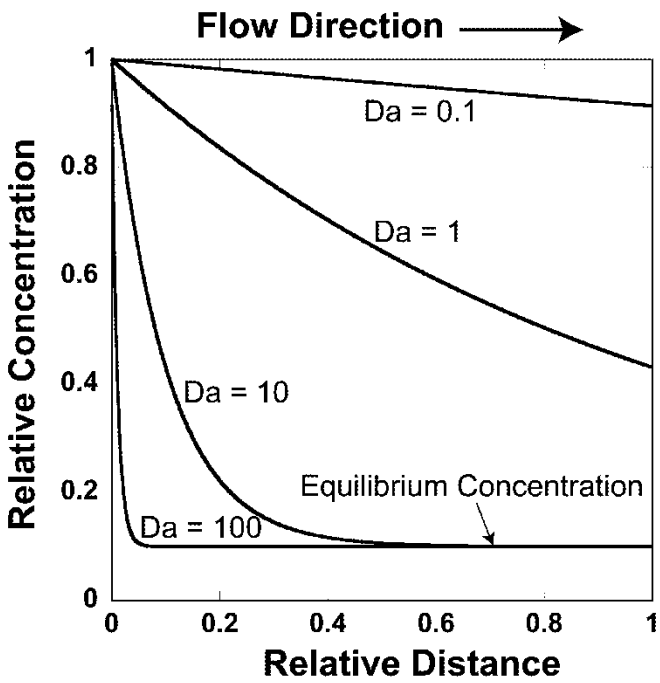

Analytical Solutions to ADR Equation

Solutions in one dimension for linear kinetics take the form

$$C' = e^{-\alpha' x'}$$

Pure advective transport

$$\alpha' = Da_I = \frac{Akl}{v}$$

Pure diffusive transport

$$\alpha' = Da_{II} = \frac{Akl^2}{D^*}$$

Mixed advective and diffusive transport

$$\alpha' = \frac{1}{2}\left(\sqrt{Pe^2 + 4Da_I \cdot Pe} - Pe\right) = \frac{1}{2}\left(\sqrt{Pe^2 + 4Da_{II}} - Pe\right) = \frac{1}{2}\left[\sqrt{\left(\frac{vl}{D}\right)^2 + 4\frac{Akl^2}{D}} - \frac{vl}{D}\right]$$

Equilibration Length Scales

$$C' = e^{-\alpha' x'}$$

Equilibration length = λ

$$\lambda' = \frac{\lambda}{l} = \frac{1}{\alpha'}$$

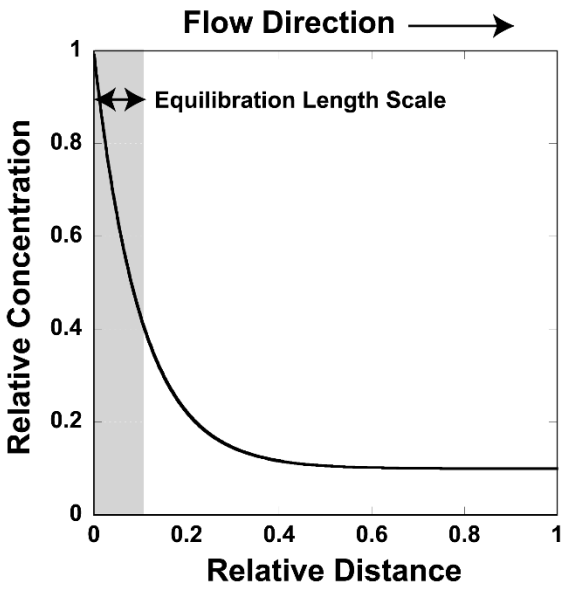

Multicomponent Geochemistry

Aqueous Speciation

Canonical Form

$$HCO_3^- \rightleftarrows CO_3^{2-} + H^+$$

Secondary Species Primary Species

$$A_i \rightleftharpoons \sum_{j=1}^{N_c} \nu_{ij} A_j \quad (i = 1, \ldots, N_x),$$

$$K_{eq} = \frac{\left[CO_3^{2-}\right]\left[H^+\right]}{\left[HCO_3^-\right]}$$

$$\left[HCO_3^-\right] = \frac{\left[CO_3^{2-}\right]\left[H^+\right]}{K_{eq}}$$

$$X_i = K_i^{-1}\gamma_i^{-1}\prod_{j=1}^{N_c}(\gamma_j C_j)^{\nu_{ij}} \quad (i = 1, \ldots, N_x),$$

Total Concentration

$$T_j = C_j + \sum_{i=1}^{N_x} \nu_{ij} X_i,$$

Primary Species

$$Al^{+++} + 4H_2O \rightleftharpoons Al(OH)_4^- + 4H^+$$

$$H^+ + OH^- \rightleftharpoons H_2O$$

$$\begin{bmatrix} 4 & -4 & 1 \\ 1 & -1 & 0 \end{bmatrix} \begin{bmatrix} H_2O \\ H^+ \\ Al^{+++} \end{bmatrix} = \begin{bmatrix} Al(OH)_4^- \\ OH^- \end{bmatrix}$$

Secondary Species

$$T_{H_2O} = C_{H_2O} + 4C_{Al(OH)_4^-} + C_{OH^-}$$

$$T_{H^+} = C_{H^+} - 4C_{Al(OH)_4^-} - C_{OH^-}$$

$$T_{Al^{+++}} = C_{Al^{+++}} + C_{Al(OH)_4^-}.$$

Michaelis-Menten (Monod) Kinetics

Dual Monod

$$R_m = k_{\max}\left[\frac{[C_E]}{[C_E]+K_{S_E}}\frac{[C_D]}{[C_D]+K_{S_D}}\right]$$

E = electron acceptor
D = electron donor

Inhibition Term

$$I_m = \left(\frac{[C_{in}]+K_{in}}{K_{in}}\right)$$

Mineral Dissolution/Precipitation Rate Laws

General Form

$$r_s = -A_s\left\{\sum_{l=1}^{N_{rs}} k_l\left(\prod_{i=1}^{N_c+N_x} a_i^{p_{il}^s}\right)\right\}\left[1-\left(\frac{Q_s}{K_s}\right)^M\right]^n,$$

Burch et al., 1993

$$R_1 = RSA\cdot k_1(1-Q/K_{eq})^1$$

$$R_2 = RSA\cdot k_2(1-Q/K_{eq})^{100,000}$$

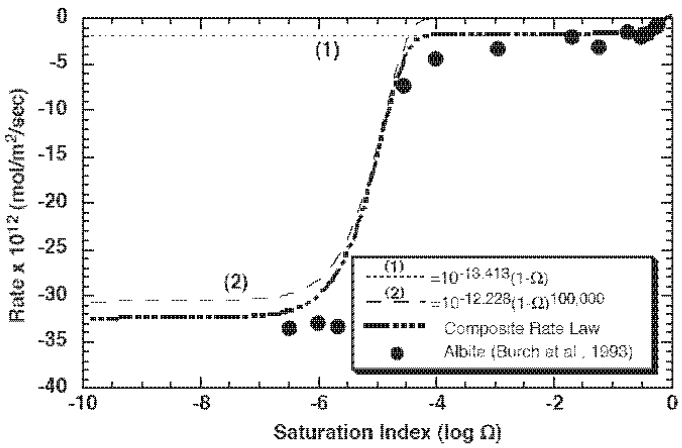

Cation Exchange

Exchange reaction involving Cs^+ and a competing cation

$$Cs^+ + \frac{1}{m} MX(i)_m \leftrightarrow CsX(i) + \frac{1}{m} M^{m+}$$

Gaines-Thomas convention for activity of an exchange species

$$\beta(i)_M = \frac{z_M q(i)_M}{\sum_M z_M q(i)_M}$$

Cation charge → z_M; Moles/g → $q(i)_M$

Selectivity Coefficient

$$K_{M/Cs} = \frac{\beta(i)_M^{1/m}[Cs^+]}{\beta(i)_{Cs}[M^{m+}]^{1/m}}$$

Cation Exchange Capacity

Single exchange site

$$CEC = \sum_M z_M q_M$$

Multiple exchange sites

$$CEC = \sum_i \sum_M z_M q(i)_M$$

Surface Complexation

Protonation-deprotonation reactions controlling surface charge

$$SOH_2^+ \rightleftarrows SOH^0 + H^+$$

$$K_{a1} = \frac{[SOH^0][H^+]}{[SOH_2^+]}$$

First Acidity Constant

$$SOH^0 \rightleftarrows SO^- + H^+$$

$$K_{a2} = \frac{[SO^-][H^+]}{[SOH^0]}$$

Second Acidity Constant

Electrostatic Effects

$$W = (+)_{\text{surface sites}} - (-)_{\text{surface sites}}$$

$$Q = W / \text{mass sorbent}$$

$$\sigma(C/m^2) = \frac{QF}{A}$$ ← Surface charge density

$$\Delta G_{ads} = \Delta G_{chem} + \Delta G_{coul}$$

$$K_a = K_{\text{intrinsic}} \exp\left[\frac{\Delta z F \Psi}{RT}\right]$$

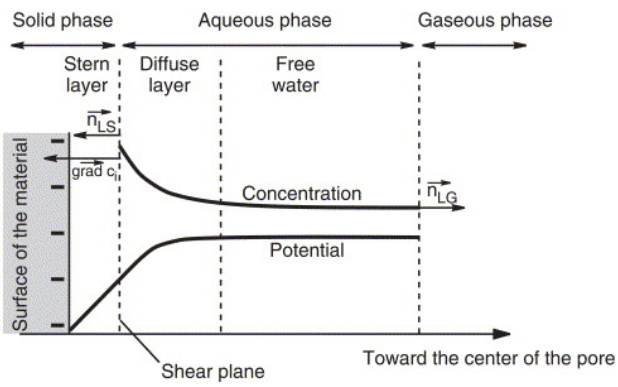

Electrical Double Layer

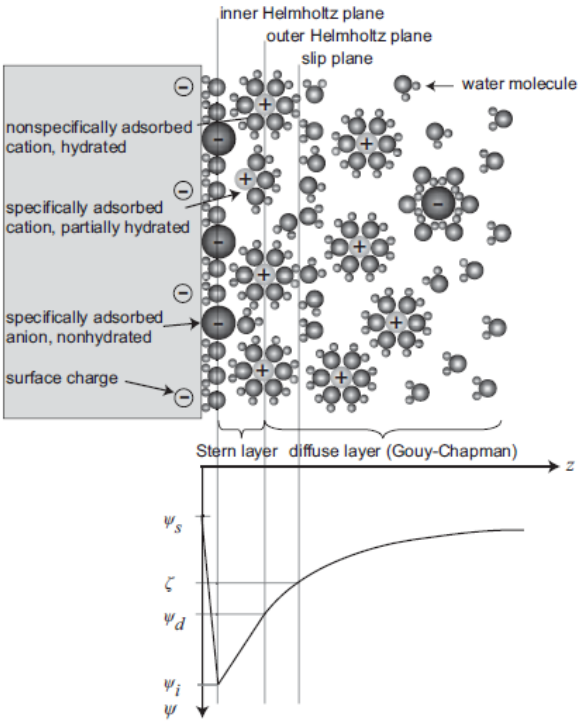

Double Layers between Charged Surfaces

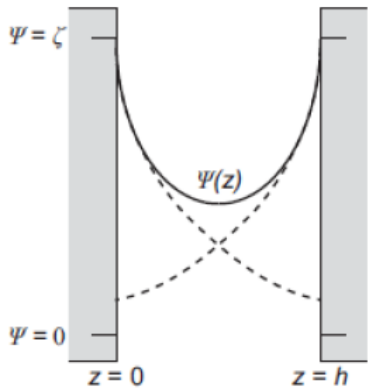

Solid line: Overlapping double layers
Dashed line: No opposite wall present

After Schoch et al, 2008

Nernst-Planck Equation

$$\mu_j = \mu_j^0 + RT \ln a_j + z_j F \psi = \mu_j^0 + RT \ln\left(\gamma_j C_j\right) + z_j F \psi$$

Chemical Potential — Electrostatic Potential

$$J_j = -u_j C_j \frac{\partial \mu_j}{\partial x} = -\frac{D_j C_j}{RT} \frac{\partial \mu_j}{\partial x}$$

Mobility

$$J_j = -D_j \nabla C_j - \frac{z_i F}{RT} D_i C_i \nabla \psi - D_j C_j \nabla \ln \gamma_j$$

Fickian Diffusion — Electrochemical Migration — Activity Coefficient Gradient

$$J_j = -D_j \nabla C_j - \frac{z_i F}{RT} D_i C_i \nabla \psi$$

Nernst-Planck Equation

Left Boundary

pH	6.0
Cl-	0.1 mM
Na+	0.1 mM
NO3-	0.001 mM

NOTE: No initial gradient in Na^+ or Cl^-, so Fick's Law would say there is no diffusion

Initial Condition

pH	4.0
Cl-	0.1 mM
Na+	0.1 mM
NO3-	0.1 mM

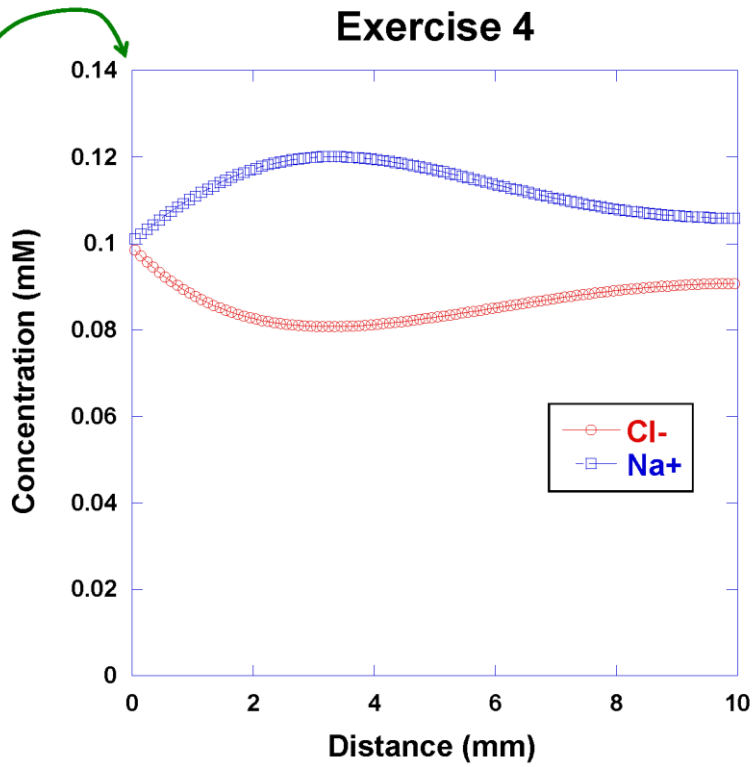

Poisson-Nernst-Planck (PNP) Equation

Poisson Equation, with summation over mobile and immobile species

$$\nabla \bullet \left[\varepsilon_0 \varepsilon_r \nabla \psi \right] = -F \sum_i^N z_i C_i$$

ψ : electrical potential

ε_0 : free space permittivity

ε_r : relative permittivity

F: Faraday's constant

$$J_i = -D_i \nabla C_i - \frac{z_i F}{RT} D_i C_i \nabla \psi$$

Leads to (unmodified) Poisson-Nernst-Planck system of equations

Tournassat & Steefel, 2015

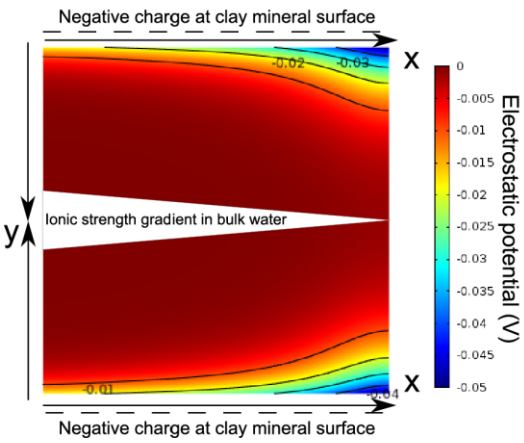

Mean Electrostatic Potential Approach

$$\mu_i^{EDL} = \mu_i^B \qquad C_i^{EDL} = C_i^B \exp\left(\frac{-z_i e \psi_m}{k_B T}\right)$$

Concentration in diffuse layer (EDL) related to concentrations in bulk water (B) through the mean electrical potential, of the diffuse layer φ_m

$$\phi^{EDL} \sum_i z_i C_i^{EDL} = Q^{SL} = \sum_k^{Ns} z_k \Gamma_k$$

Solve for mean electrical potential of diffuse layer from charge balance of mineral surface charge, Q^{SL}, and the diffuse layer

Why use a reactive transport model?

- ✓ Describes open systems where fluxes drive reactions
- ✓ Describes time dependent processes (e.g. kinetics, transport)
- ✓ Quantitative test of hypotheses

Why use a multicomponent RTM?

- ✓ Effects of multiple species and minerals on thermodynamics of (bio)reactive system (pH effects on rates, inhibition)
- ✓ Competitive effect of other ions on contaminant sorption
- ✓ Effects of dissolved, sorbed and solid phase bioavailabiltiy

Why use a coupled RTM?

- ✓ Diffusive, dispersive and advective transport rather than ad hoc mixing schemes
- ✓ Spatially distributed basis includes heterogeneity
- ✓ Relatively easy to couple to other time-dependent processes (e.g. sediment transport, salinity)

Why model contaminants with RTM?

- ✓ Considers multiple aqueous and surface complexation pathways and effects on contaminant mobility
- ✓ Degradation via multiple biogenic and abiotic pathways

SHORT COURSE EXERCISES

Short Course Exercises

Introduction to speciation
- Example using the carbonate system featuring various constraints
- Stable isotopes of carbon (^{12}C and ^{13}C) implemented to demonstrate equilibrium fractionation

Advective transport
- Introduce a non-reactive tracer into an advective flow field
- Investigate numerical dispersion

Diffusive transport
- Introduce a non-reactive tracer into a purely diffusive transport problem
- No-flux versus Dirichlet boundary conditions

Multicomponent diffusion
- Concept of charged species diffusing at different rates and electrochemical migration
- Stable isotopes of Cl are implemented to consider the influence of diffusive fractionation

Transverse dispersion
- Example based on a recent 2D dispersion experiment, including multi-ion diffusion in an advective flow field

Ion exchange
- Introduce ion exchange of cesium in a 1D sediment column with competing Na^+

Surface complexation
- Surface complexation of zinc on iron-hydroxide (PHREEQc example 8)

CO_2 attack on reservoir rocks
- Diffusion of gas and flow of water, with variable liquid saturations and multi-mineral nucleation, precipitation, and dissolution

Calcite precipitation with isotopes
- Simulation of stable isotope kinetic fractionation of calcium during carbonate precipitation

Two-dimensional flow fields
- Xie et al (2015) benchmark on porosity and permeability change due to mineral reaction

Diffusion in clay
- Tournassat & Steefel, 2016

Inverse modeling with PEST-CrunchFlow
- Steefel et al, 2003

CrunchTope Files

1) Executable: CrunchTope.exe

2) Input file: *name*.in

1) Database(s): *name*.dbs

```
TITLE
Cs exchange on Hanford sediments:  Experiment 3
END


RUNTIME
time_units          hours
timestep_max        0.1
timestep_init       0.00001
time_tolerance      0.01
solver              gmres
preconditioner      ilu
precondition_level  1
lag_activity        on
debye-huckel        on
database_sweep      off
speciate_only       false
hindmarsh           true
gimrt               true
courant_number      1.0
density_module      sodium_nitrate
graphics            kaleidagraph
screen_output       50
database            HanfordTanksColumnFit3Site-GT.dbs
save_restart        Column3NaNO3Flush1.rst
later_inputfiles    ShortCourse12b.in ShortCourse12c.in
END

OUTPUT
time_units           hours
spatial_profile      19.25
```

```
'temperature points' 8   0.  25.  60. 100. 150. 200. 250. 300.
'Debye-Huckel adh'   0.4939  0.5114 0.5465 0.5995 0.6855 0.7994 0.9593 1.2180
'Debye-Huckel bdh'   0.3253  0.3288 0.3346 0.3421 0.3525 0.3639 0.3766 0.3925
'Debye-Huckel bdt'   0.000 0.000 0.000 0.000 0.000 0.000 0.000 0.000
'H2O' 3.0  0.0    18.0153
'Ag+' 2.5  1.0   107.8682
'Al+++' 9.0  3.0    26.9815
'Am+++' 5.0  3.0   243.0000
'Ar(aq)' 3.0  0.0    39.9480
'Au+' 4.0  1.0   196.9665
'B(OH)3(aq)' 3.0  0.0    61.8330
'Ba++' 5.0  2.0   137.3270
'Be++' 8.0  2.0     9.0122
'Br-' 3.0 -1.0    79.9040
'Ca++' 6.0  2.0    40.0780
'Cd++' 5.0  2.0   112.4110
'Ce+++' 9.0  3.0   140.1150
'Cl-' 3.0 -1.0    35.4527
```

CrunchTope Files

```
OUTPUT
time_units          hours
spatial_profile     16.0  32.0
time_series         Rolle.out   11  20  1
time_series_print   K+  Mg++  Cl-
time_series_interval 1
END/
```

spatial_profile generated automatically at times specified (16, 32 hours)

time_series saved every *time_series_interval* in file `Rolle.out`

time_series_print writes species specified in file `Rolle.out`

Spatial profile files include:

1. totcon#.tec — total concentrations in solution
2. pH#.tec — solution pH
3. conc#.tec — log concentrations of individual species
4. rate#.tec — mineral reaction rates (mol/L(bulk)/s)
5. aq_rate#.tec — aqueous reaction rates (mol/L/s)
6. volume#.tec — mineral volume fraction (dimensionless)
7. porosity#.tec — (dimensionless)
8. velocity#.tec — Darcy flux ($m^3/m^2/yr$)
9. toperatio_aq#.out — per mil
10. toperatio_min#.out — per mil

4.6 Code 6 – MIN3P – Assessing far-field and near-field geochemical stability in the context of deep geologic repositories for spent nuclear fuel – Reactive transport modeling with MIN3P-THCm

MIN3P-THCm is a general-purpose reactive transport code for simulation of flow and reactive transport processes in the subsurface. In Canada, the Nuclear Waste Management Organization (NWMO) is responsible for designing and implementing the country's plan for the safe, long-term management of used nuclear fuel and is currently evaluating potential sites for a deep geologic repository (DGR) in either sedimentary or crystalline rock. MIN3P-THCm has been used to assess various aspects of long-term geochemical stability in the context of DGRs in support of site characterization in both the far-field and the near-field. The goal of the far-field simulations was to assess the geochemical stability of pore water at repository depth over long time periods (on the order of 100,000 years). Due to the geographic location of Canada, it is necessary to consider the impact of the advance and retreat of a continental ice sheet on flow and reactive transport processes. In the case of sedimentary rocks, simulations were conducted on the scale of a sedimentary basin, taking into consideration the various stratigraphic units, including shales, limestones, sandstones and evaporite units. In the case of crystalline rock, simulations were designed to evaluate the interplay between flow and reactive transport processes in fractured granitic media accounting for exchange of solute between fractures and the matrix. In both cases, the emphasis was on assessing the ingress and attenuation of dissolved oxygen in the rock. In addition, near-field simulations were conducted with MIN3P-THCm to evaluate the performance of engineered barrier systems composed of concrete and bentonite, in contact with host rock. In this presentation, we will provide an overview on the approach, challenges and outcomes of these modeling studies.

Lecturer

K. Ulrich Mayer, University of British Columbia, Department of Earth, Ocean and Atmospheric Sciences, Vancouver, BC, Canada

Kerry T.B. MacQuarrie, University of New Brunswick, Department of Civil Engineering, Fredericton, NB, Canada

Danyang Su, University of British Columbia, Department of Earth, Ocean and Atmospheric Sciences, Vancouver, BC, Canada

Mingliang Xie, University of British Columbia, Department of Earth, Ocean and Atmospheric Sciences, Vancouver, BC, Canada

Reading Material

Bea, S.A., U.K. Mayer, and T.B. Macquarrie, 2016. Reactive transport and thermo-hydro-mechanical coupling in deep sedimentary basins affected by glaciation cycles: model development, verification, and illustrative example. **Geofluids** 16:279-300.

Bea, S.A., D.Y. Su, K.U. Mayer, and K.T.B. MacQuarrie, 2018. Evaluation of the Potential for Dissolved Oxygen Ingress into Deep Sedimentary Basins during a Glaciation Event. **Geofluids** DOI Unsp 9475741, 10.1155/2018/9475741..

Spiessl, S.M., K.T.B. MacQuarrie, and K.U. Mayer, 2008. Identification of key parameters controlling dissolved oxygen migration and attenuation in fractured crystalline rocks. **Journal of Contaminant Hydrology** 95:141-153.

Su, D.Y., M.L. Xie, K.U. Mayer, and K.T.B. MacQuarrie, 2022. The Impact of Ice Sheet Geometry on Meltwater Ingress and Reactive Solute Transport in Sedimentary Basins. **Water Resources Research** 58

Xie, M.L., D.Y. Su, K.U. Mayer, and K.T.B. MacQuarrie, 2022. Reactive transport investigations of the long-term geochemical evolution of a multibarrier system including bentonite, low-alkali concrete and host rock. **Applied Geochemistry** 143.

Slides

Assessing far-field and near-field geochemical stability in the context of deep geologic repositories for spent nuclear fuel – Reactive transport modeling with MIN3P-THCm

K. Ulrich Mayer[1], Kerry T.B. MacQuarrie[2], Danyang Su[1] and Mingliang Xie[1],

[1]University of British Columbia, [2]University of New Brunswick

February 8, 2023

a place of mind | THE UNIVERSITY OF BRITISH COLUMBIA | EURAD – Geochemical & Reactive Transport Modelling for Geological Disposal

Introduction and Overview

- The MIN3P-THCm code: Main simulation capabilities
- Brief timeline of model development
- Benchmarking and model verification
- Applications: Deep geologic repositories for spent nuclear fuel in sedimentary and crystalline rocks – far-field and near-field processes
- Work was performed for the Deep Geologic Repository Program of the Nuclear Waste Management Organization (NWMO)

a place of mind | THE UNIVERSITY OF BRITISH COLUMBIA | EURAD – Geochemical & Reactive Transport Modelling for Geological Disposal

Main Simulation Capabilities

- Variably saturated flow (Richards equation)
- Multicomponent reactive transport in aqueous and gas phase
- Energy balance
- High ionic strength solutions and density effects
- Geochemical reactions
  - Homogeneous: intra-aqueous
  - Heterogeneous: gas exchange, minerals, surface reactions
  - Equilibrium and kinetic
  - Database-driven

a place of mind | THE UNIVERSITY OF BRITISH COLUMBIA | EURAD – Geochemical & Reactive Transport Modelling for Geological Disposal

MIN3P-THCm Numerical Methods

- Modified Newton-Raphson methods for flow and reactive transport solutions
- Global Implicit Approach (GIA) for reactive transport equations
- Picard iteration for density coupling
- Globally and locally mass-conservative
- Adaptive time stepping
- Efficient iterative sparse matrix solvers
- Parallelization for shared and distributed memory
- Structured and unstructured grids

a place of mind | THE UNIVERSITY OF BRITISH COLUMBIA | EURAD – Geochemical & Reactive Transport Modelling for Geological Disposal

Time Line of Model Development

1999
- Completion of first full version of MIN3P-code

2004
- Initiation of work with NWMO (formerly OPG): redox stability in fractured crystalline rock

2007
- Development of a module for gas advection and multicomponent gas diffusion

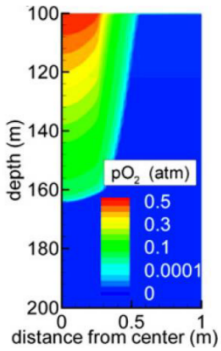

a place of mind | THE UNIVERSITY OF BRITISH COLUMBIA | EURAD – Geochemical & Reactive Transport Modelling for Geological Disposal

Time Line of Model Development

2008
- Participation in MoMaS workshop: International Model Comparison

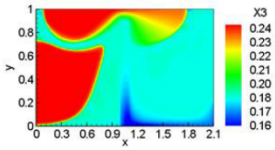

2008
- Continuation of work with NWMO: Geochemical stability in deep sedimentary basins

2009
- Coupling between reactive transport and density-dependent flow

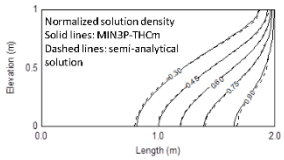

a place of mind | THE UNIVERSITY OF BRITISH COLUMBIA | EURAD – Geochemical & Reactive Transport Modelling for Geological Disposal

Time Line of Model Development

2011
- Implementation of energy balance equations
- One-dimensional vertical stress

2012
- Near field applications: Mont Terri DR-A and EBS-TF diffusion experiments
- Implementation of multicomponent diffusion and electrochemical migration

2014
- Participation in Subsurface Simulation International Code Intercomparison exercises

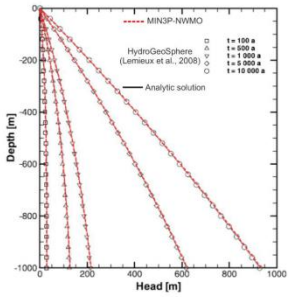

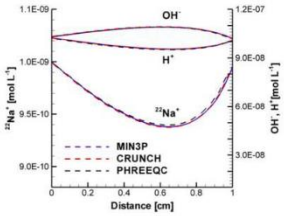

a place of mind | THE UNIVERSITY OF BRITISH COLUMBIA | EURAD – Geochemical & Reactive Transport Modelling for Geological Disposal

Time Line of Model Development

2016
- Completion of parallelization for shared and distributed memory computing platforms

2020
- Completion unstructured grid implementation in two and three spatial dimensions
- Near field simulation of reactive transport across interfaces (concrete-bentonite-host rock)

2022
- Long-term 3D-simulation of reactive transport in sedimentary basins during a period of glaciation and deglaciation

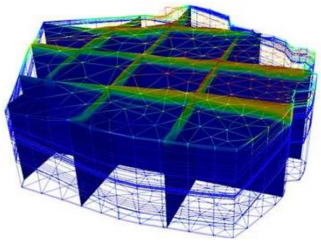

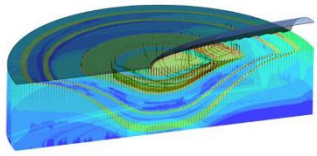

a place of mind | THE UNIVERSITY OF BRITISH COLUMBIA | EURAD – Geochemical & Reactive Transport Modelling for Geological Disposal

Benchmarking and Model Verification

- Verification by comparison to other numerical models or analytical solutions for specific code capabilities
- Participation in international benchmarking and code intercomparison exercises
  - Documented in two special issues of *Computational Geosciences*
    - 2010: MoMaS intercomparison
    - 2015: SSBench Workshop Series (2011-2014)

MIN3P-THCm Applications Relevant to Deep-Geologic Repositories

- Far-field:
  - Redox stability in fractured crystalline rocks (Spiessl et al., 2008; MacQuarrie et al., 2010)
  - Geochemical stability of deep sedimentary basins (Bea et al., 2015, Bea et al, 2018, Su et al., 2022)
- Near-field:
  - Diffusive transport in low permeability media
    - EBS-TF (NWMO TR-2014-23; Alt-Epping et al., 2015)
    - Mont Terri: DR-A experiment (NWMO TR-2014-25)
    - Reactive transport across interfaces involving low-pH concrete, bentonite and host rock (Xie et al., 2022)

Far field Geochemical Stability of Deep Sedimentary Basins

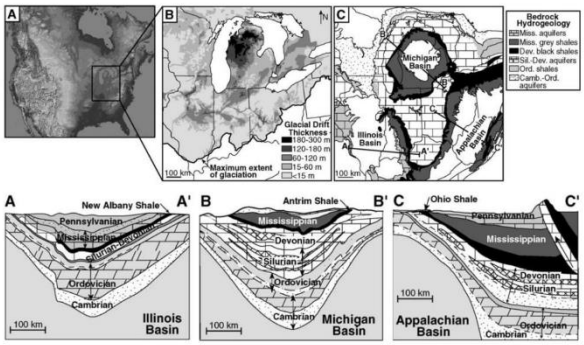

Location and main geology features for the intracratonic sedimentary basins in North America (Illinois Michigan and Appalachian basins, taken from McIntosh and Walter, 2005)

Primary goals: conduct full coupled reactive transport simulations in a sedimentary basin affected by a glaciation/deglaciation event.

Simulation of Reactive Transport in a Hypothetical Sedimentary Basin During a Glaciation/Deglaciation Cycle

- ✓ Evaluate model capabilities
- ✓ Provide an illustration of geochemical stability

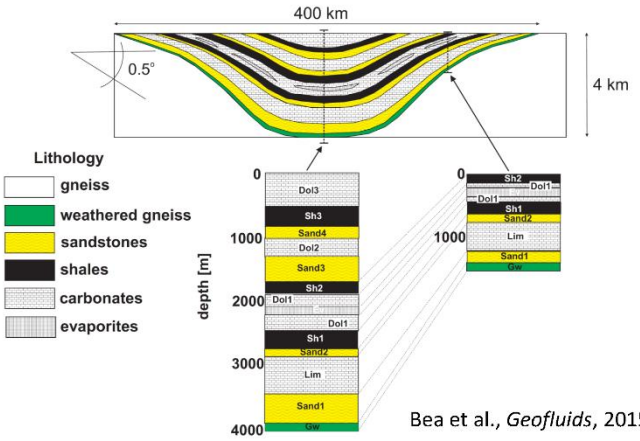

Bea et al., *Geofluids*, 2015

Model Setup and Boundary Conditions

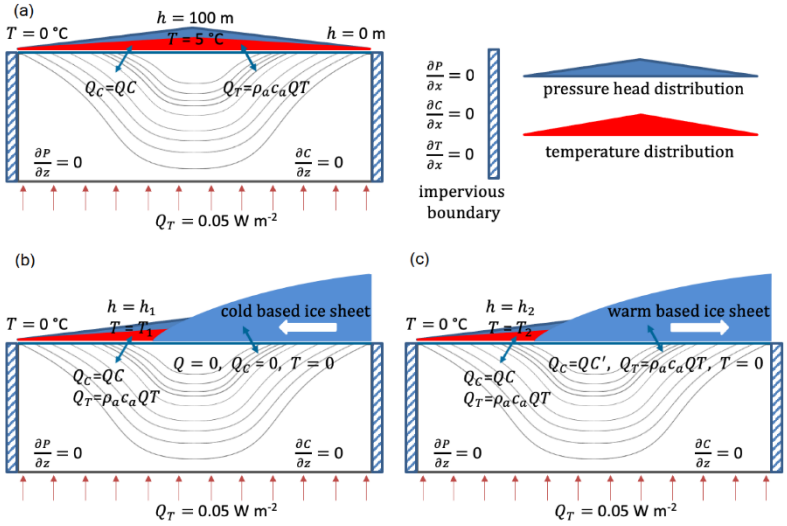

Illustration of boundary conditions during different stages

(a) pre- and post-glaciation stage (< 4000 or > 28000 yrs); hydraulic head and temperature are linearly distributed along the top boundary;

(b) ice sheet advance (4000-20000 yrs); zero-flux flow boundary and zero temperature beneath the ice sheet;

(c) ice sheet retreat (20000-28000 yrs); hydraulic head beneath the ice sheet is specified as 90% of the ice sheet thickness; zero basal temperature.

a place of mind | THE UNIVERSITY OF BRITISH COLUMBIA | EURAD – Geochemical & Reactive Transport Modelling for Geological Disposal 12

Initial Distribution of Porosity and Hydraulic Conductivity

- ✓Related to lithology
- ✓Constrained by literature data
- ✓Includes general trend of porosity and permeability reduction with depth
- ✓Permeability related to porosity via Carman-Kozeny relationship

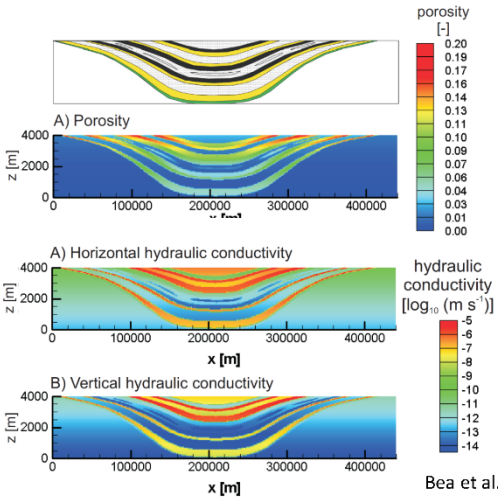

Bea et al., *Geofluids*, 2015

a place of mind | THE UNIVERSITY OF BRITISH COLUMBIA | EURAD – Geochemical & Reactive Transport Modelling for Geological Disposal

Initial Distribution of Mineral Phases

- ✓Halite and anhydrite present in evaporite units
- ✓Calcite and dolomite present in all units
- ✓Cation exchange capacity elevated in shales

Bea et al., *Geofluids*, 2015

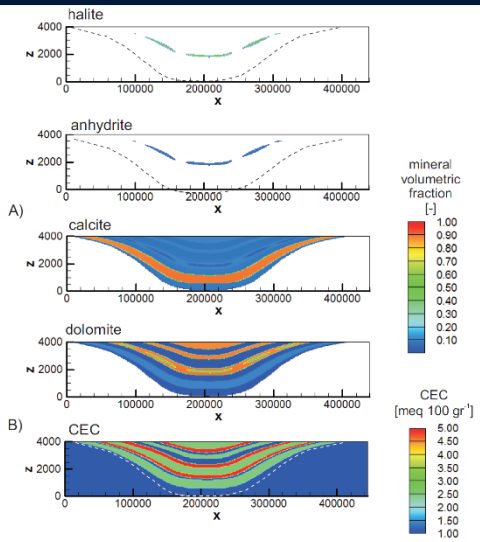

Evolution of Solution Density

- ✓"Fresh water" limited to shallow depths (e.g. < 200m mid-basin) during the entire glacial cycle
- ✓More permeable units experience some fresh water ingress
- ✓Low hydraulic conductivity of aquitards, near horizontal layering of hydrogeological units, and fluid density contrasts limit fresh water ingress beyond a few hundred metres

Bea et al., *Geofluids*, 2015

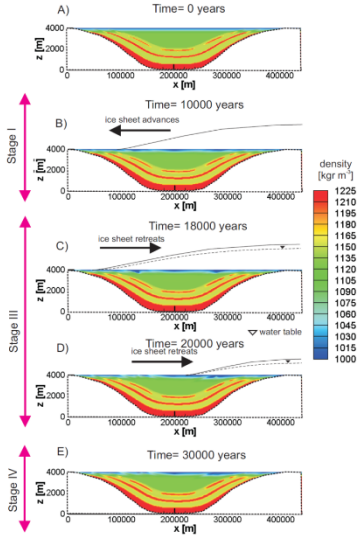

Rates of Mineral Dissolution-Precipitation During Period of Deglaciation

- ✓Shallow aquifers: dedolomitization
- ✓Deeper sedimentary units: limited dedolomitization and evaporite diss.-prec.
- ✓Rates are very slow

Bea et al., *Geofluids*, 2015

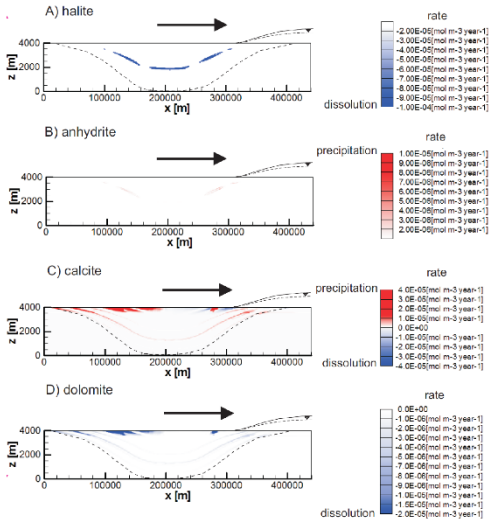

a place of mind | THE UNIVERSITY OF BRITISH COLUMBIA | EURAD – Geochemical & Reactive Transport Modelling for Geological Disposal

Simulated Porosity Changes After 32,500 Years

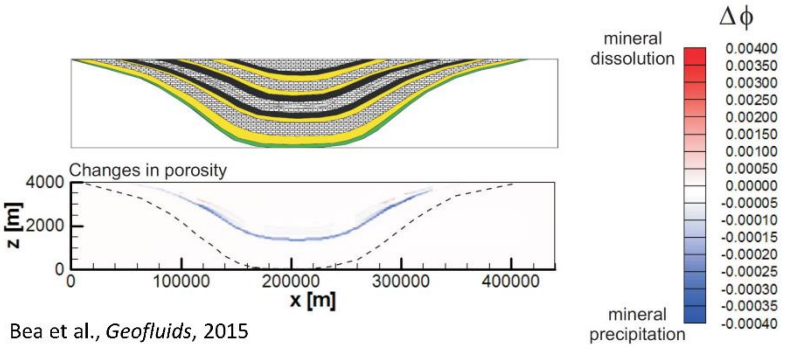

Bea et al., *Geofluids*, 2015

- ✓Simulated porosity changes are very small over the time period of 32,500 years
- ✓Limitation of spatial discretization: cell dimensions are probably inadequate to capture local-scale processes

a place of mind | THE UNIVERSITY OF BRITISH COLUMBIA | EURAD – Geochemical & Reactive Transport Modelling for Geological Disposal

Extension of Simulations to 3D

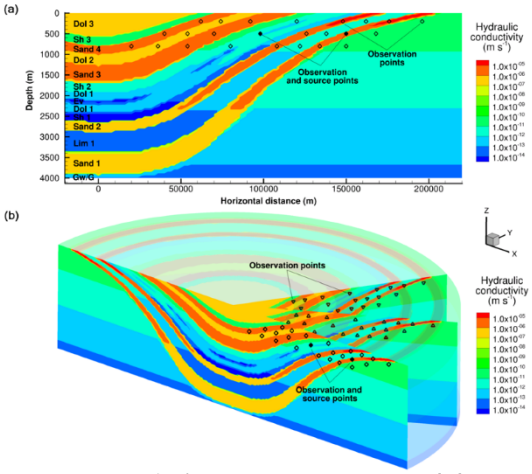

Source and observation points in (a) 2D scenario, and (b) 3D scenarios.

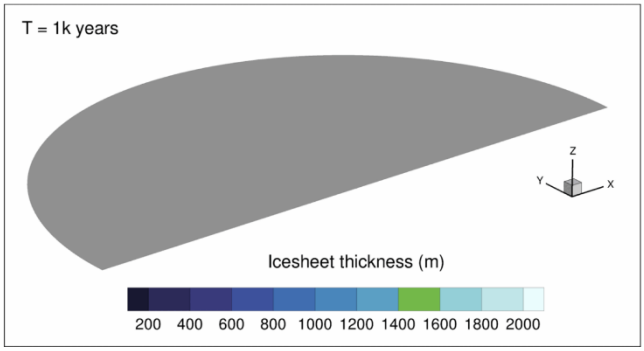

Illustration of medium width icesheet movement.

Su et al., *WRR*, 2022

Ice Sheet Geometries During Glacial Advance and Retreat

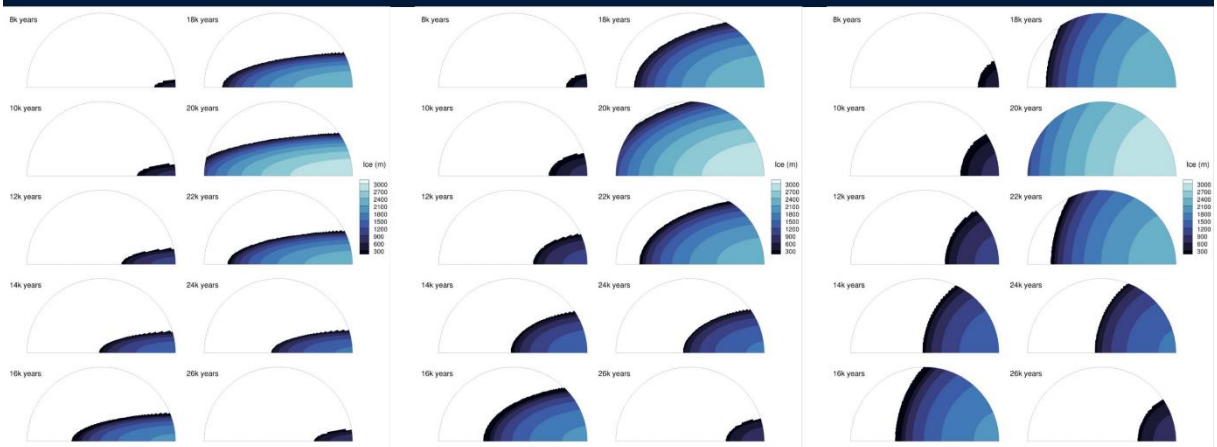

Narrow icesheet | Medium icesheet | Wide icesheet

Su et al., *WRR*, 2022

Impact of Model Dimensionality and Ice Sheet Geometry on Meltwater Penetration

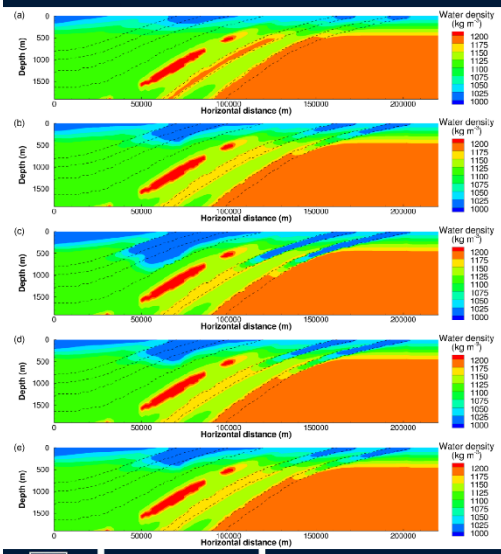

Scenario	Volume of meltwater ingress (m^3)	Percentage to groundwater in domain (%)	Penetration depth* (m)
2D	4.7×10^6	8.4	400
3D-narrow	1.6×10^{12}	23.5	750
3D-medium	9.6×10^{11}	14.1	500
3D-wide	7.3×10^{11}	10.6	450

* Estimated based on groundwater density 1025 kg m^{-3}

Su et al., *WRR*, 2022

Left: Groundwater density, (a) initial, (b) to (e) after 24000 years for 2D, 3D narrow, 3D medium and 3D wide icesheet.

a place of mind | THE UNIVERSITY OF BRITISH COLUMBIA | EURAD – Geochemical & Reactive Transport Modelling for Geological Disposal 20

Impact of Model Dimensionality and Ice Sheet Geometry on O_2 Ingress from Meltwater

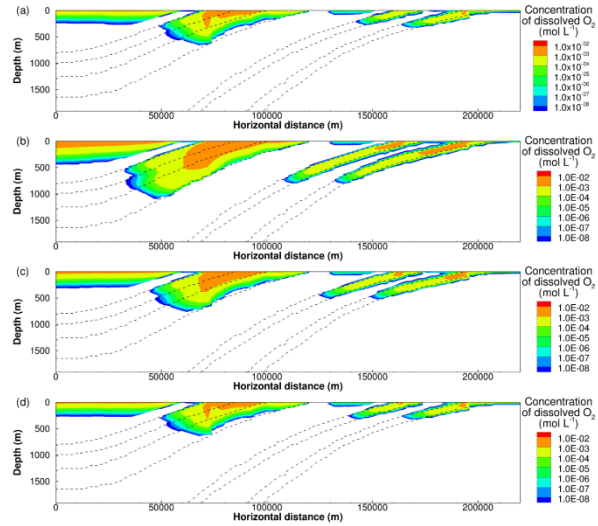

Scenario	Ingress depth in HPUs (m)	Ingress depth in LPUs (m)
2D	700	< 100
3D-narrow	1,100	< 100
3D-medium	900	< 100
3D-wide	700	< 100

* Estimated based on O_2 concentration 1.0×10^{-8} mol L^{-1}

Left: dissolved O_2 concentration after 24000 years, (a) 2D icesheet, (b) 3D narrow icesheet, (c) 3D medium icesheet, and (d)3D wide icesheet.

a place of mind | THE UNIVERSITY OF BRITISH COLUMBIA | EURAD – Geochemical & Reactive Transport Modelling for Geological Disposal 21

Impact of Model Dimensionality and Ice Sheet Geometry on O_2 Ingress from Meltwater

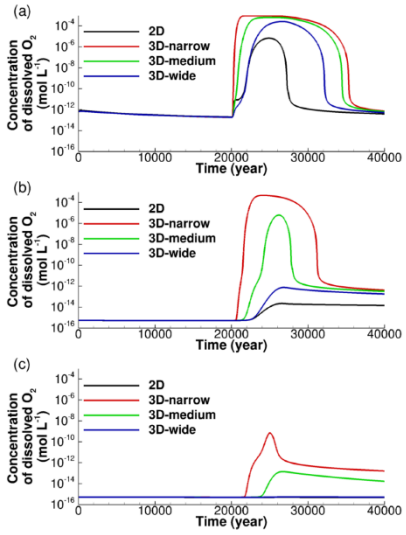

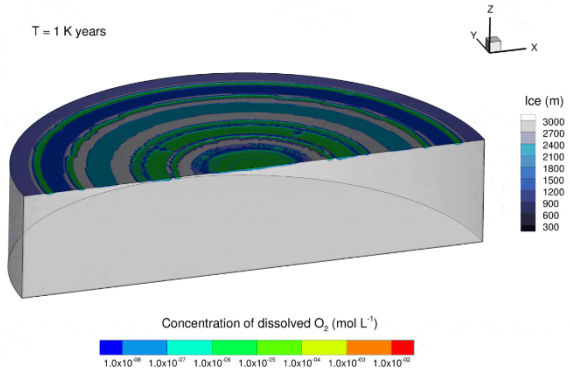

Left: O_2 concentrations at observation points in Sand 2 unit, (a) 200 m depth, (b) at 500 m depth, and (c) 800 m depth.

Right: Animation of dissolved O_2 concentration under medium-width icesheet.

Su et al., *WRR*, 2022

Reactive Transport Modeling of the Long-Term Geochemical Evolution of a Multibarrier System

- Near field scenarios
- Materials include bentonite, low-alkali concrete and host rock
- Limestone and granite
- Diffusion dominated
- Evolution of porosity at interfaces?
- Effects on solute migration?

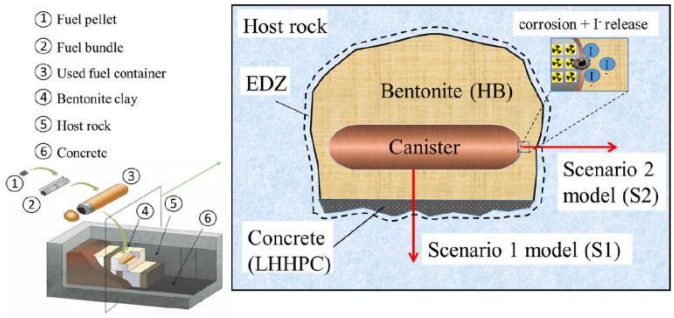

Xie et al., *Appl. Geochem.*, 2022

Scenarios Considered

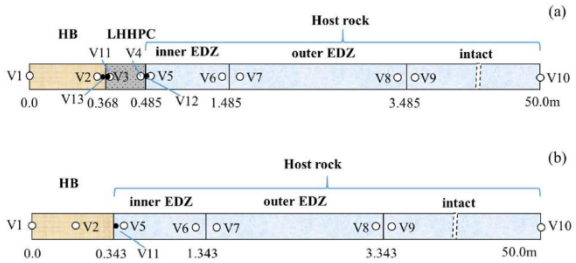

Xie et al., *Appl. Geochem.*, 2022

- HB = Highly compacted and homogenized bentonite
- LHHPC = Low Heat High Performance Concrete (low alkali)
- EDZ = Excavation Damage Zone
- Consider Scenarios with and without LHHPC
- No significant effects on porosity for case without LHHPC

Mineral Volume Fractions and Porosity after 10,000 years

Granite Case

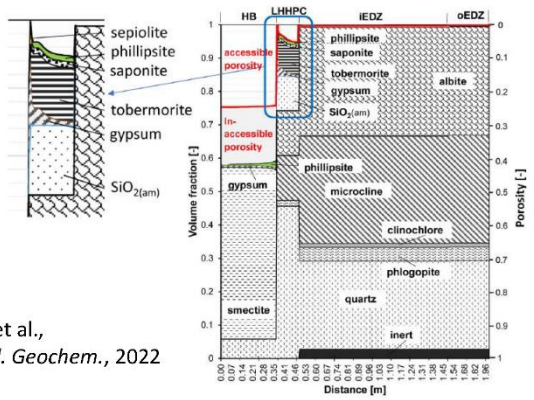

Xie et al., *Appl. Geochem.*, 2022

Clogging at LHHPC-HB interface in LHHPC due to precipitation of tobermorite, gypsum, saponite, phillipsite and sepiolite

Limestone Case

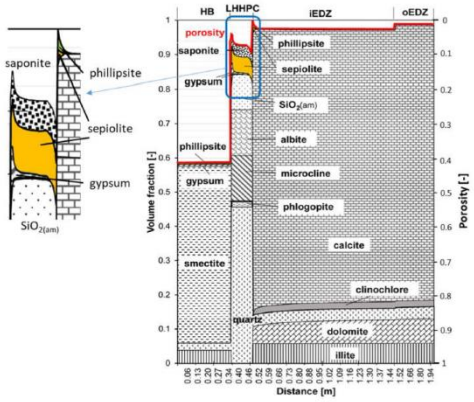

Clogging at LHHPC-host rock interface in host rock mostly due to precipitation of sepiolite and phillipsite

Effect of Secondary Mineral Formation on Solute Transport in Inner EDZ

Granite Case

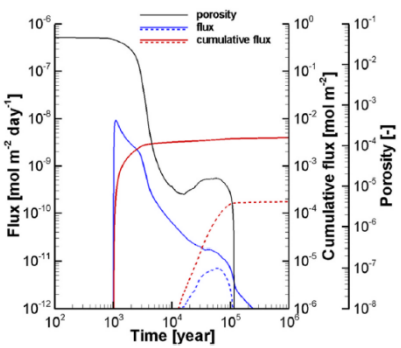

Limestone Case

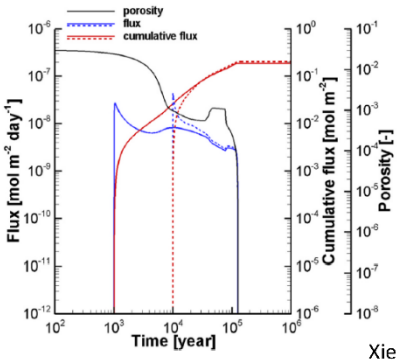

Canister failure time

1,000 years

10,000 years

Xie et al., *Appl. Geochem.*, 2022

Pronounced effect of timing of porosity reduction on absolute and cumulative solute fluxes

Conclusions and Outlook

- MIN3P-THCm has been developed and maintained for nearly 30 years
- The code has proven useful for simulating near-field and far-field scenarios related to the safe geologic storage of spent nuclear fuel
- Applied to both sedimentary and crystalline rock environments
- Simulations indicate limited O_2 ingress in far-field simulations under glaciation deglaciation conditions due to hydraulic constraints and redox buffering
- Near-field simulations of Engineered Barrier Systems indicate that secondary mineral formation is beneficial in case of canister failure
- Current efforts focus on the generation and fate of elevated dissolved sulphide in sedimentary basins and further development of simulation capabilities for fractured systems with non-orthogonal fractures

Acknowledgements

nwmo NUCLEAR WASTE MANAGEMENT ORGANIZATION SOCIÉTÉ DE GESTION DES DÉCHETS NUCLÉAIRES

NSERC CRSNG

compute canada | calcul canada

WESTGRID

Thank you!

References - Model Formulation

- Mayer, K. U., E. O. Frind, and D. W. Blowes, 2002. Multicomponent reactive transport modeling in variably saturated porous media using a generalized formulation for kinetically controlled reactions, *Water Resour. Res.*, 38, 1174, https://doi.org/10:1029/2001WR000862
- Molins, S., and K. U. Mayer, 2007. Coupling between geochemical reactions and multicomponent gas diffusion and advection – A reactive transport modeling study, *Water Resour. Res.*, 43, W05435, https://doi.org/10.1029/2006WR005206
- Henderson, T.H., K. U. Mayer, B. L. Parker, and T.A. Al., 2009. Three-dimensional density-dependent flow and multicomponent reactive transport modeling of chlorinated solvent oxidation by potassium permanganate, *J. Contam. Hydrol.*, 106:183-199, https://doi.org/10.1016/j.jconhyd.2009.02.009
- Mayer, K. U., R. T. Amos, S. Molins, and F. Gérard, 2012. Reactive Transport Modeling in Variably Saturated Media with MIN3P: Basic Model Formulation and Model Enhancements, Ch. 8 in: Groundwater Reactive Transport Models, Eds.: Zhang F., G.-T. Yeh and J. Parker, 186-211, Bentham Science, ebook, eISBN: 978-1-60805-306-3, https://doi.org/10.2174/97816080530631120101
- Su, D., K. U. Mayer and K. T. B. MacQuarrie, 2017. Parallelization of MIN3P-THCm: a high performance computational framework for subsurface flow and reactive transport simulation, Environmental Modelling and Software, 95:271-289, https://doi.org/10.1016/j.envsoft.2017.06.008
- Su, D., K. U. Mayer and K.T.B. MacQuarrie, 2020. Numerical investigation of flow instabilities using fully unstructured discretization for variably saturated flow problems, *Advances in Water Resources*, 143:103673, https://doi.org/10.1016/j.advwatres.2020.103673
- Su, D., K. U. Mayer and K.T.B. MacQuarrie, 2020. MIN3P-HPC: a high performance unstructured grid code for subsurface flow and reactive transport simulation, *Mathematical Geosciences*, 53-517-550, https://doi.org/10.1007/s11004-020-09898-7

Additional Information on code on-line (with download options):

- MIN3P webpage: https://www.min3p.com/
- MIN3Pro webpage (GUI version): https://mypage.science.carleton.ca/~richardamos/min3pro/

References - Benchmarking

- Carrayrou J., J. Hoffmann, P. Knabner, S. Kräutle, C. de Dieuleveult, J. Erhel, J. Van der Lee, V. Lagneau, K. U. Mayer, and K.T.B. MacQuarrie, 2010. Comparison of numerical methods for simulating strongly non-linear and heterogeneous reactive transport problems – the MoMaS benchmark case, *Comp. Geosci.*,14:483-502, https://doi.org/10.1007/s10596-010-9178-2
- Mayer, K. U., and K. T. B. MacQuarrie, 2010. Solution of the MoMaS reactive transport benchmark with MIN3P - Model formulation and simulation results, *Comp. Geosci.*, 14:405-419, https://doi.org/10.1007/s10596-009-9158-6
- Steefel, C. I., S. B. Yabusaki, and K. U. Mayer, 2015. Editorial: Reactive transport benchmarks for subsurface environmental simulation, *Comp. Geosci.* 19:439-443, https://doi.org/10.1007/s10596-015-9499-2
- Steefel, C.I., C.A.J. Appelo, B. Arora, D. Jacques, T. Kalbacher, O. Kolditz, V. Lagneau, P.C. Lichtner, K. U. Mayer, J.C.L. Meeussen, S. Molins, D. Moulton, D.L. Parkhurst, H. Shao, J. Šimůnek, N. Spycher, S.B. Yabusaki, and G.T. Yeh, 2015. Reactive transport codes for subsurface environmental simulation, *Comp. Geosci*, https://doi.org/10.1007/s10596-014-9443-x
- Rasouli, P., C.I Steefel, K.U. Mayer, and M. Rolle, 2015. Benchmarks for multicomponent diffusion and electrochemical migration, *Comp. Geosci*, https://doi.org/10.1007/s10596-015-9481-z
- Şengör, S.S., K.U. Mayer, J. Greskowiak, C. Wanner, D. Su, H. Prommer, 2014. A reactive transport benchmark on modeling biogenic uraninite re-oxidation by Fe(III)-(hydr)oxides, *Comp Geosci*, 19:569-583, https://doi.org/10.1007/s10596-015-9480-0
- Mayer, K.U., P. Alt-Epping, D. Jacques, B. Arora and C. I. Steefel, 2015. Benchmark problems for reactive transport modeling of the generation and attenuation of acid rock drainage, *Comp Geosci* , https://doi.org/10.1007/s10596-015-9476-9
- Perko, J., K. U. Mayer, G. Kosakowski, L. De Windt, J. Govaerts, D. Jacques, #D. Su, J. C. L Meussen, 2015. Decalcification of cracked cement structures, *Comp Geosci*, https://doi.org/10.1007/s10596-014-9467-2
- Marty, N.C.M., P. Blanc, O. Bildstein, F. Claret, B. Cochepin, #D. Su, E.C. Gaucher, D. Jacques, J.-E. Lartigue, K. U. Mayer, J.C.L Meeussen, I. Munier, I. Pointeau, S. Liu, and C. Steefel, 2015. Benchmark for reactive transport codes in the context of complex cement/clay interactions, *Comp Geosci*, https://doi.org/10.1007/s10596-014-9463-6
- Xie, M, K. U. Mayer, F. Claret, P. Alt-Epping, D. Jacques, C.I. Steefel, C. Chiaberge, and J. Simunek, 2015. Implementation and evaluation of permeability-porosity and tortuosity-porosity relationships linked to mineral dissolution-precipitation, *Comp Geosci*, https://doi.org/10.1007/s10596-014-9458-3
- Alt-Epping, P., C. Tournassat, P. Rasouli, C.I. Steefel, K.U. Mayer, A. Jenni, U. Mäder, S. Sengor, and R. Fernandez., 2015. Benchmark reactive transport simulations of a column experiment in compacted bentonite with multi-species diffusion and explicit treatment of electrostatic effects, *Comp Geosci*, https://doi.org/10.1007/s10596-014-9451-x
- Poonoosamy, J., C. Wanner, P. Alt-Epping, J. Fernández Águila, J. Samper, L. Montenegro, M. Xie, K. U. Mayer, D. Su, U. Mäder, L. R. Van Loon and G. Kosakowski, 2018. Benchmarking of reactive transport codes for 2D simulations with mineral dissolution/precipitation reactions and feedback on transport parameters, *Comp. Geosci.*, https://doi.org/10.1007/s10596-018-9793-x

a place of mind | THE UNIVERSITY OF BRITISH COLUMBIA | EURAD – Geochemical & Reactive Transport Modelling for Geological Disposal

References - RT Modeling Related to DGRs

- MacQuarrie, K. T. M., and K. U. Mayer, 2005. Reactive transport modeling in fractured rock: a state-of-the-science review. *Earth Sci. Rev.*, 72:189-227, https://doi.org/10.1016/j.earscirev.2005.07.003
- Spiessl, S.M., K.T.B. MacQuarrie, and K.U. Mayer, 2008. Identification of key parameters controlling dissolved oxygen migration and attenuation in fractured crystalline rocks, *J. Contam. Hydrol.*, 95:141-153, https://doi.org/10.1016/j.jconhyd.2007.09.002
- MacQuarrie, K. T. B., K. U. Mayer, B. Jin, and S. M. Spiessl, 2010. The importance of conceptual models in the reactive transport simulation of oxygen ingress in sparsely fractured crystalline rock, *J. Contam. Hydrol*, 112:64-76, https://doi.org/10.1016/j.jconhyd.2009.10.007
- Bea, S.A. K.U. Mayer, K.T.B. MacQuarrie, 2015, Coupling of thermo-hydro-chemical and mechanical processes in deep sedimentary basins: Model development, verification and illustrative example, *Geofluids*, https://doi.org/10.1111/gfl.12148
- Bea, S. A, D. Su, K. U. Mayer, and K.T.B. MacQuarrie, 2018. Evaluation of the potential for dissolved oxygen ingress into deep sedimentary basins during a glaciation event, *Geofluids*, 2018:9475741, https://doi.org/10.1155/2018/9475741
- Xie, M., D. Su, K. U. Mayer, K.T.B. MacQuarrie, 2022. Reactive transport investigations of the long-term geochemical evolution of a multibarrier system including bentonite, low-alkali concrete and host rock, *Applied Geochemistry*, 143:105385, https://doi.org/10.1016/j.apgeochem.2022.105385
- Su, D., M. Xie, K. U. Mayer and K. T.B. MacQuarrie, 2022. Simulation of diffusive solute transport in heterogeneous porous media with dipping anisotropy, *Frontiers in Water*, 4:974145, https://doi.org/10.3389/frwa.2022.974145
- Su, D., M. Xie, K. U. Mayer and K. T.B. MacQuarrie, 2022. The impact of ice sheet geometry on meltwater ingress and reactive solute transport in sedimentary basins, *Water Resources Research*, 58(10):e2022WR032353, https://dx.doi.org/10.1029/2022WR032353

a place of mind | THE UNIVERSITY OF BRITISH COLUMBIA | EURAD – Geochemical & Reactive Transport Modelling for Geological Disposal

4.7 Code 7 – CORE

CORE is a series of **C**omputer **C**odes for transient saturated or unsaturated water flow, heat transport and multicomponent **RE**active solute transport under both local chemical equilibrium and kinetic conditions in heterogeneous and anisotropic porous and fractured media. The codes use the finite element method. The series of codes includes: 1) VISUAL-CORE, a user-friendly version; 2) INVERSE-CORE^{2D}, a version for automatic estimation of reactive transport parameters; 3) BIOCORE^{2D}, a version which accounts for microbial processes in addition to geochemical reactions; 4) CORE^{3D},, a fully 3D version of the code; 5) INVERSE-FADES-CORE V2, a finite element code for modelling non-isothermal multiphase flow, heat transport and multicomponent reactive solute transport in deformable media; and 6) CORE^{2D}V5, the most updated version which considers the porosity feedback effect caused by mineral dissolution/precipitation reactions and the update of flow and transport parameters (Águila et al, 2020). CORE codes have been extensively verified against analytical solutions and other reactive transport codes and widely used to model groundwater flow and solute transport in aquifers, laboratory and in situ experiments and the long-term geochemical evolution of radioactive waste repositories.

The presentation of CORE codes will include: 1) A brief description of the main capabilities, features, and numerical methods; and 2) Some selected applications of the codes related to HLW radioactive waste disposal, which were performed within the context of the ACED and DONUT Work Packages of the EURAD Joint Project.

Lecturer

Javier Samper, Luis Montenegro & Alba Mon, Centro de Investigaciones Científicas Avanzadas (CICA), E.T.S. Ingenieros de Caminos, Canales y Puertos, Campus de Elviña, University of A Coruña, 15071-A Coruña, Spain

Reading Materials

Águila, J.F., Samper, J., Mon, A., Montenegro, L. (2020). Dynamic update of flow and transport parameters in reactive transport simulations of radioactive waste repositories. *Appl Geochem* 2020, *117*, 104585. https://doi.org/10.1016/j.apgeochem.2020.104585

CORE Manual: https://www.osti.gov/etdeweb/biblio/20101793

Samper, J., Xu, T., Yang, C. (2009). A sequential partly iterative approach for multicomponent reactive transport with CORE^{2D}. *Computat Geosci* 2009, *13*. http://dx.doi.org/10.1007/s10596-008-9119-5

Samper J, Yang C, Zheng L, Montenegro L, Xu T, Dai Z, Zhang G, Lu C, Moreira S (2012). CORE^{2D} V4: A code for water flow, heat and solute transport, geochemical reactions, and microbial processes. In Groundwater Reactive Transport Models (p 160-185). Bentham Science Publishers Ltd, doi 10.2174/9781608053063112010101 60.

Samper J., A. Mon, L. Montenegro & A Naves (2020). THCM numerical simulations of the engineered barrier system for radioactive waste disposal. Environmental Geotechnics. https://doi.org/10.1680/jenge.19.00104.

Slides

UNIVERSIDADE DA CORUÑA

eurad
European Joint Programme on Radioactive Waste Management

CORE
SERIES OF CODES FOR WATER FLOW & MULTICOMPONENT REACTIVE TRANSPORT

Javier Samper, Luis Montenegro & Alba Mon

University of A Coruña
j.samper@udc.es

This project has received funding from the European Union's Horizon 2020 research and innovation programme 2014-2018 under grant agreement N°847593

UNIVERSIDADE DA CORUÑA

OUTLINE

- **Introduction**
- **Main capabilities, features, and numerical methods of CORE codes**
- **Brief description of VISUAL CORE**
- **Selected applications of the codes**
  - Hydrogeology & groundwater contamination
  - HLW radioactive waste disposal
- **Models performed within ACED and DONUT Work Packages of the EURAD Joint Project**

General features of the CORE codes

- CORE: Series of computer **CO**des for saturated/unsaturated water flow, heat transfer and multicomponent **RE**active solute transport in porous and fractured media
- Saturated/Unsaturated flow through porous media
- Solute transport with geochemical reactions
- Heat transfer
- Homogeneous & heterogeneous media
- Isotropic & anisotropic media
- Dimensions: 1D, 2D & 3D axisymmetric

February 9th, 2023 CORE presentation

General features of the CORE codes

- Galerkin finite elements with linear weigting and basis functions
- Finite differences for time integration (Euler scheme)
- Newton-Raphson method for unconfined aquifers and unsaturated flow
- Direct and inverse problems
- Iterative sequential approach for reactive transport
  - Transport equations are decoupled from geochemical reactions
- Language: FORTRAN

February 9th, 2023 CORE presentation

General features of the CORE codes

Flow + Transport + Chemical Reactions = Reactive Transport

February 9th, 2023 CORE presentation

CORE series of codes

VISUAL-CORE^{2D}

CORE^{2D} V5

Most updated 2D version:

EURAD (ACED-DONUT)

(Águila, 2017)

INVERSE-CORE^{2D}

Automatic parameter estimation:

Lab & in situ tests

Bure (DIR)

CORE^{3D}

3 D version

Aspo & Mont Terri

INVERSE-FADES-CORE^{2D}

Non-isothermal and multiphase flow:

Grimsel (FEBEX; FEBEX-DP)

BIO-CORE^{2D}

Microbiological processes coupled to chemical reactions

Mol: CERBERUS

Äspö (Redox; REX)

February 9th, 2023 CORE presentation

Specific features: spatial discretization

- Uses triangular 2D elements
- 1D flow is simulated with a row of elements by specifying K_y = 1000 K_x

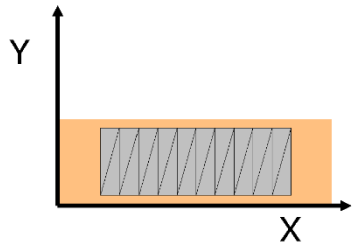

- 2D flow in horizontal plane (X,Y)
  - Confined aquifer
  - Unconfined aquifer

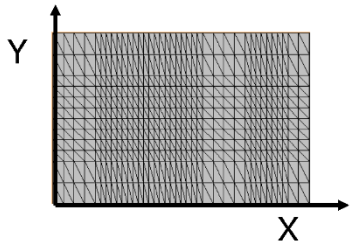

February 9th, 2023 CORE presentation

Specific features: time discretization

- Time discretization
  - Several options for time units, but one must be consistent
- The simulation time is subdivided into time periods
- Each time period is subdivided into N time increments
- For each time period
  - Duration
  - Number of time increments

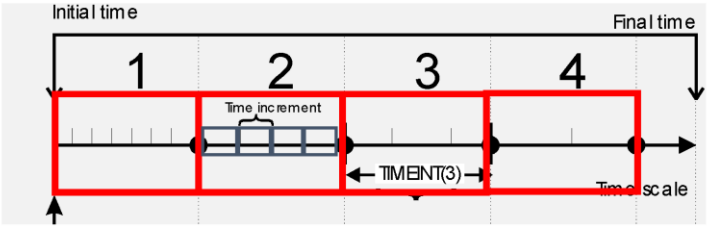

February 9th, 2023 CORE presentation

Specific features: time discretization

- Time functions for parameters and input data which vary with time
  - External head $H(t) = H_0 f_H(t)$
    - H_0 = reference head
    - $f_H(t)$ = time function for head
  - Prescribed flow $Q(t) = Q_0 f_Q(t)$
    - Q_0 = reference flow
    - $f_Q(t)$ = time function for flow
  - Areal recharge $r\ (t) = r_0 f_r(t)$
    - r_0 = reference recharge
    - $f_r(t)$ = time function for recharge
- Functions f are step functions
  - Values of f_i at each time period i

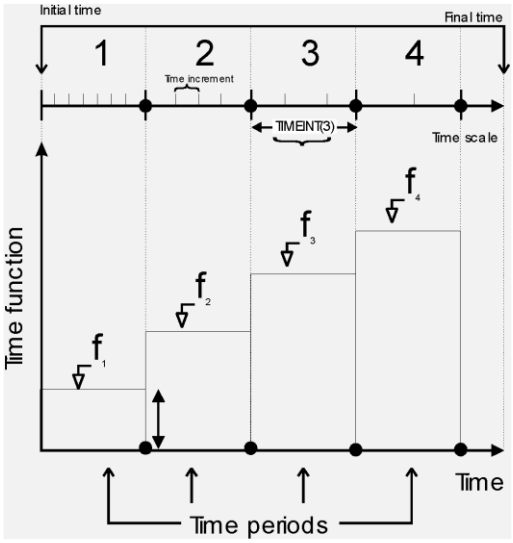

February 9th, 2023 CORE presentation

Specific features: transport parameters

- Transport parameters
  - Total porosity
  - Molecular diffusion coefficient
  - Longitudinal & transverse dispersivities
  - Dry density (for retardation)
  - Accesible porosity (for anion exclusion)

February 9th, 2023 CORE presentation

Specific features: zonation

- Flow and solute transport parameters of the medium are defined by material zones

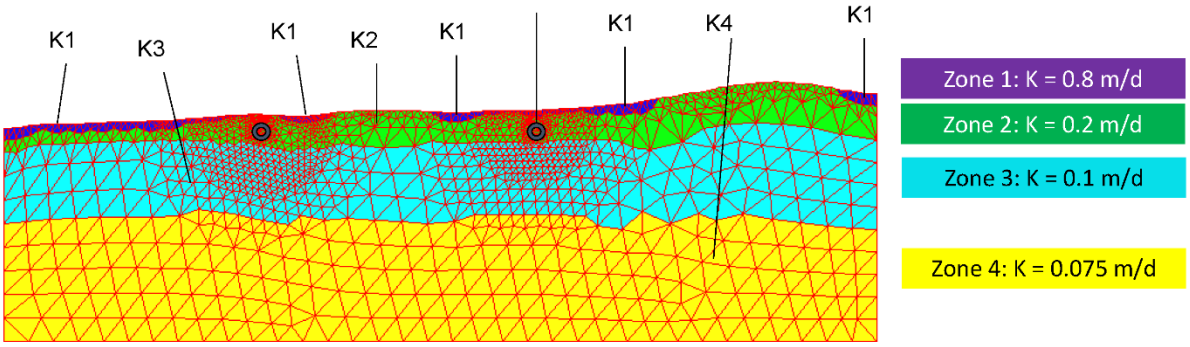

February 9th, 2023 CORE presentation

Specific features: types of water for chem. composition

- VISUAL-CORE considers several types of
  - Initial waters
  - Recharge waters
  - Boundary waters

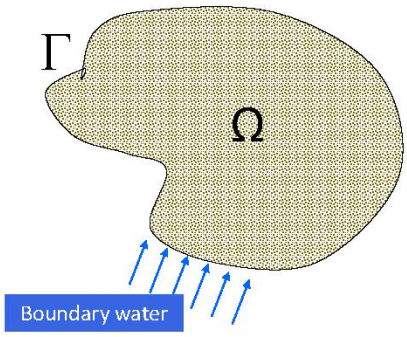

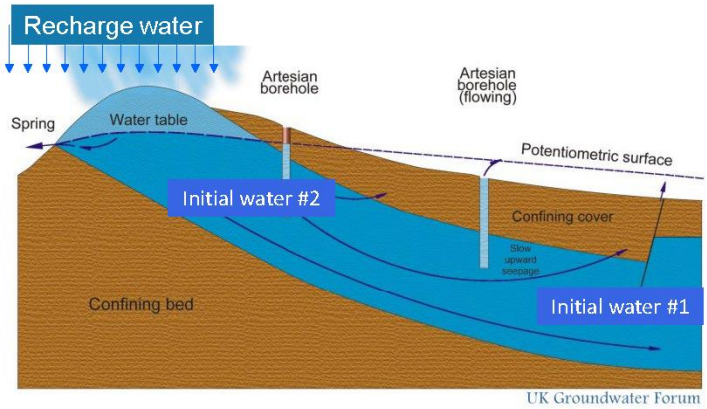

February 9th, 2023 CORE presentation

Specific features: types of chemical reactions

- Homogeneous reactions (single phase)
  - Aqueous complexation
  - Redox
- Heterogeneous (several phases)
  - Mineral dissolution/precipitation
  - Gas solution/exsolution
  - Sorption
    - Cation exchange
    - Surface complexation
- The user selects the species needed for a given problem
  - List the names of species:

```
'calcite'   -1.000 'h+'  +1.000 'ca+2'  +1.000 'hco3-'
```

February 9th, 2023 CORE presentation

Specific features: thermodynamic databases

- Selection and format of the CORE TDB
  - CORE series codes rely on several TDB such as ThermoChimie v10a or the com TDB of EQ3/6
    - The user can select the TDB
    - The selected TDB have to be used in the CORE TDB format
  - CORE TDB format: CORE codes use 2 TDB to calculate the logK for each chemical reaction
    - TDB at 25ºC: "master25.dat" with a value of logK at 25ºC
    - TDB at T variable: "masterte.dat" with 8 values of logK at 0, 25, 60, 100, 150, 200, 250 and 300 ºC

$$\log K\ (0 - 300\ ^{\circ}C) = \frac{b_1}{T^2} + \frac{b_2}{T} + b_3 \cdot \ln T + b_4 + b_5 \cdot T$$

b_1, b_2, b_3, b_4 y b_5 are coefficients calculated wiht this function for each chemical reaction by using the 8 logK values of "masterte.dat"

February 9th, 2023 CORE presentation

Specific features: thermodynamic databases

- "masterte.dat" example
  - The 2 CORE TDB contains 5 blocks of information: primary species, aqueous complexes, minerals, gases and complexation complexes
    - Components and stochiometry of the chemical reaction
    - 8 values of logK at 0, 25, 60, 100, 150, 200, 250 and 300 ºC
    - Charge and size of the ions
    - Molar volume of the minerals
  - The user can modify the CORE TDB (change a log K, add a new reaction, …)

Aqueous complex TDB format example

'nh4+' 4 -2.000 'o2(aq)' +1.000 'h2o' +1.000 'no3-' +2.000 'h+' +58.1088 +52.8591
+46.5407 +40.4988 +34.2478 +29.0289 +24.5194 +20.4271 +3.00 +1.00

Mineral TDB format example

'calcite' 36.934 3 -1.000 'h+' +1.000 'ca+2' +1.000 'hco3-' +2.2257 +1.8487 +1.3330
+0.7743 +0.0999 -0.5838 -1.3262 -2.2154

February 9th, 2023 CORE presentation

Specific features: kinetic database

- Selection and format of the CORE kinetic database
  - CORE series codes use a kinetic database with data at 25 ºC
    - "kinetics.dat"
  - The user can select between thermodynamic or kinetic control

sign

Activation energy (kJ/mol)

Catalytic or inhibition effect

Empirical kinetics parameters

$$r_m = \varsigma_m A_m e^{-\frac{Ea_m}{RT}} \sum_{k=1}^{N_k} k_{mk} \prod_{i=1}^{N_c+N_x} a_i^{p_{mki}} \left|\Omega_m^{\theta_{mk}} - 1\right|^{\eta_{mk}}$$

Dissolution/precipitation rate (mol/m³/s)

Specific surface (m²/m³)

Kinetic constant at 25ºC (mol/m²/s)

Saturation state $\Omega_m = IAP/K_m$

February 9th, 2023 CORE presentation

Selected applications

- Contaminant transport: Uranium migration in alluvial aquifer (Spain)

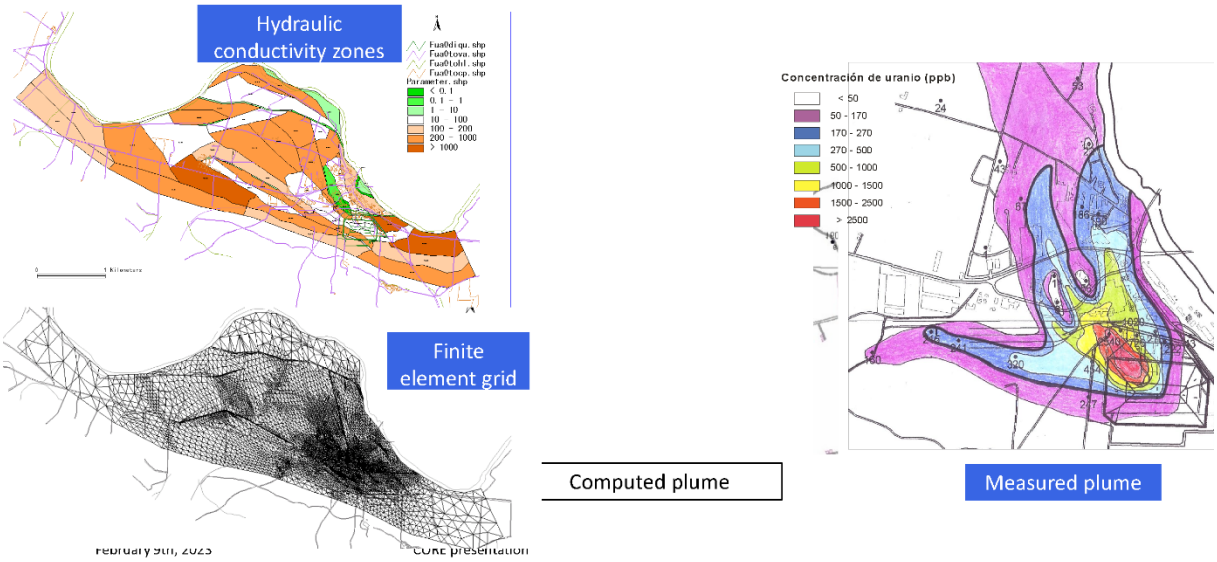

Selected applications

- Contaminant transport: Hexachlorohexane pollution in Sardas site (Huesca, Spain)

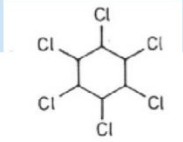

HCH

($C_6H_6Cl_6$)

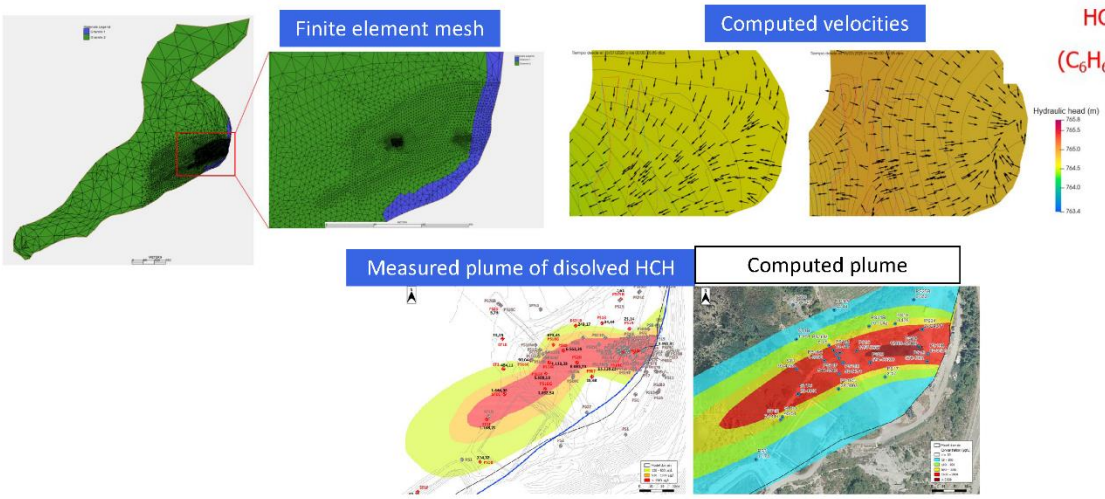

February 9th, 2023 CORE presentation

Selected applications

- 2D & 3D numerical models for the Spanish site of interim surface storage of high-level radioactive waste (HLW)

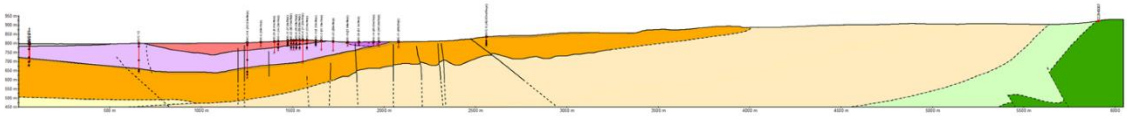

Finite element mesh

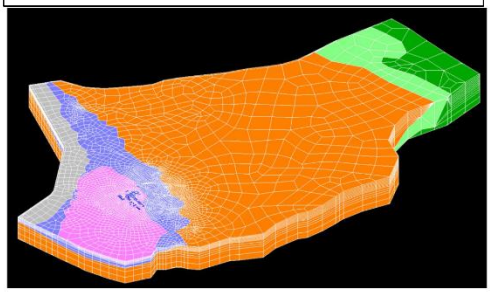

Computed hydraulic heads

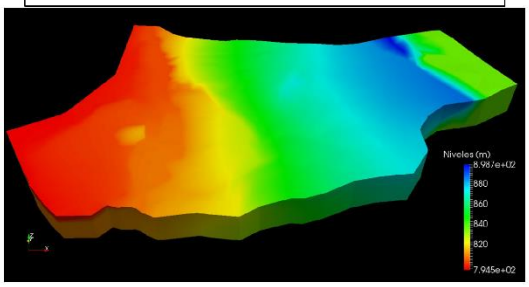

February 9th, 2023 CORE presentation

Selected applications

- Water flow & multicomponent solute transport with chemical and biological reactions for geological high-level radioactive waste disposal

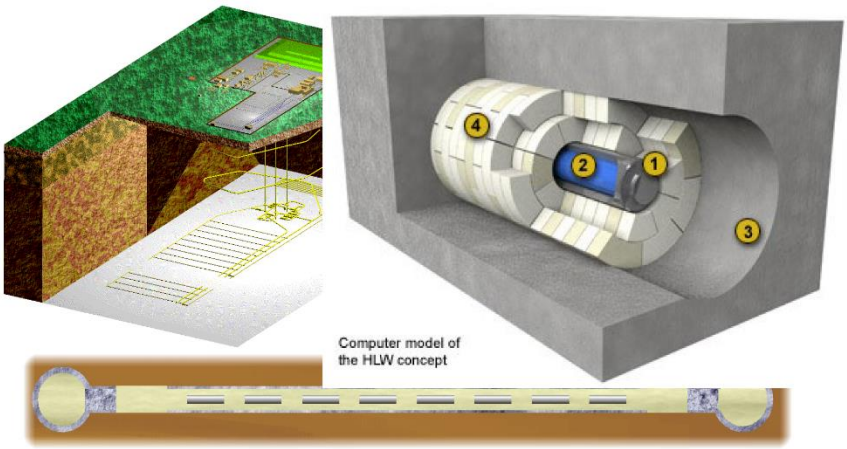

February 9th, 2023 CORE presentation

Selected applications

- Numerical models of flow and transport of laboratory and in situ experiments
- Natural clays and compacted bentonites
- Reactive transport models
  - Coupled thermal (T), Hydrodynamic (H), chemical (C), mechanical (M) and microbial (B) processes
  - Interactions of carbon-steal corrosion products with bentonites and clay host rocks
  - Interactions of concrete degradation products with bentonites and clay rocks
- CORE codes have been used within the context of many research projects of the European EURATOM Program
  - Mol: CERBERUS
  - Bure: DIR
  - Grimsel: FEBEX I, II FEBEX-DP
  - Aspo: Redox, REX, Task Force 5
  - Mont Terri: DR

Selected applications

- ACED (Assessment of Chemical Evolution in ILW & HLW repositories)
- Task 2: reactive transport models of the interactions of steel corrosion products and bentonite
- Task 4: reactive transport models for the long-term of a disposal cell in a HLW repository in granite
  - To be presented next Friday in Lecture 8

February 9th, 2023 CORE presentation

reactive transport models of the interactions of steel corrosión products and bentonite

Overall objective: Reactive transport modelling of laboratory and in situ heating and hydration tests dealing with steel/bentonite interfaces

- **Laboratory corrosion tests performed by CIEMAT**
  - FB tests: column tests containing bentonite blocks in contact with Fe powder. Sequence of tests: FB1 to FB6 with increasing durations: 0.5 (FB1) years up to 15 years (FB6)
  - FeMo test: steel sinters emplaced in holes drilled in a bentonite block. 15 years of duration
- **FEBEX in situ test**
  - FEBEX-DP provided multiple evidences of interactions of corrosion products and bentonite (NAGRA NAB 16-16)
  - 18 years of duration

FB corrosion tests

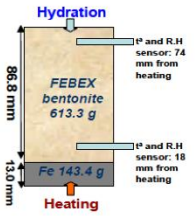

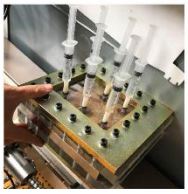

FeMo test

FEBEX in situ test

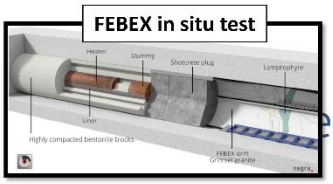

February 9th, 2023 CORE presentation

UNIVERSIDADE DA CORUÑ

FB corrosion tests model

- Non-isothermal anoxic conditions with initially unsaturated **bentonite** in contact with **Fe powder**
- **Coupled THCM models are needed** considering hydration of the bentonite on the top of the column and heating at the bottom; water evaporation near the heater; and multicomponent geochemical reactive transport for the interactions of the Fe powder with the bentonite
- 2 materials: bentonite (86.8 mm lenght) and Fe powder (13 mm)
- 1-D finite element mesh: 86 nodes in the bentonite and 13 in the Fe powder
- Geochemical reactions: aqueous complexation, acid-base, redox, cation exchange (Na, K, Ca, Mg and Fe), surface complexation (H^+ and Fe) on strong and weak sites and mineral dissolution/precipitation
- 12 primary species: H_2O, $O_2(aq)$, H^+, Na^+, K^+, Ca^{2+}, Mg^{2+}, Fe^{2+}, HCO_3^-, Cl^-, SO_4^{2-} and $SiO_2(aq)$
- 39 secondary aqueous species, 5 exchanged cations and 13 surface complexes
- 9 minerals: all assumed at chemical equilibrium except Fe corrosion
- Magnetite is assumed to be the most important corrosion product. Goethite and siderite are also considered

Cells FB: iron/bentonite

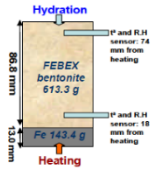

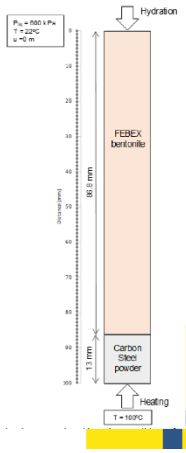

February 9th, 2023 CORE presentation

Description of the work carried out & main results

UNIVERSIDADE DA CORUÑA

Volumetric water content and porosity at the FB corrosion tests models

- Computed water content and porosity are similar for FB3, FB4 and FB5 tests
- Computed water content overestimates measured data at the bentonite-Fe powder interface

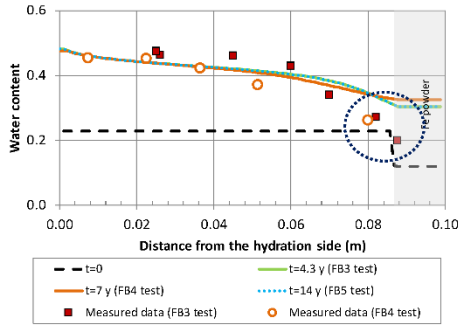

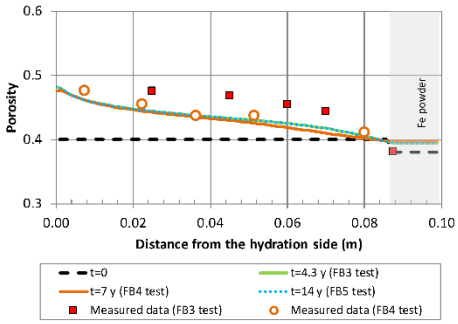

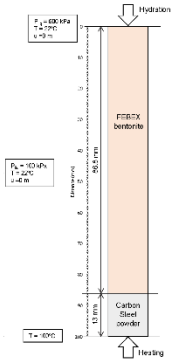

February 9th, 2023 CORE presentation

Description of the work carried out & main results

UNIVERSIDADE DA CORUÑA

Temperature and relative humidity at the FB tests models

- Computed temperature and relative humidity are similar for FB3, FB4 and FB5 tests
- Computed temperature overestimates measured data

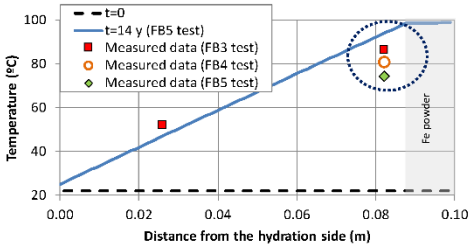

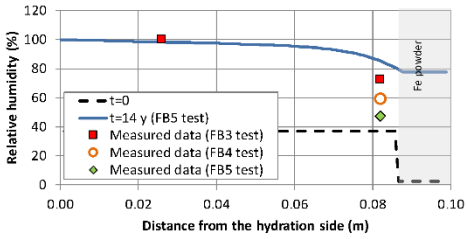

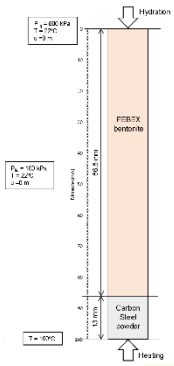

February 9th, 2023 CORE presentation

Description of the work carried out & main results

UNIVERSIDADE DA CORUÑA

Dissolved Cl^- and Na^+ at the FB tests models

- Computed dissolved concentrations capture the general trend of the measured data
  - Larger concentration near the heater and smaller concentrations near the hydration zone

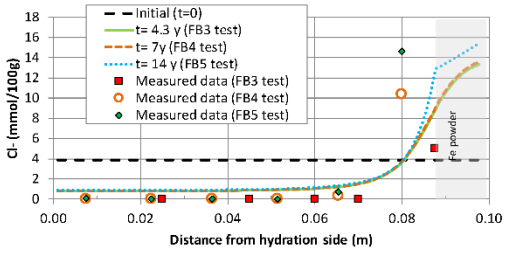

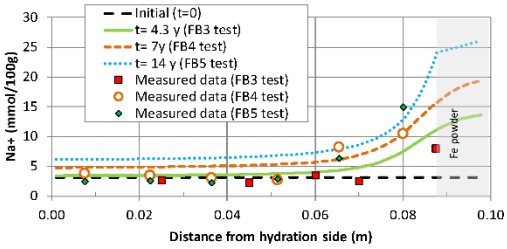

February 9th, 2023 CORE presentation

Description of the work carried out & main results

UNIVERSIDADE DA CORUÑA

Mineral dissolution/precipitation at the FB tests models

- Magnetite is the main corrosion product which precipitates in the Fe powder and penetrates few mm into bentonite

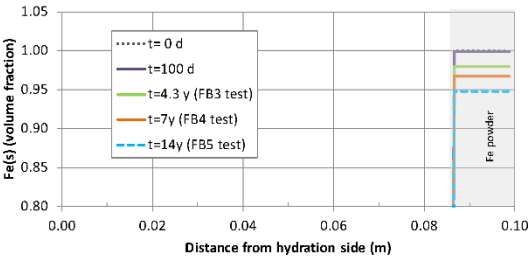

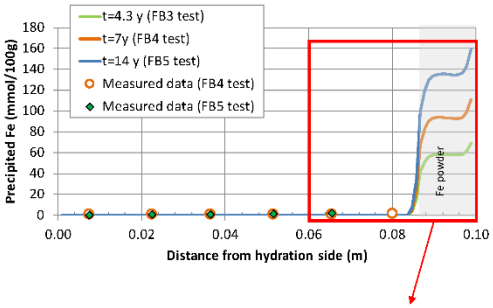

February 9th, 2023 CORE presentation

UNIVERSIDADE DA CORUÑA

REFERENCES

- Águila, J.F., Samper, J., Mon, A., Montenegro, L. (2020). Dynamic update of flow and transport parameters in reactive transport simulations of radioactive waste repositories. Appl Geochem 2020, 117, 104585. https://doi.org/10.1016/j.apgeochem.2020.104585
- CORE Manual: https://www.osti.gov/etdeweb/biblio/20101793
- Samper, J., Xu, T., Yang, C. (2009). A sequential partly iterative approach for multicomponent reactive transport with CORE2D. Computat Geosci 2009, 13. http://dx.doi.org/10.1007/s10596-008-9119-5
- Samper J, Yang C, Zheng L, Montenegro L, Xu T, Dai Z, Zhang G, Lu C, Moreira S (2012). CORE2D V4: A code for water flow, heat and solute transport, geochemical reactions, and microbial processes. In Groundwater Reactive Transport Models (p 160-185). Bentham Science Publishers Ltd, doi 10.2174/9781608053063112010101 60.
- Samper J., A. Mon, L. Montenegro & A Naves (2020). THCM numerical simulations of the engineered barrier system for radioactive waste disposal. Environmental Geotechnics. https://doi.org/10.1680/jenge.19.00104.

February 9th, 2023 CORE presentation 29

4.8 Code 8 - porousMedia4Foam: an hybrid-scale solver to model coupled processes in porous media

porousMedia4Foam is a package for solving flow and transport in porous media using OpenFOAM® - a popular open-source numerical toolbox. We introduce and highlight the features of a new generation open-source hydro-geochemical module implemented within porousMedia4Foam, which relies on micro-continuum concept and which makes it possible to investigate hydro-geochemical processes occurring at multiple scales i.e. at the pore-scale, reservoir-scale and at the hybrid-scale. Geochemistry is handled by a third party package (e.g. PHREEQC) that is coupled to the flow and transport solver of OpenFOAM®. We conducted benchmarks across different scales to validate the accuracy of our simulator. We further looked at the evolution of mineral dissolution/ precipitation in a fractured porous system. Application fields of this new package include the investigation of hydro-bio-geochemical processes in the critical zone, the modelling of contaminant transport in aquifers, as well as and the assessment of confinement performance for geological barriers.

Lecturer

Cyprien Soulaine, Centre National de la Recherche Scientifique (CNRS), Institut des Sciences de la Terre d'Orléans, Université d'Orléans, CNRS, BRGM, 45100 Orléans, France

Reading Material

S. Pavuluri, C. Tournassat, F. Claret, C. Soulaine "Reactive transport modelling with a coupled OpenFOAM®-PHREEQC platform" Transport in Porous Media 145, 475–504 (2022) link

C. Soulaine, S. Pavuluri, F. Claret, C. Tournassat "porousMedia4Foam: Multi-scale open-source platform for hydro-geochemical simulations with OpenFOAM®" Environmental Modelling and Software 145, 105199 (2021) link, pdf

Slides

porousMedia4Foam: AN HYBRID-SCALE SOLVER TO MODEL COUPLED PROCESSES IN POROUS MEDIA

CYPRIEN SOULAINE*

CNRS – Earth Sciences Institute of Orleans, France

www.cypriensoulaine.com

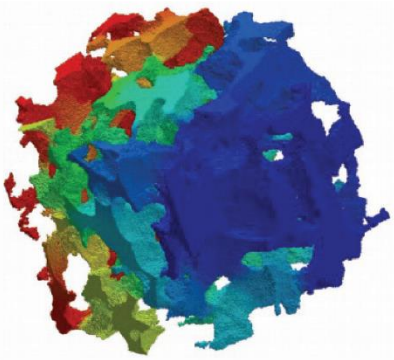

1

INSTITUT DES SCIENCES DE LA TERRE D'ORLEANS

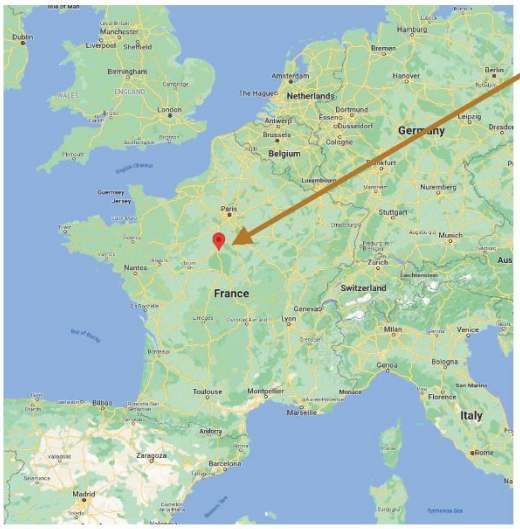

= cnrs + UNIVERSITE D'ORLEANS + brgm

120 people (faculty, PhD students, postdocs, engineers, technicians, administrative staff)

porousMedia4Foam

- OpenFOAM-based platform,
- Design to model couple processes in porous media,
- Coupled with geochemical packages such as PHREEQC,
- Multi-scale formulation,
- Open-source: https://github.com/csoulain/porousMedia4Foam

3

WHAT IS OPENFOAM?

OpenFOAM®

= **Open** **F**ield **O**peration **A**nd **M**anipulation

- Solve the Partial Differential Equations using the finite volumes method
- Multiphysics simulation platform mainly devoted to fluid flow
- Handle 3D geometries by default
- Open-source software developed in C++ (object-oriented programming)
- Can be freely downloaded at www.openfoam.org or www.openfoam.com
- Designed as a toolbox easily customizable
- Parallel computation implemented at the lowest level
- Cross-platform installation (Linux preferred)

- 1989 : First development at Imperial College London
- 1996 : First release of FOAM
- 2004 : OpenFOAM® released under GPL licence by OpenCFD Ltd.
- 2023 : OpenFOAM 10.0 ; OpenFOAM v2212 ; foam-extend5.0

4

COMPUTATIONAL FLUID DYNAMICS (CFD)

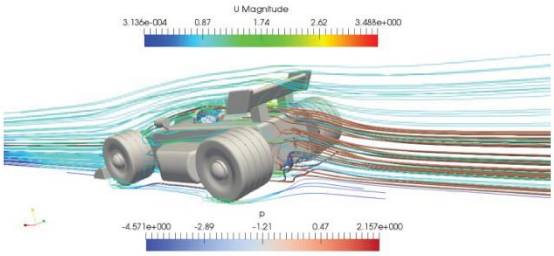

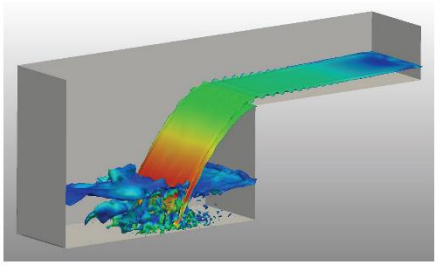

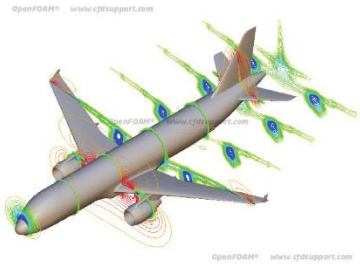

(source: SimScale)

5

PORE-SCALE VS CONTINUUM-SCALE

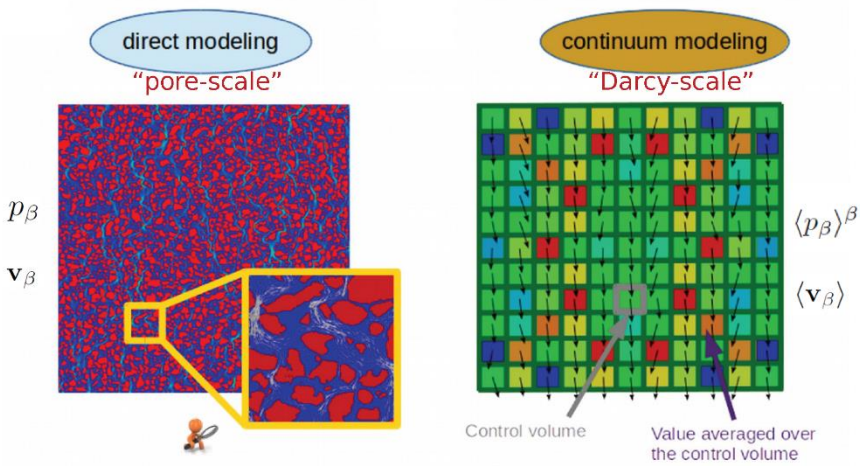

for every point of the domain

fluid **OR** solid

fluid **AND** solid

Soulaine (2015). *On the origin of Darcy's law*, Stanford University

6

porousMedia4Foam: CODE ARCHITECTURE

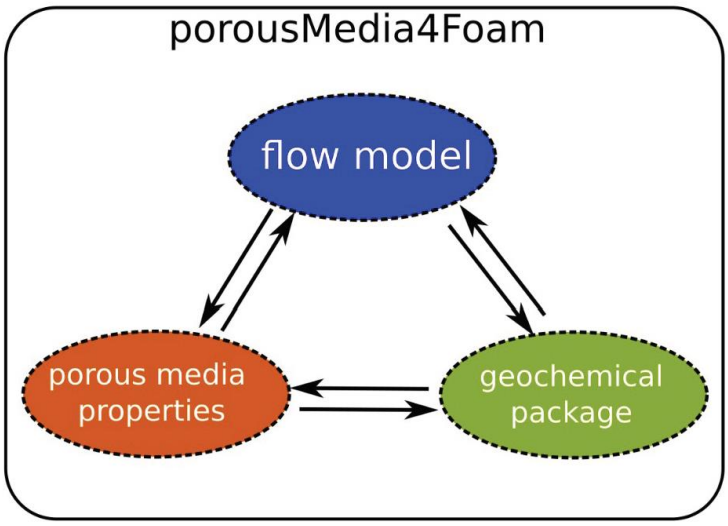

https://github.com/csoulain/porousMedia4Foam

Soulaine et al "porousMedia4Foam: Multi-scale open-source platform for hydro-geochemical simulations with OpenFOAM®" Env Modelling and Soft 145, 105199 (2021)

7

POROUS MEDIA MODELS

Absolute permeability

Name	Expression
none	$k = 0$
constant	$k = k_0$
Power-law	$k = k_0 \left(\frac{\varphi}{\varphi_0}\right)^n$
Kozeny-Carman	$k = k_0 \left(\frac{\varphi}{\varphi_0}\right)^n \left(\frac{1-\varphi_0}{1-\varphi}\right)^m$
Verma-Pruess	$k = k_0 \left(\frac{\varphi - \varphi_c}{\varphi_0 - \varphi_c}\right)^n$
Hele-Shaw	$k = \frac{h^2}{12}$

Dispersion tensor

Name	Expression
none	$\mathsf{D}_i^* = 0$
diffusionOnly	$\mathsf{D}_i^* = D_i \mathsf{I}$
archiesLaw	$\mathsf{D}_i^* = \varphi^n D_i \mathsf{I}$
linearDispersion	$\mathsf{D}_i^* = \varphi^n \left((D_i + \alpha_T \lvert \boldsymbol{v} \rvert) \mathsf{I} + \frac{(\alpha_L - \alpha_T)}{\lvert \boldsymbol{v} \rvert} \boldsymbol{v}\boldsymbol{v} \right)$

Other models

- Surface area,
- Relative permeability
- Capillary pressure
- ….

https://github.com/csoulain/porousMedia4Foam

Soulaine et al "porousMedia4Foam: Multi-scale open-source platform for hydro-geochemical simulations with OpenFOAM®" Env Modelling and Soft 145, 105199 (2021)

8

GEOCHEMICAL MODELS

Name	Model	Comments
phreeqcRM	PHREEQC	Parkhurst and Wissmeier (2015)
simpleFirstOrderKineticMole	first order kinetic, C_i in mol/m^3	Molins et al. (2020), Soulaine et al. (2017b)
transportOnly	no geochemistry	–
flowOnly	no transport, no geochemistry	–

https://github.com/csoulain/porousMedia4Foam

Soulaine et al "porousMedia4Foam: Multi-scale open-source platform for hydro-geochemical simulations with OpenFOAM®" Env Modelling and Soft 145, 105199 (2021) 9

FLOW MODELS

Name	Model	Comments
dbsFoam	Micro-continuum (Darcy-Brinkman-Stokes)	pore-scale, hybrid-scale, continuum-scale, Soulaine and Tchelepi (2016).
darcyFoam	Darcy's law	continuum-scale only.
impesFoam	Two-phase Darcy	continuum-scale only, Horgue et al. (2015)
hybridPorousInterFoam	Two-phase micro-continuum (Darcy-Brinkman-Stokes)	pore-scale, hybrid-scale, continuum-scale, Soulaine et al. (2019, 2018), Carrillo et al. (2020).
constantVelocityFoam	constant velocity profile	uniform or non-uniform velocity profiles.

https://github.com/csoulain/porousMedia4Foam

Soulaine et al "porousMedia4Foam: Multi-scale open-source platform for hydro-geochemical simulations with OpenFOAM®" Env Modelling and Soft 145, 105199 (2021) 10

DARCY-SCALE SIMULATIONS OF CALCITE DISSOLUTION

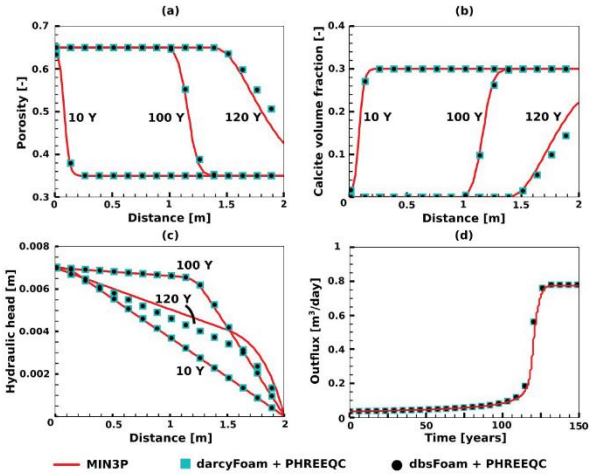

$$CaCO_3 + H^+ \leftrightarrow Ca^{2+} + HCO_3^-,$$
$$HCO_3^- \leftrightarrow H^+ + CO_3^{2-}.$$

Fig. 2. Calcite dissolution under kinetic conditions considering feedback of porous media properties. Evolution of (a) porosity, (b) calcite volume fraction, (c) hydraulic head along the channel and (d) evolution of outflux. MIN3P data is from Xie et al. (2015) for comparison.

11

REACTIVE ZONE INCLUDING CELESTITE HAVING DIFFERENT GRAIN SIZES

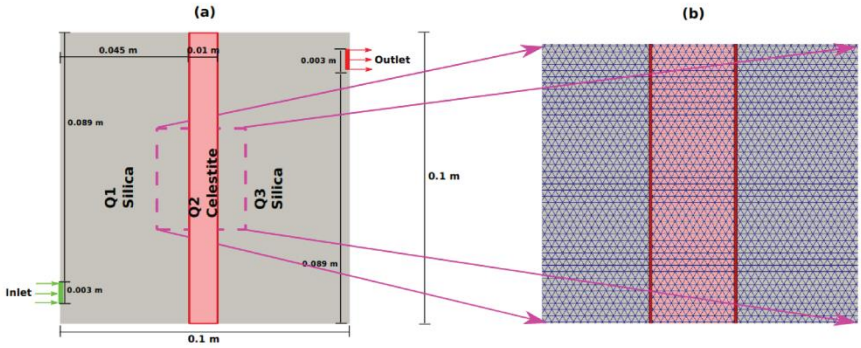

In this case, we investigated reactive transport occurring in a 2D flow cell containing celestite ($SrSO_4$) having a bimodal grain size distribution. The setup was discussed in detail in Poonoosamy et al. (2018) and is illustrated in Fig. 2a. The flow cell comprised of three compartments - Q1, Q2 and Q3. Q1 and Q3 were composed of inert mineral (quartz). Q2 comprised of a reactive mineral, celestite. An acidic solution comprising of barium (Ba^{2+}) and chloride (Cl^-), was injected continuously from the inlet at a constant rate. Once the barium ions reached the reactive zone Q2 in the flow cell, celestite dissociated into strontium (Sr^{2+}) and sulphate (SO_4^{2-}) ions. The barium ions reacted with sulphate ions resulting in the precipitation of barite ($BaSO_4$) according to the following reaction:

$$Ba^{2+} + SrSO_4 \rightarrow BaSO_4 + Sr^{2+}. \quad (18)$$

12

REACTIVE ZONE INCLUDING CELESTITE HAVING DIFFERENT GRAIN SIZES

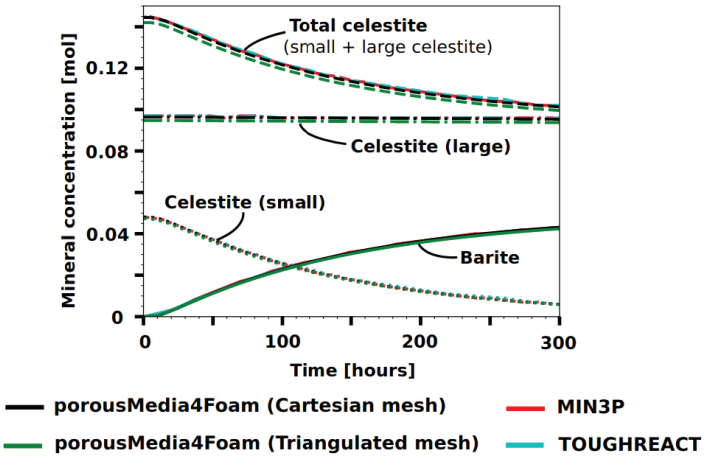

Figure 13: Case 8 – Concentration of celestite - small, large grains, total and barite in the flow cell after 300 hours. Results of *porousMedia4Foam* (with structured, unstructured mesh) was compared with the data obtained by TOUGHREACT and MIN3P from Poonoosamy et al. (2018).

S. Pavuluri, C. Tournassat, F. Claret, C. Soulaine "Reactive transport modelling with a coupled OpenFOAM®-PHREEQC platform"

13

REACTIVE ZONE INCLUDING CELESTITE HAVING DIFFERENT GRAIN SIZES

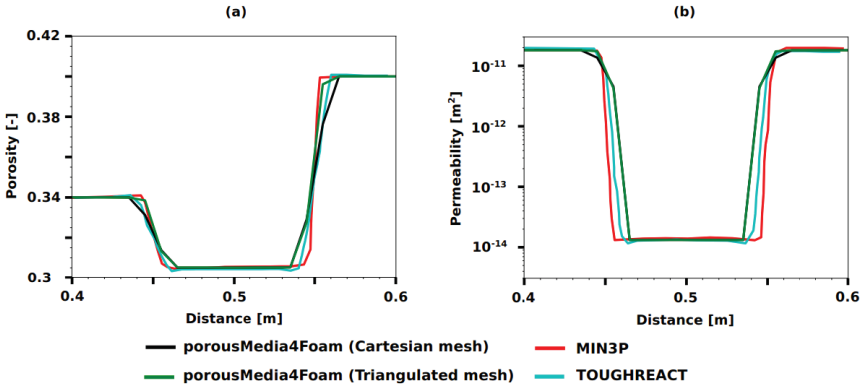

Figure 14: Case 8 – Change in porous media properties (a) porosity, (b) permeability at 300 hours due to dissolution of celestite and precipitation of barite in Q2 zone of the flow cell. The results of *porousMedia4Foam* were compared with TOUGHREACT and MIN3P which were taken from Poonoosamy et al. (2018).

S. Pavuluri, C. Tournassat, F. Claret, C. Soulaine "Reactive transport modelling with a coupled OpenFOAM®-PHREEQC platform"

14

THE MICRO-CONTINUUM APPROACH

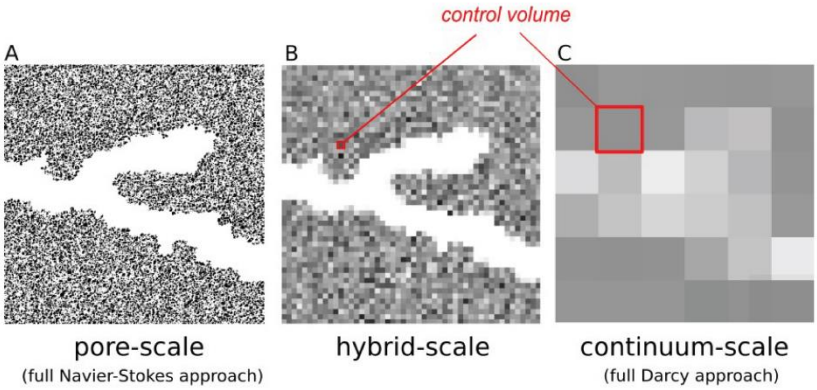

The Darcy-Brinkman-Stokes[1,2,3] equation allows a single domain formulation

$$0 = -\nabla \bar{p}_f + \frac{\mu_f}{\varepsilon_f}\nabla^2 \bar{\mathbf{v}}_f - \mu_f k^{-1} \bar{\mathbf{v}}_f$$

Vanishes in the void space

Dominant in the porous region

[1]Brinkman *A Calculation of The Viscous Force Exerted by a Flowing Fluid on a Dense Swarm of Particles* Appl. Sci. Res. (1947)
[2]Neale and Nader *Practical significance of Brinkman's extension of Darcy's law: coupled parallel flows within a channel and a bounding porous medium*. (1974)
[3]Soulaine and Tchelepi *Micro-continuum approach for pore-scale simulation of subsurface processes* Transport in Porous Media (2016)

15

MAIN FEATURES OF THE MICRO-CONTINUUM APPROACH

Two-scale

(large permeability contrast, fractured media...)

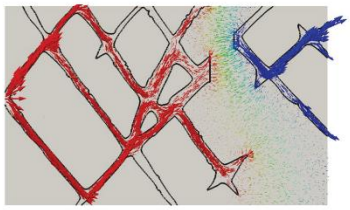

16

MAIN FEATURES OF THE MICRO-CONTINUUM APPROACH

Two-scale

(large permeability contrast, fractured media...)

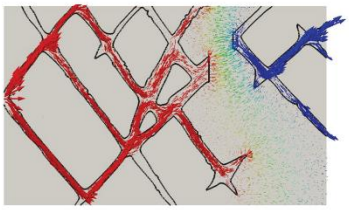

Pore-scale simulations

(penalized approach: solve complex flow on Cartesian grid)

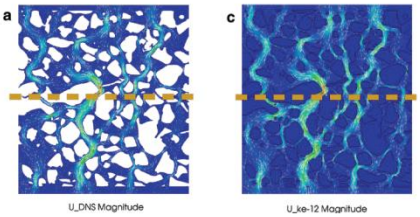

17

MAIN FEATURES OF THE MICRO-CONTINUUM APPROACH

Two-scale

(large permeability contrast, fractured media...)

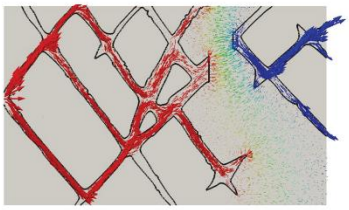

Pore-scale simulations

(penalized approach: solve complex flow on Cartesian grid)

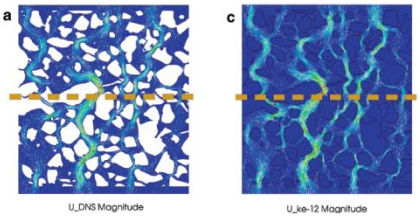

Surface reaction

(adsorption, dissolution, precipitation…)

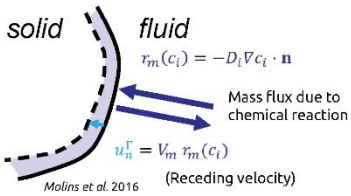

18

MAIN FEATURES OF THE MICRO-CONTINUUM APPROACH

Two-scale
(large permeability contrast, fractured media...)

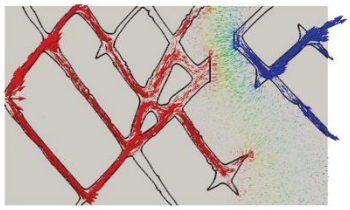

Pore-scale simulations
(penalized approach: solve complex flow on Cartesian grid)

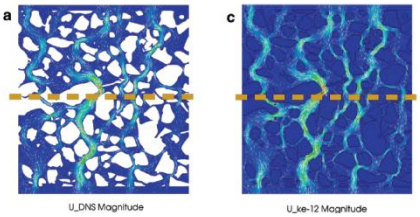

Surface reaction
(adsorption, dissolution, precipitation…)

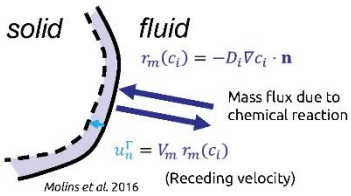

Deformable media
(swelling, fracturing..)

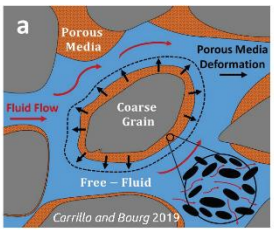

19

MAIN FEATURES OF THE MICRO-CONTINUUM APPROACH

Two-scale
(large permeability contrast, fractured media...)

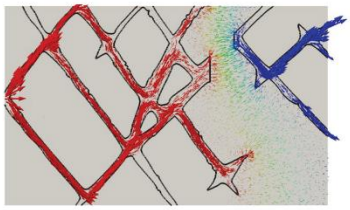

Pore-scale simulations
(penalized approach: solve complex flow on Cartesian grid)

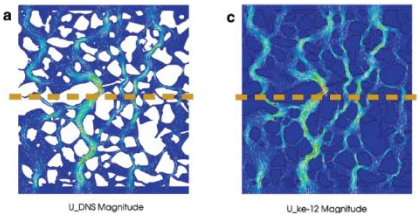

Multi-phase flow
(capillary, gravity effects…)

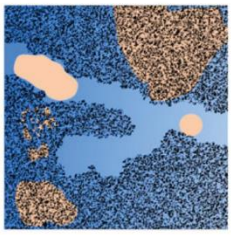

Surface reaction
(adsorption, dissolution, precipitation…)

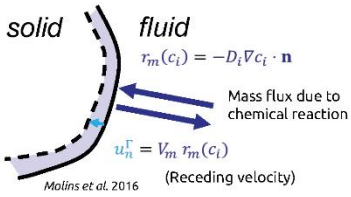

Deformable media
(swelling, fracturing..)

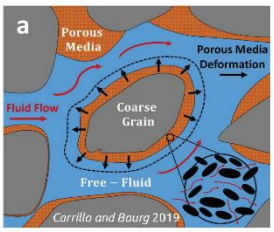

20

EXAMPLE: ACCESSIBLE REACTIVE SURFACE AREA

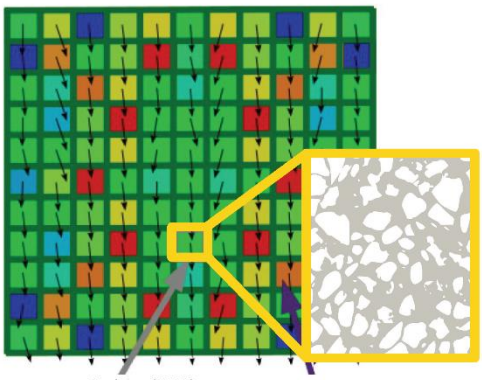

Soulaine (2015)

- Darcy scale = averaged equations with averaged properties (permeability, surface area...)
- How does the permeability evolves when the pore-structure changes due to the dissolution/precipitation?
- What is the surface area accessible to the acid component?
- What about multiphase reactive flows?

Soulaine (2015). *On the origin of Darcy's law*, Stanford University

21

EXAMPLE: ACCESSIBLE REACTIVE SURFACE AREA

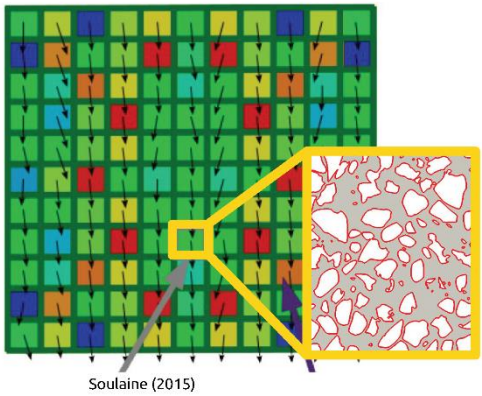

Soulaine (2015)

- Darcy scale = averaged equations with averaged properties (permeability, surface area...)
- How does the permeability evolves when the pore-structure changes due to the dissolution/precipitation?
- What is the surface area accessible to the acid component?
- What about multiphase reactive flows?

Soulaine (2015). *On the origin of Darcy's law*, Stanford University

22

EXAMPLE: ACCESSIBLE REACTIVE SURFACE AREA

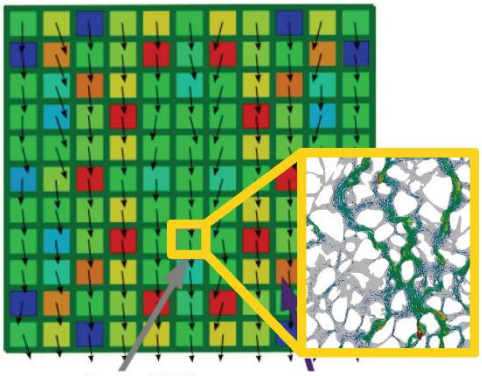

Soulaine (2015)

- Darcy scale = averaged equations with averaged properties (permeability, surface area...)
- How does the permeability evolves when the pore-structure changes due to the dissolution/precipitation?
- What is the surface area accessible to the acid component?
- What about multiphase reactive flows?

Soulaine (2015). *On the origin of Darcy's law*, Stanford University

23

MINERAL DISSOLUTION AT THE PORE-SCALE

Development of hydro-geochemical **simulation tools** at the pore-scale[1]

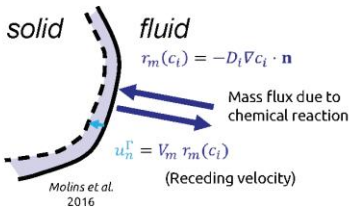

[1]Soulaine and Tchelepi, *Micro-continuum approach for pore-scale simulation of subsurface processes*, Transport in Porous Media (2016)

24

MINERAL DISSOLUTION AT THE PORE-SCALE

Development of hydro-geochemical **simulation tools** at the pore-scale[1]

↓

Validation of the numerical model using **microfluidic** experiments[2]

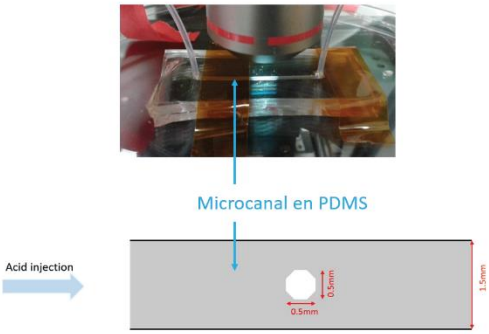

[1]Soulaine and Tchelepi, *Micro-continuum approach for pore-scale simulation of subsurface processes*, Transport in Porous Media (2016)
[2]Soulaine et al., *Mineral dissolution and wormholing from a pore-scale perspective*, Journal of Fluid Mechanics 827 (2017)

25

MINERAL DISSOLUTION AT THE PORE-SCALE

Development of hydro-geochemical **simulation tools** at the pore-scale[1]

↓

Validation of the numerical model using **microfluidic** experiments[2]

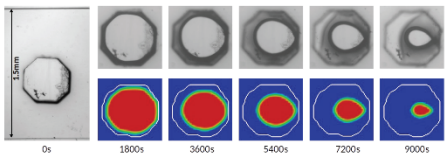

[1]Soulaine and Tchelepi, *Micro-continuum approach for pore-scale simulation of subsurface processes*, Transport in Porous Media (2016)
[2]Soulaine et al., *Mineral dissolution and wormholing from a pore-scale perspective*, Journal of Fluid Mechanics 827 (2017)

26

MINERAL DISSOLUTION AT THE PORE-SCALE

Development of hydro-geochemical **simulation tools** at the pore-scale[1]

↓

Validation of the numerical model using **microfluidic** experiments[2]

↓

Interpretation of the results and **upscaling**[2]

Péclet number	Damköhler number
$Pé = \frac{\text{advection}}{\text{diffusion}}$	$Da = \frac{\text{reaction}}{\text{diffusion}}$

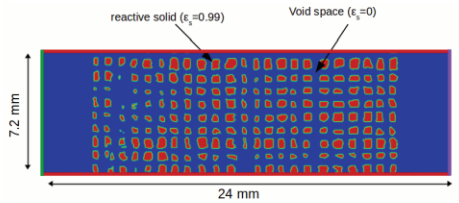

[1]Soulaine and Tchelepi, *Micro-continuum approach for pore-scale simulation of subsurface processes*, Transport in Porous Media (2016)
[2]Soulaine et al., *Mineral dissolution and wormholing from a pore-scale perspective*, Journal of Fluid Mechanics 827 (2017)

27

MINERAL DISSOLUTION AT THE PORE-SCALE

Development of hydro-geochemical **simulation tools** at the pore-scale[1]

↓

Validation of the numerical model using **microfluidic** experiments[2]

↓

Interpretation of the results and **upscaling**[2]

Péclet number	Damköhler number
$Pé = \frac{\text{advection}}{\text{diffusion}}$	$Da = \frac{\text{reaction}}{\text{diffusion}}$

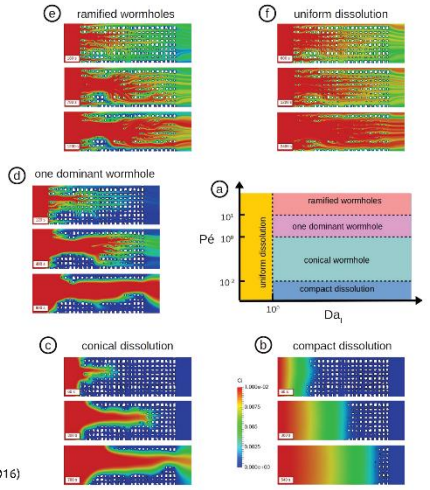

[1]Soulaine and Tchelepi, *Micro-continuum approach for pore-scale simulation of subsurface processes*, Transport in Porous Media (2016)
[2]Soulaine et al., *Mineral dissolution and wormholing from a pore-scale perspective*, Journal of Fluid Mechanics 827 (2017)

28

MINERAL DISSOLUTION AT THE PORE-SCALE

Development of hydro-geochemical **simulation tools** at the pore-scale[1]

↓

Validation of the numerical model using **microfluidic** experiments[2]

↓

Interpretation of the results and **upscaling**[2]

Péclet number	Damköhler number
$Pé = \frac{\text{advection}}{\text{diffusion}}$	$Da = \frac{\text{reaction}}{\text{diffusion}}$

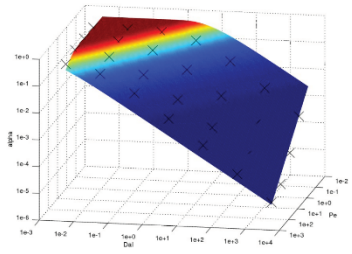

$$\frac{A}{A_0} = 1 - \exp\left(-Pe^{-n}\left(\frac{Da_{II}}{Pe}\right)^{-m}\right)$$

[1]Soulaine and Tchelepi, *Micro-continuum approach for pore-scale simulation of subsurface processes,* Transport in Porous Media (2016)
[2]Soulaine et al., *Mineral dissolution and wormholing from a pore-scale perspective,* Journal of Fluid Mechanics 827 (2017)

29

PORE-SCALE CALCITE DISSOLUTION WITH OPENFOAM-PHREEQC

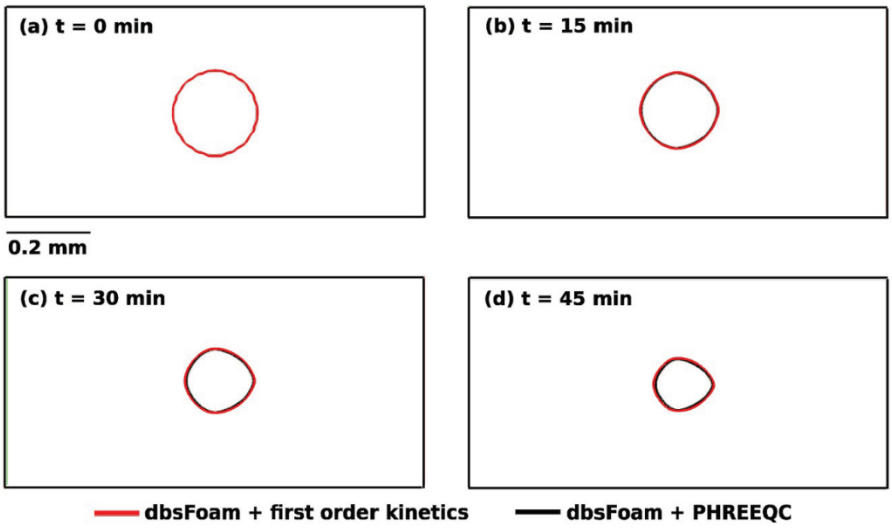

Soulaine et al "porousMedia4Foam: Multi-scale open-source platform for hydro-geochemical simulations with OpenFOAM®" Env Modelling and Soft 145, 105199 (2021)

30

DISSOLUTION OF A FRACTURED POROUS MEDIA

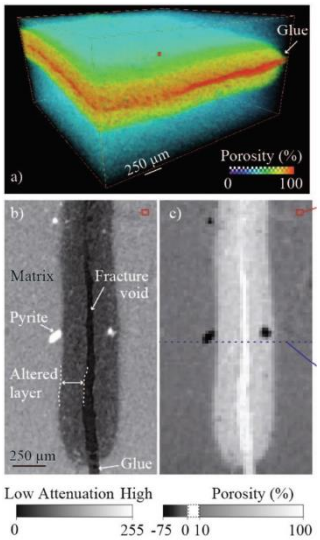

Noiriel, Madé, Gouze.: *Impact of coating development on the hydraulic and transport properties in argillaceous limestone fracture*. Water Resour. Res. 43(9), 1–16 (2007)
Noiriel and Soulaine, *Pore-Scale Imaging and Modelling of Reactive Flow in Evolving Porous Media: Tracking the Dynamics of the Fluid–Rock Interface,* Transport in Porous Media (2021)

31

DISSOLUTION OF A FRACTURED POROUS MEDIA

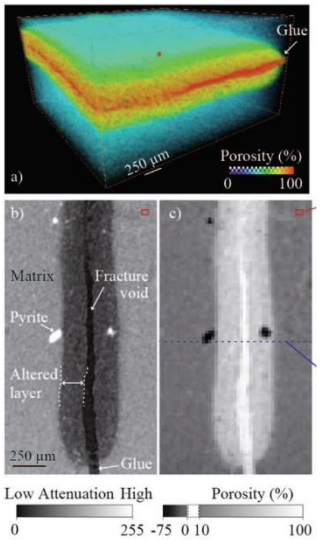

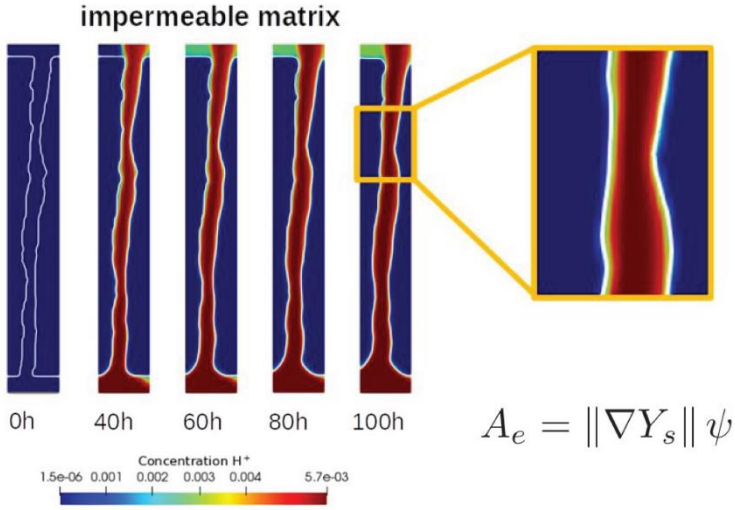

$$A_e = \|\nabla Y_s\| \psi$$

Noiriel, Madé, Gouze.: *Impact of coating development on the hydraulic and transport properties in argillaceous limestone fracture*. Water Resour. Res. 43(9), 1–16 (2007)
Noiriel and Soulaine, *Pore-Scale Imaging and Modelling of Reactive Flow in Evolving Porous Media: Tracking the Dynamics of the Fluid–Rock Interface,* Transport in Porous Media (2021)

32

DISSOLUTION OF A FRACTURED POROUS MEDIA

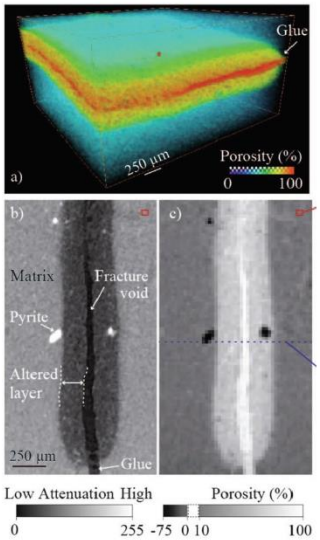

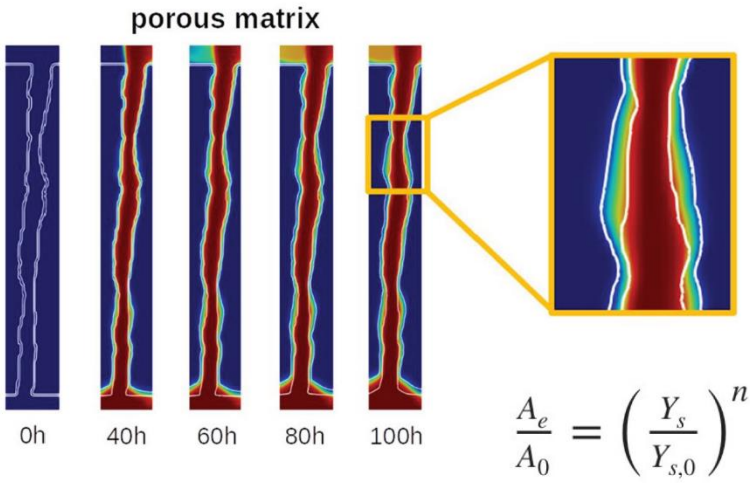

Noiriel, Madé, Gouze.: *Impact of coating development on the hydraulic and transport properties in argillaceous limestone fracture*. Water Resour. Res. 43(9), 1–16 (2007)
Noiriel and Soulaine, *Pore-Scale Imaging and Modelling of Reactive Flow in Evolving Porous Media: Tracking the Dynamics of the Fluid–Rock Interface*, Transport in Porous Media (2021)

33

CONCLUSION AND PERSPECTIVES

- The **porousMedia4Foam** package:
  - *Coupling with geochemical packages (e.g. Phreeqc) for more comprehensive geochemical reactions,*
  - *Multi-scale formulation using micro-continuum solvers,*
  - *Standard Darcy-scale solvers.*
  - *https://github.com/csoulain/porousMedia4Foam*

- Development are still pending:
  - *Reactive two-phase flow,*
  - *Hybrid-scale two-phase flow,*
  - *Simulation in geothermal wells,*
  - *Poromechanics with Darcy-Brinkman-Biot?*

34

ACKNOWLEDGEMENTS

- Funding:
- F. Carrillo and I. C. Bourg (Princeton University),
- H. Tchelepi and A. Kovscek (Stanford University),
- Experimentalists who provided the high-resolution dataset (Sophie Roman, Charlotte Garing, Catherine Noiriel)
- People involved in the code development: Saideep Pavuluri, Emmanuel LeTronc, Julien Maes, Christophe Tournassat, Laurent André, Florian Osselin

35

Thank you for your attention

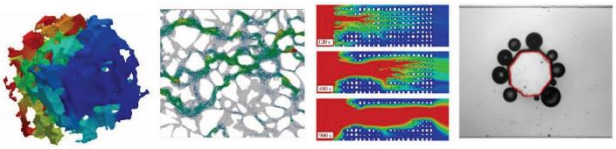

www.cypriensoulaine.com

36

Appendix A. Short career summary of lectures

Barbara Lothenbach, EMPA, Switzerland

Barbara.Lothenbach@empa.ch

Barbara Lothenbach is group leader of the Cement Chemistry and Thermodynamics Group of the Concrete & Asphalt Laboratory at Empa, the Swiss Federal Institute for Materials Science & Technology. She has graduated for ETH Zürich and now is associate professor at University Berne, Switzerland, and adjunct professor at NTNU, Norway. She plays an active role in the promotion of the use of thermodynamic modelling to predict and understand the composition of hydrated cement, fundamental to develop durable and low CO_2-cements.

Carl I. Steefel , LBNL, US

CISteefel@lbl.Gov

Dr. Carl I. Steefel is a Senior Scientist and Head of the Geochemistry Department at Lawrence Berkeley National Laboratory. He has over 30 years of experience in developing models for multicomponent reactive transport in porous media and applying them to topics in reactive contaminant transport and water-rock interaction. He developed the first routine for multicomponent nucleation and crystal growth in the Earth Sciences and the first multicomponent, multi-dimensional code for simulating water-rock interaction in non-isothermal environments. He has also worked extensively in applying reactive transport modeling to natural systems, including hydrothermal, contaminant, and chemical weathering environments. More recent work has focused on pore scale studies of reactive systems, especially faults, and modeling of Critical Zone processes in terrestrial environments. He has been involved in experimental and modeling studies of cation exchange and mineral dissolution and precipitation, as well as modeling studies of field systems focused on contaminant transport, microbially-mediated biogeochemical reactions, chemical weathering, and isotope systematics. In addition to his focus on continuum reactive transport, he has investigated pore scale reactive transport using high performance computing. He is the principal developer of the reactive transport software CrunchFlow, a widely used package in many countries around the world and a 2017 R&D100 award winner. He also has contributed significantly to CrunchClay, an offshoot of Crunch for simulating reactive transport in clayey materials where electrostatic effects are important for transport and sorption.

Diederik Jacques, SCK CEN, Belgium

djacques@sckcen.be

Diederik Jacques is Head of Unit Engineered and Geosystem Analysis at SCK CEN. He obtained his PhD in Agricultural and Applied Biological Sciences at the Catholique University of Leuven (Belgium). He worked as a post-doctoral researcher at SCK CEN in 2002 and became a group leader in 2011. His long-term experience covers such areas as flow and transport phenomena in porous media, coupled reactive transport modelling, parameter estimation, geostatistical characterization and pore-scale/continuum-scale model development. The most recent research is focused on soil-aquifer interactions, long-term evolution of cement-based materials, contaminant and colloid transport in porous media, and performance assessments of surface and deep radioactive waste disposal systems or NORM sites. A major achievement is the development of the coupled reactive transport code HPx for variable saturated porous media. Diederik Jacques is the leader of the EURAD WP2 ACED

Dmitrii Kulik, PSI, Switzerland

dmitrii.kulik@psi.ch

Dmitrii Kulik is Senior Scientist at LES PSI. His research interests include thermodynamics of (multi-site) solid solutions, adsorption and ion exchange in the context of geochemical modelling by Gibbs energy minimization (GEM); geochemical modelling of cement systems and compilation of related

thermodynamic datasets; mineral surface reactivity and kinetics in relation to reactive transport; development,maintenance and promotion of GEM software (https://gems.web.psi.ch; https://cemgems.org; https://thermohub.org; https://reaktoro.org). He has graduated from Taras Shevchenko Kyiv State University (1980) and Institute of Geochemistry and Mineral Physics ASU, Kyiv, Ukraine (1986). Since 2000, he conducts research at PSI (Switzerland). In 1980 – 2000, he worked from research assistant up to leading research associate positions in Ukraine, with multiple research stays abroad (in Germany, USA, Switzerland) in 1992 - 1999.

Emilie Coene, Amphos 21 Consulting S.L., Spain

emilie.coene@amphos21.com

Emilie Coene will be the course instructor. Emilie is a Senior Consultant of the Materials Engineering team at Amphos 21 Consulting S.L. She is a Chemical Engineer and holds a Masters in Numerical Modelling for Science and Engineering. She is an expert in numerical model development and application by using, for example, Matlab, Comsol Multiphysics and iCP. As a consultant at Amphos 21, Emilie has been involved in projects related with nuclear waste management programs in Sweden, Finland, France and Japan. These projects involved numerical models of radionuclide transport, reactive transport and multiphase flow in different media such as concrete, clay materials and host rock. She has also carried out management and development tasks of the interface iCP.

Eric C. Gaucher, University of Bern, Switzerland

eric.gaucher@geo.unibe.ch

Eric C. Gaucher is an expert geochemist working at the University of Bern. His work focuses on water–rock–gas interactions at the laboratory scale up to basin scale using experimental, field and numerical modeling methods. Geological storages (nuclear waste, CO_2, H_2) are his main domain. Although one of his main research objectives is to understand the behaviour of CO_2(g) in sediments (e.g., diagenesis, CO_2 storage), he is now researching abiotic gases (H_2, CH_4) in natural systems mainly linked to serpentinization. He has made interesting discoveries of natural H_2 in the Pyrénées and in the Alps. Prior to coming to TOTAL in 2012, he was the head of a research unit at the French geological survey (BRGM) investigating the stability of clay formations for the management of nuclear waste. In 1993 he gained his MSc in Earth sciences from the École normale supérieure in Lyon (France) and in 1998 his PhD in geochemistry from the University of Paris VII.

Erik Laloy, SCK CEN, Belgium

Eric.laloy@sckcen.be

Eric Laloy works with the Engineered and Geosystem Analysis unit at SCK CEN. He obtained his PhD in environmental engineering at the Université catholique de Louvain (UCL). After a postdoc at the University of California, Irvine (UCI), he joined SCK CEN in 2011. Currently, his main areas of research are uncertainty quantification of geoscientific simulation models, machine learning applied to the geosciences and probabilistic modelling for radiological characterization of radioactive waste.

Hans Meeussen, NRG, The Netherlands

meeussen@nrg.eu

Hans Meeussen is a Senior research scientist, Nuclear Research and consultancy Group (NRG), Petten, The Netherlands and an Associate Professor, Department of Civil Engineering University of Technology Delft, The Netherlands.

He received his MSc in Environmental Science and Software Engineering and his Ph.D. in Soil Chemistry both from Wageningen Agricultural University, The Netherlands.

His area of expertise is the chemical- and migration behavior of contaminants in reactive porous media such as soils, cementitious materials and (nuclear) waste forms, with a focus on theoretical processes and numerical modeling. He has (co-)authored over 50 scientific papers in this area and is developer of the ORCHESTRA reactive transport modeling software (www.meeussen.nl/orchestra).

The structure of this software, in which all models are user definable, makes it ideal for development of e.g. new types of adsorption models. Within the EURAD DONUT project a C^{++} version of the chemical solver was developed, from the original Java version, that facilitates integration with Python, or transport codes.

Javier Samper, University of A Coruña, Spain

j.samper@udc.es: Scopus Author ID 7004089866. http://orcid.org/0000-0002-9532-8433. https://www.scopus.com/authid/detail.uri?authorId=7004089866; Researcher ID: F-7311-2016; Google scholar = nB0YEpwAAAAJ. Web page: http://pdi.udc.es/en/File/Pdi/KF39E.

B.S. and a M.S. in Civil Engineering (Madrid Polyt Univ, 1981). Ph. D. Hydrology & Water Resources (Univ of Arizona, Tucson, 1986). Teaching in UPM (Madrid, 1986-87), UPC (Barcelona (1987-1993) and UDC (Coruña, since 1993). He chaired the Spanish Chapter of the International Association of Hydrogeologists (1997-2000). He holds the following honors: 1) Gómez Navarro Award (1981) from Polytechnic University of Madrid for best Civil Engineering undergraduate student on Hydraulics. Spain; 2) Horton Research Award (1984) from American Geophysical Union, USA.; 3) Student Departmental Honor (1985) from the Department of Hydrology and Water Resources of the University of Arizona. USA; 4) Appearance as Expert in the Senate of Spain (1997) at the Commission on Nuclear Waste Disposal; and 5) Guest Professor from Jilin University in Changchun, China (2006).

He has developed extensive research in hydrology and hydrologic engineering with special emphasis in hydrogeology, water resources evaluation, geostatistics, numerical models of groundwater flow, heat transport and contaminant transport with applications to groundwater management and protection. He has developed computational codes for surface and surface hydrology for the following topics: Water balance modeling (VISUAL-BALAN and GIS-BALAN), water flow, solute and reactive transport in aquifers ($CORE^{2D}$), non-isothermal multiphase water flow, multicomponent reactive transport in clay barriers for waste disposal (INVERSE-FADES-CORE), water flow, and reactive transport and microbial processes in porous and fractured media ($BIOCORE^{2D}$). Participation un EURATOM Research Projects since 1991. Advisor of 11 Master 20 PhD students. 110 publications; 1968 cites; h index = 28; Member of editorial board of J Contaminant Hydrology (2006-2023).

Laurent De Windt, Mines Paris, France

laurent.de_windt@minesparis.psl.eu

Dr. Laurent De Windt is a senior researcher in applied geochemistry in the Geosciences Department at Mines Paris (France), one of the French higher education institutions in engineering. Before that he spent five years in the French institute for radiological protection and nuclear safety (IRSN). His research activities focus on reactive transport modelling applied to environmental chemistry, water decontamination, material durability and radionuclide migration. He has been currently involved in the DISCO and ACED/EURAD European programs on radioactive waste disposals.

Nikolaos Prasianakis, PSI, Switzerland

Nikolaos.prasianakis@psi.ch , https://www.psi.ch/en/les/people/nikolaos-prasianakis

Nikolaos Prasianakis is the head of the transport mechanisms group at the laboratory for Waste Management at the Paul Scherrer Institut (PSI) in Switzerland. He has obtained his PhD degree in multiphysics modelling at the Mechanical and Process Engineering department of ETH-Zürich in 2008. The group activities focus on interdisciplinary approaches to merge experimental knowledge at the field and laboratory scale, geochemical and molecular modelling in order to assess geochemical and transport phenomena in geological repositories for radioactive waste. His research is relevant to multiscale multiphysics modelling, digital twins and machine learning.

Sergey Churakov, PSI, Switzerland

sergey.churakov@psi.ch

Sergey V. Churakov is Head of Laboratory of Waste Management in the Department of Nuclear Energy and Safety at the Paul Scherrer Institute and Full Professor in the Institute of Geological Sciences at the University of Bern. His research covers multidisciplinary topics of environmental geochemistry and mineralogy with specific focus on mechanistic understanding of transport and retention of hazardous contaminants and radionuclides in natural environment and geotechnical systems.

Ulrich Mayer, UBC, Canada

umayer@eoas.ubc.ca

Ulrich Mayer completed his PhD-studies at the University of Waterloo with a focus on reactive transport modeling. Since 2000, he is a professor of hydrogeology at the University of British Columbia (UBC) in the Department of Earth, Ocean and Atmospheric Sciences. His research revolves around reactive transport processes in the subsurface with applications in the oil and gas industry, mine waste management, and deep geologic repositories for used nuclear fuel. At UBC, he is teaching courses on groundwater hydrology, groundwater geochemistry and reactive transport modeling. Over the past three decades, he has led the development of the reactive transport code MIN3P-THCm, a computer model designed for the process-oriented simulation of multicomponent reactive transport. Together with his research group, he has published more than 100 articles in peer-reviewed international journals.

Vanessa Montoya, SCK CEN, Belgium

vanessa.montoya@sckcen.be

Vanessa Montoya is Research Project leader at the Engineered and Geosystem Analysis Unit as part of the Expert Group Waste & Disposal of SCK CEN. Her background is chemistry with 16 years of experience in interdisciplinary and transdisciplinary scientific projects dealing with Radioactive Waste Management and disposal applications. She obtained her PhD in Chemistry at the Universitat Autònoma de Barcelona -UAB (Spain) in 2006. After her PhD, in 2006, she started to work in the Waste Management department of the Environmental consulting company Amphos 21, in Barcelona, as a scientific consultant and project manager. After 6 years in the private sector, and from October 2012 to April 2022, she worked as a Group leader / scientist at the Karlsruhe Institute of Technology – Institute of Nuclear Waste Disposal (KIT-INE) in Karlsruhe and at the department of Environmental informatics, as part of the Smart Models and Monitoring Unit at the Helmholtz-Centre for Environmental Research (UFZ) in Leipzig, Germany. Along her professional career, her work has been mainly focused on providing numerical simulations of geochemical, reactive transport and coupled geochemical and multiphysical processes in natural and engineered barrier systems. She has mainly applied her research to Radioactive Waste Management and Disposal at laboratory, field (i.e. URL: Mont Terri and Grimsel) and long-term repository scales by using and expanding different geochemical and multiphysics finite

element codes. In addition, development of international thermodynamic databases (i.e. ThermoChimie, Thereda) in the same field of application has been part of her activities.